Françoise Gray

Umberto De Girolami

Jacques Poirier

ESCOUROLLE & POIRIER MANUAL OF

Basic Neuropathology

BH

Neurology is an ever-changing field. Standard safety precautions must be followed but as new research and clinical experience broaden our knowledge, changes in treatment and drug therapy may become necessary or appropriate. Readers are advised to check the most current product information provided by the manufacturer of each drug to be administered to verify the recommended dose, the method and duration of administration, and contraindications. It is the responsibility of the treating physician, relying on experience and knowledge of the patient, to determine dosages and the best treatment for each individual patient. Neither the Publisher nor the author assumes any liability for any injury and/or damage to persons or property arising from this publication.

Contributors

Homa Adle-Biassette, MD, PhD
Associate Professor of Pathology, Faculté de Médecine Paris VII (Bichat–Claude Bernard), Université Denis Diderot; Praticien Hospitalier, Service d'Anatomie Pathologique, Hôpital Bichat–Claude Bernard, Paris, France

Douglas C. Anthony, MD, PhD
Professor and Chair, Department of Pathology and Anatomical Sciences, University of Missouri, Columbia, Missouri

Umberto De Girolami, MD
Professor of Pathology, Harvard Medical School; Director, Neuropathology Divisions, Departments of Pathology, Brigham and Women's Hospital; Children's Hospital Boston, Boston, Massachusetts

Charles Duyckaerts, MD, PhD
Professor of Pathology, Faculté de Médecine Paris VI (Pitié-Salpêtrière), Université Pierre et Marie Curie; Praticien Hospitalier, Laboratoire de Neuropathologie Raymond Escourolle, Hôpital de la Salpêtrière, Paris, France

Férechté Encha-Razavi, MD
Associate Professor of Histology, Embryology, and Cytogenetics, Faculté de Médecine Paris V (Necker-Enfants Malades); Université René Descartes; Head, Unit of Fetal Genetic Development, Department of Genetics, Hôpital Necker-Enfants Malades, Paris, France

Margaret Esiri, DM, FRCPath
Professor of Neuropathology, Department of Clinical Neurology, Oxford University; Honorary Consultant Neuropathologist, Oxford Radcliffe NHS Trust, Oxford, United Kingdom

Rebecca D. Folkerth, MD
Assistant Professor of Pathology, Harvard Medical School; Associate in Pathology, Brigham and Women's Hospital; Consultant Neuropathologist, Children's Hospital Boston, Boston, Massachusetts

Matthew P. Frosch, MD, PhD
Assistant Professor of Pathology, Harvard Medical School; Assistant Pathologist, C.S. Kubik Laboratory for Neuropathology, Massachusetts General Hospital, Boston, Massachusetts

Jennian F. Geddes, MB, BS, FRCPath
Reader in Clinical Neuropathology, Department of Histopathology and Morbid Anatomy, Queen Mary—University of London; Honorary Consultant Neuropathologist, Royal London Hospital, London, United Kingdom

Romain K. Gherardi, MD
Professor of Histology, Faculté de Médecine Paris XII (Créteil); Université Paris–Val de Marne; Director, INSERM, Institute of Molecular Medicine; Head, Service d'Histologie and Groupe Nerf-Muscle, Department of Pathology, Hôpital Henri Mondor, Creteil, France

Bernardino Ghetti, MD
Distinguished Professor and Director of Neuropathology, Department of Pathology and Laboratory Medicine, Indiana University School of Medicine, Indianapolis, Indiana

Hans H. Goebel, MD
Professor of Neuropathology, Johannes Gutenberg University Medical Center, Mainz, Germany

David I. Graham, MB BCh, PhD, FRCPath
Professor of Neuropathology, University of Glasgow; Honorary Consultant Neuropathologist, South Glasgow University Hospitals NHS Trust, Glasgow, Scotland, United Kingdom

Françoise Gray, MD, PhD
Professor of Pathology, Faculté de Médecine Paris VII (Lariboisière–St. Louis), Université René Descartes; Director, Service d'Anatomie Pathologique, Hôpital Lariboisière, Paris, France

Brian Harding, D.Phil, BM BCh, FRCPath
Senior Lecturer, Neurosciences Unit, Institute of Child Health; Consultant Neuropathologist, Department of Histopathology, Great Ormond Street Hospital for Children, London, United Kingdom

Jean-Jacques Hauw, MD
Professor of Pathology, Faculté de Médecine Paris VI (Pitié-Salpêtrière), Université Pierre et Marie Curie; Director, Laboratoire de Neuropathologie Raymond Escourolle, Hôpital de la Salpêtrière, Paris, France

E. Tessa Hedley-Whyte, MD
Professor of Pathology, Harvard Medical School; Neuropathologist, Massachusetts General Hospital, Boston, Massachusetts

William F. Hickey, MD
The Hampers Professor and Senior Associate Dean of Academic Affairs, Department of Pathology, Dartmouth Medical School, Hanover; Attending Pathologist, Dartmouth–Hitchcock Medical Center, Lebanon, New Hampshire

James W. Ironside, MBChB, FRCPath, FRCPE
Professor of Clinical Neuropathology, University of Edinburgh; Honorary Consultant Neuropathologist, Lothian University Hospitals Trust, Edinburgh, Scotland, United Kingdom

Hart G. W. Lidov, MD, PhD
Associate Professor of Pathology and Neurology, Harvard Medical School; Staff Neuropathologist, Children's Hospital Boston and Brigham and Women's Hospital, Boston, Massachusetts

David N. Louis, MD
Professor of Pathology, Harvard Medical School; Associate Chief of Pathology, Massachusetts General Hospital, Boston, Massachusetts

James Lowe, B.Med.Sci., BM BS, DM, FRCPath
Professor of Neuropathology, School of Clinical Laboratory Sciences, University of Nottingham Medical School; Clinical Head of Service, Department of Pathology, Queen's Medical Centre, Nottingham, United Kingdom

Jacqueline Mikol, MD
Professor of Pathology, Faculté de Médecine Paris VII (Lariboisière-St. Louis), Université René Descartes; Director, Service d'Anatomie Pathologique, Hôpital Lariboisière, Paris, France

Vânia Nosé, MD, PhD
Associate Professor of Pathology, Harvard Medical School; Associate Director of Surgical Pathology, Brigham and Women's Hospital; Consultant Pathologist, Children's Hospital Boston, Boston, Massachusetts

Jacques Poirier, MD, PhD
Professor of Histology, Faculté de Médecine Paris VI (Pitié-Salpêtrière), Université Pierre et Marie Curie, Praticien Hospitalier, Laboratorire de Neuropathologie Raymond Escourolle, Hôpital de la Salpêtrière, Paris, France

Francesco Scaravilli, MD, PhD, DSc, FRCPath
Professor of Neuropathology, Department of Molecular Neuroscience, Institute of Neurology, University College of London; Honorary Consultant Neuropathologist, University College Hospital NHS Trust, London, United Kingdom

Sydney S. Schochet, Jr., MD
Professor of Pathology, Neurology and Neurosurgery, Robert C. Byrd Health Sciences Center of West Virginia University; Neuropathologist, Ruby Memorial Hospital, Morgantown, West Virginia

Danielle Seilhean, MD, PhD
Associate Professor of Pathology, Faculté de Médecine Paris VI (Pitié-Salpêtrière), Université Pierre et Marie Curie; Praticien Hospitalier, Laboratoire de Neuropathologie Raymond Escourolle, Hôpital de la Salpêtrière, Paris, France

Leroy R. Sharer, MD
Professor of Pathology (Neuropathology), Department of Pathology and Laboratory Medicine, New Jersey Medical School; Attending Pathologist, Department of Pathology and Laboratory Medicine, University Hospital, Newark, New Jersey

Thomas W. Smith, MD
Professor of Pathology, University of Massachusetts Medical School; Director of Neuropathology and Diagnostic Electron Microscopy, Department of Pathology, University of Massachusetts Memorial Medical Center, Worcester, Massachusetts

Raymond A. Sobel, MD
Associate Professor of Pathology, Stanford University School of Medicine; Staff Neuropathologist, Laboratory Service, Veterans Affairs Health Care System, Palo Alto, California

Maria Thom, MB BS, BSc, FRCPath
Senior Lecturer in Neuropathology, Department of Clinical and Experimental Epilepsy, Institute of Neurology, University College London; Honorary Consultant in Neuropathology, National Hospital for Neurology and Neurosurgery, London, United Kingdom

Jean-Michel Vallat, MD
Professor of Neurology, Faculté de Médecine de Limoges; Chairman, Department of Neurology, Hôpital Universitaire Dupuytren, Limoges, France

Harry V. Vinters, MD, FRCP(C), FCAP, FFPath (RCPI)
Professor of Pathology and Laboratory Medicine and Neurology, David Geffen School of Medicine at University of California, Los Angeles; Chief, Laboratory of Neuropathology, Department of Pathology and Laboratory Medicine, University of California, Los Angeles Medical Center, Los Angeles, California

Preface

The first French editions of the *Manuel de Neuropathologie*, published in 1971 and 1977, were conceived, written, and edited by Raymond Escourolle and Jacques Poirier. After the death of Raymond Escourolle in 1984, Françoise Gray joined Jacques Poirier for the third edition; Jean-Jacques Hauw and Romain Gherardi contributed to selected chapters as well. The first three editions reached the English-speaking public thanks to the friendship and translating ability of Lucien Rubinstein.

Neuropathology has evolved to such an extraordinary extent since 1993, the date of publication of the third English edition, that it is no longer possible for just two or three individuals to produce a high-quality, updated new edition. For this fourth edition, therefore, Umberto De Girolami has joined us as a co-editor, and we have sought the collaborative efforts of multiple experts throughout the world to write the English language text.

The compilation of a basic work designed to familiarize physicians-in-training with such a highly specialized discipline as neuropathology entails two opposing risks: in attempting to compress the maximum amount of information within the minimum space, the text is liable to become unintelligible to beginners; if, on the contrary, one tries to maintain too elementary a level, the danger is that only the obvious will be stated. In presenting to the noninitiated reader neuropathological information that some may find too simple, we have opted for the hazard of the second pitfall. Names have purposefully been avoided, with the exception of those traditionally associated with a particular disease. Discussions on the interpretation of lesions have been limited to relatively simple observations. Clinico-pathologic correlations have been reduced to essentials. Rare diseases have been glossed over or mentioned only for completeness. Despite their interest, historical data have been omitted. We have taken for granted that the reader has some familiarity with basic concepts of neuroanatomy, neurohistology, and general principles of anatomic pathology.

This manual is indeed designed not for neuropathologists, or even trained neurologists, but for students and physicians-in-training, particularly those interested in anatomic pathology, neurology, neuroradiology and neurosurgery, who have recently joined a neuropathology laboratory hoping to become familiar with the essential topics of the pathology of the nervous system. Those who do not plan a career in

neurology or neuropathology need not extend their studies much beyond the material covered herein; the others should regard this manual simply as an introduction to the textbooks and major references listed in the bibliography at the end of this text.

We hope that the readers of the fourth edition of this book will grant it as favorable a reception as that happily enjoyed by earlier editions.

Acknowledgments

The editors and authors acknowledge with pleasure Ms. Nancy Lombardi for superior editorial assistance; Ms. Susan Pioli, editor representing the Butterworth-Heinemann Company, for making this work possible; and Ms. Diane Brown and Ms. Linda Palcsey for excellent support in helping us prepare a final draft of this manuscript.

<div align="right">

Jacques Poirier, MD, PhD
Francoise Gray, MD, PhD
Umberto De Girolami, MD

</div>

neurology or neuropathology need not extend their studies much beyond the material covered herein; the others should regard this manual simply as an introduction to the textbooks and major references listed in the bibliography at the end of this text.

We hope that the readers of the fourth edition of this book will grant it as favorable a reception as that happily enjoyed by earlier editions.

Acknowledgments

The editors and authors acknowledge with pleasure Ms. Nancy Lombardi for superior editorial assistance; Ms. Susan Pioli, editor representing the Butterworth-Heinemann Company, for making this work possible; and Ms. Diane Brown and Ms. Linda Palcsey for excellent support in helping us prepare a final draft of this manuscript.

<div align="right">

Jacques Poirier, MD, PhD
Francoise Gray, MD, PhD
Umberto De Girolami, MD

</div>

Foreword

When I was learning neurology in the mid-1970s, neuroanatomy and neuropathology were the basic sciences of the field. Nearly a third of my formal neurological training was devoted to a serious study of neuropathology. I went to the autopsy room, removed the brain and spinal cord, fixed the tissue, and later examined it grossly and microscopically, ultimately generating a clinical-pathologic correlation. A formal report of the findings was written, supervised by a senior neuropathologist. These 50 personally analyzed cases formed the foundation of my entire career in clinical neurology. Through these cases I learned the anatomy of the nervous system, its reaction to disease, and the rigorous methods necessary to hone my clinical approach using the gold standard of neuropathology.

At that point in my nascent career I had no knowledge of neuropathology except for the very simple principles learned in my medical school general pathology course. Thank goodness for the then newly available *Manual of Basic Neuropathology* by Raymond Escourolle and Jacques Poirier. The original French monograph entitled *Manuel Élémentaire de Neuropathologie* had just been translated into English by Lucien J. Rubinstein and published in 1973. It was my bible and savior. With it I was able to learn approaches and techniques to analyze my cases and unlock the enormous trove of invaluable knowledge that the cases held. To this day I frequently refer back to the little blue paperback book that had such an enormous impact on the way in which I approach neurological problems.

In many ways neurology and neurological training have fundamentally changed. The basic sciences of neurology are now molecular genetics and cell biology. Current trainees must learn a great deal about structural and functional imaging of the nervous system as well as the details of a whole array of subspecialty subjects such as movement disorders, cancer neurology, stroke, demyelinating diseases, epilepsy, neuromuscular diseases, neuro-ophthalmology, cognitive and behavioral neurology, and pain. Thankfully, therapeutics is now a real part of neurology, so modern neurologists in training are faced with a dizzying array of complex treatments for nearly every category of neurologic diseases.

As the complexity of clinical neurology has increased, the subject of neuropathology has become progressively neglected. The opportunity to spend nearly a year on the study of neuroanatomy and neuropathology is unavailable; yet the lessons that can be learned are even more important than they were in the past. A

rigorous approach to neurologic disease, with the gold standard of modern neuropathology, is absolutely required for the neurologist of the future.

In this context, Jacques Poirier, one of the original authors, is joined on the editorial team by Françoise Gray and Umberto De Girolami, together with 30 distinguished neuropathologists from around the world to remodel, update, and expand *Manual of Basic Neuropathology* for the modern era. The reader will find the fourth edition to be just as clearly written and accessible as the earlier ones, but it now contains the relevant principles and advances in the fields of molecular genetics and cell biology. The old and new neuropathology are skillfully blended to enlighten the student of nervous system diseases with the basic principles and processes that underlie all of the major categories of illness.

The basic principles of pathology of the central nervous system lead the book, with a survey of modern neuropathological methods at the end. New chapters on tumors, trauma, vascular diseases, and infections follow. A new, beautifully clear chapter on the important prion diseases is followed by thoroughly updated chapters on demyelinating diseases and degenerative disorders. Three new chapters on acquired metabolic disorders, hereditary metabolic disorders, and congenital malformations and perinatal diseases replace the single small chapter in the original work on toxic, deficiency, and metabolic diseases.

Two new separate chapters on nerve and muscle neuropathology replace the single old chapter, reflecting the major changes that have occurred in this area of peripheral nervous system neuropathology. Finally, a wholly new chapter on the pituitary gland completes the book. The authors of the individual chapters are experts in their fields and write clearly and concisely.

I found the new *Manual of Basic Neuropathology* a marvelous and welcome addition to neurologic literature. I look forward to referring to this new version for many years to come. It will have an honored place on my library shelf, right next to the original little blue book that gave me such a great start so many years ago.

Martin A. Samuels, MD

Chapter 1
Basic Pathology of the Central Nervous System

Danielle Seilhean, Umberto De Girolami, and Françoise Gray

Diagnosis in neuropathology is based primarily on the gross and microscopic study of the brain, brainstem, cerebellum, and spinal cord. Three consecutive and closely interrelated steps are involved: (1) morphologic analysis of the lesions, (2) topographic analysis of the lesions, and (3) critical integration of these findings and their subsequent correlation with the clinical data and the general autopsy findings, thus permitting an etiologic diagnosis to be made in most instances.

Morphologic Analysis of Central Nervous System Lesions

With the exception of tumors and malformations, most disorders of the CNS are characterized morphologically by the combination of a number of lesions that are not diagnostic in themselves. Various pathologic processes induce neural parenchymal injuries with consequent reaction of the cellular elements of the nervous system (neurons, astrocytes, oligodendrocytes, and microglia) and supporting structures (meninges, connective tissue, and blood vessels). Reactions of the former type (basic cellular lesions) are demonstrable only on microscopic examination, whereas reactions of the latter type (tissue lesions) may be associated with more extensive changes that can be recognized macroscopically or with the help of a magnifying lens.

Although changes that occur in neurons, glia, connective tissue, and vascular structures will be described separately, for the sake of clarity, it is essential to emphasize the close functional interdependence of the various cellular elements of the nervous system in their reactions to injury. This is particularly important in the case of nerve cell alterations where, except for very acute lesions, the possibility of artifactual change may be suspected whenever the reaction is not accompanied by a glial cell response.

Basic Cellular Lesions

Neuronal Lesions

Neuronal injury may result in irreversible cell damage (cell death) or in reversible cell damage. The death of cells may be recognized morphologically as "atrophy" when the injury occurs relatively slowly. Acute neuronal cell injury (eosinophilic neuronal necrosis) and neuronophagia are manifestations of acute, lethal injuries. There are also characteristic neuronal lesions that lead to cell destruction over variable time periods (i.e., neurofibrillary degeneration, neuronal storage of metabolic products, and disorders associated with inclusion bodies). Central chromatolysis, to some extent a reversible insult, is a morphologic manifestation of a reparative response to injury.

The end stage of all irreversible processes that involve the nerve cells is neuronal loss. Nerve cell loss is said to occur when the number of cell bodies in a particular area is appreciably lower than normal. This assessment can be difficult to make in the absence of rigorous morphometric analysis, when less than 30% of the normal cell population has been lost. Further, it depends on the thickness of the section and on the normal cytoarchitectonics of the region examined.

Nerve Cell Atrophy. *Nerve cell* or *neuronal atrophy* is the descriptive term given to a wide variety of irreversible neuronal injuries that cause relatively slow cell death. Neuronal atrophy is characterized morphologically by retraction of the cell body, with diffuse basophilia of the cytoplasm and pyknosis and hyperchromasia of the nucleus in the absence of an inflammatory reaction. Neuronal atrophy occurs in many degenerative disorders that involve several interconnected neuronal systems (e.g., olivopontocerebellar atrophy, Friedreich ataxia, and amyotrophic lateral sclerosis). It is also seen in anterograde and retrograde trans-synaptic degeneration (e.g., in the lateral geniculate body following a lesion of the optic nerve).

Neuronal atrophy should not be confused with "dark neurons," an artifact seen in brain biopsies fixed in formalin by immersion. The latter are characterized by shrunken cytoplasm and by deeply stained and irregularly shaped nuclei.

Apoptosis. *Apoptosis* (programmed cell death) is an active, genetically controlled, energy-consuming process. Neurons undergoing simple neuronal atrophy or apoptosis have similar morphologic features and may show positive in situ end-labeling to identify internucleosomal DNA fragmentation (Fig. 1-1) or be demonstrable by activated caspase-3 immunostaining.

Acute Neuronal Necrosis (Anoxic/Ischemic Neuronal Change). *Acute neuronal necrosis* occurs in a variety of acute injuries, including anoxia and ischemia, but may also be found in many other acute pathologic processes, including hypoglycemia and exposure to excessive amounts of excitotoxic neurotransmitters. Unlike apoptosis, the predominant cellular changes in acute neuronal necrosis involve the cytoplasmic organelles and
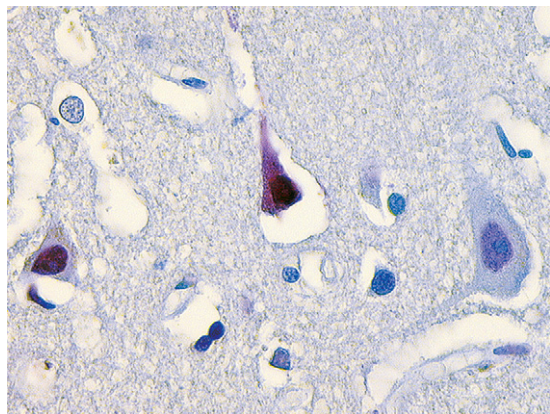

Figure 1-1. Two neurons undergoing apoptosis positively stained by in situ end-labeling to demonstrate internucleosomal DNA fragmentation. In one neuron (*left*), only the nucleus is stained, whereas in the other (*middle*), which is at a later stage of the programmed cell-death process, the entire cell body is stained. Compared to a normal neuron (*right*), both apoptotic neurons have similar morphologic features and show pyknotic nuclei and shrunken cytoplasm.

the cell membrane, which ruptures, leading to cell death.

The following sequence of changes is noted under light and electron microscopy: (1) cytoplasmic microvacuolation due to swelling of mitochondria and endoplasmic reticulum; (2) shrinkage of the cell body, with retraction of the cellular outlines and disappearance of Nissl bodies with eosinophilic condensation of the cytoplasm ("red neuron"); (3) condensation of nuclear chromatin and nuclear pyknosis (Fig. 1-2); (4) late disappearance of the nuclear chromatin, resulting in increased acidophilia of the nucleus, which appears to merge into the surrounding cytoplasm (karyorrhexis).

Occasionally, dead neurons—especially those adjacent to old (mostly hemorrhagic) infarcts, or to traumatic scars—become encrusted with basophilic mineral deposits, chiefly iron and calcium salts. This condition is referred to as mineralization or ferrugination of neurons (Fig. 1-3).

Central Chromatolysis. Central chromatolysis is characterized morphologically by swelling of the cell body; disappearance of Nissl bodies, beginning centrally and extending outward; and flattening and eccentric displacement of the nucleus to the
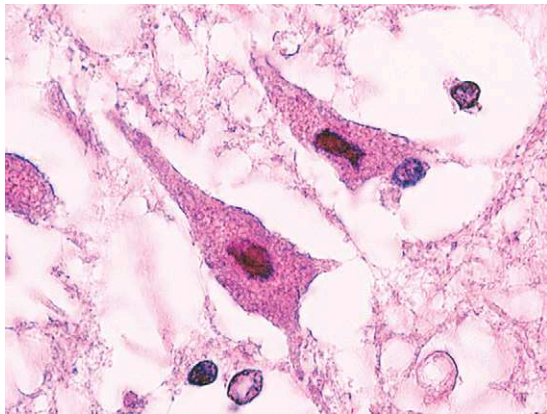
Figure 1-2. Acute ischemic nerve cell change (hematoxylin and eosin [H and E]). Eosinophilic and shrunken cytoplasm and hyperchromatic nucleus.
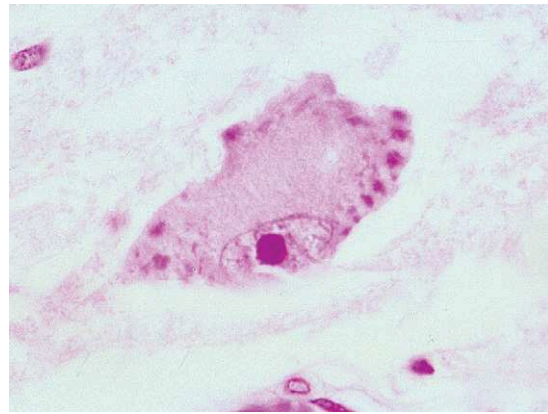

Figure 1-4. Central chromatolysis (Nissl stain). Note cellular swelling, eccentric displacement of the nucleus, and margination of the Nissl bodies.

periphery (Fig. 1-4). It is usually seen in lower motor neurons (i.e., anterior horns of the spinal cord, cranial motor nerve nuclei), where it represents a reparative reaction of the cell body to a lesion of the axon (retrograde degeneration or axonal reaction). Subsequent recovery of normal cell morphology or, conversely, further progression to nerve cell degeneration depends on the reversibility of the axonal lesion (Fig. 1-5). Central chromatolysis is sometimes seen in upper motor neurons but is then more difficult to interpret. On the one hand, axonal lesions within the central nervous system either do not produce changes in cell body morphology or result in a "simple" type of atrophy. On the other hand, some metabolic dis-

orders that do not involve axons a priori (e.g., Wernicke's encephalopathy, pellagra encephalopathy, porphyria) are accompanied by central chromatolysis. Central chromatolysis may be diagnosed only after comparison with the normal morphology of the affected nerve cell, as some nuclei (e.g., the mesencephalic nucleus of the fifth cranial nerve, Clarke's column) normally possess rounded neurons with marginated Nissl bodies.
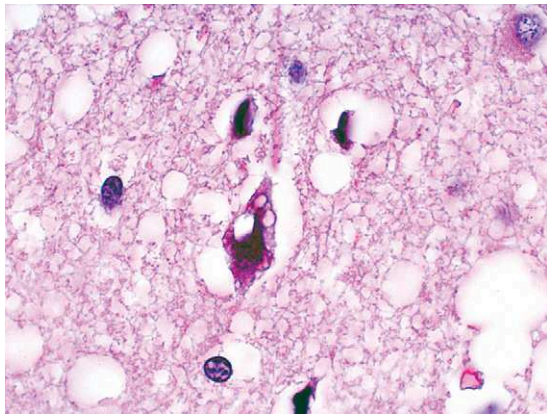
Vacuolated Neurons and Neuropil.   Vacuolated neurons and neuropil are observed in Creutzfeldt-
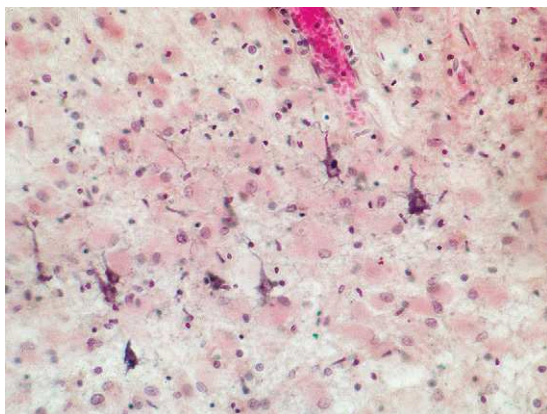
Figure 1-3. Ferrugination (mineralization) of the neurons at the edge of an old hemorrhagic infarct (H and E).
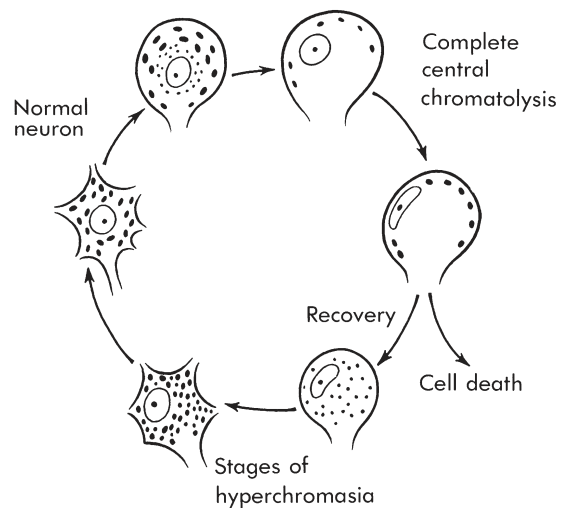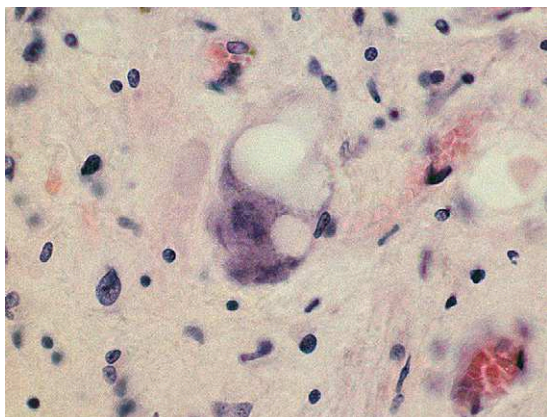

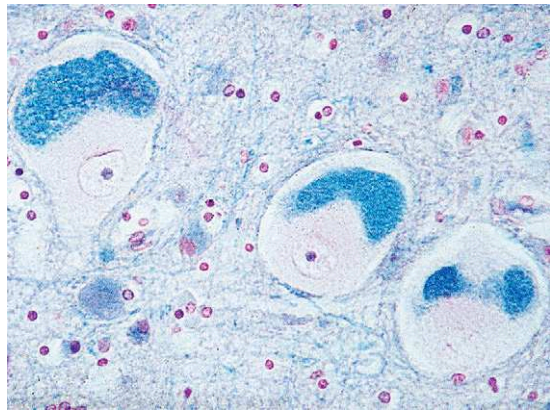**Figure 1-5.** Various nerve cell changes resulting from central chromatolysis.

**Figure 1-6.** A vacuolated neuron in a case of Creutzfeldt-Jakob disease (H and E).

Figure 1-8. Distended nerve cell bodies in a case of neurolipidosis (combined Luxol fast blue and Bodian silver impregnation).

Jakob disease (Fig. 1-6). In rare instances, swelling with vacuolation of nerve cells, so-called "fenestrated neurons" is thought to result from trans-synaptic degeneration. This is seen, for example, in the neurons of the inferior olive in olivary hypertrophy secondary to a lesion of the ipsilateral central tegmental tract or of the contralateral dentate nucleus (Fig. 1-7).

Binucleated Neurons.   These lesions are seen rather infrequently, sometimes in normal tissue or, more often, at the edges of old focal lesions such as those caused by dysplastic/malformative phenomena (e.g., tuberous sclerosis) or in certain neoplasms (e.g., ganglion cell tumors).

Figure 1-7. A fenestrated neuron in a case of olivary hypertrophy (Nissl stain).

Neuronal Storage Disorders.   In some hereditary metabolic diseases related to enzymatic defects involving synthetic or degradative pathways for lipids or carbohydrates, interruption of the pathway leads to cytoplasmic accumulation of intermediate substrates or their by-products. This accumulation results in swelling and distention of nerve cell bodies and eccentric displacement of their nucleus (Fig. 1-8). In several neuronal storage disorders, the stored material has distinctive histochemical and ultrastructural features that may help characterize clinically suspected cases. Biochemical tests on blood, leukocytes, and other body fluids are now particularly useful to more precisely diagnose many of these disorders.

Lipofuscin accumulation is a characteristic aging change (Fig. 1-9).

Alzheimer Neurofibrillary Degeneration; Granulovacuolar Degeneration.   *Alzheimer neurofibrillary degeneration* is chiefly observed in aging and in senile dementia of the Alzheimer type but has been described in a variety of cerebral disorders. Neurofibrillary tangles (NFTs) are best identified by silver impregnation, which demonstrates thickened and tortuous fibrils within the neuronal cytoplasm. The configuration may vary according to the site of the tangle, the type of neuron affected, and, possibly, the stage of its development (Fig. 1-10). Band-shaped perikaryal NFTs are seen both in large and small pyramidal cells and are perhaps an early stage of NFT
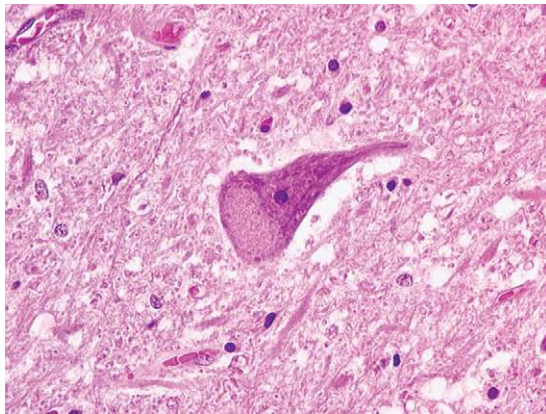
Figure 1-9. Lipofuscin in neuronal cell body (H and E).

formation (Fig. 1-10A). Triangular, flame-shaped perikaryal NFTs are seen mainly in large pyramidal cells (Figs. 1-10B and C). Small, compact, globose perikaryal NFTs are mainly seen in small cortical neurons (Fig. 1-10D). Large, globose NFTs reminiscent of a ball of yarn are more common in the nucleus basalis of Meynert and in the brainstem (Fig. 1-10E). In the final stages of the disease, the cell outline disappears and only the distorted fibrils remain as "ghost NFT" (Fig. 1-10F). The main biochemical component of neurofibrillary tangles is made of microtubule-associated tau protein in an abnormal highly phosphorylated form. The great majority of tangles are particularly well-demonstrated by anti-tau antiserum; this immunocytochemical technique is increasingly used as a routine method for detecting NFTs. A few NFTs are also immunoreactive for ubiquitin. Under electron microscopy, most NFTs consist of paired helical filaments measuring around 20 nm in diameter with a regular constriction to 10 nm occurring every 80 nm; these constrictions may also be associated with straight filaments. In progressive supranuclear palsy, tangles have been found to consist mainly of straight filaments measuring 15 nm in diameter.

Granulovacuolar degeneration is mainly found in Ammon horn and is seen in normal aging as well as in Alzheimer disease and Pick disease. It manifests as small clear vacuoles measuring 4 μm to 5 μm in diameter and containing an argyrophilic granule that is also well stained by hematoxylin (Fig. 1-11). Some of the granules are immunoreactive for phosphorylated neurofilaments, tubulin,

tau, and ubiquitin, suggesting that the vacuoles are autophagic lysosomal structures in which cytoskeletal components are being degraded.

Intraneuronal Inclusion Bodies. *Intraneuronal* (intracytoplasmic or intranuclear) *inclusion bodies* are important indicators of neuronal injury. They occur in degenerative, metabolic, and viral diseases and often have diagnostic immunocytochemical and ultrastructural features.

Pick bodies are rounded, homogenous, intracytoplasmic neuronal inclusions (Fig. 1-12). They are characteristic of Pick disease, where they may be seen in pyramidal neurons and dentate granule cells of the hippocampus as well as in affected regions of the neocortex. They are intensely argyrophilic and are immunoreactive for phosphorylated neurofilaments, ubiquitin, tau, and tubulin. Ultrastructurally, they consist of poorly circumscribed masses of intermediate filaments, 15-nm straight filaments, some paired helical filaments, and entrapped vesicular structures.

Lewy bodies are neuronal inclusions whose appearances vary according to whether they are found in the perikaryon or in the nerve cell processes, in the cortex, brainstem, or sympathetic ganglia (Fig. 1-13, p. 8). Classic (brainstem) Lewy bodies are roughly spherical, with an eosinophilic core surrounded by a paler "halo." One or more may be present in the cytoplasm of a single neuron (Figs. 1-13A and B). They may be more elongated when they occur in axonal processes or in sympathetic ganglia (Figs. 1-13C and D). Cortical Lewy bodies are less clearly defined and consist of a homogenous zone of hypereosinophilia that usually lacks a surrounding "halo" (Figs. 1-13E and F). Lewy bodies are immunoreactive for ubiquitin, αB crystallin and α-synuclein. Under electron microscopy they consist of an amorphous, electron-dense core surrounded by a halo of radiating filaments. Their presence defines several conditions termed "Lewy body disorders," the most frequent of which is Parkinson disease.

Hirano bodies are brightly eosinophilic, rod-shaped or elliptical cytoplasmic inclusions that may appear to overlap the edge of a neuron. They are mostly found in the CA1 field of the hippocampus and are particularly numerous in Alzheimer disease, Pick disease, and Guam parkinsonism-dementia. They are immunoreactive for actin and
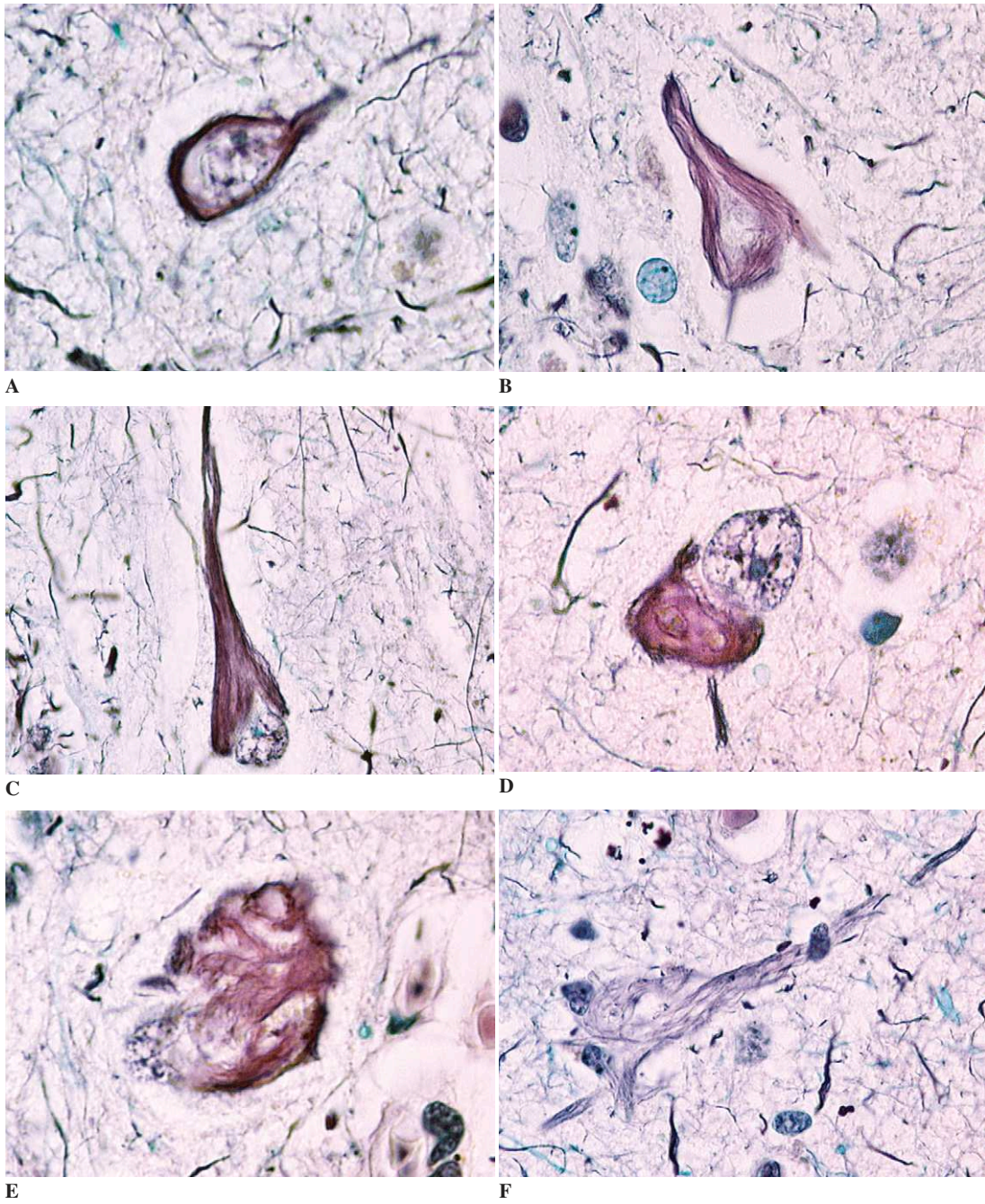
Figure 1-10. Different types of neurofibrillary tangles (Bodian silver impregnation combined with Luxol fast blue). **A**, Band-shaped perikaryal NFT. **B** and **C**, Triangular flame-shaped perikaryal NFT. **D**, Small compact globose perikaryal NFT. **E**, Large globose NFT. **F**, "Ghost NFT."
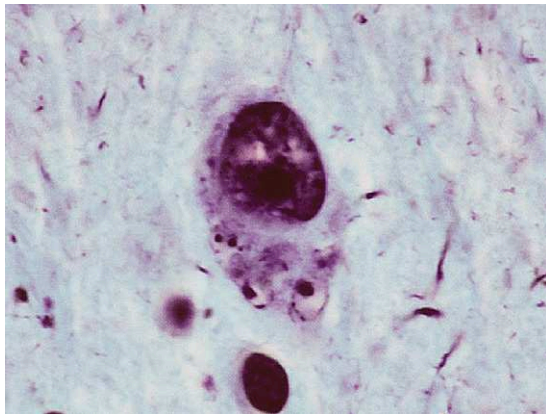
Figure 1-11. Granulovacuolar degeneration (Bodian silver impregnation).

actin-associated proteins. Ultrastructurally, they are highly characteristic and consist of parallel filaments that are 100 nm in length and alternate with a longer sheet-like material.

Bunina bodies are eosinophilic, nonviral intracytoplasmic inclusions that may be observed in motor neurons in cases of familial or sporadic amyotrophic lateral sclerosis (Figs. 14A and B). Ultrastructurally, they appear as electron-dense, membrane-bound bodies.

Skein-like inclusions are abnormal, ubiquinated, threadlike structures that appear in anterior horn cells in motor neuron diseases. Some present singly and others form networks of threads. Occasionally, the threads are aggregated to form large, dense inclusions (Fig. 1-15). Ultrastructurally, they
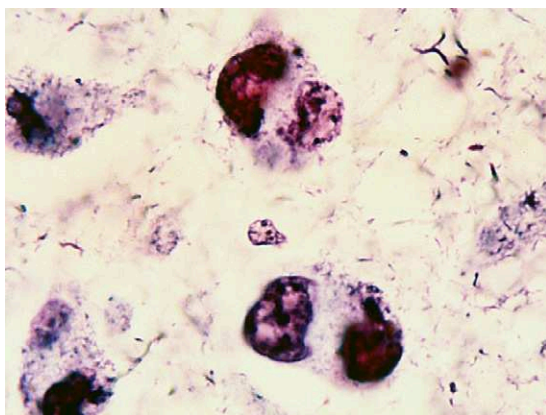
Figure 1-12. Neuronal argyrophilic inclusion in Pick disease (Bodian silver impregnation).

consist of bundles of filaments of 15 nm to 25 nm in diameter, with a tubular profile on cross section.

Marinesco bodies are small, eosinophilic, strongly ubiquitin-positive, intranuclear inclusions located chiefly in melanin-containing brainstem neurons (Fig. 1-16A). They have no known pathologic significance. However, comparable eosinophilic intranuclear, ubiquitin-positive inclusions may be observed in selected groups of neurons in various hereditary diseases with cytosine-adenine-guanine repeat expansions—including spinocerebellar degenerations (Fig. 1-16B), Huntington disease, and dentatorubral pallidoluysian atrophy—or in "familial neuronal intranuclear hyaline inclusion disease."

Lafora bodies are rounded structures composed of polyglucosan (polymers of sulfated polysaccharides) and are similar to corpora amylacea (see further on) in composition and staining characteristics. They are found in large numbers in myoclonic epilepsy in the CNS—chiefly in the dentate nucleus—and in certain peripheral tissues such as sweat glands, liver, and skeletal muscle. They usually have a dense, strongly periodic acid-Schiff (PAS)–positive core, surrounded by a filamentous, less PAS–positive region. (Fig. 1-17).

Viral inclusions are eosinophilic, intranuclear inclusions that occupy a greater or a lesser proportion of the nucleus and may be surrounded by a clear halo. They are associated with some viral infections of the CNS (see Chap. 5), being seen chiefly in herpes virus infections (particularly in the necrotizing encephalitis caused by herpes simplex virus) and in subacute sclerosing panencephalitis. Intracytoplasmic viral inclusions may also occur (e.g., Negri body associated with rabies). In rare instances (e.g., cytomegalovirus infection), both intranuclear and intracytoplasmic viral inclusion bodies may be seen. Most of these inclusion bodies are immunoreactive for specific antivirus antibodies, allowing a specific diagnosis. Electron microscopy may demonstrate the presence of characteristic viral structures; however, various other morphologic forms that do not correspond to viral structures are also frequently seen.

Axonal Alterations. Following axonal lesions, the distal part of the axon undergoes Wallerian degeneration, which will be described later (see "Basic lesions of the peripheral nervous system," Chap. 14).
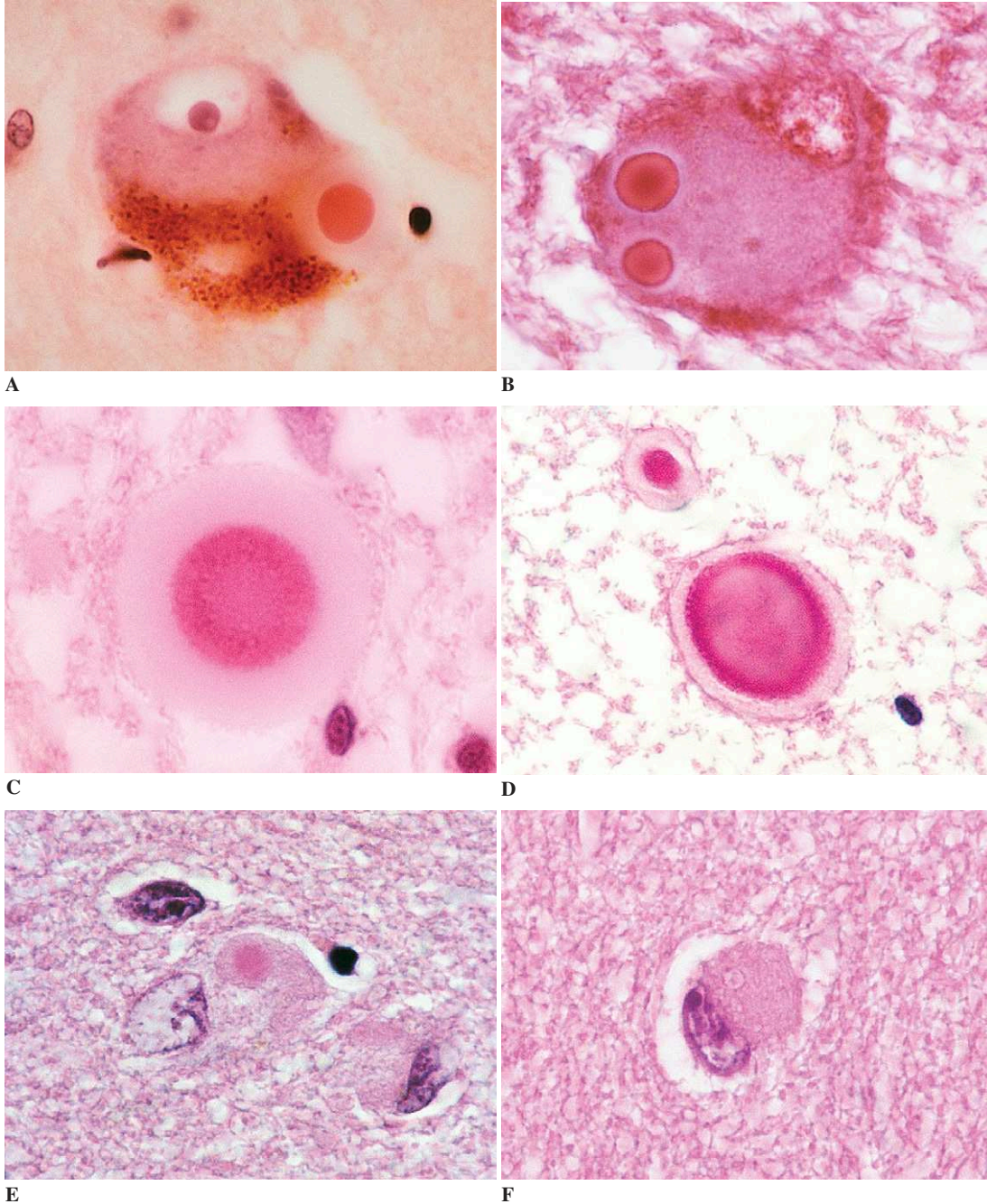
Figure 1-13. Lewy bodies (H and E). Solitary (**A**) and multiple (**B**) Lewy bodies in the perikaryon of pigmented neurons of the substantia nigra in a case of Parkinson disease. **C** and **D**, Lewy bodies in axonal processes in the dorsal nucleus of the tenth cranial nerve in a case of Parkinson disease. **E** and **F**, Cortical Lewy bodies in the perikaryon of a cortical neurons in a case of Lewy body disease.
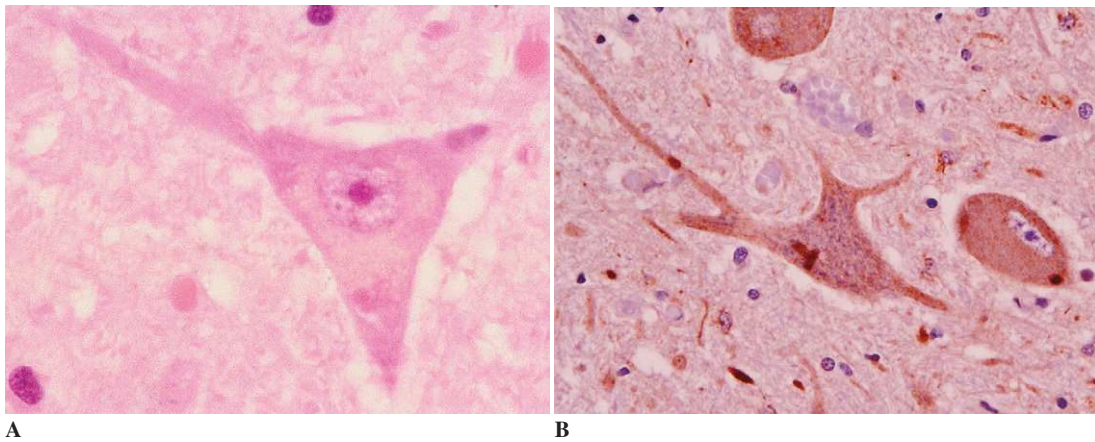
Figure 1-14. A, Bunina bodies in anterior horn cells of the spinal cord in a case of motor neuron disease (H and E). **B**, Immunocytochemistry for ubiquitin.

In neuronal atrophy, perikaryal lesions are associated with degeneration of the axon, which becomes altered and undergoes atrophy. In system degenerations, the lesions appear to begin at the distal extremities of the longest axons.

Axonal swellings or *spheroids* are localized, eosinophilic enlargements of the axon. They are composed of neurofilaments, organelles, and other materials that are normally conveyed along the axon by an anterograde transport system but accumulate focally when this transport system is interrupted. Spheroids are a feature of axonal damage, the result of diverse extrinsic insults, especially trauma and ischemia. They are well demonstrated

Figure 1-15. Skein-like inclusion in an anterior horn cell, in a case of motor neuron disease (immunocytochemistry for ubiquitin).

by silver impregnation (Fig. 1-18A) and by immunostaining with ubiquitin (Fig. 1-18B) and with the precursor of the beta amyloid protein (Fig. 1-18C). The latter is transported by axonal flow and accumulates when it is disrupted. The term *torpedoes* is applied to Purkinje cell axonal swellings, which are a feature of a wide range of metabolic and degenerative cerebellar diseases. These occur in the initial portion of the axis cylinder before the origin of the collateral branches and are well seen with silver impregnations (see Fig. 1-18C).

The axonal swellings that develop when axonal transport is disrupted by neuronal metabolic dysfunction are usually termed *dystrophic*. Transport disruption occurs in some acquired (e.g., vitamin E deficiency) or inherited metabolic diseases. The term *dystrophic neurite* is also used to describe a neuronal process within the grey matter that is distended by tau protein or other abnormal, ubiquinated material. Dystrophic neurites occur in several neurodegenerative diseases, including neuroaxonal dystrophy.

Astrocytic Lesions

Gliosis (Astrogliosis).   *Gliosis* (astrogliosis), proliferation of the astrocytes, is the best indication that a microscopic abnormality is of pathologic significance, not artifactual. It is an important astrocytic reaction to tissue damage and is seen in both acute and chronic processes. Its associated morphologic changes include expansion of the

Figure 1-16. Marinesco bodies. **A**, Small intranuclear inclusion in a pigmented neuron of the substantia nigra (H and E). **B**, Ubiquitin-positive intranuclear inclusion in a case of spinocerebellar degeneration with cytosine-adenine-guanine repeat expansion. (Courtesy of Dr. Francesco Scaravilli.)

astrocytic cytoplasmic arborization. For reasons that are not understood, mitotic figures are only rarely identified in gliotic tissue.

Depending on the location, stage of evolution, and nature of the pathologic process, gliosis assumes one of the following three forms:

(1) In *fibrillary gliosis*, the astrocytic reaction is characterized in its early stages by hypertrophy of the nucleus (which is often hyperchromatic and eccentrically placed in the perikaryon), while the cytoplasm and cell processes become visible and are found to contain excess glycogen (Fig. 1-19A). These reactive astrocytes (gemistocytic astrocytes) now show an expanded swath of homogeneous eosinophilic cytoplasm (Figs. 1-19B and C).
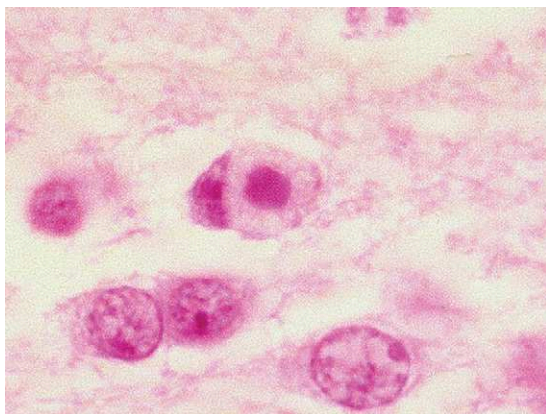
Figure 1-17. Lafora body in a case of myoclonic epilepsy (periodic acid Schiff).

(2) In chronic disease states and slowly degenerative processes, astrocyte nuclei regain, over time, their resting size and shape. Their cytoplasmic networks of cell processes are extensive and can best be appreciated with the help of special stains (i.e., Mallory's phosphotungstic acid-hematoxylin or immunostaining of the glial fibrillary acidic protein [GFAP]).

(3) In slowly-evolving degenerative conditions, the alignment of astrocyte processes conforms to the architecture of previously normal local tissue, resulting in the picture of *isomorphic fibrillary gliosis*.

Alzheimer Type II Glia. *Alzheimer type II glia* are seen in hyperammonemic states such as occur in Wilson disease and in liver failure. Astrocytic nuclei become enlarged, reaching 15 μm to 20 μm in diameter, and irregular in shape; they are pale and empty-looking because of the disappearance of chromatin granules (Fig. 1-20). One or two dense, crisp, rounded bodies resembling nucleoli are often seen next to the nuclear membrane; these are PAS-positive. The cell bodies are usually invisible on conventional preparations and stain poorly with GFAP. They occur in the deep gray nuclei, especially in the pallidum, the dentate nuclei, and (to a lesser extent) the cerebral cortex. Alzheimer type II glia are metabolically active cells engaged in the detoxification of ammonia and contain numerous mitochondria.
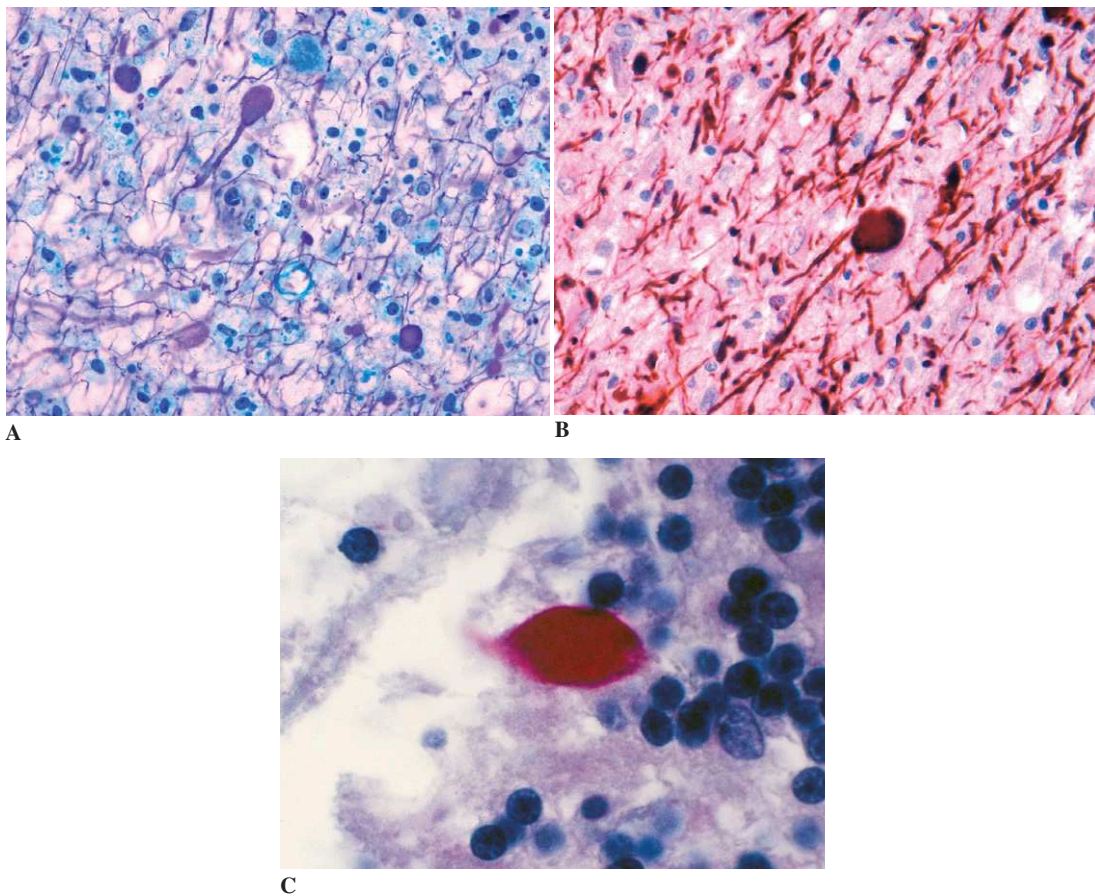
Figure 1-18. Axonal swellings in the white matter identified on silver impregnation. **A**, Bodian stain. **B**, Ubiquitin immunostain. **C**, Torpedo (axonal swelling) on a Purkinje cell axon identified by β-APP immunostaining.

**Rosenthal Fibers.** Under light microscopy, Rosenthal fibers are beaded structures—rounded, oval, or elongated—that measure 10 μm to 40 μm across and appear homogenous and brightly eosinophilic. Under electron microscopy they are seen to consist of swollen astrocytic processes filled with electron-dense amorphous granular material and glial filaments. By immunohistochemistry, they show peripheral labeling for GFAP, ubiquitin, and αB-crystallin. Rosenthal fibers are seen in various pathologic conditions that have in common intense fibrillary gliosis of long duration as seen around multiple sclerosis plaques, in the spinal cord in syringomyelia, around craniopharyngiomas, in certain neoplasms (e.g., pilocytic astrocytomas of the cerebellum or hypothalamus; see Chap. 2), and in Alexander disease (see Chap. 10).

Eosinophilic granular bodies are to some extent related to Rosenthal fibers; they are rounded hyaline droplets that occupy the cytoplasm of astrocytes and are also seen in pilocytic astrocytomas and gangliocytomas.

Inclusions and Storage Material. Accumulation of *lipofuscin* occurs in astrocytes, as in neurons, with aging. Similarly, *glial lipid storage* may accompany neuronal storage in lipid storage diseases.

Tau protein, which is the main component of neurofibrillary tangles, can also accumulate in astrocytes, particularly in progressive supranuclear palsy and corticobasal degeneration (see Chap. 8).

Tufted astrocytes are considered to be highly characteristic of progressive supranuclear palsy (PSP) (see Fig. 8-5A). The whole length of their processes contains tau protein and they are often
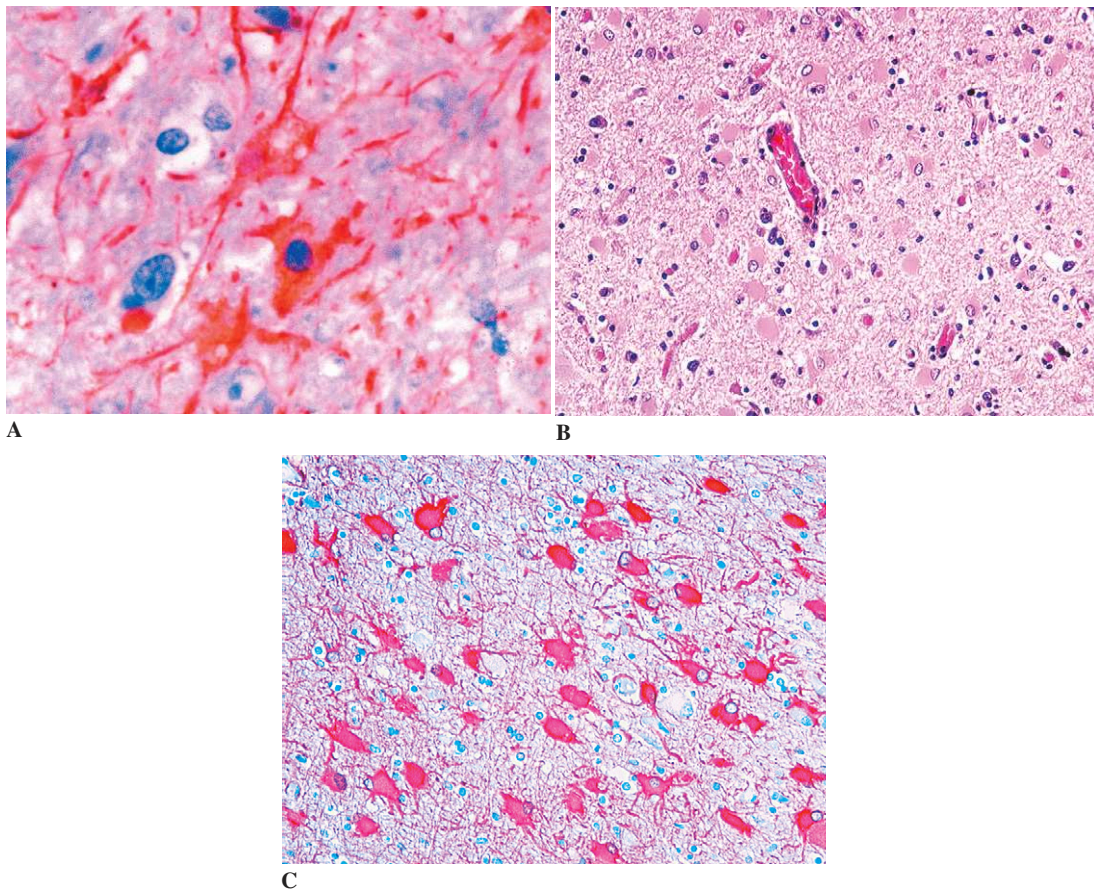
Figure 1-19. Gliosis. **A**, Fibrillary gliosis. Hypertrophy of nucleus as of cytoplasm and processes that are well visible on glial fibrillary acidic protein (GFAP). **B**, Gemistocytic astrocytes with large homogenized and eosinophilic cytoplasm (H and E). **C**, Gemistocytic astrocytes (GFAP).
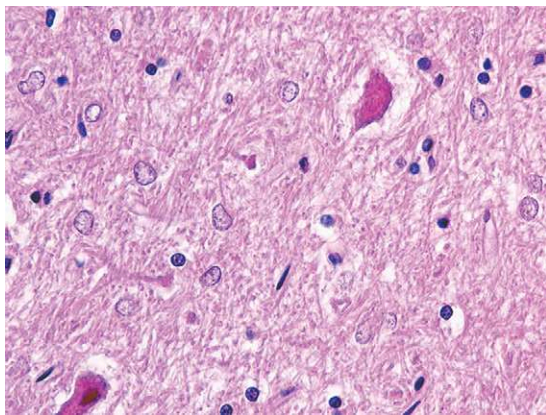
Figure 1-20. Alzheimer type II glial cells (H and E).

binucleated. They may be demonstrated by Gallyas stain or tau immunocytochemistry.

Thorn astrocytes have an argyrophilic cytoplasm with a few short processes (see Fig. 8-5B) and (often) a small, eccentric nucleus. They are commonly seen in PSP but may also be seen in other neurodegenerative conditions.

In corticobasal degeneration, accumulation of tau protein in astroglial cells in gray matter areas forms distinctive structures termed *astrocytic plaques*. Tau protein accumulates at the end of the astrocytic processes while the center of the plaque is devoid of tau immunoreactivity (see Fig. 8-11).

Viral inclusion bodies may also be found in astrocytes, particularly in subacute sclerosing panencephalitis and cytomegalovirus infection (see Chap. 5).

Corpora amylacea are spherical, basophilic, PAS-positive inclusions 10 μm to 50 μm in diameter. They are predominantly found in astrocyte processes, although they occasionally occur within axons. Ultrastructurally, they consist of densely packed filaments 6 nm to 7 nm in diameter that may be mixed with amorphous granular material and are not membrane-bound. Corpora amylacea increase in number with aging, particularly in the subpial and subependymal regions, around the subcortical blood vessels, and in the posterior columns of the spinal cord. Adult polyglucosan body disease (see Chap. 10) is characterized by diffuse accumulation of corpora amylacea occurring in the cortex and white matter and associated with diffuse and/or focal myelin damage.

Lesions of Oligodendrocytes

Like neurons and astrocytes, oligodendrocytes may be the seat of intranuclear viral inclusions (e.g., progressive multifocal leukoencephalopathy; see Chap. 5), or of lipid storage (e.g., metachromatic leukodystrophy).

Glial cytoplasmic inclusions involving mainly oligodendrocytes have been shown to be a characteristic feature of multiple system atrophy (see Chap. 8). These inclusions are usually flame- or sickle-shaped; they can be demonstrated by silver impregnation and are immunoreactive for tau-protein, ubiquitin, tubulin, and αB-crystallin.

Accumulations of tau protein in oligodendrocytes, known as "coiled bodies," may be found in PSP, corticobasal degeneration, and argyrophilic grain disease (see Chap. 8). They consist of fibrillary structures "coiling" around the nucleus.

Microglial Lesions

Microglia are cells of monocyte lineage and have important phagocytic functions. They can be demonstrated by silver impregnation, lectin-binding techniques, and immunohistochemical techniques using antibodies that react with monocyte/macrophages like CD68. Microglia found in normal brain have been subdivided into *resident* microglia (which undergo little turnover and occur throughout the CNS parenchyma) and *perivascular* microglia (which occur beside the perivascular basal lamina and undergo turnover with hematoge-

nous monocytes). Microglial activation occurs in inflammatory conditions of the CNS and involves (a) increased entry of hematogenous monocytes into the CNS, (b) proliferation of resident microglia, and (c) expression or secretion of a wide range of proteins, most of which are concerned with antigen presentation and inflammation.

Microglia play a part in three basic reactive processes, as follows.

(1) *Macrophage proliferation and phagocytosis.* In the CNS, macrophages are also known as compound granular corpuscles, foam cells, lipid phagocytes or gitter cells. Macrophage proliferation and phagocytosis is a frequent finding in brain lesions, particularly those associated with demyelinating processes or with traumatic or ischemic tissue destruction. After a destructive or demyelinating insult, macrophages appear within 48 hours of injury. They are rounded cells 20 μm to 30 μm in diameter, with small, darkly staining, and sometimes eccentric nuclei and a clear, granular cytoplasm that contains lipids or hemosiderin pigment (Fig. 1-21). These cells increase in number over days and weeks and may still be observed months after the injury. Most derive from blood monocytes.

(2) *Rod cell proliferation* (Fig. 1-22; see also Fig. 5-25) is a microglial response to subacute parenchymal injury in which necrosis is minimal or absent. Rod cells are elongated, spindle-shaped cells that can be recognized on H and E
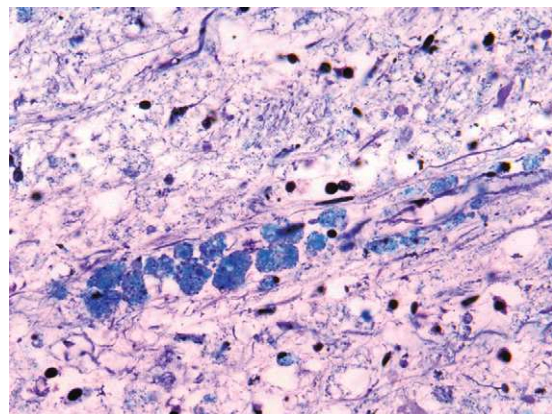
Figure 1-21. Perivascular lipid-laden macrophages (compound granular corpuscles, foam cells, or gitter cells) in a demyelinating lesion (Luxol fast blue combined with Bodian silver impregnation).
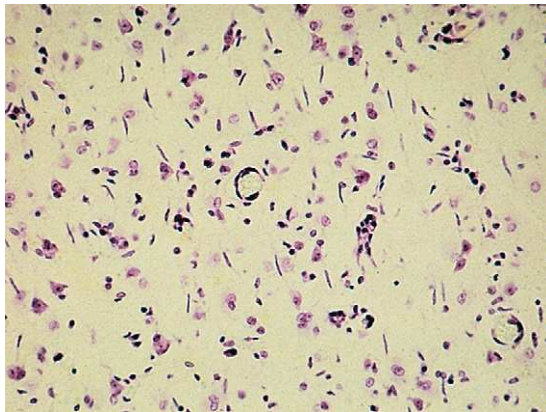
Figure 1-22. Rod-shaped microglia in a case of general paresis of the insane—tertiary syphilis (Nissl stain).

preparations by the presence of a cigar-shaped nucleus. Their presence is well-documented in the literature in descriptions of general paresis of the insane (GPI)—tertiary syphilis (see Chap. 5); the disease is seen infrequently today. They are also seen in cases of subacute encephalitis or slowly evolving ischemia.

(3) *Microglial nodules* consist of discrete clusters of microglial cells. They are typically found in chronic encephalitis, particularly in HIV encephalitis in and around sites of acute neuronal destruction (*microglial nodules*; see Chap. 5).

Ependymal Cells

In ependymal cells, as in glial cells and neurons, viral diseases, such as cytomegalovirus infection, may produce inclusion bodies. Ependyma has limited reaction to injury; in the adult CNS, ependymal cells do not proliferate in response to injury and cell loss. Destruction of ependymal cells is accompanied by proliferation of subependymal astrocytes, which form small hillocks along the ventricular surface (ependymal granulations). Surviving ependymal cells may be overgrown by the astrocytic reaction and appear as clusters of tubules buried within the proliferative foci.

General CNS Tissue Reactions to Injury

A number of general tissue reactions are known to occur in a variety of CNS diseases. These gen-

eral reactions are distinct from the reactions to specific pathologic processes (i.e., vascular, infectious, inflammatory, demyelinating, metabolic, and degenerative) that will be described in later chapters. They may accompany the microscopic cellular lesions that have just been described, or may result in more extensive changes that can be visible to the naked eye.

Cerebral Atrophy

Cerebral atrophy is the end stage of a number of brain diseases. A brain with cerebral atrophy is lighter than a normal age-matched control. Macroscopically, there is narrowing of the gyri and widening of the sulci and fissures over the cerebral convexities. The cortical ribbon is seen to be thinned on section, and ventricular dilatation is often present. The histologic substratum shows a variable loss of neurons, often associated with gliosis (depending on the underlying illness), and a variety of neuronal alterations that will be discussed in subsequent chapters.

Cerebral Edema

Cerebral edema is an increase in the brain's volume due to increased water content. Depending on its pathogenesis, cerebral edema can be classified as vasogenic, cytotoxic, or interstitial (hydrocephalic). However, combinations of different types of edema are frequent.

Vasogenic edema, probably the most common type of brain edema, complicates head injury, abscess, tumors, and hemorrhages. Both vasogenic edema and cytotoxic edema occur with ischemia. Vasogenic edema results from increased permeability of the blood-brain barrier to macromolecules, particularly proteins. Sites of vasogenic edema are marked in imaging studies by increased densities after contrast injection because the contrast medium leaks across the permeable vascular membrane. Biochemically, the edema fluid resembles a plasma filtrate. It is located chiefly in the extracellular spaces of the white matter.

In *cytotoxic edema*, excessive amounts of water enter one or more of the intracellular compartments of the CNS (neurons, glia, endothelial cells, or myelin sheaths) because the cellular concentration of osmotically active solutes is increased. This

usually results from an injury impairing the cells' capacity to maintain ionic homeostasis or is associated with systemic disturbances in fluid and electrolyte metabolism. Cytotoxic edema complicates hypoxia and ischemia because of failure of the ATP-dependent sodium pump in the affected cells. It also occurs in osmotic disequilibrium syndromes associated with hemodialysis or diabetic ketoacidosis and in acute plasma hypo-osmolality states such as water intoxication and inappropriate secretion of antidiuretic hormone. Because the cerebrovascular macromolecular barrier remains intact, cytotoxic edema is not enhanced in imaging studies by contrast medium.

Interstitial or *hydrocephalic edema* is the accumulation of cerebrospinal fluid (CSF) in the extracellular spaces of the periventricular white matter that results from obstructive hydrocephalus. As fluid collects in the obstructed ventricles, pressure increases and the CSF is forced across the ependymal lining into the adjacent extracellular spaces.

Macroscopically, edematous areas of brain are swollen and soft (Fig. 1-23). The swelling increases the volume of the intracranial contents, which causes increased intracranial pressure (see later discussion). The cut surfaces of the brain may be wet and shiny. If the edema is diffuse, the ventricles are compressed; in severe cases they are reduced to slit-like cavities.

Under light microscopy, myelin stains demonstrate pallor of the white matter. The cerebral tissue has a loose appearance and is split by vacuoles of

Figure 1-23. Cerebral edema of the left cerebral hemisphere with swelling of the parenchyma (paler parenchyma); note flattening of the gyri and narrowing of the sulci and of the left lateral ventricle.

variable size. Glial cells are swollen and perivascular spaces are dilated.

These gross and microscopic features correspond to ultrastructural features that vary according to etiologic and pathogenetic mechanisms. They also include dilatation of the perivascular and extracellular spaces, swelling of astrocytic cell processes, and splitting of the myelin lamellae (Fig. 1-24).

Hydrocephalus

Hydrocephalus is an abnormal increase in the intracranial volume of CSF associated with dilatation of all or part of the ventricular system. It is secondary to disequilibrium between CSF formation and reabsorption. On rare occasions it results from increased production of CSF (e.g., in choroid plexus papilloma). More commonly, it is the consequence of altered flow and absorption of the CSF as a result of obstruction of CSF pathways within the ventricular system (noncommunicating hydrocephalus) or in the subarachnoid space (communicating hydrocephalus). The ventricular system usually becomes obstructed at "bottleneck" areas such as the foramina of Monro, the aqueduct of Sylvius, and the exit foramina of the fourth ventricle (lateral foramina of Luschka and midline foramen of Magendie) when the ventricles become filled by tumor or blood clot. Subarachnoid pathways most often become blocked over the cerebral convexities and around the rostral brainstem (incisural block) as a result of inflammation or hemorrhage. In the acute phase, a blood clot or inflammatory exudate forms a barrier to flow. Subsequently, organization of the clot or exudate leads to fibrous obliteration of the subarachnoid space.

Hydrocephalus is often associated with increased intracranial pressure. In children, in the absence of appropriate shunting procedures, the head can become enlarged when hydrocephalus develops before the cranial sutures close. When the obstructive lesion causing the hydrocephalus is not severe and progressive, the hydrocephalic process may stabilize and the CSF pressure return to normal limits ("normal-pressure hydrocephalus").

Several alterations in the brain are common to all forms of hydrocephalus. These include dilatation of the ventricular system; interstitial edema; reduction of white matter volume; accentuation of the primary, secondary, and tertiary cerebral
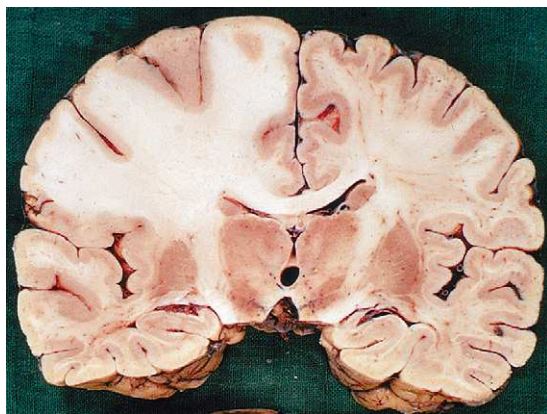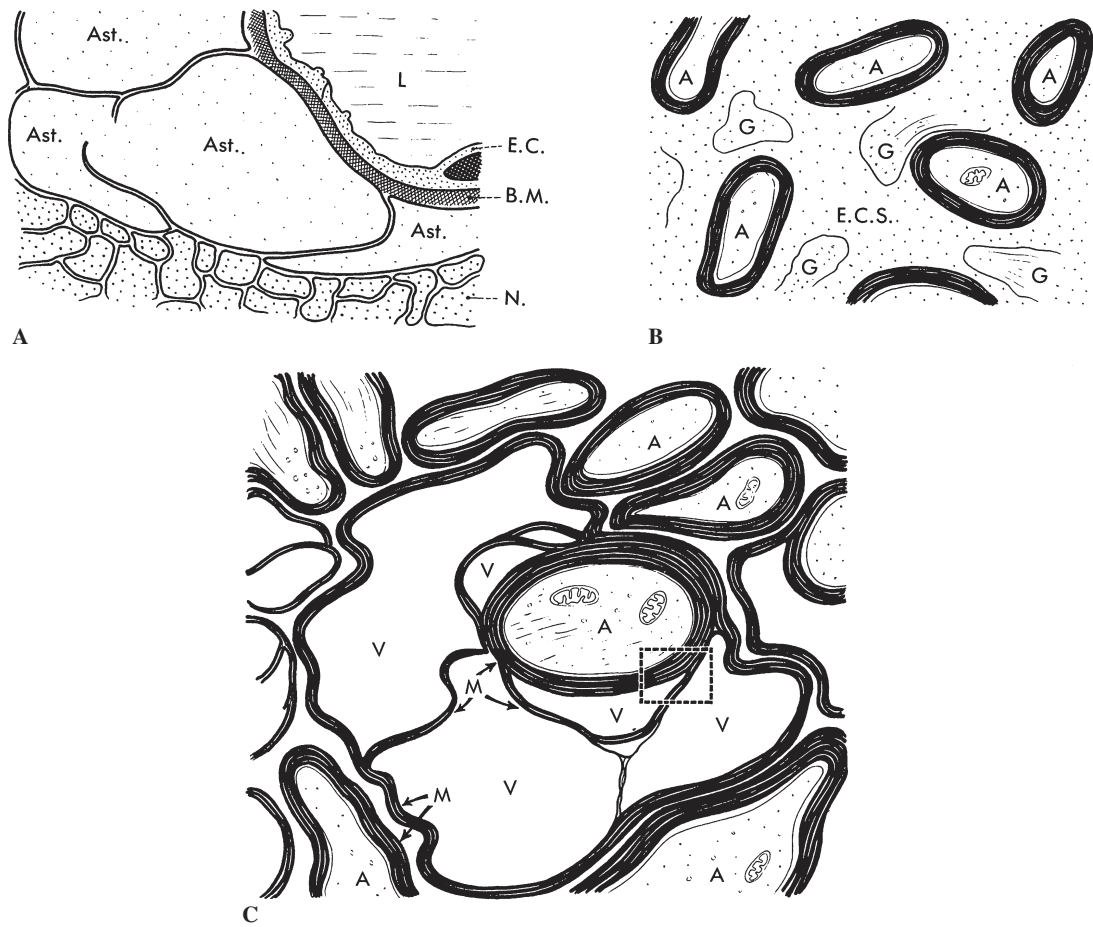
Figure 1-24. Cerebral edema: principal ultrastructural forms. **A**, Gray matter (traumatic and inflammatory edemas). Swelling of astrocytic cell processes, especially near capillaries. Ast = astrocytic cell process, EC = capillary endothelial cell, L = capillary lumen, N = neuropil, BM = basement membrane. **B**, White matter (traumatic and inflammatory edemas). Enlargement of extracellular spaces. A = myelinated axon, G = glial cell process, ECS = extracellular space. **C**, White matter (cytotoxic edema due to triethyltin poisoning). Splitting of myelin lamellae at the intraperiod line. A = myelinated axon, M = myelin, V = vacuole.

sulci, producing a prominent gyral pattern; and perforation of the septum pellucidum. Disruption and loss of the ependymal lining with localized subependymal astrocytic proliferations protruding into the ventricular cavities (*ependymal granulations*) is frequent. Proliferation of the subependymal glia may bring about stenosis of the aqueduct; this is one of the causes of obstructive hydrocephalus in childhood (see Chap. 11).

Increased Intracranial Pressure and Brain Herniation

After closure of the sutures, the volume of the cranial cavity is fixed by rigid bony walls of the skull and compartmentalized by partitions of bone and dura. The normal contents of the cranial cavity (blood, brain, and CSF) are relatively incompressible. Under these conditions, an increase in the volume of the cranial contents will result in increased intracranial pressure.

The intracranial contents may expand because of diffuse brain edema, increased cerebral blood flow and blood volume, or the development of space-occupying lesions such as tumors, abscesses, hematomas, or large, recent infarcts accompanied by edema. The effects of space-occupying lesions on intracranial pressure are caused not only by the mass of the lesion but by accompanying edema and obstruction of venous or CSF pathways. In children
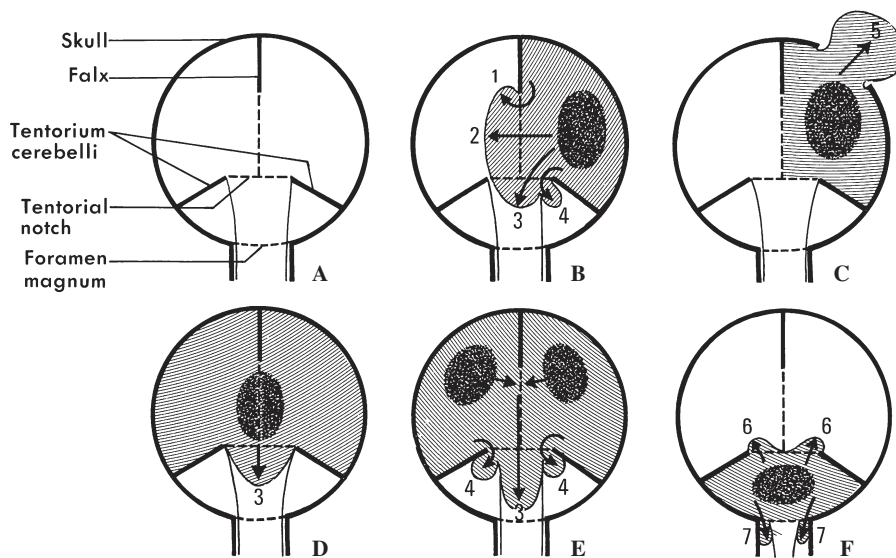
Figure 1-25. Localization of the chief types of cerebral herniation. **A**, Normal aspect of rigid structures within the skull. **B**, Unilateral hemispheric expanding lesion. **C**, Herniation through bone flap. **D**, Midline hemispheric expanding lesion. **E**, Bilateral hemispheric expanding lesions. **F**, Expanding infratentorial lesion: (1) Cingulate subfalcial herniation; (2) lateral displacement of midline structures; (3) central diencephalic herniation; (4) temporal herniation; (5) external herniation (through bone flap); (6) superior cerebellar herniation (through tentorial opening); (7) cerebellar tonsillar herniation (through foramen magnum).

with ununited cranial sutures, increase in the volume of the intracranial contents will lead to splaying of the sutures, resulting in increased skull size and in digital convolutional markings. However, in adults and in older children the bony skull can no longer enlarge, and intracranial hypertension leads to compression of the brain surfaces against the inner table of the skull with consequent flattening of cerebral gyri, narrowing of intervening sulci, and accentuation of the foraminal and tentorial markings on the inferior cerebellar and medial temporal surfaces. The expanding cerebral mass will also insinuate itself into whatever free residual openings can accommodate it. These compensatory displacements of brain from one intracranial compartment to another, caused by an increase in the volume of cranial contents, give rise to *cerebral herniation*. The form that cerebral herniation takes will differ according to whether the space occupying lesions are supratentorial or infratentorial (Fig. 1-25).

Cerebral Herniations in Supratentorial Lesions. A *unilateral lesion* (Fig. 1-26) that increases the hemispheric volume is likely to cause herniation of the cerebral hemisphere through openings limited

by the lower border of the falx and by the free edge of cerebellar tentorium on the same side of the lesion. Depending on the extent of the hemisphere enlargement and on the precise site of the expanding lesion, the herniation will either take place through both these openings or predominate in one or another direction. As a result, several main types of herniation may occur:

- Herniation of the cingulate gyrus under the falx (subfalcine herniation) with lateral displacement of the anterior cerebral arteries.
- Lateral displacement of the midline structures (e.g., third ventricle, pineal gland, vein of Galen).
- Downward herniation of the diencephalon through the tentorial notch, causing downward displacement of the floor of the hypothalamus and of the mamillary bodies (central diencephalic herniation).
- Herniation of the hippocampal gyrus in the tentorial notch between the brainstem and the free edge of the tentorium cerebelli. In this case, the herniated temporal rim is likely to compress and stretch the third and sixth cranial nerves, the cerebral peduncle (possibly
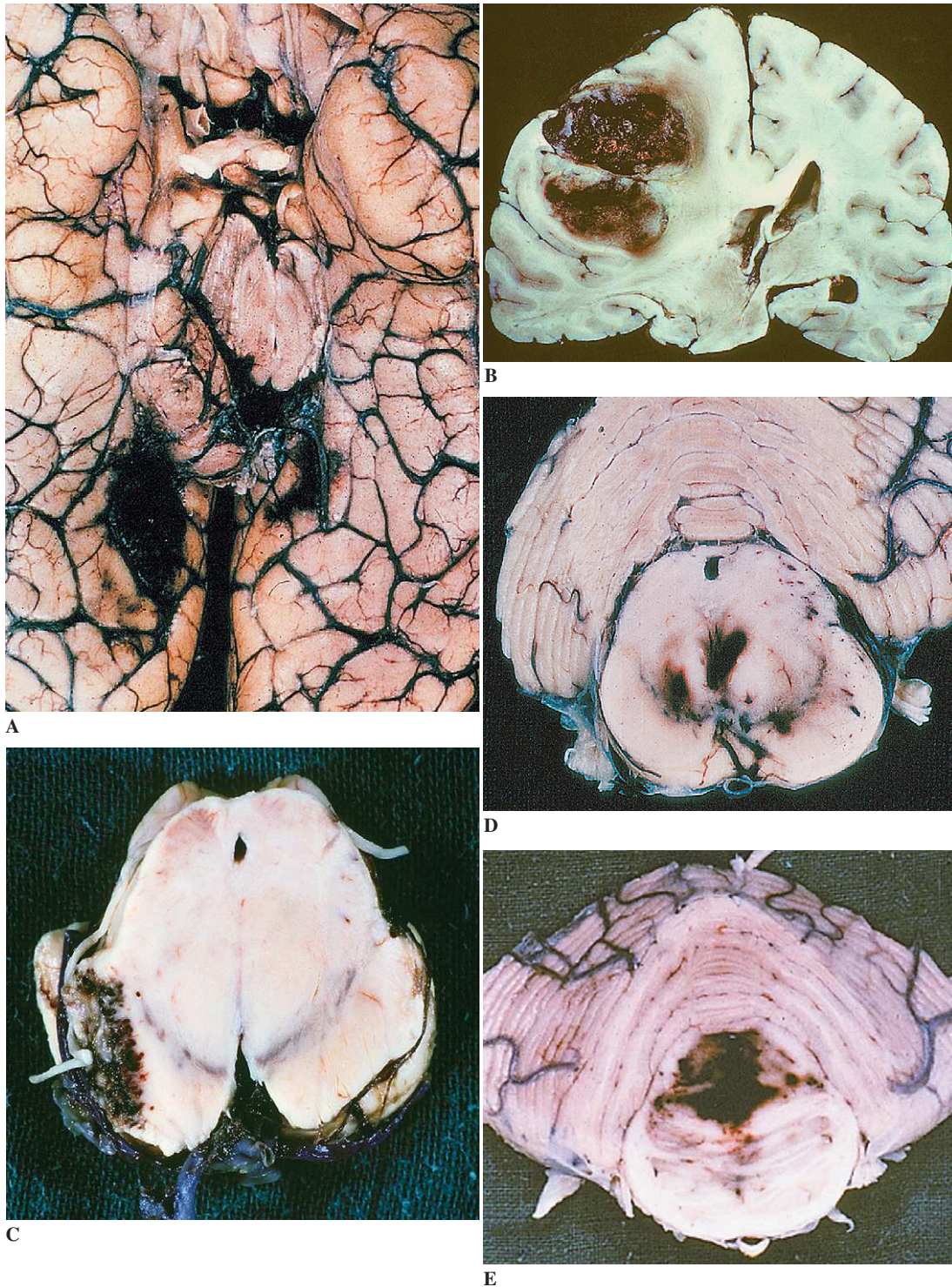
Figure 1-26. Cerebral herniations. **A**, Inferior aspect of the cerebral hemispheres. Herniated rim of the right hippocampal gyrus compressing the oculomotor nerve and displacing the brainstem. **B**, Cerebral metastases causing temporal herniation. Displacement of the midline structures and cingulate herniation. **C**, Midbrain. Hemorrhagic lesion in the crus of the peduncle contralateral to the temporal herniation (Kernohan notch). **D** and **E**, Midbrain and pontine hemorrhages involving mostly the tegmentum, secondary to temporal herniation (Duret hemorrhages).

A   B
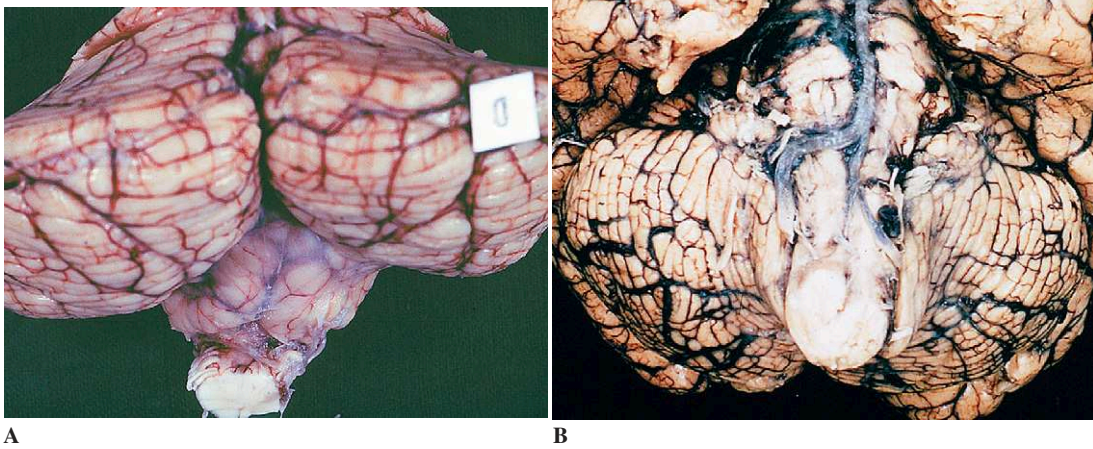
Figure 1-27. Cerebellar tonsilar herniation. **A**, Posterior view. **B**, Anterior view.

producing a lesion in the crus of the contralateral peduncle against the free edge of the tentorium, thus giving rise to Kernohan notch), and the posterior cerebral artery (with the likelihood of secondary infarction in its territory of supply). Finally, compression due to medial temporal lobe herniation and the downward thrust of central diencephalic herniation may result in stretching of the penetrating blood vessels, especially veins, which supply the midbrain and pons, thereby leading to secondary brainstem hemorrhages (Duret hemorrhages).

- External cerebral herniation through surgical or traumatic defects in the calvaria may also occur.

A *bilateral* or *diffuse lesion* that increases the volume of both hemispheres will result chiefly in central diencephalic herniation and/or bilateral temporal lobe herniation.

A *midline expanding lesion* will result chiefly in central diencephalic herniation.

Cerebellar Herniations in Infratentorial Lesions. Two types of cerebellar herniation are recognized.

(1) *Upward herniation of the mesencephalon and cerebellum through the tentorial notch.* Direct mesencephalic lesions may result from this complication, as well as secondary lesions due to vascular compression.

(2) *Cerebellar tonsillar herniation through the foramen magnum.* This is the most frequent and dangerous complication of infratentorial expanding processes, regardless of their nature or degree of severity. As a result of increased intracranial pressure in the posterior fossa, the cerebellar tonsils are thrust downward through the foramen magnum (Fig. 1-27), which they override, culminating in medullary compression and life threatening lesions in the floor of the fourth ventricle.

Topographic Analysis of CNS Lesions

Topographic analysis of lesions is just as important as the study of their morphology. It constitutes a crucial step in the attempt to arrive at an etiologic diagnosis. It necessitates a rigorous and systematic examination of all the neural structures and, by the same token, implies the need for multiple sampling at various levels. Large brain sections permit the synchronous study of the various areas of the central nervous system.

Diffuse Distribution

Diffusely distributed lesions are produced chiefly by blood-borne infective processes. Some degenerative processes may, however, also cause cerebral atrophy. It is important to emphasize that, despite

the diffuse character of these changes, lesions often show regional predominance.

Focal Distribution

Lesions may be localized to an anatomically well-defined area (e.g., cerebral lobes, basal ganglia, brainstem), and certain preferential sites of involvement are linked to specific etiologic entities (e.g., cerebral tumors). Lesions may also be localized to a vascular territory. Cerebral infarcts exemplify this type of focal lesion.

Disseminated Distribution

Disseminated distribution is seen in multifocal processes, of which multiple sclerosis is the most characteristic example.

Systematized Distribution

A number of nervous system disorders, especially degenerative diseases, cause changes that involve certain functionally related morphologic systems, for example, involvement of upper and lower motor neurons in amyotrophic lateral sclerosis or spinocerebellar involvement in Friedreich ataxia.

Integration of Morphologic and Topographic Findings

The two steps in neuropathologic examination that have been somewhat artificially dissociated under the headings of morphologic and topographic analysis must now be followed by a regrouping of the findings that will assist an etiologic diagnosis of the lesions. In fact, these findings alone are not sufficient, and it is necessary to correlate them with the clinical data, imaging studies, clinical laboratory findings, general autopsy findings, and possibly other investigative methods, including molecular studies. Full understanding of a cerebral infarct, for example, is possible only after careful and complete postmortem examination of the vascular tree, heart, and lungs and after comparing the anatomic findings with information provided by the clinical picture, the chronology of the functional disturbances, and data from cerebral and vascular imaging.

Likewise, study of the lipidoses cannot be based solely on neuropathologic findings; it requires detailed alignment with data from the general postmortem examination, neurochemical analysis, and molecular genetic investigation.

Finally, many hereditary disorders of the central nervous system, peripheral nerves, and skeletal muscles now need to be confirmed by genetic examination.

Chapter 2
Tumors of the Nervous System

Thomas W. Smith, Rebecca D. Folkerth, Jacques Poirier, and David N. Louis

Classification

The basis for classification of nervous system tumors remains the histologic appearance of a particular neoplasm by light-microscopic examination (supplemented by immunohistochemical and electron microscopic observations where appropriate). It is becoming clear, however, that information derived from cytogenetics and molecular genetics will play an increasingly important role in tumor classification, particularly with respect to providing more precise diagnostic and prognostic information about particular tumors. Underlying most histology-based classification schemes has been an implicit assumption that the phenotypic appearance of a particular tumor accurately reflects its cellular derivation (e.g., low-grade astrocytomas are derived from mature astrocytes). Recent evidence suggests, however, that at least some CNS tumors, such as primary glioblastoma, might in fact be derived from multipotential neuroepithelial stem cells that persist throughout adult life. It is also clear that, as with other human cancers, CNS tumors arise when alterations occur in growth-regulatory genes such as oncogenes and tumor-suppressor genes. It is thus paramount that any classification scheme be flexible enough to allow for the inclusion of new diagnostic categories as well as for the modification and even the removal of existing categories on the basis of information derived from newer methodologies.

The classification scheme used in this book is based on the current (2000) World Health Organization (WHO) classification of nervous system tumors.

CNS tumors can be grouped into two major categories: primary tumors and secondary tumors. Primary tumors arise from cells that are intrinsic to the CNS or its coverings, including the calvarium, and include tumors of neuroepithelial origin and non-neuroepithelial origin. Secondary tumors arise from sites elsewhere in the body and involve the brain or spinal cord mainly by hematogenous dissemination (metastases) or, less often, by contiguous extension.

CNS tumors can also be grouped according to location and their corresponding incidence by age. In adults, approximately 70% of all brain tumors occur supratentorially (i.e., within the cerebral hemispheres or coverings) and include, in order of decreasing frequency, metastases, gliomas, meningiomas, and schwannomas. In children, by contrast, approximately 70% of brain tumors are infratentorial in location (i.e., within the cerebellum or brainstem) and are neuroectodermal in origin; the most common, in order of decreasing frequency, are pilocytic astrocytoma, medulloblastoma, and ependymoma. Spinal cord tumors constitute about 15% of all primary CNS tumors and include, in order of decreasing frequency, schwannomas, meningiomas, and gliomas (i.e., ependymoma, astrocytoma).

Primary Neoplasms

Tumors of Neuroepithelial Tissue

Astrocytic Tumors

Diffusely Infiltrating Astrocytomas. As a group, *diffusely infiltrating astrocytomas* share the following features: widespread occurrence throughout the CNS, clinical presentation in adults, diffuse infiltration of adjacent and often distant brain structures, and tendency for progression to anaplasia over time.

A number of histologic grading schemes have been used for diffusely infiltrating astrocytomas; however the Ste. Anne/Mayo grading system and its adaptation to the current WHO classification has proved to be the most reproducible and predictive of tumor behavior. The Ste. Anne/Mayo criteria are based on the presence or absence of four easily recognizable histologic features: nuclear pleomorphism, mitoses, microvascular proliferation, and necrosis. While the Ste. Anne/Mayo system recognizes a grade I diffuse astrocytoma that lacks all of the preceding features, this has proved to be such a rare and controversial entity that the WHO scheme uses modifications of the Ste. Anne/Mayo criteria for only the three higher grades of diffuse astrocytoma (Table 2-1). The WHO grade I category is reserved for circumscribed astrocytomas, including pilocytic astrocytoma and subependymal giant cell astrocytoma (SEGA).

DIFFUSE ASTROCYTOMA (WHO GRADE II). *Diffuse astrocytomas* constitute about 10% to 15% of all astrocytic neoplasms. They can affect all age groups but are mainly tumors of adults, with 25% occurring in persons between the ages of 30 and 40.

They most commonly occur in the cerebral hemispheres (especially the frontal and temporal lobes), followed by the brainstem and spinal cord, and are rarely seen in the cerebellum. The clinical features reflect the location of the tumor, with seizures being a frequent presenting symptom. Imaging studies usually show an ill-defined, homogeneous, non–contrast-enhancing lesion; the presence of focal contrast-enhancement may suggest progression toward anaplasia.

Macroscopically, these tumors enlarge and distort involved brain structures, often with blurring of normal anatomic landmarks (Fig. 2-1A). Cysts of varying sizes and focal calcifications may be present.

Microscopically, diffuse astrocytomas are slight-to-moderately cellular tumors composed of well-differentiated astrocytes (Fig. 2-1B). Some degree of nuclear atypia is almost always present, which should help distinguish the neoplastic cells from reactive astrocytes. Mitoses are extremely rare or absent. Microvascular proliferation and necrosis are never present. The background matrix may be loose, vacuolated, or even microcystic. The Ki-67/MIB-1 labeling index (a measure of cellular proliferation) is usually less than a few percent.

Three histologic variants of diffuse astrocytoma have been recognized, although in practice most have a mixture of cell types.

By far the most common variant is the *fibrillary astrocytoma*, which is composed of neoplastic cells with scant perikaryal cytoplasm within a loose but consistently glial fibrillary acidic protein [GFAP]–positive fibrillary matrix.

Gemistocytic astrocytoma is defined as a tumor in which at least 20% of the neoplastic cells

Table 2-1. Grading of Diffuse Astrocytoma

WHO Grade	Designation	Histologic Criteria (Ste. Anne/Mayo)
I	(Pilocytic astrocytoma; SEGA)	(Not applicable)
II	Diffuse astrocytoma	One criterion—usually nuclear pleomorphism
III	Anaplastic astrocytoma	Two criteria—usually nuclear pleomorphism and mitoses*
IV	Glioblastoma	Three *or* four criteria—nuclear pleomorphism, mitoses, microvascular proliferation, and/or necrosis†

*The presence of a single mitosis in a diffuse astrocytoma that only exhibits nuclear pleomorphism is not sufficient to reclassify it as a WHO grade III tumor.

†Necrosis is not required for the diagnosis of glioblastoma as long as microvascular (endothelial) proliferation is present.

Source: Modified from Kleihues P and Cavenee WL. Pathology and genetics of tumors of the nervous system. Lyon, ARC Press, 2000.
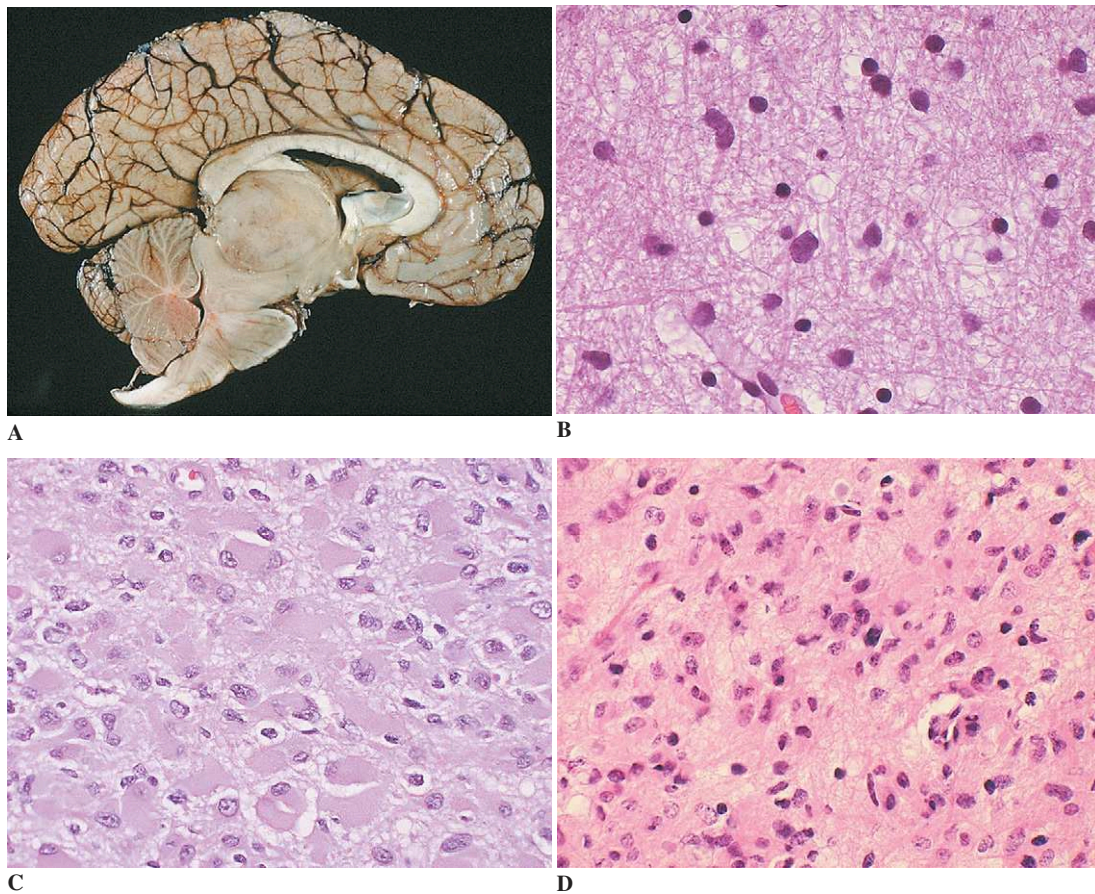
Figure 2-1. Diffuse astrocytoma. **A**, Thalamic astrocytoma (gross). Microscopic features: **B**, Low-grade fibrillary astrocytoma (H and E); **C**, Gemistocytic astrocytoma (H and E); **D**, Anaplastic astrocytoma (H and E).

resemble gemistocytic astrocytes, that is, have abundant eosinophilic cytoplasm and peripherally displaced nuclei (Fig. 2-1C). These tumor cells strongly express GFAP. Although gemistocytic astrocytomas are highly associated with progression to anaplastic astrocytoma and glioblastoma, they should not automatically be assigned a higher grade unless the appropriate histologic criteria are fulfilled.

The *protoplasmic astrocytoma* is the least common (and most controversial) variant. It is an astrocytic tumor composed mainly of small, round cells with scant, minimally GFAP-reactive processes in a prominent mucoid or microcystic background matrix. This pattern bears a striking resemblance to the loose, spongy tissue of pilocytic astrocytomas and may also be seen focally in other tumors (e.g., oligodendroglioma, dysembryoplastic neuroepithelial tumor).

Characteristic molecular changes in grade II astrocytomas include mutations of the *TP53* tumor-suppressor gene in about 50% of cases, over-expression of platelet-derived growth factor and its receptor, and loss of portions of chromosome 22. Most low-grade diffuse astrocytomas will progress to a high-grade tumor. The average interval to malignant change is about 4 to 5 years, but this may vary considerably.

ANAPLASTIC ASTROCYTOMA (WHO GRADE III). *Anaplastic astrocytomas* often arise in the setting of a preexisting low-grade diffuse astrocytoma but can also present de novo without clear evidence of a less-malignant precursor. The average age of presentation is about 10 years higher than for low-grade diffuse astrocytoma; location, clinical presentation, macroscopic appearance, and imaging features are otherwise similar except that some

contrast enhancement may be present within the tumor (but not the "ring" enhancement typically seen in glioblastoma).

Microscopically, anaplastic astrocytoma has the appearance of a diffusely infiltrating astrocytoma but shows increased cellularity, nuclear atypia, and mitotic activity compared to its low-grade counterpart. However, microvascular proliferation and necrosis are absent (Fig. 2-1D). Many but not all tumor cells may express GFAP. Ki-67/MIB-1 labeling indices are generally increased (usually by 5% to 10%) but can overlap with those for both low-grade diffuse astrocytoma and glioblastoma. These tumors are aggressive, with typical survivals of only 2 to 3 years from diagnosis.

At a molecular level, anaplastic astrocytomas have inactivation of the cell-cycle control pathway that includes the *CDKN2A/p16/ARF*, *CDK4*, and *RB* genes, as well as loss of parts of the long arm of chromosome 19.

Glioblastoma (WHO grade IV). *Glioblastoma* (previously known as "glioblastoma multiforme" and still abbreviated as GBM) is a malignant, rapidly progressive, and fatal astrocytic neoplasm. GBMs are the most common primary brain tumor, accounting for approximately 10% to 15% of all intracranial tumors and 40% to 50% of all glial tumors. They may arise de novo in the absence of a pre-existing astrocytic tumor ("primary GBM") or develop from a less-malignant diffuse astrocytoma ("secondary GBM"). GBMs occur in all age groups but most occur in adults, with a peak incidence between the ages of 45 and 70 years. They may arise in any region of the CNS; however, the cerebral hemispheres (particularly the frontal and temporal lobes, basal ganglia, and commissural pathways) are sites of predilection. The radiologic features of GBM typically include the presence of an irregular mass with a central hypodense region of necrosis surrounded by a contrast-enhancing "ring" that represents the more cellular and vascularized portions of the tumor. A classic radiologic (and macroscopic) presentation is the "butterfly" pattern caused by spread of the tumor across the corpus callosum into the opposite hemisphere. The tumor may be surrounded by considerable vasogenic edema, which manifests as hyperintensity on a T2-weighted magnetic resonance imaging scan.

Macroscopically, GBMs often appear as relatively well-defined mass lesions, although there is almost always significant microscopic infiltration of tumor into the surrounding parenchyma. They typically have a "variegated" appearance, with solid gray-pink tissue at the periphery and yellow zones of central necrosis (Fig. 2-2A); some have old or recent hemorrhage. Like other diffuse astrocytomas, GBMs may widely infiltrate adjacent tissue and extend for long distances within fiber tracts. They may sometimes form additional masses at distant sites, creating the impression of a multifocal or "multicentric" glioma on neuroimaging studies. True multifocal gliomas do occur, but their exact frequency has been difficult to establish (estimated range, 2.4% to 7.5% of all gliomas). These tumors would by definition be polyclonal and presently can be proven only by the use of molecular markers. Some GBMs extend into the subarachnoid space or ventricles with the potential for cerebrospinal fluid (CSF) dissemination, although this appears to be an infrequent phenomenon. Extracranial extension and hematogenous dissemination are very rare in patients who have not had prior surgery. GBMs are among the most malignant tumors in human beings; mean survival ranges from less than one year to 18 months, with less than 2% surviving longer than 3 years.

All GBMs display the histologic features of high cellularity, marked nuclear atypia, mitoses, microvascular proliferation, and necrosis. However, their microscopic appearance can be highly variable, with considerable regional heterogeneity. In some GBMs, the tumor cells may show considerable nuclear and cytoplasmic pleomorphism, with multinucleated, giant cells (Fig. 2-2B), whereas others may consist mainly of small, "undifferentiated" cells with scant cytoplasm and, often, poor GFAP expression. This "small-cell" pattern appears to be more characteristic of primary GBM. Many GBMs also contain zones having better-differentiated fibrillary and gemistocytic astrocytes. Other cell types that may be infrequently present in GBM include cells with glandular or epithelioid features, oligodendrocyte-like cells, periodic acid-Schiff (PAS)–positive granular cells, and heavily lipidized cells. Proliferative activity is prominent in GBM, and both typical and atypical mitoses are found; Ki-67/MIB-1 labeling indices are likewise high, commonly averaging 15% to 20%. Proliferative activity is usually greatest in tumors composed predominantly of small, undifferentiated cells.
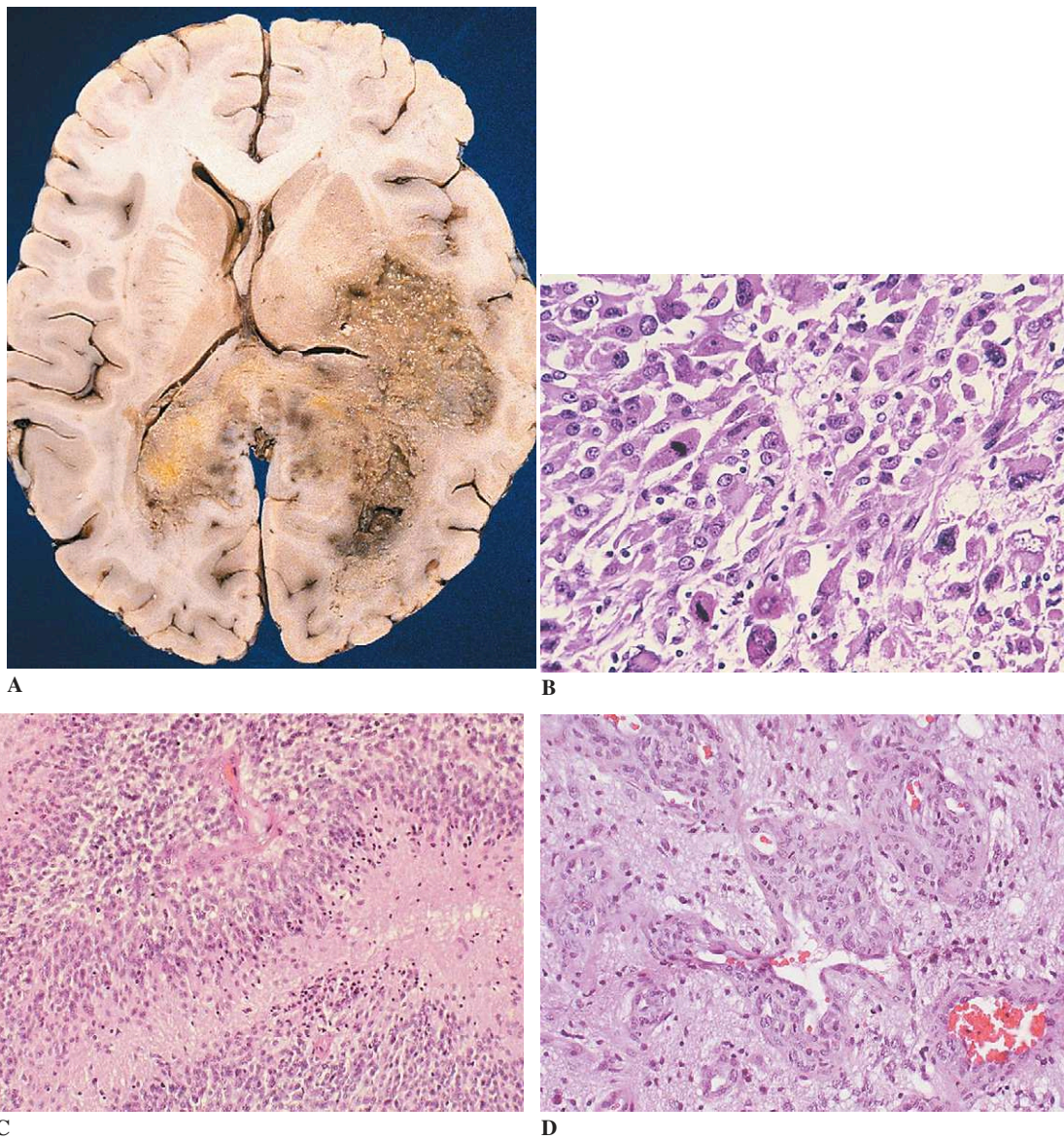
Figure 2-2. Glioblastoma. **A**, Glioblastoma (gross). Microscopic features: **B**, Cellular anaplasia, mitoses (H and E); **C**, necrosis with pseudopalisading (H and E); **D**, microvascular proliferation with glomeruloid structures (H and E).

Necrosis is a characteristic feature of GBM and can consist of either large, confluent foci of coagulative necrosis or of small, band-like or serpiginous "geographic" necrotic foci surrounded by a rim of densely packed tumor cells (imparting the characteristic and highly diagnostic "pseudopalisading" pattern; Fig. 2-2C).

Microvascular proliferation is defined as the presence of abnormal vessels with walls composed of two or more layers of mitotically active endothelial (and/or smooth-muscle/pericytic cells), often forming glomeruloid structures (Fig. 2-2D). Microvascular proliferation has also been referred to as "capillary endothelial proliferation," although it is likely that other vascular components besides the endothelial cells undergo proliferation. Some of these vessels thrombose. Occasional GBMs may show considerable connective tissue reaction,

which may be caused by meningeal invasion by tumor or organization of zones of necrosis, or as a response to marked microvascular proliferation.

The pathogenesis and molecular genetics of GBM have been an area of intense investigation in recent years. The origin of GBM remains controversial. The traditional explanation is that GBMs arise from differentiated adult astrocytes or their immediate precursors; an alternative explanation is that they arise from neuroepithelial stem cells that are present throughout adult life. The latter view finds some support in recent human and animal studies. At a molecular level, GBMs nearly always have inactivation of the cell-cycle control pathway that includes the *CDKN2A/p16/ARF*, *CDK4*, and *RB* genes as well as loss of parts of the long arm of chromosome 10. Chromosome 10 loss is sometimes associated with mutations of the *PTEN* tumor-suppressor gene. GBMs also frequently demonstrate amplification of the *EGFR* gene, along with rearrangements and overexpression of mutant *EGFR*. Molecular studies have shown that primary and secondary GBMs often have different sets of genetic alterations: primary GBMs are commonly characterized by *EGFR* gene amplification or overexpression. *EGFR* gene amplification is also particularly common in "small cell glioblastoma." Secondary GBMs arising from lower-grade precursors have a sequential series of genetic alterations, among which the most common is *TP53* gene mutation. Pediatric GBMs (most of which arise de novo) also differ genetically from primary GBMs in adults, with approximately 40% having *TP53* gene mutations and loss of chromosome 17p, particularly in children older than 4 years of age and in childhood brainstem GBMs.

Glioblastoma Variants.   *Giant cell glioblastomas* (WHO grade IV) are rare tumors that account for less than 5% of all GBMs. They arise de novo, without evidence of a pre-existing astrocytoma, and are otherwise similar in clinical presentation to typical GBMs. Radiologically and macroscopically they tend to be better circumscribed than ordinary GBMs. They are characterized histologically by the presence of giant, multinucleated cells that may show variable expression of GFAP. Many examples have an abundant stromal reticulin network. They have other histologic features typical of GBM, including mitoses, necrosis, and microvascular proliferation, which distinguishes them from the morphologically similar pleomorphic xanthoastrocytoma (see later discussion). Genetically this tumor has a high frequency of *TP53* mutations. Giant-cell GBMs generally have a poor prognosis, although some reports have suggested a somewhat better clinical outcome compared to ordinary GBMs, possibly due to their less infiltrative behavior.

Gliosarcomas (WHO grade IV) are tumors having a biphasic pattern of neoplastic glial and mesenchymal tissue. They comprise approximately 2% of all GBMs and are usually found in the cerebral hemispheres, with a predilection for the temporal lobes. Their clinical presentation is similar to that of ordinary GBMs. The radiographic appearance can be identical to typical GBMs or, if the sarcomatous component predominates, can present as a hyperdense, circumscribed, uniformly contrast-enhancing mass mimicking a meningioma. The histologic diagnosis rests on establishing the presence of unequivocally malignant glial and mesenchymal elements. The sarcomatous regions usually consist of malignant spindle cells arranged in a fascicular, herringbone, or sometimes storiform pattern (the latter resembling malignant fibrous histiocytoma), and may rarely show other types of mesenchymal differentiation including cartilage, bone, skeletal, and smooth muscle. Rare examples have shown keratin-positive epithelial and adenoid structures. GFAP immunohistochemistry is helpful in distinguishing between the glial and mesenchymal components; likewise, a reticulin stain will show abundant reticulin fibrils in the sarcomatous mesenchymal component but not the glial component. The origin of the sarcomatous component has been traditionally ascribed to malignant transformation of the proliferating blood vessels in GBM, but there is now convincing cytogenetic and molecular evidence for a monoclonal origin of both the glial and mesenchymal components of the tumor. The overall prognosis of gliosarcoma is essentially the same as that of ordinary GBM.

Circumscribed Astrocytomas

Pilocytic Astrocytoma (WHO Grade I). *Pilocytic astrocytomas* are well-circumscribed, slow-growing, often cystic gliomas that predominantly occur in children and young adults (Fig. 2-3A). They are the most common glioma in children but are much less frequent in adults and are rare after age 50. The most common sites, in
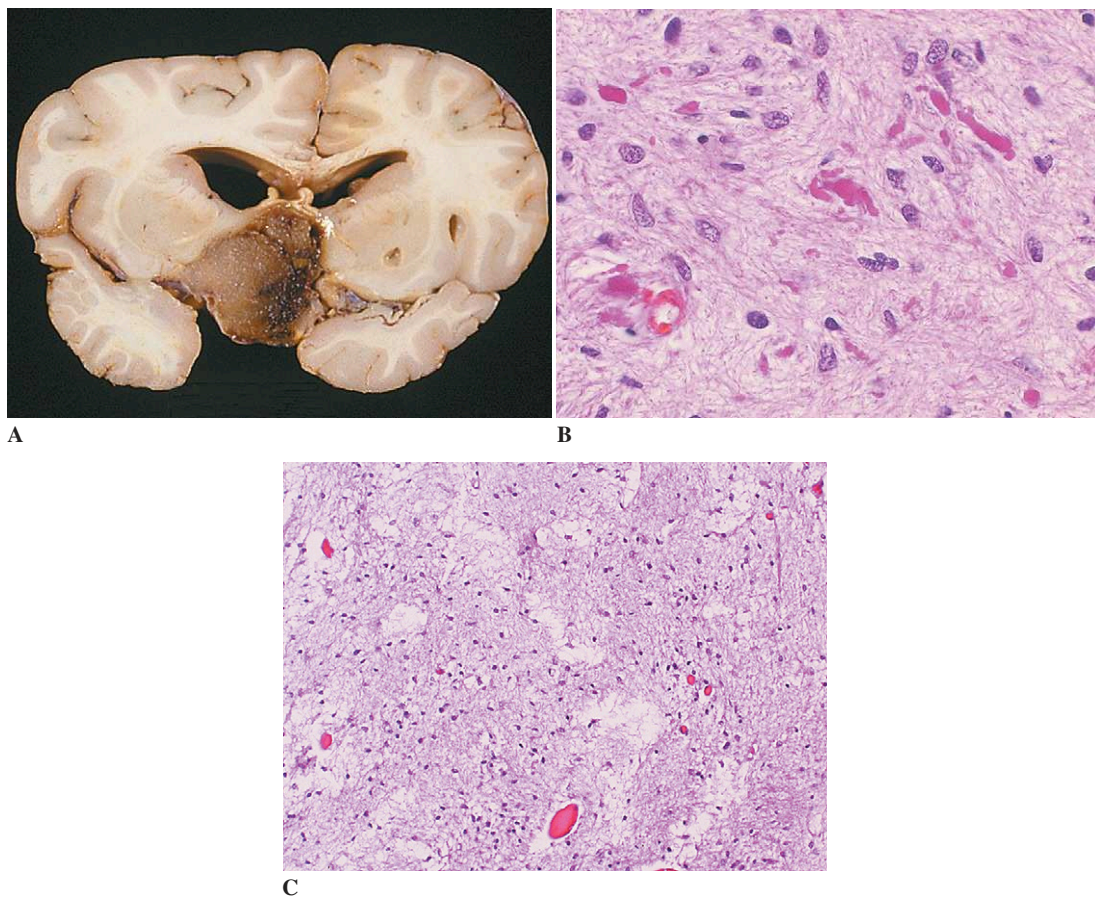
Figure 2-3. Pilocytic astrocytoma. **A**, Optic glioma (gross). Microscopic features: **B**, Rosenthal fibers (H and E); **C**, Microcystic change (H and E).

order of decreasing frequency, are the cerebellum, hypothalamus/third ventricular region, optic nerves, brainstem, cerebral hemispheres, and spinal cord. Their clinical presentation is largely dependent on tumor location, with an evolution in keeping with their slow rate of growth. Imaging studies show a circumscribed, cystic, or (less often) solid mass with contrast enhancement. In cystic examples, contrast enhancement may be localized to a mural nodule.

The histologic features of pilocytic astrocytoma are highly distinctive and classically consist of a biphasic pattern of compact and loose ("spongy") tissue (Figs. 2-3B and C). The compact zones consist of dense aggregates of elongated bipolar astrocytes with variable numbers of strongly eosinophilic irregular Rosenthal fibers, whereas the loose or spongy areas consist of small round

multipolar astrocytes in association with microcysts and eosinophilic granular bodies. However, the proportion of these two classic histologic patterns may vary within a given tumor, and some tumors (especially in small biopsies) may show a predominance of one pattern. Adding to the diagnostic difficulty is the presence of other tissue patterns (e.g., foci of oligodendrocyte-like cells) that can form part of the histologic spectrum of pilocytic astrocytoma; the reader should consult several of the suggested references for further discussion. Pilocytic astrocytomas may also contain histologic features that could be mistaken as evidence of anaplasia; these include microvascular proliferation (including glomeruloid vessels), nuclear atypia, and meningeal infiltration. Mitoses are rare and most examples have a very low Ki-67/MIB-1 labeling index (usually 0% to 1%).

The vast majority of pilocytic astrocytomas are indolent and are treated primarily by surgical excision with excellent long-term survival; however, hypothalamic and brainstem tumors can be difficult to manage and often recur, with adverse consequences. True malignant transformation of a pilocytic astrocytoma is very rare and most examples have occurred following radiotherapy. Histologically, malignant pilocytic astrocytomas show significantly increased mitotic activity (i.e., multiple mitoses per single high-power field), microvascular proliferation, and/or palisading necrosis.

No specific or diagnostically useful cytogenetic or molecular genetic alterations have been identified in pilocytic astrocytomas. In contrast to diffuse astrocytoma, *TP53* mutations do not appear to play a role in the formation of pilocytic astrocytoma. There is a well-established association between neurofibromatosis type 1 (NF1) and pilocytic astrocytomas, especially those that occur in the optic nerves (which are often bilateral in NF1). It is likely that the NF1 gene plays a role in the pathogenesis of NF1-associated and sporadic pilocytic astrocytoma.

Pleomorphic Xanthoastrocytoma (WHO Grade II). *Pleomorphic xanthoastrocytoma* (PXA) is a low-grade, slow-growing, cortical astrocytoma that occurs primarily in children and young adults, often presenting with a chronic seizure disorder. PXA characteristically involves the superficial cortex and leptomeninges, and may be solid or cystic; the latter type may have a mural nodule. Almost all PXAs are supratentorial and have a predilection for the temporal lobes. Microscopically, PXAs have a varied mix of cell types, including more-typical astrocytic cells with fibrillary processes as well as, often, strikingly bizarre giant cells with single or multiple pleomorphic nuclei and variable xanthomatous change in the cytoplasm. Mitoses are usually rare or absent, as are necrosis and microvascular proliferation. The tumor cells show consistent but often variably intense GFAP immunoreactivity. Some examples also express "neuronal" markers, including synaptophysin and neurofilament protein. Other characteristic histologic features include the presence of a conspicuous reticulin network (possibly reflecting a putative origin from subpial astrocytes), lymphocytic infiltrates, and eosinophilic granular bodies similar to those found in pilocytic astrocytomas and ganglion cell tumors. The prognosis of this tumor is excellent with surgical excision alone, with recurrence-free, 10-year survival greater than 60%. Recurrences may show the same histology as the original tumor or evidence of anaplasia, including significantly increased mitotic activity (i.e., 5 or more mitoses per 10 high-power field), necrosis, and microvascular proliferation. Characteristic molecular genetic alterations have not been detected, but the reported changes appear distinct from those of diffuse astrocytomas.

Subependymal Giant Cell Astrocytoma (WHO Grade I). *Subependymal giant cell astrocytomas* (SEGAs) are benign, slow-growing, intraventricular tumors that are characteristically associated with tuberous sclerosis. In some cases, SEGA may be the presenting feature of this disease; however, it is unresolved whether SEGAs occur in the absence of tuberous sclerosis. Most SEGAs arise during the first two decades of life and present with worsening of a seizure disorder or with symptoms of increased intracranial pressure. They typically occupy the wall of one of the lateral ventricles and can cause blockage of the foramen of Monro. Rare examples have undergone massive hemorrhage. SEGAs have a characteristic histologic appearance, being composed of large cells resembling gemistocytic astrocytes but often having "ganglioid" nuclei with prominent nucleoli (Fig. 2-4). Spindle-shaped cells with elongated fibrillar processes may also be encountered. Some tumor cells may show considerable nuclear pleomorphism
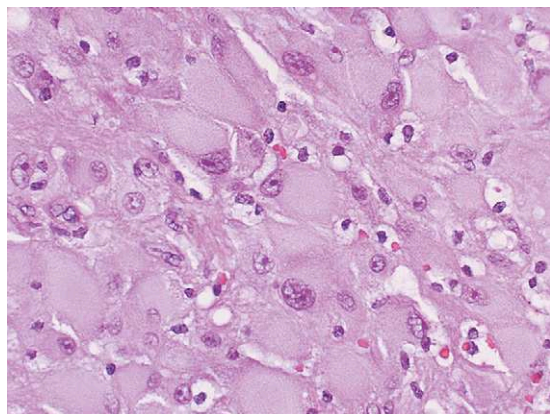
Figure 2-4. Microscopic appearance of subependymal giant cell astrocytoma (H and E).

and occasional mitoses may be present, but these features do not indicate anaplastic change. Calcifications may be present. Immunohistochemically, the tumor cells may express either or both glial and neuronal-associated antigens, which may reflect their putative origin from dysplastic bipotential cells in the subependymal region. Most genetic alterations in SEGAs relate to the two genes implicated in tuberous sclerosis, namely, the *TSC1* gene on chromosome 9q that encodes the hamartin protein and the *TSC2* gene on chromosome 16p that encodes the tuberin protein. SEGAs are treated by surgical excision alone and rarely recur.

Oligodendroglial Tumors

Oligodendroglioma (WHO Grade II). *Oligodendrogliomas* are diffusely infiltrating gliomas composed of cells morphologically resembling mature oligodendrocytes. They account for approximately 5% of all intracranial gliomas, and most occur in adults, with a peak incidence between the ages of 30 and 60. They are most often found in the cerebral hemispheres but have been reported in the cerebellum, brainstem, and spinal cord; even the leptomeninges have been reported as a primary site. Because of the relatively benign, slow-growing nature of the tumor, patients may often present with a long history of neurological symptoms, most often chronic seizures. Imaging studies usually show a well-demarcated mass, often with calcification and occasionally intratumoral hemorrhage, but peritumoral edema and contrast enhancement are not common except in the more anaplastic examples.

Macroscopically, oligodendrogliomas are usually well-circumscribed and grayish pink. They often include areas of mucoid change, which may result in a gelatinous consistency, as well as zones of cystic degeneration, focal hemorrhage, and calcification.

Oligodendrogliomas, when pure, have an easily recognizable, highly uniform histologic appearance. In paraffin sections, the tumor cells are closely packed and appear swollen, consisting of a small, round nucleus (usually slightly larger than that of a normal oligodendrocyte) surrounded by a clear halo (Fig. 2-5A). This imparts a characteristic "honeycomb" or "fried-egg" appearance to the tumor, but this pattern is not apparent in smear preparations or frozen sections and is often absent in paraffin sections made from previously frozen material. These tumors also characteristically contain a network of thin-walled branching capillaries, often described as a "chicken-wire" or "wishbone" vascular pattern (Fig. 2-5B). The presence of occasional mitoses and nuclear atypia (which may be marked in some cases) is still compatible with a WHO grade II neoplasm, however, the presence of significant mitotic activity, vascular proliferation, or necrosis indicates anaplastic transformation (WHO grade III). Most WHO grade II oligodendrogliomas have a Ki-67/MIB-1 labeling index less than 5%. Some oligodendrogliomas may contain nodules of increased cellularity; careful attention to these areas may reveal other anaplastic features. Small calcifications (calcospherites) are a characteristic histologic feature (see Fig. 2-5A) but are only seen in 20% of cases and are not specific for oligodendroglioma. Another characteristic and diagnostically useful feature is the presence of perineuronal, perivascular, or subpial tumor aggregates (secondary structures) when the tumor infiltrates cortex. It is not uncommon to find well-differentiated astrocytes with visible cytoplasm admixed with the oligodendrocytes. In most cases, their morphology and uniform distribution suggest that they are reactive rather than neoplastic. Since there is as yet no commercially available immunohistochemical marker specific for neoplastic oligodendrocytes, the histologic diagnosis of oligodendroglioma rests on its characteristic H and E appearance. GFAP immunostaining can be problematic, since reactive astrocytes in the tumor as well as some neoplastic oligodendrocytes may express GFAP. The latter cells often resemble small gemistocytic astrocytes and are referred to as *mini-* (or *micro-*) gemistocytes. These cells have no specific prognostic significance but are often seen in anaplastic oligodendrogliomas and anaplastic oligoastrocytomas. They are thought to be either a transitional form between oligodendrocytes and astrocytes or a phenotypic recapitulation of the premyelination stage of normal immature oligodendrocytes.

Oligodendrogliomas generally have a favorable outcome, with a median postoperative survival of 3 to 5 years. Some have extensive postoperative recurrences with progression to frank anaplasia.
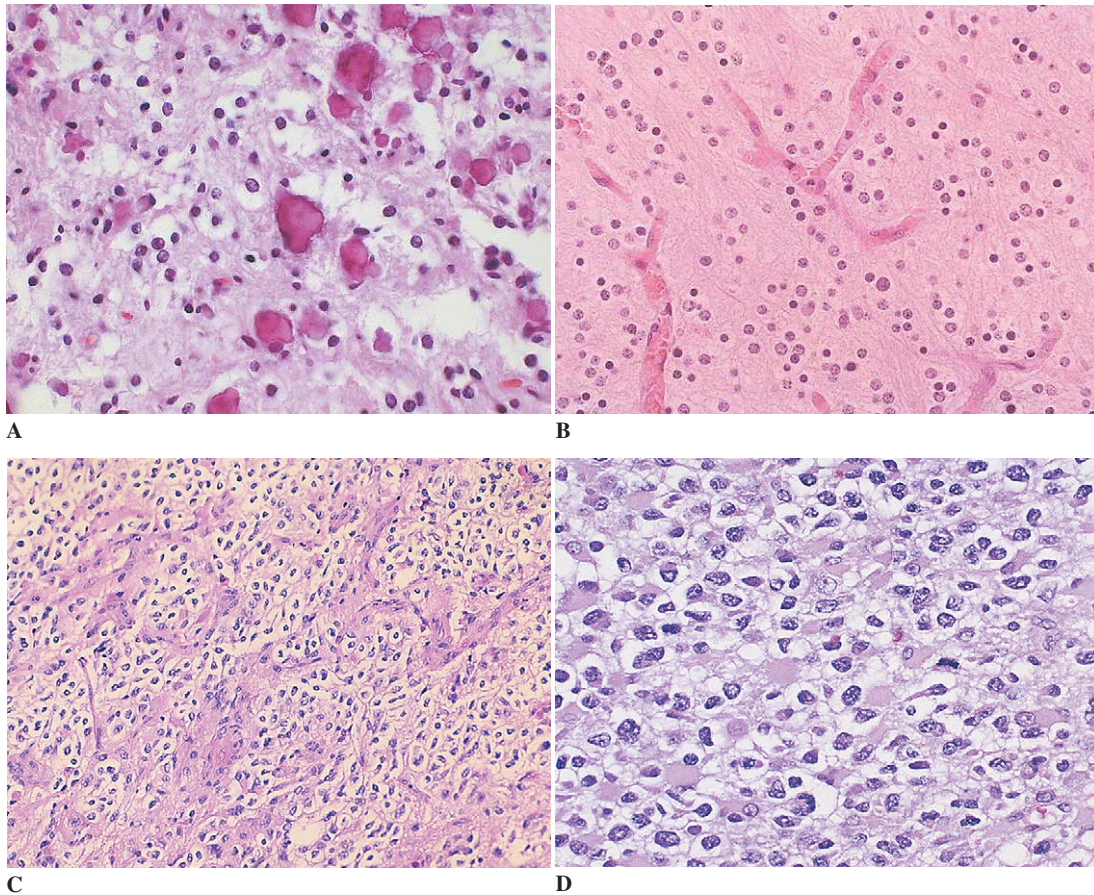
Figure 2-5. Microscopic appearance of oligodendroglioma. **A**, Oligodendroglioma with microcalcifications (H and E). **B**, "Chicken-wire" vascular pattern (H and E). **C**, Microvascular proliferation in anaplastic oligodendroglioma (H and E). **D**, Nuclear atypia, mini-gemistocytes in anaplastic oligodendroglioma (H and E).

Metastases through the cerebrospinal pathways may also occur.

Molecular genetic analysis has shown that approximately 80% of histologically classic oligodendrogliomas have concurrent loss of both the 1p and 19q chromosome arms, which has been associated with a more favorable prognosis (see following discussion of anaplastic oligodendroglioma).

Anaplastic Oligodendroglioma (WHO Grade III).   The exact incidence of *anaplastic oligodendroglioma* has been difficult to determine for various reasons, including the lack of clearcut histopathologic criteria in prior studies. Age of onset, location, and clinical features are generally similar to those of oligodendroglioma. Imaging studies usually show some degree of contrast enhancement.

The macroscopic appearance is similar to oligodendroglioma except that areas of necrosis may be present.

Microscopically, these tumors have the general histologic appearance of an oligodendrogliomas but in addition demonstrate focal or diffuse features of overt malignancy, including increased cellularity, cytologic atypia, frequent mitoses, and (often but not always) microvascular proliferation and necrosis with or without pseudopalisading (Figs. 2-5C and D). GFAP-positive mini-gemistocytes are often present but have no prognostic significance. Although the presence of a clearcut oligodendroglial pattern is a prerequisite for the histologic diagnosis of this tumor, it is acknowledged that some examples may be difficult to distinguish from GBM.

Most anaplastic oligodendrogliomas share with low-grade oligodendrogliomas the characteristic loss of chromosome arms 1p and 19q. When such changes are found in anaplastic oligodendrogliomas, the tumors show remarkable responses to combination chemotherapy with PCV—procarbazine, CCNU (1-[2-chloroethyl]-3-cyclohexyl-1-nitrosourea, also known as lomustine), and vincristine—and long median survival (over 10 years). However, other anaplastic oligodendrogliomas have genetic alterations similar to those found in high-grade astrocytomas such as glioblastoma: *PTEN* mutations and chromosome 10 loss, *EGFR* amplification, and *CDKN2A/p16/ARF* deletion. Such tumors often have a poor prognosis, with minimal responses to PCV and with median survivals less than 2 years.

Mixed Gliomas

Oligoastrocytoma (WHO Grade II). *Oligoastrocytomas* are tumors composed both of unequivocally neoplastic astrocytes and of oligodendrocytes. Their exact incidence has been difficult to determine due to lack of uniformity of the histologic criteria used to define this tumor; it probably varies between 2% and 10% of all gliomas. Age and sex distribution, location, clinical presentation, and imaging features are all similar to those of WHO grade II oligodendroglioma.

Two histologic variants have been recognized: a "compact" or biphasic variant and a "diffuse" or intermingled variant. Neither the astrocytic nor the oligodendroglial component should have anaplastic histology. The diagnosis of oligoastrocytoma is usually easier and less controversial in the biphasic variant, which shows distinct areas of oligodendroglial and astrocytic differentiation. The diagnosis of the intermingled variant is more difficult because of the occurrence of reactive astrocytes within the tumor and of GFAP-positive oligodendrocytes, that is, mini-gemistocytes or gliofibrillary oligodendrocytes. However, the presence of GFAP-positive oligodendrocytes should prompt a search for more definitive areas of astrocytoma. Because of the emphasis being placed recently on identification of an oligodendroglial component (with its prognostic implications with regard to sensitivity to chemotherapy), it is likely that some tumors may be overdiagnosed as mixed gliomas on the basis of equivocal histopathologic criteria.

Oligoastrocytomas are monoclonal tumors in which the oligodendroglial and astrocytic components have the same genetic alterations. These tumors, interestingly, have genotypic features of either oligodendrogliomas or astrocytomas. It is therefore likely that most oligoastrocytomas will be genotypically characterized as either oligodendrogliomas or astrocytomas in the future.

Anaplastic Oligoastrocytoma (WHO Grade III).
Anaplastic oligoastrocytomas consist of both neoplastic oligodendrocytes and astrocytes, where one or both components show clearly malignant histology. The most challenging aspect of the diagnosis is distinguishing this tumor from a GBM. As previously mentioned, anaplastic oligodendrogliomas may have features in common with glioblastomas, including the presence of GFAP-positive cells, often in transition with mini-gemistocytes. Likewise, otherwise typical GBMs may have foci of oligodendroglioma-like histology. Thus, the classification of these tumors may be rather arbitrary in some cases. The advent of molecular markers may play a significant role in making the diagnosis of such problematic entities more objective.

Ependymal Tumors

Ependymoma (WHO Grade II). *Ependymomas* account for approximately 6% of intracranial gliomas. Although they occur at any age, they are more frequent in childhood and adolescence. They occur at any level of the ventricular system; however, supratentorial tumors (approximately 40%) are less common than infratentorial ones (approximately 60%). In the spinal cord, ependymomas are the most common neuroepithelial tumor, accounting for approximately 60% of the spinal gliomas. They are most often found in the lumbosacral segments and region of the filum terminale/cauda equina. The clinical symptoms vary with location of the tumor and include local effects as well as hydrocephalus and symptoms of increased intracranial pressure. Imaging studies show a relatively well-circumscribed mass with varying degrees of contrast enhancement, with tumor infiltration and edema being infrequent. Hydrocephalus or displacement of ventricles or brainstem can be

observed. Some spinal ependymomas are associated with syringomyelia.

Macroscopically, ependymomas are gray-red, lobulated, and usually well-demarcated tumors that often have a relationship to a ventricular cavity (Fig. 2-6A). Some infratentorial tumors may extend into the cerebellopontine angle or within the cisterna magna along the medulla. In the spinal cord they usually present as circumscribed intramedullary tumors. Some ependymomas, especially those arising infratentorially, may spread widely throughout the CSF, though rarely outside the CNS.

Ependymomas have a characteristic and easily recognizable microscopic appearance, although cellular density and cytoarchitecture may vary among cases and within the same case. The typical tumor is moderately cellular and composed of polygonal cells having uniform nuclei. Two diagnostically important but often inconstant features include the presence of perivascular pseudorosettes (Fig. 2-6B) and true ependymal rosettes or tubules (or "canals"; Fig. 2-6C). Perivascular pseudorosettes are by far the most common pattern and consist of tumor cells arranged radially around a central vessel, with a "clear" region composed of slender cytoplasmic processes oriented perpendicular to the vessel wall. The ependymal rosettes (tubules) are composed of ependymal cells lining central lumens that recapitulate the appearance of a normal ventricle. In general, the tumor cells show minimal atypia, and mitoses are rare or absent; however, some WHO grade II ependymomas may have foci of necrosis without pseudopalisading. Occasional examples show myxoid degeneration, focal hemorrhage, and (occasionally) bone and cartilage formation. GFAP immunoreactivity is almost always present in the cytoplasmic process surrounding the perivascular pseudorosettes but is more variable elsewhere; the
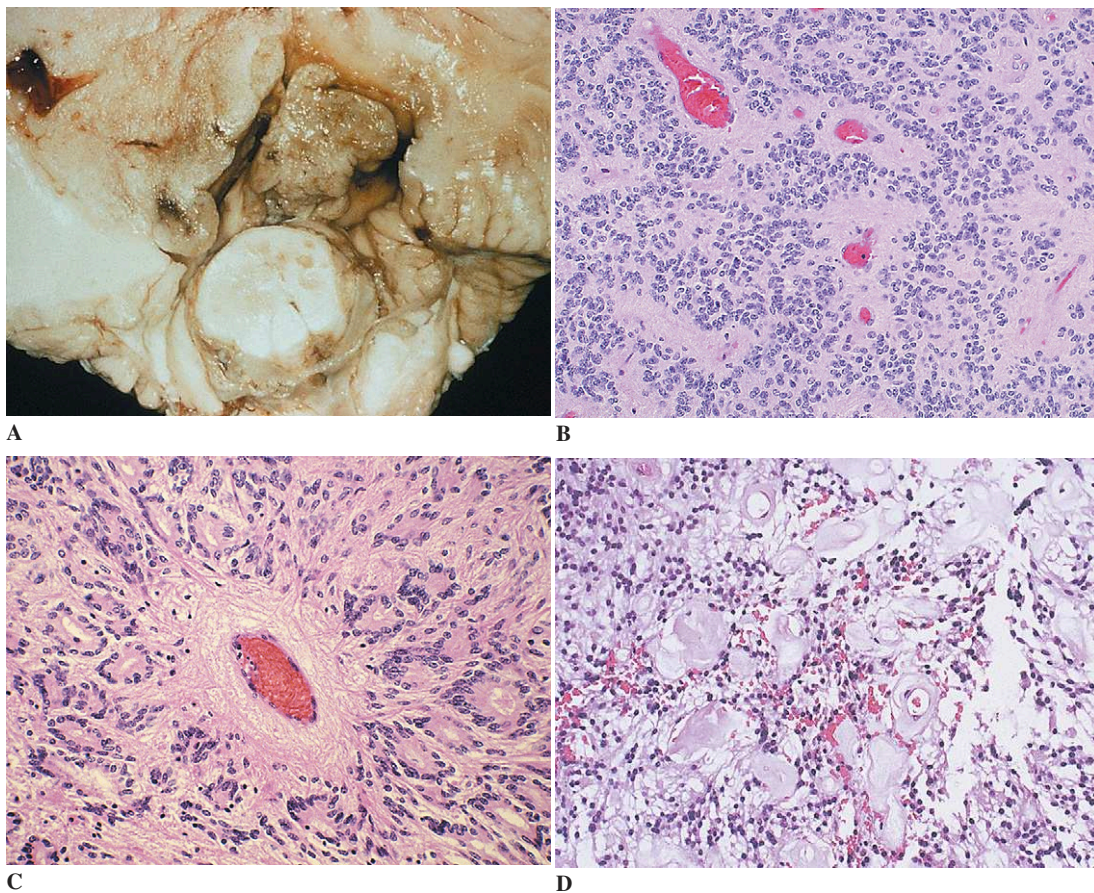
Figure 2-6. Ependymoma. **A**, Ependymoma of fourth ventricle (gross). Microscopic features: **B**, Perivascular pseudorosettes (H and E); **C**, Ependymal tubules (H and E); **D**, Myxopapillary ependymoma (H and E).

tumor cells in ependymal canals often express epithelial membrane antigen. Ultrastructurally, the tumor cells may express features of ependymal differentiation including cilia, blepharoplasts, surface microvilli, and sometimes microrosettes.

Several histologic variants are recognized: *Cellular ependymomas* show high cellularity without increased mitotic rate or other anaplastic features; perivascular rosettes and ependymal tubules are uncommon. *Papillary ependymomas* have well-formed papillary structures and are distinguished from choroid plexus papillomas by the presence of GFAP-positive processes abutting central vessels. *Clear-cell ependymomas* have tumor cells with prominent clear perinuclear halos; immunohistochemistry or electron microscopy may be needed to distinguish this variant from oligodendroglioma or central neurocytoma. *Tanycytic ependymomas* have tumor cells arranged in fascicles with ill-defined perivascular pseudorosettes and rare ependymal tubules; they most often occur in the spinal cord and may appear similar to astrocytomas or schwannomas.

Ependymomas are generally considered slow-growing "benign" tumors. However, it has been difficult to precisely correlate tumor histology with prognosis, partly due to the inability to define reliable indicators of anaplasia. CSF dissemination is associated with a poorer prognosis.

Neurofibromatosis type 2 (NF2) is associated with the occurrence of spinal cord ependymomas, indicating a role for the NF2 tumor-suppressor gene (located on chromosome 22q12) in this tumor. In sporadic tumors, spinal ependymomas more frequently have alterations of the NF2 gene.

Anaplastic Ependymoma (WHO Grade III). *Anaplastic ependymomas* are defined as ependymomas showing increased cellular density and cytologic atypia, frequent mitoses, and (usually) microvascular proliferation and necrosis. However, as noted previously, tumor histology and clinical outcome often do not correlate well. Of the anaplastic features mentioned, only high cell density, a high mitotic index, and a Ki-67/MIB-1 labeling index greater than 4% appear to independently predict a poorer outcome. The presence of necrosis alone does not indicate anaplastic change.

Myxopapillary Ependymoma (WHO Grade I). *Myxopapillary ependymoma* is a distinct subtype of ependymoma that occurs almost exclusively in the conus medullaris/cauda equina region of the spinal cord where it is thought to arise from ependymal cells in the filum terminale. They have rarely been described in other locations in the brain and spinal cord. Subcutaneous sacrococcygeal or presacral myxopapillary ependymomas arising from ectopic ependymal remnants are a well-recognized variant. Myxopapillary ependymomas occur primarily in young adults, where they usually present clinically as back pain. In imaging studies they appear as well-circumscribed lesions with strong contrast enhancement and, sometimes, cystic change and hemorrhage. Myxopapillary ependymomas have a characteristic histologic appearance, consisting of GFAP-positive cuboidal tumor cells arranged around vascularized stromal cores that exhibit variable amounts of mucoid material or fibrous tissue (Fig. 2-6D). The tumor may also contain microcystic areas. Mitoses are very rare or absent and other features of anaplasia are not present. This tumor has an extremely favorable outcome after surgical resection, with the exception of the sacrococcygeal variant, which is associated with a greater rate of regrowth and potential for metastatic dissemination.

Subependymoma (WHO Grade I). *Subependymomas* are well-demarcated, slow-growing, benign tumors composed of cells resembling subependymal glia. They are typically attached to the ventricular wall and project into the lumen. They may occur at any site but are most often encountered in the fourth ventricle. Most subependymomas are clinically silent, but some are symptomatic because of ventricular obstruction, increased intracranial pressure, or (rarely) spontaneous hemorrhage. Microscopically, they consist of small nests of glial-cell nuclei embedded in a hypocellular GFAP-positive fibrillary matrix. Mitoses are rare or absent. Additional histologic features include the presence of microcysts, calcifications, focal hemorrhage, and abnormal vasculature. Mixed tumors with features of both subependymoma and ependymoma have been described; their overall behavior is more aligned with ependymomas and they are considered WHO grade II neoplasms.

Choroid Plexus Tumors

Choroid plexus tumors (papillomas and carcinomas) account for 0.5% of all brain tumors and for 2% of the tumors of the glioma group. They are

encountered most frequently in the first decade of life, with 10% to 20% presenting in the first year of life. The ratio of choroid plexus papilloma to carcinoma is approximately 5 : 1, however, 80% of the carcinomas arise in children. These neoplasms occupy the sites of the ventricular system where choroid plexus is normally found. They occur, in order of decreasing frequency, in the fourth ventricle, lateral ventricles (more so on the left), and third ventricle. Most lateral-ventricle tumors occur in individuals less than 20 years old, whereas those in the fourth ventricle are more evenly age-distributed. Patients present clinically with signs of hydrocephalus and increased intracranial pressure. Only rarely do they produce excessive amounts of CSF. Imaging studies show these tumors to be hyperintense, contrast-enhancing intraventricular tumors. Choroid plexus tumors are treated primarily by surgical excision. The prognosis is excellent for choroid plexus papilloma (nearly 100% 5-year survival) but much less favorable for carcinoma (40% 5-year survival).

Choroid Plexus Papilloma (WHO Grade I). *Choroid plexus papilloma* is a histologically benign tumor whose structure recapitulates that of normal choroid plexus except for having slightly more crowded and elongated papillae (Figs. 2-7A and B). The papillae consist of vascular connective tissue cores (see later discussion of gliovascular cores of papillary ependymoma) lined by a simple columnar or cuboidal epithelium. Prominent mitotic

activity, necrosis, and brain invasion are absent. The majority of choroid plexus papillomas are immunoreactive for transthyretin as well as for vimentin, cytokeratin, and S100 protein, but not for epithelial membrane antigen. Focal staining for GFAP may also be present (25% to 55% of cases).

Choroid Plexus Carcinoma (WHO Grade III). *Choroid plexus carcinomas* show clear histologic features of malignancy including frequent mitoses, nuclear and cytoplasmic atypia, more solid growth pattern with at least some loss of papillary architecture, and (often) brain invasion. The diagnosis of choroid plexus carcinoma is most confidently made in children, whereas in adults the major differential diagnosis is that of metastatic carcinoma, which is distinctly more common in this age group. Immunohistochemistry may be helpful, especially if the tumor expresses markers that are considered more characteristic of choroid plexus; however, some of these markers (e.g., transthyretin) are not always expressed in choroid plexus carcinoma, or, conversely, may also be expressed by some metastatic carcinomas.

Glial Tumors of Uncertain Origin

Astroblastoma. *Astroblastoma* is a rare glial neoplasm of uncertain histogenesis. It is characterized histologically by perivascular pseudorosettes composed of GFAP-positive tumor cells with processes radiating to a central blood vessel that

A   **B**
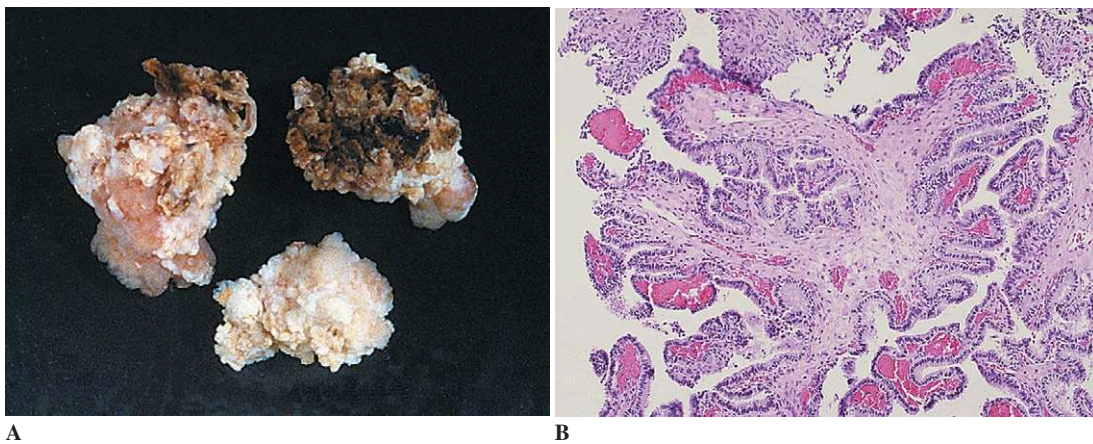
Figure 2-7. Choroid plexus papilloma. **A**, Surgical specimen (gross). **B**, Microscopic features (H and E).

often has a thickened hyalinized wall. The tumor cell processes are usually shorter, thicker, and less variable in diameter than ependymoma, to which astroblastoma shows some similarities. Most astroblastomas occur in young adults, but some have been reported in children and infants. Although both low- and high-grade examples have been described, this tumor has not been assigned a WHO grade due to its variable biologic behavior and the lack of adequate clinical correlative data. Pure astroblastoma should be distinguished from conventional astrocytomas and glioblastomas that may have focal astroblastoma-like histology.

Gliomatosis Cerebri. *Gliomatosis cerebri* is defined as a diffusely infiltrating glioma involving more than two lobes of the brain. It is frequently bilateral and may extend into posterior fossa structures and even the spinal cord. Its histogenesis remains controversial; the most popular theories are diffuse infiltration from one or several "primary" sites in the brain and a "field" transformation. From a molecular-biologic point of view, however, it seems likely that gliomatosis represents the most infiltrative example of a clonal diffuse astrocytic tumor. Until recently, the diagnosis of gliomatosis cerebri was made only at postmortem examination, but it is now often suggested clinically on the basis of magnetic resonance imaging findings and a biopsy showing an infiltrating glioma. The microscopic appearance of the tumor can be variable, with some neoplastic cells resembling astrocytes and others having more indeterminate features or, rarely, oligodendroglial histology. GFAP immunostaining can likewise be variable. The tumor nuclei usually show enough atypia to facilitate their identification as neoplastic, although mitoses may be minimal or even absent. Microvascular proliferation and necrosis are usually absent.

Chordoid Glioma of the Third Ventricle. *Chordoid glioma of the third ventricle* is a recently described glioma that occurs exclusively within the rostral third ventricle. It consists of nests and cords of strongly GFAP-positive cells within a mucinous stroma, often containing lymphoplasmacytic infiltrates. The tumor has little or no mitotic activity and a very low Ki-67/MIB-1 labeling index. Chordoid gliomas of the third ventricle are low-grade

tumors (provisionally WHO grade II) and are treated by surgical excision. They show little evidence of brain invasion, but attachment to the hypothalamus may make removal difficult.

Neuronal and Mixed Neuronal-Glial Tumors

Neuronal and mixed neuronal-glial tumors are less common than pure glial tumors and are made up either entirely or partially of cells having neural characteristics. Such characteristics may be evident at the light-microscopic level; cells may range in appearance from the small, "blue" cell reminiscent of the neuroblast to the differentiated ganglion cell, with its vesicular chromatin, prominent, round, central nucleoli, and even cytoplasmic Nissl substance. It is not unusual, however, for neural features to be appreciated only on ultrastructure or after immunostaining for neural epitopes (e.g., phosphorylated neurofilament protein, neuronal nuclear antigen [NeuN], synaptophysin). In general, tumors with neuronal elements tend to arise in children and young adults and are frequently located within or adjacent to foci of cortical dysplasia (defined as cortex having disorganized, nonlaminar architecture and bizarre cytologic features such as binucleation).

Gangliocytoma and Ganglioglioma. *Gangliocytomas* and *gangliogliomas* are tumors that occur most commonly in the temporal lobe and are often associated with seizures. Both tumors are circumscribed, homogeneous masses having an even, granular cut surface, although small cysts or calcifications can be encountered.

Gᴀɴɢʟɪᴏᴄʏᴛᴏᴍᴀ (WHO Gʀᴀᴅᴇ I). *Gangliocytomas* consist entirely of mature, readily recognized ganglion cells, some of which may be binucleated or bizarre (Fig. 2-8A). A fine reticulin network may be identified around individual cells, particularly in those occupying a very superficial cortical location. Mitoses and necrosis are absent, and vessels, while conspicuous in number, do not have multilayered walls. A variant is seen rarely in a sellar or suprasellar location, with concurrent pituitary adenomas in some instances.

Gᴀɴɢʟɪᴏɢʟɪᴏᴍᴀ (WHO Gʀᴀᴅᴇ II ᴏʀ III). *Gangliogliomas* have a neoplastic glial component that is usually astrocytic, although oligodendroglial differentiation has been reported (Fig. 2-8B). In
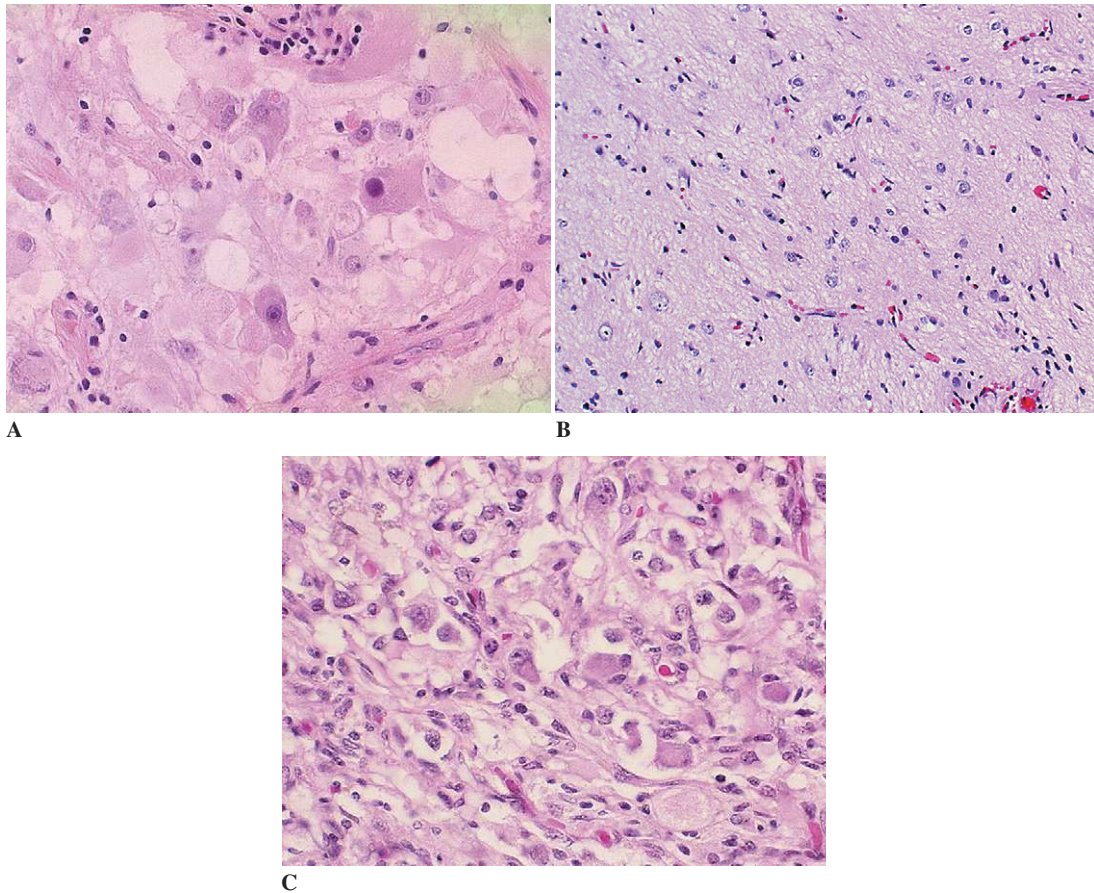
Figure 2-8. Neuronal-glial tumors (microscopic appearance). **A**, Gangliocytoma (H and E). **B**, Ganglioglioma (H and E). **C**, Desmoplastic infantile ganglioglioma (H and E).

some cases, the neuronal component may be overshadowed by the glial component and requires immunostaining for neural markers for confirmation. Care must be taken that "entrapped" neurons, for example in a segment of cortex infiltrated by astrocytoma, are not mistakenly identified as neoplastic; the presence of binucleated or other bizarre forms, as well as disorganized cytoarchitecture, serve to distinguish neoplastic from entrapped ganglion cells. The behavior of gangliogliomas is determined by the degree of anaplasia of the glial component so that documentation of necrosis, mitotic activity, and vascular proliferation must be made. The vast majority of gangliogliomas lack anaplastic features and are indolent tumors best treated by excision. Gangliogliomas that show anaplasia of the glial component would be designated as anaplastic gangliogliomas (WHO grade III).

DYSPLASTIC GANGLIOCYTOMA OF THE CEREBELLUM (LHERMITTE-DUCLOS DISEASE). *Dysplastic gangliocytoma of the cerebellum* is a distinctive lesion characterized by grossly visible expansion of the cerebellar folia, usually in only one hemisphere. The centers of the affected folia contain large, bizarre ganglion cells (with morphologic and focal immunohistochemical resemblance to Purkinje cells) and some small, granular neurons, while the surface is covered by aberrant white matter bundles; this configuration is sometimes referred to as "inverted cerebellar cortex." This lesion is best considered a hamartoma, as it does not grow or spread in the manner of true neoplasms and does not in itself constitute a threat to life. About half of all cases of Lhermitte-Duclos disease are associated with Cowden syndrome, which is a constellation of multiple verrucous skin

lesions, facial trichilemmomas, fibromas of the oral mucosa, hamartomatous polyps of the gastrointestinal tract, and thyroid and breast tumors (both benign and malignant). Cowden syndrome arises from mutations in the *PTEN* gene on chromosome 10q, and it is therefore likely that alterations of *PTEN* function are related to Lhermitte-Duclos pathogenesis. This association is supported by a recent mouse model of disrupted *PTEN* activity, which develops lesions that are histologically similar to Lhermitte-Duclos.

Desmoplastic Infantile Ganglioglioma (WHO Grade I). *Desmoplastic infantile ganglioglioma* is a rare variant of ganglioglioma which occurs up to the age of 2 years. The superficial aspect of the frontal and parietal lobes is the usual site; accompanying cysts are not uncommon. Identifying histologic features are abundant connective tissue (desmoplasia), intermixture of astrocytic and ganglion cell components, and tendency to adhere to overlying meninges (Fig. 2-8C). A similar tumor, lacking ganglion cells, is the *desmoplastic astrocytoma of infancy*. Both tumors are slow-growing and treatable by surgery.

Neurocytic Tumors

Central Neurocytoma (WHO Grade II). *Central neurocytoma* is a low-grade tumor that usually arises in the third or lateral cerebral ventricle, most commonly in older children and young adults. It is composed of small, well-differentiated neurons with uniform round nuclei, fine chromatin, and occasional nucleoli, in a loose neuropil-like background (Fig. 2-9A). An artifact of fixation results in perinuclear clearing, which results in a histologic appearance similar to oligoden-

A

B

C
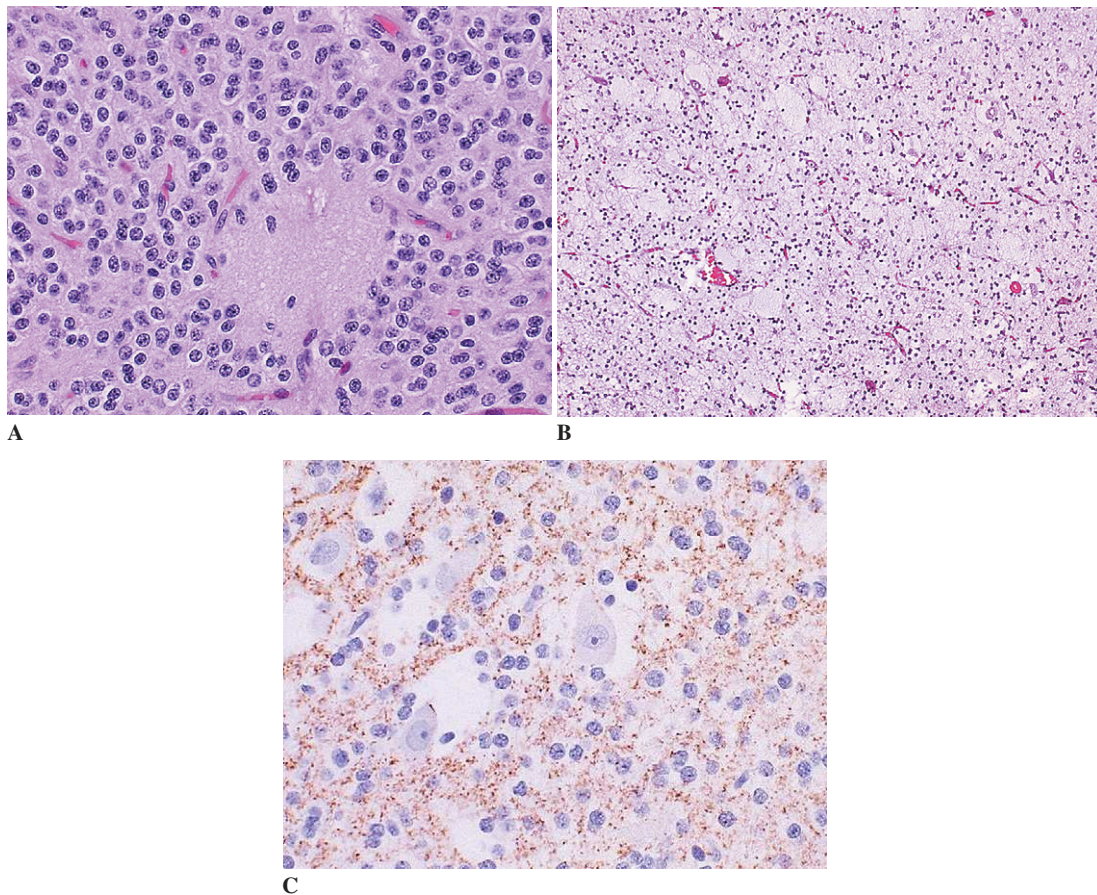
Figure 2-9. Neuronal-glial tumors (microscopic appearance). **A**, Central neurocytoma (H and E). **B**, Dysembryoplastic neuroepithelial tumor (DNT; H and E). **C**, DNT (immunostain for synaptophysin).

droglioma. Because of this appearance, these tumors were thought to be unusual intraventricular oligodendrogliomas until their neuronal character was established by electron microscopy. Currently, immunostaining for synaptophysin can confirm the neuronal nature of the lesion. Atypical and malignant phenotypes have recently been recognized; these are characterized by dense cellularity, vascular cell proliferation, mitotic activity, infiltration of adjacent brain, and a tendency to recur.

CEREBELLAR LIPONEUROCYTOMA. *Cerebellar liponeurocytoma* is a variant tumor composed of neurocytoma-like cells admixed with mature adipocytes. It arises in the cerebellum of adults. This neoplasm is a low-grade tumor (provisionally WHO grade I or II) that has a generally favorable clinical outcome following surgery.

Other Neuronal-Glial Tumors

DYSEMBRYOPLASTIC NEUROEPITHELIAL TUMOR (WHO GRADE I). The *dysembryoplastic neuroepithelial tumor* (DNT) is a low-grade tumor containing oligodendroglial-like and neurocytic areas but with a nodular (or multinodular) architecture and intracortical location. The tumor occurs mostly in children, although adult examples have been recognized. It is often heralded by medically intractable seizures. A histologic hallmark of dysembryoplastic neuroepithelial tumor is the "specific glioneuronal element," which is the microarchitectural association of the round oligodendroglial- or neurocytic-like cells with axon bundles bounding microcystic spaces in which larger ganglion cells lie ("floating neurons") (Figs. 2-9B and C). The cortex adjacent to the tumor nodules is often dysplastic, suggesting a developmental (or hamartomatous) nature. Calcifications and cysts are frequent accompaniments. Surgical excision is considered curative. The existence of anaplastic versions has been suggested, but is not universally embraced.

PARAGANGLIOMA. Within the cranial vault and spinal canal can arise tumors of extra-adrenal chromaffin tissue that are analogous to pheochromocytomas of the adrenal gland. Most often these are circumscribed nodules in the filum terminale, although cranial and spinal nerve root masses extending into skull or vertebral foramina have been noted. Those arising in the middle ear, often extending into the posterior fossa at the cerebellopontine angle, are also known as "glomus jugulare" tumors. Regardless of where they are seated within the neuraxis, these neoplasms are identical histologically to paragangliomas elsewhere in the body, being made up of nests or "zellballen" of plump neuroendocrine cells separated by fine fibrovascular septa. Tumor cells are chromogranin- and synaptophysin-positive, while interspersed sustentacular cells are S100-positive. They only rarely produce catecholamines, instead causing symptoms as a result of local compression. The biologic behavior of these neoplasms is determined more by their anatomic extent at the time of presentation than by histologic features.

Neuroblastic Tumors

PERIPHERAL NEUROBLASTIC TUMORS. Arising in the neural-crest–derived adrenal gland or sympathetic nervous system in children, *peripheral neuroblastic tumors* are typified by densely packed, small, "blue" cells, sometimes forming rosettes and neuropil stroma. The most primitive tumor of this group, the *neuroblastoma*, occurs in the first decade of life as a palpable abdominal mass or as a dumbbell-shaped mass filling a spinal foramen. The prognosis of neuroblastoma depends upon the proportion of ganglion cells, representing differentiating neuroblasts, within the tumor: those neuroblastomas with no differentiating cells are termed "undifferentiated," those with less than 5% differentiating cells are termed "poorly differentiated," and those with more than 5% differentiating cells are termed "differentiating." In general, the differentiating forms have increasing pink, fibrillary (schwannian) stroma, whereas the undifferentiated form may be entirely made up of small, "blue" cells and require electron microscopy or immunohistochemistry for the demonstration of a neural phenotype. Favorable clinical outcome is also highly correlated with age less than 1 year, confinement of tumor to the adrenal gland, and histologic parameters such as a low mitosis-karyorrhexis index. Better-differentiated tumors consisting of neuroblasts, differentiating neuroblasts, and mature ganglion cells with more abundant schwannian stroma are known as *ganglioneuroblastomas*, and tumors consisting entirely of schwannian stroma with scattered mature ganglion cells are designated *ganglioneuromas*.

OLFACTORY NEUROBLASTOMA. The *olfactory neuroblastoma* (or *esthesioneuroblastoma*) is a

neuroblastic, small (blue)-cell tumor localized to the olfactory epithelium in the upper nasal cavity. It occurs in late childhood through adulthood, with presenting symptoms of sinus obstruction or headache. Destruction of the cribriform plate may allow growth of tumor into the anterior cranial fossa, meninges, and frontal lobes of the brain. It has a characteristic broad, nodular growth pattern. As with neuroblastic tumors at other sites, the neoplastic cells have a neural immunophenotype and ultrastructure. Homer Wright–type rosettes (with central neurofibrillary processes) or, occasionally, Flexner-Wintersteiner rosettes (with central lumina) may be seen. A high mitotic rate and necrosis tend to indicate aggressive biologic behavior.

Pineal Parenchymal Tumors

The pineal gland is made up of cells having phenotypic characteristics of retinal photoreceptors, with which they share a common embryonic lineage. Neoplasms of this region may be well-differentiated and difficult to distinguish on biopsy from normal pineal gland (pineocytoma), or they may be poorly differentiated, small (blue)-cell tumors (pineoblastomas). A third category, the pineal parenchymal tumor of intermediate differentiation, may have admixed well and poorly differentiated zones or consist of cells with differentiation intermediate between the two extremes. All will demonstrate neural characteristics on immunohistochemistry (i.e., synaptophysin, neuron-specific enolase, chromogranin), and may additionally show retinal S-antigen, rhodopsin, and melatonin. Ultrastructurally, synaptic vesicles and microtubules confirm neural differentiation; cytoplasmic annulate lamellae are further reminiscent of retinal differentiation.

Pineocytoma (WHO Grade II). The *pineocytoma* occurs in young to middle-aged adults and represents about 45% of all pineal parenchymal tumors. The component cells are uniform, with round to oval nuclei and occasional fine nucleoli and have fibrillary or club-shaped eosinophilic processes that may converge in the center of rosettes. The tumor has a lobular architecture recalling the normal structure of the pineal gland, but the lobules are separated by delicate fibrovascular septa (Figs. 2-10A and B). Variable amounts

of neuropil may be present in the background. The tumor is histologically low grade and lacks mitotic activity or pleomorphism. It is well-circumscribed and slow-growing but not easily resectable because of its central location. Nonetheless, 5-year survival rates of up to 90% may be expected.

Pineoblastoma (WHO Grade IV). The *pineoblastoma* arises in children and young adults as a rapidly growing mass, with heterogeneity on neuroimaging that reflects its tendency toward hemorrhage, necrosis, and cystic degeneration. Histologically, it is a densely cellular tumor made up of oval, hyperchromatic nuclei with little visible cytoplasm, resulting in "molding" of nuclear contours. Some cells may have recognizable eosinophilic processes or form rosettes of Homer Wright or Flexner-Wintersteiner type (Fig. 2-10C). Single-cell invasion of adjacent brain structures, high mitotic activity, and necrosis are evidence of malignancy. Like other small (blue)-cell tumors of the CNS, pineoblastomas are considered "seeding" tumors that, because of their invasive phenotype, can gain access to the cerebrospinal fluid and spread within the ventricles and subarachnoid space to other sites in the neuraxis. Such malignancies are often treated prophylactically with craniospinal irradiation and systemic chemotherapy in anticipation of such a route of spread, which carries a very high mortality.

Pineal Parenchymal Tumor of Intermediate Differentiation. *Pineal parenchymal tumor of intermediate differentiation* has been recently recognized in both children and adults but is relatively rare. It has a more sheetlike architecture and atypical cytology compared to the pineocytoma, yet does not have the overt small-"blue"-cell malignant phenotype of the pineoblastoma. It may have variable amounts of eosinophilic neuropil background. Biologic behavior and clinical survival are intermediate between those of the aggressive pineoblastoma and the more indolent pineocytoma.

Embryonal Tumors

The category of *embryonal tumors* comprises neoplasms of very immature, or primitive, cells resembling neuroepithelium, the origin of the precursor cells of the nervous system. Tumors made up of
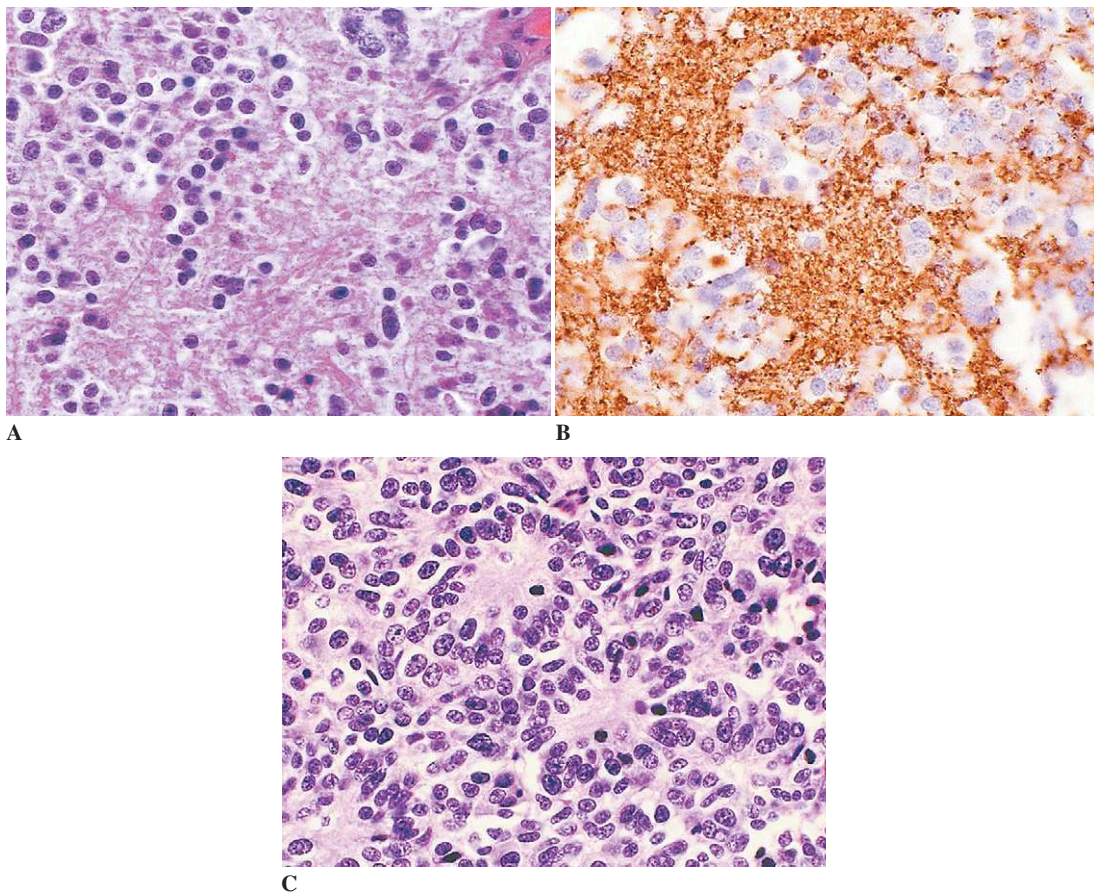
Figure 2-10. Pineal parenchymal tumors. **A**, Pineocytoma (H and E). **B**, Pineocytoma (immunostain for synaptophysin). **C**, Pineoblastoma with Homer Wright rosettes (H and E).

these cells may retain the capability to differentiate along both neural and glial lines, as detected by immunohistochemical or ultrastructural means. They tend to be large, bulky tumors that grow rapidly and spread ("seed") along cerebrospinal fluid pathways.

Medulloblastoma (WHO Grade IV). *Medulloblastomas* are the prototype of the embryonal CNS tumors, representing a significant proportion of primary brain tumors in children. A second peak in age incidence occurs in early adulthood. The tumor arises (by definition) in the cerebellum, usually the vermis, and may cause ataxia, headache, and vomiting due to acute obstruction of the fourth ventricle with hydrocephalus (Fig. 2-11A). Neuroimaging studies reveal enhancing, lobulated masses; as much as one third of patients will have leptomeningeal enhancement representing CSF seeding at presentation. Histologically, medul-

loblastomas are small (blue)-cell tumors somewhat resembling pineoblastomas (see earlier discussion). Homer Wright rosettes, with central neurofibrillary processes, are a hallmark but are not always present (Fig. 2-11B). Necrosis occurs both as single cells (apoptosis) and in confluent fields. Mitotic activity is conspicuous.

Several histologic variants exist, including the *desmoplastic medulloblastoma*, which is characterized by broad nodules of tumor cells separated by collagenous septa. The periphery of the nodules is occupied by densely arranged tumor cells, while the centers are neuropil-rich "pale islands." This variant somewhat resembles the rare *medulloblastoma with extensive nodularity and advanced neuronal differentiation* ("cerebellar neuroblastoma"; Fig. 2-11C). The latter differs from the desmoplastic subtype by less conspicuous collagen stroma and greater evidence of neural differentiation in the form of central

A   **B**

C
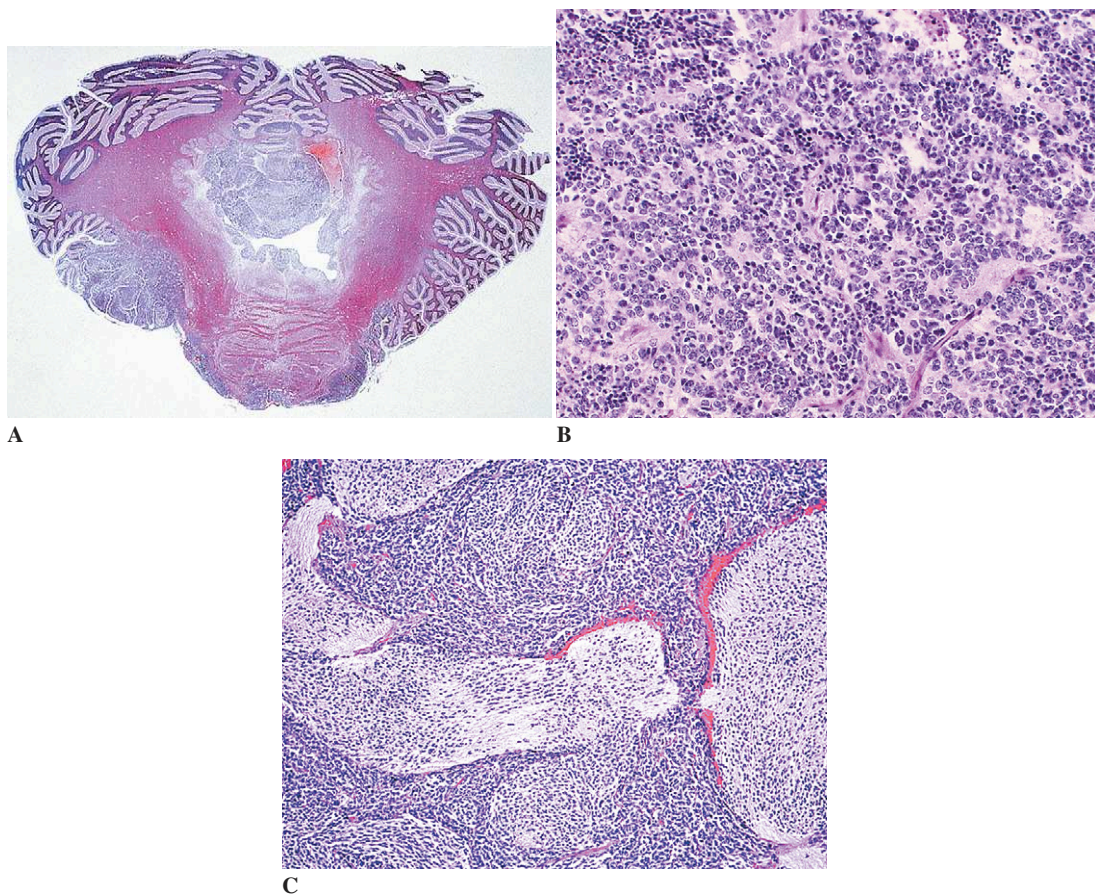
Figure 2-11. Medulloblastoma. **A**, Medulloblastoma of cerebellar vermis, with ependymal and leptomeningeal spread (H and E whole mount). Microscopic features: **B**, Homer Wright rosettes (H and E); **C**, Nodular architecture (H and E).

neurocytoma-like areas (see earlier discussion) as well as mature ganglion cells. *Large-cell (anaplastic) medulloblastoma* has a closely packed cell arrangement as in the usual type of medulloblastoma, but with nuclei of increased diameter containing prominent nucleoli. This variant also has striking immunohistochemical staining for synaptophysin. The *medullomyoblastoma* has "strap" cells representing immature rhabdomyoblasts, while the *melanotic medulloblastoma* has scattered tubular clusters of pigmented, melanosome-laden tumor cells. The latter two variants are quite rare. All subtypes are associated with malignant biologic behavior, requiring aggressive resection and craniospinal radiotherapy for control. By these means, 5-year survival has increased to about 75%.

The most common genetic alteration in medulloblastoma is isochromosome 17 q. The association of medulloblastoma with Gorlin's syndrome (basal cell nevus syndrome, from mutation of the *PTCH* gene on chromosome 9 q) and Turcot's syndrome (colon and brain tumors, due to mutation of the *APC* gene on chromosome 5 q or defects in mismatch repair genes) has implicated the SHH-PTCH-SMO and the Wnt-β-catenin pathways, respectively, in medulloblastoma tumorigenesis. Indeed, mice with targeted disruption of *PTCH* develop medulloblastoma-like tumors.

Medulloepithelioma (WHO Grade IV). *Medulloepithelioma*, which arises in infants and young children, has an unusual trabecular or ribbon-like growth pattern of primitive, small, "blue" cells recapitulating the appearance of the embryonic neural tube. Medulloepitheliomas may be found throughout the CNS but most often occur in the cerebral hemispheres in periventricular locations. On neuroimaging, the medulloepithelioma has a

heterogeneous appearance corresponding to areas of necrosis, hemorrhage, cysts, and calcification. Divergent differentiation, with areas resembling astrocytoma, neuroblastoma, or gangliocytoma, is common. It is mitotically active and clinically aggressive.

Atypical Teratoid/Rhabdoid Tumor (WHO Grade IV). The *atypical teratoid/rhabdoid tumor* (AT/RT) is a densely cellular "blue"-cell tumor often confused with medulloblastoma. The AT/RT, however, shows cells with clear cytoplasm and nucleoli that are admixed with cells having eosinophilic, rounded (rhabdoid) cytoplasmic inclusions. The rhabdoid cells stain with vimentin, epithelial membrane antigen, and sometimes desmin or cytokeratin, indicating divergent differentiation (hence the term "teratoid"). AT/RTs occur predominantly in infants and young children, and may present in the cerebral hemispheres rather than the cerebellum. AT/RTs are nearly always associated with allelic loss of one copy of chromosome 22 and mutation in the *INI1/SNF5* gene on the remaining copy of 22 q. Molecular testing for these two genetic changes can be helpful in diagnosing difficult cases of AT/RT.

Supratentorial Primitive Neuroectodermal Tumors (WHO Grade IV). The *primitive neuroectodermal tumor* is a histologic analog to the medulloblastoma but occurs in the supratentorial compartment. Like medulloblastomas, primitive neuroectodermal tumors can demonstrate multiple lines of differentiation—glial, neuronal, or sometimes mesenchymal—by ultrastructural or immunohistochemical methods. Occasionally, such elements may be visible by routine light microscopy as scattered cells with eosinophilic fibrillary cytoplasm (astrocytic differentiation) or cells with large, vesicular nuclei (ganglionic differentiation, prompting the designation "cerebral neuroblastoma" if extensive). The majority of tumor cells, however, are undifferentiated small cells with nuclear molding and high mitotic activity. Nodular growth patterns, neuropil background, geographic necrosis, hemorrhage, or calcifications may be evident.

Ependymoblastoma (WHO Grade IV). The *ependymoblastoma* tends to be seen in the cerebral hemispheres of infants and young children. Its principal distinguishing feature is the presence of multilayered rosettes with true lumina bounded by ciliated neuroepithelial cells. These rosettes may be scattered or form back-to-back arrangements amidst a population of small, undifferentiated cells. On ultrastructural analysis, ependymoblastomas are found to carry basal bodies (blepharoplasts) and cilia in the cells lining the rosettes. Tumor cells may show divergent phenotypes, including glial and neuronal characteristics, as in other embryonal tumors. The neoplasm behaves in a malignant fashion. This tumor is histologically similar to the anaplastic ependymoma (see earlier discussion) but lacks the perivascular pseudorosettes that characterize the latter tumor; furthermore, the multilayered rosettes seen in ependymoblastoma differ from the single-layered rosettes (tubules) present in ependymoma.

Tumors of Peripheral Nerves

One of the following three criteria must be met to affirm that a tumor has arisen from a peripheral nerve.

1. The tumor macroscopically arises from a nerve trunk (i.e., continuity with the nerve trunk is apparent).
2. The nature of the tumor cells may be clearly identified (by immunohistochemistry or electron microscopy) as schwannian or perineurial.
3. There are stigmata or a familial history of neurofibromatosis (NF), either NF1 (formerly called peripheral NF or Von Recklinghausen's disease) or NF2 (formerly called central or bilateral acoustic NF).

Benign Tumors of Peripheral Nerves

Schwannoma (WHO Grade I). *Schwannomas* (neurilemmomas or neurinomas) are benign tumors arising from Schwann cells. A peak of incidence may be seen in the fourth to sixth decades of life. As they originate wherever Schwann cells are present, schwannomas may be found on cranial nerves, spinal nerve roots, peripheral nerve trunks, and even at nerve endings, leading to cutaneous, subcutaneous or (less often) visceral tumors. Intracranial schwannomas most often involve the vestibular branch of the eighth cranial nerve, in
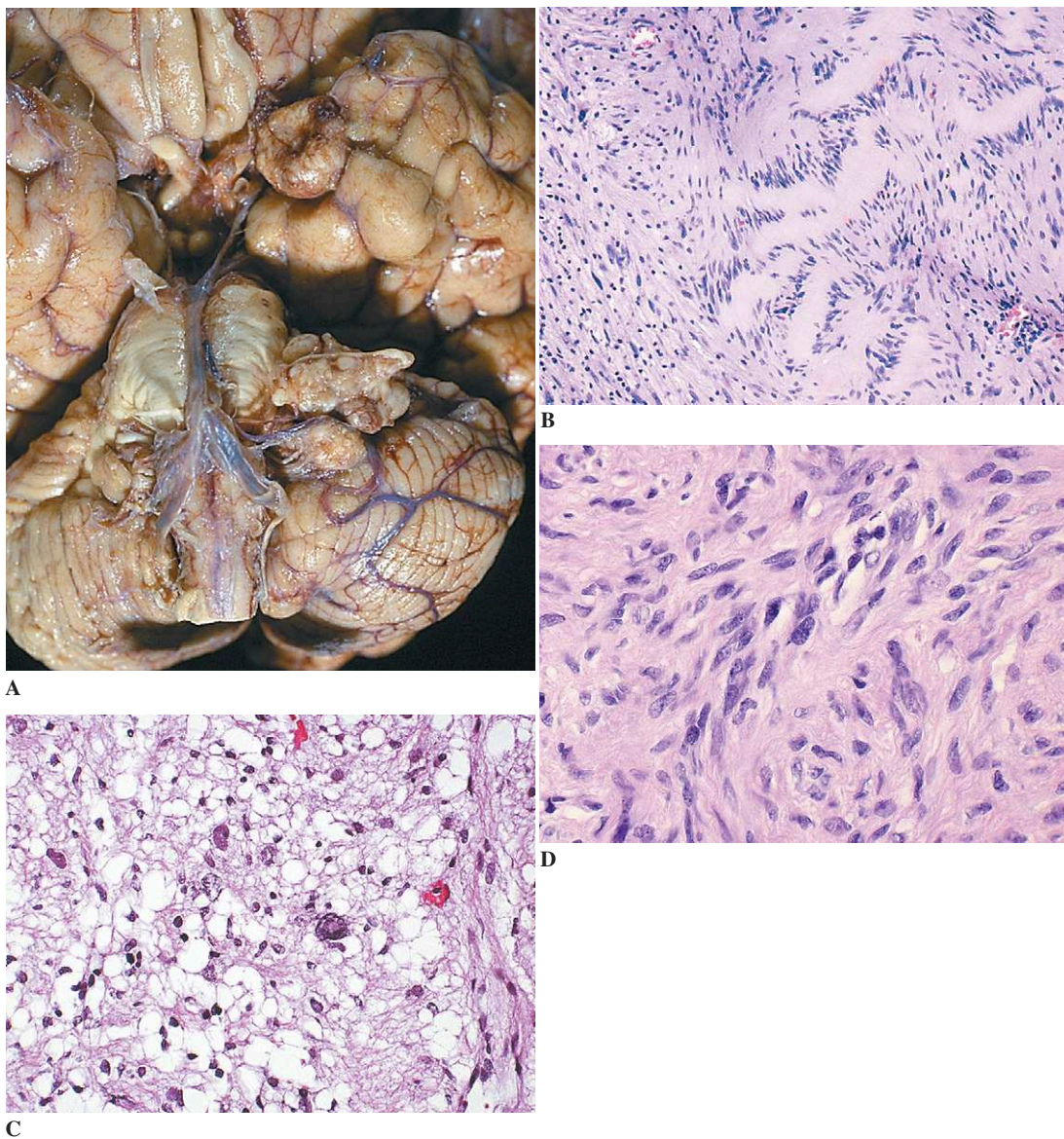
Figure 2-12. Schwannoma. **A**, Vestibular schwannoma (gross). Microscopic features: **B**, Antoni A tissue with palisading (Verocay bodies; H and E); **C**, Antoni B tissue (H and E); **D**, Pleomorphic nuclei (H and E).

which case they are referred to as *vestibular schwannomas* (Fig. 2-12A). Most vestibular schwannomas are situated in the cerebellopontine angle and, on reaching a critical size, can cause clinical symptoms due to effects on neighboring structures. These include enlargement and erosion of the internal auditory meatus, stretching of neighboring cranial nerves, and cerebellar and brainstem compression. Schwannomas of the fifth, ninth, and tenth cranial nerves are much less common. Motor cranial nerves are involved only exceptionally. Spinal schwannomas are situated most frequently on dorsal sensory nerve roots but some have also been described on the ventral motor nerve roots. The thoracic segments are most often implicated, but cervical and lumbar schwannomas are not rare. Spinal schwannomas may also be situated in the cauda equina. The tumor is usually

restricted to the subdural space but may sometimes extend through the intervertebral foramen, resulting in an hourglass appearance. Intraparenchymatous (intracerebral or intraspinal) or intraosseous schwannomas have been exceptionally reported.

Macroscopically, schwannomas are firm, well-circumscribed, encapsulated tumors of variable size. Small tumors are spherical, white, or slightly translucent and have an elastic consistency. Larger examples are irregularly lobulated and may be cystic. On section, some may show hemorrhages and yellowish foci. These tumors displace rather than invade the nerves from which they originate. Bone erosion is sometimes evident on imaging studies. As a general rule, schwannomas are solitary tumors; in NF2, however, multiple schwannomas, especially bilateral vestibular schwannomas, may be found. Multiple schwannomas in the absence of other features of NF2 are seen in schwannomatosis. The clinical evolution of schwannomas is slow; they remain histologically benign, but may recur. Half of schwannomas have a deletion of the long arm of chromosome 22 and a mutation or a deletion of the *NF2* gene on the remaining allele. Total inactivation of the *NF2* gene, with subsequent loss of merlin (schwannomin) expression, as demonstrated by immunocytochemistry or Western blotting, seems to be a crucial step in the tumorigenesis of schwannomas.

Microscopically, schwannomas consist of two characteristic tissue types that are often intermingled within the same tumor: (1) dense fibrillary (Antoni A) tissue, which consists of elongated bipolar cells having scant cytoplasm and cylindrical nuclei arranged in elongated drifts, whorls, or characteristic palisades (Verocay bodies; Fig. 2-12B), and (2) loose reticulated (Antoni B) tissue, which is less densely cellular and consists of small, round nuclei randomly arranged in a matrix containing microcysts and vacuolated cells that impart a finely honeycombed appearance (Fig. 2-12C). Reticulin fibers are present in both tissue types. Antoni B tissue usually predominates in intracranial schwannomas. Although a moderate degree of nuclear pleomorphism may be seen (Fig. 2-12D), mitotic figures are absent. Many examples show hyaline thickening of vessel walls and sometimes thrombosis and evidence of prior hemorrhage. Unlike neurofibromas, nerve fibers are usually not present within a schwannoma but are displaced and incorporated into the surrounding fibrous capsule. Ultrastructurally, schwannomas are composed solely of Schwann cells ensheathed by a continuous basal lamina in association with a variable proliferation of collagen fibers. Virtually all schwannomas show strong immunoreactivity for S100 protein; some examples may also show variable *GFAP* expression.

Several histologic subtypes of schwannoma are recognized, as follows.

(1) *Plexiform* (or *multinodular*) *schwannomas* are most often dermal or subcutaneous in location and occur on the trunk or upper extremities. Histologically, they consist of multiple nodules of varying sizes embedded in fibrous connective tissue. Occasional examples may be locally aggressive and recur but even these are not considered overtly malignant. Plexiform schwannomas are associated with NF2; they must be distinguished from plexiform neurofibromas, which are almost always associated with NF1.

(2) *Dermal nerve sheath myxoma* (or *neurothekeoma*) arises in the dermis, most often on the face or upper extremity. It consists of multiple lobules separated from one another by thin, fibrous septa and is composed of spindle and stellate Schwann cells lying within an abundant basophilic, mucoid, PAS- and Alcian-blue–positive, vacuolated matrix. Epithelioid and multinucleated giant cells may be encountered. Their clinical behavior is entirely benign. This tumor must be differentiated from rare, mucinous cysts of the peripheral nerves.

(3) *Cellular schwannomas* are characterized by spindle cells forming a compact fascicular, sometimes fibrosarcoma-like, growth pattern. The tumor is characteristically located near the vertebral column in the mediastinum or retroperitoneum. Occasionally, bone destruction and neurologic symptoms develop. Their clinical appearance, together with the high cellularity, fascicular pattern, moderate nuclear pleomorphism, and mitotic activity of this tumor, has led to the erroneous diagnosis of a soft-tissue sarcoma in some cases. However, cellular schwannomas always have a benign course and show a high degree of schwannian differentiation under electron microscopy and by immunohistochemistry.

(4) *Melanotic* (or *pigmented*) *schwannomas* consist of Schwann cells containing melanosomes.

They are divided into psammomatous and nonpsammomatous forms, the former frequently seen as part of the Carney complex (a multiendocrine autosomal-dominant disorder). Melanotic schwannomas usually have a benign course.

(5) *Granular-cell tumors*, first believed to be of myogenic origin, were originally called "granular-cell myoblastomas" or Abrikossof tumors. They are now known to be of Schwann cell origin. Several examples have been reported to originate from small, peripheral, myelinated nerves, major nerve trunks, and intracranial nerves (i.e., facial and trigeminal). They are composed of masses of large, rounded, or polyhedral cells with abundant cytoplasm filled with PAS-positive granules. Bundles of myelinated or unmyelinated fibers have been demonstrated among the granular cells. Under electron microscopy the granules are seen to correspond to collections of dense or multivesicular bodies suggesting lysosomes; the tumor cells are surrounded by a basal lamina. The tumor cells are immunoreactive for S100 protein. Most granular-cell tumors involving peripheral nerves are benign, although occasional examples display malignant behavior and develop metastases.

Neurofibroma (WHO Grade I). *Neurofibromas* may occur as sporadic, solitary tumors of nerve roots and peripheral nerves. Less often, as part of the NF1 picture, they form multiple tumors. All ages and both sexes may be affected.

Although there has been some controversy about the clonal nature of neurofibromas, they are most likely derived from Schwann cells since allelic loss can be demonstrated at the *NF1* locus in the Schwann cells of neurofibromas. The genetic basis of neurofibroma formation is unclear, but the *NF1* gene on the long arm of chromosome 17 is clearly involved in the early stages of tumorigenesis. Neurofibromas also feature hyperplasia of the fibroblastic supporting elements of the nerve, the individual fibers of which appear to be dissociated by this benign proliferation.

Under light microscopy, even at low magnification, two different zones may be clearly identified in sections of neurofibromas: a central zone containing fibroblasts, Schwann cells, dense collagen bundles and nerve fibers, either myelinated or unmyelinated (Fig. 2-13); and a less-dense, peripheral zone devoid of nerve fibers. The Schwann cells
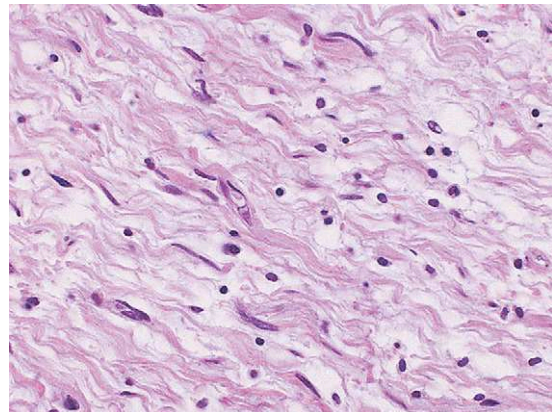
Figure 2-13. Microscopic appearance of neurofibroma (H and E).

and the fibroblasts are embedded in a clear, often myxoid-appearing matrix. Atypical nuclei may be observed, but mitoses are rare or absent. There are several histologic variants of neurofibroma: *plexiform neurofibromas* present a characteristic pattern with multiple segments of neurofibromatous nerve bundles embedded in a dense collagenous matrix. They are almost always associated with NF1. *Pacinian neurofibromas* (also known as *pacinian corpuscle neuromas* or *pacinian neuromas*) are small, papular, cutaneous tumors that occur either on the hand or foot along the course of a nerve with which they are always linked by a slight stalk. Histologically, the lobules of the tumor contain several pacinian corpuscles. These tumors are better referred to as "hyperplastic pacinian corpuscles" or "pacinian hyperplasia" than as true neurofibromas and should be distinguished from the latter, which may sometimes contain occasional Meissner's or pacinian corpuscles. *Melanotic (pigmented) neurofibromas* are exceedingly rare. *Storiform neurofibroma* has a storiform architectural pattern and its cells contain melanin in 50% of cases.

Malignant change in a neurofibroma may occur, with production of a *malignant peripheral nerve-sheath tumor* (see later discussion). Such an evolution is frequently associated with NF1 and particularly affects plexiform neurofibromas and neurofibromas of major nerves.

Intraneural Perineurioma (WHO Grade I). *Intraneural perineurioma* is an exceedingly rare neoplasm that almost exclusively affects young

subjects, without sex predilection. It consists of a localized hypertrophy of one major peripheral nerve of the extremities. Microscopically, the tumor is characterized by onion-bulb formations that closely resemble the hypertrophic neuropathy of Dejerine-Sottas disease or the hypertrophic form of Charcot-Marie-Tooth disease, but it lacks the multiplicity of nerve involvement or the genetic background of those conditions. Electron microscopy and immunohistochemistry of the cells forming the onion bulbs provide further support for their perineurial nature: they are immunopositive for epithelial membrane antigen (EMA) and negative for S100 protein. They are benign tumors with no tendency toward recurrence or metastasis. Intraneural perineuriomas are not related to NF1 or NF2; nonetheless, alterations of the long arm of chromosome 22 have been documented in these tumors, and probably involve the *NF2* gene. Some authors believe that the features of intraneural perineurioma are more suggestive of a relatively organized hyperplastic process in which the perineurial cells are selectively involved, perhaps as a reaction to minor trauma to the perineurial sheath.

Malignant Tumors of Peripheral Nerves

The exceptional involvement of peripheral nerve by lymphomas and metastatic tumors will not be considered here.

Malignant Peripheral Nerve Sheath Tumor (WHO Grade III or IV). Several terms that are more or less synonymous with *malignant peripheral nerve sheath tumor* (MPNST)—malignant schwannoma, malignant neurofibroma, malignant mesenchymoma of nerve sheath, neurogenic sarcoma, and neurofibrosarcoma—are misleading and must be avoided.

MPNSTs occur in adults and represent 5% to 10% of soft-tissue sarcomas. According to different series in the literature, 25% to 65% of MPNSTs occur during the course of NF1. (Approximately 4% of patients with NF will develop an MPNST). The most common location is along the main nerve trunks of limbs (sciatic nerve, brachial plexus, sacral plexus), on the trunk, and in the head and neck. MPNSTs of cranial nerves are uncommon and are mostly seen on the inferior dental nerve. MPNSTs may arise de novo or from a preexisting tumor—usually a neurofibroma, rarely a ganglioneuroma, ganglioneuroblastoma, or pheochromocytoma—and very exceptionally by malignant transformation of a schwannoma. Most MPNSTs have a poor prognosis, with a 10-year survival rate of about 23%.

Histologically, MPNSTs are mainly malignant spindle-cell tumors with increased cellularity, nuclear atypia, numerous mitoses, and frequent geographic necrosis. The majority of MPNSTs have a high Ki-67/MIB-1 labeling index (5% to 65%). Various forms of divergent differentiation towards osteosarcoma, chondrosarcoma, liposarcoma, angiosarcoma, or malignant Triton tumor are very inconstant. Other components can also be encountered, such as epithelial components (epithelioid, epidermoid, or glandular MPNSTs), melanocytes (melanotic malignant schwannoma), or perineurial cells. MPNSTs are pseudoencapsulated and frequently invade the adjacent soft tissues. In many cases, electron microscopy and especially immunohistochemistry will contribute to the diagnosis and facilitate the distinction between other different kinds of spindle cell tumors (i.e., fibroblastic sarcomas, leiomyosarcomas, sarcomatoid carcinomas, and some melanomas). It must be kept in mind that Schwann cells are S100 protein-positive, sometimes GFAP-positive, and usually vimentin-positive; perineurial cells are EMA-positive and S100-protein–negative; fibroblasts are vimentin-positive; smooth muscle cells are desmin-positive; carcinomas are cytokeratin-positive; and melanocytes are S100 protein-positive and HMB45-positive. MPNSTs demonstrate inactivation of both the *p53* and *p16* growth-control pathways; for instance, tumors will often have *TP53* mutations and *CDKN2A/p16/ARF* deletions.

Malignant Peripheral Neuroectodermal Tumor. *Malignant peripheral neuroectodermal tumors* (MPNETs, also called *peripheral neuroepitheliomas*, *peripheral neuroblastomas,* or *extraskeletal Ewing's sarcomas*) form a group distinct from other malignant, small round-cell tumors such as neuroblastoma, Ewing's sarcoma, rhabdomyosarcoma, and lymphoma. They arise essentially in soft tissue and bone; association with a peripheral nerve trunk is quite rare. They are more frequent in children. The histologic criteria for the diagnosis of MPNET include pseudorosette formation seen

under light-microscopic examination, positive immunohistochemical demonstration of neuron-specific enolase, or demonstration of intracytoplasmic dense-core neurosecretory granules by electron microscopy.

Other Peripheral Nerve Tumors

True Neuromas. True neuromas, in distinction to post-traumatic neuromas, result from the proliferation of nerve fibers without significant change in the endoneurial or perineurial elements. *Solitary circumscribed neuromas* are distinctive, benign, cutaneous tumors that are not associated with neurofibromatosis. These lesions almost always appear on the face or close to a mucocutaneous junction in middle-aged adults. They are composed of innumerable small axons arranged in interlacing fascicles, with a capsule composed of perineurial cells. The histologic pattern resembles a post-traumatic neuroma but there is little collagen formation. A very rare condition includes *multiple mucosal neuromas* (conjunctiva, lips, tongue, nasal, and laryngeal mucosa) eventually associated with cutaneous ones. The *type II multiple endocrine neoplasia syndrome* (autosomal dominant inheritance) includes benign and malignant endocrine neoplasms with or without true neuromas.

Intraneural Ganglionic Cyst. *Intraneural* (or *paraneural*) *ganglionic cysts* can cause compression of nerves in close contact with joints, such as the common peroneal nerve, the median nerve in the carpal tunnel, or the ulnar nerve at the elbow.

Fibrolipomatous Hamartoma of Nerve. *Fibrolipomatous hamartoma of nerve* is a rare, benign condition not associated with NF. It usually involves the upper extremities and has a striking predilection for the median nerve. The majority of patients are young adults. Macroscopically, there is a sausage-shaped or fusiform enlargement of nerve. The epineurium is expanded by fibrofatty tissue that surrounds and separates the nerve bundles; within this fibrofatty tissue, a fibroblastic proliferation with perineurial fibrosis invades the individual nerve bundles.

Neuromuscular Choristoma. *Neuromuscular choristoma* (or *benign Triton tumor*) is an un-

common peripheral nerve tumor of early childhood. Bound firmly to the involved nerve, the tumor is made up of bundles of striated muscle fibers intermingled with myelinated nerve fibers. These tumors are benign, regressing with time.

Tumors of the Meninges

Tumors of Meningothelial Cells: Meningiomas

Meningiomas are tumors originating from arachnoidal cells and attached to the inner face of the dura mater. They account for 13% to 25% of primary intracranial tumors and approximately 25% of intraspinal tumors. Most meningiomas occur in adults between the ages of 20 and 60, with a maximal incidence around 45. They are predominantly found in females (male-to-female ratio between 2 : 3 and 1 : 2), except for atypical and anaplastic meningiomas whose incidence is higher in males. Many small meningiomas are incidental findings due to the wide clinical use of computerized tomography and magnetic resonance imaging.

Meningiomas arise wherever arachnoidal cells are present, but have the following predilections: Convexity meningiomas (parasagittal, falx, lateral convexity) are the most frequent (approximately 50%); basal meningiomas (olfactory groove, intra-orbital, lesser wing of the sphenoid, pterion, para- or suprasellar) are next in frequency (approximately 40%); posterior fossa meningiomas (tentorium, foramen magnum) and intraventricular meningiomas are considerably less common (approximately 10%); spinal meningiomas are most frequently situated in the thoracic segments and are usually located in the lateral compartment of the subdural space.

Macroscopically, meningiomas are spherical or lobulated, well-circumscribed, and firmly attached to the inner surface of the dura (Figs. 2-14A and B). They displace the underlying neural parenchyma without invading it. Meningiomas *en plaque* spread along the deeper surface of the dura and tend to invade the overlying bone; this often results in hyperostosis. Meningiomas are usually single, but multiple tumors may occur either as sporadic cases or in patients with NF2. Some cases of diffuse meningiomatosis that may involve the entire leptomeningeal space have been described.
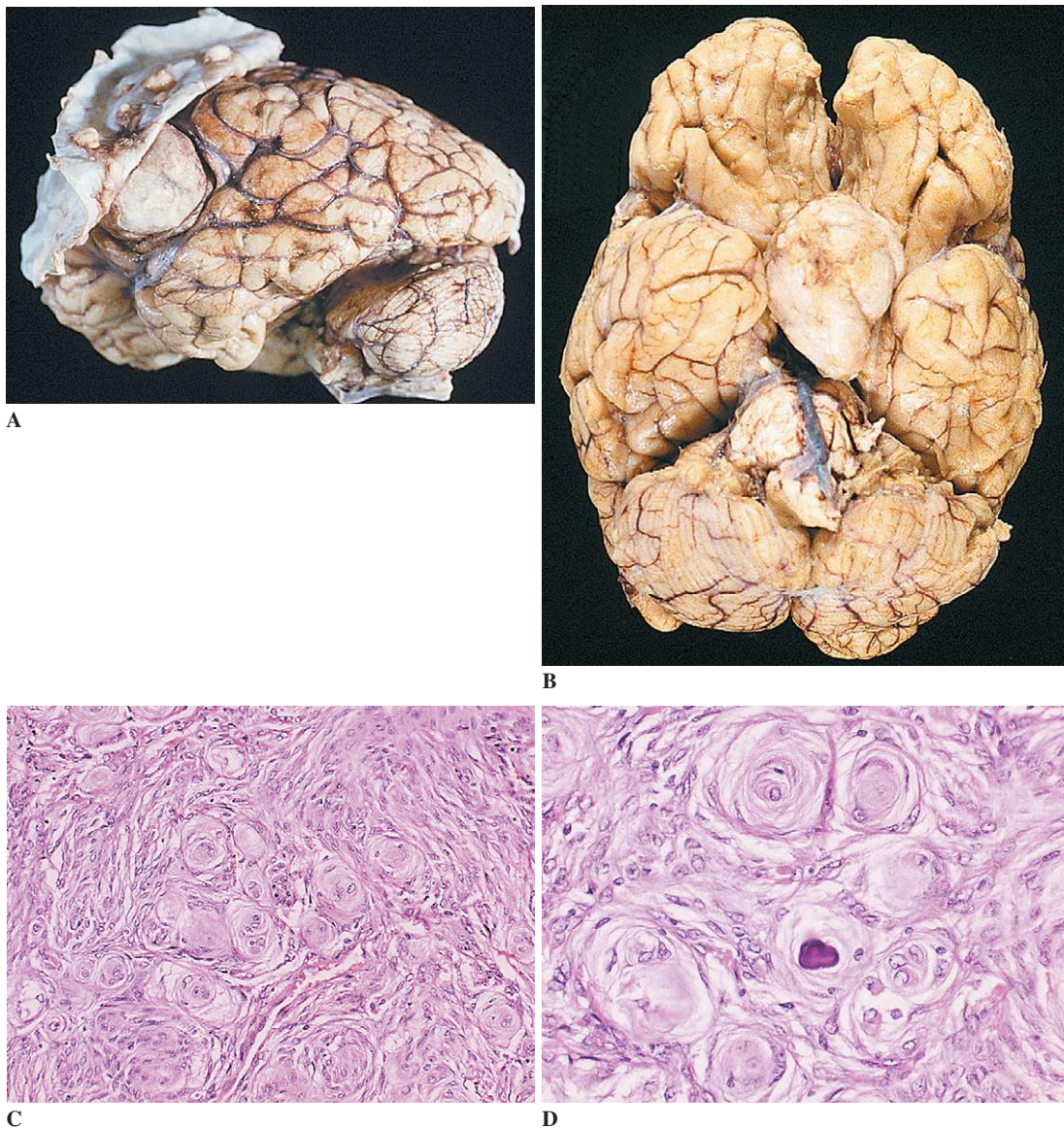
Figure 2-14. Meningioma. **A**, Convexity meningioma (gross). **B**, Meningioma of skull base (gross). Microscopic features: **C**, Cellular whorls (H and E); **D**, Whorls and psammoma body (H and E).

The formation of WHO grade I meningiomas is associated with mutations of the *NF2* gene and loss of the other *NF2* allele on chromosome 22. These alterations are more common in fibrous and transitional than in meningothelial variants (see following discussion). As meningiomas increase in grade, additional genetic events often occur, including loss of the short arm of chromosome 1 and the long arms of chromosomes 10 and 14.

The light-microscopic appearance of meningiomas can be variable and sometimes quite challenging. Nevertheless, the unitary character of meningiomas should be emphasized: the electron-microscopic appearance is always similar and demonstrates arachnoidal cells with tonofilaments, desmosomes, and a variable number of collagen fibers, and by immunohistochemistry the tumor cells of virtually all meningiomas are reactive for

vimentin, EMA, and (sometimes) S100 protein or cytokeratin. The current WHO classification recognizes a number of well-defined subtypes or variants of meningioma that have been correlated with WHO grade. By far the most frequent meningiomas are benign WHO grade I tumors of the first three subtypes described in the following section.

WHO Grade I Meningioma Subtypes. *Meningothelial meningioma* is composed of polygonal, epithelial-like cells with ill-defined cell borders, a pale cytoplasm, and a relatively voluminous spherical nucleus containing a conspicuous nucleolus and occasionally showing a pseudoinclusion in the shape of a clear, well-defined intranuclear vacuole. The distribution of the cells is fairly uniform, being diffuse and consisting of elongated sheets or in islands separated by scant vascular connective-tissue trabeculae. In some cases the tumor cell borders may be difficult to visualize, imparting a "syncytial" pattern to the tumor. A characteristic and diagnostic pattern, which is almost always present to a greater or lesser extent, is the formation of cellular *whorls* (Fig. 2-14C) in which the tumor cells are closely wrapped around one another. When whorls show a hyalinized and calcified center they are termed *psammoma bodies* (Fig. 2-14D). However, the frequency of psammoma bodies in a given tumor is variable, and some meningothelial meningiomas may have very few.

Fibrous (fibroblastic) meningioma is composed of elongated fusiform cells arranged in wavy, interlacing fascicles. A fairly well-developed network of collagen and reticulin fibers is found between the individual cells. Meningothelial cells, whorls, and occasionally psammoma bodies are also present.

Transitional (mixed) meningioma is a frequent subtype with features intermediate between those of meningothelial and fibroblastic meningioma. Whorls and sometimes psammoma bodies are numerous.

Psammomatous meningioma has exceptionally numerous psammoma bodies that may become confluent.

Angiomatous meningioma (formerly called angioblastic meningioma) shows very rich vascularization. The vessels, most often of small diameter, frequently have hyalinized walls.

Microcystic meningioma has tumor cells that show elongated processes circumscribing multiple small cysts with a mucinous content. Pleomorphic cells and nuclei are often numerous. Small vessels with thickened, hyalinized walls are frequently encountered.

Secretory meningioma is a variant characterized by the presence of eosinophilic PAS-positive globular intracellular inclusions which are immunoreactive for carcinoembryonic antigen.

Some meningiomas may contain a conspicuous, plasma cell–lymphocytic component and are known as *lymphoplasmacyte-rich meningiomas*. These must be distinguished from other intracranial masses that are rich in lymphocytes and/or plasma cells and resemble meningiomas both in imaging studies and at surgery. These cases may include extramedullary hematopoiesis-simulating parasagittal meningioma, intracranial solitary dural extraskeletal plasmacytoma, primary T cell–rich B-cell lymphoma, and a variety of pseudotumoral inflammatory or clonal meningeal masses such as plasma cell granuloma, sinus histiocytosis with massive lymphadenopathy, Castleman's giant lymph-node hyperplasia, atypical monoclonal plasma cell hyperplasia, or lymphomatoid granulomatosis.

Several secondary metaplastic changes may be observed in *metaplastic meningiomas*: (1) xanthomatous change with the presence of lipid-filled cells, (2) myxomatous change characterized by an abundant homogeneous stroma separating the individual cells, (3) cartilage or bone within the tumor, and (4) melanin pigment within the connective tissue trabeculae (pigmented meningiomas).

All of the preceding WHO grade I subtypes of meningioma display a low rate of proliferation (Ki-67/MIB-1 labeling index often less than 4% to 5%). The WHO grades II and III varieties described in the following sections have a more aggressive behavior and exhibit higher rates of recurrence.

WHO Grade II Meningioma Subtypes. *Chordoid meningioma* is a rare variant in which some parts of the tumor are similar to chordoma, with trabeculae of vacuolated cells in a myxoid matrix. Inflammatory cell infiltrates may be conspicuous.

Clear cell meningioma is a rare variant that shows a patternless proliferation of polygonal cells with clear cytoplasm. Because of this histologic feature, clear cell meningioma has also been called "pseudo-oligodendrogliomatous" meningioma. The

cells contain PAS-positive cytoplasmic glycogen granules.

The diagnosis of *atypical meningioma* is based on either increased mitotic activity (4 or more mitoses per 10 high-power fields) or the presence of three or more of the following histologic features: increased cellularity, small cells with a high nucleus/cytoplasm ratio, prominent nucleoli, patternless sheets of tumor cells, small foci of necrosis. The Ki-67/MIB-1 index is moderately high (usually less than 10%). Atypical meningiomas have a higher recurrence rate than grade I meningiomas.

WHO Grade III Meningioma Subtypes. *Papillary meningioma* is a rare subtype characterized by the presence of perivascular pseudopapillae in some parts of the meningioma. These tumors are often invasive, recurrent, and even metastatic.

Rhabdoid meningioma is an uncommon and clinically aggressive tumor that contains sheets of rounded cells with an eccentric nucleus (often with a conspicuous nucleolus) and a prominent intracytoplasmic eosinophilic "inclusion" consisting of vimentin filaments. These tumor cells resemble those found in rhabdoid tumors in other sites.

Anaplastic (*malignant*) *meningioma* is by definition a meningioma having histologic features that are clearly malignant (i.e., that resemble those of a sarcoma or carcinoma) or having at least 20 mitoses per 10 high-power fields. The histologic distinction between atypical and anaplastic meningioma is usually fairly clear-cut, but there are borderline cases that remain difficult to classify. Ki-67/MIB-1 labeling index is frequently greater than 15%. The median survival time for anaplastic meningiomas is about 2 years. Invasion of the brain parenchyma, though frequent in anaplastic meningiomas, is not by itself sufficient for the diagnosis of anaplastic meningioma, since brain invasion may also be observed in atypical or even WHO grade I meningiomas.

Meningioma Recurrence.   The clinical evolution of meningiomas is usually very slow. The most important risk is recurrence. Prediction of recurrence is difficult; numerous mitoses, a high index of cell proliferation (i.e., high Ki-67/MIB-1 labeling index), higher tumor grade, and the absence of progesterone receptors are significant factors, but

the extent of surgical removal is of paramount importance. On the whole, the rates of recurrence are about 10% to 20% for grade I meningiomas, 30% to 40% for grade II, and 50% to 80% for grade III. Anaplastic meningiomas may metastasize (principally to lung, bone, and liver); the exceptional metastases of WHO grade I meningiomas occur following surgery. Radiation-induced meningiomas are often atypical or anaplastic.

Mesenchymal Nonmeningothelial Tumors

Hemangiopericytoma (WHO Grade II or III). *Meningeal hemangiopericytomas* are much less frequent than meningiomas (approximately 2 per 100). Their histogenesis is uncertain, although light-microscopic and ultrastructural features suggest pericytic differentiation. Macroscopically, they are solid, rather firm tumors attached to the dura mater and well-delineated from the adjacent central nervous system parenchyma (i.e., resemble a meningioma). Microscopically, they consist of a highly cellular, homogeneous proliferation of elongated cells individually embedded in a dense network of reticulin fibers. The distinction between WHO grade II and III tumors is based mainly on the degree of cellular anaplasia and mitotic activity. Grade III tumors tend to have more numerous mitoses (5 or more per 10 high-power fields) along with other anaplastic features such as nuclear pleomorphism and foci of hemorrhage or necrosis. Brain invasion may also occur. The tumor cells are consistently immunoreactive for vimentin and somewhat more variably for CD34, and are negative for EMA and S100 protein. The Ki-67/MIB-1 labeling index is about 5% to 10%. They are considered to be tumors of variable malignant potential, similar to their soft-tissue counterparts, with the same tendency to recur and produce metastases.

Tumors of Adipose Tissue

Lipomas are rare, benign growths. In the cranial cavity, they favor midline sites, specifically the corpus callosum (often associated with partial or complete agenesis of that structure), quadrigeminal plate, and cerebellopontine angle. Most intraspinal lipomas are discovered in childhood and are congenital lumbosacral lipomas associated with spinal

dysraphism (spina bifida occulta) or "tethered cord" (abnormally low-lying conus tethered by the lipomatous mass). In adults, intraspinal intradural lipomas are isolated tumors composed of normal-appearing adipose tissue and most frequently located at the thoracic level; they represent less than 1% of all spinal cord tumors. Rare complex lipomas containing bundles of nerve fibers associated with muscle fibers have been described. They have been referred to as *Triton tumors* or neuromuscular hamartomas, suggesting a possible relationship with peripheral nerve fibrolipomatous hamartomas.

Angiolipomas are rare, benign, mesenchymal tumors composed of mature adipose tissue and blood vessels that are either normal or may mimic a capillary angioma, cavernous angioma, or arteriovenous malformation. It may be difficult to distinguish angiolipomas from hemangiomas, which are often accompanied by adipose tissue. They are usually found in the epidural space at the thoracic level. Invasion of surrounding tissues and especially of vertebral bodies has been noticed in rare cases; in these cases, total removal is not always possible. The exceptional *angiomyolipomas* contain a more or less conspicuous smooth muscle component intermingled with blood-vascular channels and mature adipose tissue. *Spinal angiolipomas* and *angiomyolipomas* are to be distinguished from spinal epidural lipomatosis associated with Cushing's syndrome or induced by long-term corticosteroid therapy.

Fibrous Tumors

Solitary fibrous tumor is a rare, benign tumor that involves the cranial or spinal meninges or lateral ventricles of adults and mimics a meningioma. Elongated fibroblasts, disposed in fascicles between conspicuous bands of collagen fibers, display strong immunoreactivity for vimentin and CD34 but not EMA. Some examples may have a histologic pattern that is difficult to distinguish from hemangiopericytoma, suggesting a possible histogenetic relationship between these two entities.

Intracranial *fibrosarcomas* are very rare neoplasms that account for less than 1% of all intracranial tumors. They are derived from fibroblasts, which may be situated in the dura, leptomeninges, perivascular spaces, tela choroidea, or stroma of the choroid plexus. Fibrosarcomas are most frequently attached to the meninges, but may sometimes be entirely parenchymatous. Macroscopically, they are well circumscribed but nonencapsulated, firm in consistency, and have gray, fairly homogeneous cut surfaces. In some cases, the tumor is not a well-defined mass but consists of a diffuse infiltration of the meninges (meningeal sarcomatosis). The microscopic appearance is identical with that of fibrosarcomas arising elsewhere in the body and presents the same range of cellular differentiation. The better-differentiated examples are characterized by interlacing bundles of elongated fibroblastic cells of which only the nuclei are clearly visualized; these bundles are separated by a rich network of reticulin fibers. Nuclear abnormalities are usually rare, but mitoses are common. Foci of necrosis are frequent; they may invade the neural parenchyma.

Fibrohistiocytic tumors are rare tumors composed of a mixture of spindle-shaped, fibroblast-like and round, histiocyte-like cells that may be benign (*benign fibrous histiocytoma*) or malignant with numerous mitoses and foci of necrosis (*malignant fibrous histiocytoma*). Some authors believe that exhaustive study of such a tumor by immunohistochemistry or electron microscopy will usually allow more definitive classification as a neural or myogenic sarcoma.

Muscle Tumors

Leiomyosarcoma is a very exceptional tumor, corresponding microscopically to its well-known soft-tissue counterpart. It is desmin- and smooth muscle actin–positive by immunohistochemistry. Rare examples have been described in patients with AIDS; the tumor cells in these cases often express the Epstein-Barr virus genome.

Rhabdomyosarcoma may arise in the CNS. It consists primarily of small, undifferentiated cells and resembles a primary neuroepithelial neoplasm. Immunohistochemistry results (tumor cells reactive for myoglobin, desmin, and muscle-specific actin) or electron microscopy (demonstration of myofilaments arranged in sarcomeres) may be indispensable for diagnosis.

Osteocartilaginous Tumors

Chondroma, *osteoma*, and *osteochondroma* are benign osteocartilaginous tumors, commonly arising from the bones of the skull base or spine. Their histology is similar to that of their more frequent systemic counterparts.

Chondrosarcomas are preferentially located in the petrosal, occipital, or sphenoid bones. They are histologically classified in four subtypes of increasing malignancy: grade I, grade II, mesenchymal, and myxoid. Immunohistochemistry may be necessary to distinguish chondrosarcomas from chordomas (and particularly from so-called chondroid chordomas). S100 protein is expressed in both tumors, but chordomas are vimentin-negative and EMA- and cytokeratin-positive, whereas chondrosarcomas are vimentin-positive and EMA- and cytokeratin-negative.

Osteosarcomas of the skull or spinal bones may be encountered in Paget's disease.

Blood Vessel Tumors

Hemangiomas of either the capillary or cavernous type (*cavernomas*) are not true tumors but vascular malformations.

Epithelioid hemangioendothelioma is an endothelial cell tumor rarely encountered at the level of the skull base and exceptionally in the brain parenchyma. Histologic examination reveals typical epithelioid cell cords or nests in a myxoid stroma. Tumor cells express endothelial-specific antigens such as factor VIII or CD31.

Angiosarcoma may occur as a primary CNS malignancy, often requiring immunohistochemical and ultrastructural studies for a definitive diagnosis. Cerebral involvement by Kaposi's sarcoma is metastatic, probably from primary foci in the lungs.

Primary Melanocytic Lesions

A wide variety of rare disorders, ranging from a simple increase in normal leptomeningeal pigmentation to highly malignant conditions (e.g., *diffuse melanosis* and *primary malignant melanomas*), may be encountered. However, whether they are benign (*melanocytomas*) or malignant, primary melanomas of the nervous system are extremely rare. Before this diagnosis can be considered, it is essential to exclude the possibility of small, occult, primary cutaneous, or ocular melanoma. In addition, other tumors, in particular schwannomas and meningiomas, may sometimes contain melanin pigment, and electron-microscopic study may be needed in order to distinguish them from true melanomas, whose cells have no basal lamina or desmosomes. Most often, the cells of melanocytic lesions express S100 protein and are immunopositive for HMB-45 directed against melanosomes.

Tumors of Uncertain Histogenesis

Hemangioblastoma (WHO Grade I)

Hemangioblastomas account for approximately 1% to 2.5% of all intracranial tumors. They are encountered at any age but are seen most frequently in young and middle-aged persons. They are most often situated in the cerebellum. Indeed, they represent approximately 7% of the primary tumors originating in the posterior fossa. In addition, they may be found within the parenchyma of the spinal cord, the medulla oblongata, and, exceptionally, in the supratentorial compartment.

Although hemangioblastomas are often demonstrably or apparently solitary, in approximately 25% of cases they are multiple and, in that setting, permit the diagnosis of von Hippel-Lindau disease. This inherited autosomal dominant condition is caused by mutations of the *VHL* tumor-suppressor gene located on chromosome 3p. The diagnosis of von Hippel-Lindau disease is based on the presence of a CNS or retinal hemangioblastoma that is associated with a known family history or with a pheochromocytoma, clear cell renal carcinoma, pancreatic tumor, or endolymphatic sac tumor of the inner ear.

Macroscopically, hemangioblastomas are well-circumscribed and very often cystic; they sometimes consist solely of a small, mural nodule attached to the wall of a considerably larger cyst (Fig. 2-15A). The fairly characteristic yellow color is due to its abundant lipid content. In addition, the tumor is usually vascularized and drained by
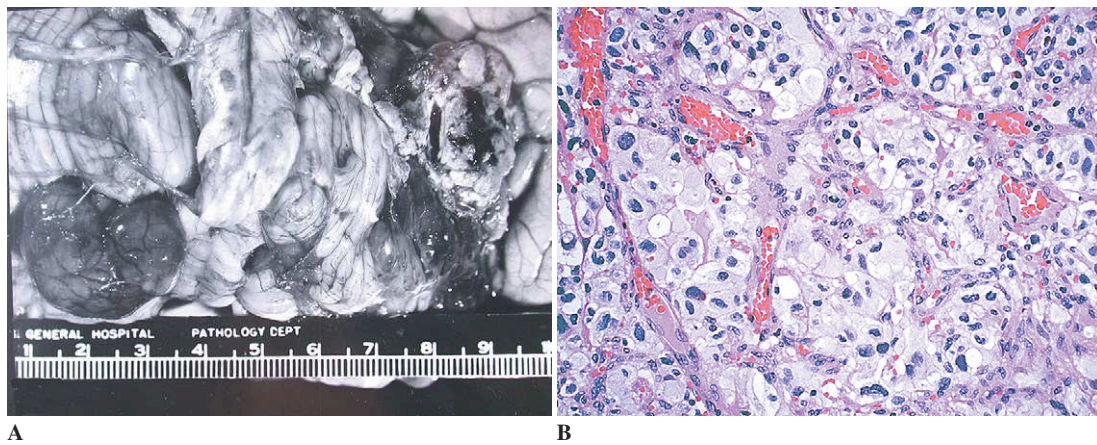
Figure 2-15. Hemangioblastoma. **A**, Multiple cerebellar tumors (gross). **B**, Microscopic appearance (H and E).

well-developed vascular pedicles which, in some cases, may erroneously suggest an associated arteriovenous malformation. This rich vascularization accounts for the frequency of bleeding within the tumor.

The histologic picture of hemangioblastoma is highly characteristic, consisting of numerous capillary blood vessels of different sizes separated by trabeculae or sheets of clear cells with round or elongated nuclei (Fig. 2-15B). These stromal tumor cells often have a spongy appearance due to an abundance of intracytoplasmic vacuoles that have been emptied of their lipid contents as a result of the embedding procedure. Mitoses are rare. A fine network of reticulin fibers surrounds the capillary blood vessels and individual tumor cells. The stromal cells have long been regarded as being derived from capillary endothelial cells, hence the classic view that these are vascular tumors. In reality, their origin remains debatable. The endothelial cells express factor VIII, CD31, CD34, and receptor to vascular endothelial growth factor (VEGF). The stromal cells do not express endothelial cell markers, GFAP, EMA, or cytokeratin. They do express vimentin, erythropoietin, and VEGF, but otherwise lack specific markers. In some cases, these immunohistochemical characteristics may be helpful in distinguishing between hemangioblastoma and metastatic clear cell renal carcinoma.

Hemangioblastomas are histologically benign tumors (WHO grade I), but postoperative recurrence and especially the appearance of hemangioblastomas at other sites may darken the prognosis.

Lymphomas and Hematopoietic Neoplasms

Lymphomas

Primary CNS Lymphomas

Primary lymphomas historically represented approximately 2% of all tumors of the CNS, but their incidence has recently increased to 6% to 7%. They occur preferentially in immunosuppressed or immunodeficient patients, especially as a complication of AIDS; approximately 10% of AIDS patients develop primary CNS lymphomas. They may occur as either single or multiple masses and infiltrate the cerebral parenchyma in a diffuse manner. Their most frequent site is the deep periventricular region of the brain (Fig. 2-16A).

Histologically, they consist of a predominantly perivascular infiltration by neoplastic lymphoid cells, most often B cells (e.g., large B lymphocytes, immunoblasts, or lymphoblastic B cells of IgM/kappa subtype) associated with perivascular reticulin hoops (Figs. 2-16B and C). Necrotic areas are frequent and reactive T-cell lymphocytic infiltrates, astrocytic gliosis, and a microglial response may also be observed. Ki-67/MIB-1 proliferation
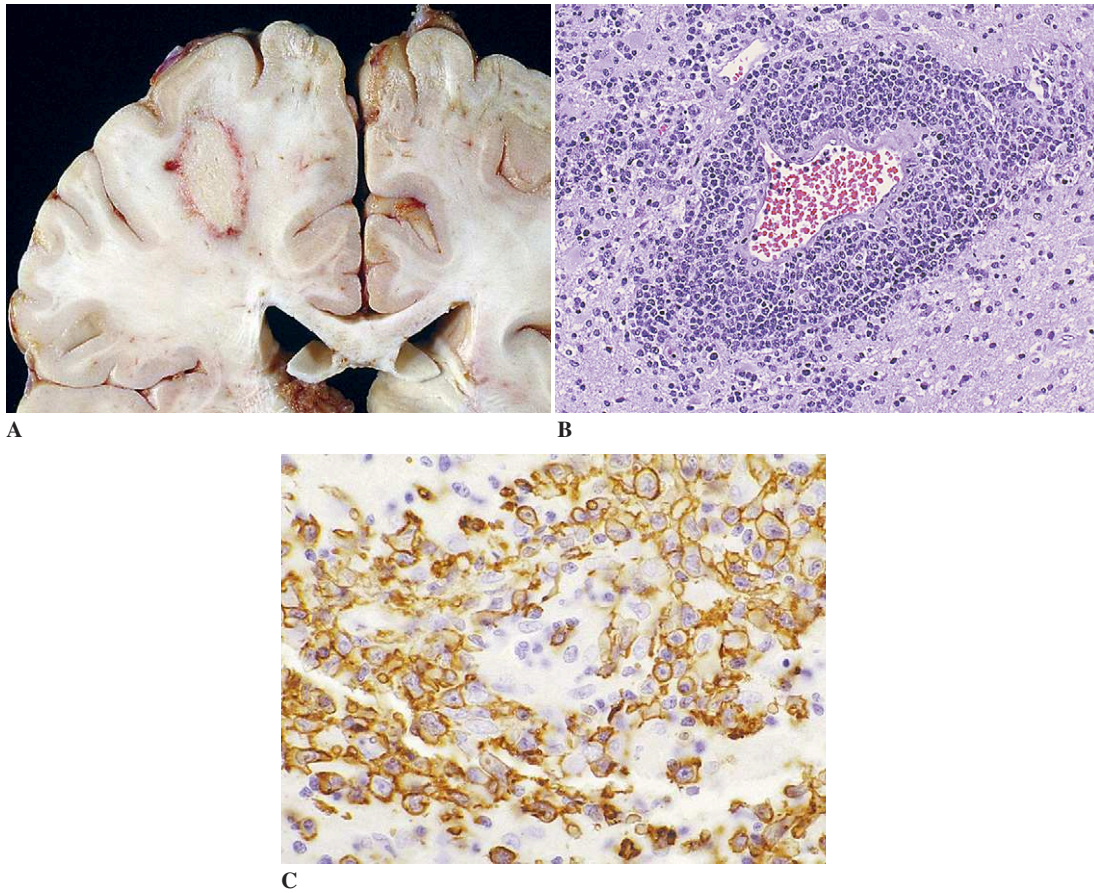
Figure 2-16. Primary CNS lymphoma. **A**, Tumor in periventricular white matter (gross). Microscopic features: **B**, Perivascular localization of tumor cells (H and E); **C**, Immunoreactivity of neoplastic lymphoid cells for B-cell marker (CD20).

indices may vary from 20% to more than 90%. In almost all cases of cerebral lymphoma in immuno-compromised patients, the Epstein-Barr virus genome is found in tumor cells. The CNS is involved in about one third of cases of intravascular (angiotropic) lymphoma. T-cell lymphomas constitute approximately 2% of all primary CNS lymphomas.

Primary lymphomas are usually tumors of high malignancy, but current therapeutic protocols suggest the possibility, in some cases, of postoperative survival of more than 5 years.

Hodgkin Disease

The diagnosis of the exceptional primary intracranial occurrence of Hodgkin disease rests upon the identification of Reed-Sternberg cells (immuno-reactive to CD30 and CD15) in an infiltrate made up of lymphocytes, plasma cells, histiocytes, and eosinophils.

Histiocytic Tumors

Langerhans Cell Histiocytosis

Langerhans cell histiocytosis, which characteristically occurs most often in children, may present either as a solitary osteolytic lesion of the skull (eosinophilic granuloma) or as a multifocal lesion involving the bone and hypothalamic region (Hand-Schüller-Christian disease). Histologically, the granulomatous infiltrates include variable proportions of eosinophils, macrophages, lymphocytes, plasma cells, Langerhans cell histiocytes,
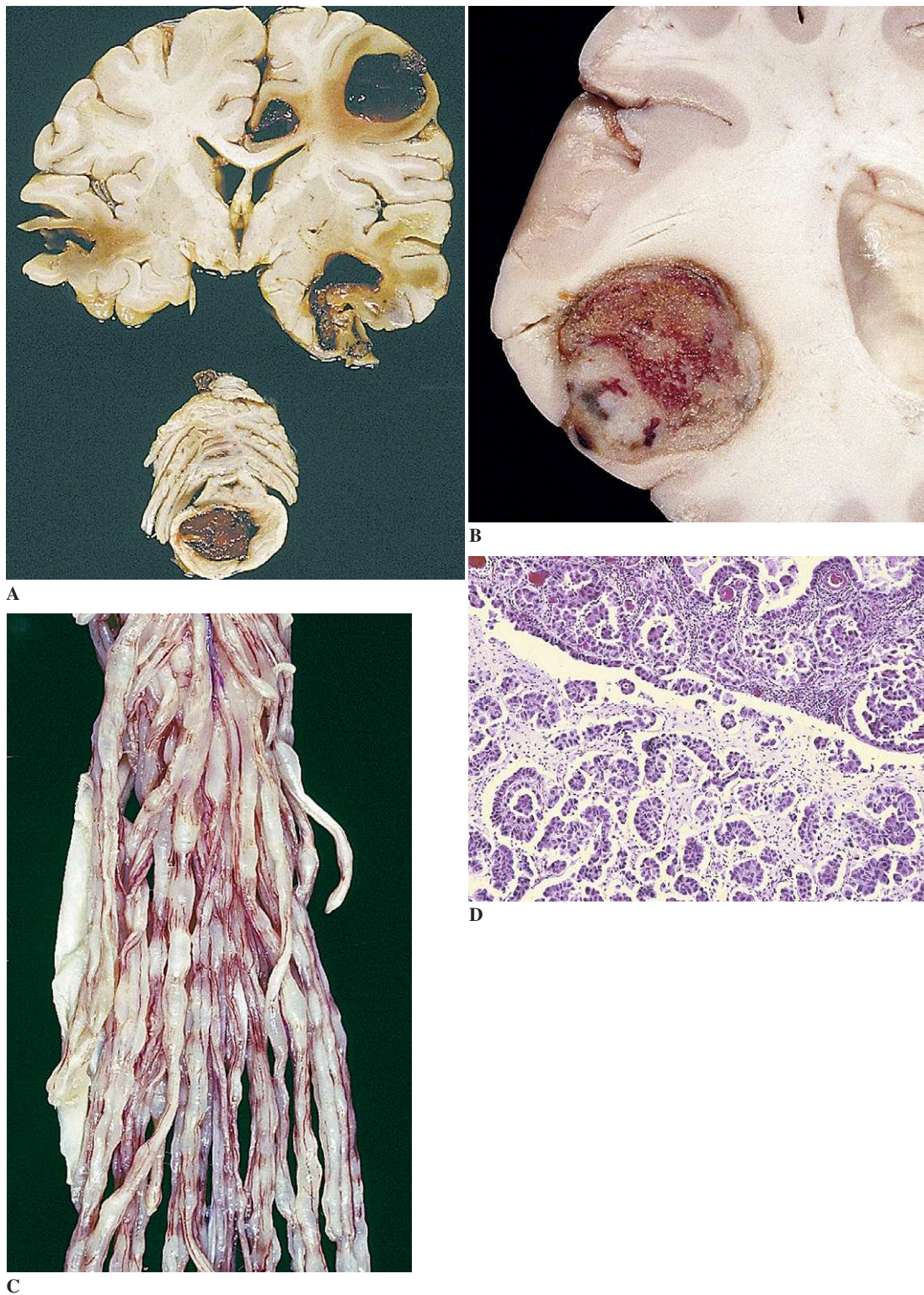
Figure 2-17. Metastatic tumors. **A**, Multiple hemorrhagic metastases from melanoma (gross). **B**, Lung carcinoma metastatic to cerebrum (gross). **C**, Meningeal carcinomatosis involving cauda equina (gross). **D**, Metastatic adenocarcinoma (lung) involving parenchyma and leptomeninges (H and E).

and sometimes Touton giant cells. The precise diagnosis of this condition requires either immunoreactivity for CD1a and/or electron-microscopic demonstration of Birbeck granules in the Langerhans cell histiocytes.

Non–Langerhans Cell Histiocytoses

This inhomogeneous group of diseases arising from mononuclear phagocytes (CD68-positive, foamy histiocytes/macrophages) includes such different entities as intracranial Rosai-Dorfman syndrome, Erdheim-Chester disease, hemophagocytic lymphohistiocytosis, juvenile xanthogranuloma, and xanthoma disseminatum, as well as (usually asymptomatic) cases of choroid plexus xanthoma and xanthogranuloma.

Secondary Neoplasms

Metastatic neoplasms from primary visceral cancer are among the most frequent intracranial and intraspinal tumors (about 20%). Their incidence increases with age. They may occur in virtually any region of the cranial cavity or spinal canal, including the central neuraxis (cerebral hemispheres, cerebellum, brainstem, or, less often, spinal cord),

spinal or cranial nerve roots; choroid plexus; or meningeal coverings (meningeal carcinomatosis, spinal epidural metastases, or dural metastases at the skull base or over the convexities; Figs. 2-17A–D, p. 55). Most metastatic CNS tumors are due to hematogenous spread of tumor cells arising from the primary neoplasm. The most common primary sources are lung carcinoma in males and breast carcinoma in females, followed in frequency by malignant melanoma, renal cell carcinoma, carcinoma of the alimentary tract, and choriocarcinoma.

Macroscopically, CNS metastases may be solitary but are most often multiple. Their size ranges from less than a millimeter to over several centimeters. They generally are well-circumscribed nodules, either firm or soft, the latter often resulting from hemorrhage within the tumor, focal necrosis, or cystic degeneration.

In most cases, metastases essentially recapitulate the histologic appearance of their primary source. However, if extensive tumor necrosis and/or highly atypical features are present, specific histologic identification of a primary site of origin may be very difficult or, occasionally, impossible, even if immunohistochemistry or electron microscopy are used.

Chapter 3
Central Nervous System Trauma

Jennian F. Geddes and David I. Graham

Closed Head Injury

The various processes that result from head injury are now collectively referred to as *traumatic brain injury* (TBI), and current evidence suggests that what defines mild, moderate, or severe TBI is not so much the nature of the lesions as their amount and distribution.

Classification and Mechanisms of Brain Damage

The neuropathological classification of TBI is based on information derived from postmortem studies in patients who have died with varying degrees of disability after TBI. Consequently, it must take into account the full spectrum of clinical presentation and outcome in fatal cases, from the patient who remains in a coma from the moment of injury until death, to the patient who is apparently normal after the initial injury but who subsequently relapses and dies as a result of a complication.

TBI may be either *primary* (occurring at the moment of injury) or *secondary* (occurring in an already mechanically injured brain). Secondary damage is often due to complications that are not unique to trauma, but similar to those seen in association with other intracranial events (Table 3-1).

Based on clinical and neuroradiological data, TBI can also be categorized as either *focal* or *diffuse*

(*multifocal*; Table 3-2). "Focal damage" implies lesions that are detectable by scans and often amenable to treatment, while "diffuse damage" refers to widespread pathology (assumed present because the patient is unconscious, but not always demonstrable neuroradiologically). This classification provides a basis for employing neuroimaging as a consistent means of predicting the clinical course after head injury.

TBIs result from two principal mechanisms, *impact* or *acceleration-deceleration* (Table 3-3). Lesions caused by impact tend to result from either an object striking the head or contact between brain and skull, while acceleration-deceleration brain injuries result from unrestricted movement of the head, leading to shear and compressive strains.

In any given patient, the outcome is a product of many factors. While focal pathologies associated with impact are likely to be sustained from a fall or an assault, and diffuse pathologies are more commonly associated with a vehicular accident, there are many examples of mixed causation and of brain damage that remain perplexing both clinically and neuropathologically.

Focal Injury

Scalp, Skull, and Dura

Lesions of the scalp, skull, and dura often provide a clue to the site and nature of underlying injury

Table 3-1. Classification of Head Injury by Clinicopathological Correlation

Primary (at Moment of Injury)	Secondary (Delayed or Complication)
• Injury to scalp	• Hypoxia; ischemia
• Fracture of the skull	• Brain swelling
• Surface contusions/ lacerations	• Infection (meningitis, abscess, subdural empyema, cranial osteomyelitis)
• Intracranial hematomas	• Raised intracranial pressure and associated vascular changes
• Diffuse traumatic axonal injury	
• Diffuse vascular injury	

Table 3-3. Classification of Head Injury by Mechanism of Production

Impact	Acceleration-Deceleration
• Lesions of scalp	• Tearing of bridging veins with formation of subdural hematomas
• Fracture of skull with or without an associated extradural hematoma	• Diffuse traumatic axonal injury including "tissue-tear" hematomas
• Surface contusions/ lacerations and associated intracerebral hematomas	• Diffuse vascular injury

and alert the clinician and pathologist to seek associated lesions and potential complications.

Bruising at the back of the skull is often associated with severe contusion of the frontal lobes; bruising around the mastoid process may be associated with traumatic subarachnoid hemorrhage; and a bruise on the temple may be associated with a skull fracture and subsequent development of an extradural hematoma. On the other hand, a scalp laceration is often of little significance, although severe bleeding in a small child may occasionally produce a risk of hypovolemia.

The occurrence of skull fracture is directly proportional to the severity of the head injury. Skull fracture may be limited to the vertex or the base, or may affect both. The great majority of skull fractures are linear, affecting the vault of the skull in some 60% of cases with extension into the base in 20%. Fractures of the skull base are important because the impact necessary to cause the fracture

is significantly greater than for other fractures, and there may be severe brain damage in addition to the bony injuries. Furthermore, structures such as cranial nerves and blood vessels are particularly vulnerable in fractures of the floor of the skull, and complications such as ascending infection or pneumocephalus may develop in survivors.

There are different types of fracture (Table 3-4). It must be stressed that a fracture of the skull is not necessarily associated with any underlying brain damage and, in contrast, the absence of a skull fracture does not imply an intact brain; in 20% of fatal head injuries there is no skull fracture. This is particularly true in pediatric practice, where the flexibility of the skull may prevent a fracture from forming but allow a great deal of underlying traumatic brain damage.

A characteristic (though unusual) lesion resulting from skull fracture in infancy is the "growing" fracture, the etiology of which is probably a tear in

Table 3-2. Classification of Head Injury by Neuroradiological and Neuropathological Features

Focal	Diffuse (Multifocal)
• Injuries to scalp	• Hypoxia; ischemia
• Fracture of skull	• Traumatic axonal injury
• Surface contusions/lacerations	• Diffuse vascular injury
• Intracranial hematomas	• Brain swelling
• Mass effect and associated vascular changes	• Meningitis
• Abscess; subdural empyema; cranial osteomyelitis	

Table 3-4. Types of Fracture of the Skull

- "Linear" or "fissure"
- "Depressed": fragments of the inner table are displaced inwards by at least the thickness of the diploë
- "Compound": depressed fracture is associated with laceration of scalp; "penetrating" if there is also a tear in the dura
- "Hinge": fracture extends across the base of the skull
- "Coup": fracture is located at site of injury
- "Contrecoup": fracture is located a distance from the point of injury
- "Growing": fracture occurs in infancy; soft tissue and meninges become interposed between edges of fracture and prevent healing

Figure 3-1. An arrested growing fracture that presented in a woman of 38. When asked about childhood injuries, she remembered that she had fallen out of her carriage as a very young child. **A**, Plain skull X-ray. **B**, The excised portion of bone.

the dura, produced at the time of the original injury, through which a small piece of arachnoid becomes extruded and interposed between the broken bone edges. Over ensuing months and years, pulsation of the CSF forces more arachnoid through the dural defect, adhesions form, and what is essentially an enlarging, CSF-filled leptomeningeal cyst continues to erode bone, preventing healing. The result is that the fracture widens as the child gets older (Figs. 3-1A and B).

Surface Contusions and Lacerations of the Brain

Surface contusions and lacerations of the brain are a hallmark of brain damage after head injury. They vary in amount, are usually asymmetrical, and have a highly characteristic appearance and distribution (Table 3-5). Contusions occur at the crests of gyri and invariably involve some bleeding into the sub-arachnoid space; many extend into white matter, comprising a mixture of hemorrhage and necrosis

with associated swelling. A frank hematoma may develop, with mass effect, and a large contusion may by itself be the immediate cause of death in patients with a lucid interval. If laceration of the pia-arachnoid has taken place, there may be bleeding

Table 3-5. Surface Contusions and Lacerations

- Pia-arachnoid intact with contusions but torn with lacerations
- Affects crests of gyri at frontal and temporal poles, inferomedial, and lateral surfaces of frontal lobes
- Cortex above and below the opercula of the sylvian fissures
- Lateral and inferior surfaces of the temporal lobes
- Inferior aspect of cerebellar hemispheres
- At vertex, are related to fractures; inferiorly, correspond to irregular bony contours of base of skull
- Coup (at point of impact)
- Contrecoup (opposite to point of impact)
- Herniation (at point of impaction between hernia and free edge of dura, falx, and/or incisura)

into the subdural space. A combination of extensive contusion and an associated subdural hematoma is referred to as a "burst lobe," and most commonly occurs in relation to the frontal and temporal poles.

The pathogenesis of contusions is complex and their distribution in a given situation depends on the circumstances of the injury, but, as with fractures and subdural bleeding, contusions may occur both at the point of impact after localized deformation of the skull, and in contrecoup sites (Fig. 3-2). Typically, contusions occur on the orbital and basal frontal gyri and at the tips of the temporal lobes, and are often accompanied by "blow-out" fractures of the roof of both orbits. In general, contrecoup contusions do not occur if the head is immobile when hit, and contusions at the site of impact are rare if the head is moving at the time of injury. Parietal or occipital contusions are unusual except where they lie directly under the site of a fracture.

Neuropathologically, the smallest contusions are merely collections of minute perivascular hemorrhages in the cortex, often only a few millimeters in diameter, without any edema (Fig. 3-3). Larger

contusions contain areas of necrosis as well as hemorrhage.

Most contusional damage does not require neurosurgical treatment and, if there is no other serious injury, is usually survivable. Indeed, healed contusions—the remnants of past head injuries, sometimes associated with subdural adhesions—are a relatively common incidental finding at autopsy in adult males (Fig. 3-4). In the weeks after an injury, hemorrhage and necrotic material are removed by macrophages, leaving the affected area of brain pigmented and shrunken. Microscopy reveals foci of atrophy and gliosis, with associated hemosiderin deposition. Old contusions can usually be distinguished from old ischemic damage because of their typical distribution on the ventral surface of the frontal and temporal lobes, and their characteristic wedge-shape appearance (with the base on the crest of the cortical gyri and apex in white matter), accompanied by evidence of previous hemorrhage.

Development of a contusion index has allowed the depth and extent of contusions in different parts of the brain to be expressed quantitatively. Such an
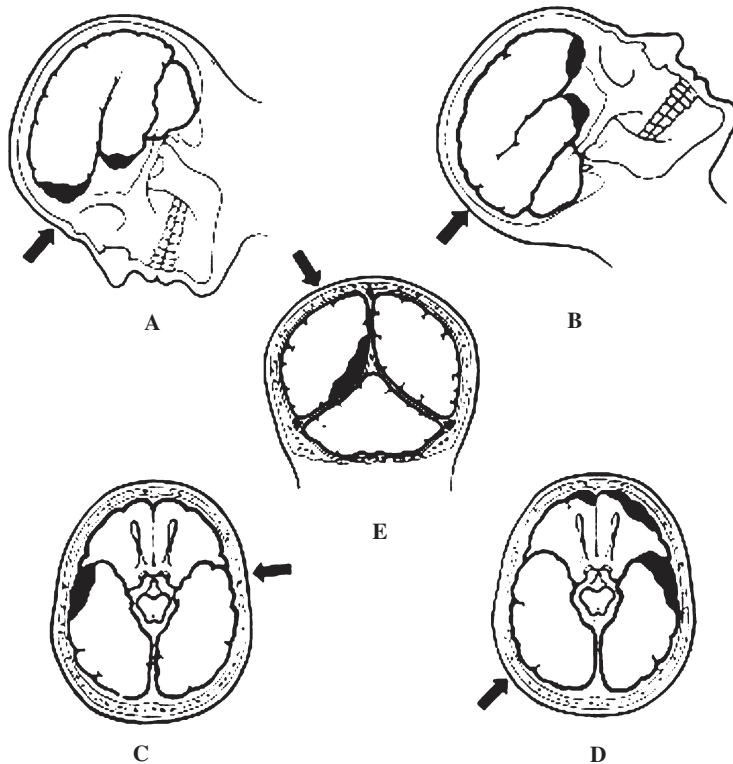
Figure 3-2. Mechanism of cerebral contusion. Arrows indicate point of application and direction of force; black area indicates location of contusion. (Reprinted from Courville CB. Pathology of the central nervous system, 2nd ed. Mountain View, CA, Pacific Press, 1937, p. 292.)
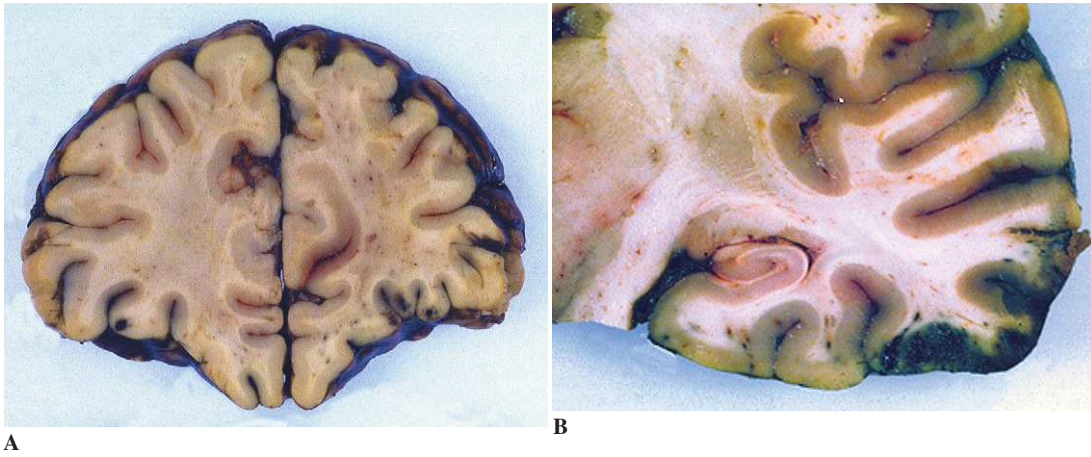
Figure 3-3. Small intracortical contusions in typical sites at the base of frontal (**A**) and temporal lobes (**B**).
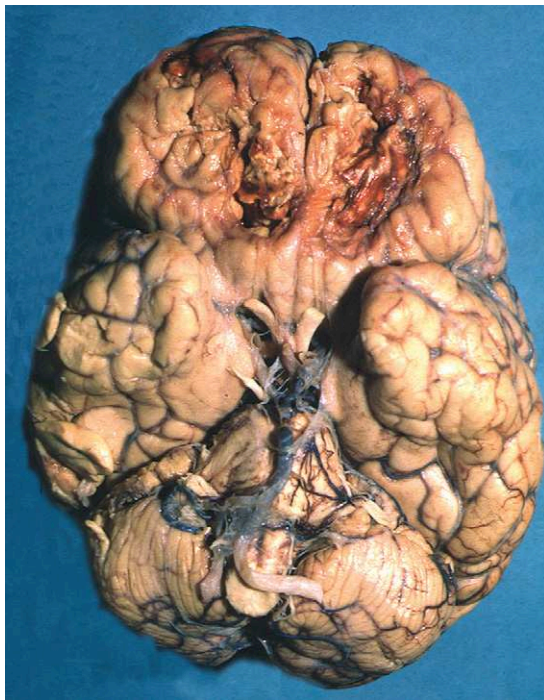
Figure 3-4. Old contusions on the base of the frontal lobes. (Reproduced with permission from Geddes JF and Whitwell HL. Head injury in routine and forensic pathological practice. In Love S, (ed.): Current Topics in Pathology: Neuropathology. Berlin, Springer-Verlag, 2001, pp. 101–124.)

index has shown that severe contusions are present in some 10% of head injury deaths, moderately severe contusions in 78%, and mild contusions in 6%. Such data confirm that contusions occur most commonly in the frontal and temporal lobes, are more severe in patients with skull fractures than in those without, are less common in patients with diffuse brain injury than in those with focal brain injury, and are more severe in patients who do not experience a lucid interval than in those who do.

Intracranial Hemorrhage

Intracranial hemorrhages are usually classified according to the anatomical compartment in which they develop.

Extradural (Epidural) Hemorrhage.   Injury to a blood vessel is a potentially serious complication of a skull fracture, as it may lead to extradural hemorrhage (EDH; Fig. 3-5). Usually a complication of impact to the head, this is most often arterial and usually involves the middle meningeal artery and its branches. These meningeal arteries lie in grooves between the undersurface of the skull and the dura. If the overlying skull is fractured, the bone pulls away from the dura, and the artery may be torn. The dura itself usually remains intact, and blood leaks under arterial pressure into the plane between it and the bone and collects around the site of the fracture. As the dura separates from the skull, the hematoma enlarges and begins to exert mass

Figure 3-5. Extradural hemorrhages. **A**, A man of 60 received a blow behind his ear. Bruising in the temporalis muscle and this linear, right-sided temporal fracture overlay a large extradural hemorrhage, which was the cause of his death 5 hours later. **B**, Gross appearance of a bifrontal extradural hematoma. **C**, Gross appearance of a classical extradural hematoma situated in the parietotemporal region.

effect, pressing on the underlying brain and rapidly causing symptoms.

Occasionally, EDH occurs without evidence of a skull fracture. This is more likely in children, whose skulls are more elastic and so more easily deformed without the bone being broken.

Less commonly, an extradural hemorrhage results from laceration of a venous sinus. Impacts to the occiput are particularly prone to result in an extradural hemorrhage, as a result of damage to dural veins in the posterior fossa. Clinical symptoms of a venous EDH tend to be slower in appearing than an arterial bleed.

Subdural Hemorrhage.   A subdural hemorrhage (SDH) is principally caused by abnormal move-

ment of the brain inside the skull. Although impact usually occurs in head injury, it is not necessary for the development of an SDH and, in patients with cerebral atrophy, there may not always be a history of antecedent trauma. Because the dura tends to be closely adherent to the skull, the plane in which most differential movement takes place is in the subdural space between the dura and the surface of the brain. Although only a potential space in subjects with normal brain size, it contains bridging veins that run from the cortical surface to the dural sinuses. If the movement of the brain inside the skull is sufficient to tear one or more of these veins, venous blood will leak out over the surface of the brain until the intracranial pressure reaches the venous pressure. Alcoholics and patients with

bleeding tendencies, particularly those on antico-agulants, have a predisposition to develop subdural bleeding after relatively minor trauma. Most SDHs lie over the convexities of the hemispheres, although subdural bleeding caused by a cerebral laceration or "burst lobe" will typically overlie the damaged area of brain. Occasionally, the subdural bleeding comes from a cortical artery rather than a vein. Previous head injury with subdural adhesions, which tend to interfere with the free movement of the brain, may predispose to this type of injury.

SDHs are classically separated into acute (Figs. 3-6A and B), subacute (Fig. 3-6C), and chronic

(Fig. 3-7) subdural bleeding. However, it is often difficult to know the exact age of a hematoma using radiological, intraoperative, and histological criteria. Imaging studies reveal that many acute SDHs involute spontaneously if left alone, and do not become chronic lesions. The process of resolution has been well documented neuropathologically. It starts with proliferation of arachnoidal cells over the surface of the hematoma, which eventually becomes encapsulated in a fibrous membrane. In the early stages, numerous thin-walled capillaries grow into the edges of the clot; there is evidence that, on occasion, rebleeding from these blood

A

B

C
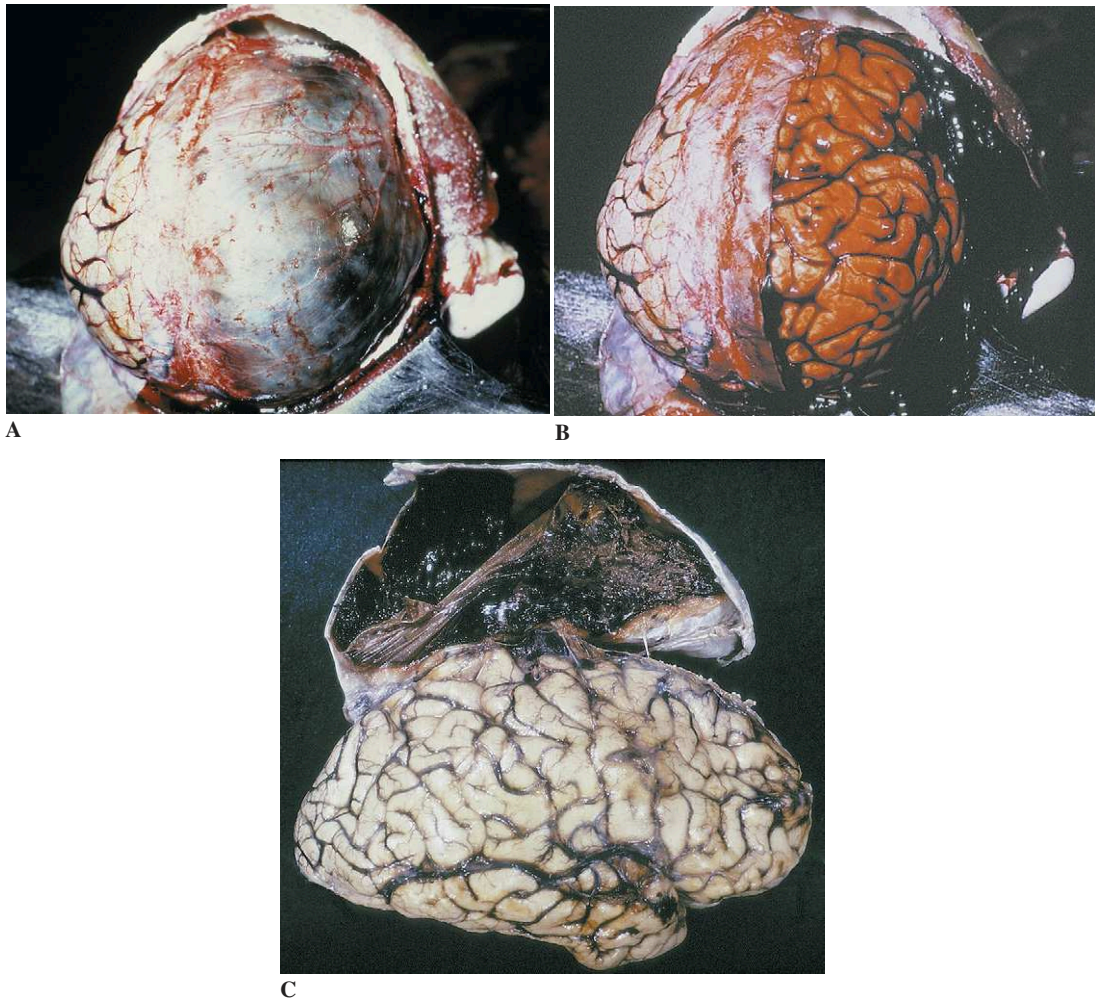
Figure 3-6. Acute and subacute subdural hematomas. **A**, Acute subdural hematoma; gross appearance before incision of the dura. **B**, Acute subdural hematoma: gross appearance after incision of the dura. **C**, Subacute subdural hematoma: gross appearance.
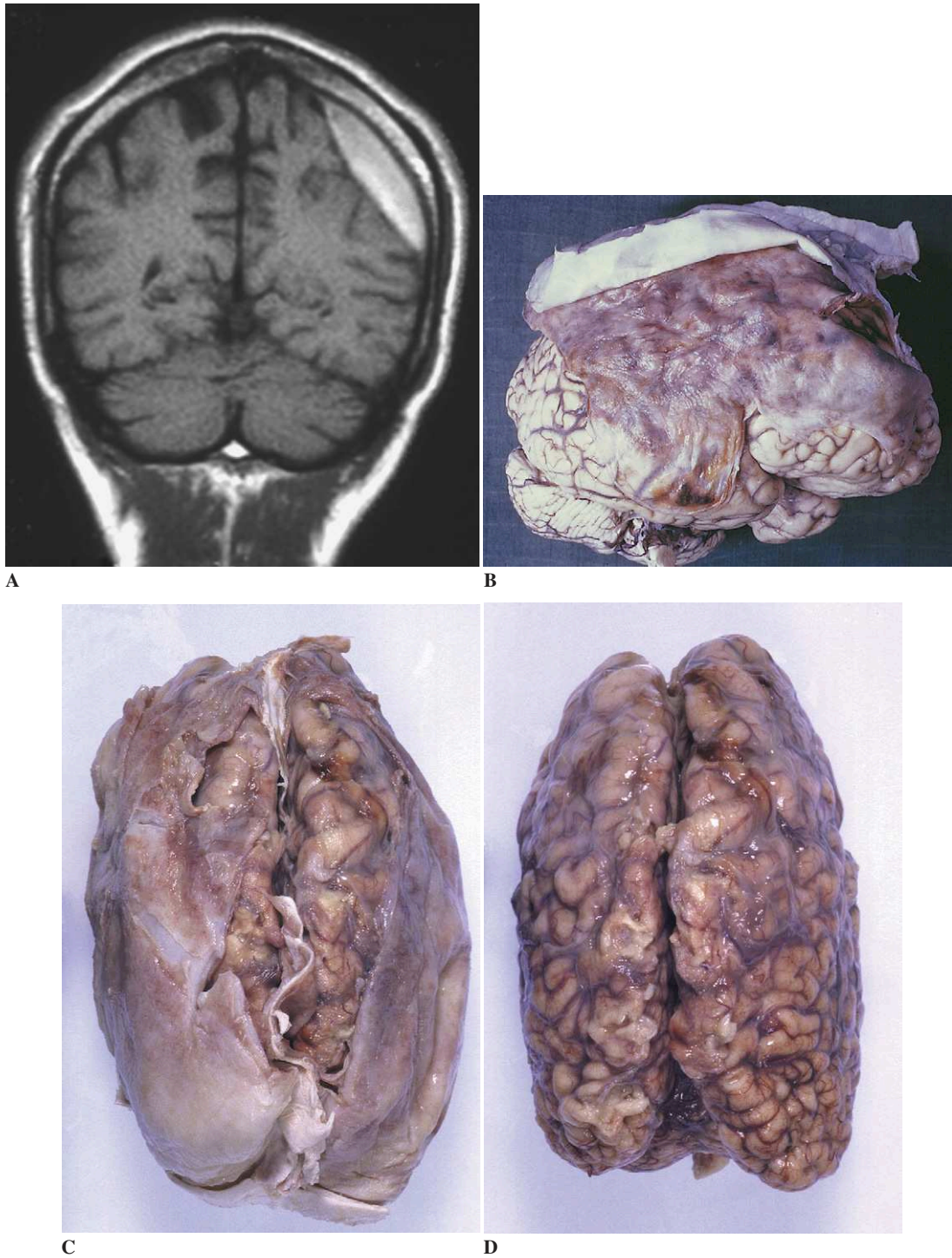
Figure 3-7. Chronic subdural hematomas. **A**, Unilateral chronic subdural hematoma, not causing midline shift but flattening the left hemisphere. **B**, Old, organized subdural hematoma, gross appearance after removal of the dura. **C**, Brain of a 6-year-old child with cerebral palsy: Bilateral chronic subdurals encapsulated by a thick collagenous membrane resembling dura. **D**, Same brain as in (**C**) after removal of the hematomas. Both hemispheres are markedly flattened.

vessels may cause a resolving hematoma to enlarge and produce symptoms. The usual end stage of SDH involution is a collapsed, pigmented, membranous sac adherent to the undersurface of the dura.

Chronic subdural hemorrhage refers to a clot that is encapsulated in fibrous membranes. Magnetic resonance imaging (MRI) is the most sensitive method of demonstrating the heterogeneous nature of such lesions (Fig. 3-7A), and MRI scans suggest that chronic subdurals may be either old hemorrhages undergoing resolution or chronic lesions into which acute rebleeding has occurred. A unilateral (or, sometimes, bilateral) SDH is not uncommonly found in an elderly person being investigated for fluctuating confusion or subtle cognitive decline. In such a patient, who may be predisposed to develop subdural bleeding because of cerebral atrophy, there may be no history of preceding trauma, and the clinical signs develop slowly because there is a relatively large subdural space to accommodate the blood. With time, the fibrous tissue encapsulating the hematoma becomes very thick (Figs. 3-7B and C). Distortion of the hemispheres is often pronounced by the time signs and symptoms are noticed (Fig. 3-7D).

Subdural Hemorrhage in Infancy. A distinct type of SDH is seen in infants who have had a head injury. (In this age group, such injuries are often inflicted by adults.) The subdural bleeding commonly extends over both hemispheres, usually with a small collection in the posterior interhemispheric fissure and posterior fossa. The amount of bleeding over the hemispheres is often small and is almost always associated with pronounced brain swelling. The origin of the subdural bleeding in these infants is believed to be the cortical bridging veins, but this has not been clearly demonstrated. A thin film of SDH with brain swelling may occur in infants in association with cortical venous and dural sinus thrombosis, presumably the result of leakage due to raised venous pressure; a thin film of blood over the hemispheres should therefore not be assumed to be traumatic in etiology. An SDH that forms a mass lesion may be seen in older children, but is rare after head injury in infants.

Subdural Hygroma. A *subdural hygroma* is not the same as a chronic subdural hematoma. The term "hygroma" refers strictly to a subdural collection of CSF, usually clear or xanthochromic, caused by a traumatic tear to the arachnoid through which CSF has leaked. Such a collection is mostly encountered in young children and in the elderly, and is often clinically indistinguishable from a subacute subdural hematoma. However, it differs from the latter both radiologically and neuropathologically. Upon MRI, hygromas have signal intensity close to that of CSF and lack encapsulation. The nature of the collection and the lack of membranes can be confirmed at surgery, if a symptomatic lesion has to be drained.

Subarachnoid Bleeding. In most cases of closed head injury, subarachnoid hemorrhage (SAH) is minimal, consisting of a thin film of venous blood resulting from injury to cortical veins running across the subarachnoid space resulting from movement between the brain and the meninges. Localized SAH is seen at the site of a contusion. The source of basal SAH may be the ventricles; if there is intraventricular bleeding, blood will find its way out of the fourth ventricle into the subarachnoid space on the ventral surface of the brain.

Fibrous organization of subarachnoid hemorrhage, resulting in either focal or widespread obliteration of the subarachnoid space, may be responsible for the development of chronic hydrocephalus.

Occasionally, traumatic damage to an artery at the base of the brain or at the craniocervical junction will produce abundant arterial subarachnoid bleeding, and if there is extensive basal hemorrhage such damage should be excluded by angiogram or by careful postmortem examination. The extracranial vertebral arteries may be the source of the bleeding, particularly if the pattern of skin or soft tissue bruising suggests that there has been a blow to the neck; they should be dissected out from the point at which they enter the foramina transversaria of the cervical vertebrae and followed up into the skull. Dissection and traumatic rupture, including pseudoaneurysm formation, should be looked for carefully.

Parenchymal Hemorrhage. There is some overlap between large contusions, "burst lobes," and parenchymal hemorrhages, and occasionally, large parenchymal bleeds that become manifest some time after injury, following perhaps after one or more negative CT scans. Such bleeding is

described as "delayed." Most delayed hemorrhages occur within the first few days of an injury, although presentation more than a week after head injury has been reported. Why bleeding from blood vessels damaged at the time of injury should be delayed is unclear, but factors such as post-traumatic vasospasm, fluctuations in systemic arterial and intracranial pressures, and post-traumatic coagulopathies may all play a part in different cases.

A distinction should be made between these larger intracerebral hemorrhages and the relatively small hematomas that occur in the deep gray matter of an unconscious patient who clinically has severe, diffuse brain damage. Such basal-ganglia hematomas do not produce mass effect, and have the same poor prognosis as the multiple, small, tissue-tear hemorrhages in the corpus callosum, rostral brainstem, and elsewhere that characterize the severest form of diffuse traumatic axonal injury (see next paragraph).

The *gliding contusion* is a particular type of traumatic parenchymal hemorrhage that, though confusingly described as a "contusion," is not primarily a surface lesion caused by impact. The name is applied to the hemorrhagic lesions in the parasagittal regions of the hemispheres, often symmetrical and predominantly involving the white matter (Fig. 3-8), that tend to be seen in severe head injuries and are associated with diffuse traumatic axonal injury (DAI). Radiologically, a gliding contusion may resemble the bilateral hemorrhagic infarction caused by sagittal sinus thrombosis.

Intraventricular Hemorrhage.   *Intraventricular hemorrhage* is seen as an isolated phenomenon that occurs in a small proportion of patients with blunt head injury. Blood may be present in the ventricles as an extension of a parenchymal hematoma or as a result of retrograde flow into the fourth ventricle from the subarachnoid space at the base of the brain. In cases where the bleeding is confined to the ventricular system, the source is presumed to be rupture of either subependymal veins or of blood vessels in the choroid plexus. Occasionally, when the brain is examined, a tissue tear in the corpus callosum, septum pellucidum, or fornix can be shown to be the cause of the hemorrhage.

Infection

While infection is always a risk after a penetrating injury, meningitis not infrequently complicates blunt head trauma. Fractures of the skull base with dural tears that provide bacteria from the sinuses access to the intracranial cavity usually are responsible. Compound vault fractures also predispose to the development of meningitis. Cranial osteomyelitis, convexity subdural empyema, and cerebral abscess are occasionally seen after penetrating injuries.

A   B
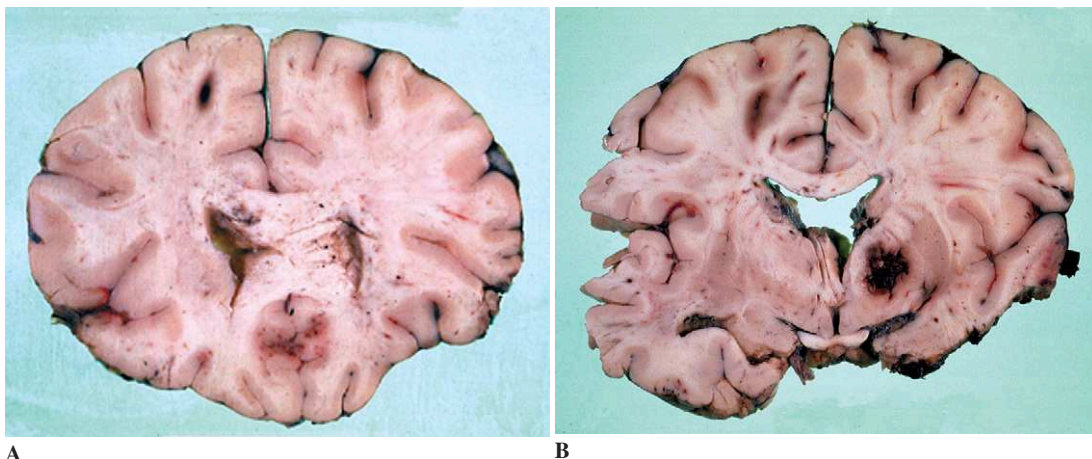
Figure 3-8. Severe head injury. **A** and **B**, Both slices show gliding contusions in the parasagittal white matter on the left and small hemorrhages in the corpus callosum. There is also a small hemorrhage in the right basal ganglia. In a patient unconscious after head injury, such lesions are the hallmark of severe DAI.

Other Focal Traumatic Damage

Damage to Blood Vessels.   Large blood vessels are liable to be damaged in a head injury, particularly when the neck has been injured. A major territory infarct occurring in the hours after a head injury may have a number of causes, but the possibility of structural vascular damage such as posttraumatic dissection or thrombotic occlusion must be rigorously investigated (Fig. 3-9). Traumatic arteriovenous fistula and pseudoaneurysm are well-recognized, though uncommon, complications of blunt trauma to blood vessels.

Damage to the Brainstem.   Localized damage to the neuraxis may occur with injuries involving the craniocervical junction. At their most severe, these are traumatic pontomedullary rents incompatible with life, although survival has been reported after partial brainstem tears. At the other end of the spectrum, the mildest detectable form of this type of damage is after hyperextension-hyperflexion injuries, which may produce axonal damage localized to the long tracts of the lower pons and medulla that is only demonstrable immunohistochemically.

Hemorrhage or hemorrhagic infarction of the brainstem may also result from transtentorial herniation secondary to raised intracranial pressure (see Chap. 1), as a result of either brain swelling
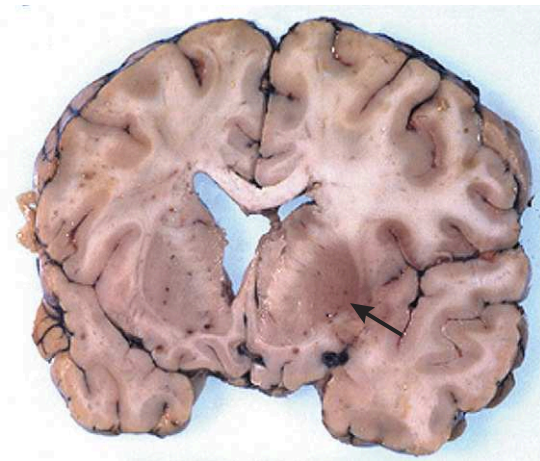
Figure 3-9. A man of 31 developed a large right middle cerebral artery territory infarct after an assault and died two days later of raised intracranial pressure. The cause of the infarct was traumatic dissection of the right middle cerebral artery with occlusive thrombus (*arrow*).

or a hematoma. Such lesions, which characteristically involve the midbrain and basis pontis in the midline, may be extensive and are morphologically quite distinct from the dorsolateral sector hemorrhages that accompany DAI.

Damage to Cranial Nerves.   Cranial nerves are at risk when the base of the skull is fractured. The site of the fracture determines which nerves are damaged. Cranial nerves may also be injured as a result of transtentorial herniation caused by raised intracranial pressure; this is usually associated with a unilateral mass lesion such as a hematoma.

Damage to the Pituitary Gland.   Derangements of pituitary function are often seen after severe head injury. The cause may be direct trauma to the stalk or secondary infarction of the gland caused by brain swelling, raised intracranial pressure, and herniation.

Diffuse Brain Injury

There are three main forms of diffuse (widespread or multifocal) traumatic brain damage: diffuse traumatic axonal injury, diffuse hypoxic-ischemic damage, and brain swelling. A fourth, less-common type—diffuse vascular damage—is, in its most severe form, incompatible with survival.

In the absence of a demonstrable by imaging structural lesion such as a hematoma, a patient in persistent coma after a head injury can be expected to have diffuse brain damage. In practical terms, in the adult, this will be widespread axonal injury, severe hypoxic-ischemic damage, or a combination of the two.

Traumatic Axonal Injury

Recent studies have shown that axons are damaged in head injuries of many different types and severities and that the distribution and amount of this damage largely determine the clinical picture, including the outcome. The concept of a spectrum of traumatic axonal injury (TAI) has evolved, with mild reversible hemispheric axonal injury resulting from concussive head injuries at one end of the spectrum and widespread or "diffuse" axonal injury at the other.

Diffuse Axonal Injury.   DAI is a clinicopathological entity corresponding to the most severe pattern of TAI, in which axons are damaged throughout the hemispheric white matter and in the rostral brainstem. By definition, the sites involved in a case of DAI are the parasagittal white matter and large fiber bundles such as the corpus callosum, internal capsule, and cerebellar peduncles, though damage is characteristically widespread and may not be limited to these sites (Table 3-6). Clinically, patients

Table 3-6. Histology in Cases Where Diffuse Brain Injury Is Suspected

Recommended Minimum Sample for a Diagnosis of DAI*
Corpus callosum with adjacent parasagittal cortex and white matter
Deep gray matter including posterior limb of internal capsule
Temporal lobe including hippocampus
Genu (anterior sections) of corpus callosum
Cerebellar hemisphere including the dentate nucleus
Midbrain at the level of the decussation of the superior cerebellar peduncles
Pons at the level of the middle cerebellar peduncles
Medulla

Recommended Stains[†]
Survival < 12 hours: H and E, βAPP
Survival > 12 hours: H and E, βAPP, silver preparation, CD68[§]
Survival > 1 week: H and E, βAPP, silver preparation, CD68
Survival > 6 weeks: H and E, CD68

Other Useful Staining Methods

Method	*Demonstrates*
Perls	Hemosiderin
Reticulin stain	Organization of a subdural
Hematoxylin van Gieson	hematoma
Cresyl-fast violet	Microglial "clusters" or "stars"
Modified PTAH[‡]	Secondary long tract degeneration
Marchi method	

H and E = hematoxylin and eosin
PTAH = phosphotungstic acid hematoxylin
* Blocks to be as large as possible; if only small blocks are taken, bilateral samples are recommended.
† Survival times given as an approximate guide.
§ CD68 in short survival cases may show (1) evidence of a previous TAI and (2) selective cortical or hippocampal damage from an episode of global hypoxia.
‡ A modification of the routine PTAH stain, which eliminates myelin staining
Source: Manlow A, Munoz DG: A non-toxic method for the demonstration of gliosis. J Neuropathol Exp Neurol 1992;51:298–302.

with the most severe grades of DAI are unconscious from the time of head injury, remain in prolonged coma, and are severely disabled or vegetative thereafter. At present, a diagnosis of DAI can only be confirmed by neuropathological examination of the brain, although it can be inferred from the clinical state; imaging provides strong support for the diagnosis when there is no mass lesion to account for the patient's prolonged unconsciousness or disability. Small tissue-tear hemorrhages in the corpus callosum (see Fig. 3-8) and dorsolateral sector of the rostral brainstem (Fig. 3-10) often accompany DAI

Figure 3-10. The upper brainstem in a case of DAI. Note that the lesions in the dorsolateral quadrant of the brainstem are very different from the brainstem hemorrhages seen as a result of raised intracranial pressure and brain shift.

Table 3-7. Frequency of Principal Macroscopic Lesions in Diffuse Axonal Injury and Their Anatomical Distribution

Location	Frequency
Rostral brainstem	95%
Corpus callosum	92%
Parasagittal white matter ("gliding contusions")	88%
Hippocampal formation	88%
Interventricular septum	80%
Thalamus	56%
Caudate nucleus and putamen	17%

and so are helpful for diagnosis. So are gliding contusions and small, parenchymal hemorrhages in the deep gray matter, both of which have been shown to be associated with DAI (Table 3-7).

Animal experiments have shown that DAI is primarily a nonimpact phenomenon resulting from angular or rotational acceleration. This explains the circumstances in which DAI primarily occurs in human injuries, namely, traffic accidents and falls from a height. In such situations, DAI is primarily the result of inertial phenomena and there is a lower incidence of skull fractures. DAI also occasionally follows accelerated falls from standing, notably assaults, but in these cases, impact plays an important role and a skull fracture is much more usual.

Other Forms of Traumatic Axonal Injury. It is not uncommon to find lesser degrees of axonal damage, usually in the cerebral white matter but not the brainstem, in patients who have had a fatal head injury but whose clinical picture was not that of DAI or, more rarely, in patients known to have had a recent mild head injury who have died of unrelated causes. However, unlike in DAI, the clinicopathological correlates of these milder, sometimes reversible, hemispheric axonal injuries are difficult to establish.

Localized TAI occasionally occurs. Traumatic damage to the spinal column may result in acute or chronic compression, with localized axonal damage in the cord at the level of the injury. Similarly, hyperflexion/hyperextension injuries to the neck that do not disrupt the craniocervical junction may cause axonal damage in long tracts in the lower brainstem or upper cervical segments. Spinal nerve roots have been reported to be damaged in cases of nonaccidental head injury in infants, possibly caused by a similar mechanism of excessive movement at the craniocervical junction, resulting in stretch to the spinal cord and nerve roots.

Microscopic Features of Traumatic Axonal Injury. The subcellular pathology of TAI is now largely known. In the mildest forms of axonal injury, temporary derangement of axonal function results from transient local disruption to axonal function; with severe damage, injury sets in train a process of breakdown in axonal transport caused by cytoskeletal collapse. During the initial stages, damage to the cytoskeleton might be theoretically reversible, but as the breakdown process evolves the axon begins to swell and eventually disconnects (i.e., undergoes axotomy), at which point the damage becomes irreversible. It is now believed that few axons rupture at the time a closed head injury occurs.

Electron microscopy has elucidated these events, but light microscopy demonstrates the gross changes well. In order to investigate the possibility of microscopic traumatic damage, the brain must be widely sampled, with careful attention to anatomical sites that are vulnerable to such injury (see Table 3-6). Using traditional neuropathological methods such as hematoxylin and eosin (H and E) and silver preparations, the earliest that axonal damage can be detected is when axonal swellings or "bulbs" become visible, from about 12 hours after injury (Fig. 3-11). However, immunocytochemical methods enable the detection of such damage from 2 to 3 hours by targeting proteins that are normally transported down the axon in undetectable quantities, but instead accumulate and so become demonstrable with anti-
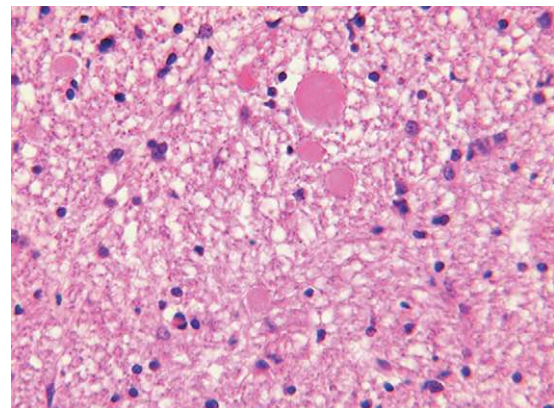
Figure 3-11. Two days' survival after injury. Damaged axons are easily seen on routine stains.

sera at the sites of damage to the axons. Many proteins could theoretically be used for this purpose, but for routine diagnostic use, greatest familiarity has been gained with β-amyloid precursor protein (βAPP); antibodies to βAPP provide a sensitive tool for diagnosing axonal damage (Fig. 3-12).

The earliest that axonal damage can now be detected is approximately 2 hours after injury, well before other histological changes become apparent. Eventually, the axon swells until it can be seen by light microscopy with H and E. Disconnection of the axon may follow and a sequence of cellular responses to the injury occurs. Microglial activation is followed by the formation of microglial "clusters" or "stars" around degenerating axons at between 5 and 10 days after injury, although timing may vary in individual cases and axonal degeneration is almost certainly a continuing process. Eventually, swellings are no longer detectable either immunohistochemically or with routine stains, and microglial nodules scattered through the white matter remain the only sign of damage; however, these are far from specific. With long-term survival after widespread TAI, long-tract degeneration can be detected by the traditional methods of Marchi or immunohistochemically, using a macrophage marker such as CD68 (Fig. 3-13). With time, gliosis (scarring) occurs in the central white matter and long tracts.

Nontraumatic Causes of Axonal Injury. None of the markers of axonal damage are specific for
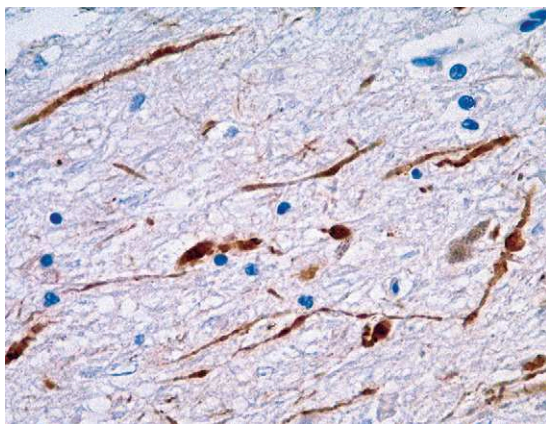
Figure 3-12. Short survival after head injury. Immunohistochemistry for βAPP delineates damaged axons and reveals early axonal swelling.

trauma. Therefore, TAI should not be mistaken for axonal damage resulting from other factors such as bleeding and ischemia. Disruption of axons by hemorrhage usually does not present diagnostic difficulties, but such areas should be avoided when sampling a brain to look for axonal injury. Ischemic damage to axons characteristically occurs as the brain swells and intracranial pressure rises. Blood vessels, often those supplying the central and deep regions of the brain—that is, much the same sites as the ones that are vulnerable in trauma—are compressed, and so many head injury cases show areas of "vascular" axonal βAPP expression caused by brain swelling. Such changes are particularly prominent in the pontine basis. They are often geographic or linear in appearance and sometimes associated with ischemic changes in neurons; however, with very short survival after injury, distinguishing white matter ischemia secondary to brain shift from traumatic damage on the basis of βAPP immunoreactivity may be difficult. Widespread sampling (see Table 3-6), a knowledge of neuroanatomy, and an appreciation of the evolution of axonal pathology are all necessary, but sometimes even these will not suffice; extreme caution should be exercised in forensic work before concluding that axonal damage in a case with short survival is definitely traumatic.

Diffuse Hypoxic-Ischemic Damage

Hypoxic brain damage is an integral part of TBI, being seen in a high proportion of severe and fatal injuries. There are a variety of possible causes (Table 3-8). While rapid resuscitation reduces its occurrence, widespread hypoxic-ischemic brain damage remains an important factor affecting the outcome after TBI; both experimental and clinical work have shown that head injury makes patients more vulnerable than non–head-injured patients to even minor alterations in cerebral perfusion or small rises in intracranial pressure. Various patterns of cerebral hypoxia may be seen in TBI, the most common of which is probably selective damage in the CA1 sector of the hippocampus. Laminar cortical necrosis, infarction in the boundary zones of the major cerebral arteries, and single-artery territory infarcts may all be seen in cases of severe head injury (see Chap. 9).

Figure 3-13. Two methods of demonstrating secondary long-tract degeneration, shown in sections from a patient with DAI who survived six months after injury. **A**, Marchi method reveals myelin breakdown products (black) in the long tracts and in the cerebellar peduncles. **B**, Immunohistochemistry for CD68 demonstrates the numbers of foamy macrophages in the corticospinal tracts in a more rostral section of the pons.

Brain Swelling

Diffuse brain swelling, an important contributor to rises in intracranial pressure, is common after moderate or severe head injury. It often involves both cerebral hemispheres, though patients with acute SDHs may have unilateral swelling of the underlying hemisphere. The cause of post-traumatic brain swelling is not always clear; both loss of autoregulation with congestive swelling and cerebral edema (cytotoxic and vasogenic) are implicated. Global hypoxia-ischemia is an important cause of brain swelling in the context of head injury, while diffuse brain swelling is a particular feature of childhood and adolescent TBI.

Table 3-8. Patterns and Causes of Hypoxic-Ischemic Brain Damage After Traumatic Brain Injury

Pattern	Cause
Diffuse	Cardiorespiratory arrest
Focal	Raised intracranial pressure, shift, distortion distortion and internal herniae
	Vasospasm
	Hypotension
	Embolism
	Penetrating injuries

Diffuse Vascular Injury

Widespread white-matter hemorrhages may be seen in the brains of patients who appear not to have survived after injury and occasionally in those who have survived for a short while. Diffuse vascular damage is only seen in the most severe injuries; it has a widespread distribution similar to the axonal damage in DAI and is therefore presumably the result of similar but more severe conditions at the time of injury (Fig. 3-14). In its most severe form, its clinical correlations are not clear.

Repetitive Head Injury and Dementia Pugilistica

While the neuropathological changes in mild head injury remain largely unknown, it is probable that cumulative damage from repeated concussive or subconcussive blows to the head of the sort sustained by boxers, jockeys, soccer and football players, and the like may cause brain damage of Alzheimer type. Neuropathological studies have shown that such subjects may show early neurofibrillary tangles in the neocortex, often around blood

A

B
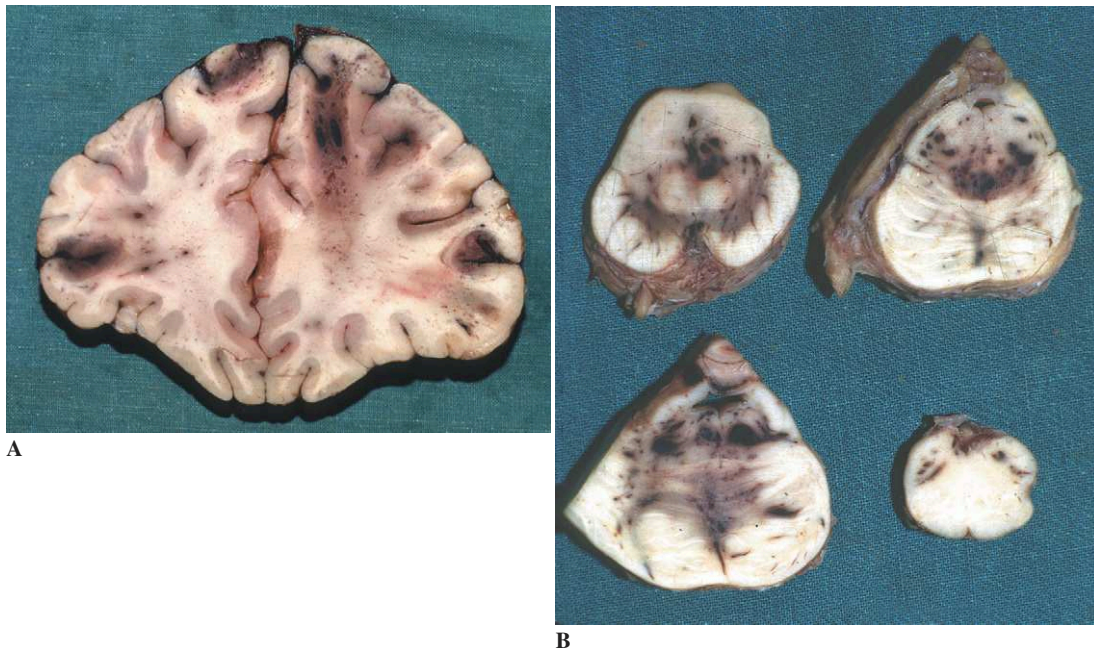
Figure 3-14. Diffuse vascular injury. Widespread small hemorrhages in the hemispheres (**A**) and brainstem (**B**) of a traffic-accident victim who died of a head injury almost immediately after the accident. Such widespread damage is believed to be incompatible with survival.

vessels in the depths of sulci (Fig. 3-15). The pathogenesis of such changes is still unknown, but they are clearly related to the development of long-term sequelae, particularly *dementia pugilistica*, a condition classically described in elderly retired boxers. Brains from such patients show damage to the interventricular septum and cavum septum, pallor of the substantia nigra, and widespread neocortical neurofibrillary tangles, neuropil threads, and diffuse amyloid plaques, but lack the neuritic plaques seen in Alzheimer disease. As in other aspects of head injury, genetic factors appear to influence the development of post-traumatic neurodegeneration.

Pediatric Head Injury

Fatal head injury is not common in young children. Accidental falls and traffic accidents are usually responsible in ambulant children, who tend to show the same types of pathology as adults with head injuries. In the infant population, inflicted ("non-accidental") injury is an important cause, and in this group head injury is rather different, presum-
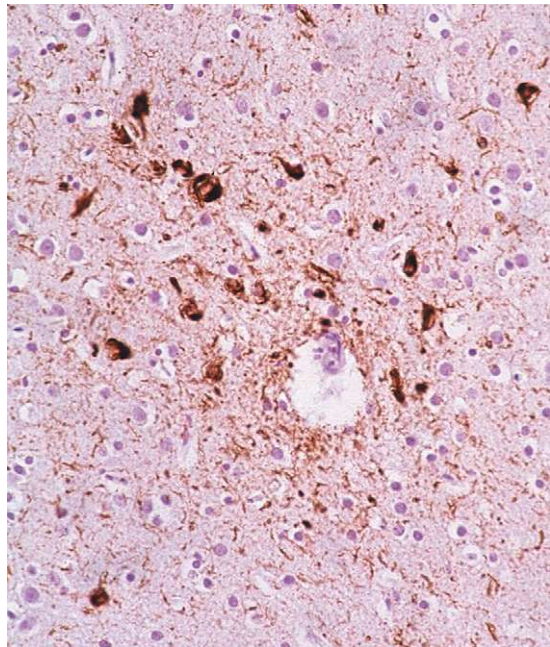
Figure 3-15. Chronic brain damage in a 23-year-old boxer dying from the effects of an acute subdural hematoma. Immunohistochemistry for tau reveals neurofibrillary tangles and neuropil threads around a small vessel in the neocortex.
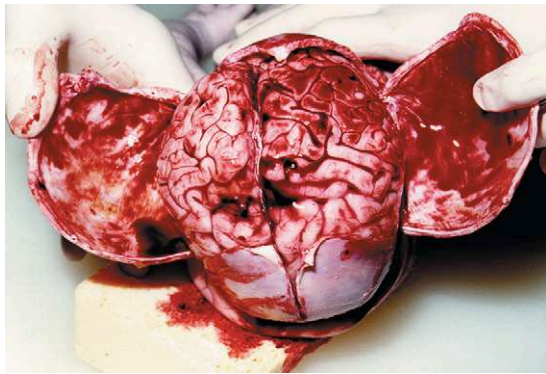
Figure 3-16. Subdural bleeding in an infant with a head injury, believed to have been inflicted. As in this case, severe brain swelling is the usual immediate cause of death. (Reproduced with permission from Geddes JF and Whitwell HL. Head injury in routine and forensic pathological practice. In Love S (ed.): Current Topics in Pathology: Neuropathology. Berlin, Springer-Verlag, 2001, pp. 101–124.)

ably because of the immaturity of both the infant's anatomy and physiology. A proportion of children believed to have been shaken show evidence of damage to the brainstem and high spinal cord; this has focused attention on the possibility of cranio-cervical injuries being responsible for the clinical picture of apnea or respiratory disturbance and the hypoxic brain swelling commonly seen post mortem. A thin film of subdural bleeding or small subdural hematoma (often midline) and retinal hemorrhages accompanies the brain swelling (Fig. 3-16), and this pathology is often considered "diag-nostic" of abusive injury. However, it has also been suggested that this unique type of SDH may some-times have a "congestive" and/or hypoxic, rather than a traumatic etiology and that retinal hemor-rhages may result from rapid rises in intracranial pressure aggravated by hypoxia. There is evidence that low-level, accidental falls in children may on occasion prove fatal. It is therefore important to develop as high a degree of certainty as possible from objective criteria before ascribing an injury to a child to nonaccidental causes.

Penetrating Injuries

While infection is an important complication of almost all penetrating injuries, the actual traumatic damage to the brain is extremely variable and depends on the type and cause of injury. In civilian life, penetrating injuries are far less common than closed head injuries, though gunshot injuries are increasingly common. In gunshot injuries the amount of damage depends on the type of gun, the size and speed of the bullet, and the direction of its path through the head. Low-velocity missiles—for example, metal instruments such as knives, screw-drivers, and drills—penetrate the brain but tend to remain embedded in it. Once again, the damage caused depends on the track of the missile.

Spinal Cord Injuries

Acute spinal cord injuries tend to be primarily the result of traffic accidents, with considerable numbers also related to sporting activities or falls (Fig. 3-17); missile injuries to the spinal

Figure 3-17. Trauma at the craniocervical junction. The patient died following transoral excision of fragments of a fractured odontoid. The lower medulla and upper cervical segments are compressed.

cord are less common. The most common mechanisms of acute spinal cord injury are vertebral fracture-dislocation and ruptured intervertebral disc. Much of the pathology of acute spinal cord trauma is similar to that of head injury. Similar progression of damage after injury occurs, though the anatomy of the spinal canal, the cord, and its blood supply is such that full recovery from injury is less usual, and small, parenchymal contusions or hemorrhages have a relatively much greater significance than in the brain. With time such a lesion cavitates, leading to the development of a syrinx.

Chronic inflammatory conditions such as long-standing rheumatoid arthritis, which affects the cervical spine in a high proportion of patients, may cause severe angulation of the vertebrae and mild chronic cord compression. A potentially lethal complication of cervical rheumatoid arthritis is instability of the craniocervical junction, which may become clinically manifest only when an unconscious rheumatoid patient is moved or intubated for surgery. Preoperative plain cervical X-rays taken in flexion and extension are essential to assess if there is any atlantoaxial or subaxial movement in such patients.

Chapter 4
Vascular Pathology

Harry V. Vinters, Umberto De Girolami,
and Jean-Jacques Hauw

Intracranial Hemorrhage

Any extravasation of blood within the brain or lep-tomeninges, whatever its cause, constitutes, respectively, a cerebral or meningeal hemorrhage.

Intracranial hemorrhages due to trauma are described in Chapter 3. Also excluded from present consideration are hemorrhages within neoplasms (Chap. 2) and brainstem hemorrhages secondary to herniation (Chap. 1). Hemorrhagic infarcts are discussed later in this chapter.

Within these limits, the two main types of intracranial or cerebral hemorrhage to be discussed here are subarachnoid hemorrhage and intraparenchymal hemorrhage.

In *subarachnoid hemorrhage* (SAH), bleeding primarily takes place in the leptomeningeal spaces, extending diffusely throughout the subarachnoid space (SAS) or is localized, as a subarachnoid hematoma. SAH may also extend into the brain parenchyma, penetrating the cortex, and can ultimately burst into the ventricular cavities.

In *intracerebral hemorrhage* or *intraparenchymal hemorrhage* (IPH), bleeding occurs first within the brain parenchyma. The hemorrhage may remain entirely within the brain substance or may burst into the ventricular cavities. In the case of hemorrhages that involve the peripheral portions of the hemisphere—lobar hemorrhages—there may be extension of the bleed into the subarachnoid space (cerebromeningeal hemorrhage). Extensive outpouring of blood into the ventricles eventually

makes its way to the subarachnoid space via the foramina of Luschka and Magendie.

Although classification of hemorrhage by various intracranial compartments provides a practical anatomic approach to assessing different pathophysiologic mechanisms (Figs. 4-1 and 4-2), the resulting groupings are arbitrary. Some causative agents and risk factors that lead to subarachnoid hemorrhage, for example, are also important in intracerebral hemorrhage. Furthermore, as mentioned previously, bleeds that originate in one compartment may extend into another.

Subarachnoid Hemorrhage (SAH)

Hemorrhage into the subarachnoid space is an important cause of morbidity and mortality in people of all age groups. Primary SAH mostly results from rupture of an aneurysm, usually on a branch of the circle of Willis. More seldom, it may complicate a vascular malformation (hemangioma) within brain parenchyma located in close proximity to the subarachnoid space. SAH may also be seen in the setting of systemic hemorrhagic diatheses, for example, severe thrombocytopenia.

Berry (Saccular) Aneurysms

An *aneurysm* is a localized pathologic dilatation of a blood vessel or of the ventricular wall of the heart that results from the giving way of components
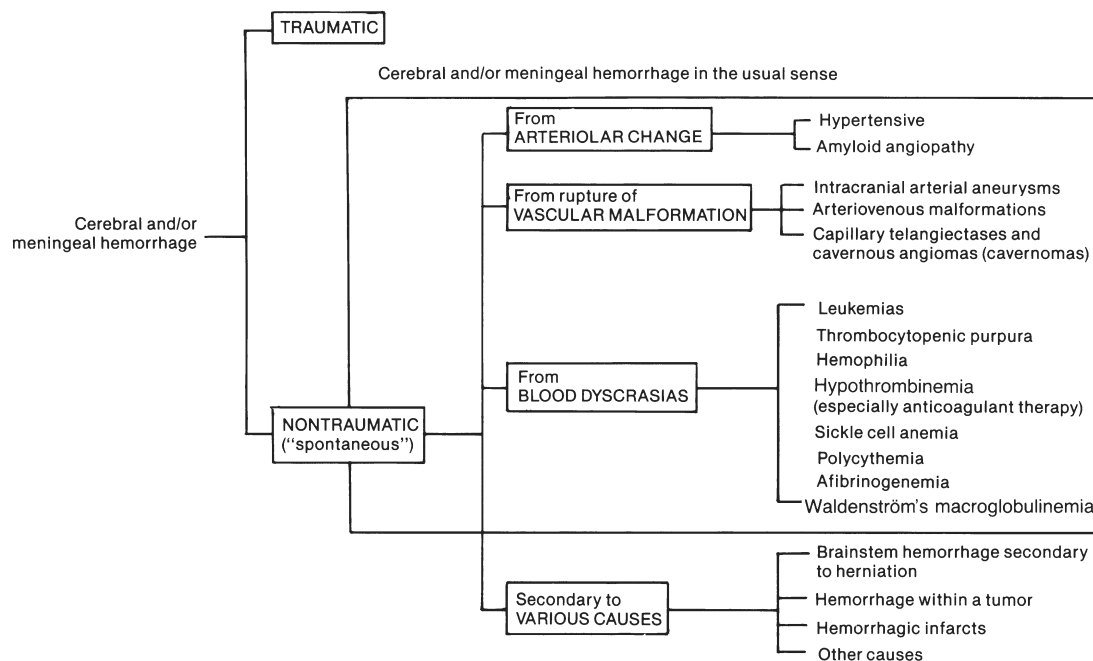
Figure 4-1. Distribution of the blood in the various forms of intracranial hemorrhages.

of the structure. *Berry* aneurysms are localized sac-like dilatations of intracranial arteries. The aneurysmal outpouching is usually connected to the artery by a narrow segment or neck; its wall is formed by thin, fibrous tissue with patchy interruption and attenuation of the elastic lamina and is associated with thinning of the media (Fig. 4-3). Berry aneurysms usually occur at major bifurcation points on the circle of Willis (Figs. 4-4 and 4-5). Most are found in the carotid anterior circulation and involve the following sites: (1) junction of internal carotid artery (ICA) and posterior communicating artery, (2) origin of the anterior choroidal artery, (3) middle cerebral artery (MCA) bifurcation or trifurcation in the Sylvian fissure, and (4) junction of anterior cerebral artery and anterior communicating artery. Ten percent of all aneurysms are found in the vertebrobasilar territory, mainly at the top of the basilar artery.

Most patients with berry aneurysms come to clinical attention between the ages of 40 and 70 years. Berry aneurysms are approximately 1.5 to 2 times as common in women as men; 10% to 30% of patients have multiple aneurysms; rarely, aneurysms are familial. Though referred to as congenital, berry aneurysms are almost never encountered in children

or infants. An aneurysm found in midlife could, however, arise from a focus of congenital muscle weakening of an artery. Berry aneurysms can also develop as the result of degenerative changes in cerebral blood vessel walls, possibly secondary to abnormal smooth muscle and connective tissues. There is an increased incidence of intracerebral aneurysms in some systemic diseases, including polycystic kidney disease, Marfan and Ehlers-Danlos syndromes, pseudoxanthoma elasticum, fibromuscular dysplasia, sickle cell disease, and coarctation of the aorta.

The clinical course of a berry aneurysm is dependent on whether the lesion goes on to rupture (Fig. 4-6, p. 80). Rupture of a berry aneurysm usually produces life-threatening SAH (Fig. 4-7, p. 80). Bleeding within the subarachnoid spaces spreads rapidly through the CSF, causing irritation of cranial nerves and spinal nerve roots. Blood products elicit vasospasm in subarachnoid arteries, which may cause multifocal infarcts or extensive anoxic-ischemic change and may be a lethal complication. Very extensive SAH may also result in rapidly increasing intracranial pressure. The hemorrhage can stop spontaneously, in which case the blood in the CSF undergoes resorption within

Cerebral ventricles—

—Cerebral parenchyma
—Subarachnoid space
—Subdural space
—Dura
—Extradural space
—Skull
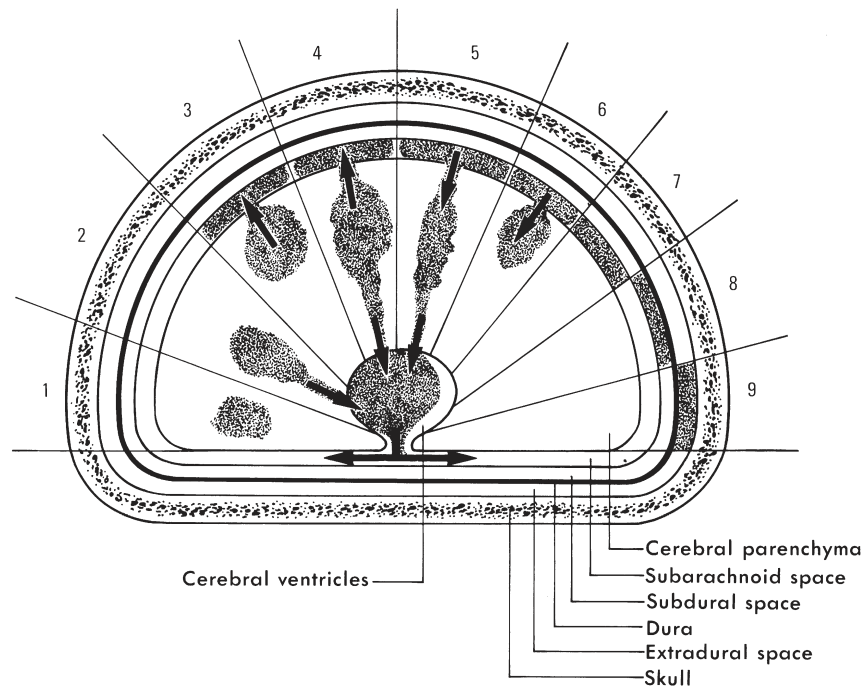
1. Pure cerebral hemorrhage (or cerebral hematoma)
2. Cerebral hemorrhage with ventricular rupture   } Cerebral hemorrhages
3. Cerebromeningeal hemorrhage
4. Cerebromeningeal hemorrhage with ventricular rupture

5. Meningocerebral hemorrhage with ventricular rupture
6. Meningocerebral hemorrhage   } Meningeal hemorrhages
7. Pure meningeal (subarachnoid) hemorrhage
8. Subdural hematoma

9. Extradural (epidural) hematoma

Figure 4-2. The chief causes of cerebral and/or meningeal hemorrhage.
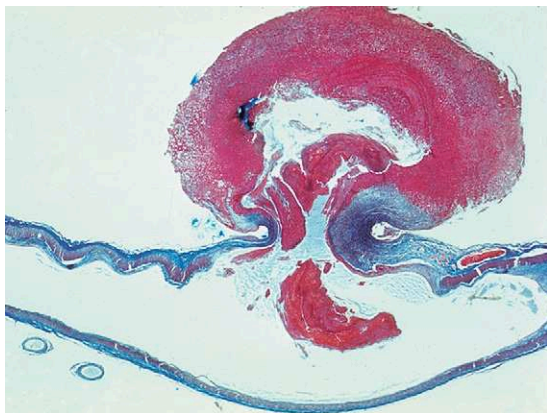
Figure 4-3. Berry aneurysm, microscopic appearance.

approximately three weeks. In some patients, rebleeding occurs 10 to 15 days after the initial bleeding. In some patients who are prone to recurrent bleeding, the spread of hemorrhage in the SAH is limited by the development of a subarachnoid hematoma; these patients may also progress to rupture of the aneurysm into the adjacent cerebral parenchyma (meningocerebral hemorrhage; Figs. 4-8 and 4-9, p. 81). Bleeding of a ruptured aneurysm may also occur directly into the brain parenchyma, especially if the site of rupture on the dome of the aneurysm is embedded within brain substance. In these patients, intraventricular rupture and intracranial hypertension may ensue.

Cerebral infarcts associated with aneurysmal rupture are frequent. Although their pathogenesis is
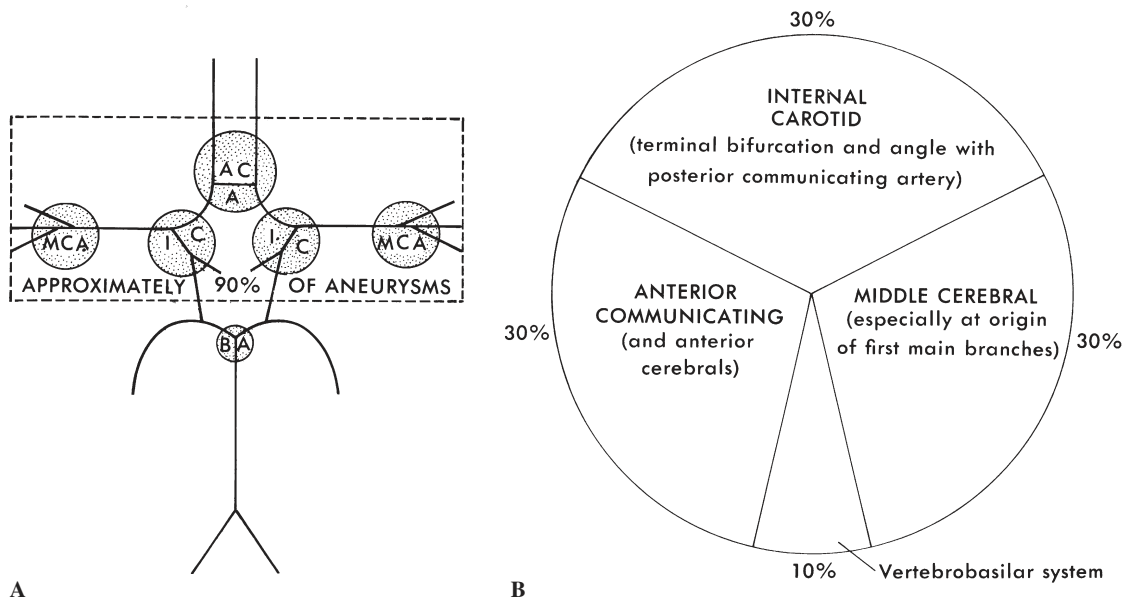
Figure 4-4. A and **B**, Distribution and frequency of arterial aneurysms. ACA = anterior communicating artery; IC = internal carotid artery; MCA = middle cerebral artery; BA = basilar artery.

uncertain, vascular compression resulting from a subarachnoid hematoma, thrombosis of the affected vessels, subsequent embolization into the sac of the aneurysm, and arterial spasm are theoretical possibilities.

Compression of structures adjacent to the aneurysmal sac—particularly cranial nerves—may occur, especially in relation to large aneurysms.

Survivors of an SAH may have significant postbleed morbidity, often associated with the development of hydrocephalus as a response to blood breakdown products in the SAS. A rare sequel of repeated episodes of smoldering SAH is subpial cerebral siderosis. This phenomenon is the result of seepage of breakdown products of red blood cells, including iron pigment, into the underlying molecular layer, with secondary toxic injury of the crests of the cerebellar folia in particular.

Unruptured aneurysms are also a relatively common "incidental" finding at autopsy and on imaging studies.

Though neurosurgical "clipping" of a ruptured aneurysm is still standard therapy in most centers, endovascular treatments (e.g., "coiling" to induce thrombosis of the aneurysm, wrapping) are increasingly being used.

Inflammatory/Infective (Mycotic) Aneurysms

Inflammatory/infective aneurysms, which account for 3% to 6% of all intracranial aneurysms, are usually associated with subacute or acute infective endocarditis and less often with spread of infection from a contiguous site (as in, for example, osteomyelitis or meningitis) into the vessel wall. The microorganisms causing the endocarditis are multiple and frequently of low virulence; both bacteria and fungi can be responsible, the latter especially in immunocompromised patients and injecting drug users. Unlike berry aneurysms, infective/mycotic aneurysms usually occupy distal branches of the arterial circulation. Rupture may result in subarachnoid or intraparenchymal bleeding. An infective aneurysm, friable and weakened because of polymorphonuclear leukocytes in the vessel wall, may be removed in the course of resection of an intracerebral blood clot and therefore must be sought in the specimen. Stainable microorganisms may be demonstrable among inflammatory cells.

Infective aneurysms secondary to endocarditis result from a septic embolus that lodges within a branch of a cerebral artery, with subsequent extension of microorganisms from the embolus into the
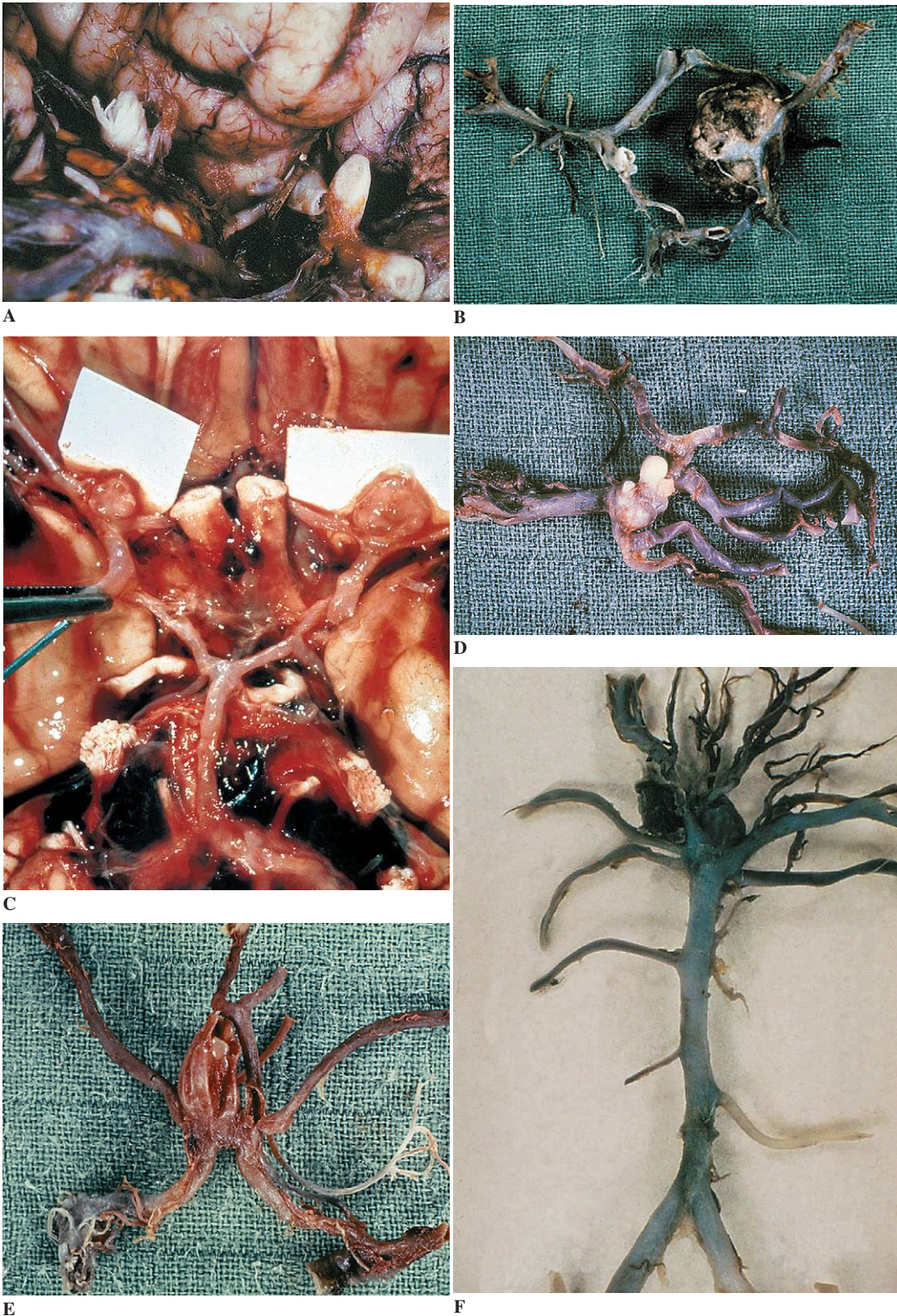
Figure 4-5. Different types of berry aneurysms. **A**, Vestigial aneurysm at the termination of the internal carotid artery, obliterated by a clip. **B**, Massive aneurysm at the termination of the internal carotid artery. **C**, Bilateral berry aneurysms at the termination of the internal carotid arteries. **D**, Middle cerebral artery aneurysm. **E**, Aneurysm of the anterior communicating artery. **F**, Aneurysm of the bifurcation of the basilar artery.
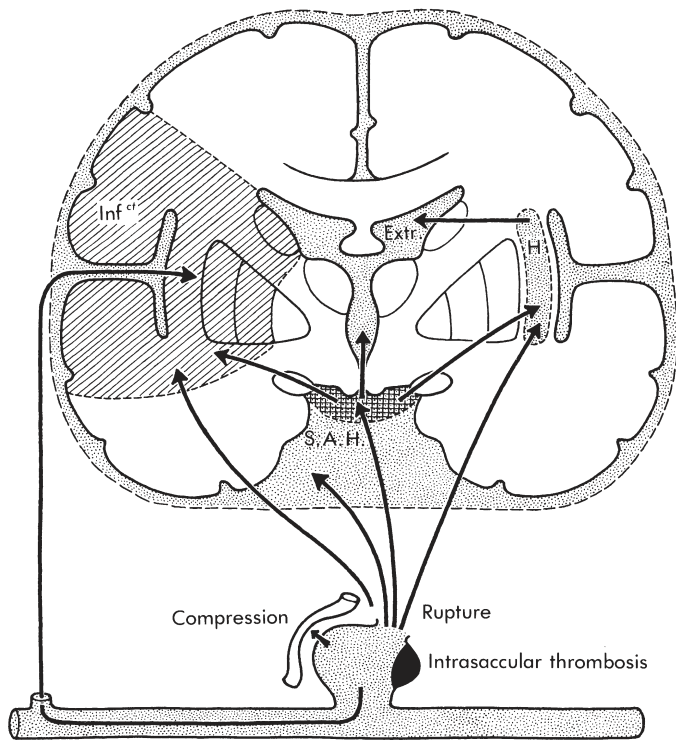
Figure 4-6. Representation of the chief complications resulting from arterial intracranial aneurysm. Inf^{ct} = infarction; Extr. = ventricular extravasation; H = intracerebral hematoma; S.A.H. = subarachnoid hematoma.
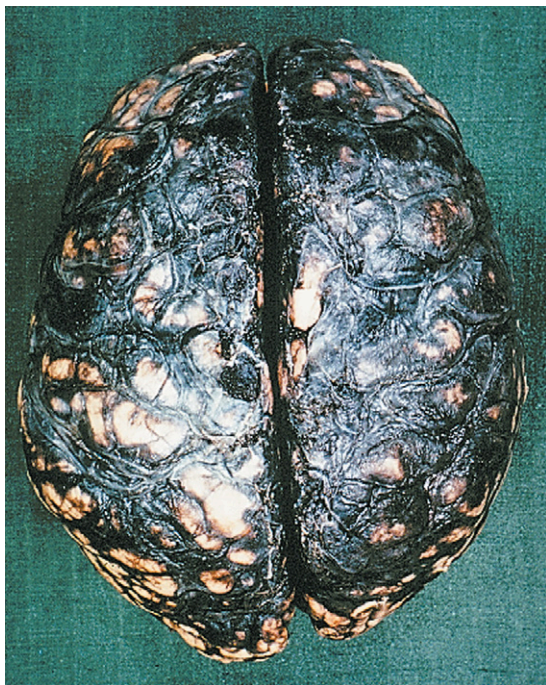
Figure 4-7. Diffuse subarachnoid hemorrhage, macroscopic appearance.

adjacent vessel wall. Septic emboli in individuals with infective endocarditis may also lead to an ischemic (bland) infarct that may undergo hemorrhagic transformation or result in a pyogenic arteritis, causing an intracerebral hematoma.

Dissecting Aneurysms (Arterial Dissections)

Dissecting aneurysms are almost always encountered in patients between 25 and 45 years and may cause both infarcts and SAH. Dissection may occur in extracranial or intracranial branches of the carotid or vertebrobasilar system. When *intracranial* dissection occurs in the anterior circulation, the site of dissection is usually between the internal elastic lamina and the media, with resultant intravascular thrombosis. When dissection occurs in the posterior circulation, transmural dissection often results in SAH.

Specific vasculopathies associated with dissection include fibromuscular dysplasia and connective tissue disorders, including Marfan syndrome and Ehlers-Danlos syndrome (type IV). Arterial dissection of cervical arteries most often occurs following
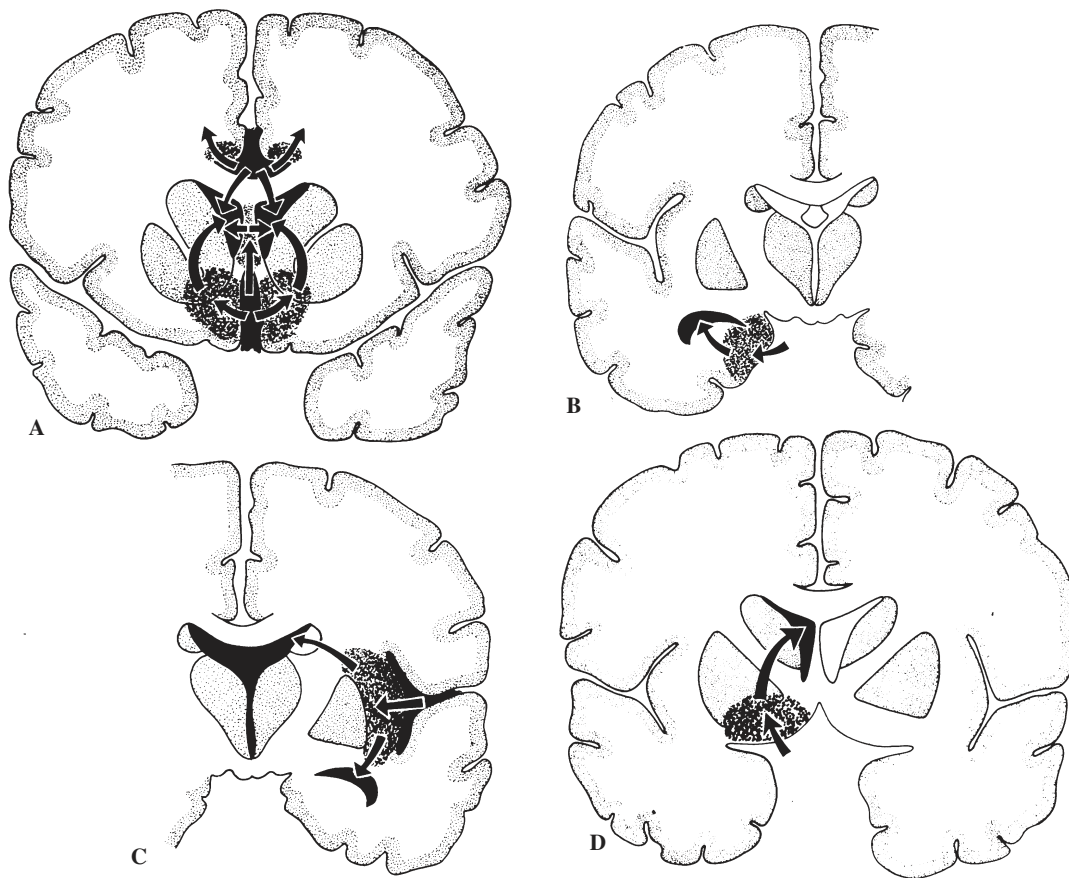
Figure 4-8. The sites of hematomas secondary to rupture of an arterial aneurysm. **A**, Aneurysm of the anterior communicating artery (and of the anterior cerebral artery). **B**, Aneurysm of the posterior communicating artery. **C**, Aneurysm of the middle cerebral artery. **D**, Aneurysm at the bifurcation of the internal carotid artery.
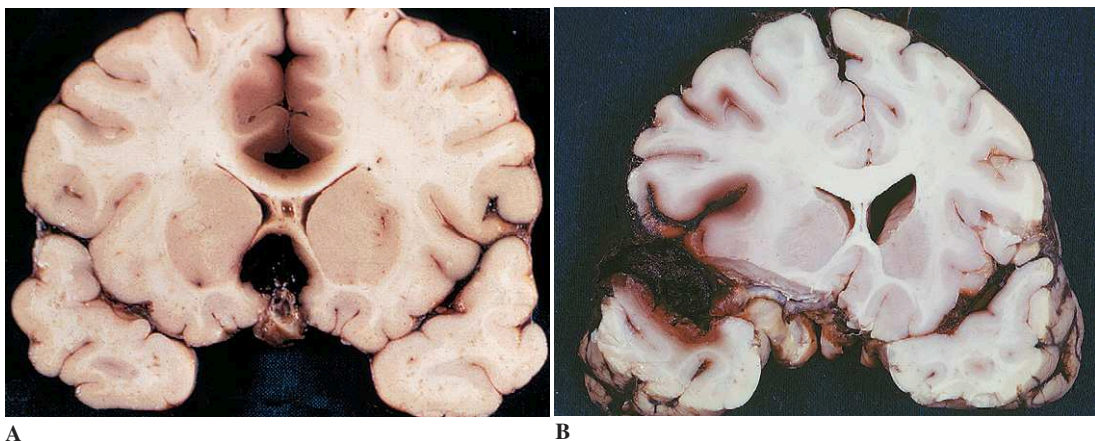
Figure 4-9. Hematomas resulting from the rupture of an arterial aneurysm. **A**, Bifrontal hematoma with ventricular rupture, following rupture of an aneurysm of the anterior communicating cerebral artery. **B**, Hematoma of the sylvian fissure following rupture of an aneurysm of the middle cerebral artery.

trauma to the neck (often perceived as quite minimal), cervical manipulation, exercise, administration of heparin, or in the context of fibromuscular dysplasia.

Fusiform Aneurysms

Fusiform aneurysms result from enlargement and widening of an arterial segment along its length. They are rare lesions and are more frequently encountered in the geriatric population, largely because of their association with complicated atherosclerosis. In young patients, they may be associated with deficiencies of the arterial muscularis and internal elastic lamina.

They are arbitrarily defined as being larger than 2.5 cm in diameter but may reach giant proportions (Fig. 4-10A). They involve most often the basilar artery (Fig. 4-10B), causing brainstem displacement and compression that can result in cranial nerve deficits.

When examined in cross section, fusiform aneurysms often have laminated thrombi within their lumen, the result of severe complicated atherosclerosis. Platelet fibrin or atheromatous emboli may travel distally in the arterial circulation to produce transient ischemic attacks or infarcts in branches of the vertebrobasilar circulation. Fusiform aneurysms only occasionally rupture to produce SAH.

Intraparenchymal Hemorrhage

The site and mechanisms of IPH vary according to etiology. The most common causes of IPH are, in roughly decreasing frequency, hypertension, cerebral amyloid angiopathy, anticoagulant administration, primary or secondary brain neoplasms, arteriovenous malformations and aneurysms, and prescription or "recreational" drug use.

Hypertension and Hypertensive Cerebrovascular Disease

Arterial hypertension has long been considered the major cause of intraparenchymal hemorrhage; however, given the increasing recognition and effective treatment of hypertension, the incidence of hypertensive hemorrhage is declining.

Mechanisms. Intraparenchymal hemorrhage resulting from hypertension is usually attributed to hypertensive cerebral microvascular disease (also known as *arteriosclerosis*, *arteriolosclerosis* [AS], *lipohyalinosis* [LH], or *AS/LH*, though the three terms are not necessarily synonymous). The molecular pathogenesis of AS/LH is even less well understood than that of atherosclerosis. Its evolution has been strongly associated with a documented history of hypertension; however, despite effective prophylactic treatment of severe and moderate hypertension in many countries, arteriosclerotic microvascular disease is still seen commonly in autopsy brain specimens, especially in the elderly.

Microscopic histopathologic features of AS include hyaline thickening (sometimes with degeneration of the internal elastic lamina), intimal fibromuscular hyperplasia, variable degrees of
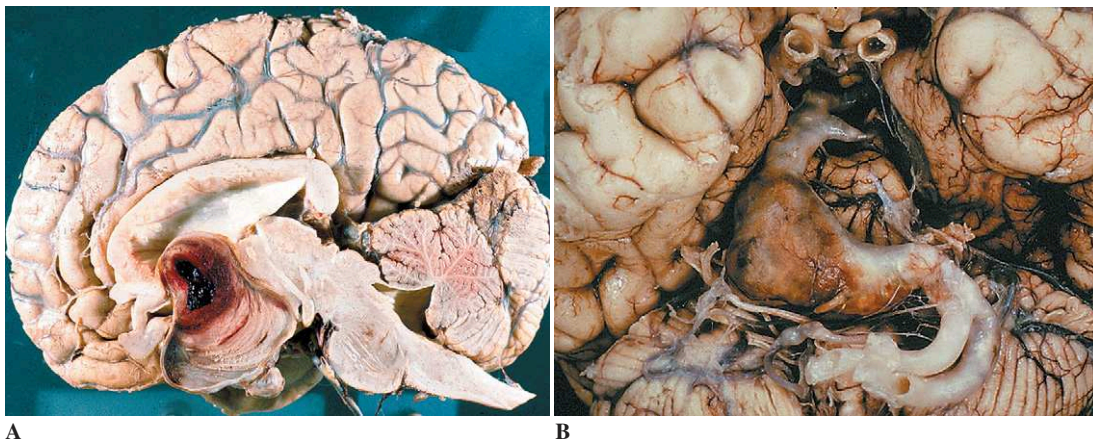
Figure 4-10. Giant atherosclerotic aneurysms. **A,** Anterior cerebral artery. **B,** Basilar artery.
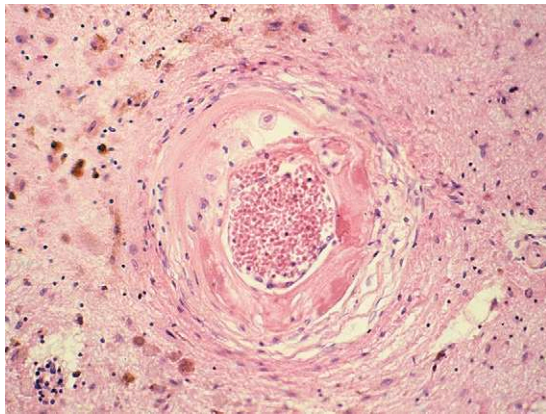
Figure 4-11. Arteriolosclerosis: narrowing of the lumen, concentric smooth muscle cell proliferation, and the presence of foamy macrophages in the arterial wall.

lumenal narrowing, thinning of the media, concentric "onion-skin" type smooth-muscle-cell proliferation, and the presence of foamy macrophages in the arterial wall (lipohyalinosis; Fig. 4-11). Fibrinoid necrosis may occur in malignant hypertension.

These microvascular lesions may lead to occlusion of arterioles or weakening of the vessel, which may rupture or become noncompliant, resulting in intraparenchymal hemorrhage, lacunes, and arteriopathic leukoencephalopathy. (See discussion of these topics later in this chapter.)

Hypertensive intraparenchymal hemorrhage is due to the rupture of small intracerebral arterioles 50 to 200 μm in diameter, the walls of which have been weakened by replacement of their normal media (muscular and elastic components) by collagenous fibrous tissue. Charcot-Bouchard microaneurysms may be found on affected arterioles (Fig. 4-12), though they may be absent, even when the brain parenchyma around a putative hypertensive hemorrhage is extensively and carefully sampled.

Evolution. The appearance of the hematoma varies depending on the duration between its onset and the time of examination.

Initially, the intraparenchymatous bleeding results in a collection of blood that is under tension, contains little parenchymatous debris, and displaces the cerebral structures (Figs. 4-13A, C, and D). Its edges are irregular, and small, petechial hemorrhages are present along its borders.

The bleeding may remain localized or may expand rapidly, resulting in increased intracranial pressure and brain herniation. It may also rupture into the ventricles, with subsequent passage of blood into the subarachnoid space. Less often, it may burst directly into the leptomeninges through the cerebral cortex.

In subacute hemorrhage (2 to 4 days), a phagocytic process occurs. The focal hemorrhage will be cleared by polymorphonuclear leukocytes and macrophages derived from blood monocytes.

A

B
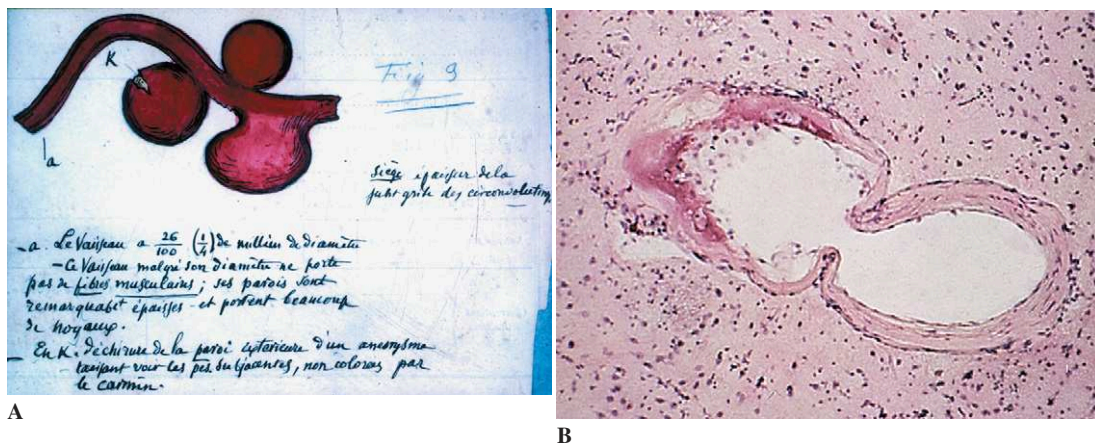
Figure 4-12. Miliary aneurysm (Charcot-Bouchard). **A**, Charcot-Bouchard microaneurysms as drawn by J. M. Charcot. The text says, in part: "Location: Hemispheric gray matter. The vessel is 26/100 (1/4) mm wide; in spite of its size, the wall is devoid of a muscle layer and is thickened." **B**, Microscopic appearance.
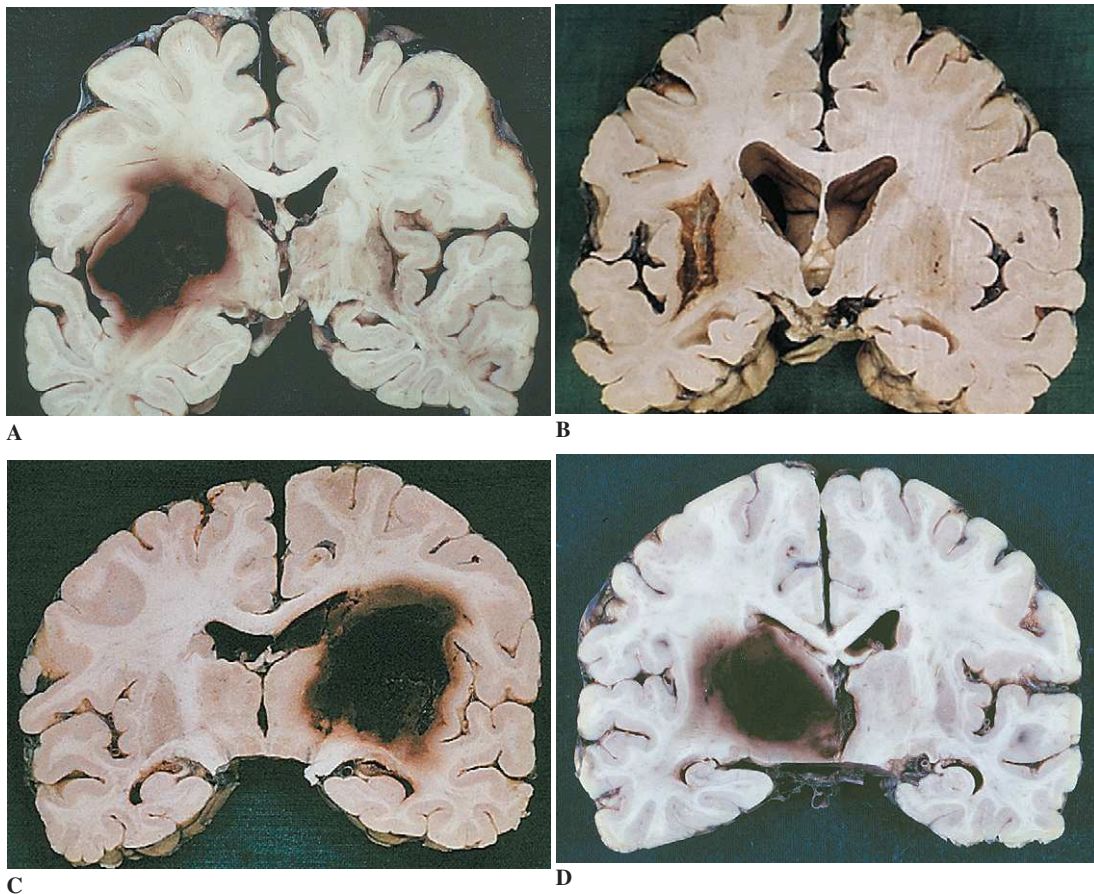
Figure 4-13. Basal ganglia hemorrhages. **A**, Lateral basal ganglia hemorrhage. **B**, Cystic scar of an old capsulolenticular hemorrhage. **C**, Massive hemorrhage. **D**, Medial thalamic hemorrhage.

Hematomas that are months to years old show only a cystic cavity with an orange/yellow margin and scarred brain tissue representing the remnants of resorbed blood (Fig. 4-13B). Microscopic sections around the edges of the hematoma show hemosiderin-laden macrophages and reactive astrocytes.

Topography. Approximately 80% of hypertensive intraparenchymal hemorrhages are situated in the cerebrum, mostly in the basal ganglia (see Fig. 4-13). Lateral basal ganglia (or putaminal) hemorrhages are the most frequent. They involve the putamen and external capsule and may extend (a) superiorly and medially into the internal capsule and lateral ventricle; (b) inferiorly into the white matter of the superior temporal gyrus; (c) medially, posteriorly, and inferiorly into the thalamus, the third ventricle, and the midbrain.

Medial hemorrhages initially involving the thalamus are rarer (10% to 20% of the hypertensive intraparenchymal hemorrhages). Hematomas may also be seen in the deep subcortical white matter.

Intracerebellar hemorrhages (Fig. 4-14) represent about 10% of all hypertensive intraparenchymal hemorrhages. The clinical evolution of these lesions is that of a space-occupying mass in the posterior fossa; rupture into the fourth ventricle may also occur.

Brainstem hemorrhages (Fig. 4-15) represent about 10% of hypertensive intraparenchymal hemorrhages. They are most often situated in the pontine tegmentum or basis pontis.

Cerebral Amyloid Angiopathy

Cerebral amyloid angiopathy (CAA) is more commonly associated with cerebral hemorrhage than

Figure 4-14. Intracerebellar hemorrhage.

with ischemia. It is characterized by the deposition of amyloid within the media and/or adventitia of small parenchymal and leptomeningeal vessels. Amyloid has a unique physicochemical structure of beta-pleated fibrils, giving it specific staining and optical properties: The deposits are metachromatic with cresyl violet or toluidine blue and give green fluorescence in ultraviolet light following staining with thioflavin T. Amyloid stains red with Congo red and gives apple green birefringence under polarized light (Fig. 4-16A). At the ultrastructural level, the deposits have a fibrillary appearance. The biochemical composition of the amyloid varies; several forms of cerebral amyloid angiopathy have been identified, based on the biochemical nature of the protein (see following discussion).

Figure 4-15. Brainstem hemorrhage.

Etiology. The most common form of CAA is that associated with deposition of Aβ protein, a small, 4.2-kDa peptide cleaved from the amyloid precursor protein (APP), which is encoded by a gene on chromosome 21. CAA has a strong association with Alzheimer disease or senile dementia of the Alzheimer type (AD/SDAT) and aging. These conditions are associated with excessive deposition of Aβ in both the brain parenchyma (as senile plaques and diffuse deposits) and vessel walls (as CAA), to a variable extent in different patient populations (see Chap. 8; Figs. 4-16B and C). Brains with moderate to severe CAA show a significantly higher frequency of ischemic and hemorrhagic lesions than do those with negligible CAA.

Relatively rare familial forms of CAA are also found in countries around the world. In a circumscribed coastal region of the Netherlands, an autosomal-dominant form of severe CAA (hereditary cerebral hemorrhage with amyloidosis, Dutch type: HCHWA-D) is attributed to a unique *APP* gene mutation (at codon 693). Massive Aβ deposition occurs within the media of cerebral arterioles, and fatal cerebral parenchymal hemorrhages frequently result.

APP codon 692 and 694 mutations appear to cause, respectively, a rare Flemish form of CAA (also with frequent intraparenchymal hemorrhage) and AD with prominent CAA in a family reported from the state of Iowa in the United States.

An Icelandic form of CAA leading to hemorrhagic stroke (hereditary cerebral hemorrhage with amyloidosis, Icelandic type: HCHWA-I), results from mutation in the gene encoding cystatin C/gamma-trace; hence, this condition is also sometimes described as *hereditary cystatin C amyloid angiopathy* (HCCAA). It causes cerebral bleeds in young and middle-aged adults. Brains from HCHWA-I patients show extensive deposition of gamma-trace protein within arteriolar walls, associated with degeneration of the affected vessel walls.

More recently, familial British and Danish forms of CAA have been described and attributed to unique mutations on the *BR12* gene, which is situated on chromosome 13. These two genetically determined forms of CAA, and others (e.g., meningovascular amyloidosis, associated with transthyretin deposition; familial amyloidosis of the Finnish type, caused by gelsolin deposition), are less consistently associated with intraparen-
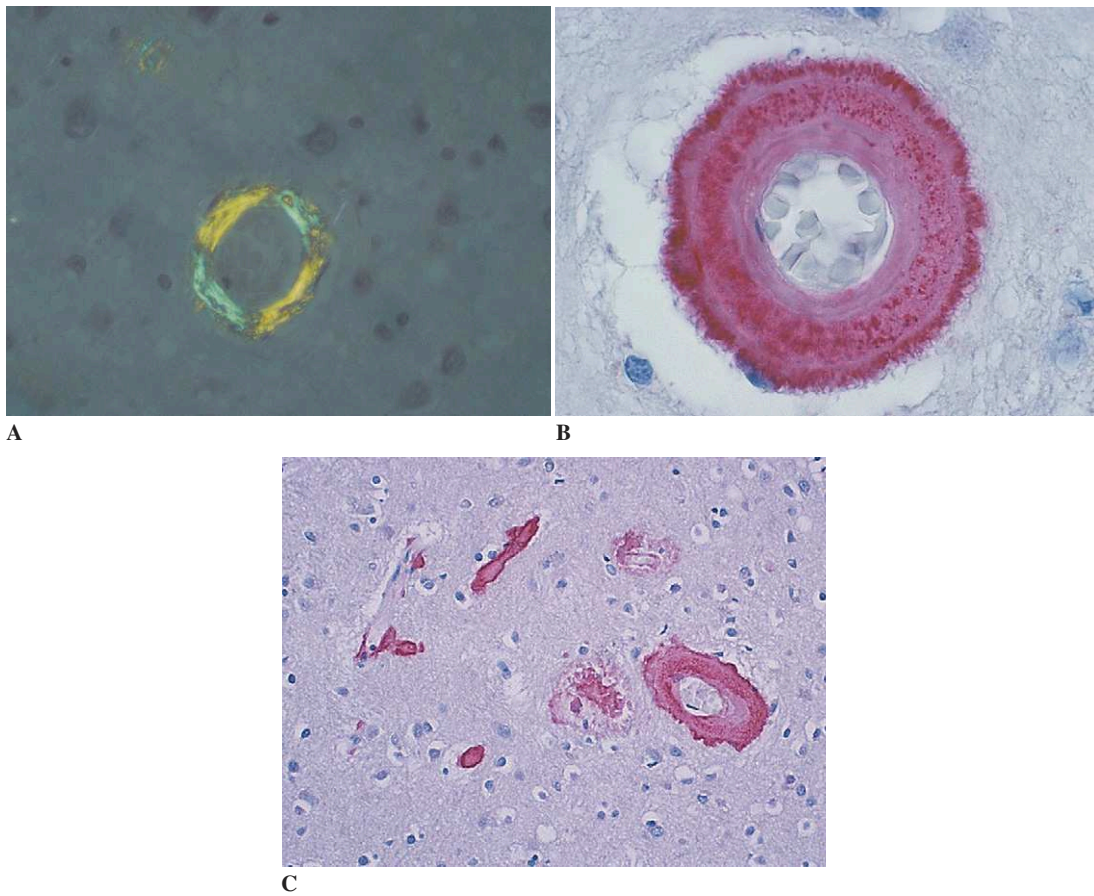
Figure 4-16. Cerebral amyloid angiopathy. **A**, Apple green birefringence of the vessel wall under polarized light with Congo red stain. **B** and **C**, Immunocytochemistry for Aβ shows diffuse infiltration of the arteriolar wall by amyloid. There is also involvement of the capillaries (dyshoric angiopathy) amyloid appearing to be "leaking" from the capillary wall into brain parenchyma (**C**).

chymal hemorrhage than are the Dutch, Flemish, and Icelandic familial variants of CAA.

Pathology.   All regions of neocortex and overlying meninges may be affected by CAA, with minor variations in the distribution of affected arteries among lobes. Whilst the cerebellum and its meninges are occasionally involved by CAA, the microvascular abnormality is almost never found within deep, central gray matter; subcortical white matter; the brainstem; or spinal cord. CAA may be patchy within the cerebral cortex and adjacent leptomeninges; it can be segmental and focally accentuated in given arterioles.

The term *CAA* encompasses amyloid deposition within the walls of small and medium-sized arteries and arterioles (congophilic angiopathy; see Figs. 4-16B, C) and capillaries (dyshoric angiopathy) where amyloid appears to be "leaking" from the capillary wall into the brain parenchyma (see Fig. 4-16C). These two types of angiopathy are almost always found together. Venous involvement is also common; however, the presence of amyloid does not always enable accurate identification of the vessel type.

Histologically, there is infiltration of the media and adventitia of small vessels by an acellular amorphous eosinophilic substance, which gives the vessel wall a homogeneous, pale appearance, often allowing the diagnosis to be made on routine stains. In addition, some affected vessels, particularly pia mater arterioles, have a "double-barrel" appearance
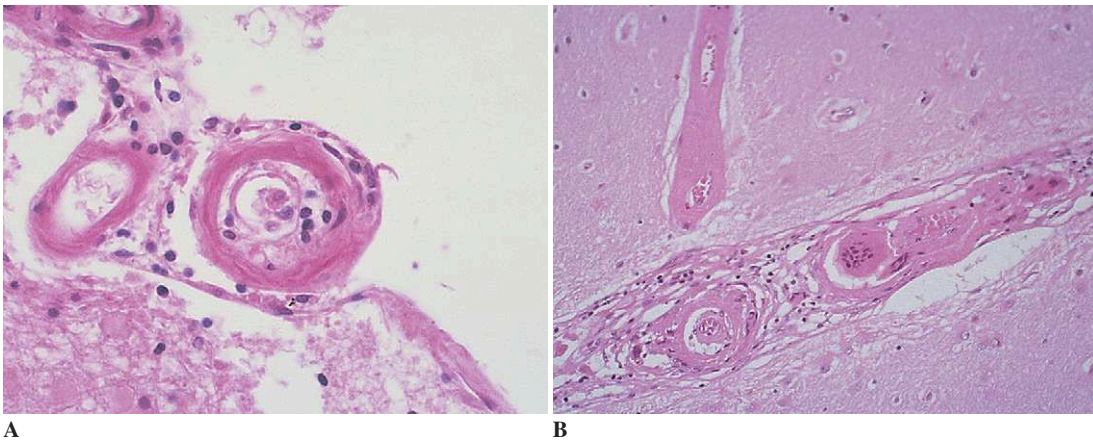
Figure 4-17. Cerebral amyloid angiopathy infiltration of the vessel wall by the acellular amorphous eosinophilic amyloid substance. Note "double barrel" appearance of a leptomeningeal arteriole (**A**) and inflammatory granulomatous reaction (**B**).

(Fig. 4-17A). Amyloid deposition in the arterial wall causes atrophy of the medial smooth muscle cells; these changes disrupt the vascular architecture and weaken the affected arterial walls. A variety of secondary changes may be found in the affected vessels, including fibrosis, microaneurysm formation, chronic inflammation (sometimes granulomatous [Fig. 4-17B]), fibrinoid necrosis, thrombosis, and (very rarely) vessel-wall calcification.

Complications of CAA. The extent of amyloid deposition within vessel walls correlates with increasing risk of intraparenchymal hemorrhage. CAA causes hemorrhages with highly distinctive clinicopathologic features (Fig. 4-18). They occur within the cortex and subcortical white matter ("lobar" hemorrhages) and often dissect into the subarachnoid space or the lateral ventricles, sometimes both. This "lobar" localization of the hemorrhages has a close correspondence to the topography of CAA, a cortical and meningeal vasculopathy. CAA may be readily detected in fragments of brain parenchyma evacuated with a hematoma. Bleeds may occur, over months or years, into different lobes of the cerebrum on both sides of the brain. As many as one third of patients with CAA-related lobar hemorrhage may also have clinical evidence of hypertensive microangiopathies
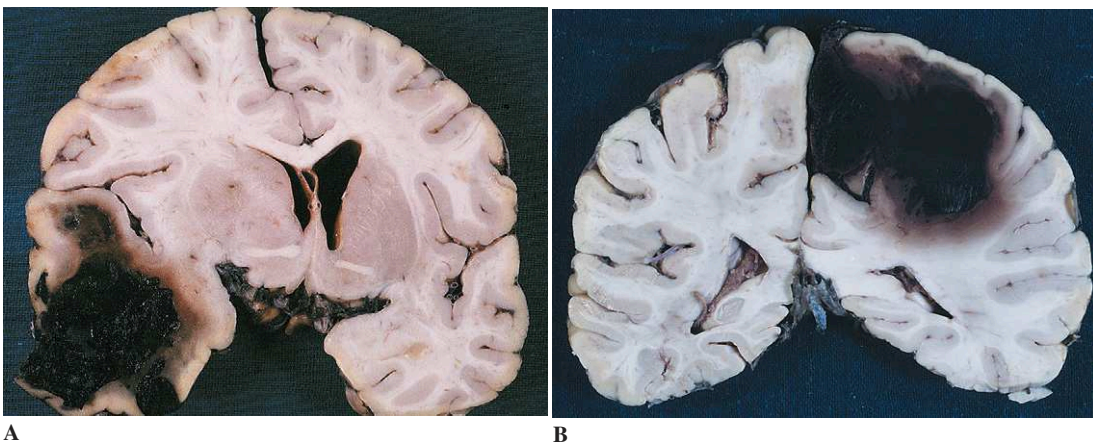
Figure 4-18. Lobar intracerebral hemorrhages in patients with cerebral amyloid angiopathy involving the right temporal lobe (**A**) and the left parieto-occipital region (**B**).

and both AS/LH, and CAA may be found in the brains of such individuals.

Other rare clinical and pathologic manifestations of CAA include SAH *without* an intraparenchymal hemorrhage, leukoencephalopathy (see later discussion), granulomatous angiitis (see Fig. 4-17B), recurrent transient neurologic symptoms (possibly due to microinfarcts and/or miliary hemorrhages in the cerebral cortex), and brain infarct.

Vascular Malformations

Vascular malformations may be found in the CNS parenchyma, overlying dura, or (rarely) at both sites.

Arteriovenous Malformations.   Clincally, *arteriovenous malformations* (AVMs) are the most important subgroup of vascular malformations. They rarely become manifest clinically beyond the age of 60 years. AVMs may cause intraparenchymal or subarachnoid hemorrhage. They usually occur in the MCA territory, often involving a wedge-shaped area of brain parenchyma and overlying leptomeninges; however, they may be seen anywhere in the CNS, including posterior fossa structures and sometimes on the circle of Willis.

An AVM represents an abnormal direct communication between one or more arteries of the brain parenchyma and one or more draining veins, without an intervening capillary bed. The shunt is often made of a core of abnormal channels called the *nidus*. Arteriovenous fistulas have single-hole arteriovenous shunts. The arterial feeders are supplied either by brain arteries or by dural arteries. The venous drainage may take place in the superficial or the deep draining systems of the brain. The morphologic features of AVM are characteristic, both grossly and microscopically (Fig. 4-19A). An AVM is recognized histologically as a collection of vascular channels of variable mural thickness and diameter, embedded within abnormal, gliotic, and occasionally malformed brain parenchyma. The brain parenchyma may show morphologic evidence of old hemorrhage, but an absence of blood breakdown products does not exclude the possibility that the AVM has bled prior to resection.
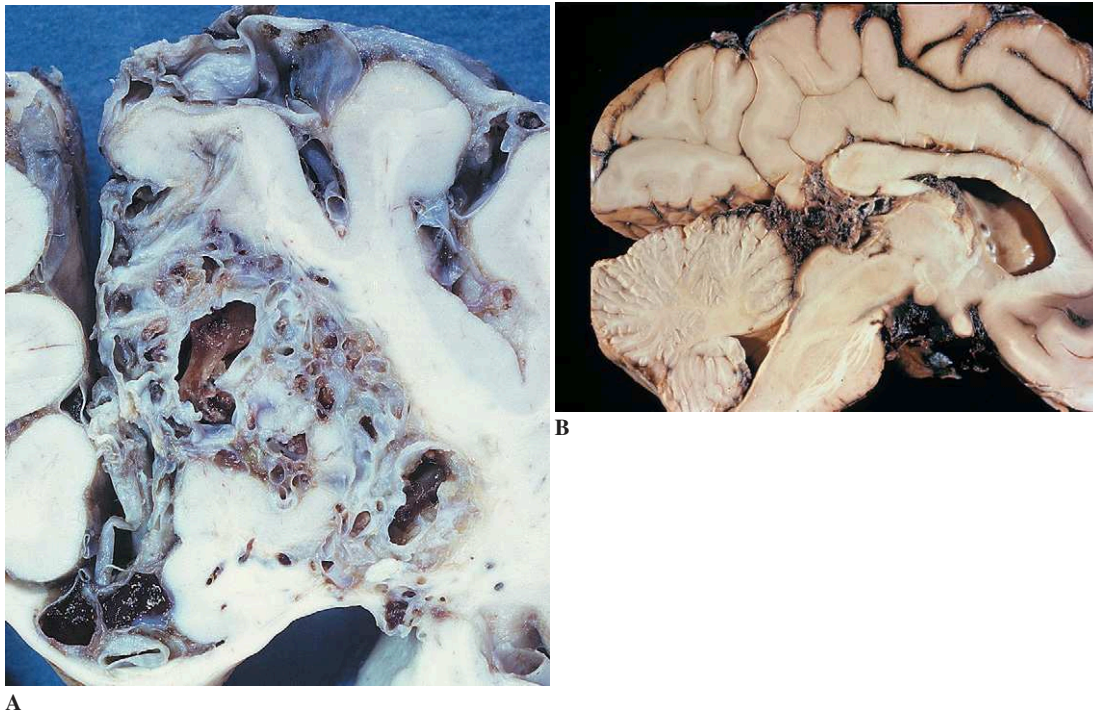
Figure 4-19.   Vascular malformations. **A**, Medial frontal cerebral arteriovenous aneurysm. **B**, Vein of Galen aneurysm.

Thrombosed and recanalized vascular channels are usually present within an AVM. Other abnormalities noted within them are hyalinized, sometimes calcified (very rarely, ossified) arterial walls or abnormalities in the blood vessels characteristic of intimal fibromuscular hyperplasia.

AVMs become symptomatic following rupture of the vessel wall and bleeding, direct pressure on adjacent brain substance, or because of a "steal" of blood from adjacent structures in the setting of arteriovenous shunting. They are associated with berry aneurysms in 10% of cases.

AVMs also occur in the spinal cord, where they manifest as dural arteriovenous fistulas.

They are usually treated by excision or iatrogenic embolization therapy (the latter performed with the intention of occluding and obliterating the AVM nidus).

Venous Angiomas. *Venous angiomas* (VAs) consist of one or more dilated, often grossly apparent veins and their smaller tributaries, lacking an obvious arterial component. A single tortuous vein (e.g., in the spinal subarachnoid space) is described as a *varix* (Fig. 4-19B). Component vessels of a VA are more dilated and have thicker walls than normal veins, and brain parenchyma between the vessels shows negligible reactive changes or old hemorrhage. VAs are usually found as an incidental lesion at autopsy.

Capillary Telangiectases. *Capillary telangiectases* are common incidental lesions at autopsy. They consist of multiple dilated capillaries without alterations of the surrounding brain substance. On macroscopic examination, both VAs and capillary telangiectases appear as small, fairly well-defined hemorrhagic lesions that initially suggest a localized region of bleeding, for example, petechial hemorrhage.

Cavernous Hemangiomas. Cavernous hemangiomas, which are less common than AVMs, appear as closely packed blood vessels (of varying wall thickness) without intervening CNS parenchyma. They have a predilection for the pons and subcortical white matter; in these loci, the clinical presentation of the patient may mimic that of a primary CNS neoplasm, behaving as space-occupying lesions, producing mass effect and seizures.
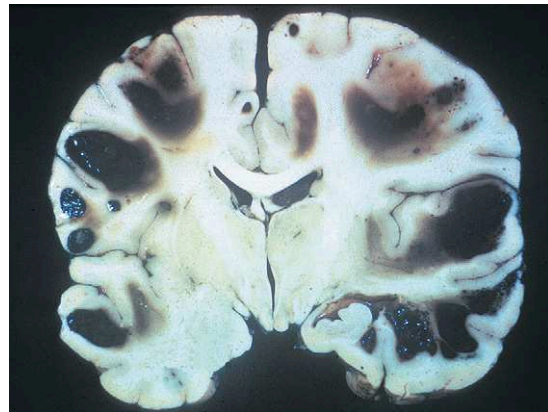
Figure 4-20. Multiple lobar hemorrhages in a patient with leukemia.

Though they do not usually cause massive hemorrhage, they are almost always surrounded by deposits of hemosiderin on histologic sections, suggesting slow or recurrent leakage of blood from component vessels. Familial syndromes of cavernous angiomas have recently been linked to genes on chromosomes 3q, 7q, and 7p.

Systemic and Miscellaneous Factors

IPH may result from systemic factors and diseases that include thrombocytopenia, coagulopathy (either iatrogenic or secondary to hepatic failure), hemophilia, disseminated intravascular coagulation (DIC), leukemia (Fig. 4-20), and abuse of "recreational drugs" such as cocaine and amphetamines. The bleeds may mimic, in terms of both their extent and topography, hematomas associated with hypertension and CAA.

Ischemic Vascular Pathology of Arterial Origin: Infarction

The terms "cerebral infarct," "cerebral softening," and "encephalomalacia" are used to denote an area of CNS tissue necrosis localized to a particular territory of vascular supply. In most cases, the infarct is due to occlusion of a branch of the feeding arterial tree. It may also follow severe decrease in blood flow in the absence of arterial occlusion. In venous infarction, the tissue ischemia is due to the occlusion of a large vein and consequent stasis.

Figure 4-21. Recent anemic or pale infarct involving the territory of the right anterior cerebral artery.

General Features

Arterial occlusion of sufficient duration produces ischemic necrosis. The gross and microscopic appearances associated with infarction are manifest by a series of sequential changes that are distinctive regardless of the site of the affected territory within the CNS.

The main types of infarction generally recognized are *anemic* (*pale*) *infarcts*, in which the cellular reactions to ischemic necrosis predominate (Fig. 4-21), and *hemorrhagic infarcts*, wherein the lesions are associated with hemorrhagic phenomena. The latter especially involve the cortical ribbon and the basal ganglia (Fig. 4-22).

Anemic (Pale, Bland) Infarction

On macroscopic examination early in the evolution of an anemic (pale, bland) infarction, the lesions are seen to be poorly circumscribed; in the first six hours or so, no alteration can be demonstrated with the naked eye, though the neural tissue might already be irreparably damaged. From about 8 to 48 hours the damaged zone becomes discolored and the demarcation between the white and gray matter is indistinct. Edematous swelling is apparent and is sometimes accompanied by vascular congestion, which is more marked in the cortex. At this stage, the softer consistency of the involved area is the only feature that permits the infarct to be recognized macroscopically (after two to three weeks of formalin fixation). From 2 to 10 days the swelling persists, progressively decreasing over time, while the softened tissue becomes more friable and the boundaries of the infarcted territory become better defined.

Microscopically, after 6 to 12 hours the neurons within the infarcted territory demonstrate the features of acute ischemic cell injury: the cytoplasm is

A   B
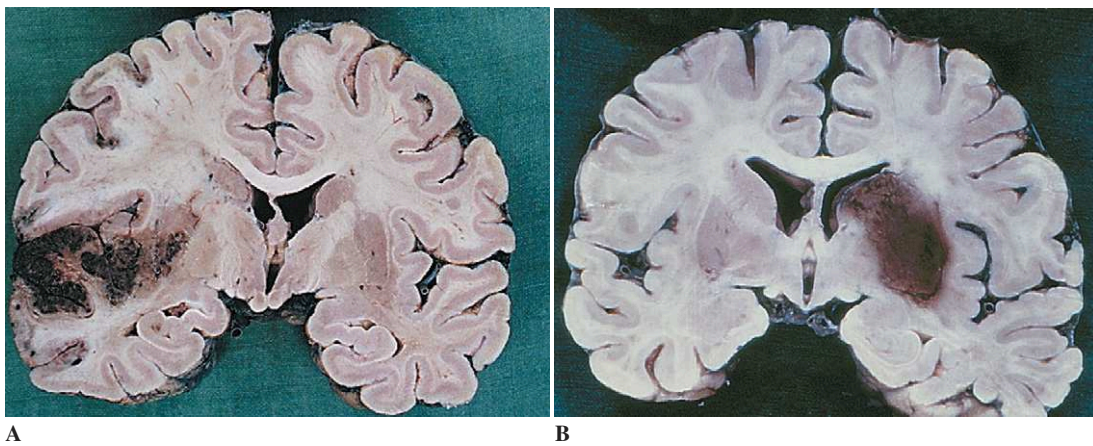
Figure 4-22. A and **B,** Hemorrhagic infarcts.
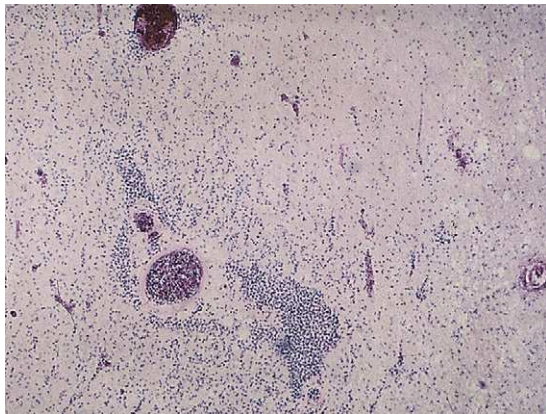
Figure 4-23. Microscopic features of cerebral infarcts. Diffusely scattered and perivascular groups of polymorphonuclear leukocytes after 35 hours.

eosinophilic, the Nissl substance is dispersed, the nucleus is shrunken, and the nucleolus is no longer visible (see Fig. 1-2). In the cortex and white matter, the capillary blood vessels show endothelial swelling accompanied by vasogenic and cytotoxic edema fluid and by some extravasation of red blood cells (even in anemic infarction). Glia also show ischemic cell damage and, somewhat later, myelinated fibers lose their usual tinctorial affinity. Between 24 and 48 hours there is evidence of an emigration of neutrophils, which can be severe and may simulate an infectious process (Fig. 4-23).

After 48 hours the leukocytes are replaced by macrophages. These cells, which are laden with sudanophilic breakdown products of myelin disintegration, cluster around the swollen walls of the capillary blood vessels. The macrophage proliferation becomes considerably more marked after five days.

After 10 days liquefaction begins, and from the third week onward the process of cavitation becomes more evident. From then on, the area of necrosis is gradually replaced by yellowish-gray tissue, which causes depression of the tissue. Macrophage proliferation persists but decreases during the subsequent months and the proliferation of reactive (gemistocytic) astrocytes increases. After a few months, the necrotic zone presents as a cystic cavity with ragged outlines, intersected by vascular connective tissue strands and covered by leptomeninges on its cortical surface (Fig. 4-24). During the phase of scar formation, the residual cystic cavity is surrounded by a glial proliferation while a few macrophages remain along the persisting vascular connective tissue strands that run across the cavity.

Hemorrhagic Infarction

This type of infarction is classically regarded as distinct from anemic (bland) infarction, although, as mentioned previously, microscopic evidence of red-blood-cell extravasation is often found in the latter. In hemorrhagic infarction, patches or
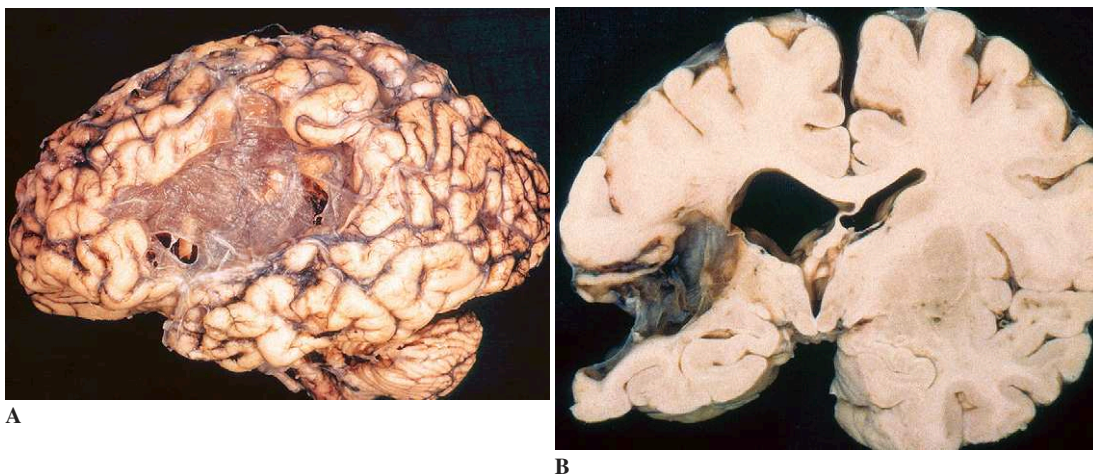
Figure 4-24. Old cystic infarct in the territory of the middle cerebral artery. **A**, Left cerebral hemisphere. **B**, Coronal section. Note the involvement of a large part of the middle cerebral artery territory, sparing the temporal lobe.
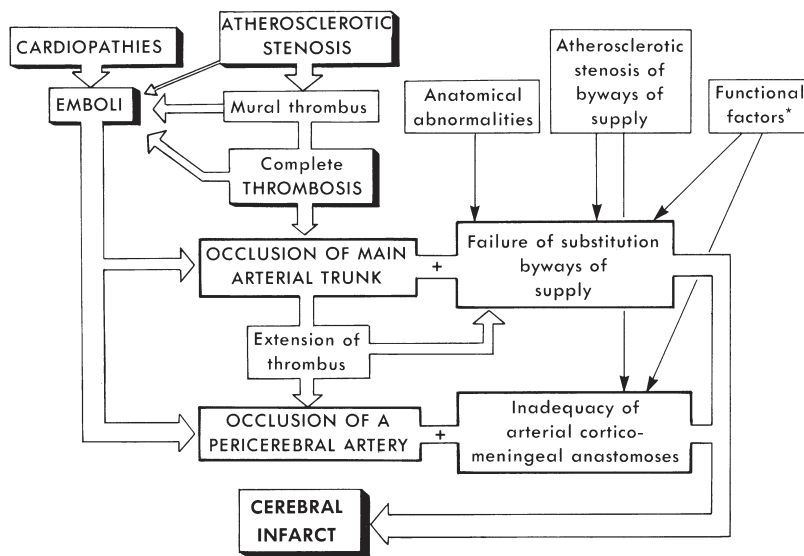
Figure 4-25. Etiological and pathophysiological factors determining cerebral infarcts. *Functional factors*: decrease in caliber of ischemic arteries; drop in blood pressure; loss of autoregulation of arterial caliber.

confluent areas of hemorrhage are evident, particularly in the cortex. These hemorrhages may involve the entire extent of the ischemic region (see Fig. 4-22A) and, in the cerebral cortex, predominate along boundary zones supplied by meningeal arterial anastomoses; in middle occlusion, the basal ganglia are involved (see Fig. 4-22B). It is generally accepted that an important pathogenetic mechanism of hemorrhagic infarction is the fact that tissue reperfusion follows thrombolysis or mobilization of the thrombus. Bleeding then occurs in a capillary bed damaged by the ischemic insult (see Fig. 4-26F). Indeed, this type of infarction most often follows cerebral embolization, where breakdown of the occluding thrombus and distal migration commonly occurs.

Pathophysiology and Etiology

Cerebral infarction caused by prolonged ischemia localized to a particular vascular territory is commonly secondary to arterial occlusion. This may be due to either thrombosis (most often due to atherosclerosis) or to embolization, often of cardiac origin. Where careful examination of the arterial tree fails to disclose an arterial occlusion, cerebral infarcts may be presumed to be caused by emboli that have undergone secondary lysis. They may also result from severe and prolonged hypotension involving arteries with extensive or multifocal

atheromatous stenosis leading to hypoperfusion of tissue, or follow stenosis associated with arterial spasm. The appearance and extent of the cerebral infarct depends on a number of modifying hemodynamic and etiological factors (Fig. 4-25).

Hemodynamic Factors

Presence and Efficacy of Anastomotic Pathways of Vascular Supply. In the course of arterial occlusion, the ischemic cerebral territory is partially reirrigated by arteries at the base of the brain (circle of Willis, ophthalmic artery) and by superficial corticomeningeal anastomoses (Fig. 4-26A). This potential arterial anastomotic reirrigation supply explains why in most cases of arterial occlusion the resulting area of cerebral softening remains limited to only part of the vascular territory that is normally served by the occluded artery (Figs. 4-26D and E). However, the extent of this reinforcement varies from case to case and anatomical variations from the norm are frequent (Fig. 4-26B). Moreover, these anastomotic pathways may themselves either be occluded by atherosclerotic lesions or become incompetent as a result of thrombus propagation (Fig. 4-26C).

Site of Occlusion. Proximal occlusion of a blood vessel such as the internal carotid artery may, because of collateral flow from the contralateral arterial network and via the ophthalmic artery,
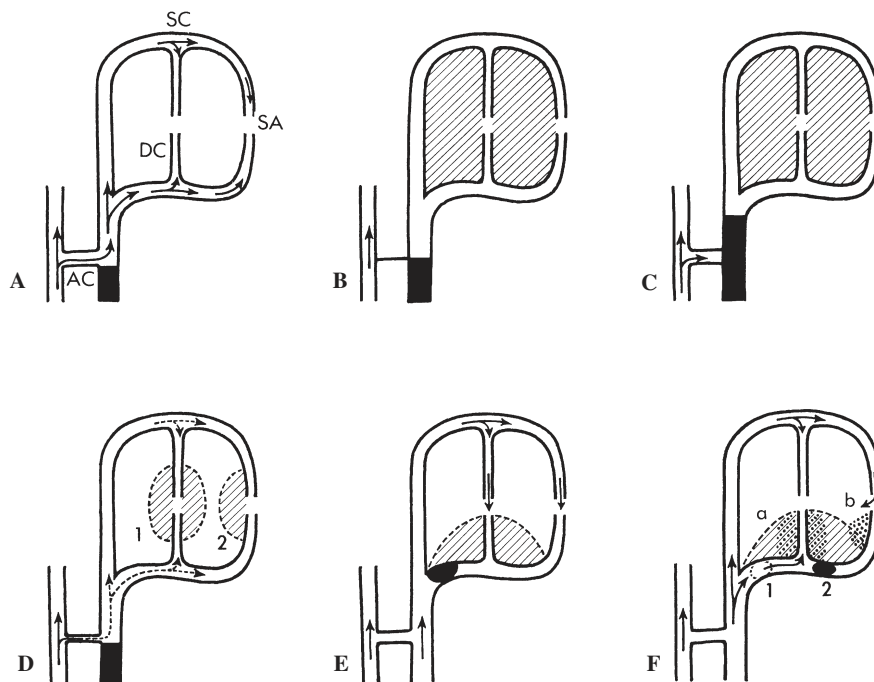
Figure 4-26. Respective roles of the anastomotic substitution pathways of circulatory supply and of the type of vascular occlusion in determining the occurrence and extent of cerebral lesions (AC = anastomotic vascular network; SC = superficial arterial circulation; DC = deep vascular territory; SA = superficial meningeal anastomoses). **A**, Arterial occlusion, but with effective and adequate anastomotic substitution network of supply: no infarction. **B**, Arterial occlusion without anatomically effective anastomotic network of supply (AC): massive infarction of the corresponding cerebral territory. **C**, Arterial occlusion extending beyond the origin of the anastomotic network of supply. No anastomotic substitution by way of vascular supply: massive infarction. **D**, Occlusion proximal to the anastomotic network of supply. Insufficient anastomotic substitution by way of arterial supply. Anemic infarct of variable extent in territory (2) distal to the junction of two vascular territories (last field of irrigation or watershed infarct) and in border zone between superficial and deep vascular territories (1). **E**, Proximal occlusion of one dividing branch; anastomotic substitution by way of vascular supply provided by superficial meningeal anastomoses: limited proximal infarction. **F**, Embolic occlusion. Mobilization of thrombus from 1 to 2. Sudden occlusion in 1, resulting in total ischemia of both deep and superficial vascular territories and in hemorrhages in the superficial territory when border zones are undergoing reirrigation (b); secondary mobilization of thrombus in 2, with hemorrhages due to secondary eruption of blood into the originally ischemic deep vascular territory (a; hemorrhagic infarct).

produce only a limited lesion. Reirrigation is generally adequate in the proximal territory; lesions will then predominate in the distal regions ("last fields of irrigation") or at the junction of two vascular territories ("watershed" or "boundary-zone infarct"; see Fig. 4-26D). Should the proximal arterial anastomotic network (circle of Willis) be anatomically incompetent (see Fig. 4-26B) or pathologically occluded (see Fig. 4-26C), the infarct will then be massive and involve the entire arterial territory.

In the case of distal occlusion involving an end artery, such as the middle cerebral artery, collateral flow is dependent on a superficial anastomotic network, which is often precarious, and as a result, the infarct proximal to the circle of Willis will usually be extensive (see Fig. 4-26E).

Type of Occlusion. In general, thrombosis, which leads to gradual occlusion of a vessel, allows for adaptive mechanisms of collateral flow. The resulting infarct is then usually pale and of relatively limited extent.

By contrast, emboli often produce sudden occlusion, with cessation of flow where reirrigation is inadequate. The resulting infarct is hence usually

extensive. In addition, migration and secondary fragmentation of the embolus is frequent. This accounts for the hemorrhagic component of the infarct frequently observed in the proximal part of the ischemic territory following sudden reentry of arterial blood into damaged tissue (see Fig. 4-26F).

Etiologic Factors

Atherosclerosis

GENERAL FEATURES. *Atherosclerosis* is the principal etiologic factor in the production of cerebral infarction. The structural features and development of atherosclerosis in the brain are comparable to those in other organs. With regard to the brain, atherosclerosis affects chiefly large intracranial blood vessels and the carotid arteries in the neck. It predominates at sites of bifurcation (particularly at the level of the carotid sinus), at sites of curvature of the arteries, and at sites where the arteries are fixed. The distribution of atherosclerosis in the thoracocervical arterial tree and in the circle of Willis is illustrated in the classical diagram by Baker and Fisher (Fig. 4-27). The internal carotid arteries and the basilar artery are the most heavily involved, both at their origins and at their terminations. The arteries over the convexity are less severely affected than the vessels at the base of the brain.

Increase in size of the plaque and local changes such as intramural hemorrhage, calcification, and mural thrombosis lead to increasing arterial stenosis (Fig. 4-28). It is generally believed that the latter must involve more than 75% of the original lumen of the artery to cause a clinically significant decrease of blood flow. The evolution of arterial stenosis is variable (Fig. 4-29); the main complication lies in the development of arterial thrombosis secondary to local changes. Thrombosis may occlude the arterial lumen completely, and as a result, a new event may take place, namely, anterograde extension of a so-called *stagnation thrombus*, usually into the first sizable collateral branch. The thrombus is ultimately replaced by loose-textured connective tissue in which new vessels of variable perfusion capacity develop. In many cases, the mural thrombus can fragment; in doing so, it gives rise to arterial emboli (artery-to-artery emboli). These emboli are believed to account for cerebrovascular accidents from which some degree of recovery is possible, particularly when the

Lesions in increasing frequency.
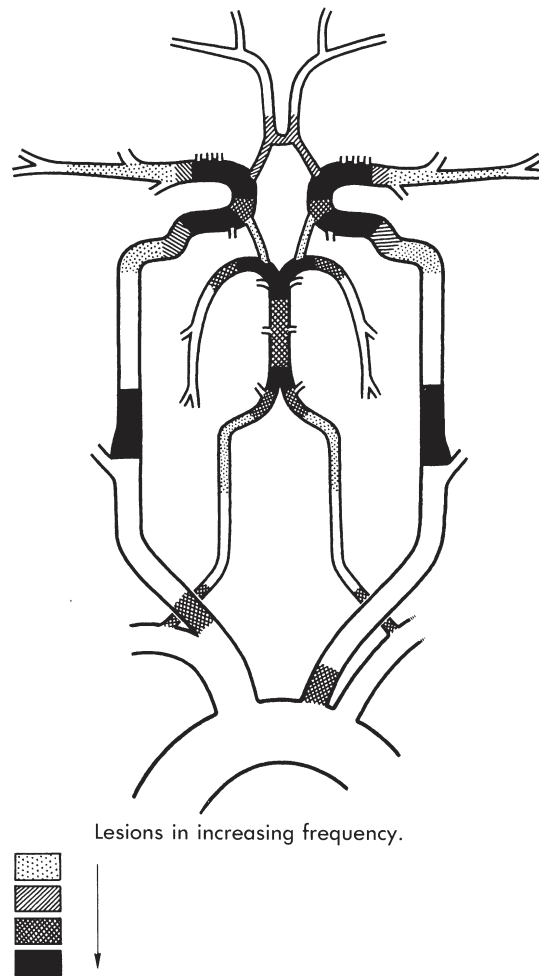
Figure 4-27. The frequency and severity of atherosclerotic lesions in the arterial cervicocerebral tree.

ischemic period is of short duration ("transient ischemic attacks"); impairment may be permanent when disintegration of the thrombus has not been sufficiently rapid.

ATHEROSCLEROTIC THROMBOSIS. *Internal carotid thrombosis* develops in a setting of stenosing atheromatous lesions (see Figs. 4-27 and 4-29). These lesions are most often observed at the carotid bifurcation or at the level of the carotid sinus. A stagnation thrombus is formed and usually extends rostrally to the ostium of the first collateral branch, namely, the ophthalmic artery; collateral contribution through the external carotid artery may ensure more or less adequate perfusion of the proximal hemispheric territory. The zone of infarction is then limited to the distal portion of the middle cerebral
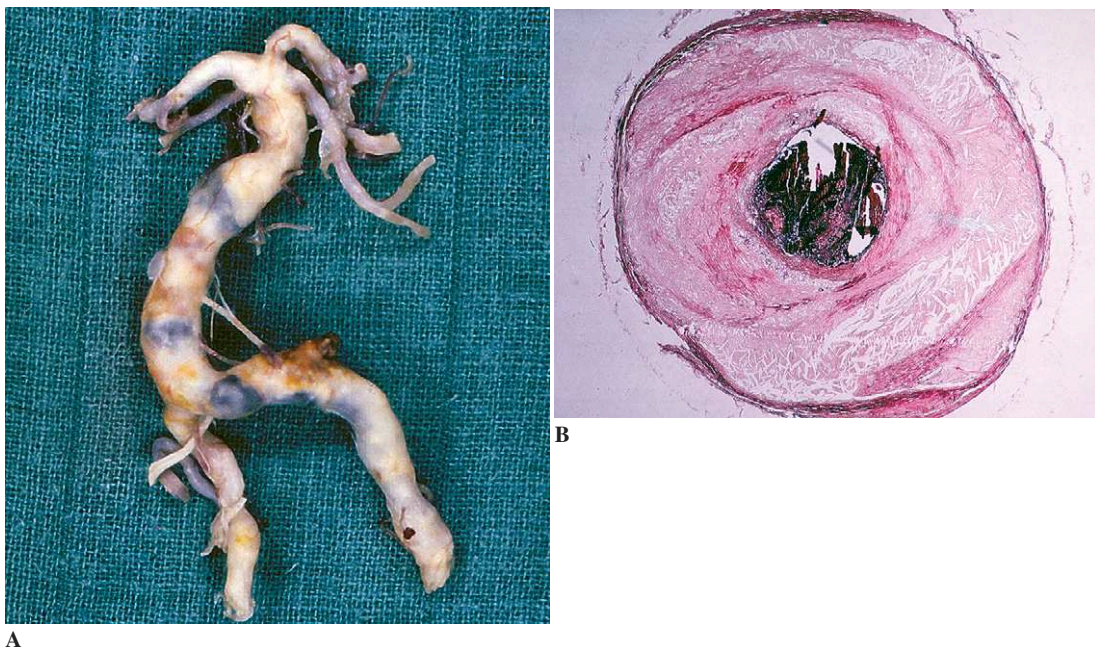
Figure 4-28. Stenosing atherosclerotic lesion. **A**, Gross appearance of atherosclerosis of the basilar artery. **B**, Microscopic appearance. Note narrowing of the arterial lumen by arteriosclerotic lesions.

artery territory and, to a lesser extent, the anterior cerebral territory. Anterograde extension of the thrombus beyond the ophthalmic artery and beyond the origin of the posterior communicating and the anterior cerebral arteries will then result in massive infarction. Less often, thrombosis takes place at the level of the carotid syphon, that is, at the termination of the internal carotid artery. Occlusion by atheromatous lesions in this terminal portion of the artery is usually accompanied by retrograde
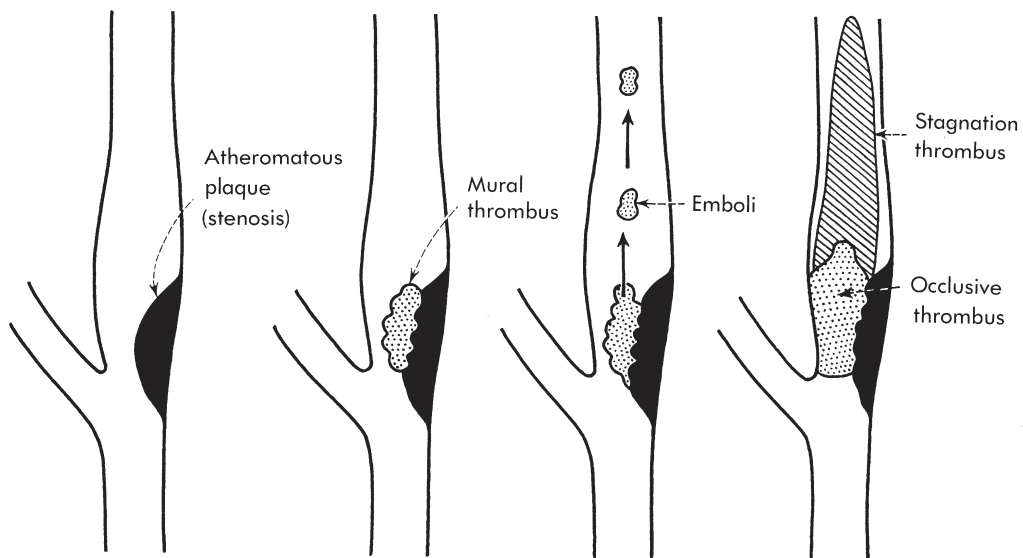
Figure 4-29. Evolution of lesions caused by atheromatous carotid stenosis.

extension of the thrombus into the carotid sinus. When the lesion is old and organized, it may be difficult to determine whether thrombosis of the carotid artery originally took place at its distal or proximal end.

Isolated thrombosis of the middle or anterior cerebral artery is much less common than internal carotid thrombosis. It often follows extension of a carotid thrombus beyond the bifurcation of the internal carotid artery.

Vertebral artery thrombus may be clinically and/or pathologically silent or, if the thrombosis does not reach the ostium of the posterior inferior cerebellar artery and provided it is unilateral, may cause discrete lesions.

Basilar artery thrombosis supervenes on atherosclerotic lesions, which are common at this site. It may also result from ascending extension of vertebral artery thrombosis and may cause infarcts in the midbrain or pons.

Thrombosis of a posterior cerebral artery is seldom an isolated event. It usually occurs as a result of anterograde extension of a basilar artery thrombosis. When the posterior cerebral artery is a tributary of the internal carotid artery, its occlusion may be secondary to extension from a thrombosed carotid. As a result, these lesions frequently result in massive hemispheric infarction.

Subclavian artery thrombosis may give rise to ischemic lesions in the vertebrobasilar territory by diverting arterial flow (so-called *subclavian steal syndrome*).

EMBOLI OF ATHEROSCLEROTIC ORIGIN.   Emboli of atherosclerotic origin are artery-to-artery emboli and play an important role in the development of cerebral infarcts (see Fig. 4-29). They can arise from ulcerated plaques anywhere along the arterial tree or from the aortic arch and spread distally. The most common sites of origin are the carotid sinus and the vertebral and basilar arteries.

Platelet emboli frequently detach as small fragments from a thrombus. They may cause transient cerebral accidents or occlude terminal arterial branches.

Fibrin emboli originate from a mural thrombus or from fragmentation of a stagnation thrombus. They often produce occlusion in the branches of larger arteries (middle, anterior, or posterior cerebral) in a setting of carotid or vertebrobasilar thrombosis.

Purely atherosclerotic emboli most often are the result of spontaneous detachment of thrombotic material from ulcerated plaques.

Cardiac Emboli.   *Cardiac emboli* are a frequent cause of arterial occlusion (Fig. 4-30). They can originate from an atrial thrombus in mitral stenosis, atrial vegetations, a mural thrombus in the course of a myocardial infarct, various forms of endocardial vegetations (e.g., bacterial endocarditis or nonbacterial thrombotic endocarditis), or a cardiac prosthesis. Emboli of noncardiac origin are less frequent.

Other Causes.   *Arteritis* is a rare cause of cerebral infarction. Syphilitic arteritis, which affects especially the basal arteries, is rarely seen today. Tuberculous and other bacterial meningitides, as well as meningitis caused by parasitic organisms, can produce occlusive arteritic lesions that may produce cerebral or spinal infarcts (see Chap. 5). "Collagen-vascular" diseases, especially polyarteritis nodosa, may sometimes affect small superficial arterioles and, more infrequently, the deep intracerebral or spinal intramedullary vessels; the resulting parenchymatous lesions consist of circumscribed, widely disseminated foci of softening. In children, otitis media and rhinopharyngitis can occasionally be a cause of internal carotid occlusion, which may result in cerebral infarction.

Granulomatous angiitis of the nervous system (GANS) is a disorder that involves multiple small- to medium-sized parenchymal and subarachnoid vessels characterized by chronic inflammation, multinucleated giant cells, and destruction of the vessel wall. It may or may not be associated with amyloid angiopathy, as discussed previously.

Figure 4-30. Arterial embolus (superficial temporal artery). Note normal appearance of the arterial wall (H and E).

Injuries to the neck or in the mouth may give rise to internal carotid occlusion.

Vascular malformations, especially AVMs, are sometimes associated with cerebral infarcts (see earlier discussion in this chapter). In addition, cerebral infarcts occur frequently in the course of severe SAH. The postulated mechanism of injury is arterial spasm induced by blood extravasation into the subarachnoid space.

Topography

Regardless of the specific cerebral or spinal territory involved by an infarct, the extent of the infarct will follow the general rules outlined previously. Within the limitations already indi-

cated, its localization will correspond to a greater or lesser portion of the relevant vascular territory.

Cerebral Infarcts

Cerebral infarcts need to be evaluated post mortem after complete anatomical study of both the carotid and the vertebrobasilar system, from the aortic arch up to the cerebral branches (Fig. 4-31). The study must also include a meticulous examination of the heart cavities, heart valves, and myocardium.

Infarcts of the Carotid Territory. Infarction may involve all or only part of each of the territories of the branches of the internal carotid artery (Fig. 4-32). A single infarct may be found, but it is

Figure 4-31. The caroticovertebral vascular tree and its chief anastomotic pathways.
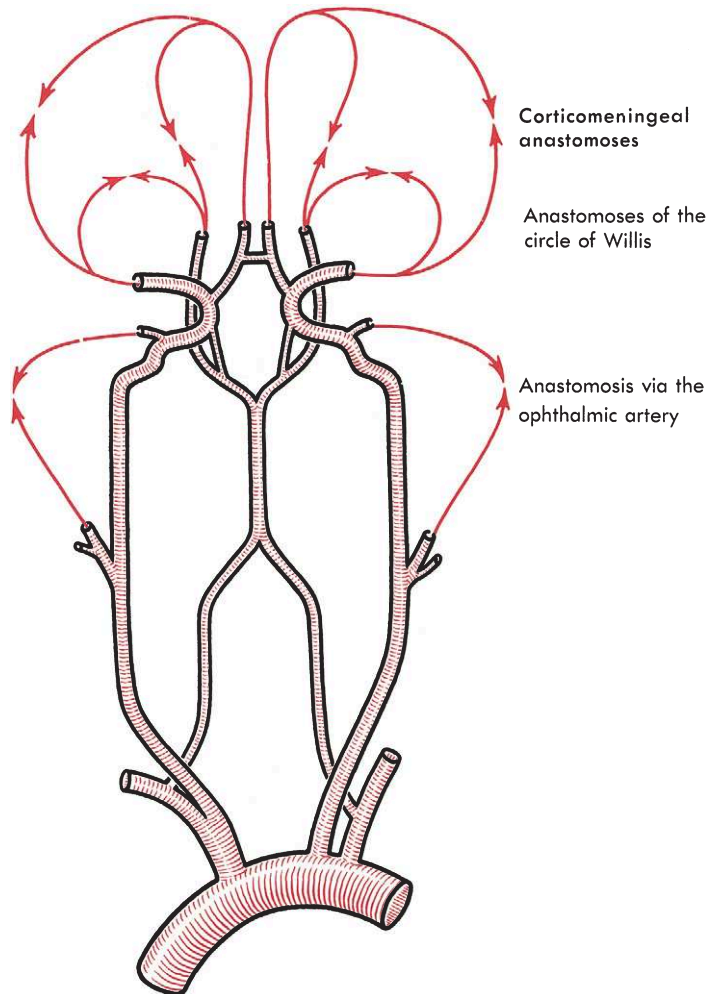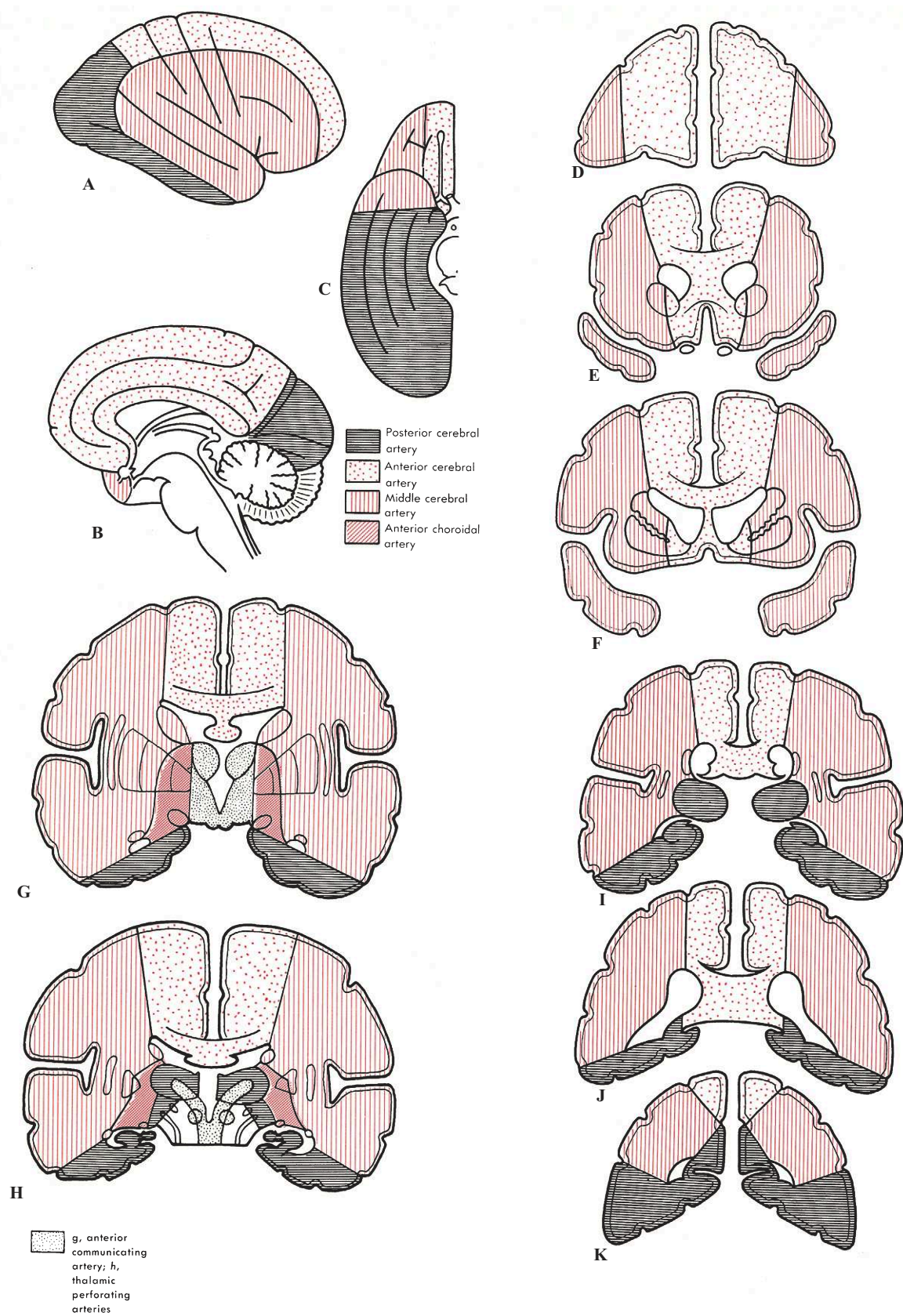
Figure 4-32. Cerebral vascular territories. **A**, Outer surface. **B**, Inner surface. **C**, Basal surface. **D–K**, Coronal slices from front to back.

important to emphasize the frequency of multiple infarcts. These can vary in size and age.

Infarct of the Anterior Cerebral Artery Territory. The anterior cerebral territory (Fig. 4-33E) includes the superior frontal gyrus, inferior and medial surfaces of the frontal lobe back to the level of the precuneus, corpus callosum, and anterior portion of the basal ganglia (supplied by the recurrent artery of Heubner). Because of collateral flow provided by the contralateral anterior cerebral artery via the anterior communicating artery, infarcts of the anterior cerebral territory are less common than those of the middle cerebral territory (discussed in the following paragraph). The existence of variations in the circle of Willis (e.g., a single anterior cerebral artery) may account for bilateral infarction in some cases. In the case of internal carotid thrombosis, infarction is also associated with involvement of the middle cerebral artery territory.
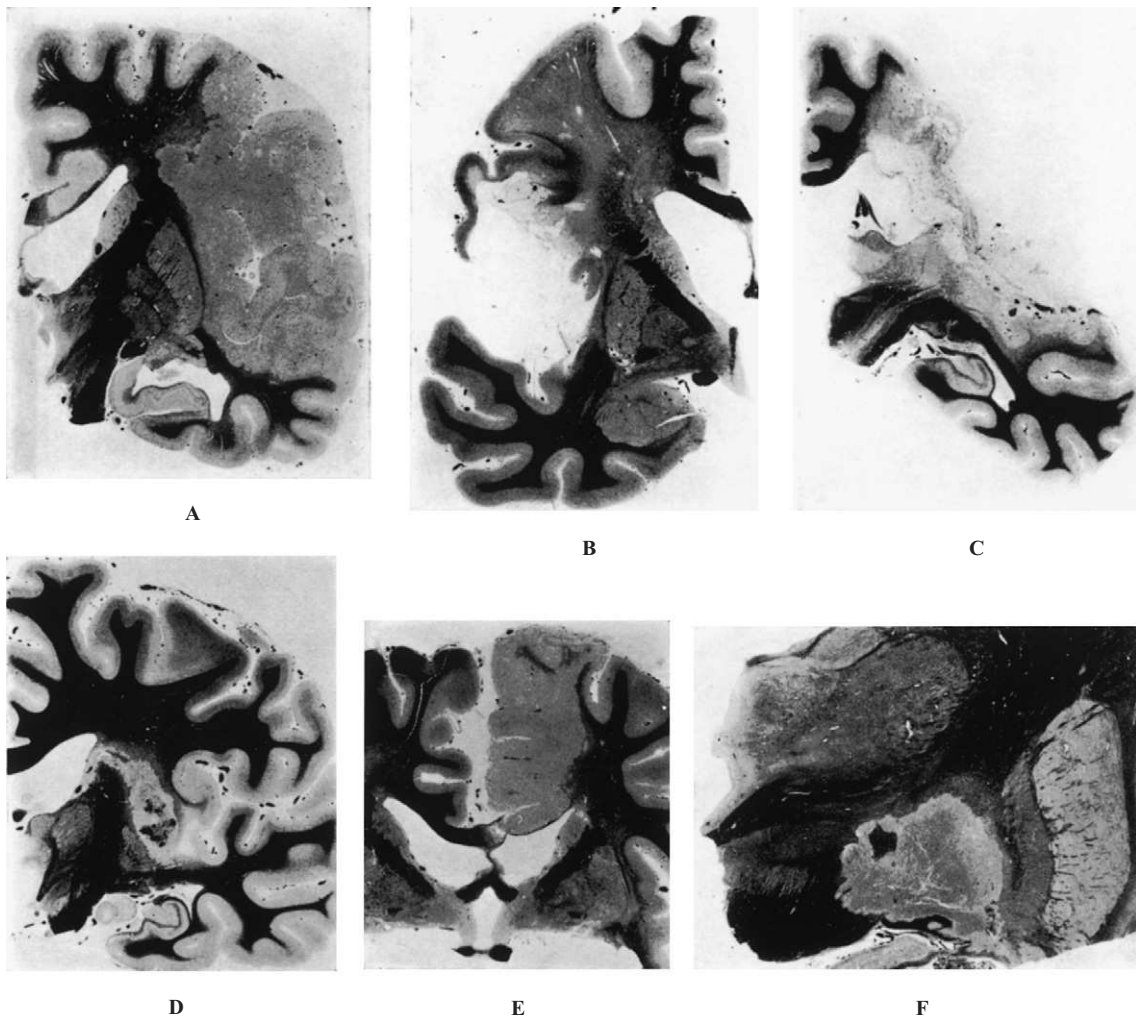
Figure 4-33. Chief topographical areas of distribution of infarcts in the internal carotid territory (Loyez stain for myelin). **A**, Recent, right-sided superficial middle cerebral infarct. Note the presence of a small associated infarct involving the corpus callosum and the cingulate gyrus (territory of the anterior cerebral artery.) **B**, Old, left-sided superficial middle cerebral infarct, sparing the temporal lobe. **C**, Old, total, right-sided middle cerebral infarct. **D**, Recent, deep, right-sided middle cerebral infarct. Note its hemorrhagic character and its association with older, more superficial lesions (insula and claustrum). **E**, Right-sided anterior cerebral infarct. **F**, Right-sided anterior choroidal infarct.

INFARCT OF THE MIDDLE CEREBRAL ARTERY TERRITORY.   The middle cerebral territory includes the lateral surface of the frontal and parietal lobes, insula, superior and middle temporal gyri, and deep striatal territory. Occlusion of the proximal part of the middle cerebral artery results in total middle cerebral infarction (Fig. 4-33C), since the superficial collateral arterial circulation is able to assume little collateral flow. The occlusion is more often the result of embolization than of primary intravascular thrombosis. Cerebral infarction restricted to the superficial branches of the middle cerebral artery results from occlusion distal to the origin of the perforating branches (superior and inferior divisions), whereas occlusion of the ostia of the latter by atherosclerosis is responsible for isolated deep middle cerebral infarcts (Fig. 4-33D). Most often, infarction involves only part of the vascular territory (e.g., territory of the ascending branches). This may result from occlusion of the terminal branches, but more often follows proximal occlusion of the internal carotid artery coupled with adequate reirrigation of the proximal territory through vascular anastomoses at the base of the brain.

INFARCT OF THE ANTERIOR CHOROIDAL ARTERY TERRITORY.   The posterior part of the internal capsule, pallidum, and optic tract are located within the anterior choroidal territory. Infarction of this deep area of supply, especially when recent, is often difficult to detect because of the limited extent of the territory (Fig. 4-33F). Isolated infarction of this area is seldom seen. In most cases, it

Figure 4-35. Old infarct at the junction of the left anterior and middle cerebral territories.

accompanies total infarction of the middle cerebral territory and is therefore part of a massive infarct.

MASSIVE HEMISPHERIC INFARCT. Massive hemispheric infarct affects the entire relevant territory of vascular supply. It is produced as the result of sudden occlusion of the terminal portion of the internal carotid artery, either by an embolus or by an extension of an internal carotid thrombus beyond the terminal bifurcation of the artery, in which case all potential collateral supply is absent. The large extent of the zone of ischemia accounts for the severity of the edematous reaction and for the risk of temporal herniation (Fig. 4-34).

"WATERSHED" OR BOUNDARY-ZONE INFARCTS. These involve mostly the boundaries between the anterior and middle cerebral territories, especially posteriorly (Fig. 4-35). Likewise, watershed infarcts may occur in the white matter of the centrum semiovale, between the deep anterior and middle cerebral territories. They may result from internal carotid thrombosis, particularly when the thrombosis is bilateral, or follow prolonged episodes of arterial hypotension (shock).

Infarcts of the Vertebrobasilar ("Posterior") Territory.   The development of infarcts of the

Figure 4-34. Recent massive hemispheric infarct. Gross appearance.

vertebrobasilar territory depends on the general pathophysiological mechanisms already described, to which should be added the special anatomical features of the posterior circulation and its system of collateral flow.

The posterior circulation system consists of a median axis (i.e., the basilar artery, which is formed by the junction of two vertebral arteries originating from the subclavian arteries that follow a tortuous course through the foramina transversaria) and of two terminal branches, the posterior cerebral arteries. The considerable anatomical variations of this vascular arrangement, especially in the size of the vertebral, posterior communicating, and posterior cerebral arteries, whose territories of supply may, as a result of narrowing or hypoplasia of their proximal segments, ultimately depend on one of the internal carotid arteries.

Variable anastomotic communications exist with the internal carotid arteries (through the posterior communicating arteries), with branches of the external carotid and subclavian arteries, and between the vertebral arteries themselves (through the spinal perimedullary arterial network). Finally, lateral anastomotic rings are formed between the cerebellar arteries.

These special anatomic features account for the frequent bilaterality and asymmetry of the ischemic lesions and for their multifocal distribution along the vertebrobasilar axis.

INFARCTS OF THE POSTERIOR CEREBRAL ARTERY TERRITORY. Infarcts of the posterior cerebral artery's hemispheric territory are often bilateral, producing necrosis of the inferomedial surface of the occipital lobe, of the cuneus, and especially of the calcarine cortex and of part of Ammon horn (Fig. 4-36A). They follow occlusion of the posterior cerebral artery beyond its junction with the posterior communicating artery. Such an occlusion is generally embolic in origin; it is then most often

A   B
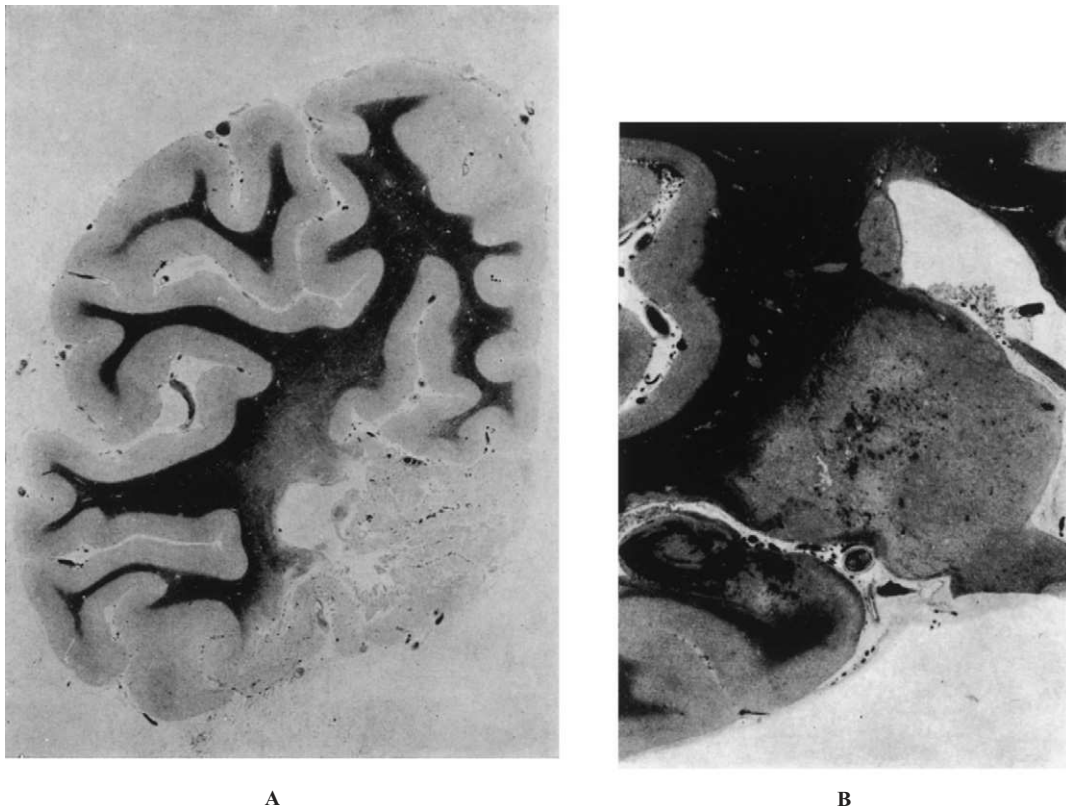
Figure 4-36. Infarcts of the posterior cerebral territory (Loyez stain for myelin). **A,** Old temporo-occipital infarct. **B,** Recent infarct of the thalamogeniculate territory. Note involvement of Ammon horn.

secondary to underlying vertebrobasilar thrombosis. Infarcts of the deep territory of the posterior cerebral artery most often affect either the thalamogeniculate territory (i.e., the ventrolateral thalamus and the pulvinar [Fig. 4-36B]) or the paramedian thalamic territory (i.e., the intralaminar nuclei). In the latter case, a bilateral butterfly-shaped lesion develops and is associated with variable involvement of the mesencephalon (i.e., a thalamomesencephalic infarct).

INFARCTS OF THE BRAINSTEM.   In the majority of cases, infarcts of the brainstem (Fig. 4-37) are secondary to atherosclerotic thrombosis of the vertebral or basilar artery, but they may also derive from an embolism originating from the heart. The general pattern of arterial supply is that of a relatively constant and simple arterial intraparenchymal network associated with a highly variable and complex extraparenchymal network. This explains why these lesions often defy classification. They fall roughly into the following types:

Localized lesions corresponding to necrosis of a particular vascular territory. These lesions involve either paramedian branches of the basilar artery (i.e., midline infarct of the midbrain tegmentum, with or without associated thalamic lesions; paramedian thalamic infarct; paramedian infarct of the pontine tegmentum with massive softening; or paramedian infarct of the medulla), short circumferential branches of the basilar arteries (i.e., infarct of the middle cerebellar peduncle), or especially the lateral medullary region (causing Wallenberg syndrome).

Multiple and diffuse lesions. These may involve many vascular territories and sometimes consist of lesions of different ages. They may also form relatively localized lesions that extend beyond the usual topographical limits of irrigation.

CEREBELLAR INFARCTS. Cerebellar infarcts are three to five times more common than cerebellar hemorrhages. These lesions frequently appear as territorial infarcts caused by occlusion of the long circumferential branches of the vertebral and basilar arteries (Fig. 4-38A). These may involve (1) the territory of the superior cerebellar artery, which comprises the superior portion of the cerebellum down to the dentate nucleus and the posterolateral portion of the pontine tegmentum (Fig. 4-38B); (2) the territory of the posterior inferior cerebellar arteries, on the ventral surface of the hemisphere; or (3) the territory of the anterior inferior cerebel-lar artery, which usually supplies the flocculus, the middle cerebellar peduncle, and the inferior lateral territory of the pontine tegmentum (Fig. 4-38C).

About 10% to 25% of cerebellar infarcts are due to emboli. The infarcts can be of considerable size; they may be associated with multiple other foci of infarction in the brainstem, and behave as space-occupying masses that can induce cerebellar herniation with brainstem compression. Border-zone infarcts, situated at the boundaries between the territories of distribution of the different cerebellar arteries, are not uncommon.

SPINAL INTRAMEDULLARY INFARCTS.   Spinal intramedullary infarcts are much rarer than cerebral infarcts. Because it is usually difficult to carry out a complete and satisfactory anatomical study of the blood supply of the spinal cord, these infarcts may raise complex problems of pathophysiological interpretation.

Arterial organization of the spinal cord.   A number of distinguishing features in the arterial organization of the spinal cord determine the chief pathological outcomes (Figs. 4-39 and 4-40). The general pattern is that of a relatively constant and simple arterial intramedullary network associated with a highly variable and complex extramedullary network.

The intramedullary network depends on one major anterior spinal artery that extends downward along the ventral aspect of the spinal cord and ensures the supply of the anterior two thirds of the cord (including, therefore, most of the gray matter) through the sulcocommissural arteries. Two posterior spinal arteries irrigate the dorsal three fourths of the posterior columns. A perimedullary anastomotic network gives off a few branches to the periphery of the cord. The extramedullary network is fed by radicular arteries.

The following territories are recognized:

1. A superior, or cervicothoracic, territory corresponding to the cervical and upper two or three thoracic segments and supplied by arterial twigs originating from the vertebral arteries or from branches of the subclavian arteries.
2. An intermediary, or middle thoracic, territory extending from T4 to T8, with a poor blood supply.
3. An inferior, or thoracolumbar, territory whose abundant vascularization is supplied by a
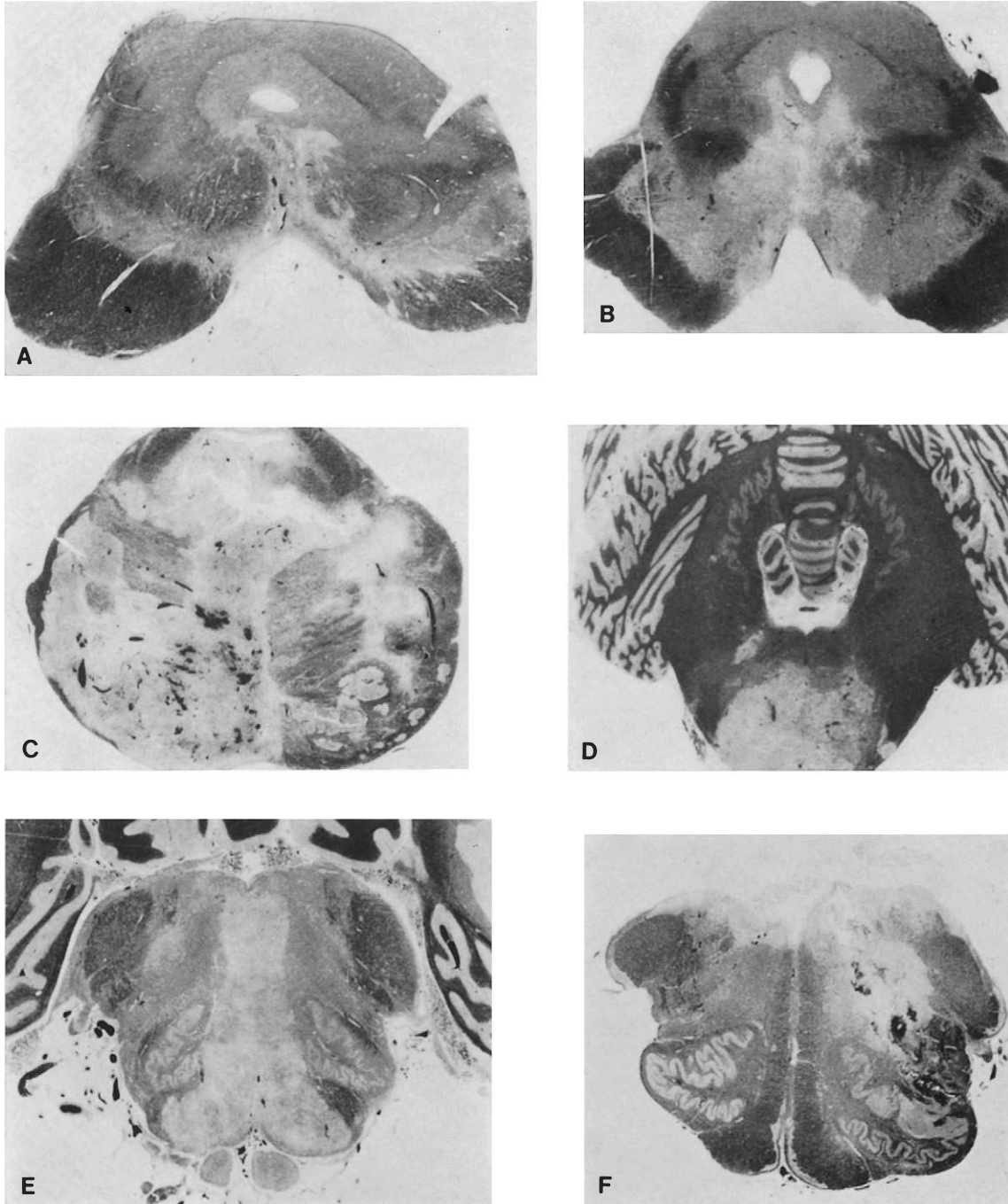
Figure 4-37. Infarcts of the brainstem (Loyez stain for myelin). **A**, Midbrain infarct. **B**, Massive infarct of the midbrain tegmentum. **C**, Massive upper pontine infarct with right-sided paramedian predominance. **D**, Massive infarct of the basis pontis. **E**, Central medullary infarct. **F**, Lateral medullary infarct (causing Wallenberg syndrome).
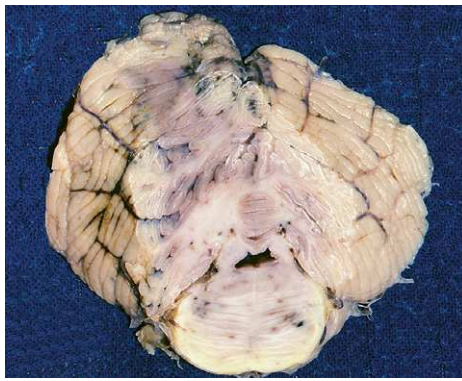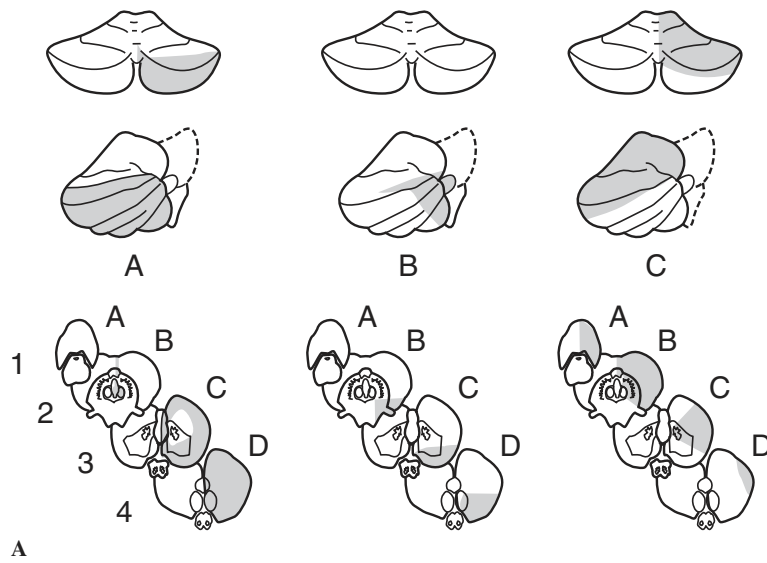
Figure 4-38. Cerebellar infarcts. **A**, Extent of lesions in cerebellar infarcts. From top down in each column: Posterior view; lateral view; and four serial sections perpendicular to the brainstem axis through (1) the upper cerebellum and pons, (2) middle cerebellum and lower pons, (3) middle cerebellum and middle medulla oblongata, and (4) lower cerebellum and medulla. Posterior inferior cerebellar artery territory (A), anterior inferior cerebellar artery territory (B), and superior cerebellar artery territory (C). **B**, Right-sided, recent, pale infarct of the superior cerebellar artery. **C**, Left-sided, hemorrhagic infarct of the posterior inferior cerebellar artery. (**A**, Modified with permission from Amarenco P, Hauw JJ: Anatomie des artères cérébelleuses. Rev Neurol [Paris] 145:267–276, 1989.)

single lumbar artery, that is, the artery of the lumbar enlargement (artery of Adamkiewicz). This artery is situated on the left and most frequently accompanies one of the lower thoracic or upper lumbar nerve roots; it is sometimes reinforced by an upper or a lower branch.

Topographical features.   Massive infarction (Fig. 4-41A) usually occurs in the middle thoracic zone, which is normally poorly vascularized. It is presumably the result of sudden total ische-mia with inadequate perfusion of the middle thoracic segments by the abundant cervical and lumbar networks. The infarct extends over several segments and is often lengthened into a proximal and a caudal fusiform pencil of centromedullary softening situated in the ventral part of the posterior columns, at the boundary between the anterior and posterior spinal territories (Figs. 4-41B and C).

Anterior spinal artery infarction involves a greater or lesser portion of the anterior spinal terri-
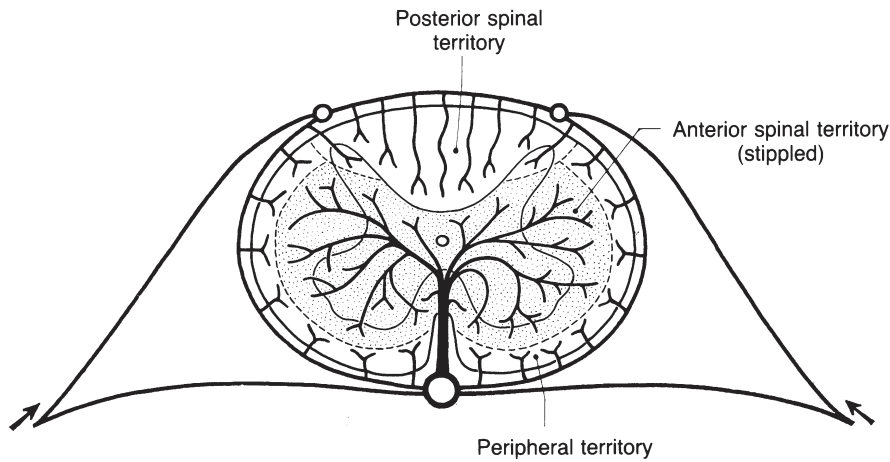
Figure 4-39. The three transverse arterial territories of the spinal cord.

tory and especially the ventral horns (Fig. 4-42). It is the most frequent type of infarct in the spinal cord. It is found in the cervical region, and more often in the lumbar region because of the special vulnerability of this territory, which depends on a single artery without potential collateral supply from an invariably slender middle thoracic arterial network.

Infarcts of the posterior spinal territory (Fig. 4-43) are considerably rarer.
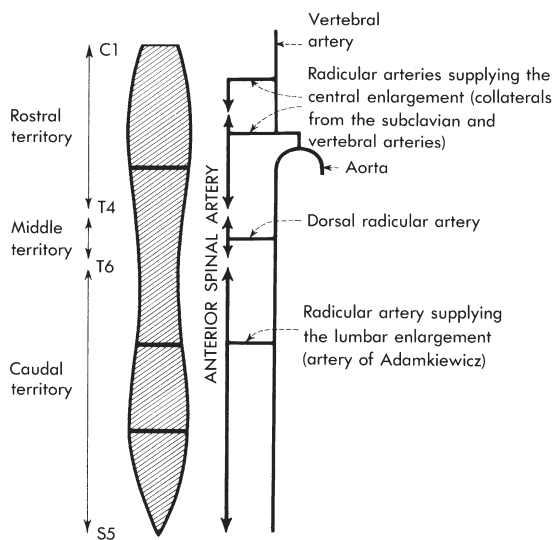
Figure 4-40. The three principal longitudinal arterial territories of the spinal cord.

Microscopic features. The microscopic lesions associated with spinal intramedullary infarcts are identical to those of cerebral infarcts, that is, they consist of an initial edematous stage and of secondary processes of liquefaction and tissue resorption through the mobilization of macrophages.

Chief etiological factors. Atherosclerosis and arterial thrombosis involving either the feeding vessels or the aorta itself play an important role. The pathological changes may operate either by obstructing the orifices of the intercostal and lumbar arteries or via an aortic aneurysm.

Except for cholesterol emboli originating from ulcerated aortic atheromatous plaques, arterial embolism can seldom be demonstrated to be an etiological factor. Cartilaginous emboli following relatively minor trauma to the spine have been recorded as a mechanism of cord infarction.

Thoracic surgery, aortography, and massive dissecting aneurysm of the aorta may be special etiological factors in vascular disorders of the spinal cord.

Other Cerebrovascular Lesions of Arterial Origin

Aside from infarcts and hemorrhages, which are the most frequent manifestations of cerebrovascular disease, other lesions may be seen which have different pathophysiological mechanisms.
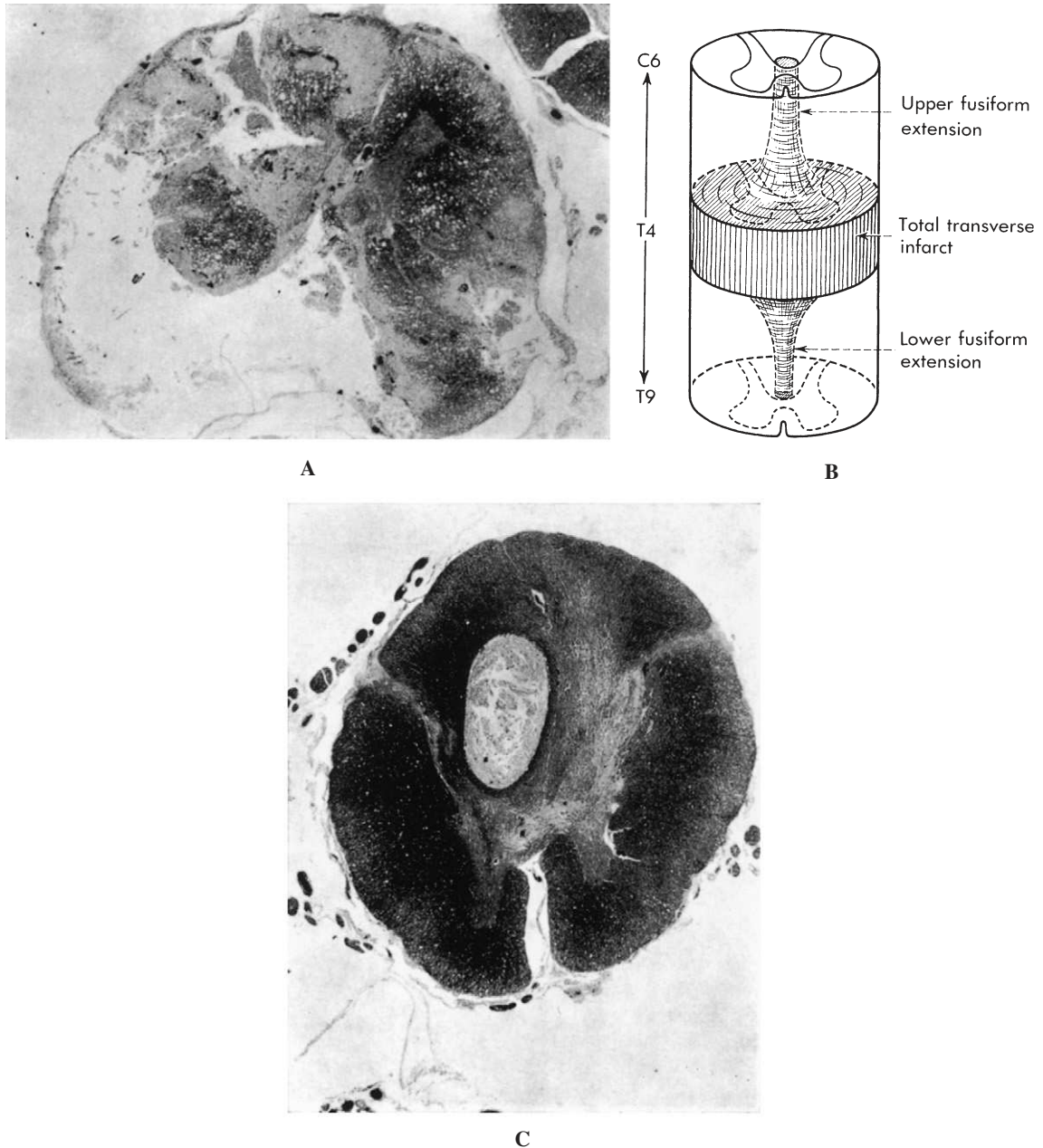
Figure 4-41. Transverse infarct of the spinal cord. **A**, Maximal extent of the lesion (Loyez stain for myelin). **B**, Diagram of fusiform extensions of the lesion. **C**, Upper fusiform extension of the lesion (Loyez stain for myelin).
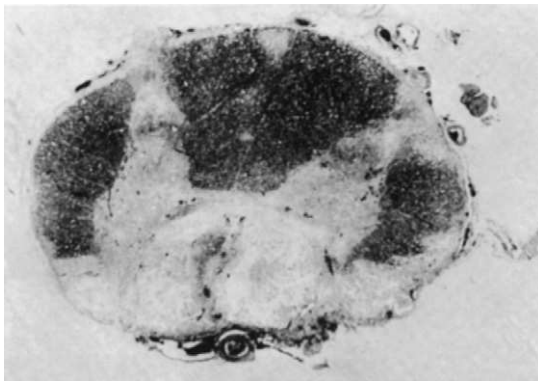
Figure 4-42. Focal infarcts of the spinal cord (Loyez stain for myelin). Anterior spinal artery infarct.

Lacunes

Lacunes are small cavities that are the result of destructive lesions of vascular origin (Fig. 4-44). They are mostly associated with hypertensive cerebral microvascular disease (see earlier in this chapter).

Lacunar Infarcts (Type 1 Lacunes)

Type I lacunes are small, old, cerebral infarcts. They are irregular, ragged cavities that on microscopic examination have all the characteristics of ischemic necrosis. They contain small, parenchymatous debris and lipid-filled macrophages, and occasionally macrophages filled with hemosiderin. Like all infarcts, most lacunar infarcts are traversed by blood vessels of small caliber and are surrounded by more or less intense reactive astrocytic gliosis. These lacunes may be solitary or multiple; they involve preferentially the basal ganglia, the pons,
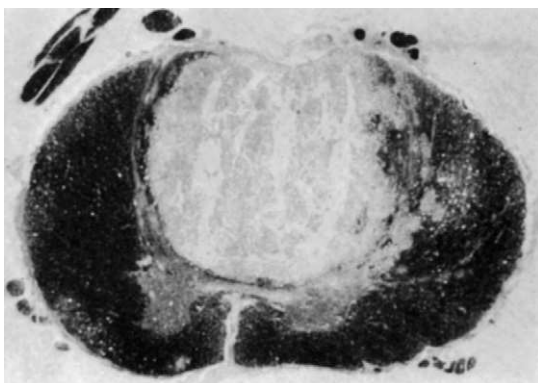
Figure 4-43. Focal infarct of the spinal cord (Loyez stain for myelin). Posterior spinal artery infarct.

and the hemispheric white matter but may be seen in any location in the CNS. Their diameter is variable, but ranges up to 15 mm or 20 mm in diameter. In the majority of cases, lacunar infarcts result from occlusion of a perforating artery by a segmental process of arteriosclerosis (or lipohyalinosis) linked to arterial hypertension. They may also be related to atherosclerosis involving arterial trunks when plaque occludes the ostium of a perforating artery. Likewise, artery-to-artery emboli or emboli of cardiac origin may cause lacunar infarcts.

Small Hemorrhages (Type 2 Lacunes)

Type 2 lacunes are cavitated scars resulting from small, old hemorrhages. Their outlines are usually more regular than those of type 1 lacunes. Their walls are the site of ocher-yellow pigmentation that corresponds to aggregates of hemosiderin-laden macrophages; these are found also inside the cavity. Type 2 lacunes are usually solitary and located in the basal ganglia or, more seldom, in the hemispheric white matter. They are thought to be due to the rupture of microaneurysms; fibrinoid necrosis or amyloid degeneration of the vessel wall has also been implicated in their pathogenesis.

État Criblé

État criblé is a condition where numerous small cavities result from dilatation of the perivascular spaces. The cavities are rounded and with a smooth outline. They always contain one or two cross-sections of an artery with an open lumen. The cavity is lined by simple flattened cells, which are none other than the normal lining cells that form the outer walls of the Virchow-Robin spaces and correspond to the invaginated pial covering surrounding the blood vessels. The cerebral parenchyma that surrounds them is devoid of gliosis. No single mechanism can explain état criblé.

Clinical Features of Lacunes

While often asymptomatic, both lacunar infarcts and small hemorrhages can give rise, when clinically significant, to a picture of "lacunar stroke," which is characterized by focal deficits and variable course, depending on the size and location of the lesions. Diffuse progressive neurological deficit may be seen when there is a multiplicity of lacunes; the most classical clinical consequences are a pseudobulbar syndrome or vascular dementia.
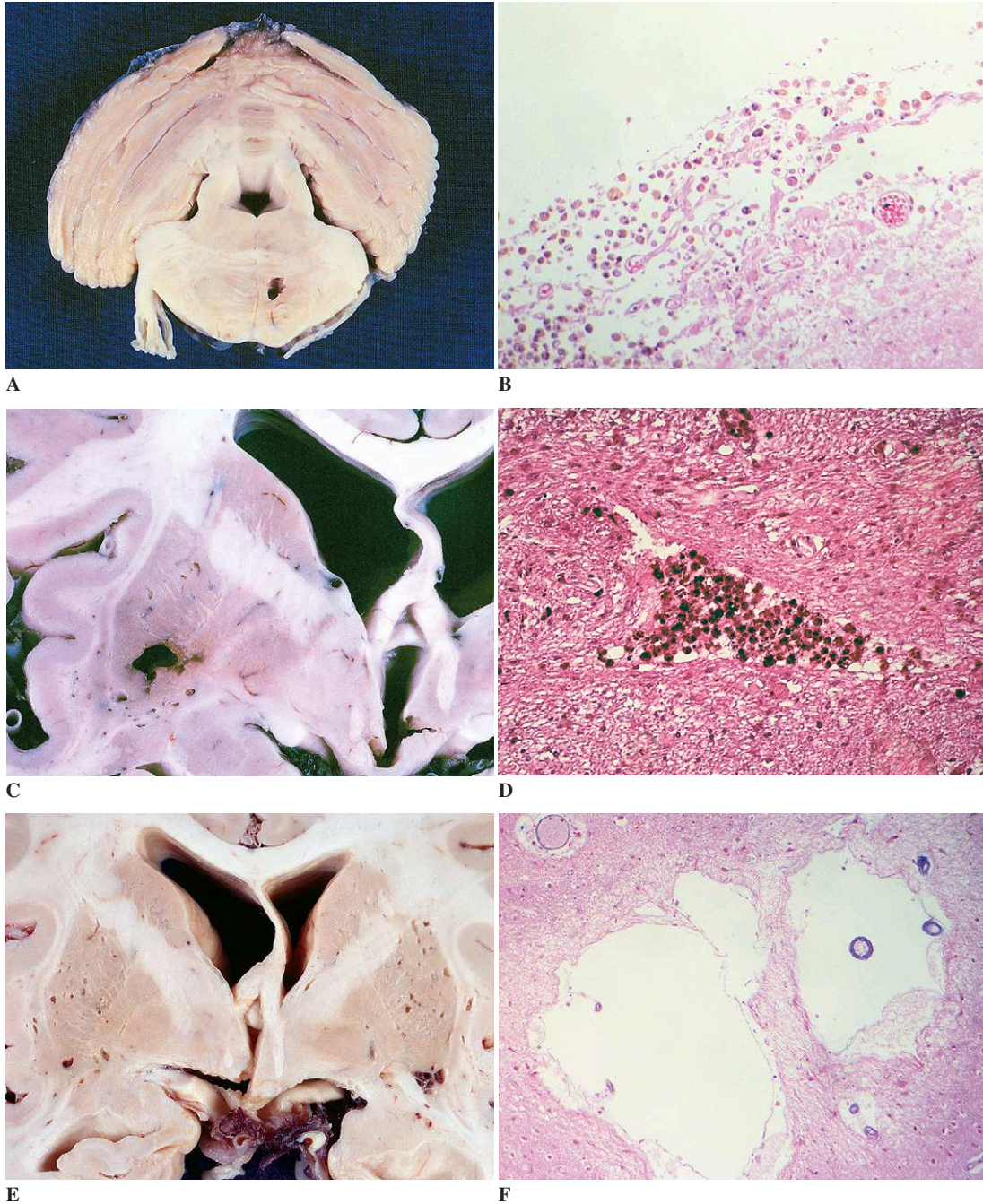
Figure 4-44. Cerebral lacunes. Macroscopic features: **A**, Type 1 lacune; **C**, Type 2 lacune; **E**, État criblé. Microscopic features: **B**, Type 1 lacune; **D**, Type 2 lacune; **F**, État criblé.

Granular Atrophy of the Cerebral Cortex of Arteriopathic Origin

Granular atrophy of the cerebral cortex of arteriopathic origin is seen in rare forms of vascular dementia. It is characterized by the presence of small, chronic, ischemic lesions forming punched-out foci of cavitated cicatricial softening, or focal glial scars, situated entirely in the cortex (Fig. 4-45). The distribution of the lesions is remarkable; they are bilateral and involve the watershed territories at the junction of the middle and anterior cerebral territories, along the crest of the gyri from the frontal to the occipital pole, along the superior frontal and interparietal sulci, and at the junction of the middle and posterior cerebral territories on the inferior surface of the temporal lobes.

The distribution of the lesions is indicative of global chronic watershed ischemia related either to bilateral internal carotid thrombosis or to cardiac insufficiency.

Arteriopathic Leukoencephalopathies (Binswanger Disease)

Arteriopathic leukoencephalopathies are diffuse white-matter lesions seen in certain forms of vascular dementia (Fig. 4-46). The changes consist in diffuse myelin pallor of the white matter with

Figure 4-45. Granular atrophy. Old ischemic lesion involving the watershed territories at the junction of the middle and anterior cerebral territories at the crest of the gyrus along the superior frontal sulcus (Loyez stain).

sparing of the U fibers, the corpus callosum, and the internal capsule. On microscopic examination, incomplete myelin destruction, astrocytic gliosis, and dilatation of the perivascular spaces with thickening of the arteriolar walls are seen. In some cases, especially in hypertensive subjects, numerous lacunes are also seen in the white matter and the basal ganglia, and the arterioles of these regions are the seat of severe arteriosclerotic lesions.

Comparable white-matter changes may be observed in other cerebral microngiopathies such as cerebral amyloid angiopathy (see earlier in this chapter) and cerebral autosomic dominant arteriopathy with subcortical infarcts and leukoencephalopathy (CADASIL), a hereditary disease of the brain vessels due to a mutation of the *Notch 3* gene on chromosome 19. It is characterized by the pathognomonic granular osmiophilic material in arterial walls (Fig. 4-47) including dermal arteries (where the deposit can easily be identified by electron microscopy on skin biopsy), since the arteriopathy is generalized. It has also been demonstrated that the extracellular domain cleaved from *Notch 3* in response to ligand binding accumulates outside the degenerating vascular smooth muscle cells and can be identified immunohistochemically. This deposition is associated with degeneration of vascular smooth muscle cells with progressive wall thickening and fibrosis and luminal narrowing in small and medium-sized penetrating arteries. Multiple small infarcts in the white matter or deep gray matter are frequent. The cerebral cortex is usually preserved and intracerebral hemorrhages are uncommon.

Vascular Pathology of Venous Origin

The study of cerebral venous lesions (Fig. 4-48) cannot be separated from that of the pathology of infectious diseases in the brain, as cerebral phlebitis is most often secondary to infectious lesions. It may also occur in a number of generalized conditions, in which it may be associated with disturbances of coagulation. Venous occlusion leads to circulatory stasis, diapedesis of red blood cells, and hemorrhages proximal to the site of vascular occlusion. A venous infarct is the final outcome of this process. In contrast to arterial hemorrhagic infarcts, which predominate in the cortex,

A

B

C

D
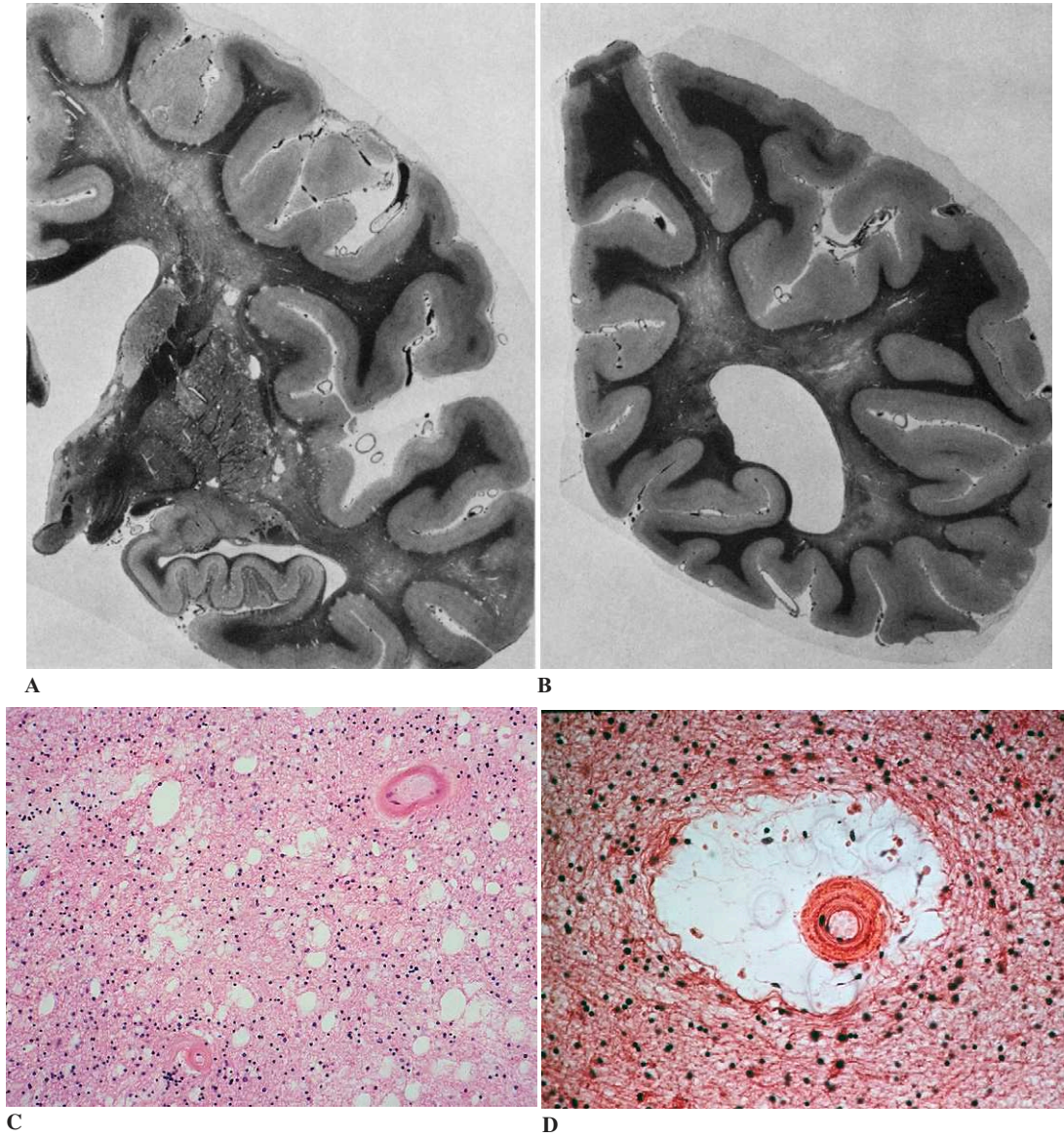
Figure 4-46. Binswanger arteriopathic subcortical encephalopathy. **A** and **B**, Macroscopic apparance on Loyez stain for myelin. Note the presence of myelin pallor of the deep white matter and type I lacune in the basal ganglia (**A**) and in the posterior white matter (**B**). **C** and **D**, Microscopic features (H and E). Edema and glial swelling (**C**), dilatation of perivascular space and arteriolar hyalinosis (**D**).
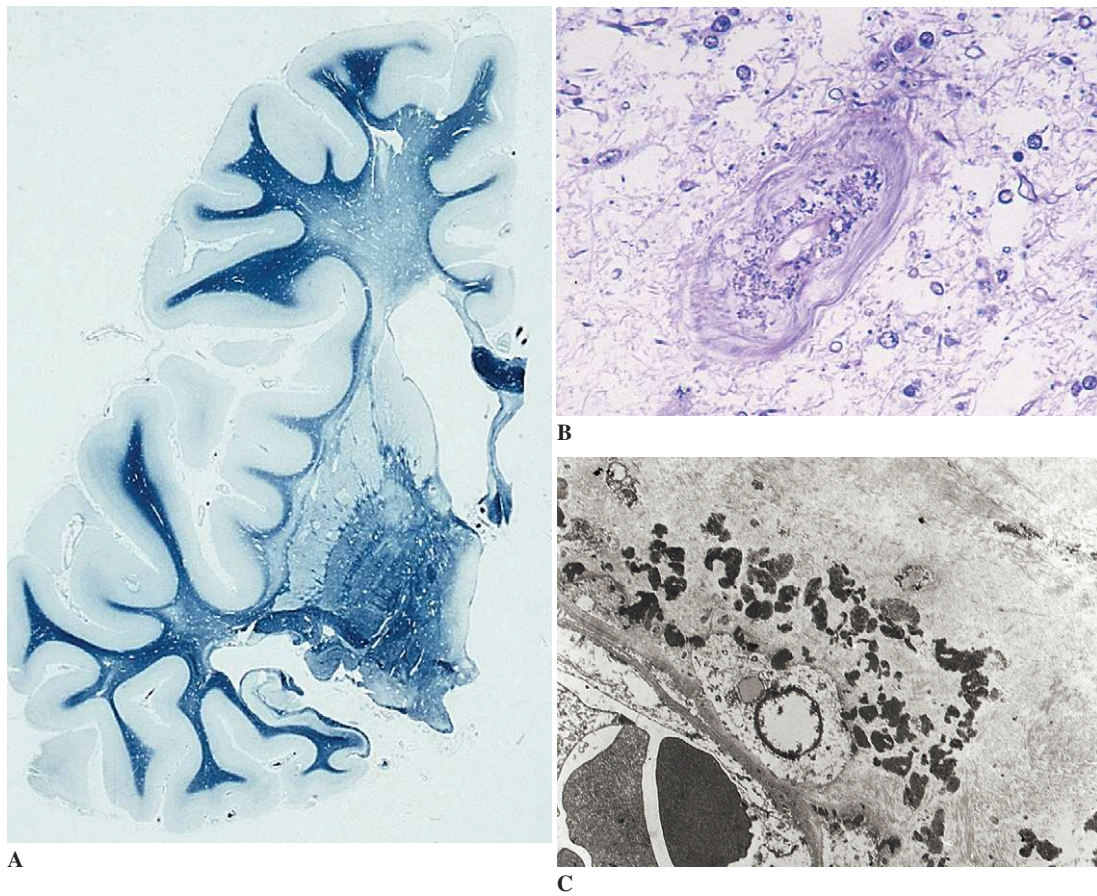
Figure 4-47. Cerebral autosomal dominant arteriopathy with subcortical infarcts and leukoencephalopathy (CADASIL). **A**, Gross appearance of the subcortical infarcts and leukoencephalopathy (Woelcke stain). Granular osmiophilic material in arterial walls on semithin section (**B**) and at ultrastructural examination (**C**).
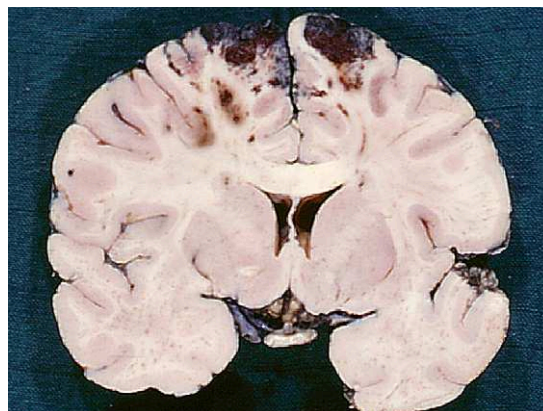
Figure 4-48. Bilateral venous infarction resulting from thrombosis of the superior sagittal sinus.

hemorrhages in venous infarction involve simultaneously the leptomeninges, the cortex, and the white matter. In superior sagittal sinus thrombosis, hemorrhagic lesions involve symmetrically the hemispheric white matter and predominate in the centrum semiovale. In thrombosis of the vein of Galen, they involve the periventricular regions and the thalamic areas. In superficial phlebitis, lesions are often seen in the hemispheric gray matter and the underlying white matter.

Chapter 5
Infections of the Central Nervous System

Francesco Scaravilli, Margaret Esiri, Leroy Sharer, and Françoise Gray

A wide variety of infectious agents—bacteria, fungi, parasites, viruses, or prions—may affect the central nervous system (CNS). Organisms can be classified as either pathogenic or opportunistic. Infections by agents in the former group cause diseases in every individual; those by agents in the latter group affect patients with lower resistance. Infectious agents can enter the CNS in many ways: through the blood, by retrograde spread via peripheral nerves, or by direct invasion. The hematogenous route is the most common, either by direct spread or via host cells.

The brain and spinal cord are relatively well protected from infective agents by the skull and vertebral column, meninges, and blood-brain barrier. However, once the pathogen enters the CNS, host defense mechanisms to control its replication and pathogenicity are suboptimal. In addition, immunodeficiency conditions in the host are increasingly frequent. This may account for the continuing high mortality and morbidity rates from infections of the CNS despite the advances in diagnosis and treatment that have been made in recent years.

Bacterial Infections

Depending on their virulence/pathogenicity determinants, bacteria can induce (1) purulent lesions involving the recruitment and lysis of polymorphs; (2) cellular inflammatory reactions, with influx of mononucleated leukocytes; or (3) inflammatory edema caused by toxins and other inflammatory substances released by bacterial secretion or lysis, in the absence of bacterial replication.

Pyogenic Infections

The bone, dura mater, arachnoid, and pia mater delimit four compartments and tend to prevent the spread of infection from one to another; accordingly, infections can occur in each of the four compartments (epidural, subdural, subarachnoid, and intraparenchymal).

Epidural Abscesses

Infection of the subdural space is rare. It usually causes circumscribed abscesses and is localized more commonly to the epidural space of the vertebral canal rather than to the intracranial subdural space. It spreads frequently from an osteomyelitis secondary to frontal or mastoid sinusitis, trauma, or surgery, and may complicate epidural analgesia. Spinal epidural abscesses usually extend over several vertebral levels. Intracranial subdural abscesses are biconvex, sharply outlined by the skull and the displaced dura.

Subdural Abscesses or Empyema

Infection of the subdural space most often extends from an adjacent sinusitis, otitis, or osteomyelitis. Infection from a purulent leptomeningitis is the main cause of subdural empyema in infants. The infections tend to spread over the convexities but are prevented by the falx from crossing the midline. In most cases an empyema is situated over the tentorium, occasionally adjacent to the falx cerebri. Empyema occurs less commonly in the posterior fossa, and rarely in the spinal canal.

Acute Bacterial Meningitis

Purulent infections of the leptomeningeal spaces are the most frequent pyogenic infections of the CNS. The overwhelming majority of cases of pyogenic meningitis are secondary to hematogenous dissemination of bacteria. Meningitis may also complicate trauma, surgery, or developmental malformations. A variety of bacterial species—gram-positive or gram-negative, aerobic or anaerobic—can be incriminated in acute bacterial meningitis. Some species are most often found in children older than one year and in adults; in these cases, infection results from a primary respiratory infection (e.g., otitis, sinusitis, rhinopharyngitis, or pneumonia). Three major agents—pneumococcus, meningococcus, and *Haemophilus influenzae*—account for about one third of recorded cases each. Other species, such as *Streptococcus agalactiae*, *E. coli*, *Citrobacter koseri*, and *Listeria monocytogenes,* are most frequently isolated in young children or newborns and are transmitted from mother to infant.

Purulent exudate may be macroscopically seen in the leptomeninges (Fig. 5-1). Microscopically, large numbers of polymorphs invade the leptomeningeal and Virchow-Robin spaces (Fig. 5-2). Bacteria may be seen either free or within polymorphs. Later, in the absence of early resolution, the polymorphs degenerate and disappear, to be replaced by a fibrinous exudate containing lymphocytes, plasma cells, histiocytes, and macrophages. After a few weeks, the exudate organizes into a fibrous connective tissue.

All CNS structures in contact with the CSF participate in the infectious process. Thus, there is: (1) a polymorphic inflammatory cellular infiltrate in the walls of the leptomeningeal blood
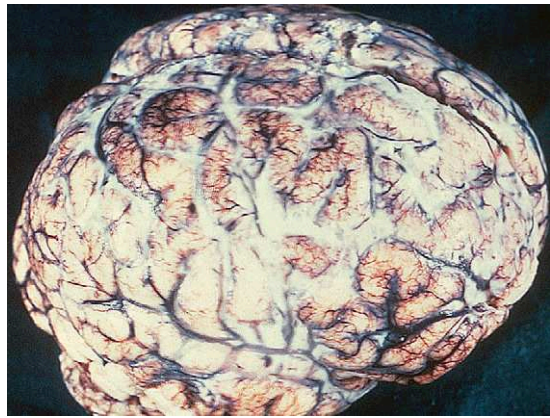
Figure 5-1. Gross appearance of purulent leptomeningitis.

vessels, mainly the veins, which may undergo thrombosis and cause cerebral infarcts; (2) cellular infiltration of the cranial nerves and spinal roots, with consequent development of demyelination; (3) invasion of the ventricular walls, with consequent purulent ventriculitis (Fig. 5-3). The infectious process may also spread to the subpial and subependymal neural parenchyma. Cerebral abscesses secondary to purulent meningitis are not unusual in infants and newborns. The production of a fibrinocellular exudate and its subsequent fibrous organization may obstruct the path of outflow of the CSF and result in the development of hydrocephalus, even pyocephalus.

Listeria monocytogenes infections deserve separate mention because of the frequency with which
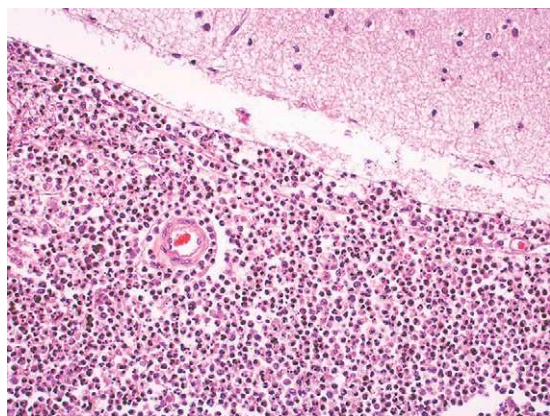
Figure 5-2. Microscopic appearance of purulent leptomeningitis (H and E).
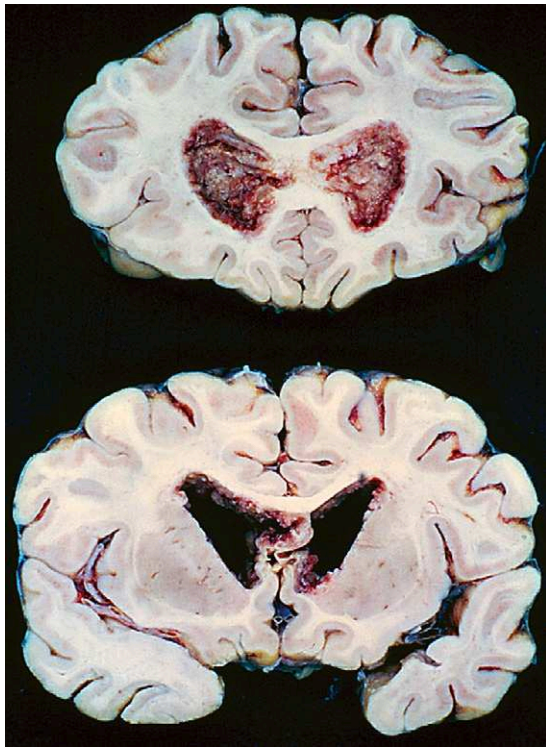
Figure 5-3. Gross appearance of purulent ventriculitis.

microabscesses ("listeria nodules"), localized particularly in the brainstem, are associated with this type of purulent meningitis.

Brain Abscesses

Brain abscess is the second most common infection of the CNS after bacterial meningitis and is the most frequent space-occupying infection. Neuroimaging has greatly helped the diagnosis of brain abscess, resulting in significant decrease of the mortality rate. It has also become possible to treat many cases with antibiotics alone.

As in leptomeningitis, the source of infection producing brain abscesses may be local or blood-borne, resulting in particular localizations. Post-traumatic abscesses occur at the site of craniocerebral wounds or neurosurgery. Abscesses of hematogenous origin tend to occur at junctions between the gray and white matter (Fig. 5-4) and are often multiple. They are secondary to septic emboli from bacterial endocarditis or chronic suppurative intrathoracic infection. Paradoxical

cerebral septic emboli may also occur in congenital cyanotic heart disease. Abscesses resulting from direct spread from an adjacent suppurative focus are usually situated in the temporal lobe (Fig. 5-5A) or cerebellum, following otitis media or mastoiditis, or in the frontal lobe, following sinusitis.

The initial stage of *focal cerebritis* (day 1 to day 3 after inoculation) appears macroscopically as an ill-defined region of hyperemia surrounded by edema. Microscopically, it is characterized by early parenchymal necrosis with vascular congestion, petechial hemorrhages, microthromboses, perivascular fibrinous exudate, and infiltration by polymorphs. Surrounding edema is invariably associated and adds to the mass effect of the abscess itself. *Late cerebritis* (day 4 to day 9) is characterized by a necrotic purulent center resulting from the confluence of adjacent foci of necrosis. The pus is surrounded by a narrow, irregular layer of inflammatory granulation tissue infiltrated by polymorphs, lymphocytes, and some macrophages. The
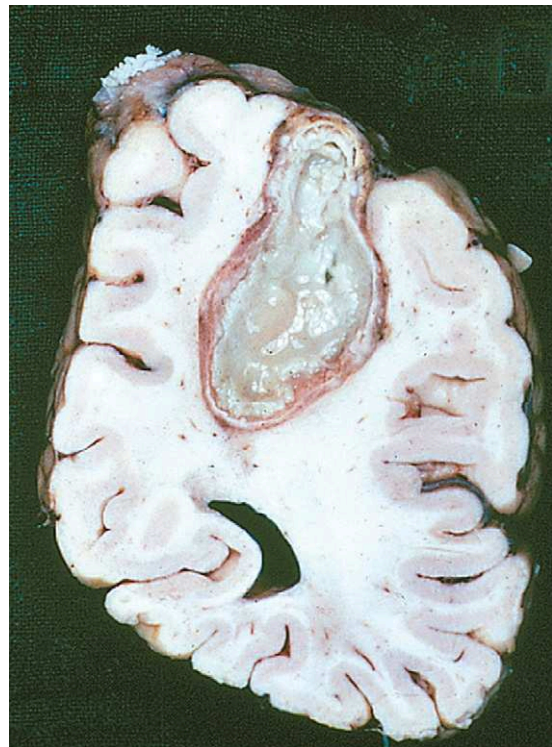
Figure 5-4. Parietal lobe abscess arising at the cortico-subcortical junction with central necrosis, and surrounding peripheral capsule composed of granulation tissue.
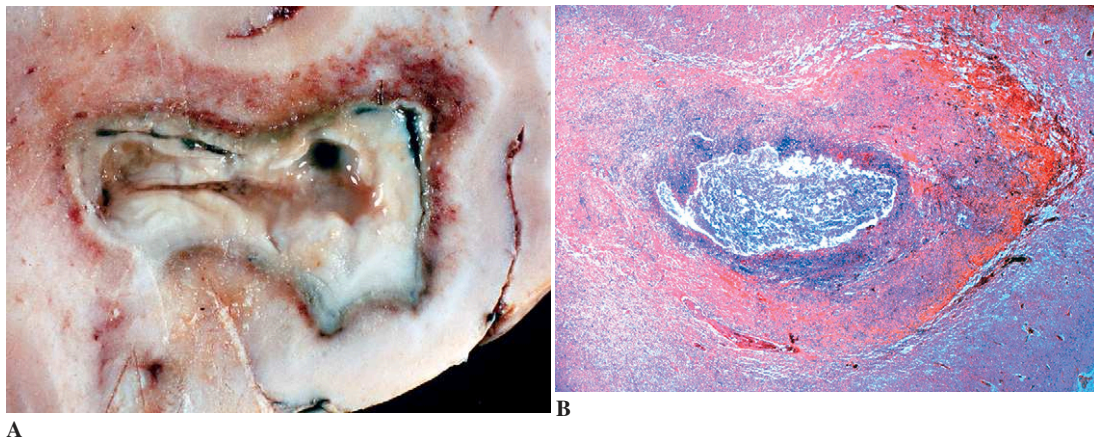
Figure 5-5. Temporal lobe abscess with purulent necrosis in the center and surrounding granulation tissue. **A**, Gross appearance. **B**, Microscopic appearance (HES).

perivascular spaces in the vicinity become cuffed with polymorphs and lymphocytes.

The *early abscess capsule* appears between day 10 and day 13 and is made up of granulation tissue that includes lymphocytes, plasma cells, monocytes, and macrophages; numerous newly formed blood vessels; and scattered fibroblasts. The developing capsule is at first poorly defined; it is thickest on its cortical surface and often very thin or even deficient on its ventricular surface. For this reason, abscesses tend to expand inward and rupture into the ventricular system, resulting in ventriculitis. As time passes (day 14 and later), the capsule becomes firmer and can be stripped easily from the surrounding, edematous white matter. Microscopically, more fibroblasts appear, so that a well-encapsulated abscess consists of five layers: (1) a necrotic center invaded by macrophages; (2) granulation tissue with proliferating fibroblasts and capillaries, and long, radially oriented blood vessels; (3) a zone of lymphocytes and plasma cells in granulation tissue; (4) dense fibrous tissue with embedded astrocytes; and (5) a surrounding, edematous area of gliosis (Fig. 5-5B).

The two major and most serious complications of brain abscesses are raised intracranial pressure (with the risk of cerebral herniation) and rupture of the abscess into a ventricle (resulting in ventricular empyema).

Septic Embolism

Apart from cerebral abscesses, septic emboli may, when of sufficient size, cause cerebral infarction that is liable to become infected by extension from the septic embolus. Implantation of a septic embolus in a cerebral artery may result in a mycotic aneurysm due to local infection and weakening of the arterial wall. (Despite their name, mycotic emboli are usually due to pyogenic bacteria rather than to fungi.) This may rupture, causing hemorrhages into the brain or subarachnoid space and meningitis.

Suppurative Intracranial Phlebitis

Septic intracranial thrombophlebitis most frequently follows infection of paranasal sinuses, middle ear, mastoid, face, or oropharynx. The infection spreads centrally along the emissary veins. Septic thrombophlebitis may also occur in association with epidural abscess, subdural empyema, or meningitis. Septic intracranial phlebitis may cause hemorrhagic infarction. In addition, local suppuration may produce venous hemorrhage, venous necrosis, epidural abscess, subdural empyema, meningitis, and brain abscess.

Tuberculosis

Epidural or Subdural Tuberculous Abscesses

Epidural tuberculous abscess is a common complication of tuberculosis of the spine (Pott disease), involving either the vertebral bodies or the intervertebral discs. Subdural tuberculous abscess is also frequent.

Tuberculous Meningitis

Tuberculous meningitis is the most common form of tuberculosis of the CNS. In most cases, it complicates the initial hematogenous dissemination that follows primary infection; it may also follow late reactivation of latent infection elsewhere in the body. Tuberculous meningitis may be associated with miliary tuberculosis.

Purulent meningitis spreads to the convexities, but in tuberculous meningitis the meninges over the base are most often involved. There may be some gray-green opacity of the meninges over the cerebral convexities, but a much thicker exudate fills the basal cisterns, covers the basis pontis, and extends into the sylvian fissures and the cisterna magna (Fig. 5-6). The spinal cord may also be enveloped by exudate. Tubercles are not easily found in the exudate, but can sometimes be seen under the banks of the sylvian fissures and near the pre- and post-central veins over the convexities.

Microscopically, the inflammatory infiltrate involves the leptomeninges, subpial regions, ependyma, and subependymal parenchyma. It is mostly composed of lymphocytes, mononuclear cells, and epithelioid nodules, with few giant cells and tubercles. The latter consist of a central area of caseous necrosis surrounded by an epithelioid

Figure 5-7. Tuberculous meningitis. Tubercles consisting of a central area of caseous necrosis surrounded by an epithelioid macrophage reaction, with a peripheral ring of lymphocytes.

macrophage reaction with a peripheral ring of lymphocytes (Fig. 5-7). Acid-fast bacilli may be abundant or scanty.

Arterial lesions of reactive endarteritis obliterans (Fig. 5-8A) are constant and are frequently responsible for the production of ischemic parenchymal lesions (particularly within the basal ganglia) because of involvement of the perforating blood vessels (Fig. 5-8B).

In treated patients dying several weeks after onset of the illness, the exudate is more fibrous. It is especially thick over the base (Fig. 5-9A) of the brain and in the cisterna ambiens, where it may obstruct the flow of CSF and lead to hydrocephalus (Fig. 5-9B).

Tuberculomas of Brain and Spinal Cord

Tuberculomas were formerly a very common type of intracranial mass lesion and remain a serious problem in areas of the world where tuberculosis is rife.

Tuberculomas may be single but are more often multiple (Fig. 5-10A). Their sites of predilection are the cerebellum, the pontine tegmentum, and the paracentral lobule. They have occasionally been described in the spinal cord. They are spherical or multilobular lesions with a caseous center (necrotic but firm and of a creamy color) surrounded by a granulomatous reaction that includes giant cells, lymphocytes, and fibrosis of variable extent

Figure 5-6. Tuberculous meningitis. Thick exudate involving the basal meninges. (Courtesy Dr. Leila Chimelli.)
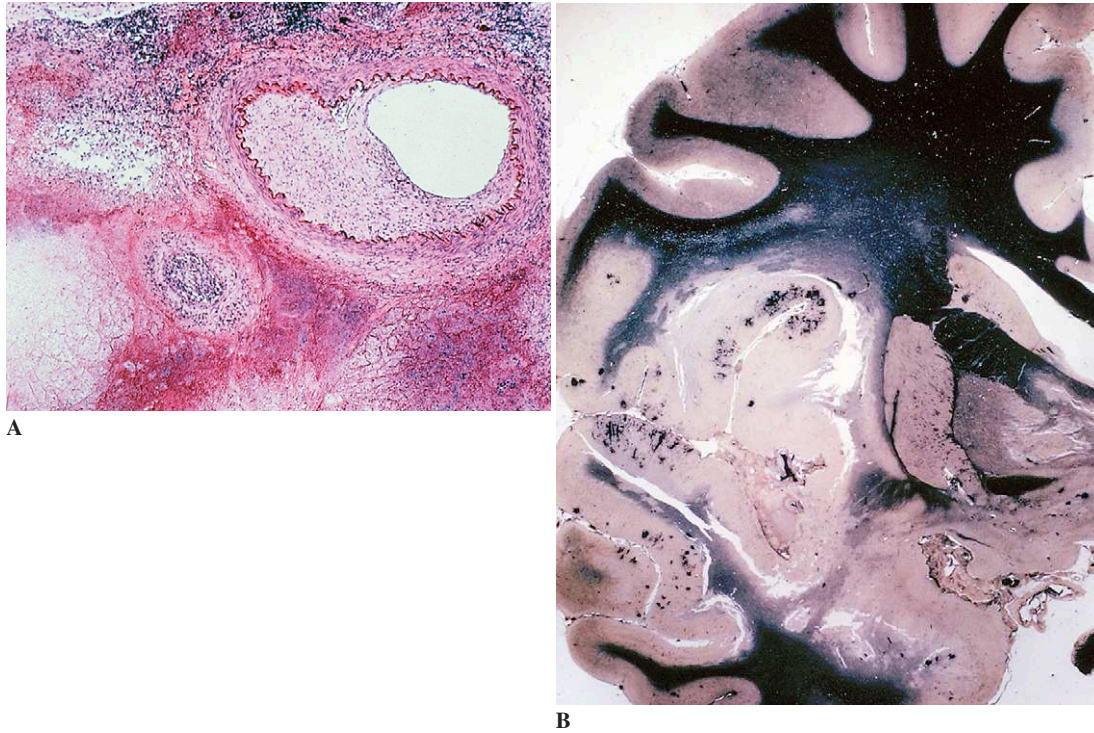
Figure 5-8. Tuberculous meningitis. **A**, Marked vascular changes forming endarteritis obliterans (H and E). **B**, Arterial lesions causing extensive cerebral infarction (Loyez stain).
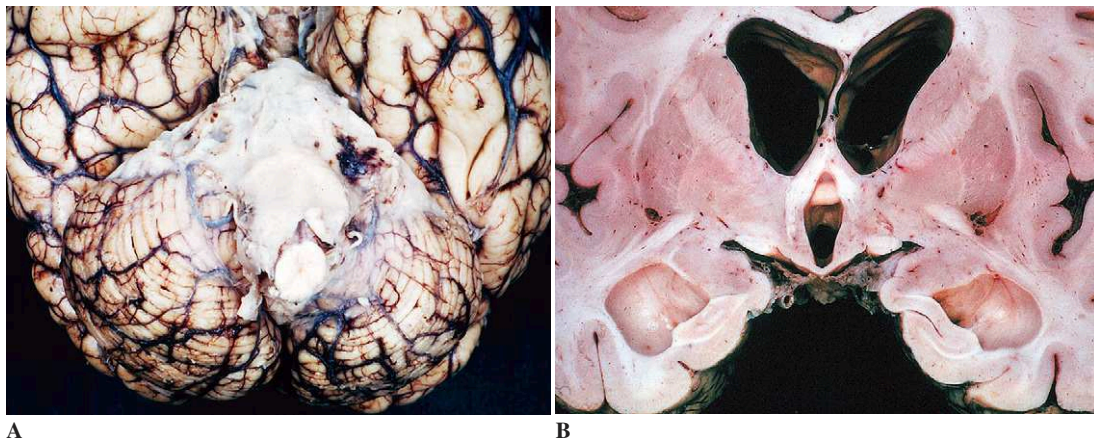
Figure 5-9. Chronic tuberculous meningitis. **A**, Massive fibrous infiltration of the basal meninges. **B**, Basal obstruction with ventricular dilatation.

A   **B**
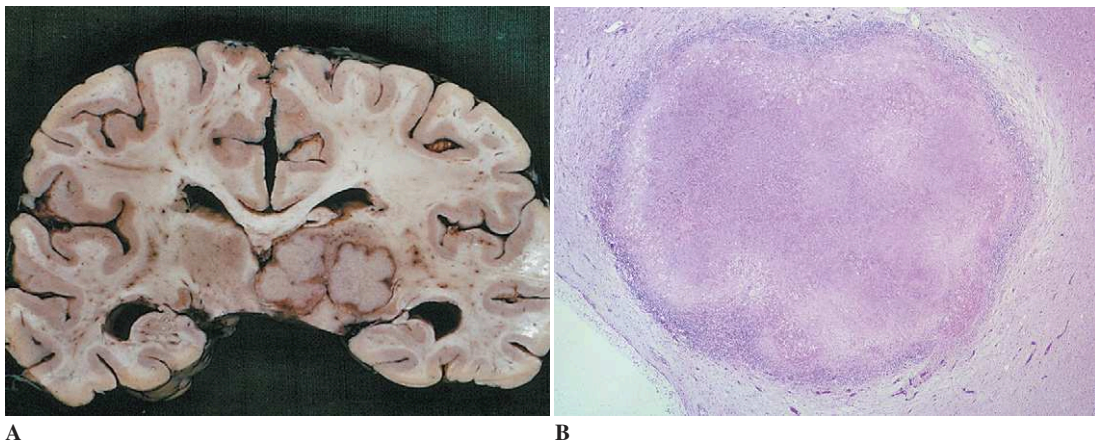
Figure 5-10. Tuberculomas. **A**, Gross appearance of multiple tuberculomas in the thalamus. **B**, Microscopic appearance. The caseous center is surrounded by a granulomatous reaction (H and E).

(Fig. 5-10B). There is much less swelling than around cerebral abscesses.

Tuberculomas, particularly of supratentorial location, may spontaneously become cystic, fibrous, or calcified; bacilli may be difficult to detect and inflammatory exudates can be scant. Tuberculomas may rupture into the meninges.

Tuberculous Abscess

True abscesses of the brain, as opposed to tuberculomas, are composed of a necrotic center containing pus in which *Mycobacteria tuberculosis* are abundant. They are surrounded by a capsule similar to that in pyogenic abscesses but lacking the characteristic granulomatous reaction. Tuberculous abscesses of the CNS are usually multiple. In true abscesses, the absence of a granulomatous epithelioid reaction suggests the failure of immune mechanisms. In our experience, we now see tuberculous abscesses most often in patients with AIDS.

Atypical Mycobacteriosis

Nontuberculous mycobacteria—"atypical mycobacteria"—were considered in the past to be saprophytic organisms. The *Mycobacterium avium* complex, including *M. avium* and *M. intracellulare*, is now recognized as one of the more common causes of opportunistic infection in AIDS patients in whom it produces disseminated systemic infection. However, in most cases with generalized *M. avium-intracellulare* infection, involvement of the CNS is asymptomatic. Neuropathological examination only reveals diffuse perivascular macrophages containing clusters of acid-fast and periodic acid-Schiff (PAS)–positive mycobacteria. Symptomatic infection of the CNS due to *M. avium-intracellulare* or *M. fortuitum* and brain abscesses due to *M. kansasii* have been recorded in rare case reports in patients with AIDS.

Whipple Disease

Whipple disease is a multisystem disorder often involving the intestine and caused by a gram-positive actinomycete, *Tropheryma whipplei*. Involvement of the CNS is uncommon and is usually associated with systemic disease. In rare instances, Whipple disease may be confined to the brain.

At neuropathological examination, small lesions are disseminated throughout the entire CNS but are especially abundant in the cortex, with a predilection for the subpial regions, the basal ganglia, the hypothalamic nuclei, the periaqueductal gray matter, the nuclei of the brainstem, and the dentate nuclei of the cerebellum. They may become confluent to form more extensive foci.

Microscopically, there are meningeal and parenchymal lymphocytes and macrophages
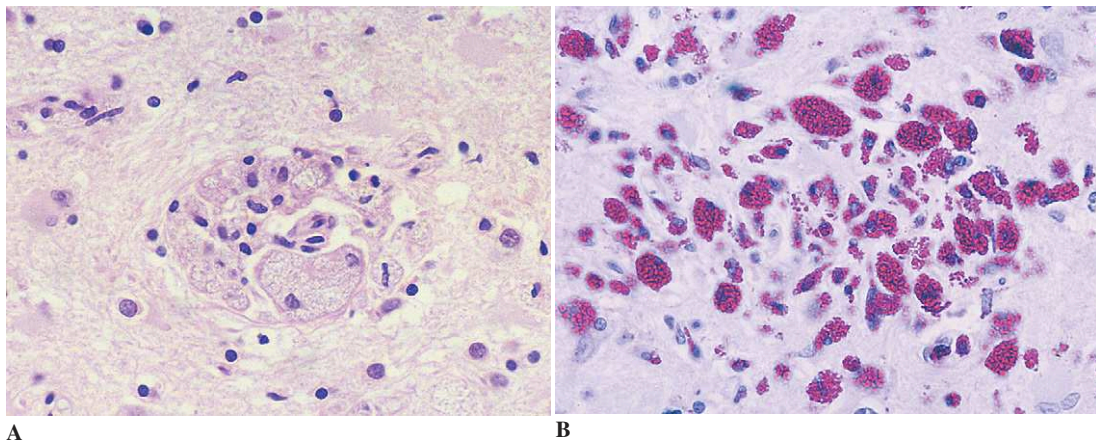
Figure 5-11. Whipple disease. **A**, Perivascular accumulation of lipid-laden macrophages surrounded by reactive astrocytosis (H and E). **B**, The foamy macrophages contain periodic acid-Schiff–positive inclusions in the cytoplasm.

(Fig. 5-11A). The macrophages with lipid-filled cytoplasm contain sickle-shaped inclusions that are PAS-positive (Fig. 5-11B), gram-positive, and methenamine-silver–positive. Bacteria are also present extracellularly in the tissue. Under electron microscopy, lamellar, partially degraded bacterial cell walls and better-preserved bacilli are seen to be present in macrophages, astrocytes, and pericytes.

Actinomycosis

Actinomyces are small, anaerobic, gram-positive organisms whose appearance as thin, branching filaments has long led to their inclusion (with *Nocardia*) amongst fungi. Actinomyces have a world-wide distribution but occur predominantly in rural areas. Most infections in man are produced by *Actinomyces israelii* and *A. bovis* and are acquired from organisms situated in the oral cavity or in the large intestine; they invade the tissues through a break in the mucosa. Bone (mainly the mandible) is the most commonly affected site. Lesions of the CNS are rare and are usually secondary to a focus elsewhere in the body that spreads to the nervous system either by direct extension or via the blood stream. Multilocular abscesses are formed, with central necrotic inflammatory exudate containing polymorphs, necrotic debris, and colonies of branching organisms forming "sulfur granules" surrounded by granulation tissue.

Nocardiosis

Nocardia asteroides is a ubiquitous aerobic organism that in most cases produces infections in immunosuppressed patients. The nervous system is usually invaded through the hematogenous route from a primary pulmonary lesion. In the brain, *Nocardia* produces abscesses or meningitis. Microscopically, the abscesses have fibrous walls and consist of polymorphs. The organism appears as thin branching filaments, about 1 µm in diameter. It cannot be recognized in routinely stained preparations but can be identified using a modified Grocott methenamine-silver stain.

Neurosyphilis

Involvement of the CNS is a sequel of a primary luetic disease that either has been undetected or has been inadequately treated. Although invasion of the leptomeninges during secondary syphilis is relatively common, symptomatic neurosyphilis occurs predominantly in the tertiary stage of the disease. Classically, neurosyphilis may be separated into meningovascular (inflammatory) syndromes occurring within a few years of infection and parenchymatous (degenerative) syndromes that have a latency of decades. However, considerable overlap of these syndromes is commonly observed.

Meningovascular Neurosyphilis

Meningovascular neurosyphilis is due to a combination of chronic meningitis, multifocal arteritis, and gummatous necrotic lesions.

Chronic meningitis composed of lymphocytes and plasma cells often leads to fibrous organization and ultimate occlusion of the CSF pathways, with consequent hydrocephalus. Extension of the inflammatory process into cranial and spinal nerves and periarteritis may also cause optic atrophy or cranial nerve palsies.

The vascular component of meningovascular syphilis, "Heubner arteritis," consists of an infiltration of the arterial wall by lymphocytes and plasma cells associated with intimal proliferation (endarteritis obliterans). This arteritis involves large and medium-sized blood vessels; it may cause ischemic lesions in the brain or spinal cord.

Cerebral gummas are rarely seen in practice; they seldom occur in the meninges. They can involve the cerebral convexity but may be found in the cerebral midbrain, hypothalamus, and spinal cord. They are usually attached to both the dura mater and the brain and consist of round, red-tan-gray lesions that are focally firm, rubbery, and have a central area of necrosis (Fig. 5-12). Microscopically, they consist of central gummatous necrosis in which ghost-like outlines of dead cells can be discerned. This is surrounded by a granulomatous reaction that includes epithelioid cells and fibroblasts with scattered multinucleated foreign body giant cells. Spirochetes are difficult to demonstrate.

Parenchymatous Neurosyphilis

Parenchymatous neurosyphilis takes two forms, paretic dementia (general paralysis of the insane, or GPI) and tabes dorsalis. Both forms may coexist as "taboparesis."

In former days, the brains of patients dying after several years of GPI dementia showed characteristic macroscopic changes. It was shrunken, firm, and covered by a thick and opaque pia-arachnoid. These lesions were most marked frontally, decreasing posteriorly. The ventricles were enlarged, and the ependyma showed diffuse, granular ependymitis. At the present time, GPI is rarely seen. In the healed stages of the disease, the

Figure 5-12. Cerebral gumma in an AIDS patient. (Courtesy Dr. Marius Valsamis.)

brain is usually grossly normal except perhaps for ependymal granulations.

On microscopic examination of classic cases, meningeal thickening and striking involvement of the cerebral cortex (which is atrophic, with loss of the normal laminar pattern) are seen. There is neuronal loss with proliferation of astrocytes and rod-shaped microglia. The lesions are distributed in scattered foci of different age, giving a "bush-fire" or "windswept" appearance. Perivascular cuffing by lymphocytes and plasma cells is found in the cortex and leptomeninges. Specific silver impregnation may occasionally demonstrate the spirochetal organism of *Treponema pallidum*.

Tabes dorsalis consists in degeneration of the posterior columns (Fig. 5-13) and spinal nerve roots, with involvement of the dorsal roots and ganglia. It is apparently the result of inflammatory meningovascular lesions localized to the subarachnoid portion of the dorsal nerve roots. Spinal-cord involvement is secondary to radiculoganglionic lesions. It is characterized by wallerian degeneration of the dorsal columns. Unlike in GPI, no inflammatory reaction is demonstrable in the cord parenchyma and *T. pallidum* is absent.
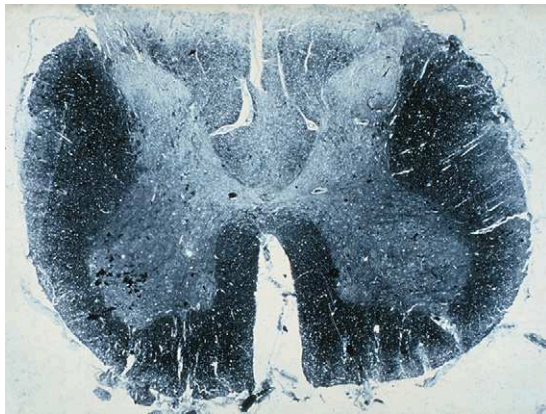
Figure 5-13. Tabes dorsalis. Horizontal section of the lumbar cord, showing the degeneration of the posterior columns (Loyez stain).

Syphilis and Human Immunodeficiency Virus Infection

Neurosyphilis is not uncommon in patients with AIDS. Coinfection with human immunodeficiency virus (HIV) may modify the clinical spectrum of syphilis. Patients with HIV infection are likely to progress to symptomatic neurosyphilis and to show an accelerated disease course; treatment failure is also more frequent. The most common manifestations of symptomatic neurosyphilis in HIV-infected patients are syphilitic meningitis and meningovascular syphilis. General paresis, syphilitic meningomyelitis, syphilitic polyradiculopathy, and cerebral gummas have been reported in occasional cases.

Borreliosis

This condition is due to an infection by a spirochete of the *Borrelia* group and transmitted to humans by insect bites. They include relapsing fever and Lyme disease. The latter is a multisystem disorder due to the spirochete *B. burgdorferi*. It involves the skin, cardiovascular system, joints, and central and peripheral nervous system (see Chap. 14). Neurological signs usually develop several weeks after a tick bite, which may cause a typical erythema chronicum migrans and culminate in a lymphocytic meningitis rich in plasma cells. Involvement of the spinal and/or cranial nerve roots is frequent. Encephalomyelitic complications are much rarer. Tertiary neu-

rological complications, occurring years after inoculation, include axonal neuropathies and low-grade encephalopathy. The pathogenesis of CNS lesions is unclear; they may result from an immunopathological process rather than as a direct effect of the bacterial invasion.

Brucellosis

Brucellosis, or Malta fever, is a zoonosis transmitted to humans by raw dairy products or by direct contact with animal products such as the placenta. The disease is endemic in cattle-breeding countries. Leptomeningeal involvement is common in the septicemic phase of the disease. Either spontaneously or after inadequate treatment, the disease may give rise to subacute neurological manifestations, either infectious or hyperergic. The different forms of neurobrucellosis correspond to a variety of clinicopathological features, including meningoencephalitis, meningomyelitis, and meningomyeloradiculitis, with frequent involvement of the cranial nerves, particularly the acoustic nerves.

Sarcoidosis

Sarcoidosis is a granulomatous multisystem disorder of unknown etiology. The lung is predominantly affected; skeletal muscle or peripheral nerve involvement is not uncommon. CNS involvement occurs in about 5% of cases.

The lesions may affect any part of the CNS, but involve preferentially the base of the brain (especially the suprasellar and the hypothalamic regions), the optic nerves and the optic chiasm, the basal ganglia, and the posterior fossa. Hydrocephalus may result from thickening of the basal meninges or aqueductal obstruction by a periventricular parenchymal lesion.

The sarcoid granulomas consist of a central mass of epithelioid cells and multinucleated giant cells surrounded by lymphocytes, monocytes, and fibroblasts (Fig. 5-14A). The granulomatous changes involve predominantly the leptomeninges; they are often perivascular and may extend to the underlying parenchyma along the Virchow-Robin spaces. Cerebral vasculitis may give rise to vascular occlusion and brain infarction. Within the brain,
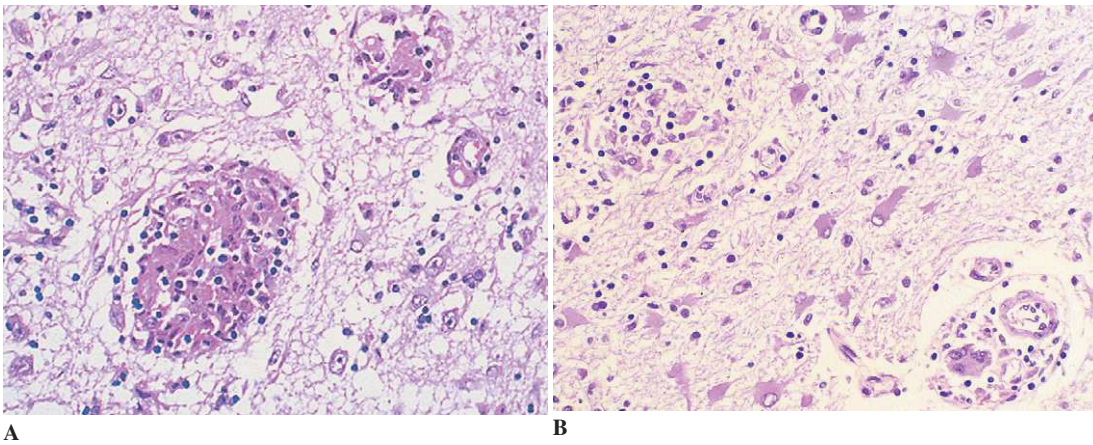
Figure 5-14. Sarcoidosis. **A**, Intraparenchymatous epithelioid granulomas (H and E). **B**, Perivascular granuloma, including lymphocytes, monocytes, and multinucleated cells. Note marked reactive astrocytosis (H and E).

granulomas may be confined to the perivascular spaces (Fig. 5-14B). Parenchymal lesions may also involve the periventricular areas, particularly around the third ventricle, and choroid plexus; they are often surrounded by marked astrocytic proliferation. Coalescence of granulomas may form larger meningeal or parenchymatous masses, simulating neoplasms.

Toxin-Induced Neurological Disease

In addition to direct invasion of the CNS, bacteria can cause neurological damage indirectly by producing neurotoxic substances. A number of neurotoxins have been identified in specific bacterial infections (e.g., diphtheria, tetanus, botulism); in other instances (e.g., shigellosis, *Bordetella pertussis* infection, melioidosis, legionellosis), because of the clinical features and persistent negative cultures of the CSF, the possibility of a toxin-induced involvement of the CNS has been postulated. In either case, although the encephalopathy may be lethal, there are few neuropathological descriptions and CNS changes are usually discrete or nonspecific.

Mycoses and Parasitic Infections

A number of different fungi, protozoa, and metazoa may affect the central and peripheral nervous system. These infections used to be relatively uncommon in everyday neuropathological practice in industrialized countries and were restricted to certain geographical areas or involved small groups of individuals. However, increased intercontinental travel, loosening of health controls, and the AIDS epidemic have made it possible for some infections to spread into previously nonaffected areas. On the other hand, the incidence of some opportunistic infections (in particular mycoses and toxoplasmosis) has increased in the last decades owing to considerable increase in the number of immunocompromised individuals.

Mycotic Infections

Although fungal infections of the CNS are usually secondary to a primary focus elsewhere (e.g., respiratory system or gastrointestinal tract) or to direct extension from the sinuses or bone, in some instances they may represent the only localization. In histological specimens, organisms may be present as yeasts (up to $20\,\mu m$ in diameter), branching hyphae (sometimes quite long), or pseudohyphae of intermediate size. The morphological differences determine the type and size of the lesions, namely, meningitis in infections by the smallest fungi, extensive infarcts following occlusion of the vessels by the largest fungi, and multiple, small infarcts in case of infection by organisms of intermediate size (with infection of

Table 5-1. Main Fungal Infections Affecting the Central Nervous System

Mycosis	Organism	Type of Action	Geographic Distribution	Neuropathology
Aspergillosis	*Aspergillus* (*flavus, fumigatus, niger*)	Predominantly opportunist	Ubiquitous	Usually secondary to foci in lungs and gastrointestinal tract. Abscesses and granulomas; vascular involvement, with extensive hemorrhage (Fig. 5-15A). Branching and septate hyphae (Fig. 5-15B).
Blastomycosis	*Blastomyces dermatitidis*	Predominantly pathogen, mainly in agricultural workers	North America, Africa	Primary focus in lungs. Meningeal lesions, epiduritis, pachymeningitis, purulent or granulomatous meningitis (mimicking tuberculosis). Central, basophilic body with wall; single bud.
Coccidioidomycosis	*Paracoccidioides brasiliensis*	Predominantly pathogen	Brazil	Primary focus in the lungs. Space-occupying lesions; meningitis. Multiple budding.
Candidiasis	*Candida albicans*	Opportunist, mainly in premature infants and immunosuppressed and diabetic patients	Ubiquitous	Saprophite in digestive and genital mucosae. Abscesses or granulomas; vascular involvement. Sometimes meningitis. Chains of elongated cylindrical pseudohyphae.
Cladosporiosis	*Cladosporium trichoides* (*bantianum*)	Predominantly pathogen	Ubiquitous	Isolated from skin, conjunctiva, lymph nodes, GI and urinary tracts. Abscesses or meningitis. Hyphae.
Coccidioidomycosis	*Coccidioides immitis*	Predominantly pathogen	South America, Mexico, south-western USA	Primary foci in lungs. Basal meningitis with nodules; vasculitis. Hyphae.
Cryptococcosis (Fig. 5-16).	*Cryptococcus neoformans*	Predominantly opportunist	Ubiquitous, but predominates in southern USA and Australia	Usually secondary to a focus in the lungs. Meningitis with occasional tubercles. Amount of inflammation depending on degree of immunosuppression. Spores with capsule.
Histoplasmosis	*Histoplasma capsulatum*	Pathogen, but for CNS infections acts as opportunist	Ubiquitous, but common in the USA	Secondary to pulmonary infection. Meningitis with vasculitis. Granulomas are rare. Small, ovoid budding bodies.
Pseudallescheriasis	*Pseudallescheria boydii*	Opportunist (immunodeficiency, diabetes)	Ubiquitous	Associated with disorders of the respiratory system. Meningitis and abscesses; vasculitis; sometimes granulomas. Septate hyphae and clamidospores.
Zygomycosis	*Rhizopus, Mucor, Absidia*	Opportunist, mainly in diabetic patients but also in drug users and patients on antibiotics and corticosteroids.	Ubiquitous	Secondary to focus in skin, nasal mucosa, or lungs. Necrosis and polymorphs with giant cells. Vasculitis with hemorrhage. Broad, branching, nonseptate hyphae.
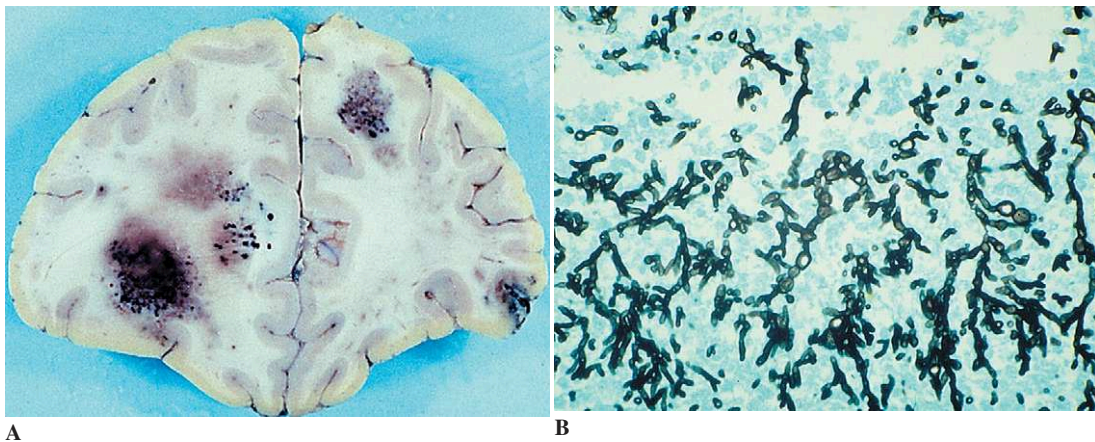
Figure 5-15. Aspergillosis. **A**, Gross appearance. Coronal section of the frontal lobes, showing multiple hemorrhagic abscesses. **B**, Presence of branching and septate hyphae (methenamine silver).

the ischemic lesions in turn causing abscesses and granulomas).

The classic classification of fungi into pathogens and opportunists is not absolute, as some can manifest in both ways.

The main fungal infections that may affect the CNS are summarized in Table 5-1.

Protozoal Infections

The main protozoa responsible for human infections are summarized in Table 5-2.

Amebiasis

Cerebral lesions are produced in human beings by *Entamoeba histolytica* and by free-living amebae. *Entamoeba histolytica* is rarely responsible for hematogenous brain abscesses that are usually associated with liver and/or pulmonary involvement. Free-living organisms may produce primary meningoencephalitis (*Naegleria fowleri*) and granulomatous encephalitis (*Acanthamoeba* and *Leptomyxid*).

Primary meningoencephalitis due to *Naegleria fowleri* is usually contracted during the summer by healthy young people swimming in infected water. Parasites reach the CNS through the nasal mucosa and the olfactory epithelium. The pathology consists of encephalitis with hemorrhagic necrosis,

identifiable parasites, and basal leptomeningitis. Virtually all cases are fatal.

Granulomatous encephalitis presents with brain swelling, moderate meningitis, and confluent areas of hemorrhagic necrosis. Histologically, it is a chronic vasculitis with presence of parasites and occasional granulomatous reaction (Fig. 5-17).

Cerebral Malaria

Responsible for 800,000 deaths a year in Africa alone, *cerebral malaria* is prevalent in 100 countries. There is marked heterogeneity among cases, probably reflecting host susceptibility.

Macroscopically, the brain is swollen, with dusky leptomeninges; on section it appears pale or slate-gray. Microscopically, the commonest feature is sequestration of parasitized blood cells within cerebral microvessels that also contain dark malarial pigment (Fig. 5-18A, p. 128). Petechial hemorrhages of various types are also frequent. Focal necrosis within the white matter is followed by a gliotic reaction (Dürck granuloma; Fig. 5-18B).

Toxoplasmosis

Toxoplasmosis can present as congenital toxoplasmosis (see Chap. 11) or as acquired or primary toxoplasmosis in adults.

Congenital toxoplasmosis is secondary to transplacental infection. It causes diffuse necrotic
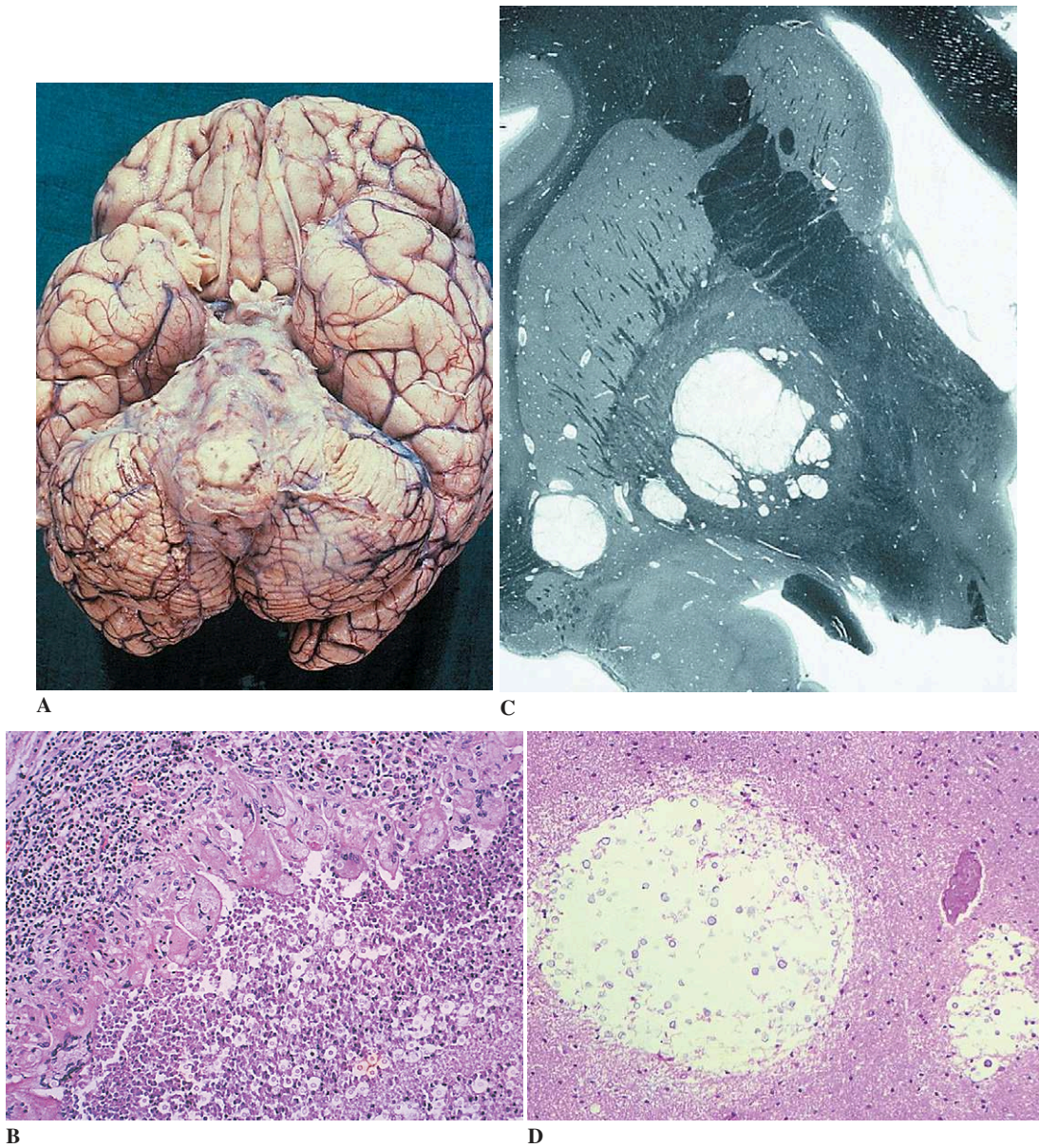
Figure 5-16. Cryptococcosis. **A**, Cryptococcus meningitis, gross appearance. Chronic meningitis involving the basal leptomeningitis. **B**, Cryptococcus meningitis in an immunocompetent patient. Marked lymphocytic and giant cell inflammation (H and E). **C**, Parenchymal cysts in an AIDS patient (Loyez stain). **D**, Microscopic appearance. Dilatation of the perivascular space, forming a cystic cavity filled with cryptococci. Note absence of inflammation or astrocytic reaction in the surrounding parenchyma (H and E).

Table 5-2. Main Protozoa Responsible for Human Infections

1. Amebiasis
   a. *Entamoeba histolytica:* cerebral amebic abscesses
   b. Primary amebic encephalitis
      i) Primary amebic meningoencephalitis (*Naegleria fowleri*)
      ii) Granulomatous amebic encephalitis (*Acanthamoeba* spp. and *Leptomyxid*)
      iii) *Acanthamoeba* keratitis
2. Cerebral malaria (*Plasmodium falciparum*)
3. Toxoplasmosis (*Toxoplasma gondii*)
4. Trypanosomiasis
   a. African trypanosomiasis (*Trypanosoma brucei* spp.)
   b. South American trypanosomiasis (*Trypanosoma cruzi*)
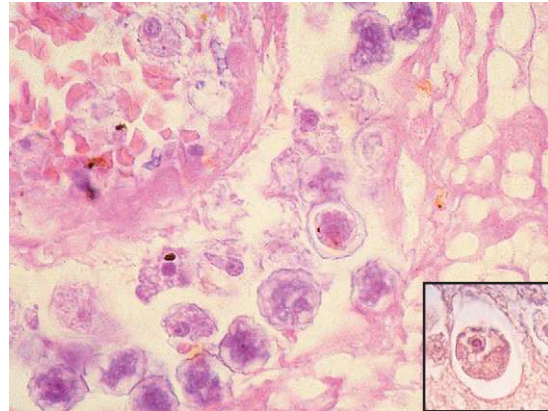
Figure 5-17. Amoebiasis, granulomatous encephalitis. Chronic vasculitis with presence of parasites (H and E).

and inflammatory lesions of the cortex and white matter that are accompanied by calcifications, especially in the periventricular regions.

In primary toxoplasmosis in immunocompetent adults, CNS involvement is uncommon, usually benign or (more often) asymptomatic. In contrast, toxoplasmosis is often fatal in immunocompromised patients (e.g., those with HIV infection, congenital immunodeficiencies, or graft recipients). Cerebral toxoplasmosis is one of the most frequent CNS complications of AIDS and is the main cause of focal cerebral lesions in these patients. Typically, it presents as multiple abscesses involving predominantly the cerebral hemispheres, particularly the basal ganglia and the cortico-subcortical junction. These abscesses contain central, eosinophilic, and acellular pseudo-ischemic necrosis surrounded by a cellular inflammatory reaction. Parasites are seen either within pseudocysts (bradyzoites; Fig. 5-19D) or as free forms (tachyzoites; Fig. 5-19C). Associated hemorrhages are frequent. These abscesses can undergo transformation during the illness and in the course of treatment and appear at post-mortem as (1) necrotizing abscesses (Fig. 5-19A), (2) organizing abscesses (Fig. 5-19B), or (3) chronic, "treated" lesions with a central cystic space. Rarely, in AIDS patients, diffuse "septicemic" encephalitic forms may occur with a dissemination of microglial nodules, some containing encysted bradyzoites or tachyzoites.

Trypanosomiasis

African trypanosomiasis is caused by *T. brucei* subspecies transmitted to humans by the tsetse fly. It is characterized neuropathologically by meningoencephalitis. There is perivascular inflammation with microglial nodules. Mott cells, characteristic of this form, are plasma cells with prominent eosinophilic cytoplasmic Russell bodies. No parasites are usually seen in the brain tissue.

South American trypanosomiasis (Chagas disease) remains a health problem in many areas of Central and South America, where it affects up to 18 million individuals. The agent, *Trypanosoma cruzi*, is responsible for both an acute and a chronic disease. The former can be asymptomatic or present as a mild meningoencephalitis with microglial nodules in the brain, sometimes containing parasites. The chronic form includes a "chagasic" encephalopathy with neuronal loss and focal inflammatory changes and, more commonly, a peripheral autonomic and occasionally somatosensory neuropathy with ganglion cell loss. In AIDS patients, *T. cruzi* infection may cause multifocal necrotizing encephalitis in which abundant
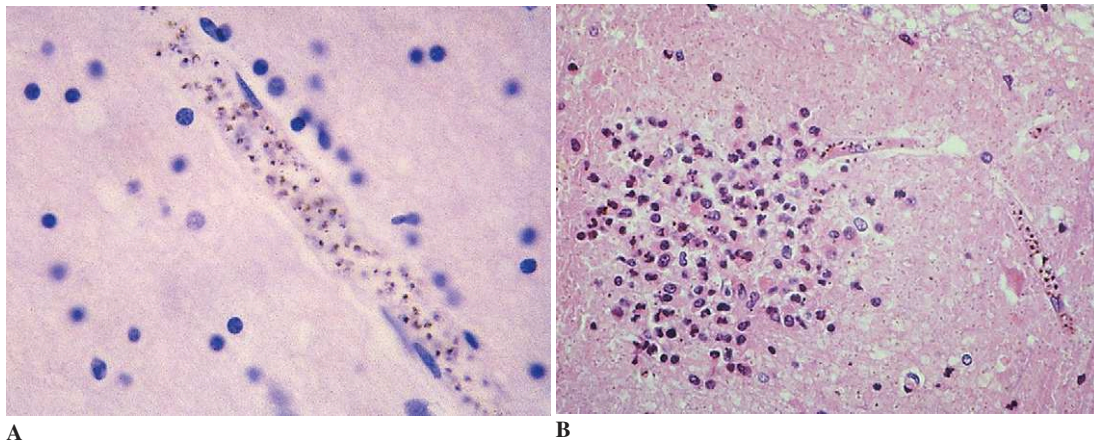
Figure 5-18. Cerebral malaria. **A**, Sequestration of parasitized blood cells within cerebral microvessels that also contain dark malarial pigment. **B**, Dürck granuloma (H and E).
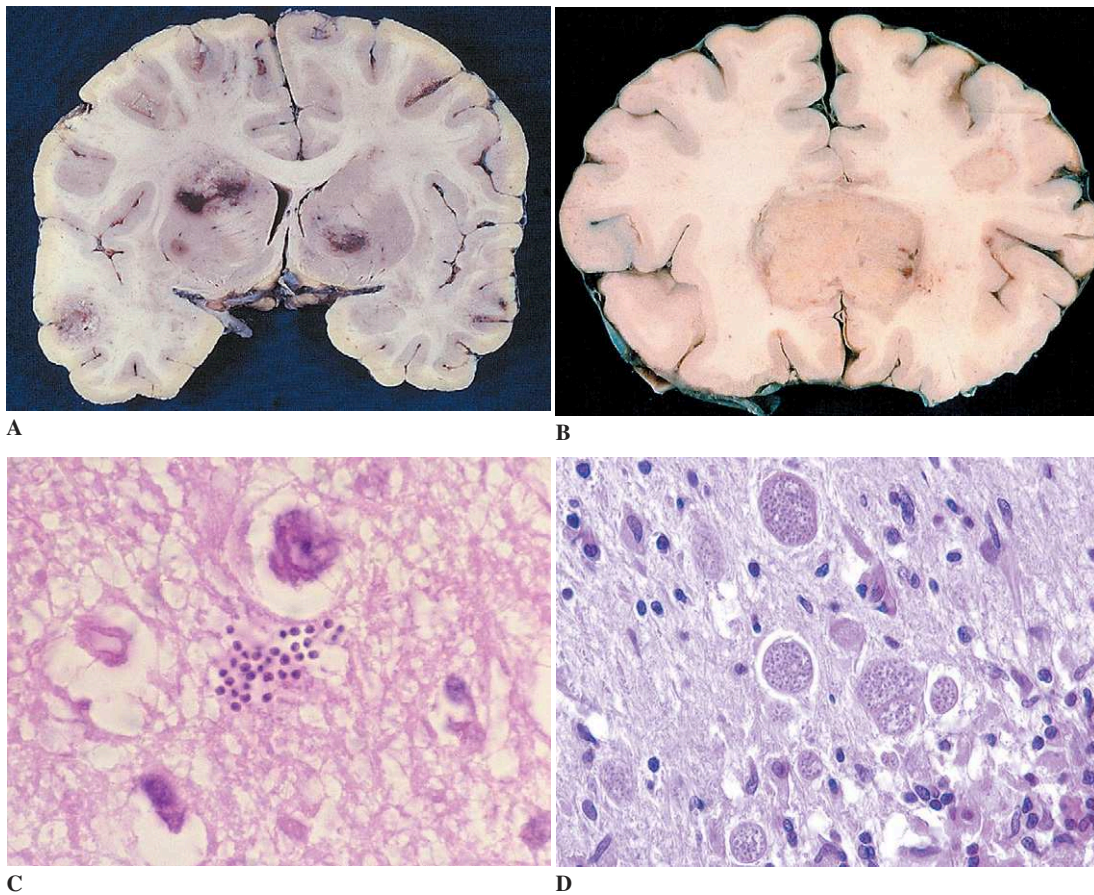
Figure 5-19. Toxoplasmosis. **A**, Multiple necrotizing abscesses, some of which are hemorrhagic, involving the basal ganglia and the cortico-subcortical junction. **B**, Organizing abscesses with central necrosis and hyperemic border in the genu of corpus callosum and in the white matter of the right frontal lobe. **C**, Free tachyzoites at the periphery of a necrotic lesion (H and E). **D**, Numerous pseudocysts (bradyzoites) around a necrotic lesion (H and E).
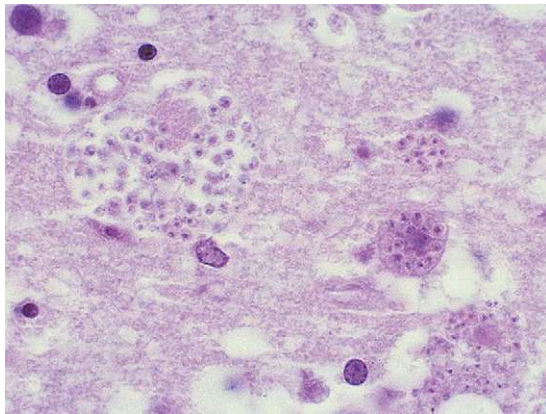
Figure 5-20. Trypanosomiasis. Abundant amastigote parasites are present within glial cells in a case of multifocal necrotizing encephalitis (H and E). (Courtesy Dr. Leila Chimelli.)

amastigote parasites are present, particularly within glial cells and neurons (Fig. 5-20).

Metazoal Infections

The major helminthic infections of the CNS can be classified as summarized in Table 5-3.

Table 5-3. Major Helminthic Infections of the CNS

1. Cestodes
   a. Neurocysticercosis (*Taenia solium*)
   b. Hydatid cyst (*Echinococcus granulosum*)
   c. Coenuriasis (*Taenia multiceps*)
   d. Sparganosis (*Spirometra*)
2. Trematodes
   a. Paragonimiasis (*Paragonimus westermani*)
   b. Schistosomiasis (*Schistosoma mansoni, japonicum, hematobium*)
   c. Other trematode infections
3. Nematodes
   a. Eosinophilic meningoencephalitis
      i) *Angiostrongylus cantonensis*
      ii) *Gnathostoma spinigerum*
   b. Toxocariasis (visceral larva migrans); other forms of larva migrans (*Trichinella spiralis*)
   c. Human filariases
      i) Loa-loa
      ii) *Dracunculus medinensis*
      iii) *Onchocerca volvulus*
   d. Nematodes and immunosuppression (*Strongyloides stercoralis*)

Cysticercosis

Cysticercosis is the most common parasitic infection of the CNS and is endemic in all countries, particularly in Latin America. It is caused by the larval stage of the pig tapeworm; the disease occurs between 2 months and 30 years after initial infection. The number of cysts in the CNS varies from one to several hundred (Fig. 5-21A). All have similar structure; they contain a single scolex with four suckers and a double row of hooklets (Fig. 5-21B). The cyst walls consist of three layers: (1) outer or cuticular; (2) middle or cellular, with pseudoepithelial appearance; and (3) inner or reticular or fibrillary (Fig. 5-21C).

Hydatidosis

Hydatid cysts are endemic in the Mediterranean regions, the Middle East, and Latin America. Dogs and other canids are the definitive hosts. Cysts in the brain are usually solitary and unilocular. Their wall consists of two layers, namely, the outer, laminated, cuticular layer and the inner, germinal layer.

Schistosomiasis

Schistosomiasis is caused by flukes of the genus *Schistosoma,* which have man and other mammals as definitive hosts. The infection is endemic in South America, the Middle and Far East, and Africa. CNS lesions involve predominantly the spinal cord. Macroscopic changes are uncommon. Histological examination reveals three main appearances: (1) necrotic-exudative, with variable number of eggs (the area is surrounded by eosinophils, lymphocytes, plasma cells, and macrophages); (2) a productive stage, in which eggs have lost the embryo; and (3) a late stage, with granulomatous reaction and giant cells (Fig. 5-22).

Eosinophilic Meningitis

Eosinophilic meningitis is due to infection by *Angiostrongylus cantonensis* or *Gnathostoma spinigerum*. Larvae may be demonstrated in the brain or meninges, which show a predominantly eosinophilic infiltrate.

Toxocariasis

Toxocara canis is a common agent and important canine zoonosis that occurs worldwide. It may occasionally affect humans, particularly children.

A **B**

C
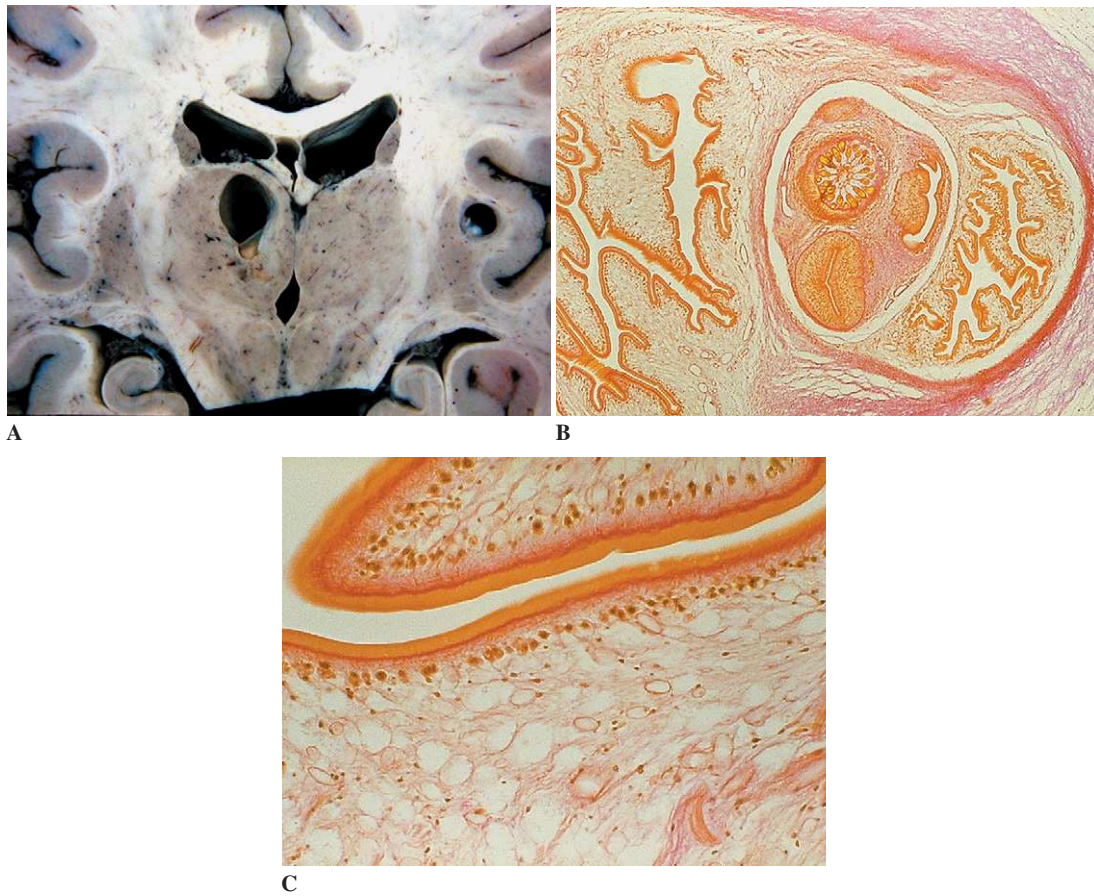
Figure 5-21. Cysticercosis. **A**, Gross appearance. Two cystic cavities containing a parasite are present in the thalamus and insular cortex. **B**, Microscopic appearance of the scolex with suckers and a double row of hooklets. **C**, Higher magnification, showing the three layers of the cyst walls (HES). (**A**, Courtesy Dr. Leila Chimelli.)
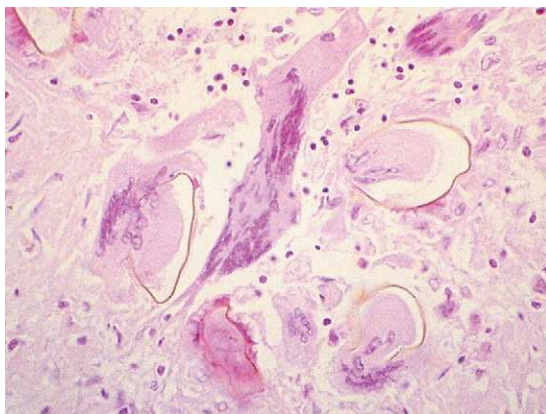
Figure 5-22. Schistosomiasis. Eggs within a granulomatous reaction with giant cells (H and E).

The death of the parasite in the brain is followed by a nonencapsulated granulomatous reaction consisting of lymphocytes, eosinophils, plasma cells, fibroblasts, and epithelioid and giant cells.

Trichinosis

Trichinosis exists mostly in North and South America, but outbreaks have also been reported in Europe and in some Mediterranean countries. Involvement of the striated muscle is the main complication (see Chap. 13). Involvement of the CNS is uncommon. Macroscopic features may be limited to nonpurulent meningitis, mild edema, and occasional, small hemorrhages. Histological findings include granulomatous nodules (predomi-

nating in the white matter and consisting of lymphocytes), microglia, and histiocytes. Larvae are only rarely identified in nodules, suggesting an immune-mediated pathogenesis of the lesions.

Strongyloides stercoralis *Infection*

Strongyloides stercoralis infection should be considered in the presence of severe immunosuppression, during which larval infection can affect every organ. In these circumstances, larvae can be seen in the subarachnoid spaces and microinfarcts may be produced by obstruction of capillaries by the parasite.

Viral Infections

The lesions of the CNS induced by viral infections may result from various mechanisms. Some of these are nonspecific and are due to immunoallergic reactions that are secondary to the viral infection; they involve the leptomeninges and especially the white matter (leukoencephalitides). Other, more specific lesions are directly caused by the infection of the CNS by the virus. They involve mainly, but not exclusively, the gray matter (polioencephalitides). Most viral encephalitides run an acute course. However, special immunological phenomena may modify the course of the disease and result in the development of a latent infection, notably as in herpes, or a persistent infection, as in subacute sclerosing panencephalitis, which is presumably caused by a defective measles virus. In AIDS, infection by the retrovirus HIV causes both a subacute encephalitis and immunodeficiency.

Nonspecific CNS Involvement in Viral Infections

Acute Viral Lymphocytic Meningitis (Aseptic Meningitis)

Acute viral lymphocytic meningitis (*aseptic meningitis*) is common with several types of viral infections, mainly enteroviruses (e.g., echovirus, coxsackieviruses, enterovirus 71), but also mumps virus, herpes simplex virus 2 (HSV-2), arboviruses, lymphocytic choriomeningitis (LCM) virus, measles, parainfluenza, adenoviruses, and others. It

is characterized by vascular congestion and a scanty infiltrate of lymphocytes in the leptomeninges, perivascular spaces surrounding some of the superficial cortical blood vessels, and choroid plexus.

Acute Disseminated Encephalomyelitis

Acute disseminated encephalomyelitis (*ADEM*), also known as *acute disseminated leukoencephalitis* or *acute postinfectious/post-vaccinial perivenous encephalitis*, may complicate a variety of systemic viral diseases, including measles, mumps, chickenpox, rubella, influenza, and infectious mononucleosis caused by Epstein-Barr virus (EBV). It was also well documented following smallpox or rabies vaccination. It closely resembles experimental allergic encephalomyelitis produced by injecting experimental animals with myelin proteins and adjuvant and is believed to be due to a T-cell-mediated hypersensitivity reaction. Clinically, it presents as an acute, disseminated encephalomyelitis that is separated by a latent period of a few days to three weeks' duration from the causative viral infection or vaccination.

The histological features are highly stereotyped and consist of lymphocyte, plasma cell, and macrophage infiltrates around the venules of the neural parenchyma. These involve mainly the white matter, where they are associated with perivenous foci of demyelination (Figs. 5-23A and B) with relative sparing of the axons. There may also be small, perivascular hemorrhages. Arteries are relatively free of inflammation, but there are often inflammatory cells in the leptomeninges.

Acute Hemorrhagic Leukoencephalopathy of Hurst

Acute hemorrhagic leukoencephalopathy of Hurst is a fulminant, usually fatal disorder regarded by some as a hyperacute form of ADEM. It is characterized by the presence of numerous, scattered, hemorrhagic foci that are more prominent in the cerebral (Fig. 5-24) and cerebellar white matter and in the pons. Microscopically, many small blood vessels undergo fibrinoid necrosis and are surrounded by a narrow zone of necrotic tissue and a larger zone of hemorrhage (ring- or ball-shaped perivascular hemorrhages). Still-recognizable vessels are veins or venules, which may be surrounded by fibrin and an inflammatory
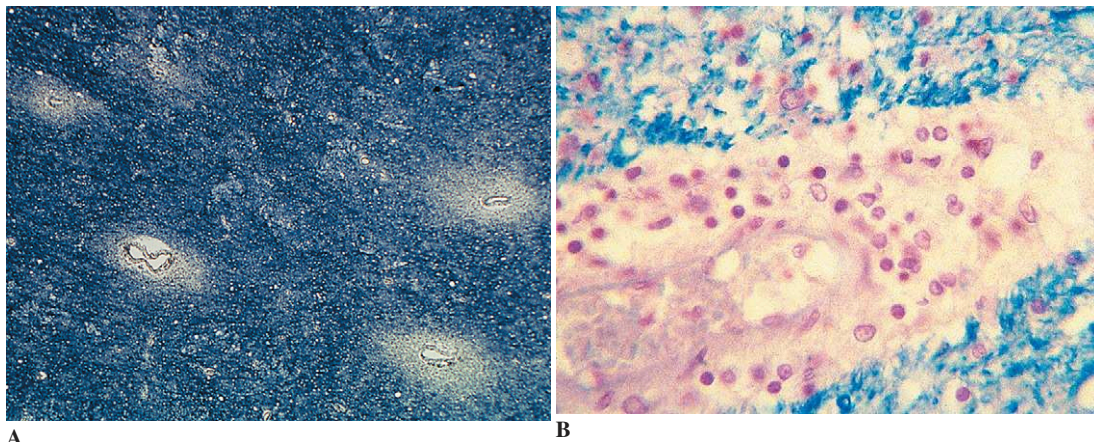
Figure 5-23. Acute perivenous encephalitis. **A**, Perivenous foci of demyelination in the white matter (Loyez stain). **B**, Higher magnification, showing perivenous inflammatory infiltrates (Klüver and Barrera stain).

infiltrate including neutrophils and mononuclear cells. Some fibers within the infiltrate are demyelinated, but many show axonal fragmentation.

Infective Viral Encephalitis and Encephalomyelitis

Viral encephalitis—in the strict meaning of the term—is due to infection of the brain by a virus. However, viral infection also quite often involves the meninges (meningoencephalitis) and/or the spinal cord (encephalomyelitis, meningoencephalomyelitis) as well as the nerve roots (meningoencephalomyeloradiculitis).
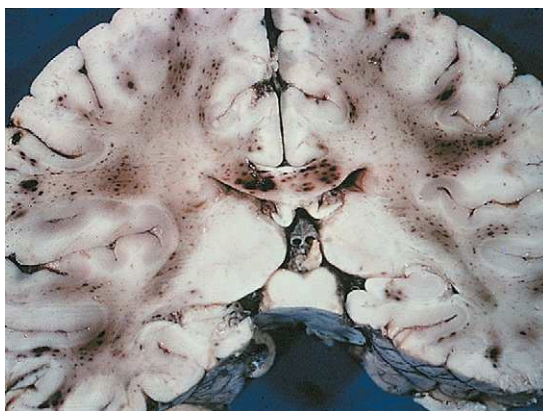
Figure 5-24. Gross appearance of acute hemorrhagic leukoencephalopathy.

Nervous system involvement is always secondary to infection elsewhere in the body. In fact, most viral infections of the CNS are rare complications of common systemic viral diseases. The portal of entry that has been directly exposed to infection may be the skin (direct contact or by an animal or insect bite), the airways (inhalation), or the alimentary tract (ingestion). The virus may spread to the CNS directly along the olfactory or peripheral nerves or, in the course of viremia, by the hematogenous route. This is followed by obligatory intracellular viral replication in one or more of the cell types in the CNS—neurons, glial cells, microglial cells, or macrophages—depending on whether they possess receptors that allow entry of the virus into the cell.

Whatever the causative virus, the basic neuropathological picture of viral encephalitis includes the following:

- Involvement of the neuronal cell bodies, resulting in their destruction and engulfment by macrophages (neuronophagia; Fig. 5-25A).
- Perivascular cuffing of inflammatory cells, mainly lymphocytes, macrophages, and plasma cells (Fig. 5-25B).
- Microglial proliferation, with the formation of microglial nodules and the appearance of rod cells (Fig. 5-25C).
- In some cases, intranuclear or intracytoplasmic inclusion bodies are indicative of the presence of virus in neurons and/or glia.
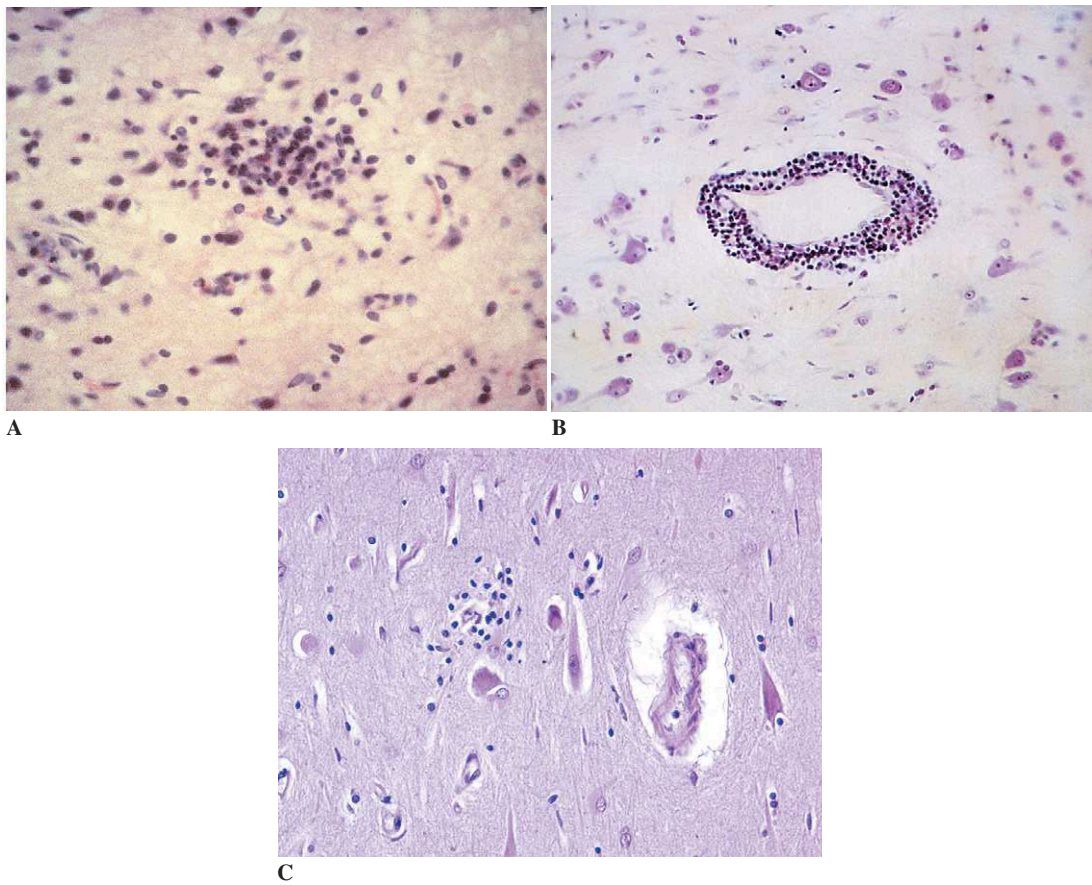
Figure 5-25. Chief microscopic features of encephalitis. **A**, Neuronophagia (Nissl stain). **B**, Lymphocytic perivascular cuffing (Nissl stain). **C**, Proliferation of rod-shaped microglia (H and E).

According to the type of virus responsible, one may separate encephalitides into those caused by RNA viruses (enterovirus, arbovirus, rabies, paramyxovirus, rubivirus, retrovirus), DNA viruses (herpesvirus, papovavirus), and (possibly) as-yet-unidentified viruses (encephalitis lethargica, Behçet uveomeningoencephalitis, chronic localized encephalitis of Rasmussen).

Encephalitides Caused by RNA Viruses

Poliomyelitis. *Poliomyelitis* is due to infection of the CNS by a poliovirus, a small RNA virus of the genus *Enterovirus*.

The most frequent form of the disease, "acute anterior poliomyelitis," is characterized by lytic infection of the motor neurons. The lesions selectively involve the motor neurons of the anterior horns and the cranial nerve nuclei but may extend to the frontal gyri, the hypothalamus, the reticular formation, and the posterior horns. As a result of viral infection and lysis of the neurons, there is neuronophagia and microglial nodules with microglial and macrophagic proliferation. Inflammation in the leptomeninges and affected gray matter is intense (Figs. 5-26A and B). There is edema, vascular congestion (which may be associated with perivascular hemorrhages), and, occasionally, focal necrosis.

Following resolution, the residual lesions consist of atrophy of the anterior horns with neuronal loss and astrocytic gliosis. There is atrophy and fibrosis of the anterior nerve roots, which appear thin and grayish at gross examination. The corresponding skeletal muscles show wasting with severe denervation atrophy.
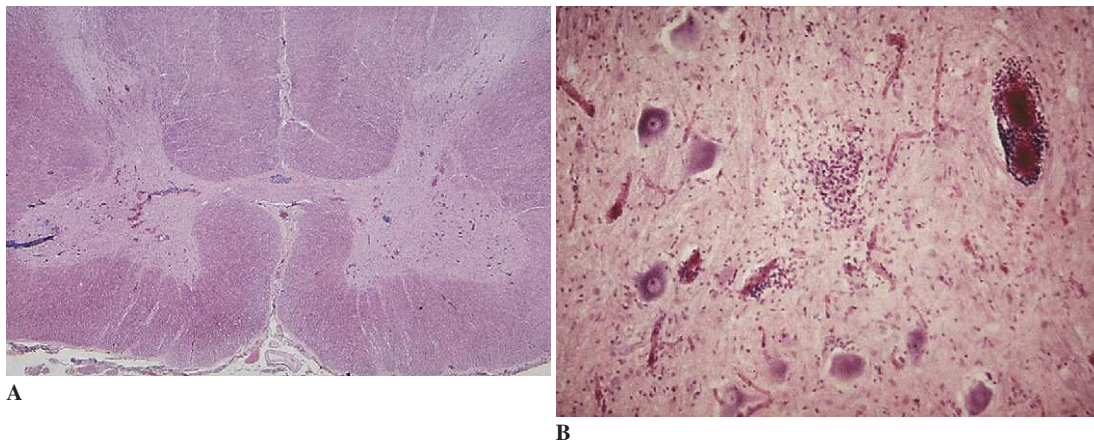
Figure 5-26. Poliomyelitis. **A**, Horizontal section of the cervical level of the spinal cord, showing inflammation in the anterior horns. **B**, Higher magnification, showing neuronophagia, microglial proliferation, and perivascular cuffing of lymphocytes (H and E).

The introduction of a vaccine has resulted in a sharp decline in the incidence of poliomyelitis. However, outbreaks of paralytic infection by wild-type poliovirus still occur in developing countries. In vaccinated populations, poliomyelitis is usually caused either by the rare reversion to neurovirulence of attenuated vaccine-related strains of poliovirus, or by other groups of enteroviruses, especially group A coxsackieviruses and enterovirus 71.

Arbovirus (Arthropod-Borne Virus) Encephalitides. *Arbovirus* (*arthropod-borne virus*) *encephalitides* are transmitted by insects. Each has a distinct geographical distribution that is often indicated by the name of the virus.

The best-known forms of the mosquito-borne encephalitides include St. Louis encephalitis and the Eastern, Western, and Venezuelan equine encephalitides in America; Japanese B encephalitis in the Far East; Murray Valley encephalitis in Australia; and West Nile fever, primarily in Africa but also in Europe, Asia, and America. In these various forms, the typical lesions of encephalitis are widely distributed throughout the neuraxis.

Tick-borne encephalitides, which include Russian spring-summer encephalitis and Central European encephalitis, are characterized by meningoencephalitic lesions and by involvement of the lower cranial nerves and anterior horns, especially at cervical levels.

Rabies. *Rabies* is caused by a rhabdovirus that is transmitted to humans by the bite of a rabid animal. The animal reservoir includes foxes, skunks, coyotes, jackals, and bats. However, dog remains the main source of human infection. The disease may present as "furious" rabies or "dumb" (paralytic) rabies. Once declared, the disease is almost always fatal.

On neuropathological examination, rabies is characterized by the presence in the neurons of diagnostic cytoplasmic inclusions called *Negri bodies* (Figs. 5-27A and B). These are mainly found in the pyramidal neurons of the hippocampus and in Purkinje cells. Accompanying lesions include leptomeningeal and perivascular inflammation, microglial nodules (Babès nodules), and microglial hyperplasia. These lesions are variable, but there may be striking disparity between the abundance of virus and the limited degree of inflammation.

Measles Encephalitides. *Measles virus*, a paramyxovirus (like the viruses that cause influenza and mumps), is known to cause two rare forms of subacute encephalitis: subacute sclerosing panencephalitis (SSPE) and immunosuppressive measles encephalitis. In addition, it may provoke postinfectious encephalitis (see earlier in this chapter).

SSPE occurs in children, several years after an episode of measles. About half of the patients are known to have had measles before the age of two.
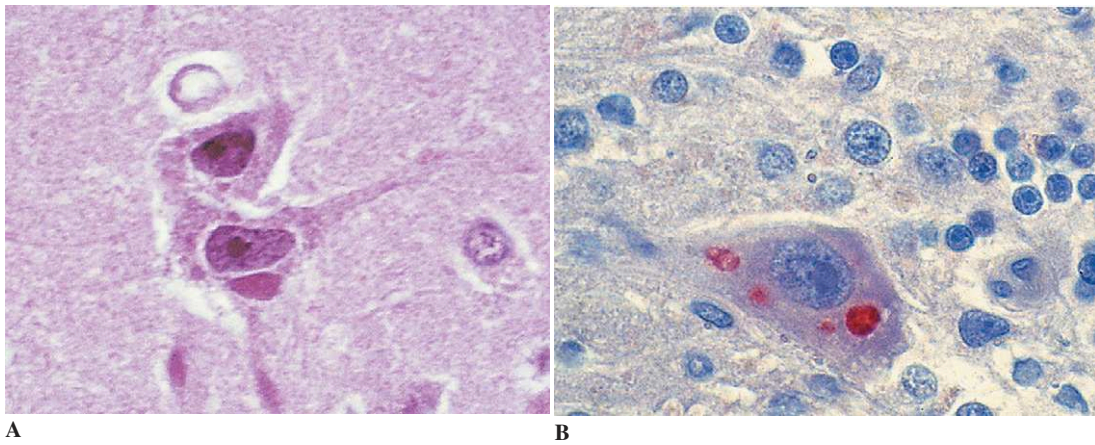
Figure 5-27. Rabies. **A**, Negri bodies in a pyramidal neuron of the hippocampus (H and E). **B**, Negri bodies in a Purkinje cell stained in red using a specific antibody.

The lesions involve both the gray and the white matter. In the gray matter, the cortex is predominantly affected but involvement of the basal ganglia, mainly the thalamus, is frequent, and there may sometimes be extension to the brainstem. Microscopic examination shows the features of subacute encephalitis. There is neuronal loss, occasional neuronophagia, and astrocytic and microglial hyperplasia. Inclusion bodies may be found in neuronal and glial nuclei (Fig. 5-28A). The white-matter lesions are variable, including marked astrocytic proliferation with inclusions in the glial nuclei and patchy myelin loss. Leptomeningeal, perivascular, and parenchymal inflammatory infiltrates are present both in the gray and white matter. In late cases there may be considerable neuronal loss with atrophy of the cortex and basal ganglia, and neurofibrillary degeneration of the Alzheimer type has been reported. The white matter shows thinning and demyelination with severe gliosis (Fig. 5-28B). Inflammatory cells may be very scanty, as may be inclusion bodies, which may be better detected immunohistochemically.

Although the measles virus has been demonstrated to be the causative agent by electron microscopy (Fig. 5-29), in tissue culture, and by immunological and virological assays, the pathogenesis of this type of prolonged viral infection remains uncertain. A viral mutation resulting in defective M-protein expression, enabling the virus to elude the host immune response, has been postulated.

Measles inclusion-body encephalitis develops within months of the initial systemic infection in patients with impaired cell-mediated immunity. In AIDS patients, similar changes have also been reported to occur after measles vaccination. The brain may be normal or may show extensive zones of necrosis of gray and white matter; thus, the diagnosis can be made only on microscopic examination. The lesions may be focal or widespread throughout the brain; involvement of the spinal cord has been found in children with AIDS. The diagnostic feature is the presence of eosinophilic inclusion bodies that are readily seen on routine stain (Fig. 5-30) but can also be demonstrated by immunohistochemistry and electron microscopy. These are mostly intranuclear and involve predominantly neurons and, to a lesser extent, astrocytes and oligodendrocytes. Occasionally, virus containing multinucleated giant cells may be found. There may be accompanying inflammatory infiltrates and reactive astrocytes and microglia, but these may be very scanty (even absent), and the presence of inclusions may thus be missed.

Progressive Rubella Panencephalitis. *Progressive rubella panencephalitis* is a very rare delayed complication of congenital or childhood rubella infection. At neuropathological examination there is (1) widespread neuronal loss with gliosis and leptomeningeal and perivascular inflammation containing lymphocytes and macrophages and (2) vasculitis with fibrinoid necrosis and mineral

A

B
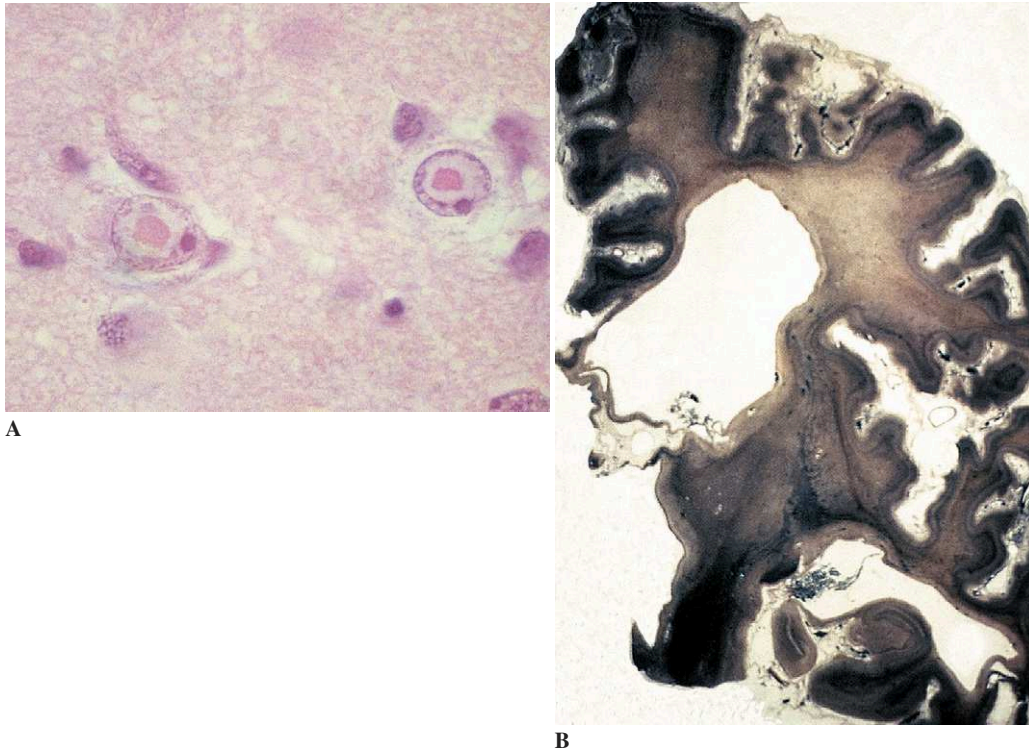
Figure 5-28. Subacute sclerosing panencephalitis. **A**, Intranuclear inclusion bodies in neurons (H and E). **B**, Massive demyelination of the white matter and severe cortical atrophy (Loyez stain).
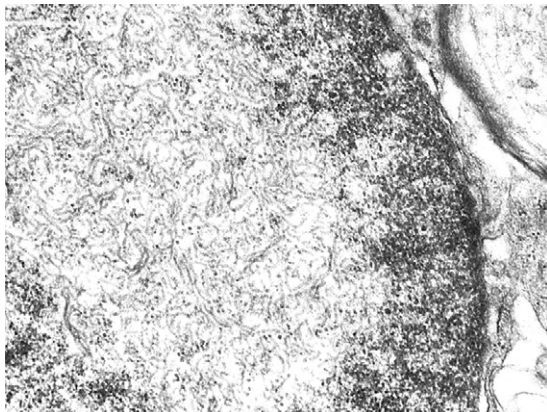
Figure 5-29. Electron microscopy showing intranuclear tubular formations characteristic of measles myxovirus in a case of subacute sclerosing panencephalitis.
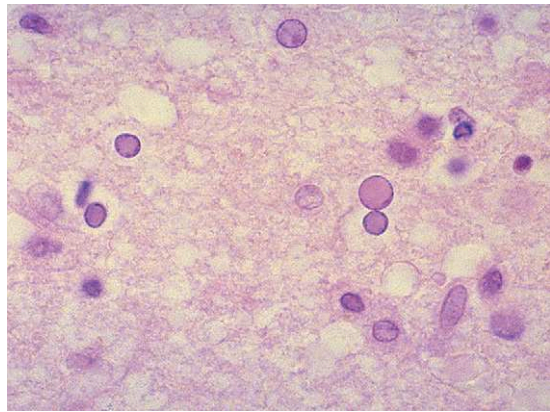
Figure 5-30. Measles inclusion-body encephalitis. Presence of numerous eosinophilic intranuclear inclusion bodies (H and E).

deposition. There is also extensive myelin destruction with relative sparing of axons. Inclusion bodies are not found, and rubella virus is not detected by either electron microscopy or molecular techniques. The lesions may result from vasculitis produced by immune-complex deposition.

Infection by HIV. HIV is a retrovirus of the lentivirus subfamily. This virus infects cells that carry on their surface the CD4 antigen, which is present both in CD4+ helper T lymphocytes and monocytes/macrophages. On the one hand, infection of the lymphocytes leads to their destruction and to cell-mediated immunodeficiency (i.e., the acquired immune deficiency syndrome, AIDS). On the other hand, it invades the CNS via infected macrophages, which represent a major cell type capable of supporting viral replication and thus potentially serving both as a reservoir for the virus and as an agent for its dissemination.

CNS neurological complications of HIV infection are frequent and result from various mechanisms. Apart from lesions directly related to infection of the CNS by the virus, opportunistic infections and lymphomas may occur as a result of the immunodeficiency syndrome. HIV-associated systemic disorders may also cause neuropathological changes. They include cerebrovascular disease (marantic endocarditis, thrombocytopenia, and coagulopathy); metabolic and nutritional abnormalities (hypoxia; vitamin deficiencies causing Wernicke encephalopathy and, possibly, vacuolar

myelopathy; electrolytic disturbances responsible for central pontine myelinolysis); liver failure, causing hepatic encephalopathy; and increased levels of circulating pro-inflammatory cytokines, likely to be responsible for multifocal necrotizing leukoencephalopathy. Finally, neurological complications of treatment, particularly those involving the peripheral nervous system and skeletal muscles, are increasingly frequent.

HIV-induced CNS lesions are unique and specific changes that have never been observed before the AIDS epidemic and are found only in HIV-infected individuals, without evidence of another cause. They include HIV encephalitis resulting from direct infection of the CNS by the virus, HIV leukoencephalopathy, and diffuse poliodystrophy, which is uncommon.

HIV encephalitis caused by productive infection of the CNS by the virus is the most characteristic of these lesions. It includes marked astrocytic and microglial activation with frequent multinucleated giant cells (Fig. 5-31A) and abundant viral load (demonstrable by immunocytochemistry; Fig. 5-31B) or in situ hybridization. Multinucleated giant cells are a hallmark of HIV encephalitis. They are of macrophage lineage, contain HIV in their cytoplasm, and result from the cell-fusing capacity of the virus. Thus, their presence provides evidence of productive HIV infection and of a cytopathic effect of the virus. The lesions consist of multiple disseminated foci that may affect any part of the CNS but are more frequently found in the deep white matter and basal ganglia.

A   B
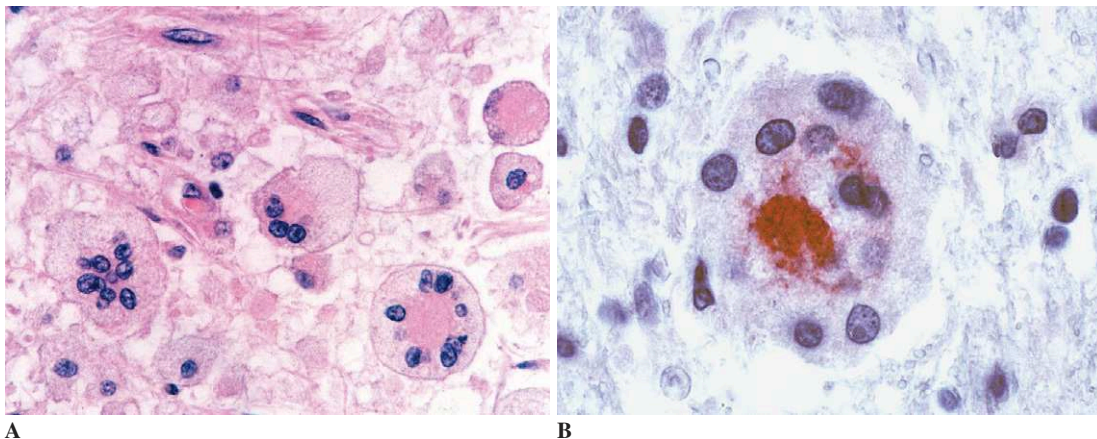
Figure 5-31. HIV encephalitis. **A**, Presence of abundant multinucleated giant cells (H and E). **B**, Immunocytochemistry using an anti–HIV p24 antibody demonstrates the presence of HIV-antigen in the cytoplasm of a multinucleated giant cells.

Figure 5-32. HIV leukoencephalopathy (Loyez stain).

Involvement of the white matter—HIV leukoen-cephalopathy—is also a prominent feature of HIV-specific neuropathology (Fig. 5-32). It is often but not invariably associated with HIV encephalitis. It is characterized both by diffuse myelin pallor (involving predominantly the deep white matter and usually sparing the U fibers) and by widespread axonal damage. The pathogenesis of the lesion is unknown, but it is thought to be secondary to alterations in the blood-brain barrier.

Involvement of the gray matter—diffuse poliodystrophy—is characterized by diffuse reactive astrocytosis and microglial activation in the cerebral gray matter. It is associated with neuronal loss resulting, at least partly, from an apoptotic process and, when severe, may cause macroscopic cortical atrophy.

None of these HIV-induced CNS lesions can be precisely correlated with the specific progressive cognitive/motor syndrome "HIV dementia," suggesting that HIV dementia more likely reflects a specific neuronal dysfunction resulting from the combined effects of several neurotoxic factors (including those produced by HIV itself as well as by substances produced by activated glial and microglial cells), some of which may be reversible.

Human T Cell Leukemia/Lymphotrophic Virus-1–Associated Myelopathy. *Human T cell leukemia/lymphotrophic virus-1* (*HTLV-1*) was the first human retrovirus to be identified. It is endemic in the Caribbean, the southern United States, South America, parts of Africa, and Japan. In rare cases, it may cause a myelopathy characterized by progressive spastic paraparesis with sphincter and sensory disturbances.

In longstanding cases, there may be macroscopic meningeal thickening, spinal cord atrophy and degeneration of the lateral columns. Microscopic examination shows myelin loss and some axonal degeneration in the long tracts of the spinal cord, particularly in the lateral columns. There is fibrosis and lymphocytic infiltration of the leptomeninges and astrocytosis and mononuclear inflammation in the spinal cord, more marked in the lower thoracic region.

Encephalitides Caused by DNA Viruses

Encephalitides caused by DNA viruses include encephalitides due to herpesviruses and papovaviruses. The main herpesviruses causing CNS infection in human include herpes simplex virus (HSV) type 1 and type 2, varicella-zoster virus (VZV) or human herpesvirus (HHV) type 3, and cytomegalovirus (HHV type 5). The main human infection caused by papovaviruses is progressive multifocal leukoencephalitis (PML) due to JC virus.

HSV Encephalitis. HSV is the most common cause of sporadic acute encephalitis. Most cases are due to infection by HSV type 1, but in immuno-suppressed individuals and neonates HSV type 2 may also cause encephalitis. Following a primary infection (oropharyngeal for HIV-1, genital for HIV-2), HSV establishes a latent infection in the sensory ganglia, with periodic reactivation of the virus leading to recurrent lesions at mucocutaneous junctions at or near the site of primary infection. The mechanism of entry of HSV-1 into the CNS to cause encephalitis is debated; possibilities include

spread along olfactory nerve fibers, either during primary nasopharyngeal infection or after reactivation of a latent virus in the olfactory bulbs; reactivation of a latent virus in the trigeminal ganglia and axonal spread into the brain; and reactivation of a previously established latent infection in the CNS, mainly in the temporal lobes.

In patients who died at the acute stage of the disease, gross examination has shown generalized swelling and bilateral asymmetric necrotic and hemorrhagic lesions involving predominantly the temporal lobes and the limbic regions (insulae, cingulate gyri, and posterior orbital-frontal cortex; Fig. 5-33A). At microscopic examination, the earliest lesions consist of meningeal, perivascular, and scanty parenchymal inflammation with scattered cells (neurons and glial cells) containing intranu-

clear inclusion bodies. The presence of HSV may be identified by immunohistochemistry or electron microscopy (Fig. 5-33D). At a more advanced stage the lesions are more characteristic and include foci of hemorrhage and necrosis with parenchymal infiltration by lymphocytes and macrophages (Fig. 5-33B). Changes more characteristic of meningoencephalitis (i.e., mononuclear inflammation of the leptomeninges, perivascular cuffing, neuronophagia, and diffuse microglial hyperplasia) are also present. Nuclear inclusions (Fig. 5-33C) are usually sparse, and thus better identified by immunohistochemistry.

In long-term survivors of untreated or unsuccessfully treated herpes encephalitis, the affected parts of the brain are shrunken and cavitated and show yellow-brown discoloration. The entire
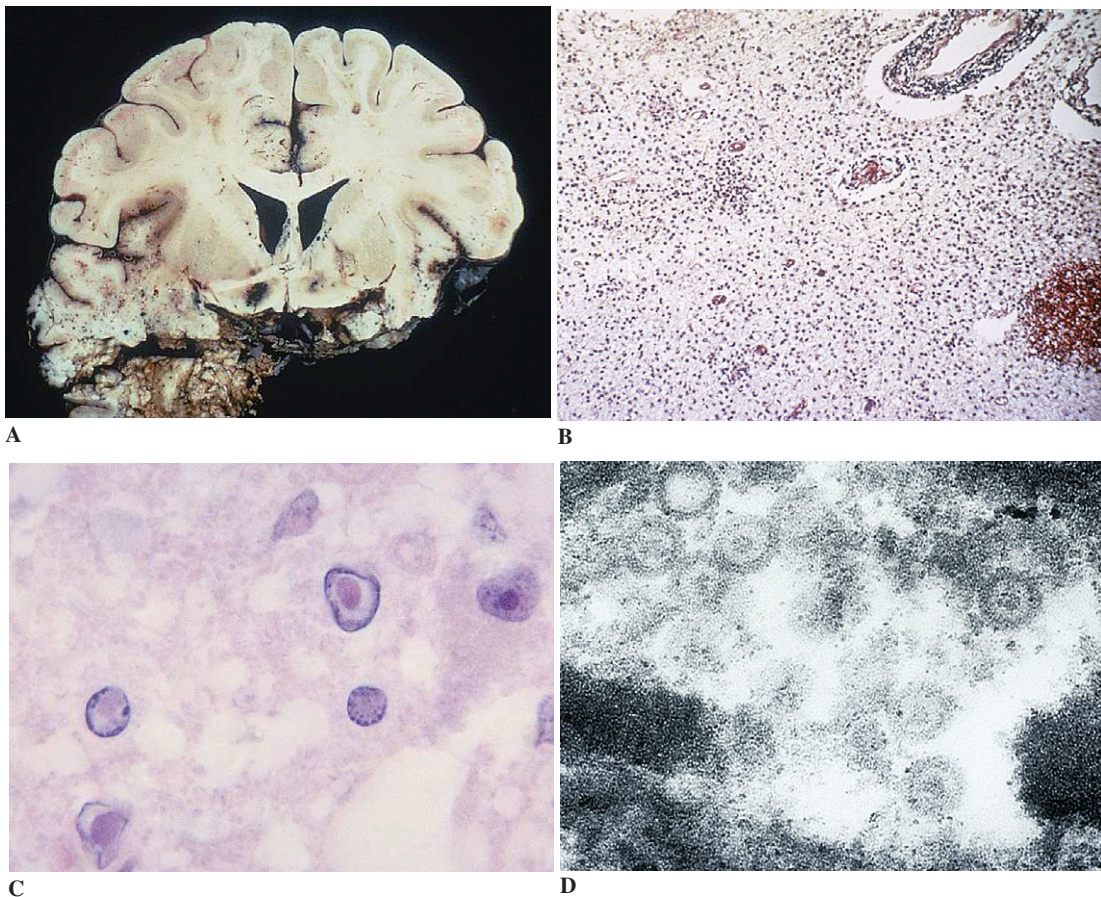
Figure 5-33. Herpesvirus encephalitis. **A**, Necrosis of the left temporal lobe (the right temporal lobe was surgically excised). **B**, Microscopic appearance: necrosis with parenchymal infiltration by macrophages. Note presence of hemorrhage and perivascular cuffing by lymphocytes (H and E). **C**, Characteristic intranuclear inclusion bodies (H and E). **D**, Electron micrograph showing typical "target-like" intranuclear viral particles.

parenchyma is replaced by cavitated glial scar tissue. Occasional clusters of lymphocytes are still seen in the leptomeninges and brain parenchyma. The virus is no longer demonstrable by culture, immunohistochemistry, or electron microscopy, but viral DNA may be identified by polymerase chain reaction.

Neonatal HSV encephalitis differs from the adult disease in that it is usually due to HSV-2 and causes more generalized encephalitis without any predilection for any part of the brain. It also presents as a necrotizing encephalitis. Nuclear inclusions, viral antigen, and DNA are usually demonstrable in abundance.

Varicella-Zoster Virus Infection.   Primary infection by varicella-zoster virus (VZV) causes chickenpox. Latent infection is subsequently established in the dorsal root or trigeminal ganglia. Reactivation of latent virus usually manifests as shingles.

The pathological changes in zoster infection are usually limited to the dorsal root ganglia or to the ganglia of a sensory cranial nerve and the nerve root, but may extend to the corresponding metameric segment of the spinal cord. There is intense lymphocytic inflammation that may be associated with vasculitis and necrosis. Arteritis of large arteries may cause extensive infarction of neural tissue.

In immunocompromised patients, particularly AIDS patients, several patterns of VZV encephalitis and myeloradiculitis have been described, including multifocal lesions predominantly involving the white matter (probably caused by hematogenous spread of the virus); ventriculitis secondary to ventricular spread; and encephalitis (involving the visual system or brainstem) and myeloradiculitis, resulting from spread from ophthalmic, trigeminal, or dorsal-root zoster, respectively. In all cases, inflammatory necrotizing lesions are associated with vasculitis. Intranuclear inclusion bodies are present, and the virus may be identified by immunohistochemistry or in situ hybridization. In addition, granulomatous, necrotizing, or noninflammatory (endarteritis obliterans) lesions involving small or large intracranial vessels may cause infarcts or hemorrhages.

Cytomegalovirus Infection.   In children, early fetal *cytomegalovirus* (*CMV*) *infection* may result

in necrotizing encephalitis or ventriculoencephalitis. Residual lesions in those surviving the acute neonatal illness include microcephaly microgyria, porencephalic cysts, hydrocephalus, and periventricular calcifications.

In adults, CMV may cause an opportunistic infection. Diffuse, non-necrotic encephalitic lesions consisting of a dissemination of microglial nodules, some of which contain characteristic cytomegalic cells (Fig. 5-34), have been described especially in transplant recipients. In AIDS patients, other lesions in addition to microglial nodule encephalitis have been observed, including necrotizing ventriculoencephalitis, necrotizing encephalitis with large cystic foci of encephalomalacia, and acute meningomyeloradiculitis, the latter usually with numerous polymorphs. Cytomegalic cells containing intranuclear and intracytoplasmic inclusion bodies are numerous and involve all types of cells (i.e., neurons, glial cells, endothelial cells, and macrophages). The virus may be identified by immunohistochemistry, in situ hybridization, or electron microscopy, but these are usually not necessary for the diagnosis.

Progressive   Multifocal   Leukoencephalitis. Progressive multifocal leukoencephalitis (PML) is due to infection by JC virus. This is an opportunistic infection occurring most often in patients with immunodeficiency, particularly AIDS. The virus infects oligodendrocytes specifically, causing a demyelinating disease. The lesions are usually bilateral but may be asymmetrical. They involve predominantly the subcortical hemispheric white matter (especially in the parieto-occipital regions), but the cerebellum, brainstem, and even spinal cord may be affected. They form limited, spotty foci that often coalesce to form larger, confluent demyelinating areas (Fig. 5-35A). They contain lipid-laden macrophages, and only scanty perivascular lymphocytes. The presence of giant astrocytes with bizarre hyperchromatic nuclei (Fig. 5-35B) and oligodendrocytes with enlarged nuclei containing viral inclusions (Fig. 5-35C) is a striking characteristic feature. The virus may be identified in oligodendrocytes by immunocytochemistry, in situ hybridization, or electron microscopy.

Since the AIDS epidemic began there has been a considerable increase in the incidence of PML. The disorder is relatively frequent in AIDS patients, in
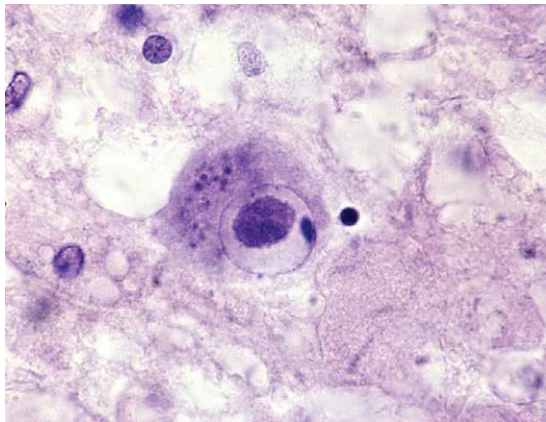
Figure 5-34. Cytomegalic cell in a case of cytomegalovirus encephalitis in an AIDS patient (Nissl stain).

whom the lesions may be particularly severe, with sometimes necrotic, very extensive changes involving particularly the cerebellum (Fig. 5-35D). Viral inclusions are particularly abundant and may be found in cells other than oligodendrocytes.

Encephalitis of Uncertain Origin

Encephalitis Lethargica. *Encephalitis lethargica* (epidemic encephalitis of von Economo), originally thought to be viral disease, was rampant from 1915 to 1927. Attempts were made using the limited techniques then available to implicate a virus and to relate the encephalitis with the contemporaneous pandemic of influenza; however, these attempts were unsuccessful. The disorder was characterized by preferential involvement of the midbrain and basal ganglia. In a large number of cases, a postencephalitic parkinsonism has been the sequel.

Behçet Uveomeningoencephalitis. Uveomeningoencephalitides present as inflammatory encephalitis, meningitis, and uveal lesions involving the choroids, ciliary body, and iris. Their etiology is uncertain.

Behçet disease is a rare disease that most commonly presents as recurrent ulceration of the mouth and genitalia accompanied by uveitis or iridocyclitis. An encephalitic syndrome may occur occasionally that consists of multifocal, necrotizing lesions involving predominantly the thalamus,

hypothalamus, and midbrain. The inflammatory changes are often necrotic and sometimes hemorrhagic. Vasculitis is considered to be the underlying lesion, but cerebral blood vessel changes are nonspecific. Attempts to demonstrate a virus as the cause of Behçet disease have failed.

Chronic Localized Encephalitis of Rasmussen. *Chronic localized encephalitis of Rasmussen* is a rare form of encephalitis that affects mainly children and is characterized by focal seizures that are refractory to treatment and show a centrifugal progression (see Chap. 12). The lesions, which are unilateral and localized, have a concentric distribution. They are necrotic and destructive in their centre, whereas at the periphery they have all the features of active encephalitis. Attempts to demonstrate a viral infection have been unsuccessful.

Rickettsiosis

Some forms of rickettsial infection (e.g., murine/endemic typhus due to *R. prowazekii*, exanthematic/epidemic typhus due to *R. typhi*, Rocky Mountain spotted fever due to *R. rickettsii*) may cause encephalitides characterized histologically by perivascular mononuclear cuffing and microglial nodules that preferentially involve the gray matter of the cerebral hemispheres and the brainstem. The agents, which are obligatory intracellular microorganisms that have the staining property of gram-negative bacilli, may be demonstrated in the cytoplasm of endothelial cells.

Opportunistic Infections

By definition, an opportunistic infection (OI) is an infection that takes the opportunity of a deficiency in the immune response of the host to develop. It may be either a primary infection or a reactivation of a latent infection. Classically, OIs are due to saprophytic organisms that do not cause diseases in immunocompetent individuals and that differ from primary pathogens by several characteristics (Table 5-4). However, one tends to include in this group infections by common pathogens such as tuberculosis, syphilis, measles, or VZV, which may behave as OIs in patients with impaired lymphocyte
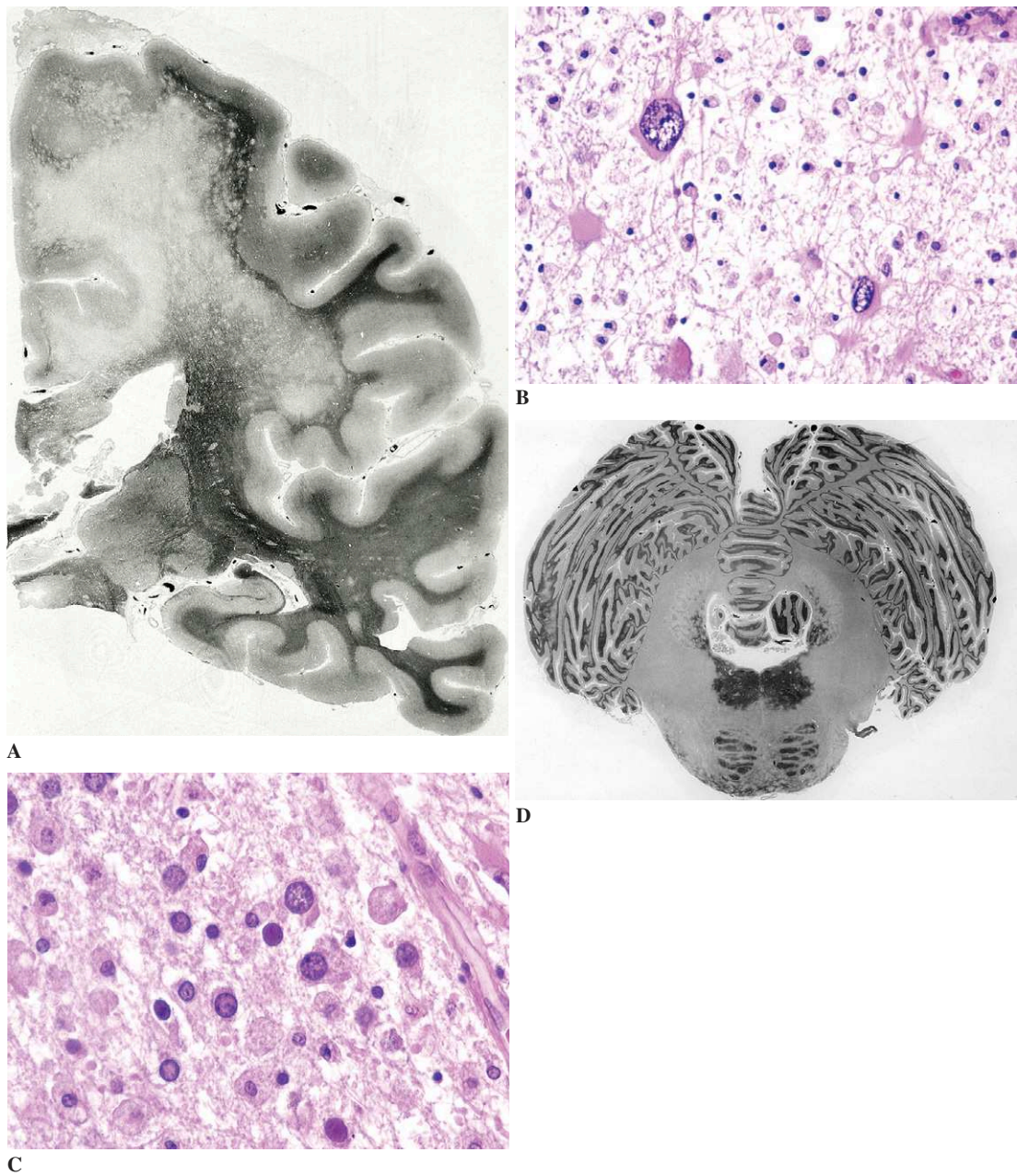
Figure 5-35. Progressive multifocal leukoencephalitis. **A**, Gross appearance. Confluent demyelination in the subcortical white matter of the parietal lobe (Loyez stain). **B**, Presence of giant, "bizarre" astrocytes in a demyelinated area (H and E). **C**, Presence of abnormal oligodendrocytes with enlarged nuclei containing viral inclusions (H and E). **D**, Extensive demyelination of the cerebellum and pons in an AIDS patient (Loyez stain).

function. One may also extend the concept of OIs to some neoplasms related to a specific viral infection, which develop only in immunocompromised individuals; one such neoplasm is Kaposi sarcoma of AIDS patients, related to infection by HHV type 8 (also known as Kaposi sarcoma–associated virus or KSHV), and another is primary brain lymphoma related to infection by EBV (HHV type 4), which occurs in AIDS patients and organ-transplant recipients.

In addition to more or less steady rates of the exceptional congenital and idiopathic immuno-

Table 5-4. Differential Characteristics of Primary and Opportunistic Pathogens

Primary Pathogens	Opportunistic Pathogens
• Induce specific diseases in immunocompetent hosts with identified reservoirs and routes of infection.	• Induce atypical infections in immunocompromised patients—present in wide environmental reservoirs or in commensal (endogenous) floras.
• Interact with specific cellular or humoral target molecules.	• Lack defined cellular or humoral host-receptors.
• Share specific virulence/pathogenicity determinants.	• May express potentially virulent and pathogenic molecules (constitutive or inducible), once they have colonized the host.
• Can be transmitted from host to host and induce the same disease (potential for epidemics).	• Are acquired from the environment, from food sources, or from the endogenous flora, and, for nosocomial infections, are communicable to susceptible contacts.
• Clonal origin with limited genetic variability. Induce specific immune responses, allowing for specific immunological diagnoses and vaccines.	• Genetic diversity and plasticity, which hamper indirect diagnosis and specific immunotherapies and vaccines. High frequency of genetic variations and rearrangements, allowing acquired resistance to antimicrobial agents.

deficiency disorders, there has been a dramatically increasing number of patients with acquired immunodeficiencies in the last 20 years or so. This situation has resulted from the steadily increasing age of the population as well as from growing numbers and longer survival times of patients with debilitating diseases such as diabetes, alcoholism, and lymphoid neoplasms. In addition, many patients have received immunosuppressive drugs for rheumatic and neoplastic diseases and for organ transplantation. Finally, the occurrence of the AIDS epidemic has represented a major cause of acquired immunodeficiency.

Different types of immunodeficiency may be associated with particular OIs, as described in the following sections.

Opportunistic Infections of the CNS in Patients with Granulocytic Disorders

Severe depletion of granulocytes is usually the consequence of decreased or absent production in the bone marrow. This may occur in myeloid leukemia or, more often, in the course of treatment with cytotoxic drugs. More rarely, severe granulocytopenia may result from peripheral sequestration, as in hypersplenism, or as an idiosyncratic reaction to medication. In people who develop severe granulocytopenia, the most common OIs are mycoses, particularly those due to *Aspergillus* spp. and *Candida* spp., and certain bacterial infections, particularly *Pseudomonas aeruginosa*, *Listeria monocytogenes*, and *Nocardia asteroides*.

Opportunistic Infections of the CNS in Patients with Combined Granulocytic and Lymphocytic Disorders

Immunodeficiency resulting from both granulocytic and lymphocytic impairment is the rule in transplant recipients. It may also occur in patients with lymphoid neoplasms (Hodgkin disease or lymphoid leukemia) or other malignancies treated with chemotherapy or in patients on prolonged high-dose corticosteroid therapy.

In addition to mycoses (e.g., aspergillosis, cryptococcosis) and bacterial infections (e.g., listeriosis, nocardiosis), other cerebral OIs may occur, including toxoplasmosis, PML, and cytomegalovirus infection. Primary malignant non-Hodgkin lymphomas of the brain, related to EBV infection, may also be seen. It is of historical interest that these tumors were first recognized as an opportunistic event in patients who had undergone renal transplantation.

Opportunistic Infections of the CNS in Patients with Lymphocytic Disorders, Particularly in AIDS

Prior to the introduction of highly active antiretroviral therapy (i.e., combination therapy including an HIV protease inhibitor), OIs secondary to the depletion in CD4+ T cells causing the cell-mediated immunodeficiency syndrome characteristic

of AIDS were the more frequent complication of the disease. They usually occurred during the late stages (i.e., in full-blown AIDS) in people with depletion of CD4 cells and with high viral loads, and included multiple parasitic (*Toxoplasma*), fungal (cryptococcal), bacterial (mycobacterial) and viral (cytomegalovirus, PML) infections, as well as primary brain lymphomas. Unlike the situation with granulocytopenia, these patients, by and large, did not have frequent infections due to *Aspergillus* spp. While bacterial infections were rare, it should be noted that a brain abscess in a patient with AIDS who did not have bacterial endocarditis was more likely to be due to *Nocardia* spp. than to any other agent.

The occurrence of many opportunistic infections in immunosuppressed patients, particularly in those with AIDS, has modified the presentation of these complications and has consequently made their diagnosis difficult for the following reasons: (1) There is an increased range of organisms involved. (2) A particular patient may have successive or simultaneous infections by different agents. (3) There can be involvement of several organs at the same time, with an increased incidence of neurological disease. (4) There is generally reduced inflammatory reaction.

The occurrence of OIs of the CNS in AIDS patients varies with the geographical location (i.e., where the patient has lived), with the age of the patient, and with therapy both for OIs and for HIV infection itself.

With regard to geographic location, several points can be made. Cerebral toxoplasmosis is more frequent in France and in Germany than in either the United States or the United Kingdom. In addition, this CNS complication has been reported in patients from sub-Saharan Africa, South America, and India. CNS histoplasmosis, blastomycosis, and coccidioidomycosis are much more frequent in America than in Europe. Acute or reactivated cerebral trypanosomiasis causing devastating necrotic lesions occurs only in South America. Mycobacterium tuberculosis infection of the CNS is especially common in patients with AIDS living in developing countries that have a high incidence of tuberculosis, particularly in Africa.

Children up to 13 years of age have, in general, a lower incidence of CNS OIs than do adults. This phenomenon is particularly manifest in AIDS, probably because children have had less time than adults to be exposed to common opportunist pathogens. This is especially true for toxoplasmosis, which is a much less common cause of CNS mass lesion than is primary brain lymphoma in children with AIDS in the United States. For this reason, it is recommended that children with mass lesions in the CNS be biopsied at presentation, rather than after a trial of anti-*Toxoplasma* therapy. Cryptococcal meningitis and PML are also rare in children with AIDS. The most common opportunistic pathogen in this age group, even in young children, continues to be CMV. Children with AIDS are also at risk for developing bacterial meningitis, including that caused by *S. pneumoniae*.

In the developed world, where highly active antiretroviral therapy is readily available and where there have been progressive improvements in the management of OIs in general, the incidence of CNS OIs has declined dramatically from the 1980s. However, people with undiagnosed or unsuspected HIV infection are still at risk of presenting with a CNS OI, as are HIV-infected individuals who are not compliant with their antiretroviral and prophylactic therapy. In addition, this complication of AIDS can be seen in people who develop mutations of HIV resistant to antiretroviral agents. Finally, and of great importance, CNS OIs also continue to be a major problem in developing countries, where these types of therapy are not usually available.

Chapter 6
Human Prion Diseases

James W. Ironside, Matthew P. Frosch,
and Bernardino Ghetti

Prion diseases, also known as transmissible spongiform encephalopathies, are rare, fatal neurodegenerative disorders that occur in mammals.

The human prion diseases are distinct from other neurodegenerative disorders in that they may be sporadic (idiopathic), inherited, or acquired (Table 6-1). They may be characterized pathologically by spongiform changes (vacuolation of the gray matter due to distention and swelling of neuronal cell processes), neuronal loss, reactive gliosis (involving microglia and astrocytes), and prion protein (PrP) deposition. These features are markedly variable from case to case and within different brain regions in a single case. The diagnosis of prion disease requires a neuropathologic examination combined with biochemical and genetic analysis.

Biology of Prions

The Infectious Agent

The transmissible agent in prion diseases is different from any known infectious pathogen in both its structure and its remarkable resistance to conventional forms of decontamination. While attempting to identify the agent responsible for scrapie (a prion disease affecting animals, particularly sheep and goats), it was determined that the agent was smaller than conventional viruses, did not have RNA or

DNA, and accumulated in the CNS. The prion hypothesis, proposed by Stanley Prusiner in 1982, stated that the transmissible agent (prion) was a protein with a molecular weight of 27 to 30 kDa, was partially resistant to proteolytic cleavage, and was consistently associated with infectivity in purified extracts of scrapie-infected brain. It was subsequently demonstrated that this protein was an abnormal isoform of a protein that normally occurs in the mammalian brain. The normal protein is encoded by the prion protein gene (*PRNP*), which in humans is located on the short arm of chromosome 20.

The Normal Prion Protein

The normal prion protein (PrP^c) is a 253-residue peptide that is translated from a single exon within *PRNP*. The peptide undergoes a series of post-translational modifications, including cleavage of a signal peptide, addition of up to two *N*-linked oligosaccharide chains (at residues 181 and 197), and attachment of a GPI anchor. *PRNP* contains five octapeptide repeats from codons 51 through 91. Four putative alpha helices in PrP^c are located from amino acid 109 to 122, 129 to 140, 178 to 191, and 202 to 218. Most PrP^c is membrane-associated and, being sensitive to proteolytic digestion, has a short half-life within the cell. PrP^c is expressed in a wide

Table 6-1. Classification of Human Prion Disease

Idiopathic	Sporadic Creutzfeldt-Jakob disease
	Sporadic fatal insomnia
Familial	Familial Creutzfeldt-Jakob disease
	Gerstmann-Sträussler-Scheinker disease and variants
	Prion disease associated with octapeptide repeat region insertional mutations (variable phenotype)
	Fatal familial insomnia
Acquired from human	Kuru
	Iatrogenic Creutzfeldt-Jakob disease
Acquired from bovine	Variant Creutzfeldt-Jakob disease

Figure 6-1. Western blot analysis. **A,** Western blot analysis of PrP in variant Creutzfeldt-Jakob disease (CJD) brain tissue with (+) or without (−) prior digestion with proteinase K. Proteinase K results in complete degradation of PrP^c and in *N*-terminal truncation of PrP^{Sc}. The remaining protease-resistant PrP (PrP^{res}) occurs in di-, mono-, and nonglycosylated forms. **B,** Western blot analysis of PrP^{res} in sporadic (S) and variant (V) CJD brain. Nonglycosylated PrP^{res} occurs as either a 21-kDa band ("type 1") or a more extensively truncated 19-kDa band ("type 2"). Variant CJD exhibits a characteristic predominance of the diglycosylated band (*) and this protein isotype is termed "type 2B" to distinguish it from the type 2A isotype seen in sporadic CJD, where the diglycosylated form does not predominate. The cases shown were homozygous for methionine (MM) or valine (VV) at codon 129 of the *PRNP* gene.

variety of tissues, but the highest levels of expression are found in neurons in the CNS. The precise function of the normal protein is uncertain, but studies on *PRNP* "null" mice, which do not express PrP^c, have indicated that it has a likely role in synaptic function and long-term potentiation, and may be involved in the control of circadian rhythms. PrP^c can act as a copper-binding protein, and a protective role for PrP^c in oxidative cell stress has been proposed. Several polymorphisms have been identified, of which the most significant are M129V and E219K, since these affect susceptibility to prion disease (Table 6-2).

The Abnormal Prion Protein

In prion disease, an abnormal isoform of the prion protein, designated PrP^{Sc}, accumulates in the CNS. Alternative terms include PrP^{CJD}—which refers to Creutzfeldt-Jakob disease—and PrP^{res}, which refers to the prion protein's property of proteinase K resistance. PrP^{Sc} has the same amino acid sequence and molecular weight as PrP^c but has a much longer half-life and is partially resistant to proteolytic digestion (Fig. 6-1A). Structural studies have indicated that PrP^{Sc} has a predominant beta-pleated sheet structure, with loss of the alpha helices that are present in PrP^c. These structural differences are thought to confer resistance to proteolytic degradation, and also allow PrP^{Sc} to accumulate as amyloid within the central nervous system. In the prion hypothesis, PrP^c is converted to PrP^{Sc}, which then accumulates in the CNS and

Table 6-2. Prion Protein Gene Polymorphisms in the Normal Population and in Prion Disease

	Prion Protein Gene Codon 129 Polymorphisms (%)		
	MM	**MV**	**VV**
Normal population	37	51	12
Sporadic CJD	71	15	14
Variant CJD	100	—	—

M = methionine, V = valine, CJD = Creutzfeldt-Jakob disease.

is neurotoxic. This results in the death of groups of neurons within the brain and eventually leads to the death of the organism.

The mechanisms and sites of conversion of PrP^c to PrP^{Sc} are not fully understood. Conversion can be achieved in a cell-free system, but the reaction is relatively inefficient. It has therefore been suggested that other factors, perhaps chaperones or cofactors, may facilitate this process in vivo.

Similarly, the mechanisms of neurotoxicity of PrP^{Sc} are not fully understood, although a range of possibilities exist, from a direct toxic effect on neurons to indirect toxicity mediated by microglia and possibly astrocytes. No pathological changes occur outside the CNS in prion diseases, although in some diseases PrP^{Sc} can be identified in the peripheral nervous system and lymphoid tissues (see later discussion).

Human Prion Diseases

Sporadic Creutzfeldt-Jakob Disease

Sporadic Creutzfeldt-Jakob disease (CJD, SCJD) is the most commonly diagnosed human prion disease, occurring with a relatively uniform incidence of around one individual per million per annum in the countries in which it has been studied. Although a wide range of ages at onset has been reported, most cases of SCJD occur in the seventh decade of life, with males and females being affected equally. The disease usually presents as a rapidly progressive dementia accompanied by other neurological abnormalities, among which ataxia, myoclonus, visual abnormalities, and pyramidal and extrapyramidal signs are common. The average duration of the clinical illness of SCJD is approximately 4 months, but both shorter and, in some cases, markedly longer clinical courses have been observed.

Diagnostic tests for SCJD include the electroencephalogram (EEG), which shows a characteristic abnormality with periodic triphasic complexes in approximately 65% of patients. Cranial magnetic resonance imaging (MRI) scans in SCJD often show an increased signal in the basal ganglia, with variable patterns of intensity in the cerebral cortex. In the CSF, levels of the protein 14-3-3 are increased in at least 90% of patients, making this a useful test that has recently been incorporated into the diagnostic criteria for this disorder.

The etiology of SCJD is unknown. It has been suggested that this disease might occur as a consequence of a random event that results in the generation or spontaneous conversion of PrP^{Sc} within the brain. Case-control studies have failed to identify any consistent predisposing factors in terms of occupation or diet, although recent reports have indicated that SCJD appears to be significantly higher in patients with a past history of surgery (not specifically neurosurgery) than in controls. Analysis of *PRNP* has shown that most patients with sporadic CJD are methionine homozygotes at codon 129, in contrast to the normal population (see Table 6-2). This finding has been reproduced consistently in different ethnic groups, but the significance of this genetic predisposing factor remains uncertain.

Clinical and pathological heterogeneity have long been associated with SCJD, and a wide range of eponyms have been applied to some of these clinical subgroups (e.g., Heidenhain variant, with a short clinical history and cortical blindness as a prominent feature; Brownell-Oppenheimer variant, with prominent cerebellar ataxia). Recent studies on large cohorts of patients with sporadic CJD have identified an association between the clinicopathological phenotype, the *PRNP* codon 129 genotype, and the PrP^{Sc} isotype on Western blot analysis.

The resistance of PrP^{Sc} to protease digestion forms the basis for biochemical detection of the pathological hallmark of prion diseases. When tissue homogenates are examined by Western blot analysis with antibodies to PrP, samples containing PrP^{Sc} will show immunoreactivity even after treatment with proteinase K. The size of the immunoreactive protein fragment that remains after protease digestion, along with the pattern of glycosylation, is used to define PrP^{Sc} isotypes. In general, two major PrP^{Sc} isotypes can be identified (see Fig. 6-1B), giving a possibility of classifying six different genotype/isotype combinations with distinct clinical features (Table 6-3). Although this is an interesting and in many ways an attractive proposition, there is no current uniformity in the nomenclature or classification of PrP^{Sc} isotypes, and the identification of multiple PrP^{Sc} isotypes in the brain in a significant minority of SCJD cases makes it

Table 6-3. Summary of Genotypes and Phenotypes of Sporadic Human Prion Disease

Clinical Disease	PRNP Mutation	PRNP Codon 129	PrP^{pres} Isotype	Proposed Histological Correlate
Sporadic CJD (myoclonic, Heidenhain variants)	None	MM, MV	Type 1A	Synaptic and coarse granular PrP staining in cortex
Sporadic CJD (Brownell-Oppenheimer variant)	None	VV	Type 2A	Plaque-like, focal and perineuronal staining
Sporadic CJD (kuru-plaque variant)	None	MV	Type 2A	Amyloid plaques in the cerebellum
Sporadic CJD (sporadic fatal insomnia)	None	MM	Type 2A	Thalamic atrophy. PrP staining faint and variable
Sporadic CJD (cortical variant)	None	MM	Type 2A (Basic glycans)	Cortical perivacuolar staining
Sporadic CJD	None	VV	Type 1A	Faint synaptic staining
Variant CJD	None	MM	Type 2B	Florid and cluster plaques

CJD = Creutzfeldt-Jakob disease, M= methionine, PrP = prion protein, V = valine.

difficult to establish these correlations with certainty in all cases at present.

Cases of SCJD exhibit the typical neuropathological features of prion diseases (Figs. 6-2A and B). The histological features in the six major subgroups of SCJD are summarized in Table 6-3. It is interesting to note that within one subgroup (MM2) there appear to be two distinct clinical presentations, one with features characteristic of SCJD and the other with features indicative of progressive thalamic and hypothalamic dysfunction. The term "thalamic variant of SCJD" is sometimes applied to the latter subgroup, although a proposal has recently been made to name cases within the subgroup as "sporadic fatal insomnia" because of pathologic similarity to a familial disorder.

Familial Prion Diseases

Familial prion diseases occur as autosomal dominant disorders with high penetrance and include a wide range of clinicopathological phenotypes. These phenotypes are categorized as familial CJD, Gerstmann-Sträussler-Scheinker disease (GSS), fatal familial insomnia (FFI), and variable pheno-
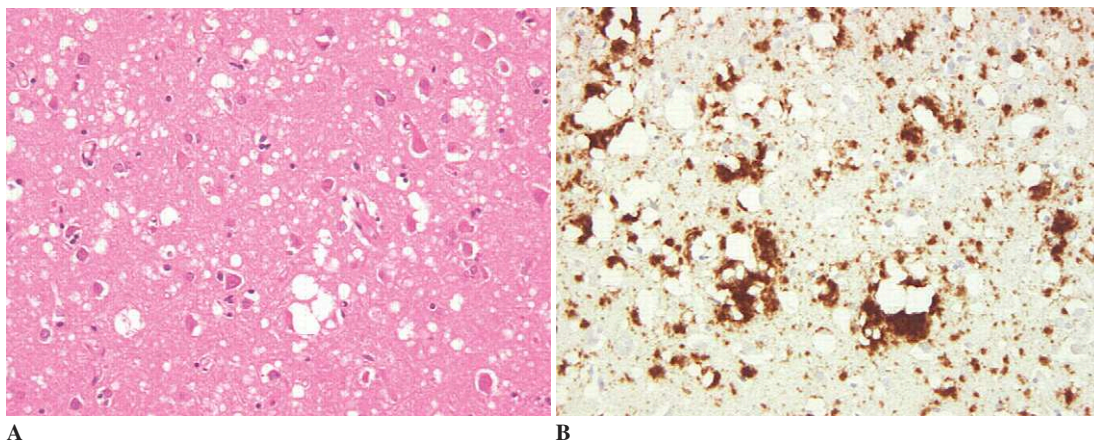
Figure 6-2. Sporadic Creutzfeldt-Jakob disease (SCJD), microscopic features. **A**, Spongiform change in the cerebral cortex in SCJD MM, type 1A consists of multiple small vacuoles in the gray matter that occasionally join to form larger cyst-like spaces (hematoxylin and eosin [H and E]). **B**, Immunocytochemistry for PrP in the same case as Fig. 6-1A shows accumulation of PrP in amorphous deposits around areas of spongiform change.

Table 6-4. Most Common Haplotypes and Phenotypes of Familial Human Prion Disease

Clinical Disease	PRNP Haplotype	PrP^{res} Isotype	Histological Correlates
Familial Creutzfeldt-Jakob disease	D178N-129V	Type 1B	Cortical spongiform degeneration
	E200K-129M	Type 1B	Diffuse PrP staining
	E200K-129V	Type 2B	Diffuse PrP staining in cortex, focal deposits in the cerebellum or plaque-like deposits in the cerebellum
Gerstmann-Sträussler-Scheinker disease	P102L-129M	Type 1B and 8 kD	Spongiform change, synaptic PrP, amyloid plaques
		8 kD only	PrP-amyloid plaques, no spongiform changes
	P105L-129V	8 kD	Multicentric amyloid plaques
	A117V-129V		
	H187R-129V		
	F198S-129V	8 kD	Multicentric amyloid plaques and neurofibrillary tangles
	Q217R-129V		
Fatal familial insomnia	D178N-129M	Type 2B	Thalamic atrophy

PrP = prion protein, PrP^{res} = prion protein (resistant).

types. The first genetic abnormality to be identified in a familial prion disease was the *PRNP* P102L mutation in GSS in 1989. Since then, over 40 different *PRNP* mutations, including missense, deletion, nonsense, and insertion mutations (in the octapeptide repeat region), have been identified. In addition to these mutations, the polymorphic codons at 129 and 219 on both the mutant and non-mutated alleles of *PRNP* can influence disease phenotype. These polymorphisms can markedly affect the clinical and pathological features of the disease when present on the mutant allele (*cis*); on the non-mutant allele (*trans*), the major effects are on age at onset and disease duration. For this reason, it has been proposed that each mutation should be identified not only with details of the mutation, but also with the codon 129 polymorphism on the mutated allele (i.e., haplotype).

Familial Creutzfeldt-Jakob Disease

In familial CJD, the clinical and pathologic phenotypes may resemble those associated with SCJD. Some cases, initially suspected to be SCJD in the apparent absence of a positive family history, have subsequently been found to be associated with a *PRNP* mutation. The *PRNP* haplotypes most often associated with CJD are E200K-129M and D178N-129V (Table 6-4). Phenotypic variability does occur within affected families in terms of both the clinical and pathological features of the disease.

Gerstmann-Sträussler-Scheinker Disease

GSS is a progressive spinocerebellar syndrome that is accompanied by pyramidal signs and progressive cognitive decline and may result in dementia. The histological feature common to the initial kindred, first reported in 1928 and 1936 by the investigators whose names are given to this disease, is the presence of multicentric PrP-amyloid plaques in the cerebral and cerebellar cortex (Figs. 6-3A and B). A number of point mutations resulting in a similar clinicopathological phenotype has been described (see Table 6-4). The F198S and Q217R mutations are associated with widespread multicentric and unicentric PrP amyloid plaques and neurofibrillary tangles (similar to those occurring in Alzheimer disease) in the neocortex.

Prion Diseases Associated with Octapeptide Repeat Region Insertional Mutations (Variable Phenotypes)

In patients with insertional mutations in the octapeptide repeat region of the *PRNP*, the clinical manifestations are highly variable both in terms of disease duration and in the disease phenotype.
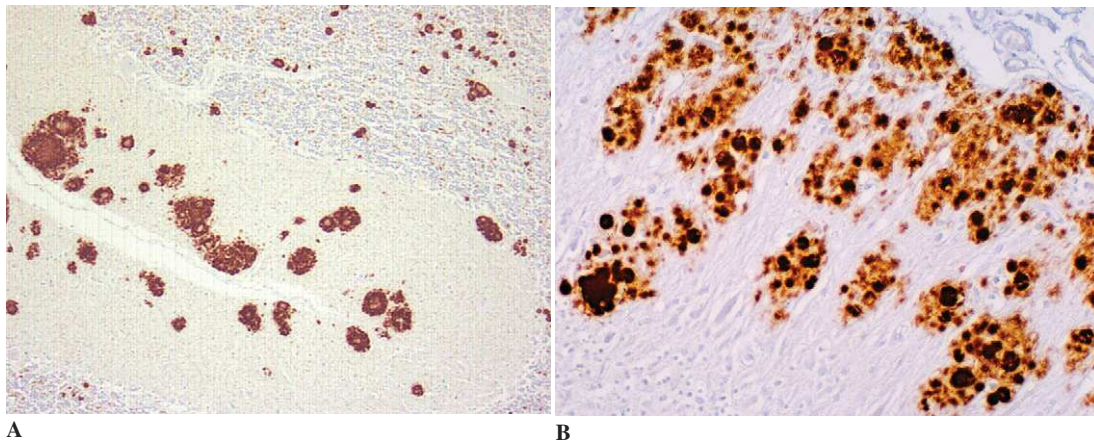
Figure 6-3. Gerstmann-Sträussler-Scheinker disease. **A** and **B,** Immunocytochemistry for PrP shows multicentric PrP plaques in the cerebellar molecular layer, with smaller plaques in the granular layer (**A**).

In general, patients with up to four octapeptide insertions have a clinical phenotype similar to sporadic CJD, with rapidly progressive dementia and characteristic EEG abnormalities. In patients with five or more octapeptide inserts the clinical phenotype is more variable, often with progressive ataxia and other movement disorders. Histologically, these cases often show unusual linear PrP deposits in the molecular layer of the cerebellum (Fig. 6-4); however, the other histological features are somewhat more variable.
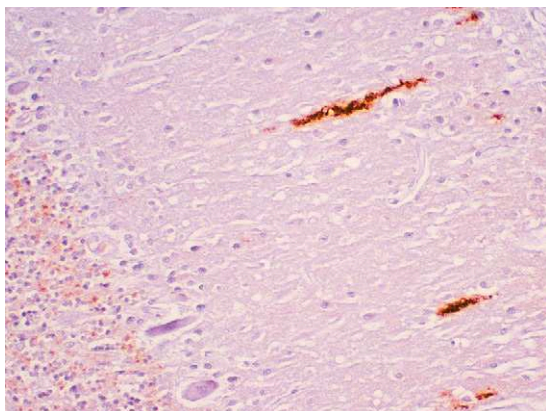
Figure 6-4. Prion disease with octapeptide repeat region insertional mutations. Immunocytochemistry for PrP shows linear PrP deposits in the molecular layer of the cerebellum.

Fatal Familial Insomnia

FFI is a disorder characterized by sleep disturbance, dysautonomia, motor signs, and cognitive abnormalities (often relatively mild). The neuropathology of FFI includes severe neuronal loss and gliosis in the anterior nucleus of the thalamus (Figs. 6-5A and C) and hypothalamus, with an absence of spongiform change. Neuronal loss and gliosis are also evident in the inferior olivary nuclei (Fig. 6-5D) and to a lesser (but variable) extent in the cerebral and cerebellar cortices. Spongiform changes can be remarkably difficult to detect in this disorder, but are usually apparent on careful study of the cerebellar cortex. In some cases, tissue blots obtained from sections of paraffin embedded tissue may help to identify PrP^{Sc} deposition, particularly in the entorhinal cortex (Fig. 6-5E).

FFI was described as a clinical entity in 1986, but not until 6 years later was the underlying *PRNP* abnormality responsible for this disorder identified as a D178N-129M haplotype (see Table 6-3). This point mutation (D178N) is also found in some patients with familial CJD; however, the amino acid present at the residue 129 polymorphic site is different. Thus, when the D178N mutation coexists in *cis* with methionine at residue 129, it is associated with FFI; however, when the D178M mutation is paired with valine at residue 129, it is associated with CJD. Phenotypic variability has been described within FFI, usually under the influence of the codon 129 genotype on the nonmutated allele (*trans*).
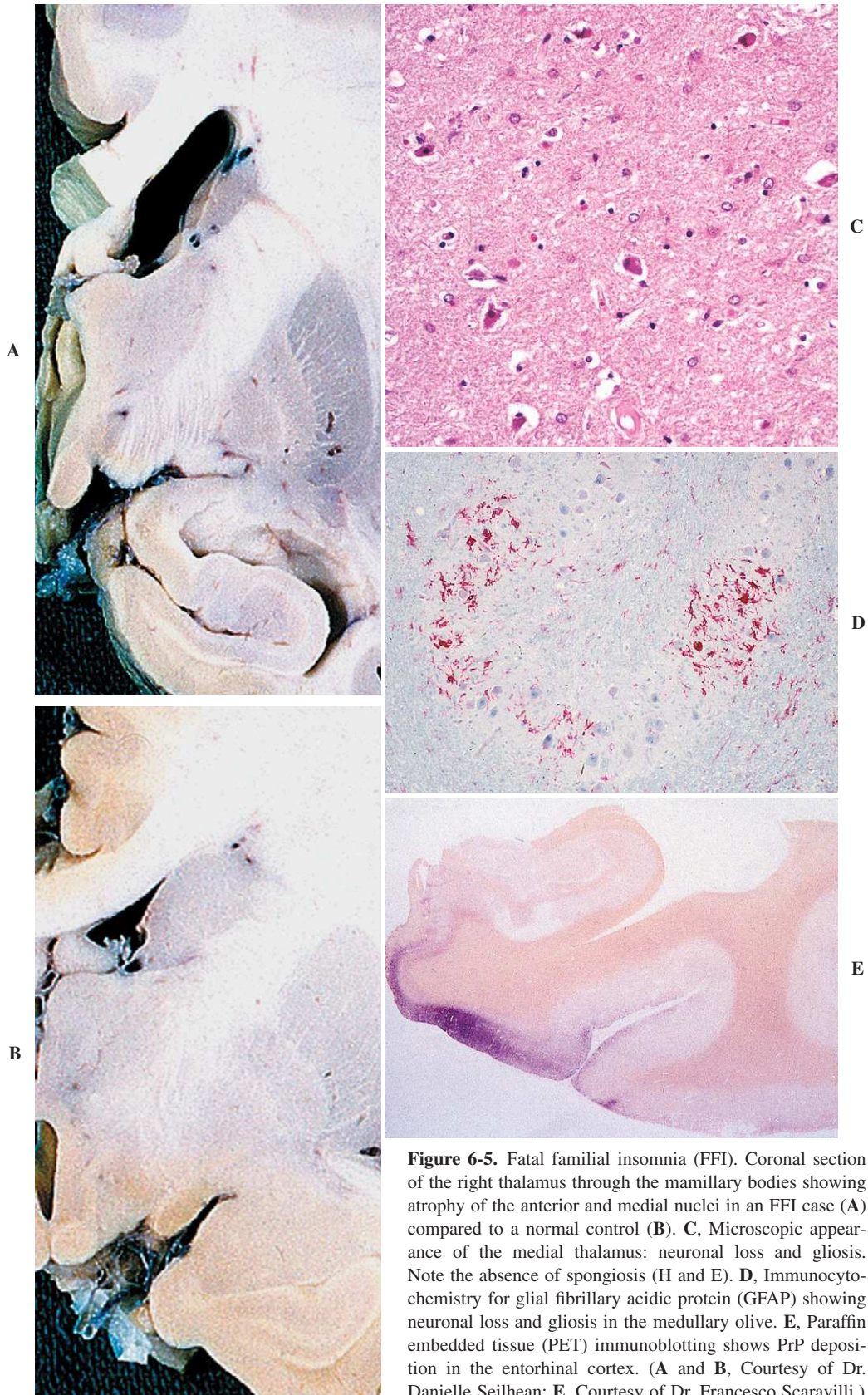
Figure 6-5. Fatal familial insomnia (FFI). Coronal section of the right thalamus through the mamillary bodies showing atrophy of the anterior and medial nuclei in an FFI case (**A**) compared to a normal control (**B**). **C**, Microscopic appearance of the medial thalamus: neuronal loss and gliosis. Note the absence of spongiosis (H and E). **D**, Immunocytochemistry for glial fibrillary acidic protein (GFAP) showing neuronal loss and gliosis in the medullary olive. **E**, Paraffin embedded tissue (PET) immunoblotting shows PrP deposition in the entorhinal cortex. (**A** and **B**, Courtesy of Dr. Danielle Seilhean; **E**, Courtesy of Dr. Francesco Scaravilli.)
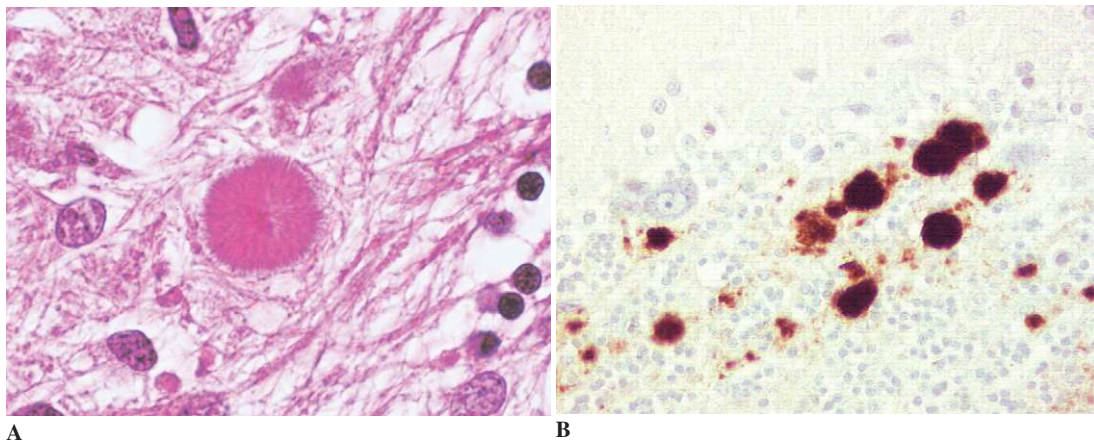
Figure 6-6. Kuru. **A**, Kuru plaque in the molecular layer of the cerebellum (H and E). **B**, Small, rounded PrP amyloid plaques, well-identified on PrP immunostain, are a characteristic feature in the granular layer of the cerebellum.

Acquired Prion Disease

Kuru

Kuru was described as an endemic disease among the Fore tribe of Papua New Guinea in the 1950s. The disease was characterized by progressive ataxia and tremor with marked emotional instability, but rapidly progressive dementia was not a common feature. The disease was associated with ritualistic cannibalism; since this practice has been discouraged the incidence of disease has declined significantly. The disease is not yet extinct and some recently symptomatic patients have sustained incubation periods of around 40 years.

The pathology of kuru is similar to that of sporadic CJD VV2 and MV2 subsets, with amyloid plaques, so called "kuru plaques," present in the cerebellum, particularly in the granular cell layer (Fig. 6-6A), and spongiform change noted in the cerebellum, basal ganglia, and thalamus, with a variable distribution in the cerebral cortex. Immunocytochemistry for PrP has highlighted the presence of the amyloid deposits in the cerebellum (Fig. 6-6B), but has also demonstrated diffuse deposits that are not identifiable on routine stains.

Iatrogenic CJD

In 1974, the occurrence of iatrogenic CJD was reported in a recipient of a corneal transplant. Since then, well over 200 cases of human-to-human transmission of CJD have been identified. The majority have been recipients of human pituitary hormones (mostly growth hormone) or human dura mater grafts. A summary of the routes of transmission of iatrogenic CJD is given in Table 6-5. In general, cases with a central route of infection have the shortest incubation times, whereas those with peripheral route of infection (particularly in growth hormone recipients) have a more lengthy incubation period, which can be over three decades in some cases.

The clinical features of iatrogenic CJD are variable. Some patients (particularly those with a central route of transmission) resemble sporadic CJD, whereas others (including the human pituitary hormone recipients) often present with a progressive cerebellar ataxia and other focal neurological

Table 6-5. Routes of Iatrogenic Transmission of Creutzfeldt-Jakob Disease

Source of Infection	Number of Reported Cases	Incubation Period (Months)
Neurosurgical instruments	5	12–28
Intracerebral electrodes	2	16–20
Dura mater graft	120	18–216
Corneal graft	4	16–320
Human growth hormone	142	550–456
Human gonadotrophin	5	144–192
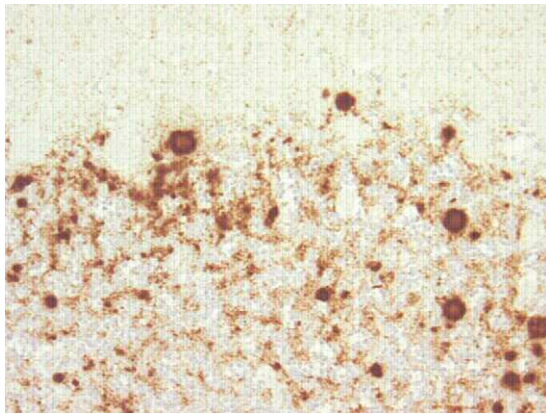
Figure 6-7. Iatrogenic Creutzfeldt-Jakob disease in a growth hormone recipient. The cerebellum contains small "kuru-type" plaques as well as more diffuse PrP deposits well identified on PrP immunostain.

symptoms as well as dementia occurring only later in the illness.

Histologically, iatrogenic CJD is similar to sporadic CJD, although the cerebellar pathology in the pituitary hormone recipients tends to be more severe than in sporadic CJD (Fig. 6-7). In the United Kingdom, iatrogenic CJD in growth hormone recipients has most frequently occurred in individuals who were homozygous for valine at residue 129; however, in France, iatrogenic CJD occurs most frequently in individuals receiving human growth hormone who are homozygous for methionine at residue 129. These differences may reflect differences in the strain of the contaminating agent, since the routes of transmission were similar (i.e., intramuscular or subcutaneous) in most cases.

Variant CJD

In 1996, a novel form of prion disease with unusual clinical, biological, and pathological features was identified by the National CJD Surveillance Unit in the United Kingdom. A causative relationship with the epidemic of bovine spongiform encephalopathy (BSE) in cattle seemed likely. Since then, over 120 patients with this disease, subsequently known as *variant CJD* (vCJD), have been identified.

Clinically, there is a relatively young age at onset (mean 27 years, range 12 to 74 years). The

lengthy duration of illness (13 months) and the clinical presentation are also characteristic. The latter includes psychiatric and/or sensory manifestations at onset followed by severe progressive ataxia, extrapyramidal and pyramidal signs, and a progressive dementia that in some cases is severe. In vCJD the EEG is abnormal but does not exhibit the characteristic abnormalities seen in sporadic CJD. Cranial MRI scans show a symmetrical area of hyperintensity in the posterior thalamus (the "pulvinar sign"; Fig. 6-8) that is highly characteristic and has been incorporated into the clinical diagnostic criteria for vCJD. Analysis of protein 14-3-3 levels in CSF has not proven helpful in making a diagnosis of vCJD.

Pathologically, vCJD differs from other forms of human prion disease in the presence of large numbers of "florid" plaques with a widespread distribution in the cerebral cortex (Figs. 6-9A and B) and in the cerebellum. These lesions comprise a central eosinophilic amyloid core with radiating
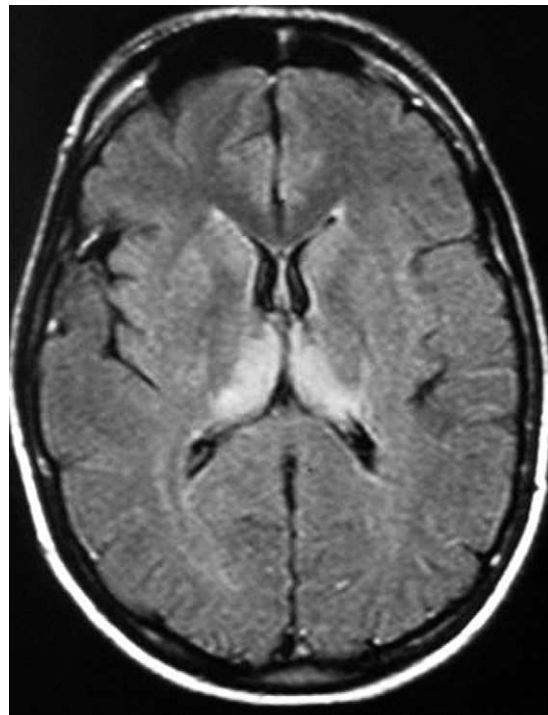
Figure 6-8. Axial MRI FLAIR image at the level of the basal ganglia, showing bilateral hyperintensity of the pulvinar and dorsomedial thalamic nuclei in variant Creutzfeldt-Jakob disease.
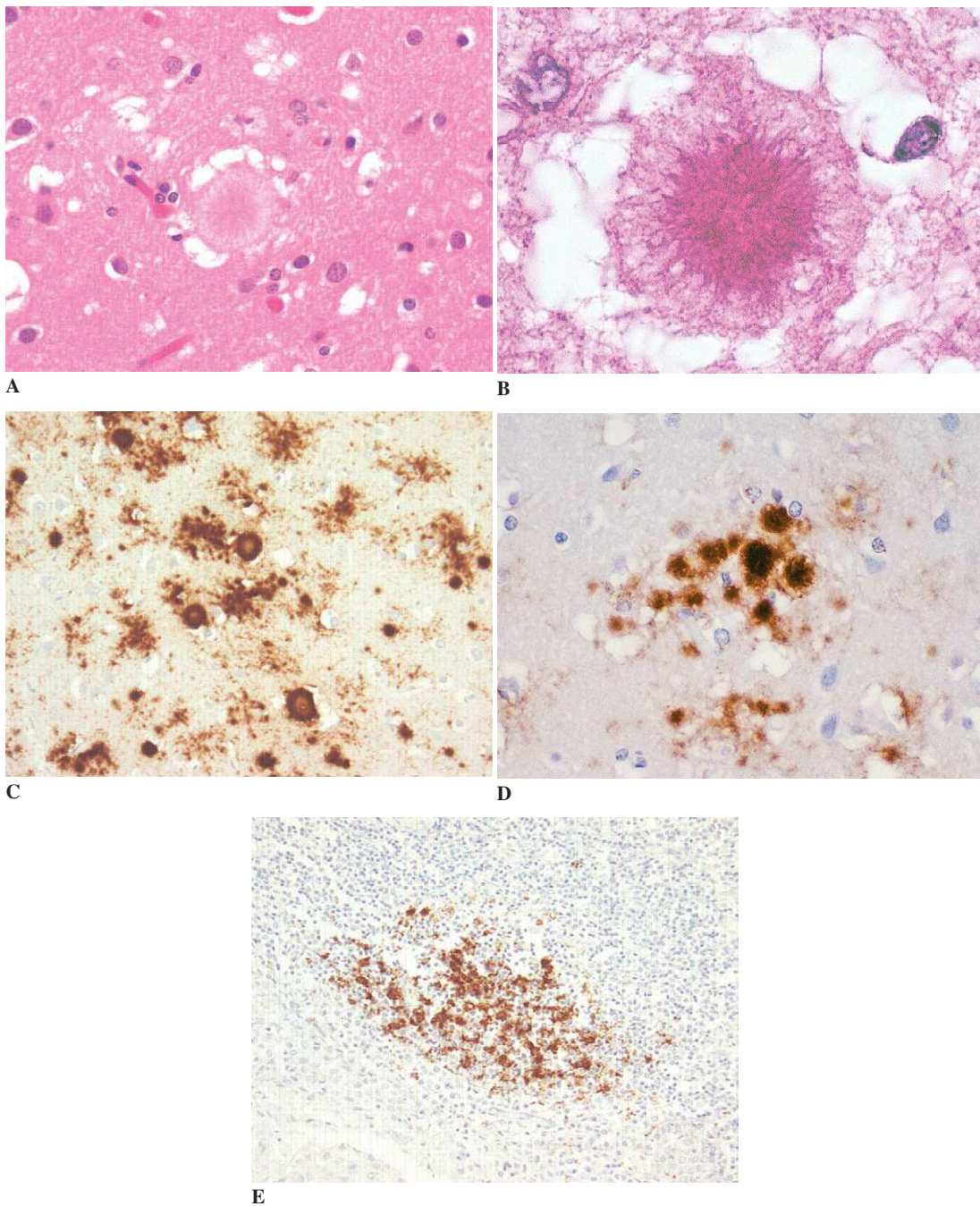
Figure 6-9. Variant CJD, microscopic features. **A** and **B**, The florid plaque in the cerebral cortex in variant CJD comprises a dense core with a paler outer layer of amyloid fibrils, surrounded by spongiform change (H and E). **C** and **D**, Immunocytochemistry for PrP shows strong staining of the florid plaques as well as multiple smaller plaques and diffuse PrP deposits. **E**, PrP accumulation in the tonsil in variant CJD within follicular dendritic cells and macrophages in a germinal center is demonstrated by PrP immunocytochemistry.

bundles of amyloid fibrils that is surrounded by marked, local spongiform change. Apart from the florid plaques, other characteristic neuropathological features of vCJD include extensive accumulation of PrP^{Sc} as both small, clustered plaques and diffuse deposits (Figs. 6-9C and D), with spongiform changes most marked in the caudate nucleus and putamen. In the thalamus, there is extensive neuronal loss and gliosis in posterior nuclei, corresponding to the abnormalities on MRI.

In vCJD, Western blot analysis of the brain shows a characteristic PrP^{Sc} isotype with a predominant diglycosylated band and an unglycosylated band that averages around 19 kD (see Fig. 6-1B). This glycosylation pattern is similar to that in Western blots for PrP^{Sc} in cattle with BSE and in other species (e.g., cats) that have been infected with BSE.

At the time of the original description of vCJD, it was suggested that the most likely hypothesis for the emergence of vCJD is exposure of the human population to the BSE agent. A number of independent investigations have demonstrated that the "strain" of the transmissible agent in vCJD is quite similar to that for BSE, but shares no similarities with the strains of sporadic CJD. On this basis, it is assumed that most human cases of vCJD result from exposure to BSE through the food chain, that is, by the consumption of contaminated meat products. There is also evidence from a case-control study to suggest that consumption of certain meat products is higher in patients with vCJD than in controls, although this data needs to be interpreted with great caution.

Since the most likely route of human exposure to BSE is oral, studies have been performed on tissues outside the CNS in order to investigate the peripheral pathogenesis of this disease. PrP^{Sc} is detectable in follicular dendritic cells within germinal centers in lymphoid tissues including the tonsil (Fig. 6-9E), lymph nodes, spleen, thymus, and the gut-associated lymphoid tissues in the appendix and small intestine. On the basis of this finding, it has been proposed that a tonsil biopsy is an important diagnostic test for patients suspected of having vCJD, particularly when characteristic MRI changes are absent. Recent investigations have confirmed the presence of infectivity in the spleen and tonsil of individuals with vCJD; however, the level of infectivity is two to three times lower than that in the brain.

The potential number of future cases of vCJD is highly uncertain; estimates range from a few hundred to many thousands. Since all patients identified with vCJD are homozygous for methionine at residue 129 in the PrP, estimates are restricted to that genotype; however, the appearance of the disease in individuals with methionine/valine heterozygosity at residue 129 or an another genetic subgroup (who may have a longer incubation period) would significantly increase the potential number of future cases.

Chapter 7
Primary Diseases of White Matter

Raymond A. Sobel, William F. Hickey,
and Danielle Seilhean

Complex and heterogeneous pathological processes mediate diseases that occur in the CNS white matter. Primary demyelination is the major feature of demyelinating diseases. Injury, breakdown, and loss of myelin sheaths with relative sparing of axons are features of primary demyelination; the injured myelin is phagocytosed, catabolized, and removed by macrophages and microglia. Primary demyelination is distinguished from secondary demyelination, in which myelin loss is a consequence of axon injury and loss, as, for example, following infarction, trauma, and hemorrhage. Secondary demyelination occurs in neurodegenerative diseases in which the neuron soma, its axon, or both undergo degeneration. Therefore, axonal (wallerian) degeneration in both the peripheral and central nervous systems is associated with myelin breakdown along the course of injured or dying axons.

General Considerations

CNS Myelin

In the CNS, the myelin sheath (Fig. 7-1) is formed from the fusion of oligodendrocyte membranes that are concentrically wrapped around the axon and compacted to form a multilamellar coating. Each oligodendrocyte sends out multiple cell extensions that ensheath intermodal segments of from 1 to 20 or more axons. CNS myelin performs many functions. It facilitates electrical conduction by the axon; orchestrates the molecular interactions between axons and myelin, promoting mutual stability; and helps define the distribution of ion channels in the axonal membrane. Therefore, myelin provides physiologic, structural, and metabolic support of axons. In its absence, axons become vulnerable to injury and may eventually degenerate.

Major Mechanisms of Primary Demyelination

Myelinoclastic Processes

In *myelinoclastic* (myelin-destructive) processes there is selective destruction of myelin by catabolic breakdown and subsequent phagocytosis by macrophages. These processes specifically target the myelin sheaths and/or the oligodendrocytes. Multiple sclerosis and related conditions are the most common demyelinating diseases in which primary demyelination occurs as a consequence of myelinoclastic processes. In these disorders, there is generally an inflammatory component which plays a part in the myelin injury (Table 7-1).

Other Primary Demyelinating Conditions

In several other primary demyelinating diseases, myelinoclastic pathogenic cellular mechanisms of injury are also known to occur. Examples of these are selective infection of oligodendrocytes by papovavirus in progressive multifocal
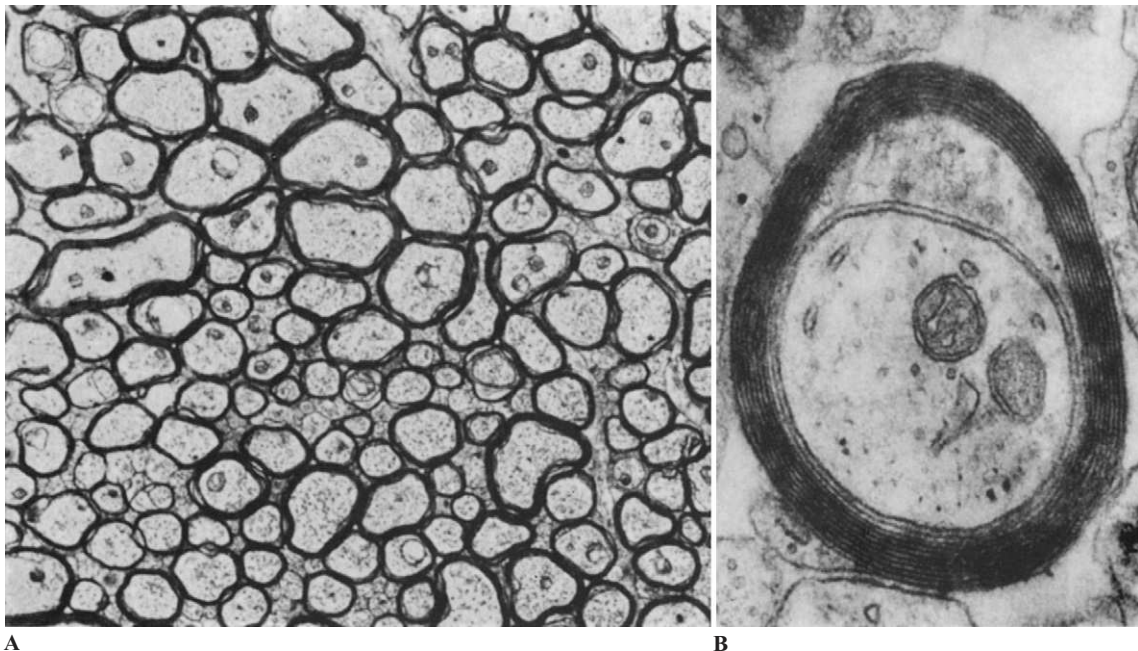
Figure 7-1. Electron-microscopic appearance of normal white matter. **A**, Low magnification (original magnification ×10,500). **B**, Myelinated axon at high magnification (original magnification ×163,500). (Courtesy of Dr. B. Berger.)

Table 7-1. Histologic Features of Primary Demyelinating Diseases

Pathologic Process	Histologic/Immunohistochemical Findings
Immune activation of CNS resident cells	Increased activation marker expression (e.g., Class II MHC) on resident microglia
Mononuclear cell infiltration	T cell, B cell, inflammatory infiltrates
Myelin injury	Swelling, breakdown of myelin
Breakdown of blood-brain barrier	Leakage of serum proteins into tissues, detectable by immunohistochemistry
Phagocytosis and disappearance of myelin	Myelin droplets in macrophages by myelin stain and oil red O
Glial scarring	Increased immunostaining for glial fibrillary acidic protein
Depletion of oligodendrocytes	Loss of oligodendrocyte-specific antigens/depletion
Axon injury and loss	Axon retraction balls/depletion

leukoencephalopathy (PML; see Chap. 5) and toxic injury to oligodendrocytes in cyanide and hexachlorophene poisoning (see Chap. 9). In other myelinoclastic conditions the exact mechanisms of myelin destruction are not known, but these conditions stand out as distinctive because of their specific pathological and clinical features. For example, *Grinker myelinopathy* is characterized by a destruction of white matter weeks after an episode of carbon monoxide exposure; *central pontine myelinolysis* is a focal damage to brain myelin that occurs following metabolic disturbances and rapid correction of hyponatremia; and *Marchiafava-Bignami disease* is characterized by demyelination in the corpus callosum and anterior commissure, which occurs in chronic alcoholics (see Chap. 9).

Leukodystrophies

Leukodystrophies (also called "dysmyelinating diseases") are genetic diseases that result in primary demyelination. However, the myelin being removed is inherently abnormal. Most of these disorders are due to defects in genes affecting myelin structural proteins or enzymes affecting myelin turnover. The

result is an abnormal or unstable myelin. Although many leukodystrophies are evident in infancy or childhood, onset of the disease in adults can result from degeneration of myelin that was apparently normal and functional at earlier ages. In some of the leukodystrophies with early onset and massive demyelination, there is nearly a complete lack of normal myelin production. These are described in Chapter 10.

Myelin Catabolism

The major components of myelin are phospholipids, glycolipids, cholesterol. and proteins (Fig. 7-2). When myelin is catabolized, the lipids are converted to triglycerides and cholesterol esters that can be identified using histochemical stains including Sudan black and oil red O (Fig. 7-3). These neutral lipids become apparent and indicate foci of acute myelin breakdown within hours after an injury, but the overall catabolic process may extend for much longer periods of time. Therefore, neutral lipids may be identified in macrophages for many months following a myelinoclastic injury.

In some of the leukodystrophies, myelin catabolism is abnormal. Consequently, in these disorders complex nonsudanophilic, (i.e., non-neutral) lipids may accumulate in the tissues. These disorders can be identified by their distinct appearances and special histochemical features, such as metachromasia (see Chap. 10). In contrast, in "sudanophilic (or orthochromatic) leukodystrophies," the macrophages accumulate sudanophilic neutral lipid myelin degradation products.

Multiple Sclerosis and Related Demyelinating Diseases

Multiple Sclerosis

Multiple sclerosis (MS) is the most common demyelinating disease. The classic lesions of
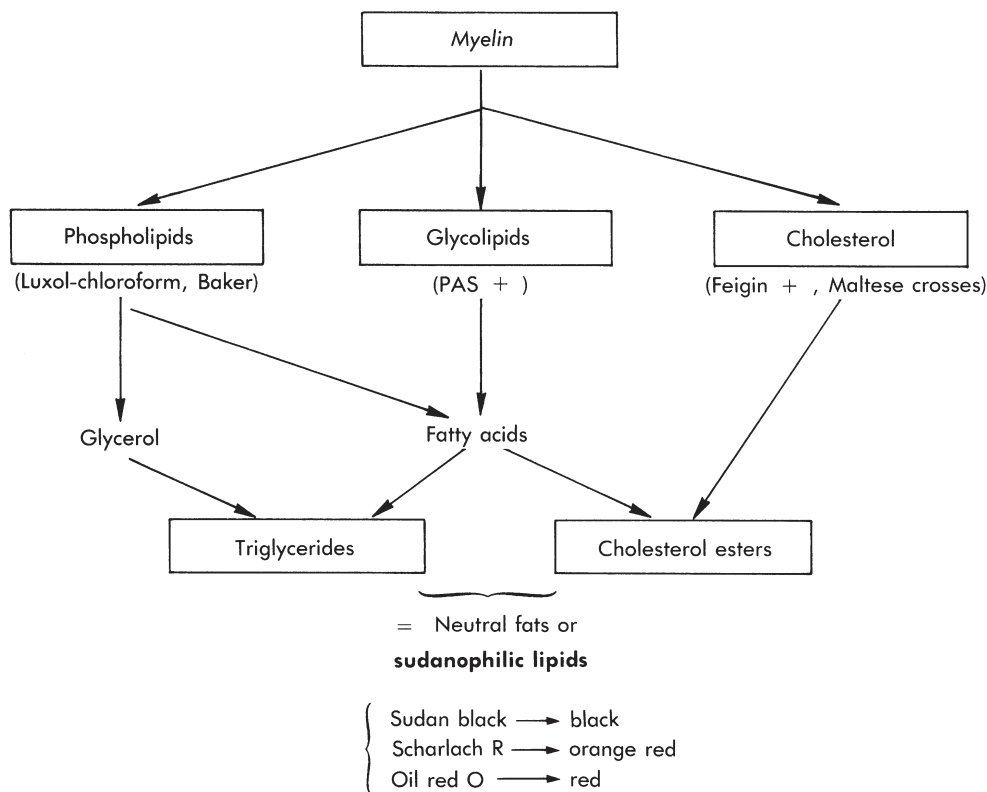
Figure 7-2. Biochemical data and chief histochemical reactions in orthochromatic degeneration of the myelin sheath.
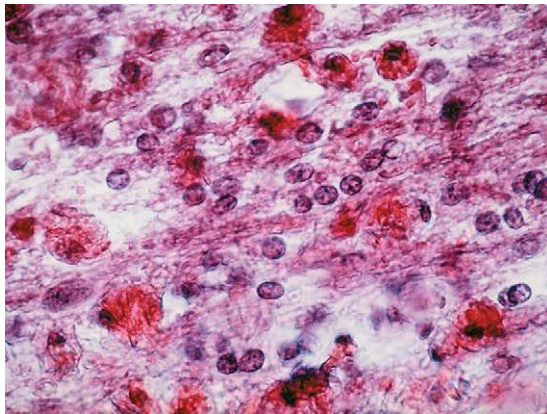
Figure 7-3. Oil red O stain in a frozen section of an active multiple-sclerosis plaque showing the sudanophilic (orthochromatic) catabolism of the myelin. Macrophages containing myelin debris are strongly stained by oil red O.

multiple sclerosis, as originally described by Charcot and Vulpian, are discrete areas of demyelination called "plaques." These are usually disseminated throughout the entire neuraxis and are associated with gliosis. In an individual patient, the plaques have many similar features but they generally vary in age. Although injury and loss of axons within lesions is always present, early axon loss within plaques and in adjacent white matter progresses over time and can lead to diffuse white matter atrophy.

Distribution of Lesions

Random dissemination of plaques throughout the white matter is an essential feature of MS (Fig. 7-4A). However, there are a number of preferential sites of involvement. In the cerebral hemispheres,
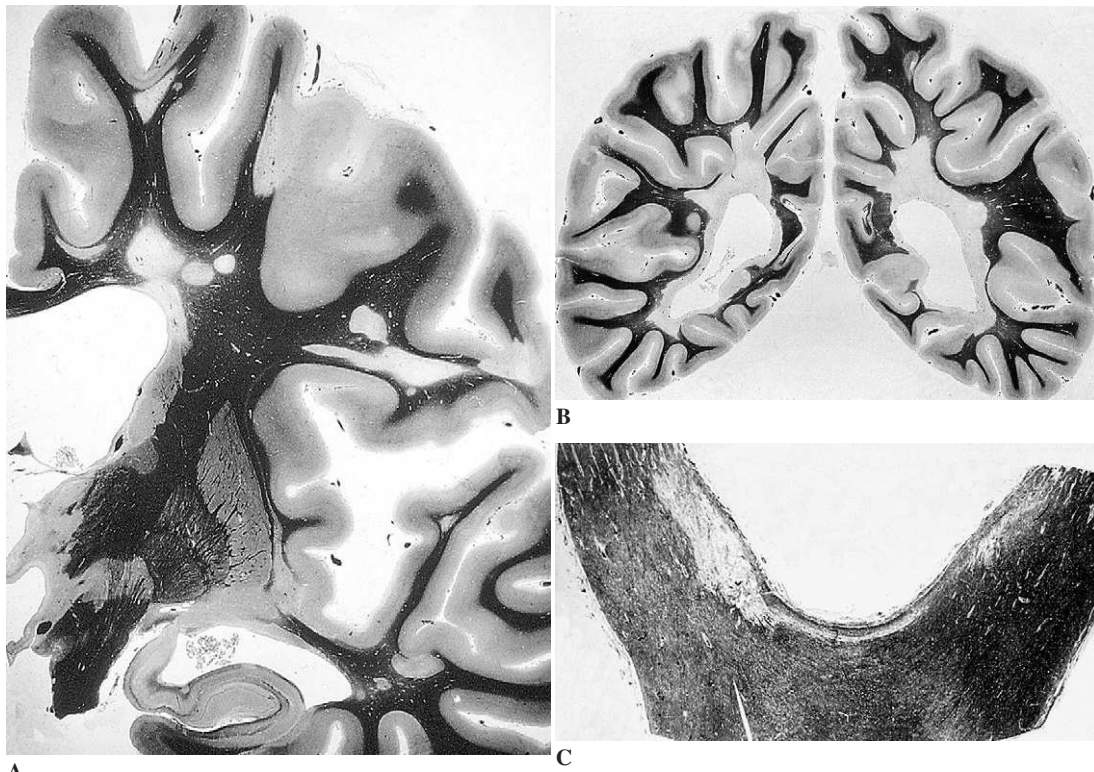
Figure 7-4. Chief topographical features of multiple sclerosis (Loyez stain for myelin). **A**, Right cerebral hemisphere: disseminated plaques. **B**, Cerebral hemispheres through the parieto-occipital region. Note periventricular distribution of the lesions. **C**, Optic chiasm. **D**, Left hemicerebellum and pons. Plaques in the anterior aspect of the fourth ventricle and in the cerebellar white matter. **E**, Plaques involving the spinal cord.

the periventricular regions are frequently involved (Fig. 7-4B). The optic pathways (i.e., optic nerves, chiasm, and tracts; Fig. 7-4C), the periventricular regions in the brainstem, the cerebellum (Fig. 7-4D), and the spinal cord (Fig. 7-4E) are also often severely affected.

There is no predilection of the plaques for specific neuroanatomic tracts, functional systems, neurons which use a particular neurotransmitter, or vascular territory.

Structure of Lesions

Gross Appearance. On gross examination of the CNS, the plaques, which become more visible after a few minutes' exposure to air, are seen to be localized predominantly in the white matter but may extend into gray matter also. They appear as rounded, geographic, sharply demarcated zones.

Recent lesions tend to be pink or yellowish, whereas older lesions tend to have sharp borders and are grayish or translucent and firm (Fig. 7-5).

Microscopic Appearance. On microscopic examination, several pathological processes are recognized in the plaques.

Inflammatory Cell Infiltration. Perivenular and pericapillary mononuclear cell infiltrates are often conspicuous (Fig. 7-6A). Inflammation is accompanied by breakdown of the blood-brain barrier, which normally excludes antibodies, complement, and coagulation factors. This permits plasma components that are normally excluded from the CNS to enter into the tissues. These may initiate pathogenic molecular cascades that result in myelin breakdown. Therefore, tissue injury is caused both by inflammatory cells that infiltrate the CNS and soluble factors from the plasma.

D

E
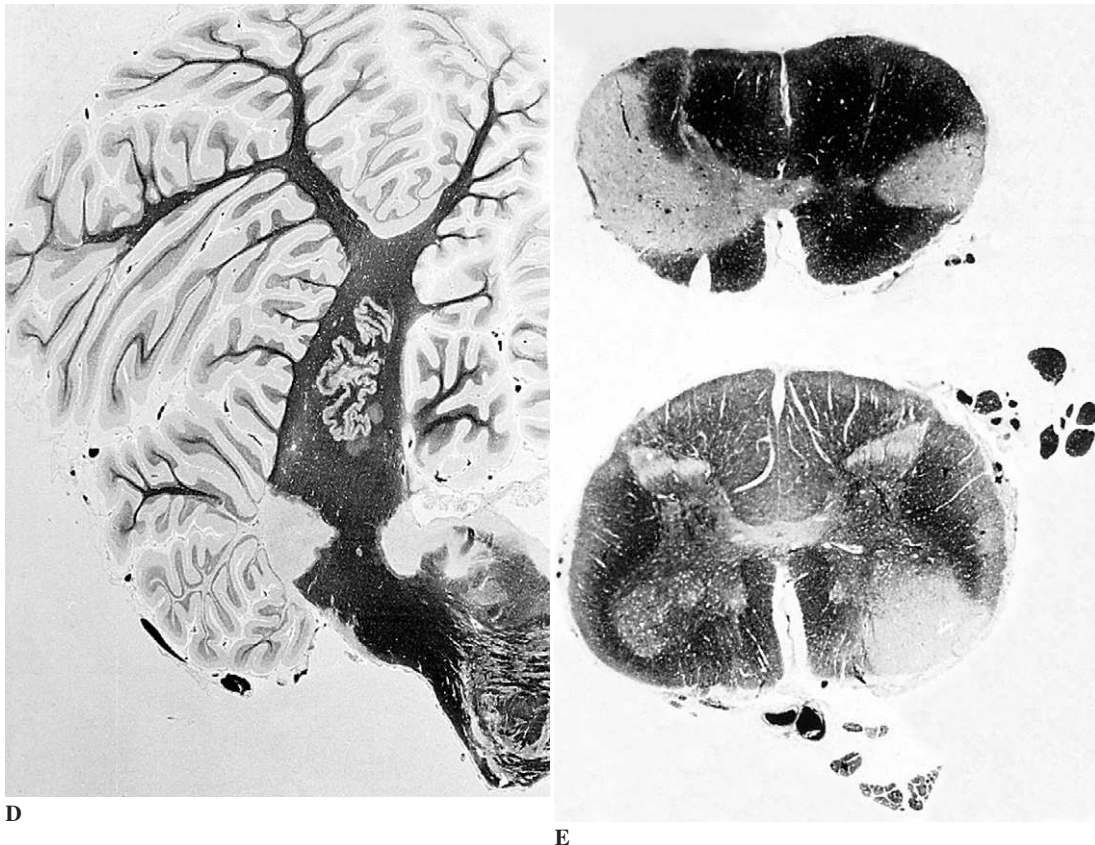
Figure 7-4. *Continued.*
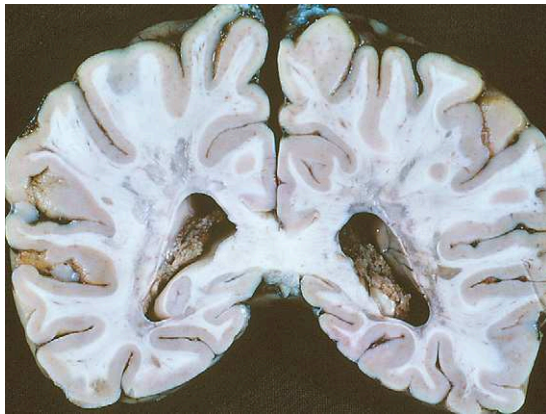
Figure 7-5. Gross appearance of parieto-occipital slice. Note periventricular distribution of the plaques.

DEMYELINATION AND AXON INJURY. This is characterized by discoloration of the myelin in discrete, well-circumscribed areas, giving a punched-out appearance in myelin stains such as Loyez stain or Luxol fast blue. Silver impregnations demonstrate a network of preserved axons in the plaque (Figs. 7-6B, 7-7B) with some axonal swellings or "spheroids" that indicate acute axon injury (Fig. 7-6C). The relative preservation of axons, as well as neuronal cell bodies in plaques encroaching on the grey matter (Fig. 7-7C), raises the possibility of repair, at least in early stages.

GLIAL CELL ALTERATIONS. Glial cells are intimately involved in the pathology of MS lesions. Perivascular cells and parenchymal microglia show
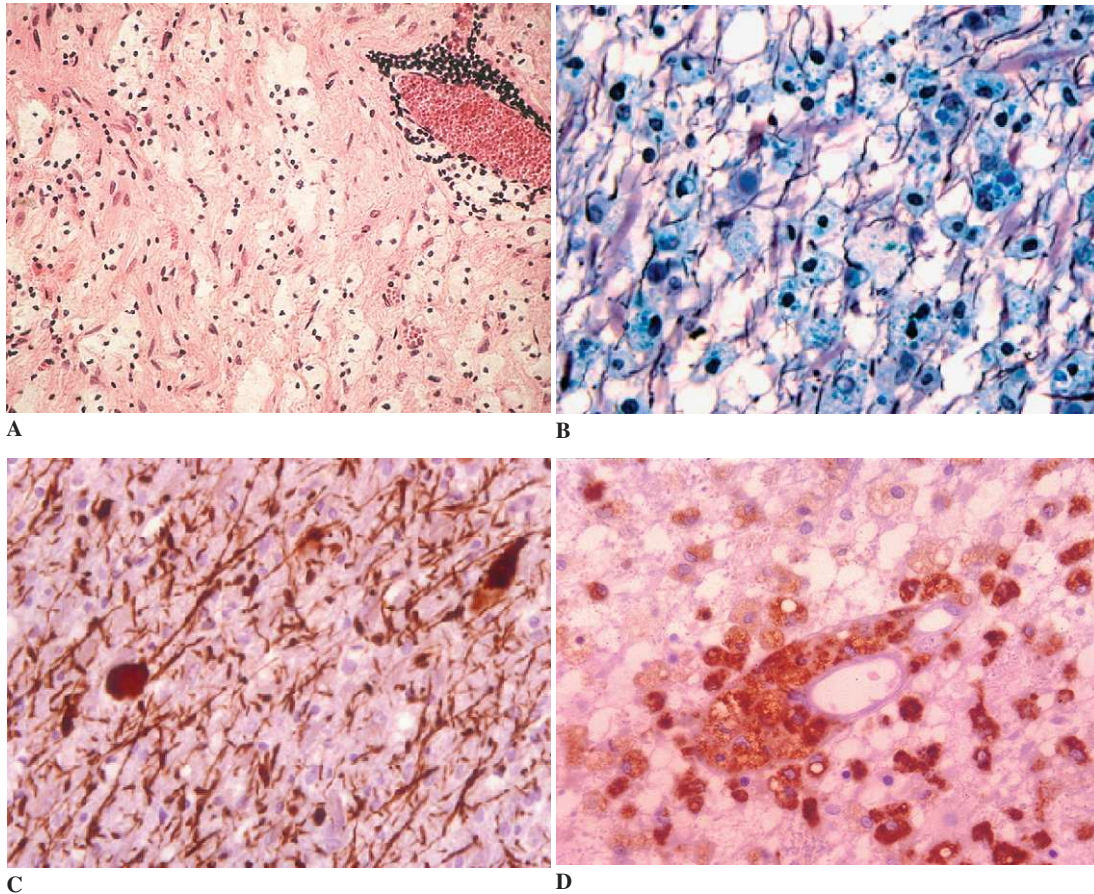
Figure 7-6. Microscopic features of multiple sclerosis (recent plaque). **A**, Perivascular lymphocytic infiltrate associated with macrophage infiltration and reactive astrocytosis. **B**, Bodian silver impregnation combined with Luxol fast blue shows diffuse infiltration by macrophages containing myelin debris and relative preservation of axons. **C**, Immunostaining for neurofilaments in the same plaque as in (**B**), showing axonal swellings. **D**, HLA-DR immunostaining shows immune activation of perivascular macrophages/microglial cells.
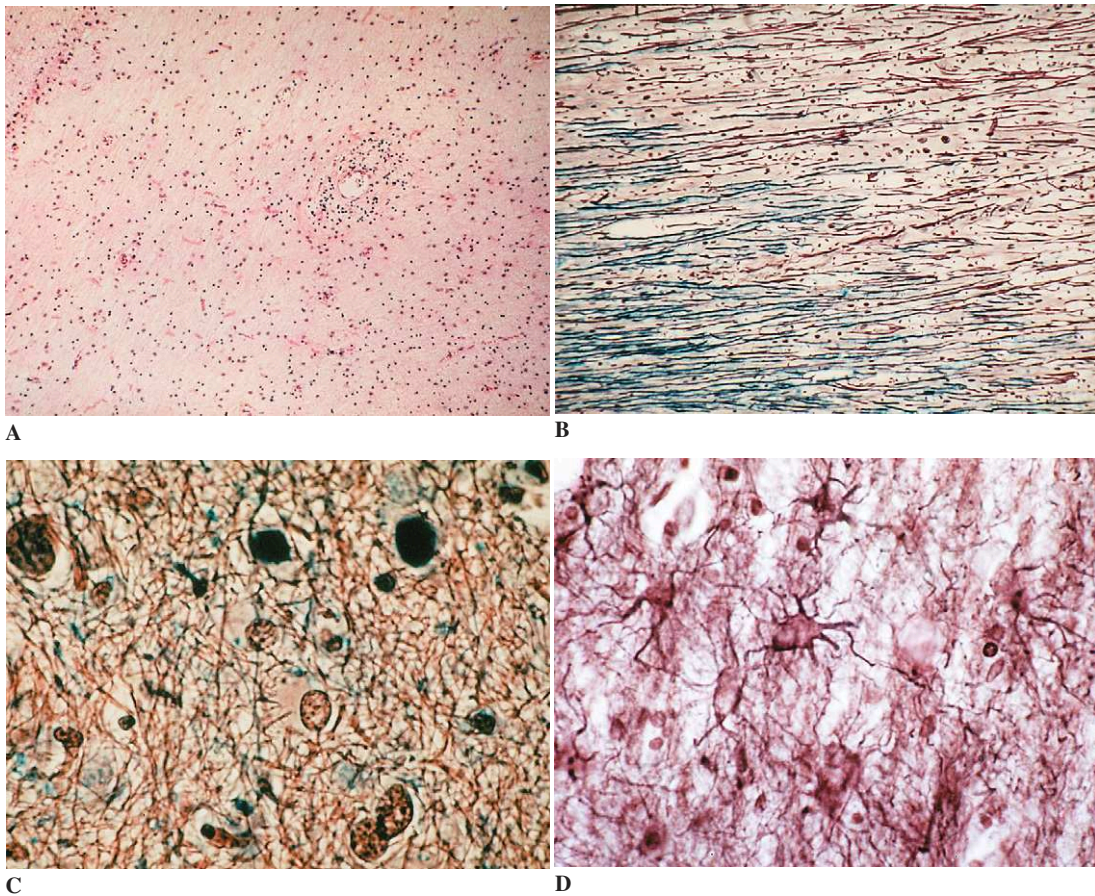
Figure 7-7. Microscopic features of multiple sclerosis (old plaque). **A**, Gliosis with Rosenthal fibers and absence of inflammation. Note residual perivascular macrophages. **B**, Bodian silver impregnation combined with Luxol fast blue at the periphery of an old plaque shows myelin-axonal dissociation with relative preservation of axons. Note normal staining of myelin on the left. **C**, Bodian silver impregnation combined with Luxol fast blue in a subcortical plaque encroaching on the cortex shows preservation of nerve cell bodies. **D**, Bielschowsky stain in the midst of an old plaque shows fibrillary gliosis.

evidence of immune activation (see Figs. 7-6B and D) and astrocytes show marked hypertrophy and proliferation. Gliosis is maximal at the edges of the plaques. Toward the center of the plaques, gliosis tends to become more fibrillary (Fig. 7-7D), with dense scar consisting of thickened astrocyte processes.

Acute Versus Old Lesions. Recent plaques show conspicuous inflammatory cell infiltrates with a marked microglial/macrophage reaction (see Figs. 7-6A, B, and D). Chronic plaques have more dense fibrillary gliosis with fewer mononu-

clear cells and macrophages (see Figs. 7-7A and D). Oligodendrocytes are depleted, particularly in chronic lesions. Axonal transection is evident in acute lesions and total loss of axons can be found in the centers of chronic plaques. Axon loss both within lesions and diffusely in normal-appearing white matter is now considered to be a major cause of chronic CNS dysfunction in MS patients. Some chronic plaques may be partly myelinated or remyelinated; however, the thickness of individual myelin sheaths never regains its original, normal diameter. In such "shadow plaques," myelin pallor is less evident.

Etiologic Factors

The etiology and pathogenesis of multiple sclerosis are not understood. Damage to the CNS white matter is mediated by immunopathologic mechanisms, including T cell–mediated and antibody-mediated injuries. There is considerable evidence supporting an autoimmune pathogenesis, but an infectious or parainfectious etiology is also possible, and MS may have different causes and pathogenetic pathways in different patients. In fact, the pathogenesis of MS appears clearly to be multifactorial.

Genetic factors, gender, and environmental factors appear to contribute to susceptibility to multiple sclerosis. Although MS may rarely occur in children and the elderly, it most frequently occurs in young adults, with a peak age of onset in the twenties. Moreover, it has a greater incidence in certain ethnic populations with particular tissue type antigens, for example, HLA DR2 and/or DW2 in European Caucasians. Furthermore, patients with close relatives with MS have a higher risk of developing MS than the general population. Yet, even in monozygotic twins, the coincidence of disease typically is only about 50%. Gender also plays a significant role in susceptibility; approximately two thirds of MS patients are women. Because of its increased prevalence in cold regions and because of its higher frequency in persons who have recently migrated from high- to low-incidence areas, a hypothetical environmental factor acquired early in childhood (e.g., virus infection) has been suggested.

An autoimmune pathogenesis is supported by a large body of literature on experimental autoimmune disease models that mimic the clinical, immunologic, and histopathologic features of MS. Experimental allergic encephalomyelitis (EAE) is a model induced by sensitization of animals with myelin or its components, thereby inducing an autoimmune reaction that mediates the CNS disease. In this model, the immune system generates T cells and/or antibodies that are truly autoimmune. Yet, it remains possible that MS arises from a response to an infectious agent. Indeed, brain viral infection models (e.g., infection by Theiler encephalomyelitis virus) induce a similar type of CNS pathology.

These models are highly useful for dissecting immunologic and pathologic mechanisms and genetic factors that impart susceptibility. Involvement of adhesion molecules, proinflammatory cytokines, chemokines, and proteases in the recruitment of inflammatory cells into the nervous tissue; the modulating effect of T cells; and glial cells are major aspects of these processes that experimental models have helped to understand. They are also important for testing potential therapies for the human disease.

Given the many questions about the nature of MS and the mechanisms responsible for tissue damage in this disorder, it is impossible to determine whether the disease represents only one specific entity. Some evidence supports the hypothesis that MS is etiologically and pathogenetically heterogeneous, though having features of inflammation and demyelination in common.

It has also been shown that different patterns of demyelination can occur in active plaques from different patients, although they were homogenous in each patient. A classification for the lesions based on histopathologic findings from diagnostic biopsies and autopsies of patients with MS has been proposed.

Pattern I and *II lesions* are characterized by radial perivenous expansion of the lesions and by inflammatory infiltrates composed of T cells and macrophages. Activated macrophages and microglia are associated with degenerating myelin, suggesting that demyelination is induced by macrophage toxins and results from a T cell–mediated inflammation with macrophage/microglia activation. In pattern II there is, in addition, massive deposition of activated complement at the site of active myelin destruction; this is suggestive of a T cell-plus-antibody–mediated autoimmune mechanism.

Pattern III and *IV lesions*, in contrast, are highly suggestive of a primary oligodendrocyte involvement. In pattern III, there is striking small-vessel vasculitis with endothelial cell damage and microvessel thrombosis. Degeneration of distal oligodendrocyte processes is followed by oligodendrocyte apoptosis and demyelination. In this pattern, it seems that demyelination is, to a large extent, mediated by focal tissue ischemia. Pattern IV lesions are similar to those of patterns I and II, but prominent oligodendrocyte degeneration is found in a small rim of periplaque white matter; this suggests that the demyelination induced by macrophage toxins occurs in the background of metabolically, perhaps genetically, impaired oligodendrocytes.

These different patterns of demyelination and inflammation are not closely linked to specific relapsing-remitting or progressive disease courses, and only Patterns I and II have clear similarities with experimental models. But the pathogenetic heterogeneity of plaques from different MS patients may explain the discrepancies in genetic susceptibility, clinical presentation, and response to treatment observed between individuals.

Acute Forms of MS

The designation *Marburg type* has been given to MS that follows a rapidly progressive, monophasic course and is usually fatal in a few months (often within one year of onset). It is most common in children and young adults but has also been described in older patients.

Neuropathological examination shows multiple plaques, the edges of which may be poorly defined, making it difficult to see them macroscopically. All the plaques are active and hypercellular with prominent perivascular lymphocytic cuffing, numerous foamy macrophages, and scattered reactive astrocytes. Edema may be present in the surrounding white matter, with mass effect in occasional cases. Necrotic changes may be found and, in cases with a prolonged course, cavitary lesions may occur (Fig. 7-8).

In "Schilder type" MS, a closely allied form of the disease most frequently involving children and running a relatively progressive course, the lesions are characterized by extensive, acute plaques with sharp borders. These plaques are often asymmetrical and spare the subcortical white matter (Fig. 7-9). Axonal lesions may be prominent, and wallerian degeneration is frequent. The cases originally described by Schilder included not only several forms of MS, but also what is now known as *adrenoleukodystrophy* (see Chap. 10). There are also forms of "transitional sclerosis," wherein extensive hemispheric lesions may be associated with typical disseminated MS lesions.

Baló Concentric Sclerosis

Baló concentric sclerosis is a very rare disease that usually presents in the second or third decade of
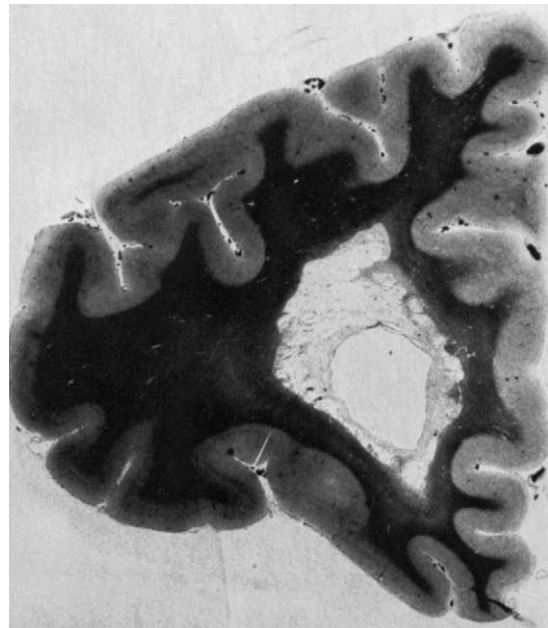
Figure 7-8. Cavitating multiple sclerosis. Wide, clean-cut periventricular plaque with sharp borders.

life and usually has a rapidly fatal course. It is characterized by alternating rings of demyelinated foci with zones in which the myelin is preserved, thereby resulting in a concentric pattern of demyelination (Fig. 7-10). The demyelinating lesions have all of the histologic features of acute plaques, and axonal injury is often prominent. Rare, cavitating forms have been reported. The disease is generally regarded as a variant of MS.

Devic Neuromyelitis Optica

Devic neuromyelitis optica is characterized by the distinct anatomic localization of the majority of lesions to the optic nerves and spinal cord. The plaques tend to be more inflammatory and destructive than in ordinary MS and may be associated with extensive lesions in the cerebral hemispheres and elsewhere in the neuraxis. Although clinically distinct, whether this disorder differs fundamentally from MS is not known.
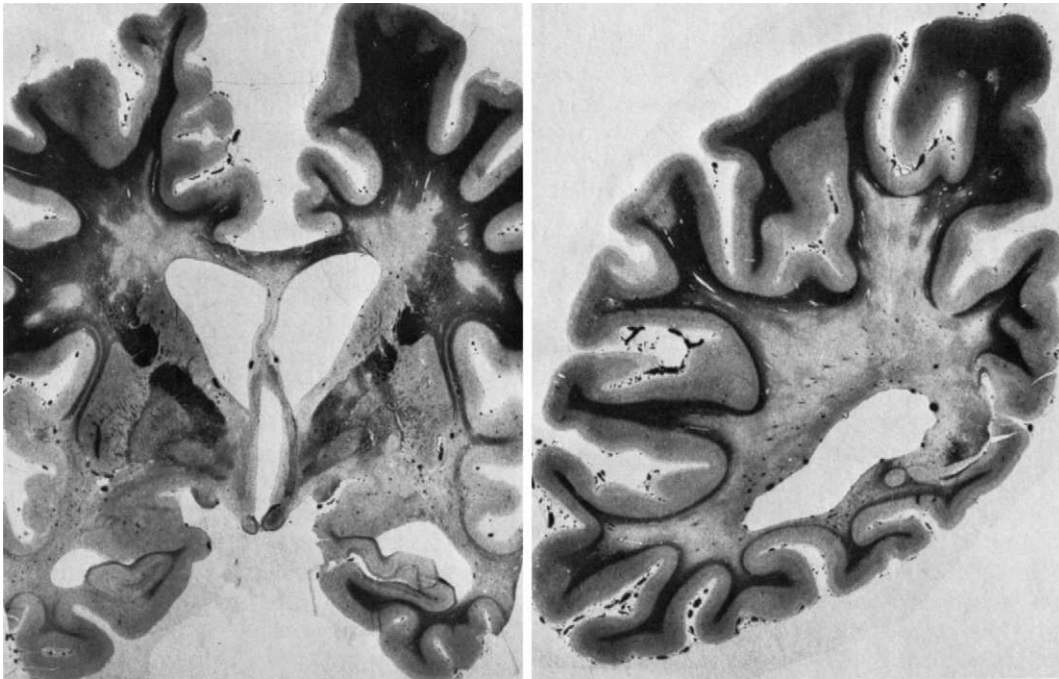
Figure 7-9. Schilder type MS. Wide hemispheric periventricular plaques (Loyez stain for myelin). Note presence of smaller plaques at a distance from large lesion.
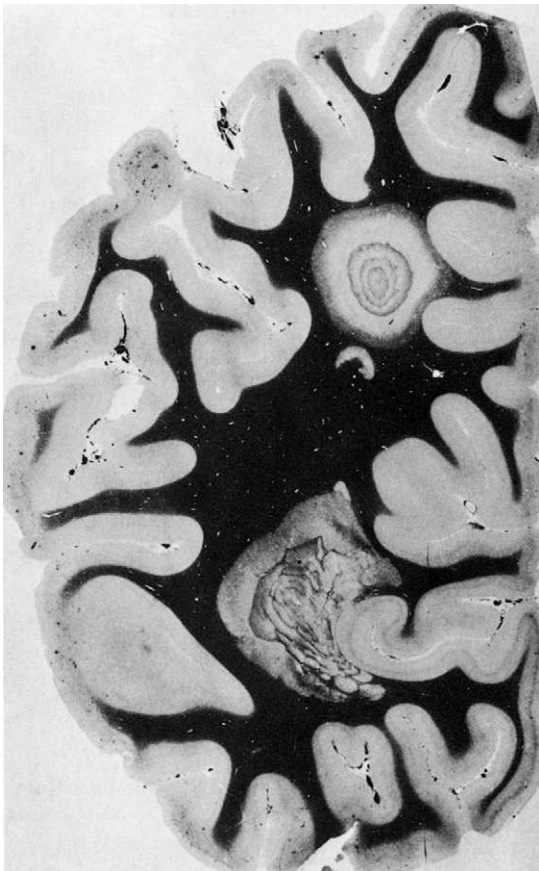
Figure 7-10. Baló concentric sclerosis.

Acute Disseminated Encephalomyelitides

In contrast to typical multiple sclerosis, *acute disseminated encephalomyelitides* are monophasic illnesses that follow an infection (e.g., measles, smallpox) or rabies vaccination. In patients who survive the acute episode, there is usually rapid recovery without neurological sequelae. They are acute CNS lesions characterized by small, perivenous, inflammatory, demyelinating lesions without large confluent MS-like plaques. These disorders are thought to be immune-mediated complications of a non-CNS infection. They include acute disseminated encephalomyelitis (or "acute disseminated leukoencephalitis"), acute postinfectious/postvaccinial perivenous encephalitis, and acute hemorrhagic leukoencephalopathy of Hurst (see Chap. 5).

Chapter 8
Pathology of Degenerative Diseases of the Nervous System

James Lowe, Charles Duyckaerts, and Matthew P. Frosch

Introduction and Background

The degenerative diseases of the nervous system are characterized by several common pathologic factors:

- They are commonest in old age.
- Each disease affects specific neuronal groups, and the clinical features of the disease relate to the anatomy and function of the affected areas. As the disease progresses, there is often atrophy of these areas, which may be detected on imaging or on macroscopic examination of the brain following death. The regional pattern of atrophy may be so distinctive for some diseases as to be considered pathognomonic.
- Histopathology is generally characterized by neuronal loss associated with variable gliosis. It is believed that in many cases neurons die by one of the mechanisms of non-necrotic, often apoptotic, cell death. Microglial activation may be seen in association with some disorders, raising the possibility that a low-level inflammatory mechanism contributes to certain disorders.
- Microscopic examination may reveal the presence of distinctive cellular inclusions containing specific proteins in either neurons or glial cells. Examples include neurofibrillary tangles, Lewy bodies, and Papp-Lantos inclusions.

Degenerative diseases of the nervous system were previously enigmatic conditions whose pathogenesis was little understood. This position is now being reversed thanks to insights from cell biology and genetics, which have led to reorganization of the classification schemes for some disorders. It is now clear that several disorders are characterized by the accumulation of an abnormal protein in cells, corresponding to the presence of inclusion bodies. One hypothesis for such diseases suggests that proteins in abnormal conformations or aggregates are toxic to cells and are not eliminated by the normal lysosomal and nonlysosomal ubiquitin-proteasomal systems. For some diseases, there are now well-characterized genetic abnormalities; in some such diseases all cases are associated with mutations, while in others both inherited and sporadic forms occur.

Classification

There are several approaches to classification, each of which has its own advantages. The one adopted here is to classify disorders by dominant presenting clinical features into three broad categories: movement disorders, cortical degenerations, and autonomic failure (Table 8-1). This approach mirrors the neurologist's approach to patients, which is based on clinical features. It is important to realize that

Table 8-1. Classification of Neurodegenerative Diseases

Movement Disorders
   The Akinetic/Rigid Syndromes
      Parkinson disease
      Progressive supranuclear palsy
      Multiple system atrophy
      Corticobasal degeneration
   Diseases of Motor Systems
      Motor neuron disease
      Hereditary spastic paraparesis
   Hyperkinetic Syndromes
      Huntington chorea
      Dystonias
   Cerebellar Ataxias
      Inherited
      Sporadic
Cortical Degenerations
   Alzheimer Disease
   Dementia with Lewy Bodies
   Frontotemporal Lobar Atrophy
   Dementia Linked to Chromosome 17
Autonomic Failure
   Lewy Body Disorders
   Multiple System Atrophy

there is great overlap in neurodegenerative diseases, so that a disease that generally presents as an akinetic rigid syndrome may also have cortical pathology leading to dementia.

Another emerging classification of neurodegenerative diseases is that which groups diseases according to type of abnormal protein accumulation.

Tauopathies are disorders characterized by accumulation of the microtubule-associated protein tau. In some of these disorders, there are mutations in the tau gene. This group includes Alzheimer disease, progressive supranuclear palsy, corticobasal degeneration, dementia linked to chromosome 17, and argyrophilic grain disease.

Alpha synucleinopathies are disorders in which there is accumulation of the synaptic-associated protein alpha synuclein. This group includes Parkinson disease, other Lewy-body diseases, and multiple system atrophy.

Polyglutamine diseases are disorders in which a mutation causes an expansion of a CAG triplet repeat in the coding region of a specific gene corresponding to a polyglutamine tract. Proteins with an expanded polyglutamine tract generally accumulate as nuclear inclusions. This group of diseases includes Huntington disease as well as some of the inherited spinocerebellar ataxias.

Movement Disorders

Movement disorders are extremely common and can be divided into four main groups (Table 8-2). It is important to remember that an apparently distinct clinical phenotype can have several underlying pathologic causes.

Akinetic Rigid Syndromes

Akinetic rigid syndromes are disorders characterized by the clinical features of parkinsonism, namely rigidity, bradykinesia, and tremor. Not all features are present in patients. While most patients with parkinsonism have Parkinson disease, some may have another pathologic condition that has produced an identical clinical picture. The clinical features of the movement disorder are related to abnormalities in the nigrostriatal system that are associated with striatal loss of dopamine.

Parkinson Disease

Parkinson disease is associated with the presence of distinctive spherical or rounded intraneuronal inclusions termed *Lewy bodies*. It is a degenerative disease mainly seen in old age. The annual incidence of Parkinson disease ranges from about 7.0 to 19 per 100,000 population and the pre-

Table 8-2. Classification of Movement Disorders

Akinetic/Rigid Movement Disorders
   Parkinsonism
Hyperkinetic Movement Disorders
   Chorea
   Myoclonus
   Dystonia
Ataxic Movement Disorders
   Spinocerebellar degenerations
Motor Neuron Disorders
   Motor neuron disease
   Spinal muscular atrophy and related disorders
   Hereditary spastic paraparesis

A   **B**
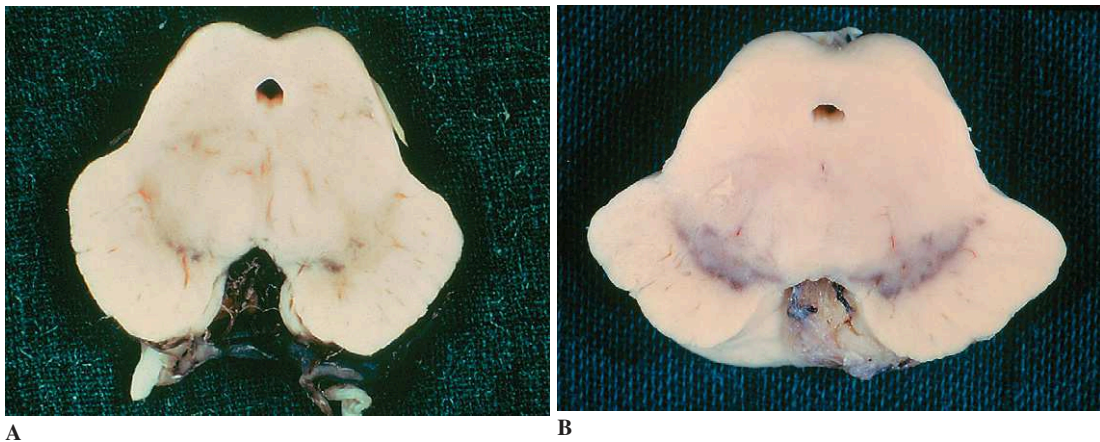
Figure 8-1. Parkinson disease. Macroscopic appearance of midbrain. Note pallor of the substantia nigra (**A**) compared with normal substantia nigra (**B**). Pallor is the result of loss of neurons containing neuromelanin.

valence ranges from about 30 to 190 per 100,000 population. There are very rare cases of familial Parkinson disease, but the cause in most cases is not known. Present studies are concentrating on oxidative stress causing damage to vulnerable neuronal populations; there may be genetic polymorphisms that place certain individuals at higher risk of developing disease.

Macroscopic Features. Macroscopic examination generally reveals normal brain weight. There is generally pallor of the substantia nigra in the midbrain (Fig. 8-1) as well as pallor of the locus ceruleus in the upper pons.

Microscopic Features. Microscopic examination shows neuronal loss and astrocytic gliosis in pigmented nuclei of the brainstem (i.e., the substantia nigra [Fig. 8-2], ceruleus-subceruleus area.) Neuromelanin pigment may be seen in macrophages, glia, or free in the neuropil. The loss of dopaminergic pigmented neurons from the substantia nigra is the pathologic basis for striatal loss of dopamine. Importantly, the striatum and pallidum are macroscopically and histologically normal. Other regions may be affected by Lewy-body pathology and may relate to other clinical features of disease. The dorsal vagal nuclei are commonly affected and may be associated with dysphagia. The nucleus basalis of Meynert is frequently affected. Lewy bodies may be seen in the

cerebral cortex, and extensive pathology has been related to a distinctive form of dementia (termed *dementia with Lewy bodies*) that is discussed in detail later in this chapter. Lewy bodies may also be encountered in the neurons of the intermediolateral columns of the spinal cord and relate to clinical features of autonomic failure, also discussed later in this chapter. They have also been found in neurons outside the nervous system, including those in the sympathetic and parasympathetic ganglia, enteric nervous system, cardiac plexus, pelvic plexus, and adrenal medulla.
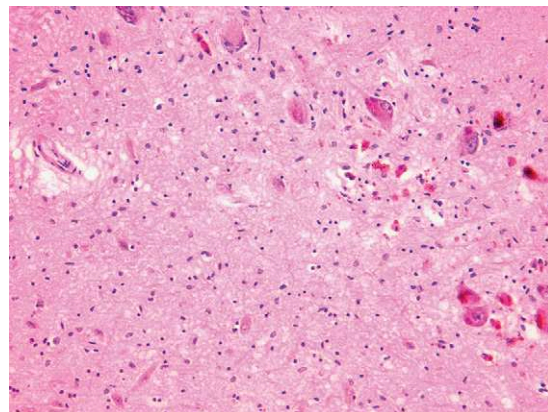
Figure 8-2. Histology of the substantia nigra, showing loss of pigmented neurons and astrocytic gliosis. Pigment can be seen in macrophages (H and E).

Molecular and Cell Biology of Lewy Bodies.
Lewy bodies are, by definition, seen in all cases of
Parkinson disease; they are by themselves highly
suggestive of the condition. However, while a
constant component of the pathology, they can be
present in low numbers. They are intraneuronal
inclusions that have a variable appearance depend-
ing on whether they are located in the perikaryon
or cell processes or in the brainstem, sympathetic
ganglia, or cortex (see Chap. 1 text and Fig. 1-13).
Their appearance is mostly characteristic in the
substantia nigra (see Figs. 1-13A and B). In the
nucleus basalis of Meynert, the dorsal nucleus of
the vagus, the locus ceruleus, the hypothalamus,
and especially the sympathetic ganglia one may
observe, in addition to the typical Lewy bodies
situated in the neuronal perikarya, hyaline acido-
philic inclusions situated in the cell processes. The
outline and the halo of these elongated inclusions
(termed *intraneuritic Lewy bodies*; see Figs. 1-13C
and D) may be less distinctly defined than those of
typical Lewy bodies. Finally, cortical (cerebral)
Lewy bodies are situated in the perikaryon of cor-
tical neurons, have an irregular outline, are less
eosinophilic, and usually have no central core or
peripheral halo (see Figs. 1-13E and F).

Immunohistochemical studies have shown that
Lewy bodies and neurites contain the protein alpha
synuclein (Fig. 8-3). This is a normal synaptic
protein, and the reason for its accumulation as
Lewy bodies is still a subject of study. Neuro-
filament protein, ubiquitin, and elements of the
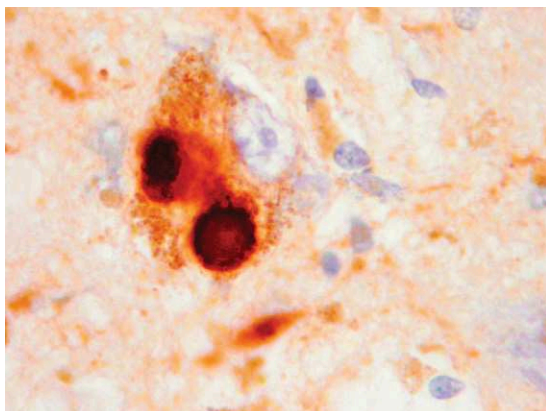
Figure 8-3. Immunohistochemistry for alpha synuclein,
showing Lewy bodies in a nigral neuron.

ubiquitin-proteasome system are also present in
Lewy bodies. Immunostaining for alpha synuclein
and ubiquitin have been recommended as methods
for the detection of cortical Lewy bodies, which
can otherwise be hard to detect.

Several familial forms of Parkinson disease
have been documented, and the genes for some of
these have been characterized. Mutations in the
alpha synuclein gene have been linked to some
of the rare autosomal dominant familial forms of
Parkinson disease. Mutations of the gene for
parkin, an E3 ubiquitin ligase, explain most of
the recessive cases of Parkinson disease, which
usually present at a young age and are sensitive to
L-dopa therapy. In these cases, Lewy bodies are
absent, although neuronal loss is severe in the
substantia nigra.

As well as being the central abnormality in
several diseases, Lewy bodies may be seen in asso-
ciation with other disorders (coincidental Lewy
body disorders) or in cases in which Parkinson
disease was not known clinically (incidental Lewy
bodies). Incidental Lewy bodies are usually con-
sidered to be evidence of preclinical Parkinson
disease.

Progressive Supranuclear Palsy

Progressive supranuclear palsy (PSP), also termed
Steele-Richardson-Olszewski syndrome, is clini-
cally characterized by parkinsonism (usually
without tremor) associated with supranuclear
ophthalmoplegia. Pseudobulbar palsy and cognitive
abnormality leading to dementia are common. The
average age of onset is about 64 years, with a
prevalence of about 7 per 100,000 population.

Macroscopic Features.   Macroscopic examina-
tion shows atrophy of the midbrain and pontine
tegmentum with loss of pigment from the substan-
tia nigra and locus ceruleus. There is variable
atrophy of the globus pallidus. The cerebral cortex
is usually spared, although some cases show
atrophy of frontotemporal regions.

Microscopic   Features.   Microscopy   shows
regional neuronal loss and astrocytic gliosis. The
main abnormalities seen in affected areas in PSP
are neuronal and glial accumulation of tau protein,
which can be highlighted by special stains.
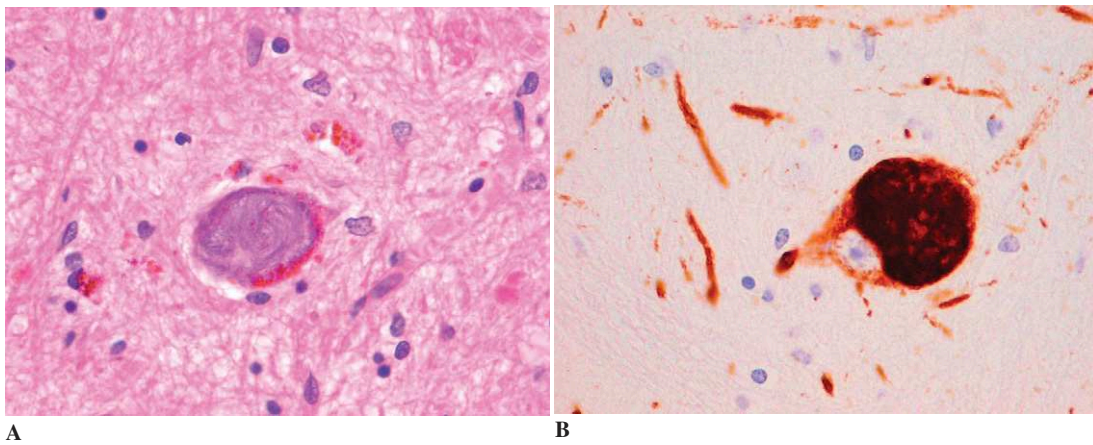
Figure 8-4. **A**, Neuron containing a globose neurofibrillary tangle (H and E). **B**, Neuron containing a globose neurofibrillary tangle (immunostaining for tau protein).

In neurons, tau protein forms neurofibrillary tangles having a characteristic globose appearance (Figs. 8-4A and B). Tufted astrocytes, considered highly characteristic of the disease, develop in affected areas (Fig. 8-5A). The whole length of their processes contains tau protein and they are often binucleated. Thorn astrocytes (Fig. 8-5B; see Chap. 1) are commonly seen but are not specific and may be seen in other neurodegenerative conditions. Accumulation of tau protein in oligodendrocytes, which also occurs in PSP but is less specific of it, is known as "coiled body." In the substantia nigra, neuronal loss is attested by the presence of pigment-containing phagocytes. Remaining nigral neurons contain basophilic, globose tangles.

The substantia nigra, the globus pallidus, and the subthalamic nucleus are always involved, but to variable degrees. The superior colliculi, the pretectal areas, the periaqueductal gray matter, and the mesencephalic and pontine reticular formations are generally markedly affected, and such changes are responsible for the atrophy of the mesencephalic and pontine tegmenta as seen on gross examination or by imaging. The dentate nucleus, locus ceruleus, oculomotor nuclei, pontine nuclei, reticular formation in the medulla, inferior olives,
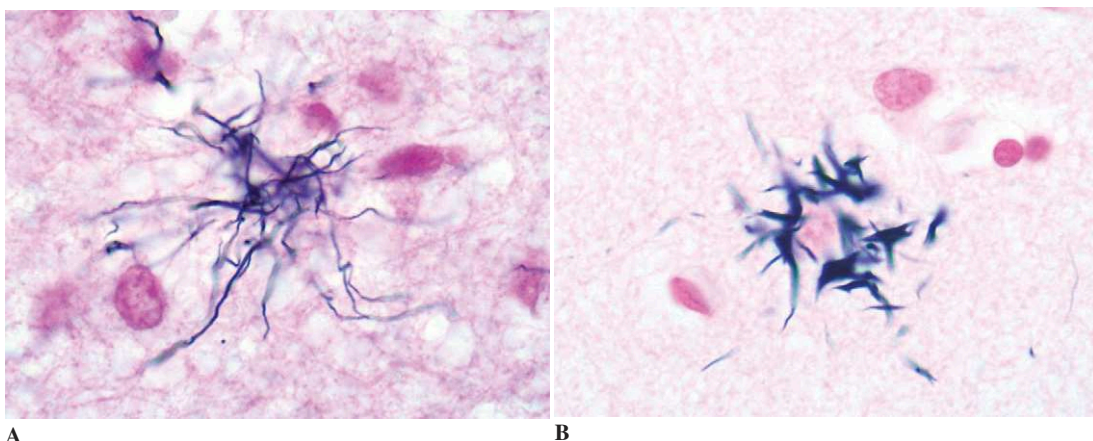
Figure 8-5. Glial pathology in progressive supranuclear palsy. **A**, Tufted astrocytes are seen in gray matter regions and have some specificity (Gallyas silver stain). **B**, Thorn astrocytes are commonly seen but are not specific and may be seen in other neurodegenerative conditions (Gallyas silver stain).

corpus striatum, and thalamus are inconsistently and usually moderately affected. Tufted astrocytes and neurofibrillary tangles are also frequently seen in the motor and premotor areas of the cerebral cortex. Other cortical areas are less severely involved. Cortical cerebellar and anterior-horn lesions are rarer.

Genetics of PSP. Genetics and cell biology point to mutations in the tau gene in rare cases, the phenotype of which cannot be distinguished from usual sporadic PSP cases, and implying overlap with the pathology of dementia and parkinsonism linked to chromosome 17 (see later in this chapter). Two haplotypes of the tau gene occur in the population, H1 and H2. H1 is the most prevalent (78% of the population), but its frequency reaches 94% among PSP cases.

Postencephalitic Parkinsonism

Cases of *postencephalitic parkinsonism* followed a pandemic of encephalitis lethargica (von Economo disease) between 1915 and 1927. Half of the individuals who survived the acute encephalitic phase of the illness developed a parkinsonian syndrome, typically after a latent period of about nine years. Contemporary cases are regarded as very rare. Macroscopic examination shows changes similar to those described in progressive supranuclear palsy. Microscopic examination shows the presence of neurofibrillary tangles; these are widely distributed but particularly affect the substantia nigra, locus ceruleus, nuclei of reticular formation, hypothalamus, and nucleus basalis of Meynert. Affected regions show neuronal cell loss with astrocytic gliosis.

Multiple System Atrophy

Multiple system atrophy (MSA) is the diagnostic term used to group three disorders formerly considered separate conditions: *sporadic olivopontocerebellar atrophy* (clinically characterized by prominent cerebellar ataxia), *primary autonomic failure* (Shy-Drager syndrome), and *striatonigral degeneration* (clinically characterized by prominent parkinsonism). These disorders are grouped as MSA because they share distinctive inclusion bodies in glial cells first identified by Papp and

Figure 8-6. Multiple system atrophy. Macroscopic examination of the fixed brain shows shrinkage of basal ganglia and discoloration of the putamen, which acquires a gray-green color.

Lantos. Macroscopically, cases presenting with parkinsonism show atrophy of the pons and midbrain with loss of pigment from the substantia nigra. There is usually atrophy of the putamen, which becomes shrunken and gray-green in color (Fig. 8-6). In cases with a predominantly ataxic presentation, there is generally cerebellar atrophy associated with atrophy of the pons (see later discussion). Microscopy shows neuronal loss and astrocytic gliosis in affected areas. On routine stains, inclusion bodies cannot be seen. A special silver stain such as Gallyas (Fig. 8-7A) or Bodian (Fig. 8-7B) shows characteristic glial cytoplasmic inclusions in oligodendroglial cells. These are widely distributed in the brains of affected patients and appear as flame- and sickle-shaped structures in glial cells. Neuronal cytoplasmic inclusions and neuronal nuclear inclusions may also be seen but are generally much less obvious.

Inclusions contain fibrils of alpha synuclein (Figs. 8-8A and B), so multiple system atrophy is classed as one of the synucleinopathies. However, no mutations of alpha synuclein have been found in MSA.

Corticobasal Degeneration

Corticobasal degeneration (CBD) is a clinicopathologic entity in which there is degeneration of cortical areas, the basal ganglia, and the substantia nigra. It is characterized by accumulation of tau
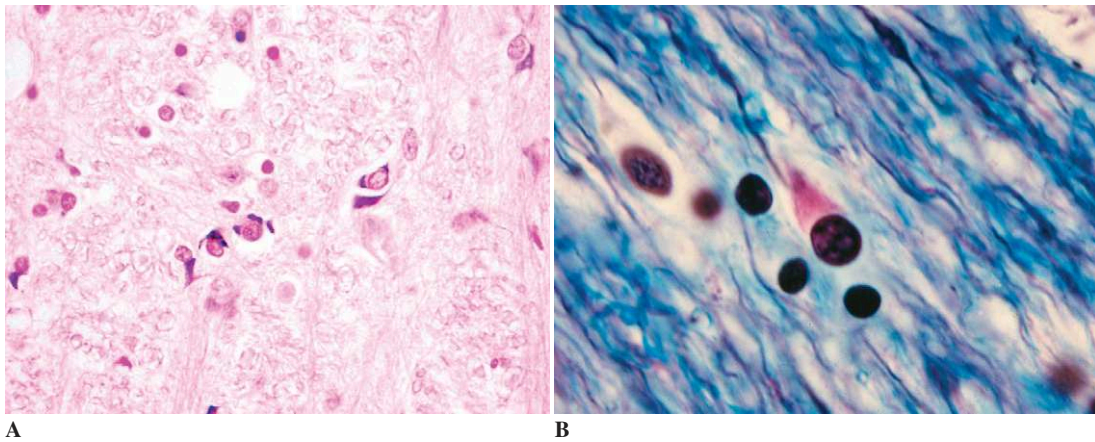
Figure 8-7. Multiple system atrophy. Glial cytoplasmic inclusions of multiple system atrophy, which have been termed Papp-Lantos inclusions, can be detected by Gallyas staining (**A**) or Bodian silver impregnation (**B**).

protein in neurons and glia and is classed as one of the tauopathies. In some cases, mutation in the tau gene has been described, and so there is overlap with the pathology of parkinsonism and dementia linked to chromosome 17 (see later in this chapter).

Clinically, patients present with rigidity, clumsiness, and stiffness or jerking of the arm or (less commonly) leg. Many patients develop progressive apraxia and the "alien limb" phenomenon, in which a limb moves without their voluntary control and in which the patient often has the feeling that the affected limb does not belong to them. Difficulty with walking develops due to apraxia of leg movement together with pyramidal deficits caused by upper motor neuron involvement. Cognitive

abnormalities occur in some patients, with aphasia and dementia of the frontotemporal type. Some patients present with cognitive abnormalities without movement disorder, highlighting the overlap with those disorders due to a mutation in the tau gene.

Macroscopically, there is asymmetric atrophy of the cerebral cortex, most prominent around the sylvian fissure. There may be frontotemporal cortical atrophy. The substantia nigra shows loss of pigment. There may be atrophy of the basal ganglia. Microscopy shows variable cortical neuronal loss and astrocytic gliosis. A characteristic feature is the presence in the cortex of swollen "achromatic" neurons that have lost their Nissl
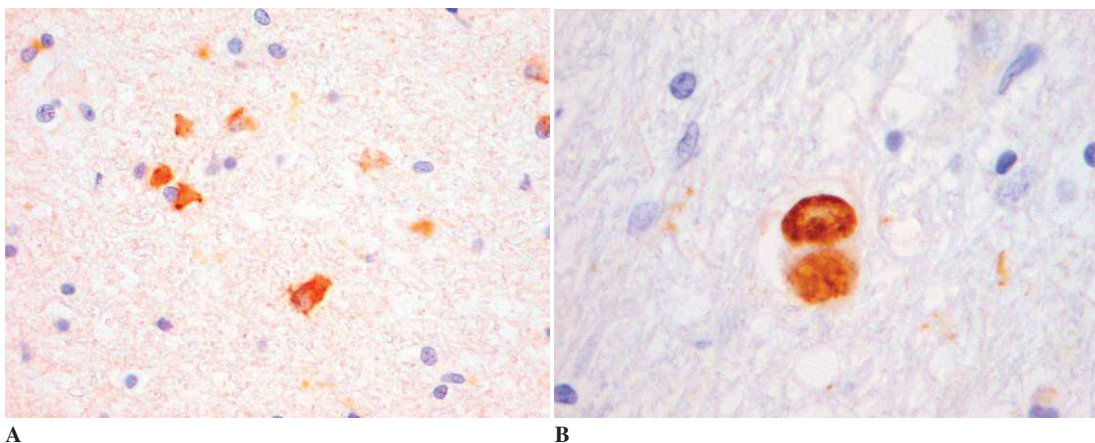
Figure 8-8. Multiple system atrophy. Alpha synuclein can be detected in glial cytoplasmic inclusions (**A**), neuronal nuclear inclusions, and neuronal cytoplasm. The neuron shown in (**B**) has both nuclear and cytoplasmic inclusions.
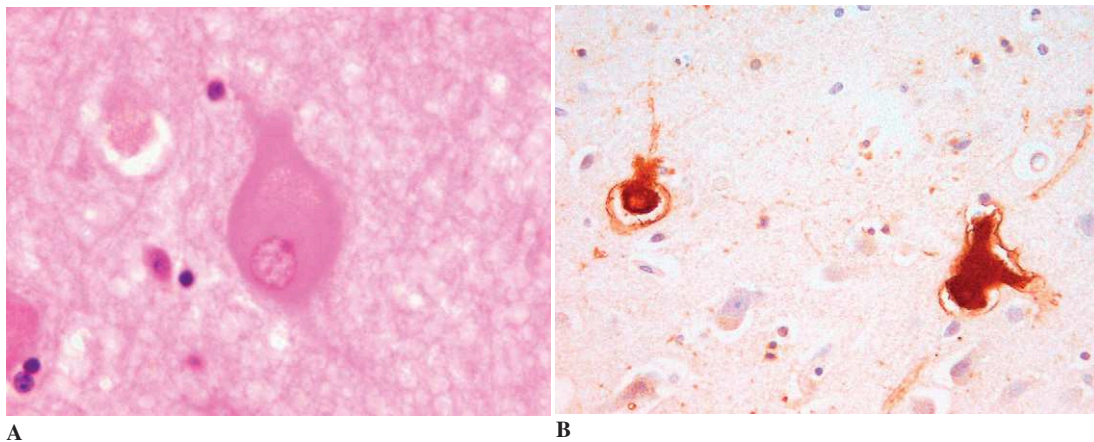
Figure 8-9. Corticobasal degeneration. **A**, A swollen achromatic neuron in the cerebral cortex (H and E). **B**, Swollen neurons show immunoreactivity for αB crystallin, which is a useful method for detection.

bodies (Figs. 8-9A and B). In the substantia nigra, cell loss is associated with astrocytic gliosis. Remaining nigral cells show large globose, pale-staining neurofibrillary tangles (Fig. 8-10). Immunostaining for tau protein shows tangles in neurons as well as immunoreactivity in many swollen neurons. Glial pathology is seen with accumulation of tau protein in astroglial cells in gray-matter areas to form distinctive structures termed *astrocytic plaques*; tau protein accumulates at the end of the astrocytic processes, while the center of the plaque is devoid of tau immunoreactivity (Fig. 8-11).

There is molecular-pathologic as well as morphologic and clinical overlap between cases of PSP, CBD, and dementia and parkinsonism linked to chromosome 17 with mutations in the tau gene.

Secondary Parkinsonian Syndromes

A number of nondegenerative pathologic processes, usually involving the striatonigral system, may result in the development of a parkinsonian syndrome.

Drug Therapy.   Parkinsonian syndromes linked to drug therapy represent the vast majority of the
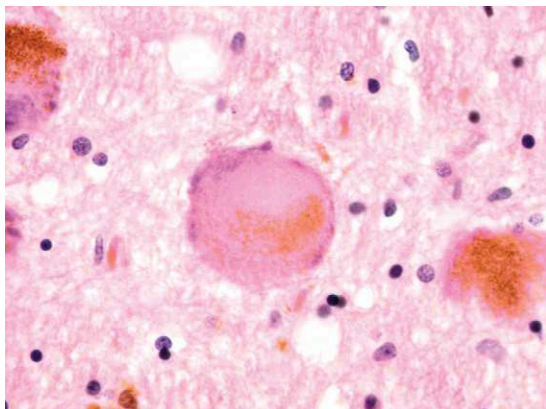
Figure 8-10. Corticobasal degeneration. Nigral neurons contain pale areas that displace the neuromelanin. These are large, globose tangles composed of tau protein (H and E).
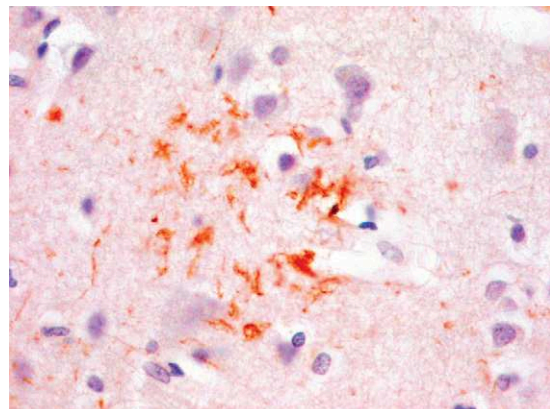
Figure 8-11. Corticobasal degeneration. Astrocytic plaques can be detected in gray matter by tau immunostaining, as here, or by Gallyas staining.

secondary parkinsonian syndromes. Extrapyramidal disturbances are often seen in the course of prolonged treatment with neuroleptics, but the anatomical substrate is poorly defined. A few cases of long-lasting parkinsonian syndrome have been observed after intoxication by 1-methyl-4-phenyl-1,2,3,6 tetrahydropyridine (MPTP); neuropathologic examination has shown nerve cell loss involving the substantia nigra in a highly selective manner and the presence of eosinophilic cytoplasmic inclusions resembling Lewy bodies.

Carbon Monoxide Poisoning. Parkinsonian syndromes following carbon monoxide poisoning are most frequently produced by bilateral necrotic pallidal lesions. Lesions in the substantia nigra are inconstant and usually moderate (see Chap. 9).

Vascular Disease. Parkinsonian syndromes caused by vascular disease are seen occasionally. Most cases present with a clinical picture that resembles pseudobulbar palsy; lacunae are commonly seen in the basal ganglia, with variable ischemic myelin loss involving fibers from the frontal lobes.

Head Injury. Parkinsonian syndromes—either pure or, more often, associated with progressive dementia (dementia pugilistica)—have been noted after repeated head injury, especially in boxers (see Chap. 3).

Diseases of Motor Systems

Several disorders are characterized by a predominant degeneration of motor neurons. Motor system degeneration may be seen in a variety of nondegenerative conditions, including toxic, infective, and metabolic disorders.

Motor Neuron Disease (Amyotrophic Lateral Sclerosis)

Motor neuron disease (MND) is characterized by a primary degeneration of motor neurons, which causes weakness and wasting of the affected muscles. The most common pattern of MND is *amyotrophic lateral sclerosis* (ALS), which is characterized by degeneration of both upper motor

neurons and lower motor neurons. In some cases, ALS begins with bulbar symptoms and may be termed *progressive bulbar palsy*. *Progressive muscular atrophy* is characterized by lower motor neuron signs with preservation of upper motor neurons and corticospinal tracts. *Primary lateral sclerosis* is characterized by upper motor neuron signs with loss of corticospinal tracts, and neuronal loss restricted to the motor cortex.

Five to ten percent of patients with MND have a familial form of disease with an autosomal dominant mode of transmission, but X-linked and recessive patterns of inheritance also occur. Mutations of the copper-zinc-superoxide dismutase (*SOD 1*) gene have been shown to cause ALS in some families.

Macroscopic Appearance.   Macroscopically, the brain usually appears normal. In a very few cases, atrophy of the precentral gyrus is seen. In patients who have developed clinical dementia, atrophy of frontal and temporal lobes may be present. The spinal cord is usually thinner than normal and the anterior nerve roots are generally shrunken and gray in comparison with the posterior sensory roots (Fig. 8-12).

Microscopic Appearance.   On microscopy, the main change seen is loss of motor neurons with associated astrocytosis in the anterior horns of the
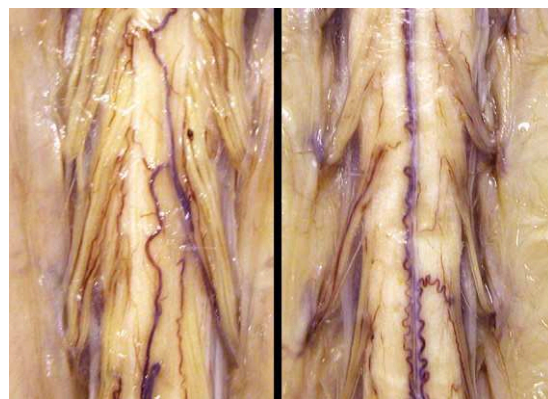
Figure 8-12. Motor neuron disease. On the left, the spinal cord (viewed from the back) shows normal-sized posterior (sensory) nerve roots. On the right, the same spinal cord (viewed from the front) shows marked atrophy of anterior (motor) nerve roots in a case of amyotrophic lateral sclerosis.
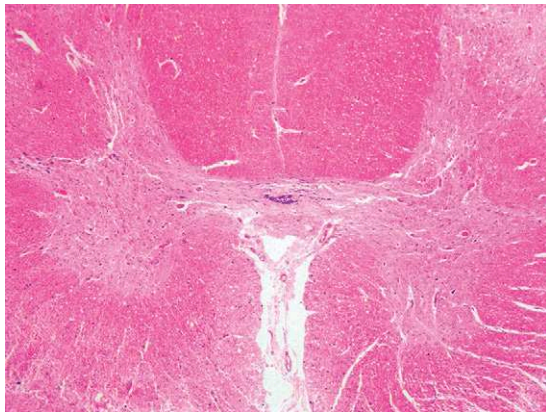
Figure 8-13. Motor neuron disease. This low-magnification view shows severe loss of motor neurons from the anterior horns of the spinal cord.

spinal cord, in the brainstem, and in the motor cortex (Fig. 8-13). In the spinal cord, there is generally severe loss of motor neurons, especially in the cervical enlargement. Among cranial nerve nuclei, the hypoglossal nucleus, nucleus ambiguus, motor nucleus of trigeminal nerve, and facial nerve may be involved. In most cases the nuclei of the third, fourth, and sixth cranial nerves nuclei appear normal. In the motor cortex, loss of Betz cells may sometimes be detected. Bunina bodies may be seen in surviving motor neurons; these are small, eosinophilic inclusions, 2–5 μm in size, located in the cell body (see Figs. 1-14A and B). Inclusion bodies can be detected in surviving motor neurons by immunocytochemical staining for ubiquitin. The commonest type of inclusion appears as an aggregate of thread-like structures termed *skeins* (see Fig. 1-15). Axonal spheroids are frequently seen in the anterior horn of spinal cord in ALS, but spheroids at the lumbar level of the spinal cord are frequent in apparently normal individuals.

In ALS and primary lateral sclerosis, the white matter of the spinal cord shows pallor in the corticospinal tracts that is related to their degeneration. Pallor of myelin staining may not be confined to the corticospinal tracts and may extend in the anterior and lateral columns (Figs. 8-14).

Involvement of nonmotor systems is well-recognized in MND. Neuronal loss and inclusion formation may be seen in Clarke column, the dorsal root ganglia, the intermediolateral nucleus in the thoracic cord, and the reticular formation.

Onufrowicz (Onuf) nucleus, located in the sacral spinal cord and controlling the bladder sphincter, is relatively spared in ALS; this might explain why incontinence is rare in this disease. Neuronal loss may be seen in subcortical structures, including the basal ganglia, locus ceruleus, substantia nigra, thalamus, subthalamic nucleus, red nucleus, cerebellar dentate nucleus, and nuclei of pontine tegmentum. The nonmotor cortex, particularly in the anterior temporal, frontal, and insular regions, may show microvacuolation (associated with neuronal loss) in the superficial layers. Ubiquitin-reactive inclusions may be seen in small cortical neurons in affected areas as well as in dentate granule cells of the hippocampus. This change has been linked to the development of cognitive abnormality and dementia in MND, as discussed later with non-Alzheimer dementias.

Spinal Muscular Atrophy

The *spinal muscular atrophies* (SMAs) are conditions in which spinal motor neurons progressively degenerate. The commonest forms are seen in childhood. In general, forms with earlier onset are more severe. Autosomal recessive SMA was originally described by Werdnig and Hoffmann and is the commonest neuromuscular disease of childhood. It is characterized by loss of anterior horn cells, which results in symmetrical weakness and wasting of muscles, and is now known as SMA type 1. SMA type 2 (chronic infantile spinal muscular atrophy) has a longer course. SMA type 3, also known as Kugelberg-Welander syndrome, is a milder form of type 2 that starts later (i.e., in adolescence) and has a longer course. An adult form (type 4) has also been described.

Macroscopically, there is atrophy of skeletal muscles and of anterior nerve roots. Nerve cell loss is especially seen in the cervical and lumbar expansions of the cord.

SMA types 1, 2, and 3 are generally linked to a deletion of the *SMN* (survival motor neuron) gene located on chromosome 5q13.

Hereditary Spastic Paraparesis

Hereditary spastic paraparesis is a heterogeneous condition with autosomal dominant, autosomal recessive, or X-linked recessive inheritance. In the commonest types, patients develop slowly pro-

Figure 8-14. Amyotrophic lateral sclerosis. **A**, Pallor of myelin staining in the medullary pyramid. **B**, Sections of the spinal cord at cervical, thoracic, and lumbar levels show pallor of myelin staining in uncrossed and crossed pyramidal tracts (Loyez stain).

A
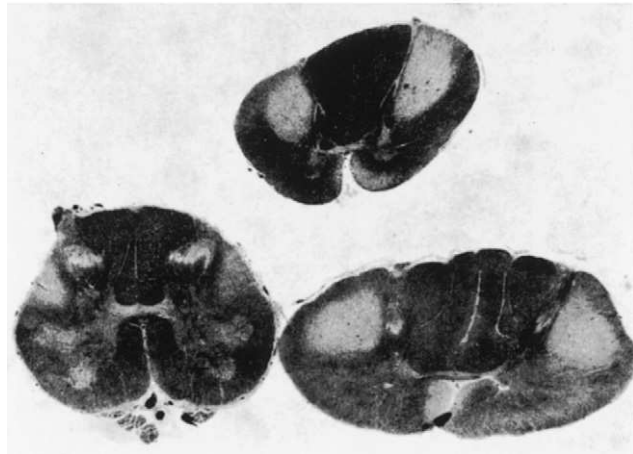
B

gressive paraparesis in which spasticity is more dominant than weakness. Pes cavus is often seen. Genetic linkages have been established in many kindreds and some genes have been identified.

There is degeneration of corticospinal tracts, most marked in the lumbar and lower thoracic cord. Degeneration of dorsal columns is also prominent, being most marked in the upper thoracic and cervical cord.

Hyperkinetic Movement Disorders

The clinical signs and symptoms of *hyperkinetic movement disorders* are chorea, ballism, myoclonus, dystonia, and tics. Chorea is characterized by nonrhythmic rapid involuntary movements. These disorders may be separated into two main groups—hereditary and sporadic—with a wide range of causes, the commonest being the inherited condition Huntington disease.

Huntington Disease

Huntington disease (HD), a disorder of autosomal dominant transmission, is caused by mutation in the gene coding for the huntingtin protein, located on the short distal arm of chromosome 4. Huntingtin is widely expressed in a variety of tissues and contains a polyglutamine tract that varies in

size from 9 to 37 copies of the amino acid, encoded by a CAG repeat in the gene. In patients with HD the repeat sequence is expanded, with the average repeat length around 46 (range, 36 to 86). Age of onset of HD correlates inversely with repeat length. There is expansion of the CAG repeat upon parental transmission to offspring, so that the disease develops earlier in subsequent generations (anticipation). The disease usually starts in middle or late life, but may occur earlier with longer expansion. It is characterized by chorea and mental deterioration leading to dementia. In some juvenile or early onset forms, chorea is replaced by hypertonia. The frequency of HD varies in different populations, with levels of between 4 and 7 per 100,000 population.

Macroscopic Appearance.   Macroscopically, the brain usually shows mild to moderate cerebral atrophy. On inspection of cut surfaces, the main neuropathologic abnormality of HD is seen to be atrophy of the caudate nucleus and putamen. Atrophy of the caudate nucleus is most evident in coronal slices; the normal convexity bulging into the lateral ventricle is replaced by either a flat or concave profile (Fig. 8-15).

Microscopic Appearance.   Microscopically, there is neuronal loss from the basal ganglia and astrocytic gliosis. The medium spiny neurons are the most severely affected. With conventional staining the cortex generally appears unremarkable, although some degree of neuronal loss and gliosis has been repeatedly documented. Immunostaining for huntingtin or ubiquitin shows accumulation of abnormal protein as nuclear inclusion bodies. Abnormal protein also accumulates in cortical neurites (Fig. 8-16). The neuritic aggregates are more common than the nuclear inclusions, which are more abundant in the cortex than in the striatum. Only about 2% of striatal neurons have nuclear aggregates.

Cellular Mechanism of Neurodegeneration. The cellular mechanism of neurodegeneration in HD remains unexplained. Proposed mechanisms contributing to pathology include loss of huntingtin function, gain of toxicity by mutant protein, transcriptional dysregulation caused by nuclear

Figure 8-15. Huntington disease. Loyez stain showing atrophy of the caudate nucleus and putamen with dilatation of frontal horn and cortical atrophy.
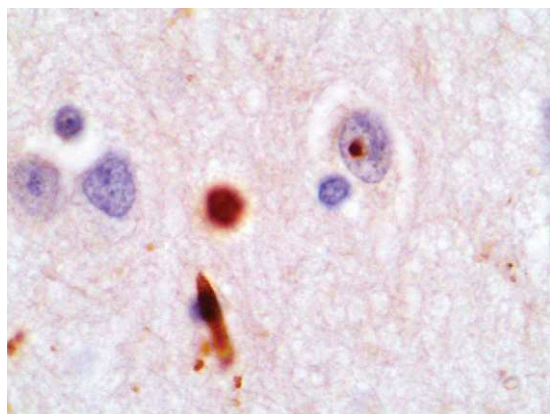
Figure 8-16. Huntington disease. Neurites can be detected in the cerebral cortex with immunostaining with anti-huntingtin or anti-ubiquitin. Nuclear inclusions are also identified by these stains.

inclusions, excitotoxicity, oxidative stress, impaired proteolysis, and stimulated apoptosis.

Choreoacanthosis

Chorea, dystonia, and tics are associated with the presence of acanthocytes in the blood. *Choreoacanthosis* is genetically heterogeneous and is usually of autosomal recessive transmission. Some cases are associated with abetalipoproteinemia; some are linked to Macleod syndrome and the Kell blood group. Hematologic examination of a fresh film reveals acanthocytes, that is, red blood cells showing "thorny" malformation. Their detection may require repeated examination or scanning electron microscopy.

Macroscopically, the lateral ventricles are expanded. The caudate nucleus and putamen are atrophied. Histology consistently shows loss of neurons associated with astrocytic gliosis in affected areas.

Sydenham Chorea

Sydenham chorea presents following a streptococcal infection, often as part of classical rheumatic fever. The neuropathology of this condition is uncertain because the findings in the few reported cases are difficult to interpret.

Degenerative Ataxic Disorders

Classification of the Spinocerebellar Ataxias

Cerebellar and spinocerebellar degenerations can be divided into two broad groups, primary and secondary, as outlined in Table 8-3. The cerebellar disorders seen as part of developmental disorders in childhood are discussed in Chapter 11.

Cerebellar Atrophies

Cerebellar atrophies, as considered here, include all the degenerative diseases that predominantly involve the cortex and the deep nuclei of the cerebellum as well as its efferent pathways (in *cerebellofugal* atrophies) and afferent pathways (in *cerebellopetal* atrophies). In early studies, morphologic classification relied on analysis of the

Table 8-3. Classification of Ataxias

Primary Cerebellar and Spinocerebellar Degenerations
Inherited
Autosomal recessive
Autosomal dominant
Sex-linked
Sporadic
Multiple system atrophy
Idiopathic cerebellar degeneration
Secondary Cerebellar and Spinocerebellar Degenerations
Neurometabolic
Prion disease
Toxic
Infective
Vascular
Paraneoplastic cerebellar degeneration

cerebellar systems involved; however, it was soon noted that there could be wide phenotypic variation in cases that were genetically identical. Morphologic neuropathologic characterization of these diseases therefore needs to be supplanted with biochemical/genetic investigation to precisely define the illnesses. Nevertheless, neuropathologic characterization has played an important part in the evolution of classification of this group of diseases.

The neuropathologic patterns of cerebellar degeneration presented here are to be considered prototypic. Overlaps are frequent and many disorders defy classification.

Three main patterns of cerebellar degeneration are recognized: *cerebellar cortical atrophy*, *cerebellopetal atrophy*, and *cerebellofugal atrophy*. These are summarized diagrammatically in Fig. 8-17 and are described in the following three subsections.

Cerebellar Cortical Atrophies. By definition, loss of Purkinje cells is the predominant change in cerebellar cortical atrophy. Lesions in the inferior olives are frequently associated and may be secondary in many instances (Fig. 8-17B). Macroscopically, the atrophy of the cerebellar cortex is often more prominent in the superior vermis and adjacent portions of the lateral lobes. In contrast, the inferior surfaces of the cerebellum are often relatively normal.
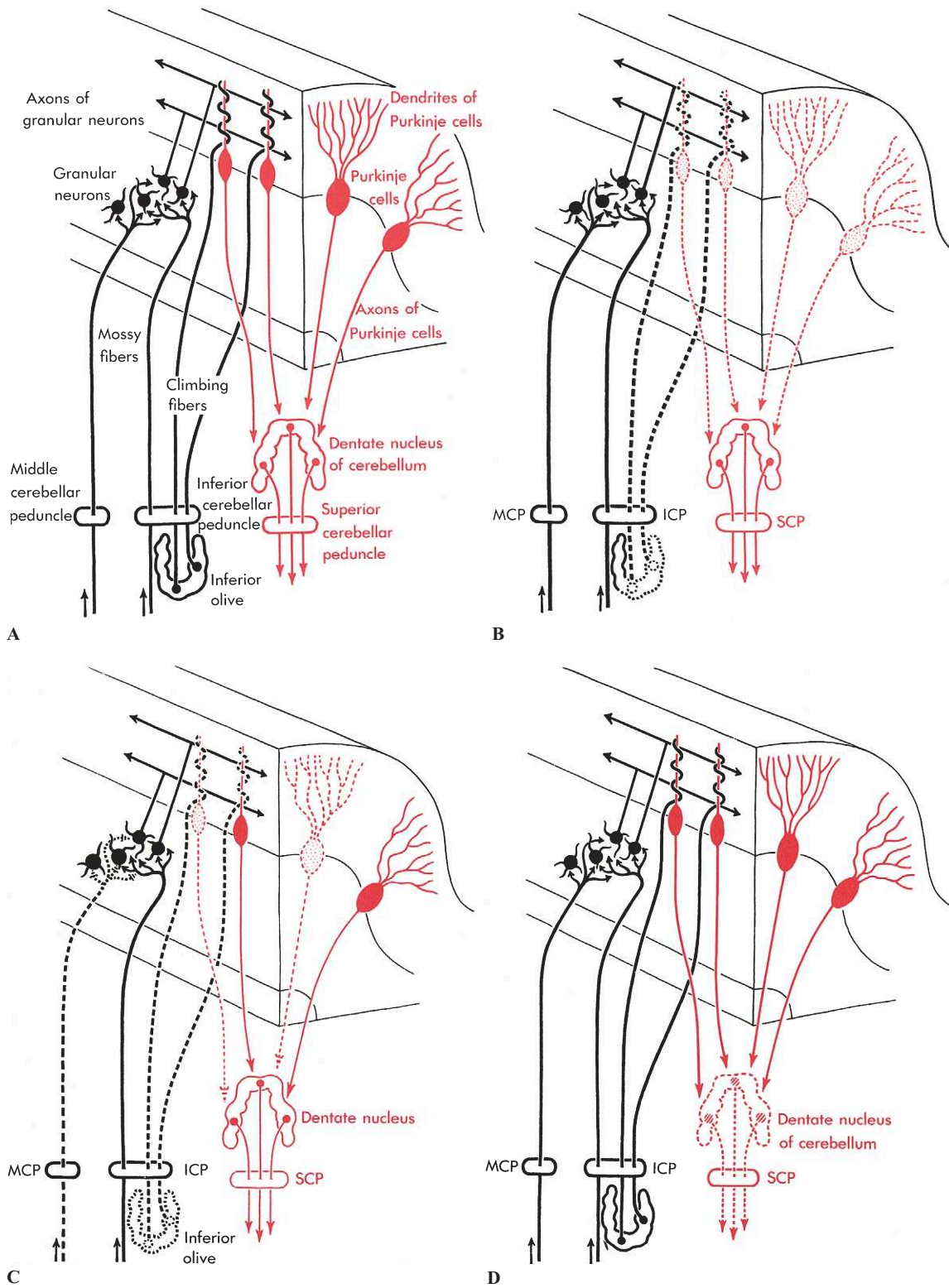
Figure 8-17. The principal neuropathologic patterns of cerebellar atrophies. **A**, Normal cerebellum. **B**, Cerebellar cortical atrophy. **C**, Cerebellopetal atrophy. **D**, Cerebellofugal atrophy. (Main afferent pathways are black; main efferent pathways are red; lost pathways are stippled.)

On microscopic examination, the loss of Purkinje cells can be complete. The neuronal cell loss may extend to the granular layer. Astrocytic gliosis in the molecular layer is variable and, at least in part, secondary to the loss of Purkinje cells and granule cells. In severely affected regions, myelin pallor in the fleece (amiculum) of the dentate nucleus indicates degeneration of Purkinje cell axons. Loss of Purkinje cells is associated with variable proliferation of Bergmann glia, visible as a layer of astrocytic cells replacing the Purkinje cell layer or located between the surviving neurons. More subtle Purkinje cell loss may be highlighted by silver staining to reveal the processes of basket cells. These processes enwrap the cell bodies of Purkinje cells; when Purkinje cells are lost, the processes remain as "empty baskets."

In the inferior olives, loss of neurons accompanied by gliosis is observed in the dorsal lamellae. The lesions are variable and are likely to be the result of retrograde trans-synaptic degeneration, secondary to slowly progressive Purkinje cell loss.

The presence of associated lesions depends on the etiology. This picture can be seen in certain hereditary forms of spinocerebellar atrophy as well as in alcoholic cerebellar degeneration (see Chap. 9).

It must be remembered that widespread loss of Purkinje cells may also be seen as a result of some other pathologic process, whether hypoxic-ischemic, toxic (e.g., phenylhydantoin intoxication), or immunopathologic (e.g., paraneoplastic cerebellar atrophy; see Chap. 9). In all of these settings, there is a characteristic cerebellofugal atrophy with massive loss of Purkinje cells, proliferation of Bergmann glia, sparing of the basket fibers, and degeneration of the cerebellar white matter.

Cerebellopetal Atrophies. *Olivopontocerebellar atrophy*, classically regarded as the prototype of cerebellopetal atrophy, is characterized by the selective involvement of fibers of pontine and olivary origin (Fig. 8-17C). The condition is characterized by pontine and cerebellar lesions with variable degeneration of the inferior olives.

Atrophy of the basis pontis is evident on macroscopic examination. There is neuronal loss from the pontine nuclei and degeneration of the pontocerebellar fibers that constitute the middle cerebellar peduncles. In myelin stains there is pallor of the pontocerebellar fibers, which is in contrast with preserved staining of the uninvolved superior cerebellar peduncles, tegmentum, and pyramidal tracts (Fig. 8-18).

The cerebellar atrophy is characterized by severe degeneration of the cerebellar white matter with astrocytic gliosis (caused, to a large extent, by loss of pontocerebellar fibers). The relative sparing of the amiculum of the dentate nucleus indicates the preservation of Purkinje cell axons. Involvement of Purkinje cells and granular neurons is variable and depends on the etiology.

Inferior olivary involvement, which is seen in only some cases, is characterized by neuronal cell loss and degeneration of the olivocerebellar fibers.

The neuropathologic picture described as olivopontocerebellar atrophy is seen in several types of inherited spinocerebellar atrophy as well as multiple system atrophy, which is sporadic (see earlier in this chapter).

Cerebellofugal Atrophies. *Dentatorubral atrophy* is characterized by atrophy of the dentate nucleus and its efferent fibers in the superior cerebellar peduncles and of the red nucleus (Fig. 8-17D). It may be associated with pallidal atrophy in the inherited condition dentate-rubro-pallido-luysial atrophy, a polyglutamine disorder.

In between these apparently distinct patterns of disease are many cases with overlapping pathologic features, making pathologic diagnostic classification difficult. Importantly, there have been great advances in understanding the molecular genetic causes of cerebellar diseases, and this has produced a genetic classification, which has superseded the previous clinical and pathologic ones (Table 8-4).

Secondary Cerebellar Atrophies. Although, strictly speaking, the following two patterns of pathology are not degenerative diseases, they are classically considered in this context.

Crossed Cerebellar Atrophy. This unilateral general atrophy of all the neocerebellar structures is secondary to massive destruction of the efferent corticopontine pathways. It is a rare consequence of extensive contralateral cerebral hemispheric lesions and seen only when the survival after the initial lesions has been long. Crossed cerebellar
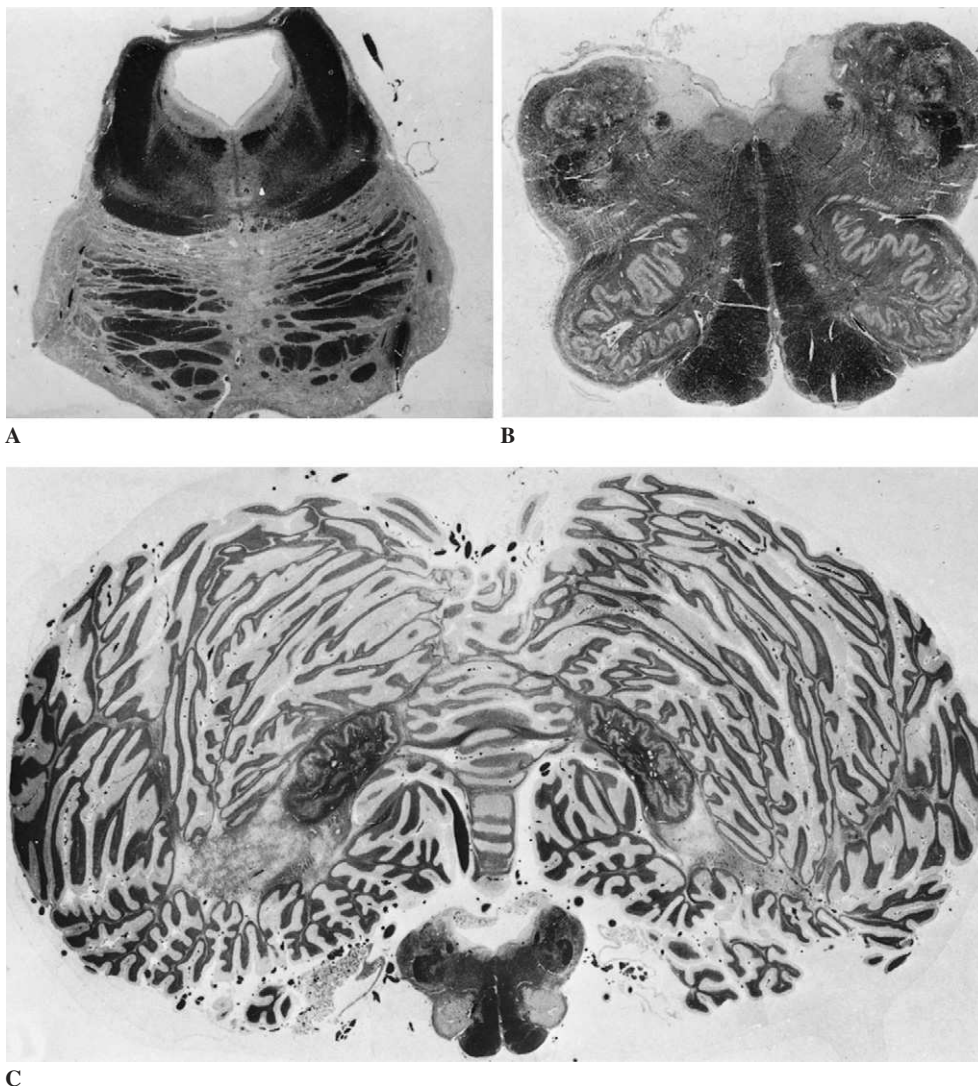
Figure 8-18. Olivopontocerebellar atrophy in a case of multiple system atrophy (Loyez stain for myelin). **A,** Upper pons. Massive myelin loss of pontocerebellar fibers with sparing of the superior cerebellar peduncles, tegmentum, and pyramidal tracts. **B,** Medulla. Loss of olivocerebellar fibers. Note wedged appearance of the median raphe due to loss of crossing fibers. **C,** Medulla and cerebellum. Myelin loss of the cerebellar white matter with relative sparing of the fleece (amiculum) of the dentate nucleus.

atrophy has been occasionally described in adults but is particularly striking when the responsible lesion has developed in utero or in the neonatal period.

OLIVORUBROCEREBELLAR ATROPHY. This associates atrophy of the dentate nucleus, superior cerebellar peduncle, and red nucleus with a loss of Purkinje cells and olivary hypertrophy. It is always the result of a longstanding lesion, usually vascular, that destroys the decussation of the superior cerebellar peduncles.

Autosomal Recessive Cerebellar Ataxias

Most of early onset cerebellar ataxias show autosomal recessive inheritance, and the most common of these is Friedreich ataxia.

Friedreich Ataxia.   *Friedreich ataxia* is a spinocerebellar degeneration mapped to chromosome 9 and caused by mutations in the gene coding for the protein frataxin. Normal frataxin is an 18-kDa

Table 8-4. Classification of Inherited Spinocere-bellar and Cerebellar Ataxias

---

Autosomal Recessive Cerebellar Ataxia
  Friedreich ataxia
  Early onset ataxia with retained reflexes (EOCA)
  SCA with vitamin E deficiency
  Ataxia-telangiectasia
  Ataxia-telangiectasia–like disorder (ATLD)
  Other rare recessive ataxias
X-linked Cerebellar Ataxia
  Several rare causes
Autosomal Dominant Cerebellar Ataxia
  Spinocerebellar ataxias (SCA 1–SCA 17)
  Dentato-rubro-pallido-luysial atrophy (DRPLA)
  Episodic ataxias (EA1 and EA2)

---

mitochondrial protein with 210 amino acids and is homologous with proteins that regulate iron metabolism in mitochondria. The commonest mutation is expansion of an intronic GAA repeat in the gene, which may reach 1,000 copies (range: from 67 to around 1,700; normal: between 6 and 34).

The spinal cord and dorsal roots are macroscopically atrophic. The peripheral sensory nerves are severely affected. The loss of large, myelinated axons and dorsal root ganglion cells and degeneration of the dorsal columns explain loss of deep sensibility and of tendon reflexes, two hallmarks of the disease. Involvement of the spinocerebellar tracts is also characteristic (Fig. 8-19). Clarke column, from which the dorsal spinocerebellar tract arises, shows neuronal loss and the dorsal spinocerebellar tract appears degenerated, atrophied, and pale in myelin stains. The ventral spinocerebellar tract is generally less severely involved. There is severe cell loss in the dentate nuclei, with consequent marked atrophy of the superior cerebellar peduncle and expansion of the rostral portion of the IVth ventricle. The cerebellar white matter is generally gliotic. The cerebellar cortex is usually normal, as are the inferior olives. The pyramidal tract often shows myelin pallor. Neuronal cell loss may be present in some of the cranial nerve nuclei (VIII, XI, XII). In some cases, optic atrophy has been noted. Cardiomyopathy with fibrosis is frequently present and may lead to cardiac failure. The incidence of diabetes mellitus is increased.

Cerebellar Ataxia with Isolated Vitamin E Deficiency. *Cerebellar ataxia with isolated vitamin E deficiency* is a neurologic condition clinically similar to that seen in Friedreich ataxia. It has been described in patients with mutations of the α-tocopherol transfer protein gene leading to low availability of vitamin E.

Neuropathology shows axonal spheroids with degeneration at the rostral ends of the posterior columns and lipofuscin accumulation in neurons, especially those of dorsal root ganglia. There may be Purkinje cell loss. Early treatment with vitamin E may prevent the occurrence of lesions.

Ataxia-Telangiectasia. *Ataxia-telangiectasia* (AT, also termed Louis-Bar disease) is the most common cause of progressive ataxia in infancy and is caused by mutations in a gene (*ataxia-telangiectasia mutated*, or *ATM*) on chromosome 11q. Histologic examination shows bizarre, large, irregular, hyperchromatic nuclei in many tissues; in the nervous system, these are most commonly found in the endothelium, dorsal root ganglia, and pituitary gland.

The cerebellar cortex shows extensive loss of the Purkinje and granule cells. Surviving Purkinje cells may contain eosinophilic cytoplasmic inclusion bodies; larger inclusions resembling Lewy bodies are occasionally seen in the substantia nigra. There is cell loss in the inferior olives. There may also be degeneration of the posterior columns and loss of satellite cells in the dorsal root ganglia.

Ataxia-telangiectasia is associated with telangiectasias of the skin and conjunctiva, immune deficiency, and increased incidence of cancers, mostly hematologic (see Chap. 10).

Autosomal Dominant Cerebellar Ataxias

The *autosomal dominant cerebellar ataxias* usually present in adult life. Neuropathology is variable even within families. Many cases show the neuropathologic pattern of olivopontocerebellar atrophy, while others show cerebellar cortical atrophy with olivary involvement.

These diseases are termed *spinocerebellar atrophy* (SCA); at the time of writing there are 16 genetically distinct types (SCA 1 through SCA 17; there is no SCA 9). Dentato-rubro-pallido-luysial atrophy (DRPLA) is also included in this group. Many of these diseases (SCA 1–3, 6, 7, 12, and 17; DRPLA) are caused by expansions of CAG repeats leading to expanded polyglutamine tracts in proteins.
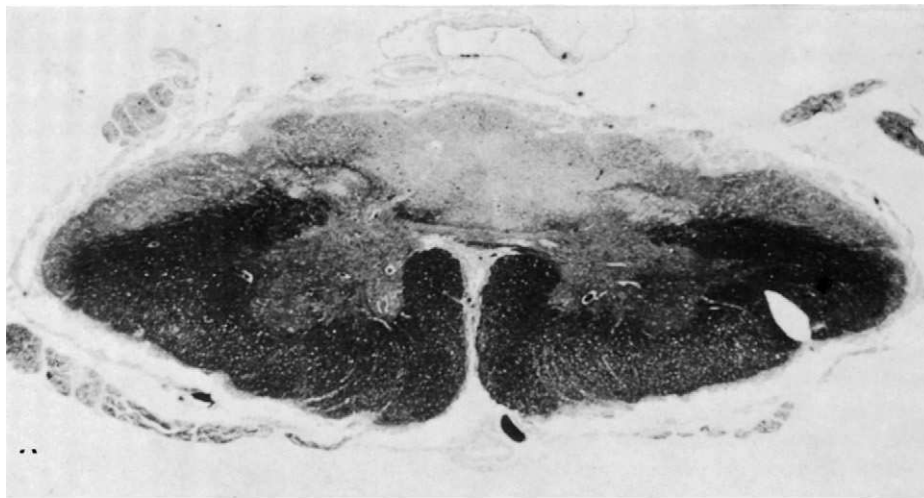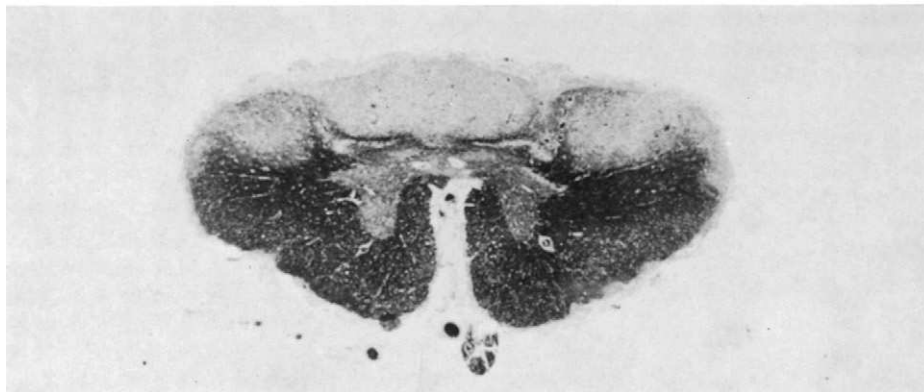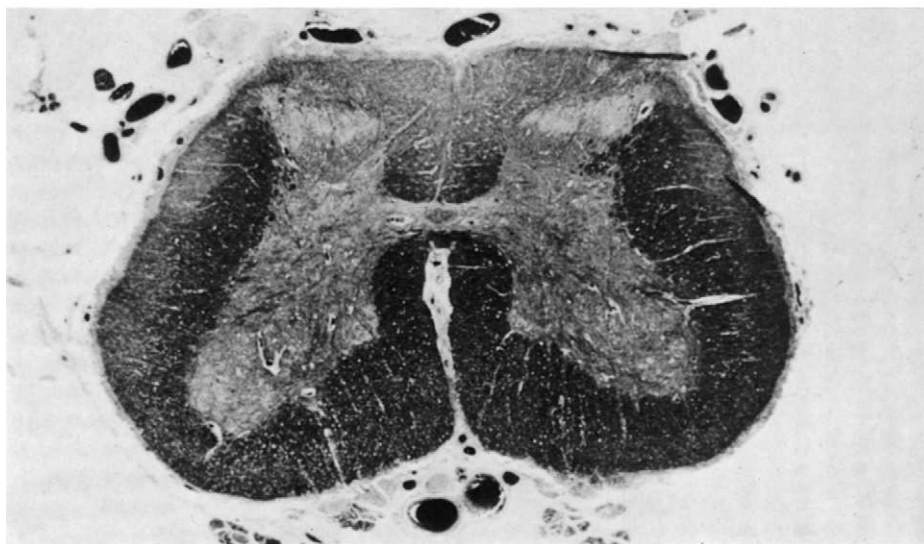
Figure 8-19. Friedreich ataxia (Loyez stain for myelin). Sections of the spinal cord at cervical (**A**), thoracic (**B**), and lumbar (**C**) levels. Involvement of the spinocerebellar tracts, mostly dorsal, and of the dorsal columns. Note discrete involvement of the pyramidal tracts in this case.

Clinically, most of these diseases show anticipation. The length of the CAG repeat expansion is generally correlated positively with clinical severity or inversely with age of onset. In several of these conditions, accumulated abnormal proteins form neuronal intranuclear inclusions, which can be detected using antibodies against polyglutamine tracts, the protein itself (when the epitope belongs to a part of the protein that accumulates), or ubiquitin. A summary of the present classification of autosomal dominant cerebellar ataxias is presented in Table 8-5.

Pathologically, the cerebellar system, extrapyramidal system, and spinal cord are affected to variable extents. Following are the main neuropathologic aspects of the most common forms of autosomal dominant ataxias.

SCA 1

CEREBELLAR SYSTEMS.   Grumose degeneration of the dentate nucleus is common, as is degeneration of the inferior olives. Mild to moderate degeneration of the Purkinje cells is also encountered.

EXTRAPYRAMIDAL SYSTEMS.   The external segment of the globus pallidus and the red nucleus are mildly affected.

SPINAL CORD.   Loss of motor neurons from the spinal cord may be pronounced in advanced cases.

SCA 2

CEREBELLAR SYSTEMS.   The three layers of the cerebellar cortex are degenerated. There is also severe degeneration of olivopontocerebellar systems. The dentate nucleus is spared.

EXTRAPYRAMIDAL SYSTEMS.   Neuronal loss is severe in the substantia nigra and less marked in the striatum.

SPINAL CORD.   Some degree of neuronal loss is seen in the anterior horn. The posterior columns are pale.

SCA 3 (Machado-Joseph Disease)

CEREBELLAR SYSTEMS.   There is neuronal loss and astrocytic gliosis in the dentate nucleus and the superior cerebellar peduncle. The olivary nucleus is spared, as is the cerebellar cortex.

EXTRAPYRAMIDAL SYSTEMS.   The globus pallidus (pars interna) is constantly affected. Less marked is neuronal loss and astrocytosis in subthalamic nucleus and substantia nigra.

SPINAL CORD.   Anterior horn cells, dorsal columns, and spinothalamic tract are variably affected.

Dentato-rubro-pallido-luysial Atrophy.   DRPLA is a dominantly inherited ataxia caused by a CAG repeat expansion in the gene coding for the protein atrophin-1. The typical disease expansion includes 49 to 75 repeats (normal, between 7 and 23).

Table 8-5. Autosomal Dominant Forms of Cerebellar Ataxia

Disorder	Chromosome	Product	Typical Disease Repeats	Typical Normal Repeats
SCA 1	6p23	Ataxin-1	42–81 (CAG)	16–36
SCA 2	12q24	Ataxin-2	35–64 (CAG)	15–24
SCA 3/MJD	14q	Ataxin-3	68–79 (CAG)	13–36
SCA 4	16q22.1	Unknown	—	—
SCA 5	11p12–q12	Unknown	—	—
SCA 6	19p	CACNA1A	21–30 (CAG)	6–17
SCA 7	3p21	Ataxin-7	38–130 (CAG)	7–17
SCA 8	13q21	Transcribed but untranslated	16–37 (CTG)	107–127
SCA 10	22q13	Transcribed but untranslated	800–4,500 (ATTCT)	10–22
SCA 11	15q14–21.3	Unknown	—	—
SCA 12	5q31	PPP2R2B	66–93	<29
SCA 13	19q13.3	Unknown	—	—
SCA 14	19q13.4	Unknown	—	—
SCA 15	Unlinked	Unknown	—	—
SCA 16	8q23–24	Unknown	—	—
SCA 17	6q27	TBP	63 (CAG)	25–42

In affected patients, the abnormal protein forms intranuclear ubiquitinated inclusions as well as diffuse nuclear accumulation.

The pathology of DRPLA is centered on the cerebellar and pallidal efferent pathways. Most cases show severe neuronal loss and associated astrocytic gliosis in the dentate nucleus and the external segment of the globus pallidus and their respective projections to the red nucleus and the subthalamic nucleus. The superior cerebellar peduncles, containing the efferent tracts from the dentate nuclei, are generally atrophic. There is generally mild to moderate cell loss from the red nucleus and severe cell loss from the subthalamic nucleus. Milder atrophic changes occur in the caudate nucleus, putamen, thalamus, substantia nigra, and inferior olives.

Mitochondrial Encephalopathies

Cerebellar ataxia may be a prominent feature of encephalopathy due to maternally inherited mutations of the mitochondrial DNA. There is usually severe neuronal loss and astrocytosis in the dentate nucleus and inferior olives with milder atrophy in the cerebellar cortex, red nucleus, and dorsal columns (see Chap. 10).

Sporadic Degenerative Ataxia

About 60% of cases of degenerative ataxia with onset after the age of 20 years appear sporadic. Some are due to multiple system atrophy (see earlier in this chapter). The remainder generally have idiopathic late-onset cerebellar ataxia, which is characterized by cerebellar cortical atrophy that is most marked in the cerebellar vermis and olives and by some degenerative changes in the spinal tracts.

Pathology of Degenerative Cortical Diseases and Dementias

Neurodegenerative disorders affecting the cerebral cortex are the most frequent cause of organic dementia. The main causes of dementia and an indication of their frequency is presented in Table 8-6.

Alzheimer Disease

Alzheimer disease (AD) is the most common of the degenerative diseases and increases in incidence

Table 8-6. Main Causes of Dementia and Their Frequencies

Disorder	Frequency
Alzheimer disease	Very common
Sporadic	Very common
Familial	Uncommon
Vascular and mixed dementia	Very common
Dementia with Lewy bodies	Common
Frontotemporal lobar degenerations	Not rare
Dementia with ubiquitin pathology	Not rare
Dementia with motor neuron disease	Not rare
Dementia with neurofilament inclusions	Uncommon
Frontotemporal degeneration	Uncommon
Dementia related to mutations in tau gene	Uncommon
Argyrophilic grains	Common; lesions uncommonly diagnosed clinically
Tangle-only dementia	Uncommon

with age. Clinically, patients tend to present with memory failure and later develop apraxia, aphasia, and agnosia. Great insights have been gained into the disease mechanism thanks to the application of molecular studies.

Gross Appearance

Cerebral atrophy is often striking, with shrinkage of gyri and widening of sulci. It involves predominantly the hippocampus (Fig. 8-20) and medial temporal structures, with parietal and frontal lobes being next most severely affected. The occipital lobe is generally spared. In some cases, especially late-onset types, the cerebral atrophy is inconstant

Figure 8-20. Alzheimer disease. On the right is the hippocampus of a patient with Alzheimer disease; on the left, the hippocampus of an age-matched patient with no cognitive abnormality. Note atrophy of cortex, shrinkage of white matter, and widening of the temporal horn of the left ventricle.
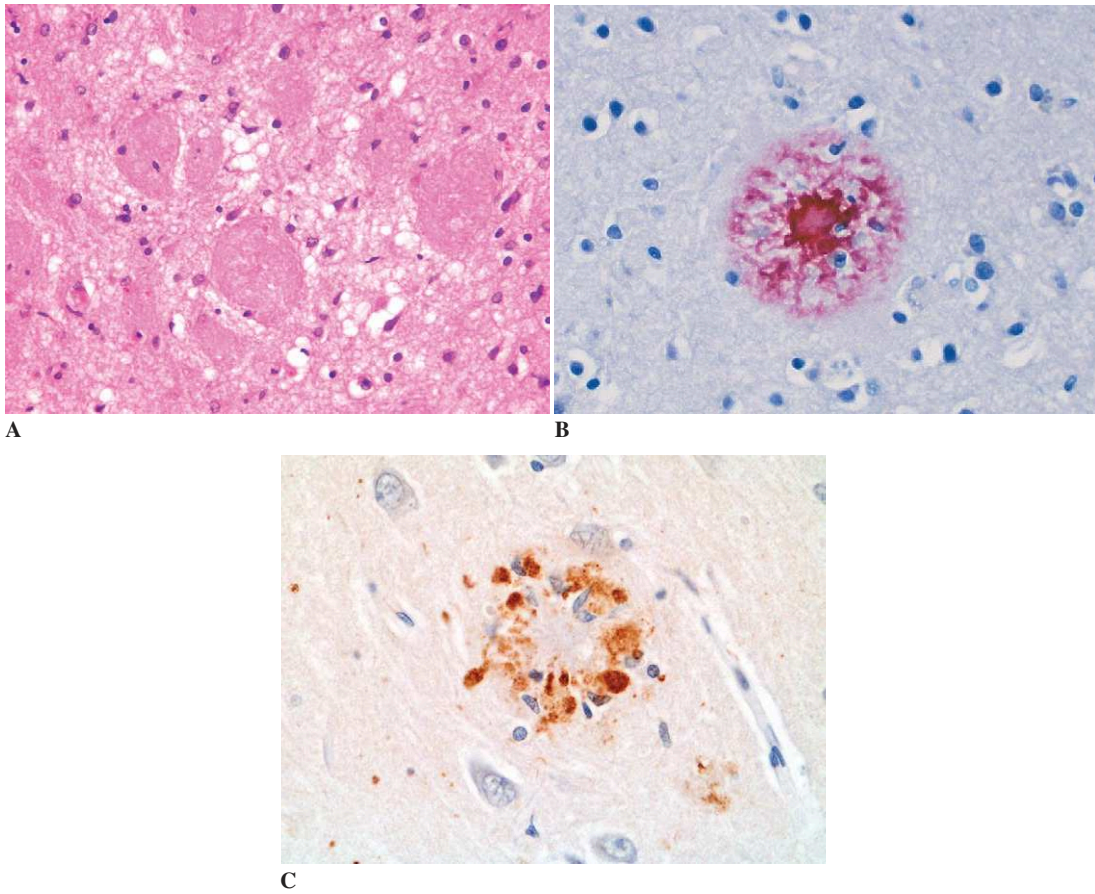
Figure 8-21. Alzheimer disease plaques. **A**, In H and E staining, focal plaques can be sometimes seen as compact, rounded alterations in the texture of the neuropil. **B**, Immunostaining for the Aβ peptide positively stains the core of the plaque. **C**, Tau immunostaining reveals neurites containing tau protein surrounding the central amyloid core material.

and often mild, and is marked by a symmetric slight reduction in the volume of the temporal gyri. On cut surface, the ventricular dilatation, generally of moderate degree, parallels the severity of the cortical atrophy.

Microscopic Lesions

AD is characterized by the development of several pathologic features, none of which is pathognomonic. The main histologic findings are senile plaques, neurofibrillary tangles, neuronal loss, and reactive glial changes. It is the combination of pathologic changes in an appropriate density and distribution that allows a neuropathologic diagnosis to be made. Several neuropathologic criteria for the diagnosis of AD have been developed.

Plaques. *Plaques* are deposits in the neuropil defined by the presence of a peptide (Aβ) derived from a fragment of a normal neuronal protein termed APP (amyloid precursor protein), which is coded by a gene on chromosome 21.

In senile or neuritic plaques (Figs. 8-21A, B, and C), the Aβ is present as round, dense accumulation forming amyloid (e.g., showing an apple green birefringence after Congo red stain). The plaques are surrounded by a corona of degenerating nerve cell processes, mostly axons immunoreactive for tau protein (see Fig. 8-21C). The neuritic plaque also elicits an astrocytic and microglial reaction.

Diffuse deposits of Aβ are also present in AD and are wispy, ill-defined structures. They are not seen on H and E or Congo red stains but can

be found by silver staining or immunostaining for Aβ.

Neuritic plaques are typically found in entorhinal cortex, hippocampus, and neocortex. The caudate and cerebellum have only diffuse plaques.

Tangles.   *Neurofibrillary tangles* are intracellular inclusion bodies primarily containing tau as well as other proteins (Fig. 8-22). Tangles may be detected by immunostaining for tau protein or by silver impregnation techniques (see Fig. 1-10). Nerve cell processes in the cortical neuropil may become swollen and also accumulate tau protein, in which case they are called *neuropil threads*. Nerve cell processes running through neuritic plaques also accumulate tau protein, in which case they are termed *dystrophic neurites*. When nerve cells die, tangles may be left behind in the neuropil as so-called "ghost tangles." A high density in wide distribution is predictive of the presence of a clinical cognitive abnormality in late life. Neurofibrillary tangles are also found, with equal frequency, in layers III and V of the neocortex and in some of the deep ganglia: the amygdaloid nucleus, limbic nuclei of the thalamus (anterior complex, laterodorsal nucleus, and some intralaminar nuclei), basal nucleus of Meynert, reticular formation of the mesencephalon, and locus ceruleus. In the same areas, neuronal cell loss, varying according to the severity of the disease, may also be seen.
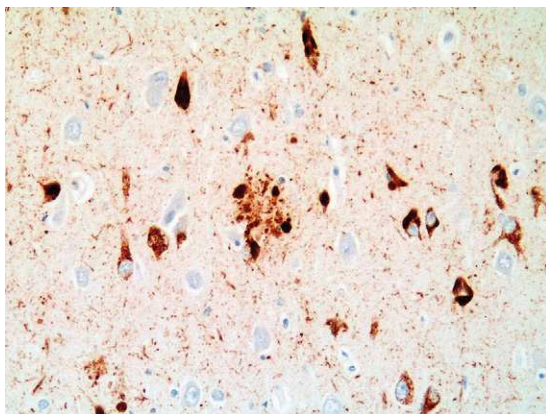
Figure 8-22. Alzheimer disease tangles. Tau immunostaining shows neurofibrillary tangles within neuronal cell bodies. In addition, neurites around plaques are detected. Fine threads in the cortex are termed *neuropil threads*.
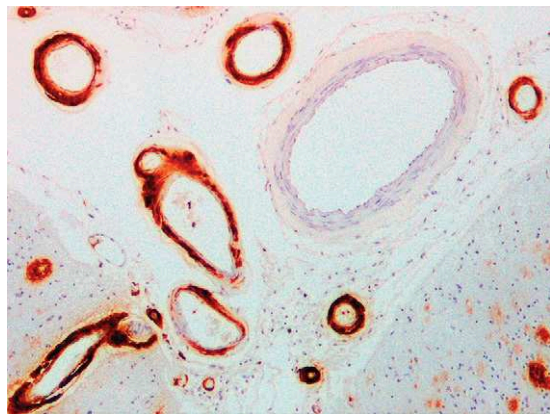
Figure 8-23. Alzheimer disease amyloid angiopathy. Immunostaining for Aβ peptide shows vessels affected by amyloid deposition.

Amyloid Angiopathy.   Accumulation of Aβ peptide in the vessel walls causes *amyloid angiopathy* (Fig. 8-23). It is especially seen in occipital cortex and, though less often, in Ammon's horn. The amyloid deposit culminates in irregular thickening of the terminal vascular bed and often extends into the adjacent parenchymatous tissue (dysphoric angiopathy). In the superficial cortical layers and in the meninges, it may also affect the small arteries and veins (congophilic angiopathy). This lesion, which may also be seen in nondemented, aged individuals (cerebral amyloid angiopathy; see Chap. 4), is, however, much more frequent in AD, where it has been considered nearly constant.

Diagnostic Criteria and Staging of AD

All the lesions of AD may be seen, though in smaller number and with more restricted distribution (usually to Ammon's horn), in normal aging. They are then especially found in Ammon's horns. Diagnostic criteria for AD have been proposed; there has been wide acceptance of NIA-Reagan and CERAD (Consortium to Establish a Registry for Alzheimer Disease) criteria. Plaque and tangle pathology develop in a predictable fashion, starting in the mesial temporal lobe (low stage) and later extending to the temporal lobe to involve wider cortical areas (high stage). This is the basis of the Braak staging scheme for AD, a high stage correlating well with

the presence of cognitive changes in late life, while low stage is generally asymptomatic.

AD pathology is often seen in association with vascular pathology; it is then considered as a mixed dementia.

Molecular Pathology

Many of the molecular steps involved in the generation of Aβ fragments from APP have been characterized. Several factors are recognized to promote or cause amyloid deposition. Rare, late-onset, familial cases of AD are caused by mutations in the APP gene on chromosome 21. It is believed that the association between trisomy 21 and AD relates to the extra copy of the APP gene 21. Mutations in genes coding for the presenilin proteins (PS1, PS2) are also known to cause early onset familial AD. These proteins are involved in the pathways of cleavage of APP to generate Aβ, with mutations giving rise to excess production of Aβ. Genotype at the apolipoprotein E locus influences risk of AD: individuals with one or two copies of the apoE4 allele have an increased risk of developing AD compared to those carrying apoE2 or apoE3 alleles.

Dementia with Lewy Bodies

Dementia with Lewy bodies (DLB) is a form of dementia that has found increasing clinical and neuropathologic recognition in recent years.

Neuropathologic changes are related to those encountered in Parkinson disease and with overlap with neuropathologic changes seen in AD. Clinically, patients develop a dementia with early hallucinations and a prominent fluctuation in cognition. There are variable clinical motor features of Parkinson disease and a high sensitivity to neuroleptics.

Macroscopic Features

Cerebral atrophy is generally not as severe as that seen in a case of AD of equivalent severity. There is usually pallor of the substantia nigra, as would be seen in typical Parkinson disease. Atrophy of the limbic system may be prominent.

Microscopic Features

Brainstem Lewy bodies, together with pale bodies, are seen in the substantia nigra and locus ceruleus. There may be cell loss equivalent to that seen in Parkinson disease.

Lewy bodies seen in neurons of the cerebral cortex ("cortical Lewy bodies") appear as ill-defined inclusions displacing the nucleus. They are found in the deeper cortical layers of temporal, insular, and cingulate cortices. They are best detected by immunohistochemistry for alpha synuclein or ubiquitin (Figs. 8-24A and B).

Lewy neurites are nerve cell processes that contain alpha synuclein and ubiquitin. They are seen in areas of Lewy body degeneration but also
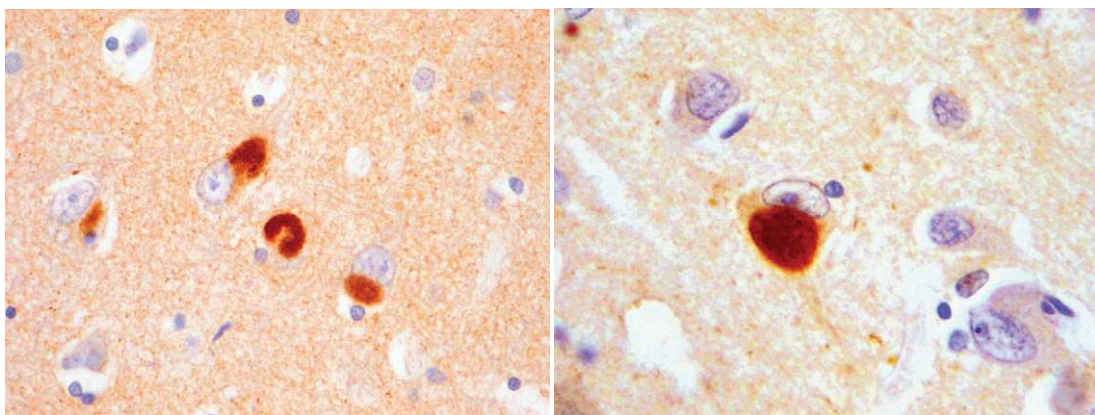
Figure 8-24. Dementia with Lewy bodies. **A,** Cortical Lewy bodies are immunoreactive for alpha synuclein. **B,** Cortical Lewy bodies may also be detected by anti-ubiquitin.
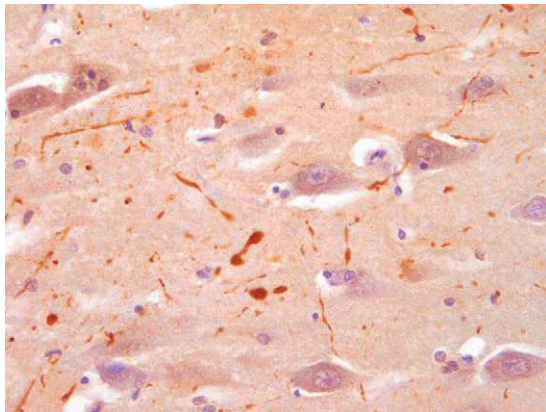
Figure 8-25. Dementia with Lewy bodies. Lewy neurites (visible here) may be detected by ubiquitin immunostaining in both demented and nondemented patients with Lewy body diseases.

may be the only alteration, particularly in the CA2 and CA3 sectors of the hippocampus (Fig. 8-25).

Alzheimer changes are seen in the majority of cases of dementia with Lewy bodies. However, in most instances the severity of changes is not as extensive as in AD. Plaques tend to be diffuse rather than neuritic.

Spongiform changes may be seen in a restricted distribution in the superficial layers of the mesial temporal cortex. These changes may be indistinguishable from those seen in Creutzfeldt-Jakob disease using conventional stains, but prion protein immunostaining is negative.

Diagnostic Classification

Lewy body diseases (e.g., dementia with Lewy bodies and Parkinson disease) can be neuropathologically separated into three groups: *brainstem* (when Lewy bodies are restricted to brainstem structures), *transitional* (when there is involvement of limbic structures), and *neocortical* (when there is additional involvement of the neocortex).

Frontotemporal Lobar Degenerations

Several diseases are characterized by neurodegeneration concentrated in the frontal and temporal lobes with relative sparing of the parietal and occipital lobes. The clinical features of these diseases relate to behavioral disturbances due to loss of frontal-lobe function with later memory defects. These conditions have been termed the *frontotemporal lobar degenerations* (FTD). The term *Pick disease* was once applied to many of these disorders but is now used to refer to a specific pattern of neuropathology (described in the following subsection).

Several of these frontotemporal lobar degenerations are now recognized as characterized by abnormal accumulation of tau protein in the brain, and some are associated with mutations in the tau gene. For cases linked to tau mutations, the term is now *frontotemporal degeneration with parkinsonism linked to chromosome 17* (FTDP-17). There is a relationship between certain types of non-tau FTD and the neuropathology of motor neuron disease with emerging genetic linkages.

Pick Disease

Pick disease presents mostly in the fifth and sixth decades of life; although most cases are sporadic, familial forms have been described. Cognitive abnormalities are due to the predominant early involvement of the frontal lobes with later additional involvement of temporal lobes.

Macroscopic Appearance.   Grossly, the cerebral atrophy, which is often considerable, is circumscribed and most evident in the frontal lobes; it often spares the posterior two thirds of the superior temporal gyrus, thus accounting for the rarity of aphasic phenomena of the sensory type. Severe involvement of Ammon's horn, which may be responsible for memory loss, may be present. The parietal cortex is seldom involved, and the occipital cortex is always spared. Anterior frontotemporal ventricular dilatation, which is considerable, corresponds to the zones of cortical atrophy.

Macroscopic Appearance

Cortical Lesions.   A massive degree of neuronal cell loss is associated with dense astrocytic gliosis and may be accompanied by cortical microvacuolation. It is currently accepted that the diagnostic feature of the disease is the presence of Pick bodies, which are cytoplasmic inclusions that appear as rounded homogeneous bodies just visible on H and E staining (Fig. 8-26). Immunohistochemical studies show that these inclusions contain
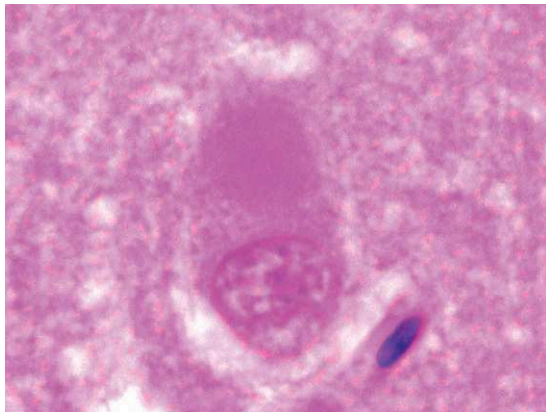
Figure 8-26. Pick disease. Pick bodies can just be seen on H and E staining as rounded, slightly basophilic inclusions in the neuronal cytoplasm.

tau protein (Figs. 8-27A and B) that is biochemically distinct from that seen in AD, CBD, and PSP. Pick bodies are strongly argyrophilic and well-detected using appropriate silver stains (see Figs. 1-12A and B). Ballooned neurons ("Pick cells") are also frequent (Fig. 8-28).

WHITE MATTER LESIONS. Myelin pallor with gliosis involves the centrum ovale and the temporal lobe, especially the frontopontine and temporopontine bundles.

BASAL GANGLIA LESIONS. Neuronal cell loss with gliosis is frequently seen in the head of the caudate nucleus, which may be extremely atrophied. Similar changes may be found in the rostral portion of the putamen, some of the thalamic nuclei (anterior, dorsomedian, and centromedian), the substantia nigra, and, less often, the pallidum.

Frontotemporal Lobar Degeneration with Motor Neuron Disease

Some patients with MND develop dementia and have a distinct set of pathologic findings. Similar changes can be found in some FTD patients without MND.

Macroscopic Appearance. At gross examination, the frontotemporal atrophy is generally severe, with associated ventricular dilatation. There may be atrophy of the caudate nucleus (Fig. 8-29).

Microscopic Appearance

CORTICAL LESIONS. On H and E staining, microvacuoles are often seen in layer 2 of the frontal cortex (Fig. 8-30). In some cases there is severe neuronal loss, involving all the cortical layers with microvacuolation and astrocytic gliosis. Immunochemical staining shows ubiquitinated intraneuronal inclusions in remaining layer II neurons as well as in hippocampal dentate granule cells (Figs. 8-31A and B). The presence of these inclusions has given rise to the term *MND inclusion dementia*. In some cases, ubiquitin-immunoreactive neurites are seen in the areas of neuronal loss and microvacuolation.

A   **B**
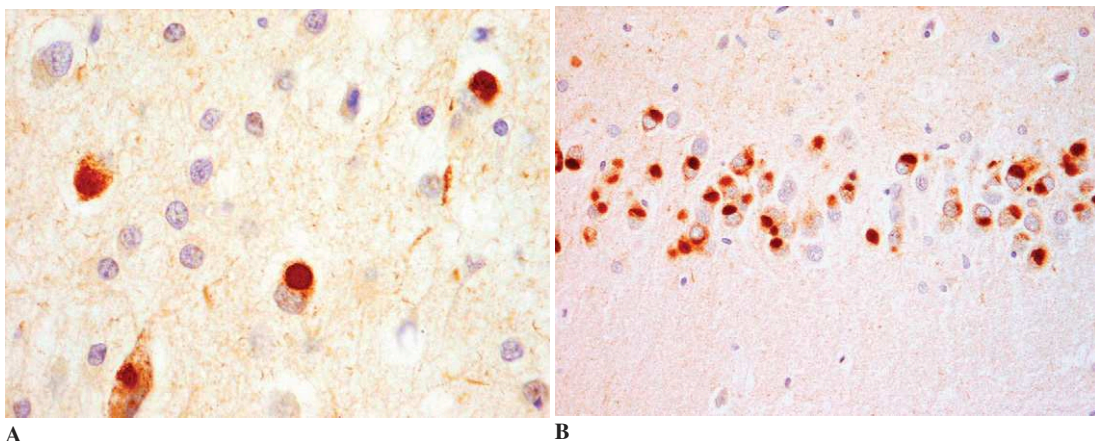
Figure 8-27. Pick disease (tau immunostaining). **A**, Pick bodies are seen on tau immunostaining in neurons in the cerebral cortex. **B**, The hippocampal dentate gyrus is characteristically heavily involved.
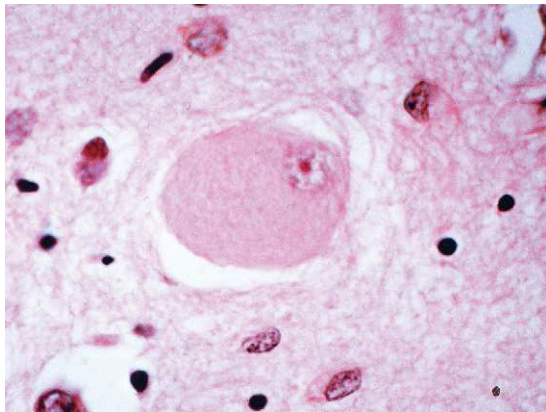
Figure 8-28. Pick disease. Swollen cortical neurons are a characteristic, but nonspecific, feature of this disease (H and E).

SUBCORTICAL LESIONS.   There may be neuronal loss and astrocytic gliosis in basal ganglia and substantia nigra. Skein inclusions may be seen in motor neuron groups, as described in classical MND.

Dementia Lacking Distinctive Histopathology

The diagnosis of *dementia lacking distinctive histopathology* is presently applied to cases lacking a marker, more specifically where tau and ubiquitin staining do not reveal any neuronal inclusions.

Macroscopic Appearance.   Grossly, the frontotemporal atrophy is moderate to severe with ventricular dilatation. There may be atrophy of the caudate nucleus.

Figure 8-29. Frontotemporal lobar degeneration. Severe cerebral atrophy with marked temporal lobe involvement is evident in this slice.
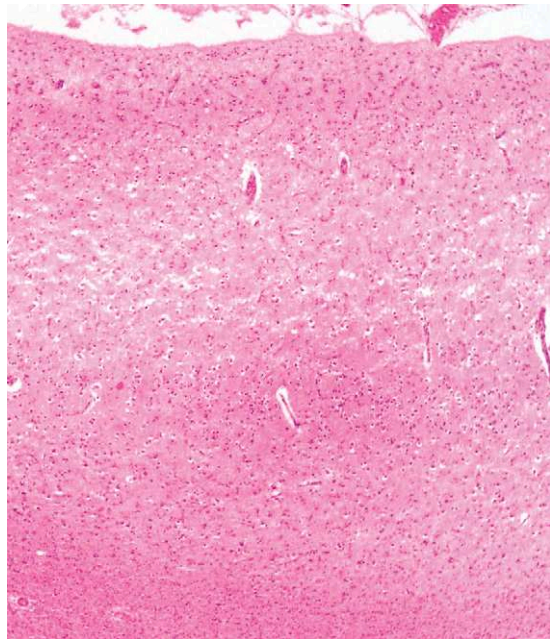
Figure 8-30. Frontotemporal lobar degeneration. Neuronal loss and microvacuolation in the outer cortical layers is often seen. In more advanced disease, there is severe neuronal loss and transcortical vacuolation (H and E).

Microscopic Appearance.   On H and E staining there is often cortical microvacuolation of layer 2 of the frontal cortex. In some cases there is severe neuronal loss involving all layers, with microvacuolation and astrocytic gliosis. Ubiquitin immunostaining may show neurites in areas of cortical neuronal loss, but no inclusions of MND are seen. Tau immunostaining is negative.

Frontotemporal Degeneration with Parkinsonism Linked to Chromosome 17

FTDP-17 is marked by accumulation of abnormal tau protein in the brain and is linked to mutations in the tau gene. The clinical picture is variable even within a given family. The pathology of this condition may overlap with that seen in PSP and CBD (see earlier in this chapter).

Macroscopic Appearance.   The frontotemporal atrophy and the ventricular dilatation are of variable severity. The caudate nucleus may be atrophic. The substantia nigra is sometimes pale.
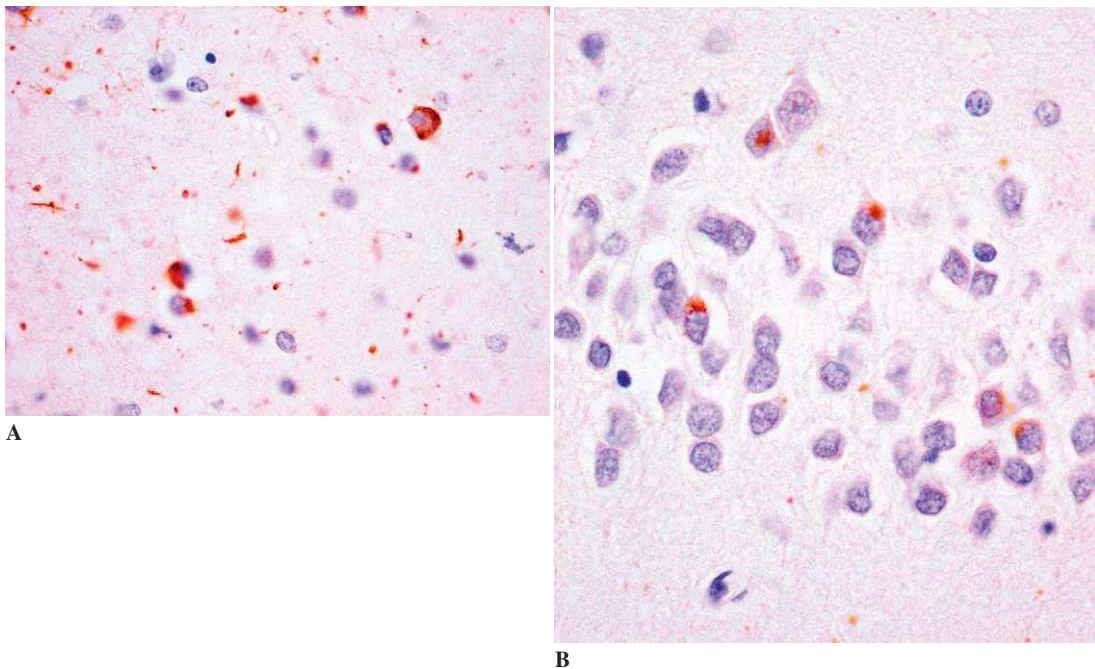
Figure 8-31. Frontotemporal lobar degeneration. **A**, Ubiquitin-immunoreactive inclusions in layer II neurons as well as accumulation in small neuritis. **B**, Ubiquitin-immunoreactive inclusions in hippocampal dentate granule cells.

Microscopic Appearance.   On H and E staining, cortical microvacuolation of layer 2, neuronal loss, and astrocytic gliosis are seen in the frontal cortex. Swollen, ballooned neurons are sometimes present. Tau immunostaining shows accumulation, characteristics of which are variable according to the mutation; some changes may resemble the astrocytic tuft of PSP, the astrocytic plaque of CBD, or the neurofibrillary tangle of AD. In most cases, the glial accumulation, particularly in the white matter, is marked. The neuronal accumulation of tau protein without tangle formation ("pretangle") is also common.

Depending on the mutation, tau accumulation may also be seen in the brainstem, particularly the substantia nigra. Tau accumulation in the reticular nuclei, the inferior olivary nucleus, and the dentate nucleus may also be seen.

Dementia with Neurofilament Inclusions

Dementia with neurofilament inclusions is a rare sporadic disease that resembles Pick disease in many aspects. The patients, sometimes starting as early as their thirties, develop a frontal syndrome and signs of involvement of the brainstem (visuomotor symptoms, swallowing difficulties). Spherical inclusions, approximately the size of the nucleus, are found in the cell body of neurons in the cerebral cortex, basal nuclei and brainstem. They are strongly labeled by the antineurofilament antibody but do not contain tau or ubiquitin.

Argyrophilic Grain Dementia

The clinical symptoms of *argyrophilic grain dementia* are largely unknown. Behavioral disorders have been described. A clinical diagnosis of AD has usually been made in those patients who are demented.

Macroscopic Appearance

There are no distinctive changes regarded as diagnostic for this condition. The brain may be atrophic and there may be selective atrophy of the hippocampus.

Microscopic Appearance

Argyrophilic grains are ovoid, spindle-shaped structures that are revealed by Gallyas silver stain;

they are mainly found in the hippocampus and amygdala. Tau immunohistochemistry strongly labels the grains and also shows accumulation of tau protein in the cell body of neurons (pretangle). Grains and pretangles are associated with "coiled bodies," that is, the accumulation of tau protein in the cytoplasm of oligodendrocytes.

Alzheimer lesions are frequently present. Argyrophilic grains have been shown to be frequently associated with PSP.

Tangle-Only Dementia

In *tangle-only dementia*, neuropathologic examination reveals the presence of neurofibrillary tangles in the hippocampus and temporal lobe, with absence of other pathologic changes. Such pathology overlaps with some of the features noted in PSP.

Hippocampal Sclerosis

Neuronal loss and gliosis limited to the CA1 sector of the hippocampus are sometimes found in aged patients. Clinically, the predominant symptom of memory loss may have led to the diagnosis of AD. Ischemic-anoxic episodes have occurred in a large proportion of cases. The lesions are frequently associated with Alzheimer changes.

Vascular Dementia

It is being increasingly recognized that vascular pathology may be a substrate for dementia (i.e., vascular dementia). Various mechanisms have been identified, including the presence of large infarcts leading to massive tissue destruction (multi-infarct dementia); one or more small infarcts localized in strategic areas (e.g., the thalamus); pathology of the white matter (as seen in Binswanger leukoencephalopathy, which is most often associated with hypertension); or in hereditary diseases of the brain vessels such as CADASIL, due to a mutation of the *Notch* gene (see Chap. 4); or multiple hemorrhages, such as those due to amyloid angiopathy (see earlier in this chapter and Chapter 4).

In many instances, pathologic changes of AD are associated. A neuropathologic diagnosis of mixed dementia is then appropriate.

Other Causes of Dementia

Many other disorders may be accompanied by clinical features of dementia. Some of these may be degenerative disorders in which lesions in the cortex and in the basal ganglia coexist (e.g., HD). In others, the lesions essentially involve the basal ganglia and the brainstem, as in progressive supranuclear palsy; these conditions may be categorized as examples of subcortical dementia. Dementia associated with various neurologic disorders may also be seen in nonconventional infections (e.g., Creutzfeldt-Jakob disease); inflammatory infectious processes (e.g., general paralysis of the insane, Whipple encephalopathy, and the subacute encephalitis of AIDS); primary demyelinating disease (e.g., multiple sclerosis with extensive hemispheric plaques or leukodystrophy of late onset); metabolic disorders (e.g., the lipidoses); and chronic hydrocephalus (in which the mechanism may be diverse).

Abnormalities of Central Autonomic Systems

There are many causes of autonomic failure, which may be divided into primary and secondary types. Some are caused by lesions of the central nervous system and others by peripheral neuropathology. Patients who have autonomic failure with parkinsonism almost always have either MSA with glial cytoplasmic inclusions or Lewy body pathology. In MSA cases, it is not uncommon for other clinical features of MSA (such as cerebellar ataxia) to develop over time. In both types of cases, autonomic dysfunction is related to loss of cells from the intermediolateral column of the spinal cord. Patients who have primary progressive autonomic failure without any other clinical neurology generally have sympathetic neuronal Lewy body pathology, MSA pathology in the absence of clinical involvement of other systems, or a peripheral cause for autonomic failure.

Chapter 9
Acquired Metabolic Disorders

Sydney S. Schochet, Jr. and Françoise Gray

A number of major general pathologic processes, including metabolic disturbances (e.g., hypoxia and some vitamin deficiencies), exogenous intoxications, and various visceral lesions, can produce changes in the central and/or peripheral nervous system. These changes, which are usually nonspecific, may show regional variation in the central nervous system (CNS). The pathophysiologic bases of this phenomenon, which is often referred to as "selective vulnerability," are unclear. It has been suggested that selective vulnerability can be explained by vascular patterns and resulting alterations in regional perfusion. Regional variations in the biochemical characteristics of the brain or (most likely) in the distribution of receptors for various excitatory amino acids may also explain this phenomenon.

Cerebral Hypoxia

The brain normally receives about 15% of the cardiac output, consumes about 20% of blood oxygen, and consumes about 10% to 20% of blood glucose. Various types of deficient oxygen supply and utilization or deficient substrate may produce cerebral hypoxic changes:

- *Anoxic or hypoxic hypoxia* results from decreased pulmonary access to oxygen. This may be due to insufficient oxygen in the inspired air; it also may result from upper-airway obstruction or pulmonary disorders that impede the uptake of oxygen.
- *Anemic hypoxia* results from decreased oxygen transport caused by either reduced hemoglobin levels or by reduced capacity of the hemoglobin to transport oxygen (e.g., in carbon monoxide poisoning).
- *Stagnant hypoxia* follows reduction or cessation of blood flow. This can be the result of impaired cardiac output (producing global ischemia) or of cerebral infarcts (with focal effects). The cerebral lesions that result from stagnant hypoxia are due to a combination of an inadequate supply of oxygen and glucose and an accumulation of lactic acid.
- *Histotoxic hypoxia* results from intoxicants, such as cyanide and hydrogen sulfide, which render the neural parenchyma incapable of utilizing oxygen and substrates.
- *Oxyachrestic hypoxia* results from severe hypoglycemia. Oxygen is not utilized because of the severe metabolic substrate deficiency.

Basic Cellular Lesions

The basic cellular lesions (see Chap. 1) consequent to cerebral hypoxia are mostly neuronal (i.e., ischemic nerve cell change), but they may also be astrocytic (glial necrosis, astrocytic gliosis) and microglial (rod-shaped microglia, macrophagic proliferation).

Figure 9-1. Laminar cortical necrosis. This is often most severe in the posterior frontal and parietal lobes.

Selective Tissue Lesions

The cellular changes resulting from hypoxia are maximal in those areas of the brain regarded as showing selective vulnerability.

In the cerebral cortex, the neuronal changes are more pronounced in the third, fifth, and sixth layers of the neocortex. In addition, the changes are more severe in the depths of the sulci than along the banks or the apices of the gyri. Widespread, severe destruction of the deeper layers of the cortex leads to laminar necrosis (Fig. 9-1). This may be especially evident in the parietal and occipital lobes, where impaired perfusion may exacerbate the effects of hypoxia. In the most severe cases, the cortical necrosis is nonselective.

The hippocampus (Ammon's horn) often shows selective involvement by hypoxia. This is most evident in the CA1 sector (an area that corresponds to the grossly defined Sommer sector; Figs. 9-2A and B). The CA3 area (also referred to as the *endplate*) is often less severely affected. The CA2 area tends to be relatively resistant to hypoxic changes. The regional variation in the susceptibility of the hippocampus is now thought to be best explained by the distribution of excitotoxic receptors.

Among the basal ganglia, the pallidum (especially the inner half; Fig. 9-3); the striatum, especially the outer half of the putamen; and the thalamus are selectively vulnerable to hypoxia. The mamillary bodies may be severely vulnerable in infancy.

In the cerebellum, cortical involvement is frequent and affects chiefly the Purkinje cells with secondary proliferation of Bergmann glia. The dentate nucleus is also frequently involved.

In the brainstem, the olives represent vulnerable areas. In children, the brainstem is sometimes severely damaged, especially in the medial and lateral reticular formations and in the adjacent cranial nerve nuclei.

Various types of white matter lesions may be seen, either alone or in association with gray matter lesions. Some of the white matter lesions consist predominantly of extravasation of fluid with maintenance of intact endothelial cells. Currently, these lesions are designated *reversible leukoen-*
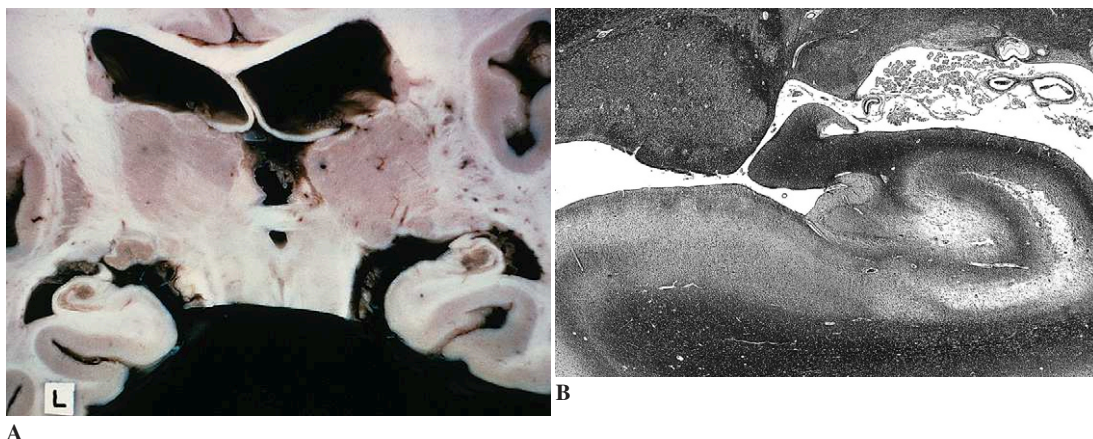
Figure 9-2. Cerebral anoxia, involvement of the hippocampus. **A**, Gross appearance. **B**, Microscopy. Note tissue loss from the CA1 sector and to a lesser extent, the endplate (Luxol fast blue myelin stain).

Figure 9-3. Bilateral necrosis of the pallidum, gross appearance.

cephalopathy; they may be seen in hypoxia and other acquired metabolic disturbances or intoxications. Other white matter lesions, often designated collectively as *hypoxic encephalopathy*, consist of varying proportions of demyelination and white matter necrosis. The lesions include small, perivascular foci of demyelination, focal plaque-like areas of demyelination and necrosis, and large, confluent areas of demyelination and necrosis. The lesions tend to be most severe deep in the white matter, with relative preservation of the subcortical U fibers (Fig. 9-4).

Variation of Lesions According to Etiology

Survival time of approximately 24 to 48 hours is necessary for the gross lesions of cerebral hypoxia to become apparent. Before that time, some degree of cerebral swelling may be observed inconstantly. In cases of early death or only moderate cerebral hypoxia, unquestionable signs of hypoxia may be discerned solely on histologic examination; these consist of ischemic neurons in the most vulnerable areas, where they appear after 4 to 12 hours of survival.

Depending on the mechanism of cerebral anoxia, distinctive ischemic changes may be distinguished as follows.

Cerebral Infarcts

Cerebral infarcts are the result of localized ischemic hypoxia due to arterial occlusion (see

Chap. 4). Infarcts and/or ischemic lesions in the boundary zone areas are the result of a number of factors leading to global oligemic hypoxias, especially evident in cases of low cerebral blood flow of sudden onset and of short duration. They are one of the possible consequences of acute heart failure (cardiogenic shock), drug-induced hypotension, and general anesthesia.

Total Cardiovascular Arrest

Total cardiovascular arrest exceeding several minutes at normal temperature causes diffuse cortical lesions with Ammon's horn involvement and variable lesions of the basal ganglia and brainstem (Fig. 9-5).

Comparable lesions are caused by profound hypoglycemia (insulin shock) and status epilepticus.
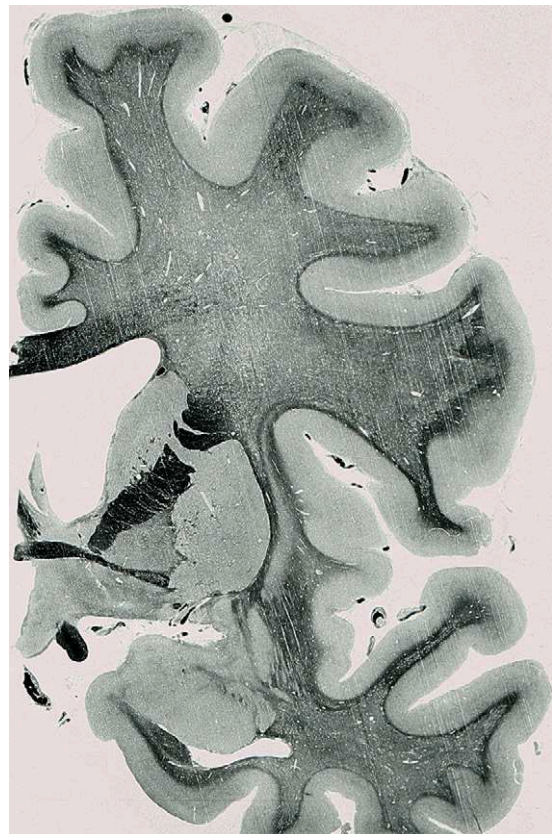
Figure 9-4. Large section at the level of the anterior commisure showing white matter demyelination with preservation of the U fibers following hypoxia (Loyez stain).
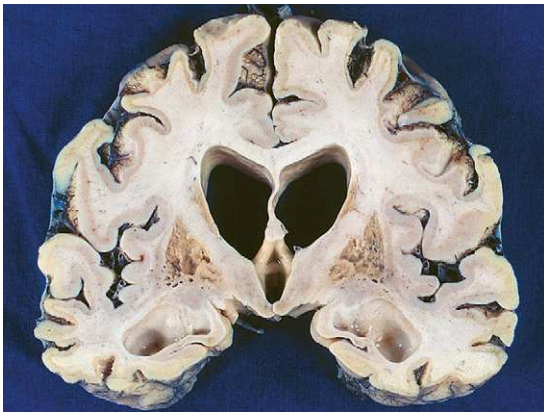
Figure 9-5. Diffuse cortical and basal ganglia lesions in a patient who died after several weeks following a cardiovascular arrest.

Carbon Monoxide Poisoning

Carbon monoxide (CO) is produced by incomplete combustion of carbon-containing substances. Humans are exposed to CO primarily through automobile exhaust, improperly ventilated stoves or heaters, and tobacco smoke. The toxic effects of CO result primarily from the decreased capacity of blood to transport oxygen.

Brains from individuals who die of CO poisoning within a few hours are generally swollen and congested. Blood within vessels has a characteristic cherry-red color of carboxyhemoglobin and imparts that color to the gross brain (Fig. 9-6). Petechial hemorrhages may also be present. The red color of the fresh brain becomes less prominent with prolonged formalin fixation.

Some individuals can recover from acute CO intoxication but may develop, a few days to weeks later, delayed neuropsychiatric manifestations, including personality changes, parkinsonism, dementia, incontinence, and psychosis.

Pallidal necrosis is classically associated with delayed deaths from CO intoxication. Grossly discernible foci of tissue damage are encountered most often in those individuals who have survived for 6 or more days. Microscopic foci of ischemic or hemorrhagic necrosis may develop even sooner. The pallidal lesions are usually bilateral but are often asymmetrical. The necrosis usually involves the anterior portion and inner segment of the pallidum but may extend into the outer segment or dorsally into the internal capsule. Although pallidal necrosis is characteristic of and frequently seen in delayed deaths from CO, it may also be seen in a wide variety of other conditions that are accompanied by hypoxia or anoxia (Figs. 9-3, 9-7, and 9-8). The selective involvement of the globus pallidus in CO poisoning has been attributed variously to selective vulnerability of pallidal neurons, hypotension and impaired circulation through the pallidal branches of the anterior choroidal arteries, or the relatively high iron content of this portion of the brain.

Other gray matter lesions noted include hemorrhagic or ischemic neocortical and hippocampal necrosis in the cerebrum and loss of Purkinje cells and internal granular layer cells in the cerebellum.

Lesions of the white matter are also encountered in individuals with delayed death from CO poisoning. These lesions consist of varying proportions of demyelination and necrosis. They may be small, perivascular foci found mainly in the deep white matter; large, confluent areas that extend from the frontal to occipital poles in the periventricular
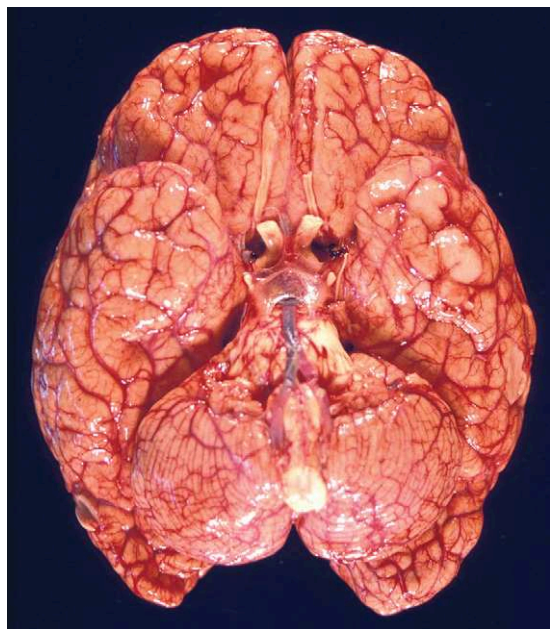
Figure 9-6. Gross brain from patient with acute carbon monoxide (CO) poisoning. The postmortem blood CO saturation was 60%. The cherry-red color of carboxyhemoglobin imparts a red hue to the entire brain.
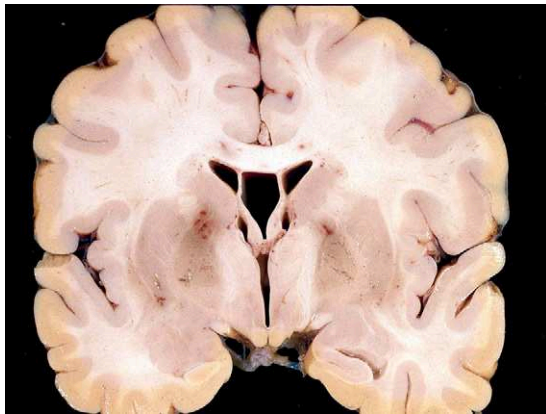
Figure 9-7. Coronal section showing bilateral pallidal necrosis. This can be seen following delayed deaths from carbon monoxide and other hypoxic conditions.

white matter; or sharply demarcated foci of demyelination with relative sparing of axons in the deep white matter ("Grinker myelinopathy"; see Fig. 9-8). All of the lesions tend to spare the arcuate fibers.

Cyanides

Cyanides are histotoxic or cytotoxic agents whose toxicity is due to bonding between the cyanide ion and the ferric iron of intracellular cytochrome oxidase. This leads to cessation of cellular respiration. Acute intoxication can result from either ingestion or inhalation of cyanides, and causes respiratory arrest. Rarely, survivors of cyanide intoxication may develop parkinsonism or dystonia.

When death is rapid, the brain may be edematous and occasionally harbor focal subarachnoid hemorrhages. If death is delayed, the brain may show foci of necrosis in the basal ganglia and white matter and loss of Purkinje cells.

Vitamin Deficiency Disorders

Thiamine Deficiency

Wernicke-Korsakoff syndrome is caused by thiamine (vitamin B_1) deficiency, resulting from (a) inadequate B_1 intake in an otherwise adequate diet (e.g., beriberi, prolonged intravenous therapy
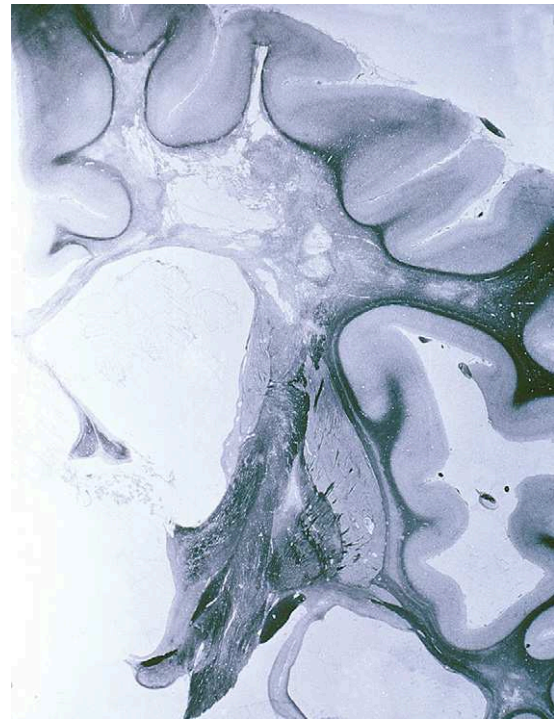
Figure 9-8. Carbon monoxide poisoning. Necrosis of the pallidum and white matter necrosis in a case of Grinker myelinopathy (Loyez stain).

without vitamin supplementation) or significant nutritional deficit (e.g., fasting or famine), or (b) gastric absorption defect, such as in hyperemesis gravidarum, gastrointestinal neoplasms, and gastric plication for morbid obesity. It also complicates chronic dialysis and treatment with tolazamide or zidovudine. It is most often encountered in patients with chronic alcoholism, probably as the result of gastric lesions.

The distribution of the lesions of *Wernicke encephalopathy* is characteristic (Figs. 9-9 and 9-10) and accounts for the symptoms; these include disturbances of wakefulness, hypertonia, and ocular palsies. The lesions are found in the periventricular areas, including the medial aspect of the thalamus, hypothalamus, and mamillary bodies; the periaqueductal region at the level of the third cranial nerve; the reticular formations of the midbrain and the inferior corpora quadrigemina; and the floor of the fourth ventricle. The mamillary bodies are the most frequently affected structures and are involved in virtually all cases.
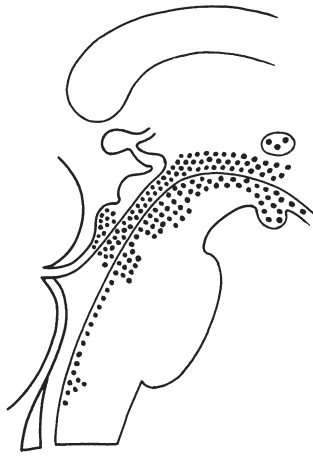
Figure 9-9. Diagram showing topographical distribution of the lesions in Wernicke encephalopathy.

The changes vary with the stage and severity of the disease. When patients die during the acute stages of the disease, petechial hemorrhages seen on gross examination involve predominantly the mamillary bodies (Fig. 9-11) but may sometimes be more extensive (see Fig. 9-10). Patients with less severe, chronic, or previously treated disease may have mildly atrophic mamillary bodies that are gray to brown in color as a result of hemosiderin deposition (Fig. 9-12). A narrow band of tissue immediately adjacent to the ventricular system and around the aqueduct usually remains unaffected.

Under light microscopy, the acute lesions display edema, petechial hemorrhages, myelin loss, and reactive astrocytosis. Neurons are generally

A

B

C

D
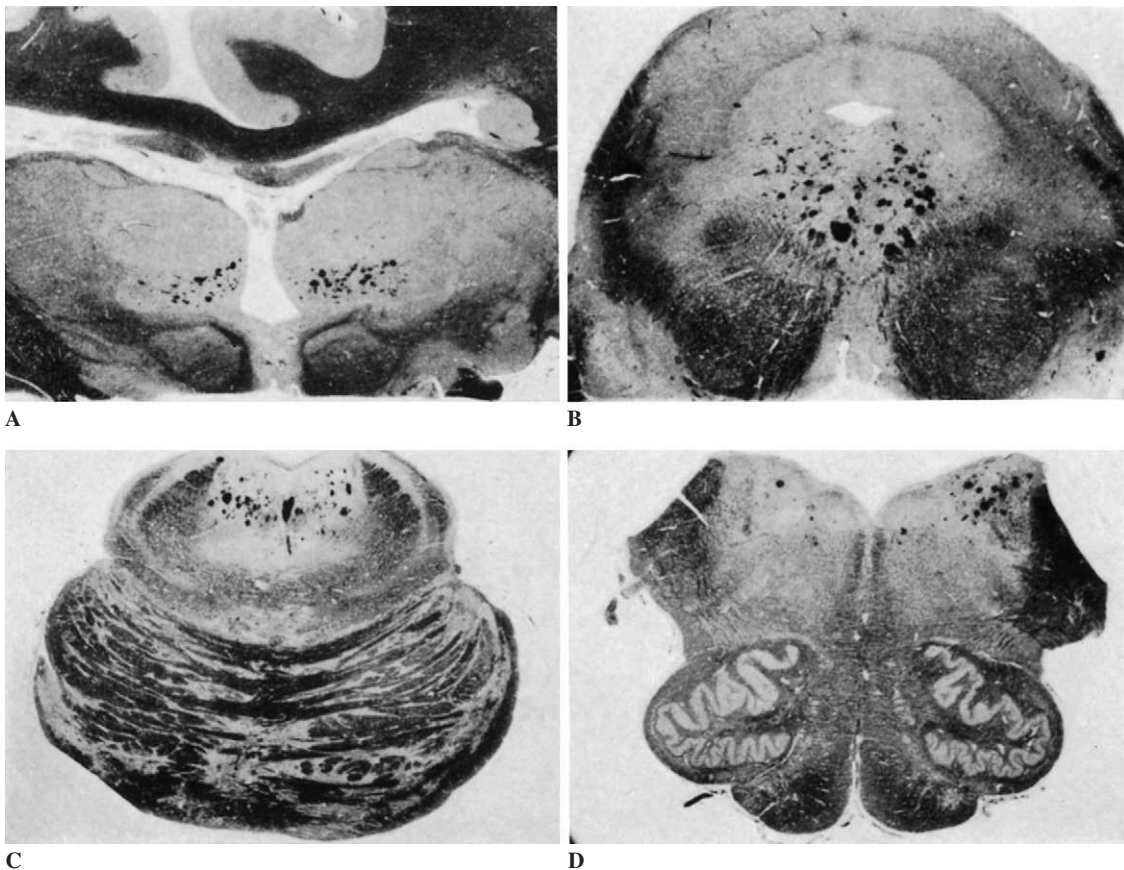
Figure 9-10. Wernicke encephalopathy: topographical distribution of the lesions (Loyez stain). **A,** Periventricular hemorrhagic thalamic lesions. **B,** Lesions in the tegmentum of the midbrain at the level of the third cranial nerve nuclei. **C,** Hemorrhages in the tegmentum of the upper pons. **D,** Hemorrhagic lesions in the medullary floor of the fourth ventricle.
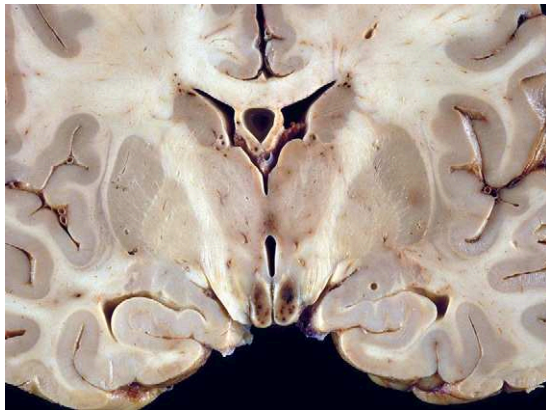
Figure 9-11. Acute Wernicke encephalopathy. Note the petechial hemorrhages in the mamillary bodies and, to a lesser extent, the walls of the third ventricle.
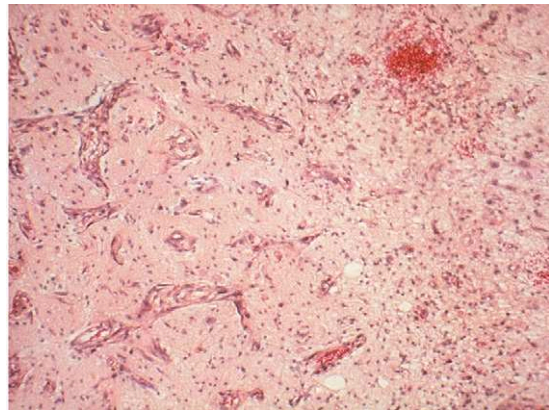
Figure 9-13. Microscopic appearance of the mamillary bodies from a patient with Wernicke encephalopathy. Note the petechial hemorrhages and the swelling of the endothelial cells.

preserved. Swelling and hyperplasia of endothelial cells make the capillaries abnormally prominent (Fig. 9-13). The perivascular spaces may contain lipid-laden macrophages. Extravasated erythrocytes and hemosiderin-laden macrophages are seen in the cases with grossly discernible petechial hemorrhages. In the chronic stages of the disease and in treated patients, the affected regions may show little more than mild loss of neurons and gliosis. Central chromatolysis of neurons may result from associated niacin deficiency (see later in this chapter).

Korsakoff psychosis, which is defined clinically as retrograde amnesia and an impaired ability to acquire new information, is usually encountered in alcoholic patients with chronic Wernicke encephalopathy. The pathologic basis of that syndrome is debated. It does not seem to result from lesions of the mamillary bodies only. Involvement of the medial dorsal nuclei (Figs. 9-10A and 9-14) and/or midline region of the thalamus also seems to play a causative role.

Thiamine deficiency also produces peripheral neuropathies, including beriberi neuropathy and

Figure 9-12. Shrunken, discolored mamillary bodies in a patient who had been treated for previous episodes of Wernicke encephalopathy.
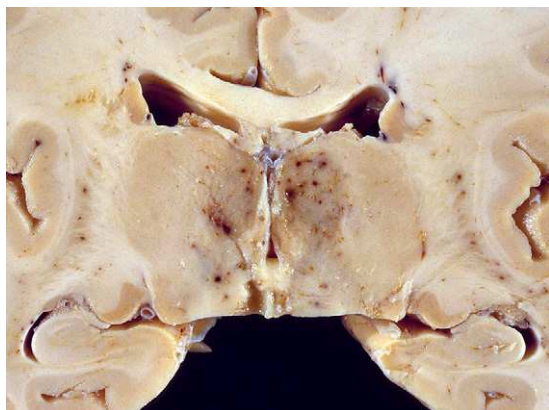
Figure 9-14. Petechial hemorrhages and myelin loss in the thalamus from a patient with Korsakoff syndrome.

at least some cases of so-called alcoholic poly-neuropathy (see Chap. 14).

Pellagra

Pellagra is manifest typically by dermatitis, diarrhea, and dementia. The disease has long been recognized among malnourished individuals who depended on corn as a major part of their diet. It results from lack of P-P (pellagra preventive) factor (nicotinic acid or niacin). It is now known that either deficiency of niacin itself, or of tryptophan, an amino acid precursor of niacin that is deficient in corn, leads to pellagra. The disease has become very rare as the result of enriching common foods, such as bread, with niacin. This vitamin deficiency is now encountered most often in patients with chronic alcoholism; the resulting disease may be clinically atypical, lacking the characteristic skin lesions.

The neuropathologic changes resulting from niacin deficiency consist of isolated neuronal changes of central chromatolysis type (Fig. 9-15) without associated glial or vascular alterations. They affect, in order of decreasing frequency, the Betz cells of the cerebral motor cortex, the pontine nuclei, the dorsal nucleus of the vagus, the gracile and cuneate nuclei, the nucleus ambiguus, the trigeminal nerve nuclei, the oculomotor nuclei, the reticular formations, and the anterior horn motor neurons of the spinal cord. Some cases of niacin deficiency may show degeneration of the posterior columns and corticospinal tracts.

Vitamin B$_{12}$ Deficiency

Vitamin B$_{12}$ is obtained primarily from meat and dairy products. The vitamin must be bound to "intrinsic factor," a glycoprotein produced by the gastric parietal cells prior to being absorbed by the body through the ileum. Most cases of vitamin B$_{12}$ deficiency actually result from inadequate production of intrinsic factor. In pernicious anemia, it is secondary to autoimmune atrophic gastritis; it is more rarely due to gastric neoplasms or gastrectomy. Vitamin B$_{12}$ deficiency also can result from impaired ileal absorption because of malabsorption syndromes, intestinal tuberculosis, regional enteritis, or lymphomas. Rare cases result from competitive utilization of the vitamin within the intestine by the fish tapeworm (*Diphyllobothrium latum*) or by bacterial overgrowth in intestinal blind loops or diverticula. Very similar changes ("vacuolar myelopathy") have been observed in AIDS patients, most likely the result of abnormalities of Vitamin B$_{12}$ metabolism.

Vitamin B$_{12}$ deficiency affects the hematopoietic (causing megaloblastic anemia), gastrointestinal (causing glossitis, anorexia, diarrhea, and weight loss), and nervous systems. Neurologic
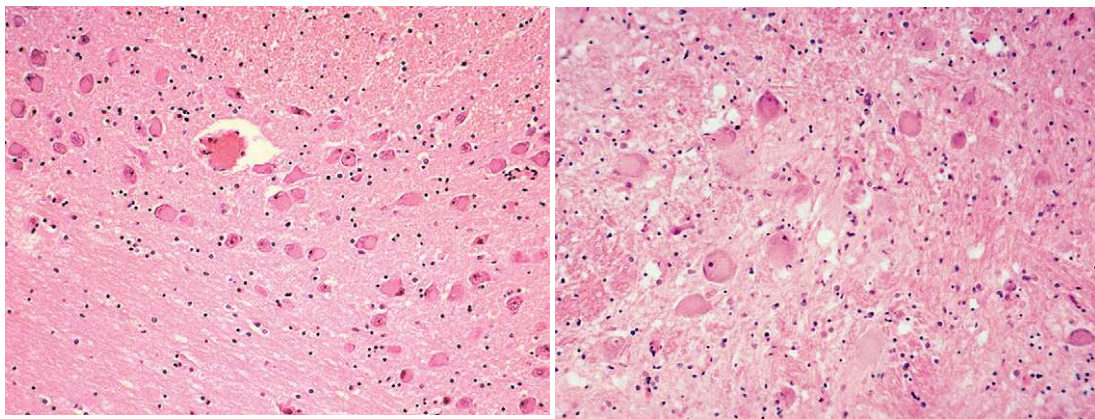
Figure 9-15. Pellagra encephalopathy. Microscopic picture of cell chromatolysis (H and E). **A**, In the pontine nuclei. **B**, In the gracile nucleus.
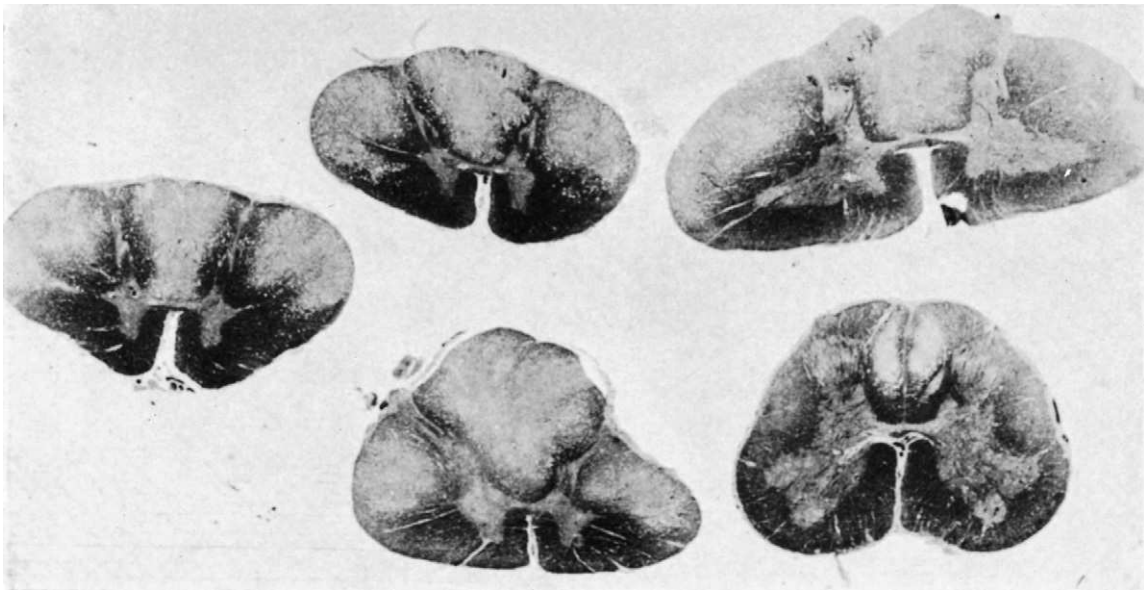
Figure 9-16. Subacute combined degeneration of the spinal cord. Note demyelination of the posterior and lateral columns of the spinal cord (Loyez myelin stain).

complications develop in 40% of untreated cases and can occur in the absence of hematologic abnormalities. Nervous system involvement (neuroanemic syndrome) elicits subacute combined degeneration of the spinal cord.

The spinal cord from patients with longstanding severe vitamin B_{12} deficiency may be mildly shrunken and show discolored posterior and lateral columns. Histologically, the earliest lesions consist of vacuolar distention of myelin sheaths resulting in a characteristic spongy appearance of the affected white matter. With further demyelination, lipid-laden macrophages are found scattered throughout the lesions. Some of the axons traversing the lesions undergo wallerian degeneration. Initially, astrocytosis is not marked, but dense gliosis may be seen in longstanding cases. The distribution of the lesions is remarkably constant. They are bilateral and symmetrical and involve chiefly the long spinal tracts. Initial lesions are found in the central part of the posterior column of the thoracic cord, from whence they extend peripherally and affect the corticospinal and spinocerebellar tracts in the lateral columns. In severe cases, the lesions may involve virtually all the white matter, including the anterior columns, sparing only the fibers adjacent to the gray matter. The severity of the lesions usually decreases towards the cervical and lumbar levels, where they are restricted to the dorsal and lateral columns, often sparing a small peripheral zone (Fig. 9-16). However, secondary ascending and descending tract degeneration may be associated findings at those levels. Rarely, the lesions may extend rostrally into the medulla. Occasionally, similar lesions may be seen in the optic nerve and cerebral white matter.

Toxic Encephalopathies

Ethanol

Ethanol has many effects upon the central nervous system. It is well known that alcoholism potentiates infections, contributes to traumatic injuries, and may increase the risk of stroke, especially hemorrhagic stroke. Alcoholism is also implicated in associated peripheral neuropathy and myopathy (see Chaps. 13 and 14).

Acute Alcohol Intoxication

Ingestion of large quantities of alcohol can lead directly to death from cardiorespiratory paralysis.

Blood alcohol levels over 450–500 mg/dl are generally considered potentially lethal, although there is considerable individual variation. Brains from individuals dying of acute alcohol intoxication usually show only cerebral edema or no morphologic abnormalities.

Cerebral Lesions in Chronic Alcoholism

Whereas a direct neurotoxic effect of alcohol on the nervous system remains controversial, the effects of chronic alcoholism on various visceral organs have an important role in determining the cerebral lesions.

Hepatic encephalopathy may result from decompensated cirrhosis that has culminated in hepatic coma and/or is accompanied by portocaval shunt (see later in this chapter).

Cerebral lesions due to vitamin deficiency include Wernicke-Korsakoff encephalopathy secondary to deficiency of vitamin B$_1$ absorption caused by alcoholic gastritis and pseudopellagra encephalopathy, with which it is frequently associated (see earlier in this chapter).

Alcoholic cerebellar degeneration may occur as an isolated lesion or in association with other alcohol-related lesions, such as Wernicke encephalopathy. Its pathogenesis is unclear. Morphologically similar but generally milder cerebellar vermal atrophy can also occur as an age-related phenomenon independent of alcoholism. The clinical manifestations evolve slowly over months to years and include truncal instability, a wide-based stance, and ataxic gait. The vermal atrophy can be demonstrated by computed tomography (CT) and magnetic resonance imaging (MRI), but the degree of atrophy does not correlate well with the severity of clinical manifestations. The lesions involve the rostral vermis (Fig. 9-17) and, to a lesser extent, the superior surface of the cerebellar hemispheres (Fig. 9-18). The folia are pale, sclerotic, and separated by widened interfolial sulci. The atrophy affects the crests of the folia more severely than the depths of the interfolial sulci. The lesions consist of loss of Purkinje cells with proliferation of Bergmann glia and variable depopulation of the internal granular cells. They are associated with lesions of the dorsal laminae of the inferior olives. The cerebellar white matter remains relatively unaffected.

Central pontine myelinolysis is a form of myelin damage that was first described in chronic alco-

Figure 9-17. Superior vermal atrophy from a patient with chronic alcoholism.

holics but which may be seen in other conditions in which severe metabolic or electrolyte disturbances are present, especially following excessively rapid correction or overcorrection of chronic hyponatremia. The clinical manifestations of central pontine myelinolysis vary from a lack of symptoms to coma, depending on the size of the lesion. The diagnosis can be made by MRI. At autopsy, the typical lesion of central pontine myelinolysis appears as a discolored, necrotic area in the basis pontis that may be centrally cavitated (Fig. 9-19). The lesions are often triangular, T-shaped, or diamond-shaped and vary from a few millimeters across (Fig. 9-20) to lesions that involve nearly the entire basis pontis. Generally, at least a thin rim of intact myelin is present at the lateral and ventral
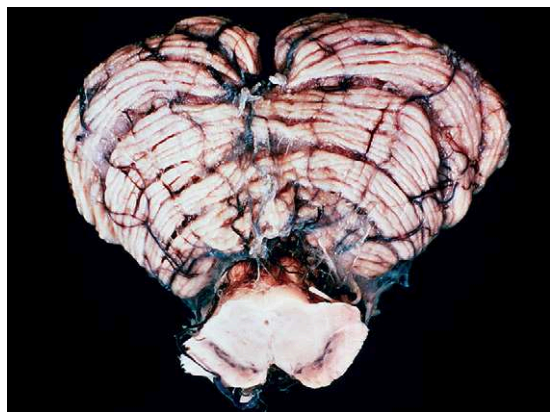
Figure 9-18. Atrophy of the rostral vermis and superior surface of the cerebellar hemispheres in a chronic alcoholic.

Figure 9-19. Cross-section of pons from patient with central pontine myelinolysis. Note ill-defined brown discoloration of the lesion.

Figure 9-21. Section of pons from a patient with extensive central pontine myelinolysis (Loyez stain).

margins of the pons (Fig. 9-21). Damage is usually maximal in the middle and rostral portions of the pons. Lesions may extend to the cerebellar peduncles. Histologically, central pontine myelinolysis is characterized by demyelination with relative preservation of axons and neuronal perikarya (Fig. 9-22). Acute lesions contain numerous lipid-laden macrophages but few or no inflammatory cell infil-

trates. Occasionally, foci of necrosis and cavitation are present in the center of the more severe lesions. Sometimes, especially in more severe cases, central pontine myelinolysis is accompanied by comparable extrapontine lesions. These may involve the subcortical white matter, striatum, anterior commissure, internal and external capsules, lateral geniculate bodies, and cerebellar folia.

Marchiafava-Bignami disease is a rare disorder of unknown pathophysiology. It is observed only in patients with chronic alcoholism of long duration and great severity. Occasionally, Marchiafava-Bignami disease has accompanied Wernicke encephalopathy or central pontine myelinolysis. It is characterized by varying degrees of myelin loss
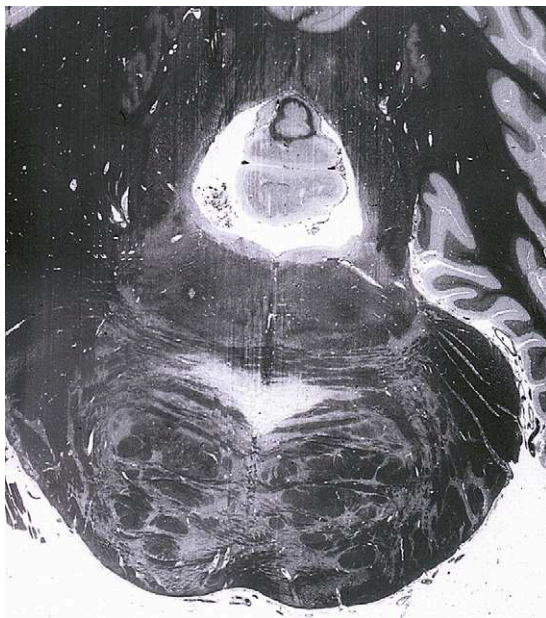
Figure 9-20. Limited triangular lesion of central pontine myelinolysis (Loyez stain).
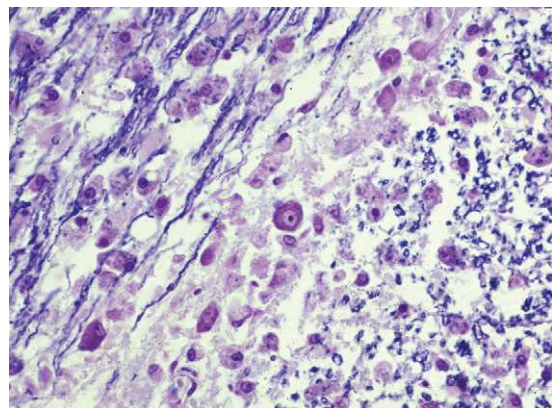
Figure 9-22. Microscopic section of pons from patient with central pontine myelinolysis. Note intact neuron in the midst of an area of myelin loss (Klüver-Barrera stain).

and white matter necrosis involving the corpus callosum and, occasionally, other white matter structures. The disease is usually diagnosed at autopsy, but the lesions have been seen by CT and MRI. Grossly and microscopically, they are regions of myelin loss or partial necrosis involving the interior of the corpus callosum with relative preservation of thin layers of myelin on its dorsal and ventral surfaces. The involvement is maximal in the genu and body of the corpus callosum (Fig. 9-23) and may be accompanied by similar involvement of the optic chiasm, anterior commissure (Fig. 9-23B), centrum semiovale (Fig. 9-23A), and middle cerebellar peduncles. Histologically, the lesions show loss of myelin with abundant lipid-laden macrophages and variable sparing of axons.

Morel laminar sclerosis is the best-known of the cortical disorders in chronic alcoholism. It is characterized by a glial astrocytic bandlike proliferation localized to the third cortical layer, especially in the lateral frontal cortex. This disease is usually associated with, and probably secondary to, the callosal lesions of Marchiafava-Bignami disease.

A wide variety of other cortical neuronal changes have been described; formerly they were attributed to alcoholism but are now regarded as nonspecific or even artifactual.

Methanol

Methanol poisoning resulting from oral intake, most often as a substitute for ethanol, may cause acute cerebral and ocular lesions. Methanol itself is neurotoxic but its catabolites formaldehyde and formic acid are even more so. Formic acid and formates block cellular respiration and contribute to the metabolic acidosis that is so characteristic of this intoxication.

The ocular pathology of the blindness has been investigated extensively. The main lesions include optic disc edema, retrolaminar myelin loss, and optic nerve necrosis. Pathologic changes in the brain include cerebral edema and necrosis of the subcortical white matter, lateral aspects of the putamen and claustrum (Fig. 9-24). The putamenal

A

B

Figure 9-23. Marchiafava-Bignami disease. **A**, Gross appearance: necrosis of the interior of the corpus callosum. Note involvement of the adjacent white matter. **B**, Large section showing lesions of the corpus callosum and anterior commissure (Loyez myelin stain).

Figure 9-24. Methanol intoxication. Necrosis of the putamen and head of the caudate nucleus and damage to the subcortical frontal white matter (Loyez stain).

necrosis is often hemorrhagic and may even evolve into a hematoma. The necrosis of the claustrum is generally nonhemorrhagic. The white matter lesions and the retrolaminar damage of the optic nerves represent histotoxic myelinoclastic damage caused by formates. The pathogenesis of the putamenal lesions remains unclear.

Ethylene Glycol

Ethylene glycol is a dihydroxy alcohol that is widely used as a solvent and component of certain antifreezes and coolants. Intoxication with this compound is encountered most often when it is consumed as a substitute for ethanol or with suicidal intent. Ethylene glycol is progressively oxidized to more toxic compounds including glycoaldehyde, glycolic acid, and glyoxylic acid. Eventually, a small proportion is oxidized to oxalic acid. The clinical manifestations include central nervous system dysfunction with severe metabolic

acidosis, cardiopulmonary failure, and acute renal failure.

Brains from fatal cases show edema, meningeal congestion, and, occasionally, petechial hemorrhages. Microscopically, acute inflammatory cells may be seen in the meninges and around intraparenchymal blood vessels. Deposits of calcium oxalate may be seen in and around blood vessels in the meninges, neural parenchyma, and choroid plexus. These crystals are birefringent under polarized light (Figs. 9-25A and B).

Phenytoin

Patients with seizure disorders who have been treated with phenytoin for prolonged periods of time may show loss of Purkinje cells and gliosis of the cerebellar cortex. Attributing these histologic changes to the phenytoin therapy is often difficult, since loss of Purkinje cells may result from hypoxia during seizures or from preexisting brain damage. Furthermore, some authors believe that Purkinje-cell loss may occur in patients with epilepsy independently of the effects of generalized hypoxia. Occasional, reports of cerebellar atrophy and degeneration in patients who had long-term treatment with phenytoin but few or no seizures support the view that phenytoin itself may be neurotoxic. The cerebellar atrophy has been documented by CT and MRI studies. Histopathologic studies have shown folial atrophy, loss of Purkinje cells throughout the cerebellum, and mild loss of internal granular layer cells (Fig. 9-26).

Intoxication by Heavy Metals and Certain Metalloids

Many metals and certain metalloids, in sufficient concentration and appropriate form, are toxic to humans. The CNS displays a varying degree of protection from toxic substances that is attributable, in part, to the blood-brain barrier. The neuropathologic picture is highly variable, reflecting the selective vulnerability of neural structures to these diverse substances. It is usually difficult to correlate a particular set of lesions with a specific etiology. In hyperacute forms of intoxication, the course may be
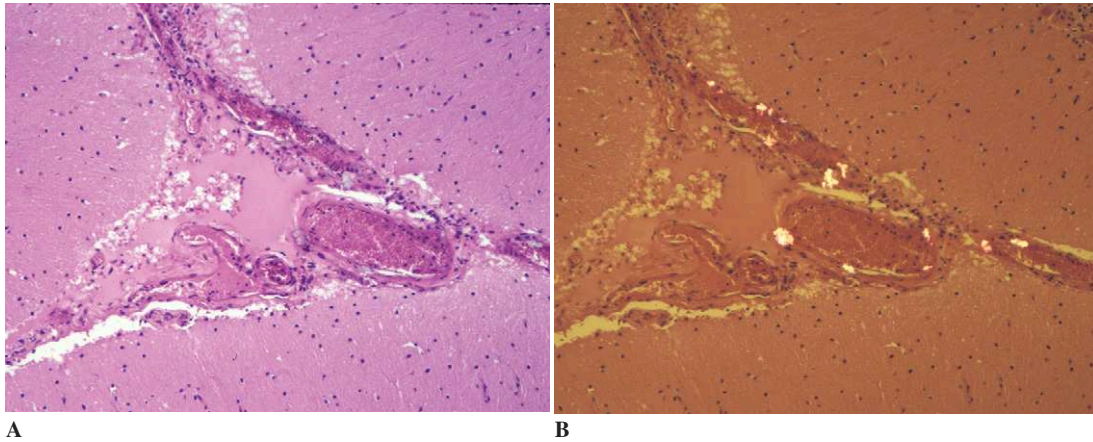
Figure 9-25. Microscopic sections showing cerebellar cortex and leptomeninges from a patient with ethylene glycol intoxication. **A**, Note refractile calcium oxalate crystals in the vessel walls (H and E). **B**, Note birefringence of the same crystals when viewed with polarized light.

so rapid that there is no time for histologic changes to appear. Commonly observed changes, such as edematous or hemorrhagic lesions, are nonspecific. Furthermore, in the majority of cases the lesions are the consequence of the multiple visceral disturbances caused by the intoxication. Finally, it is necessary to stress the frequently associated involvement of the peripheral nervous system, which is most often directly caused by toxic damage (see Chap. 14).
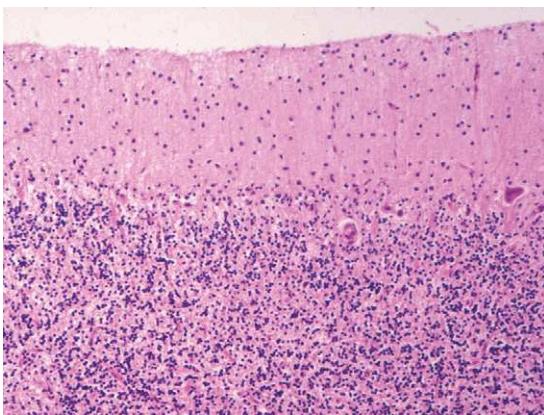
Figure 9-26. Microscopic section of cerebellar folium from a patient who had been treated for a long time with high-dose phenytoin. Note loss of Purkinje cells and mild loss of internal granular cell layer neurons.

Aluminum

The neurotoxicity of aluminum is controversial. Various aluminum compounds applied directly onto or injected into the cerebral cortex of certain laboratory animals produce seizures and neurofibrillary tangles, but these experimental paradigms are quite different from the evolution of Alzheimer disease in humans.

Aluminum toxicity is most common in patients undergoing chronic hemodialysis and is due to exposure to aluminum in the dialysate and the use of oral phosphate-binding compounds that contain aluminum. Dialysis dementia is characterized by dyspraxia, asterixis, myoclonus, and dementia and may prove fatal. The brain aluminum content may become elevated to levels even greater than those reported in Alzheimer disease, but neurofibrillary tangles are not present.

Arsenic

Arsenic intoxication is encountered most often as the result of occupational exposure or after ingestion with homicidal or suicidal intent. Acute trivalent arsenic poisoning is characterized clinically by abdominal pain, nausea, vomiting, and diarrhea followed by renal failure. Death may occur in severe cases. Chronic arsenic intoxication is clinically manifest by gastrointestinal and der-

matologic symptoms. A mixed sensory and motor neuropathy is a well-known and often disabling sequel of both acute and chronic arsenic intoxication. Encephalopathy also has been reported with acute and chronic arsenic intoxication. Acute hemorrhagic leukoencephalopathy has been reported in patients treated with organic pentavalent arsenicals. This may have been the result of a hypersensitivity reaction to the drug.

Lead

Lead can enter the body through the gastrointestinal and respiratory tracts and, when in organic compounds, the skin. Lead encephalopathy is now encountered predominantly in young children who chew on items coated with lead paint. Acute lead encephalopathy produces irritability, seizures, altered consciousness, and increased intracranial pressure. The intoxication usually responds to sedation and chelation therapy but can lead to permanent damage. Many authors attribute the encephalopathy to vascular injury, which seems to be more severe in the immature nervous system.

At gross examination, the brain is diffusely swollen. The histologic changes include congestion, petechial hemorrhages, and foci of necrosis. Intraparenchymal capillaries may show necrosis, thrombosis, and swelling of endothelial cells. There is a proteinacous exudate in the perivascular space extending into the adjacent brain tissue. Periodic acid-Schiff–positive globules may be seen within the exudates and within astrocytes. Diffuse astrocytosis has been reported even in the absence of capillary changes.

Manganese

Manganese exposure may result from inhaling dust in manganese mines or the vapor released during ferromanganese smelting. The clinical manifestations include headaches, transient psychiatric disturbances, and a hypokinetic extrapyramidal dysfunction resembling Parkinson disease, but nonresponsive to L-dopa.

Pathologic studies in humans are limited but document degenerative lesions in the pallidum, subthalamic nucleus, and, to a lesser extent, the striatum. The substantia nigra is infrequently involved.

Mercury

Acute poisoning from inorganic mercury compounds is manifested predominantly by gastrointestinal tract and renal tubular injury. Pulmonary injury is caused by inhalation of metallic mercury vapors. Neurotoxicity is also a prominent manifestation of chronic inorganic mercury poisoning and manifests clinically by behavioral changes, intention tremor, and movement disorders. Occasionally, patients also develop peripheral neuropathy.

Organic mercury intoxication is usually caused by ingestion of contaminated food. In Japan, a large number of people developed chronic organic mercury intoxication from fish contaminated by methyl mercury (Minimata disease). Other large outbreaks have resulted from the consumption of grain treated with an organic mercury fungicide. The clinical manifestations include cortical blindness, impaired proprioception, movement disorders, mental retardation, and quadriparesis.

It seems that the lesions caused by organic and inorganic mercury are essentially the same. The slight differences may simply reflect variations in the rate of entry of mercury into the nervous system. The lesions involve the neurons predominantly. There is cerebral atrophy involving predominantly the anterior portions of the calcarine fissures with loss of neurons, especially from the outer cortical layers, and gliosis. Cerebellar atrophy is also frequent with predominant loss of granule cells, mild loss of Purkinje cells, and proliferation of Bergmann glia.

Thallium

Most cases of thallium intoxication result from accidental or deliberate ingestion of thallium pesticides used for insect and rodent control. The clinical picture resembles that of trivalent arsenical poisoning. The only consistent abnormalities in the CNS are chromatolysis of spinal motor neurons and degeneration of the posterior columns related to a sensorimotor distal axonopathy.

Tin

Inorganic tin is not neurotoxic, but two organotin compounds (triethyltin and trimethyltin) are.

Triethyltin causes striking white matter edema due to accumulation of fluid in vacuoles within the myelin sheaths, which become separated along the intraperiod line (see Chap. 1 text and Fig. 1-24C). Trimethyltin does not cause intramyelinic edema but is toxic to neurons in the hippocampus, entorhinal cortex, and amygdala.

CNS Changes Secondary to Systemic Diseases

Respiratory Encephalopathies

Generally secondary to chronic bronchopulmonary disease and essentially due to hypoxia and hypercapnia, respiratory encephalopathies are characterized by diffuse vasodilatation, microscopic perivascular hemorrhages, and anoxic neuronal changes of variable intensity.

In acute asphyxia with rapid death, there is congestion of the meninges and cortex due to venous and capillary dilatation ("lilac brain"; Fig. 9-27). Hemorrhages of perivascular type predominating in the white matter may be associated.

Hepatic Encephalopathy

Hepatic encephalopathy occurs in the course of severe hepatic insufficiency with terminal coma in cases of severe hepatic cirrhosis or hepatitis, in portocaval anastomosis, and in Wilson hepato-

Figure 9-27. Lilac brain in a patient who died from acute asphyxia. Note petechial hemorrhages and laminar necrosis.

lenticular degeneration. It is characterized by the presence of Alzheimer type II glia (see Chap. 1 text and Fig. 1-20). The lesions predominate in the pallidum but may also involve the cerebral cortex and the dentate nuclei.

Disorders of Iron Metabolism

In primary or secondary *hemochromatosis*, the blood-brain barrier provides effective protection against the diffusion of pigment into the CNS. Therefore, the lesions are limited to impregnation by hemosiderin of regions outside the brain-barrier, including the choroid plexuses, the area postrema, the pineal and pituitary glands, dorsal root ganglia, and a number of vestigial remnants such as the paraphysis and the subfornical organ. These regions have a rusty gross appearance and show marked Prussian blue reaction with ferrocyanide.

Disorders of Calcium Metabolism

Massive perivascular deposits of calcium (Fig. 9-28A), iron (Fig. 9-28B), and other minerals, may be observed in the basal ganglia and sometimes in the dentate nucleus, the white matter, and Ammon's horn (Fahr disease) in a variety of circumstances, including hypoparathyroidism and conditions accompanied by hypercalcemia.

Multifocal Necrotizing Leukoencephalopathy

Multifocal necrotizing leukoencephalopathy is characterized by the development of multiple, usually microscopic foci of necrosis in the white matter. It often affects the basis pontis (focal pontine leukoencephalopathy). Its pathogenesis is unclear but it occurs predominantly in conditions in which there are increased levels of circulating proinflammatory cytokines (e.g., AIDS, neoplasms treated with radiotherapy and chemotherapy, sepsis). In most cases it is recognized only at autopsy.

Lesions are most often only evident on microscopic examination and consist of well-demarcated areas of necrosis disseminated in the white matter, particularly in the transverse pontine fibers (Fig. 9-29A). There is loss of myelin staining, proliferation
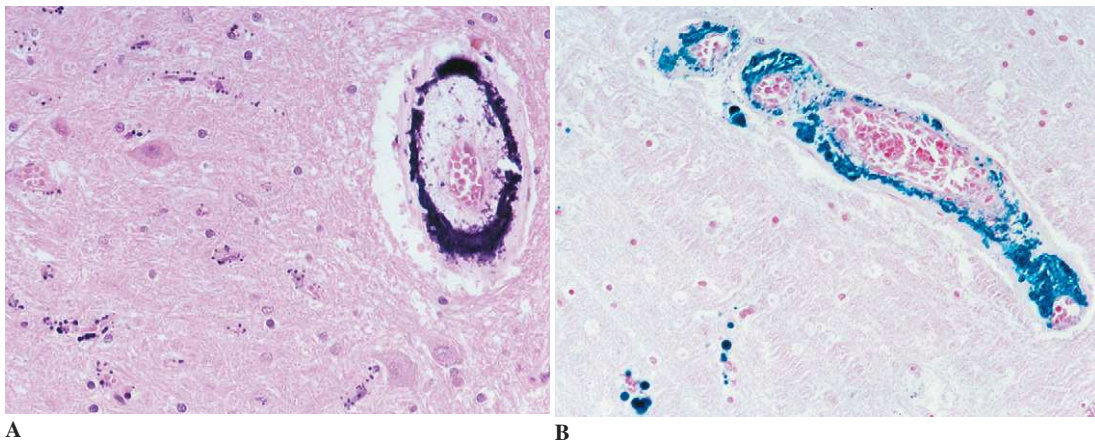
Figure 9-28. A, Massive perivascular mineral deposits in a case of Fahr disease (H and E). **B**, Iron perivascular deposits in the same patient, revealed by Perl's method for iron.

of macrophages, and lesions of axons (which appear swollen and fragmented and tend to calcify; Fig. 9-29B).

Paraneoplastic Syndromes

The *paraneoplastic syndromes* are a group of disparate disorders associated with systemic malignancies that do not directly involve the nervous system by compression, invasion, or metastasis. Also excluded are the iatrogenic complications of radiotherapy or chemotherapy; opportunistic infections related to immunodepression secondary either to the neoplastic process itself (especially in tumors of the lymphoid system) or to treatment or to both; and the metabolic or deficiency disorders and vascular disorders linked to the development of malignant disease. The paraneoplastic syndromes are rare but important entities. In some instances, the neuromuscular or neurologic complications are the initial manifestation of the neoplastic process; in other cases, they contribute significantly to the patient morbidity.

The pathogenesis of these disorders is incompletely understood and probably multifactorial. Current evidence suggests that most of the parane-
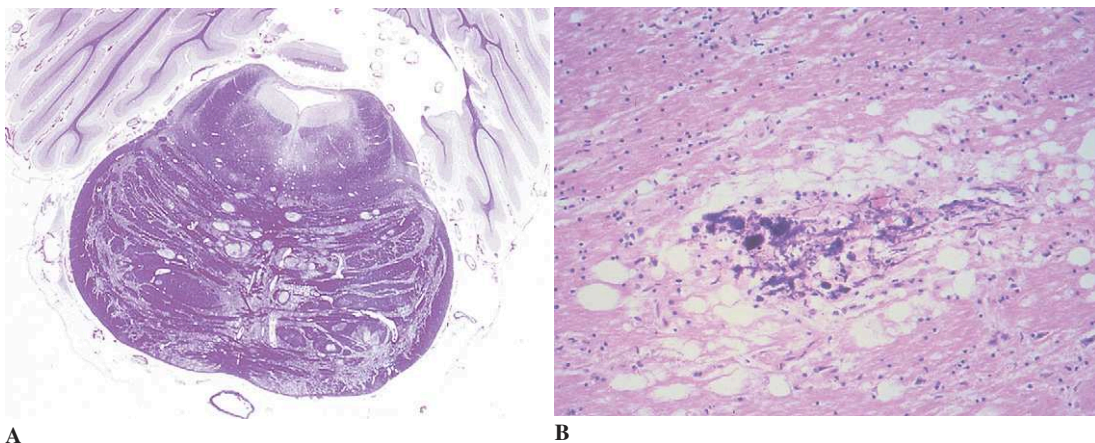
Figure 9-29. Multifocal necrotizing leukoencephalopathy. **A**, Macrosection of the pons showing disseminated necrotic foci in the transverse pontine fibers (Klüver-Barrera stain) **B**, Microscopic section showing a necrotic lesion with vacuolation and central calcification (H and E).

oplastic degenerative diseases occur when system neoplasms aberrantly express antigens that are normally found only in neurons. The strongest evidence for an autoimmune mechanism is found in the case of Lambert-Eaton myasthenic syndrome. In this condition, patients develop antibodies against voltage-gated calcium channels in neuromuscular junctions. In other conditions, the antibodies are not directly pathogenic and the neuronal degeneration may be mediated by cytotoxic T cells. Individual paraneoplastic antibodies are often (but not exclusively) associated with specific neoplasms and neurologic syndromes (Table 9-1).

The principal CNS paraneoplastic syndromes are paraneoplastic cerebellar degeneration, par-

Table 9-1. Paraneoplastic Antibodies, Associated Neoplasms, and Corresponding Neurologic Syndromes

Antibody	Tumor	Neurologic Syndrome
Anti-Hu (ANNA-1)	SCLC	Paraneoplastic neuropathy
		Paraneoplastic encephalomyelopathy
		Gastrointestinal dysmotility
Anti-Ri (ANNA-2)	SCLC, breast	Opsoclonus-myoclonus
		Paraneoplastic neuropathy
ANNA-3	SCLC	Paraneoplastic neuropathy
		Cerebellar degeneration
		Encephalopathy
Anti-Yo (PCA-1)	Ovary, breast	Subacute cerebellar degeneration
PCA-2	Lung carcinoma	Limbic encephalitis
		Cerebellar degeneration
		Lambert-Eaton syndrome
CRMP-5	SCLC, thymoma	Neuropathies
		Cerebellar degeneration
		Subacute dementia
Anti-Tr	Hodgkin disease	Subacute cerebellar degeneration
Anti-amphiphysin	Breast, SCLC	Stiff-person syndrome
Anti-voltage-gated calcium channel	Small cell lung carcinoma lymphoma	Lambert-Eaton syndrome
Anti-Ta	Testicular tumors	Limbic encephalitis
Anti-Ma1	Testicular tumors	Limbic encephalitis
Anti-Ma2	Testicular tumors	Brainstem encephalitis

aneoplastic encephalomyelitis, and opsoclonus-myoclonus.

Paraneoplastic Cerebellar Degeneration

The course of *paraneoplastic cerebellar degeneration* is generally subacute. It manifests as gait ataxia, incoordination, dysarthria, and, often, nystagmus. The cerebellum may be atrophic but is usually macroscopically normal. Histologically, there is massive, diffuse loss of the Purkinje cells with proliferation of Bergmann glia (Figs. 9-30A and B) and sparing of the basket fibers and, to a lesser extent, of the granular neurons (Fig. 9-30C). The degeneration of Purkinje cells axons often produces myelin pallor of the fleece (amiculum) of the dentate nucleus (Fig. 9-31). Microglial nodules and perivascular mononuclear cuffs in the leptomeninges and parenchyma are frequent, but inflammation may be sparse or absent.

Paraneoplastic Encephalomyelitis

Subacute polioencephalomyelitis, in the majority of cases, complicates bronchial carcinoma, especially small-cell anaplastic carcinoma. The lesions involve predominantly the gray matter and include, in variable proportion, neuronal loss, nodules of neuronophagia, proliferation of rod-shaped microglia, astrocytic gliosis, and infiltration by B and T lymphocytes. The latter are mainly of the CD4 inductor/helper type in the perivascular cuffs and of the CD8 cytotoxic type in the parenchymal infiltration. The lesions have a characteristic distribution and show a predilection for the medial temporal cortex (in limbic encephalitis), rhombencephalon (in brainstem encephalitis), cerebellum, gray matter of the spinal cord, and spinal root ganglia (in sensory neuropathy). These different localizations may be variously combined and associated with inflammatory lesions in the myenteric plexuses, the peripheral nerves (see Chap. 14), and/or the skeletal musculature.

Patients with paraneoplastic limbic encephalitis display behavioral changes, memory loss, and hallucinations. Limbic structures including the hippocampi, cingulate gyri, insular cortex, amygdala, and parts of the temporal lobe may be affected (Figs. 9-32A and B). The midbrain (Fig. 9-33) and thalamus may show similar changes.

Figure 9-30. Paraneoplastic cerebellar degeneration. **A** and **B**, Massive loss of Purkinje cells and proliferation of Bergmann glia (H and E). **C**, Loss of Purkinje cells; preservation of basket fibers and of granular neurons (Bielschowsky silver impregnation).
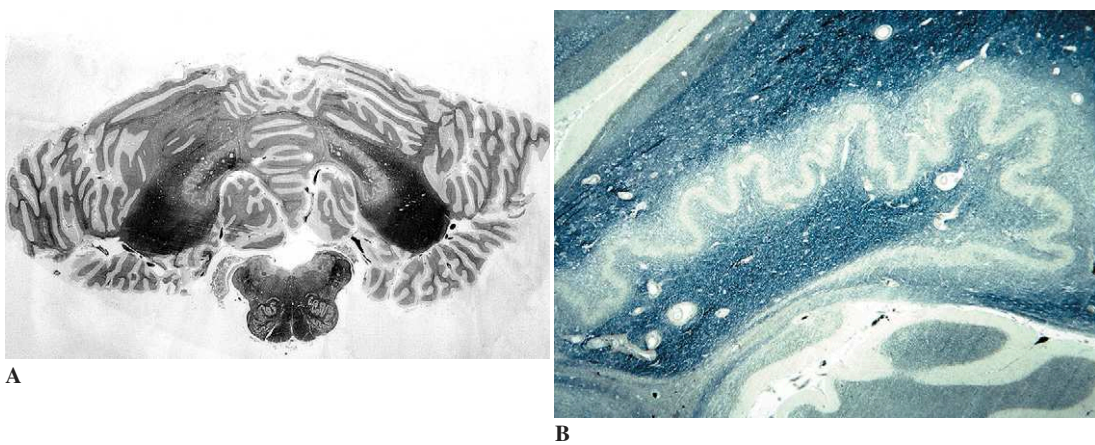
Figure 9-31. A and **B,** Paraneoplastic cerebellar degeneration. Myelin pallor of the fleece of the dentate nucleus, which is the site of projection of Purkinje cell axons (Loyez myelin stain).
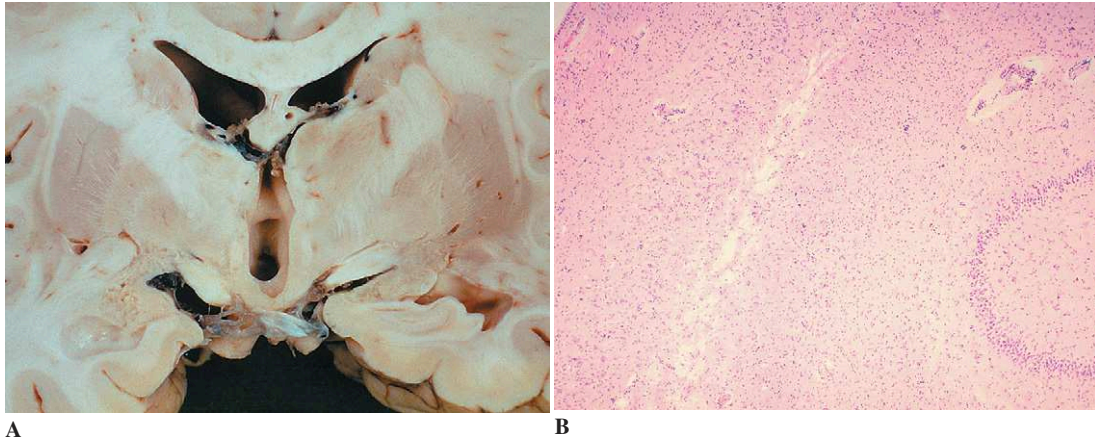
Figure 9-32. Limbic encephalitis. **A**, Gross appearance: bilateral necrosis of the hippocampus and cerebral amygdala. **B**, Microscopic section showing massive loss of pyramidal cells, astrocytic gliosis, and mononuclear perivascular infiltrates.
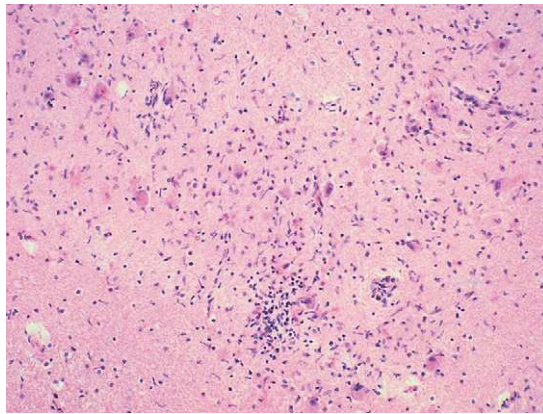
Figue 9-33. Brainstem paraneoplastic encephalitis. Microscopic section showing nodules of neuronophagia, proliferation of rod-shaped microglia, astrocytic gliosis, and mononuclear infiltration in the medullary olive.
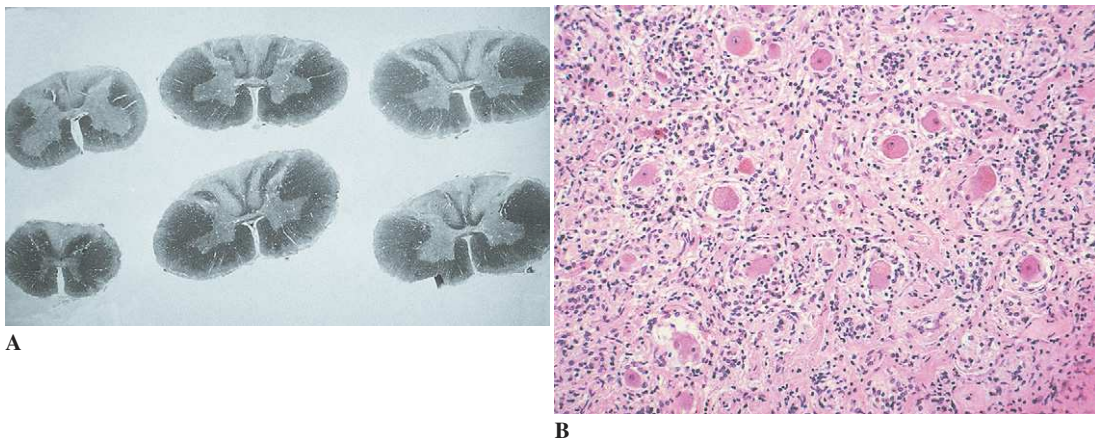
Figure 9-34. Paraneoplastic sensory neuropathy. **A**, Note demyelination of the posterior columns (Loyez myelin stain). **B**, Spinal ganglion. Loss of ganglion cells, proliferation of satellite cells, and interstitial lymphocytic infiltration.

The sensory neuropathy is a frequent component of an encephalomyeloneuropathy. Clinically, it is manifest by numbness, paresthesias, dysesthesias, and reduced or absent reflexes. The peripheral nerves show axonal degeneration with varying degrees of secondary segmental demyelination. Additional pathologic changes include degeneration of posterior roots, degeneration and demyelination of the posterior columns of the spinal cord, and degeneration of dorsal root ganglia (Fig. 9-34A). Mild perivascular and intraparenchymal infiltrates of mononuclear inflammatory cells are often present. In the ganglia, inflammatory cell infiltrates may be especially prominent. The number of ganglion cells is reduced, and nodules of Nageotte are found where the ganglion cells have been lost (Fig. 9-34B). Autonomic ganglia may be involved as well as dorsal root ganglia, but show less severe changes.

Paraneoplastic Opsoclonus-Myoclonus

The *opsoclonus-myoclonus syndrome* is rare but is best known in association with neuroblastomas in children. Even more rarely, the syndrome also occurs in association with small-cell carcinoma of the lung or, in the adult, breast carcinoma. Neuropathologic studies of the brains in these individuals may show no histopathologic abnormalities or demonstrate only Purkinje cell loss and/or mild periaqueductal infiltrates of inflammatory cells.

Chapter 10
Hereditary Metabolic Diseases

Douglas C. Anthony, Hans H. Goebel,
and Jacqueline Mikol

Introduction

Classically, a metabolic disease was defined based on an abnormality in a metabolic pathway. Identification of an abnormal metabolic pathway led to the identification of the aberrant enzymatic activity, the abnormal enzyme, and eventually to the involved gene. However, modern molecular genetics has allowed the identification of pedigrees with a known inherited disease, linkage to a genetic locus, cloning of the involved gene, determination of the protein sequence, and establishment of a putative protein function. As a result, some diseases that were previously classified as inherited "neurodegenerative" diseases of unknown etiology are today recognized as genetic defects, even though the protein function is not fully understood. These disorders are classed in this chapter as *hereditary metabolic diseases*.

Many of the hereditary metabolic diseases are associated with genetic defects involving specific cellular organelles. Three major organelles are associated with specific metabolic disorders: *lysosomes*, *peroxisomes*, and *mitochondria*.

As a general rule, disorders involving lysosomal proteins tend to involve catabolic pathways, and the lack of a lysosomal enzymatic function is often associated with accumulation of a metabolite for which the catabolic pathway is defective. The accumulation of the nondegraded metabolite in lysosomes is often referred to as a "storage" disease and may lead to distention of nerve cell bodies and their processes, glia, blood-vessel walls, or visceral cells.

Other disorders involve peroxisomes. In peroxisomal disorders, which commonly involve catabolism of a specific metabolite, serum levels of the metabolite are often increased. In contrast to lysosomal disorders, however, there is less tendency for intracellular storage of the metabolite.

In mitochondrial disorders, serum levels of intermediary metabolites are often normal, although impairment of oxidative phosphorylation may lead to elevations of lactic acid. In addition, the mitochondrial genes encoded in nuclear DNA have a mendelian pattern of inheritance, but genes encoded in mitochondrial DNA (mtDNA) have a maternal pattern of inheritance.

Metabolic disorders of the nervous system are also often classified on the basis of the region of the nervous system that is involved. Diffuse involvement of the brain creates a clinical picture of mental retardation or encephalopathy. Involvement of the cerebellum is often associated with ataxia, and involvement of the peripheral nervous system with a peripheral neuropathy.

Some disorders tend to affect neurons, and may do so within specific regions. Disorders which involve gray matter (i.e., neuronal cell bodies) are termed *poliodystrophies*, whereas those involving the white matter are termed *leukodystrophies*. The

latter disorders are characterized by loss of myelin (demyelination). Genetic leukodystrophies in which the renewal of myelin may be impaired due to abnormalities in the structure of myelin are often considered "dysmyelinating" disorders rather than "demyelinating" disorders. Pathologically, however, the process is characterized by loss of myelin with a relative preservation of axons.

The characteristics and staining properties of the myelin breakdown products have also been used in the classification of the leukodystrophies (see Chap. 7), leading to the distinction between a majority of "orthochromatic" or "sudanophilic" leukodystrophies, in which the normal catabolism of myelin results in the accumulation of neutral lipids, and a "metachromatic" leukodystrophy, in which the abnormal catabolism of myelin results in accumulation of sulfated cerebrosides. These shift the absorption spectrum of light such that the color of the stained tissue is different from the color of the stain, a property known as *metachromasia*.

Lysosomal Enzyme Deficiencies (Storage Diseases)

Deficiency of a specific lysosomal enzyme required for the lysosomal catabolism of a particular metabolite (usually a lipid) is often accompanied by the accumulation of the lipid metabolite (*storage disease*). Current classifications refer to the lipids involved and to the enzyme defects responsible for their accumulation, rather than to clinical features. However, distinct clinical syndromes are recognized, and are often named after the author of the first clinical description.

The chief lesions in the CNS involve both the cerebrum and cerebellum; they often consist of neuronal storage (with enlargement of the neuronal cell body) and, ultimately, neuronal loss and gliosis. When involvement of white matter is the predominant abnormality, the disease is characterized as a *leukodystrophy*. In some diseases, brain lesions are accompanied by peripheral nerve disease caused by injury of the Schwann cells and peripheral myelin sheaths. Storage of the metabolic product in lysosomal storage diseases also often occurs in the heart, liver, kidney, spleen, or eye. Ocular storage may be seen on ophthalmic examination as a "cherry red" spot as a result of storage

within retinal ganglion cells, and involvement of viscera may be detected as hepatosplenomegaly or cardiomyopathy.

Deficiencies in specific lysosomal proteins cause the accumulation of sphingolipids (gangliosides, cerebrosides, and sulfatides), mucopolysaccharides, and neutral lipids.

Sphingolipidoses

Sphingolipidoses are the most common lysosomal storage diseases. The catabolic enzyme defect is located in lysosomes and impairs the breakdown of the sphingolipid. Accumulation of the sphingolipid is the most common result, although "shunting" of the metabolite into another pathway may also occur (see later discussion of Krabbe disease). Sphingolipids are defined by the presence of a ceramide (*N*-acylsphingosine) and either a sugar or phosphocholine moiety. When a sugar moiety is present (galactose or glucose), the metabolites are cerebrosides; when a phosphocholine is present, the metabolite is sphingomyelin; when a sulfated sugar is present, the metabolite is a sulfatide; and when multiple sugar moieties are present, including sialic acid (*N*-acetylneuraminic acid), the metabolites are gangliosides.

Gaucher Disease

Gaucher disease (or *glucoceramidosis*) is an autosomal recessive disease caused by a deficiency of glucocerebroside β-glucosidase, which catabolizes glucosylceramide into ceramide and glucose. The disease is characterized by the accumulation of glucocerebroside within lysosomes and involves the bone marrow, liver, and spleen. The most common form (type I) has an onset in adults and the CNS is not affected. Involvement of the nervous system occurs only in the infantile severe (neuronopathic) form. The relevant gene (*GBA*, for *glucosidase, beta acid*) is located on chromosome 1q21. Mutations in this gene are responsible for all clinical forms of the disease. Although specific mutations are associated with specific clinical phenotypes, there is no correlation with enzyme activity measured in vitro.

In the typical form (type I Gaucher disease), hepatosplenomegaly is common and pancytopenia

results from replacement of the marrow with storage cells. The storage cells are predominantly macrophages and are known as *Gaucher cells*. They are found in large numbers outside the nervous system, sometimes appearing to have almost replaced the normal parenchyma of the liver, lymph nodes, marrow, and especially spleen. These large (30 to 40 μm) cells are distended with cerebrosides. The parallel cleft vacuoles give the cells a distinct appearance that has been described as resembling crumpled tissue paper. Under electron microscopy, the cells contain tubular, sickle-shaped profiles measuring 12 to 30 nm in diameter.

In the neuronopathic form (type II Gaucher disease) and in the rare juvenile form (type III, which has a prolonged course characterized by dementia), Gaucher cells are present in the brain, where they are distributed chiefly around blood vessels. Accumulation of glucocerebroside within the neurons themselves is variable and usually discrete.

Survival in type I Gaucher disease is variable, usually depending on the severity of liver and bone marrow involvement. Type II neuronopathic Gaucher disease has a severe and rapidly progressive course, with death usually occurring before the age of 2.

Krabbe Disease

Krabbe disease (also termed *globoid-cell leukodystrophy* or *galactocerebroside-β-galactosidase deficiency*) is an autosomal recessive leukodystrophy caused by a deficiency of the enzyme galactosyl ceramidase (galactocerebroside-β-galactosidase, GALC), which is necessary for the catabolism of galactosyl ceramide (galactocerebroside), an integral component of myelin. A gene located on chromosome 14q31 encodes GALC. Krabbe disease is a rare condition and is the only sphingolipidosis in which accumulation of the metabolite (galactocerebroside) does not occur. Rather, the block in catabolism of galactocerebroside leads to shunting of galactocerebroside to psychosine (galactosylsphingosine), with consequently elevated levels of psychosine. This has a toxic effect on oligodendrocytes in culture, and has been postulated to impair the maintenance of myelin. Instead of neuronal storage of galactocerebroside, there is destruction of white matter, result-

ing in an infantile leukodystrophy. Usually the onset is before the age of 6 months and the clinical course is rapidly progressive, with death occurring before the age of 2 years.

Demyelination is widespread, resulting in atrophy of the white matter of the cerebrum and cerebellum and marked fibrillary gliosis. A common feature of the disease is the presence of rounded macrophages with a large amount of cytoplasm, known as "globoid" cells. They may measure up to 40 μm, with irregular outlines, and are often multinucleated. Globoid cells occur throughout the white matter of the CNS (but are not present in the peripheral nervous system [PNS]). They may be found singly, but are more often grouped to form perivascular collections (Figs. 10-1A and B). Under electron microscopy, globoid cells are seen to contain intracytoplasmic inclusions that appear as elongated, cleftlike, empty spaces, sometimes bordered by an osmiophilic limiting membrane; they are variably needle- or splinter-shaped or gently curved, 10–100 nm in width, and of indeterminate length.

Involvement of the PNS may also be found. The clinical manifestation referable to the PNS is hyporeflexia, particularly in the childhood variants of the disease. Loss of myelinated fibers and relative preservation of unmyelinated axons are the outstanding findings, though segmental demyelination and remyelination also occur. Under electron microscopy, inclusions similar to those seen in globoid cells may be seen in histiocytes and Schwann cells (Fig. 10-1C).

There is no storage of galactocerebroside in the liver or spleen and no visceral enlargement or dysfunction. Death usually occurs before the age of 2.

Niemann-Pick Disease

Niemann-Pick disease is an autosomal recessive, multiorgan storage disease with several forms, each sharing the defining feature of accumulation of sphingomyelin. Sphingomyelinase is the enzyme that catalyzes the breakdown of sphingomyelin to phosphocholine and ceramide. There are at least three distinct genetic loci, and multiple distinct clinical forms of the disease at the different loci. Clinical forms A and B involve the gene for acid sphingomyelinase (chromosome 11p15.4-p15.1) and are the forms of "classic" Niemann-Pick
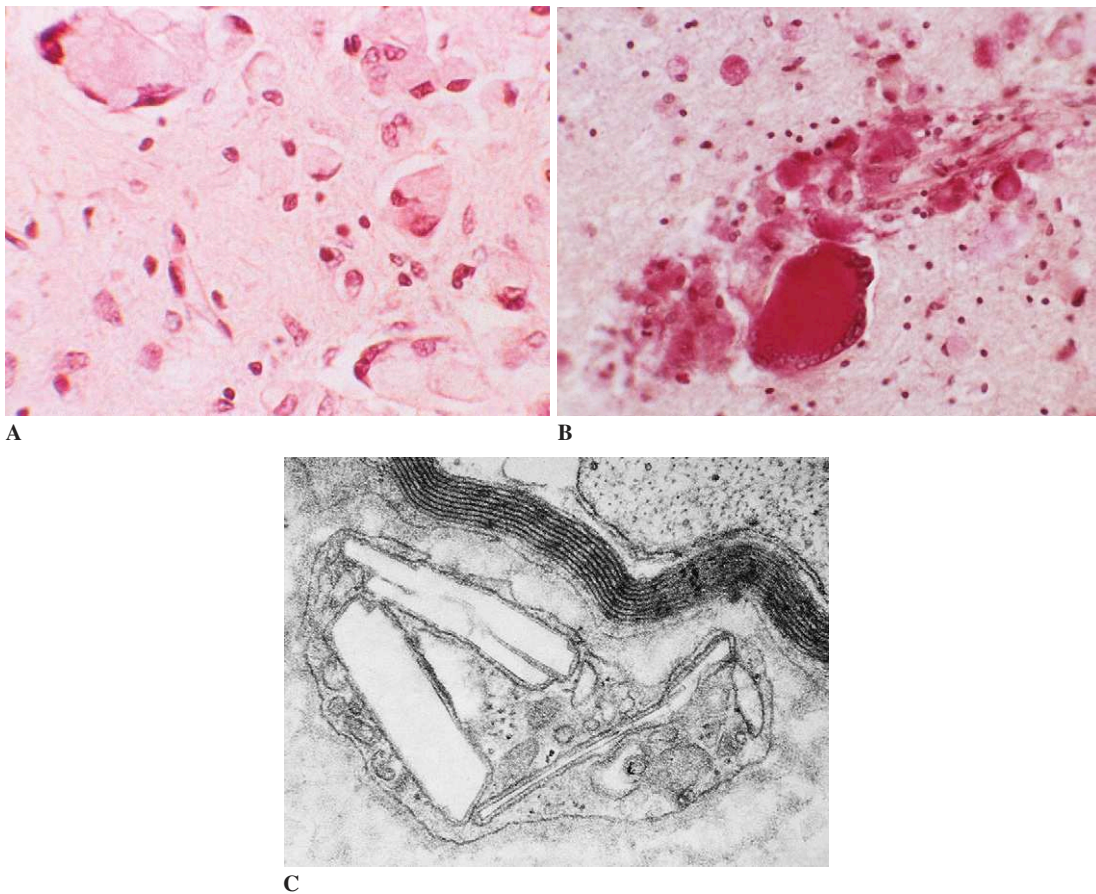
Figure 10-1. Krabbe disease. **A**, Globoid cells (H and E). **B**, Globoid cells with a perivascular distribution (PAS). **C**, Electron microscopy of peripheral nerve showing characteristic inclusions in a Schwann cell.

disease with sphingomyelinase deficiency. Clinical forms C and D involve the gene encoding pro-saposin (chromosome 18q11-q12), a cofactor required for sphingomyelinase catabolism. In type D (Nova Scotia variant), there is sphingomyelin storage but normal sphingomyelinase activity.

The nervous system is prominently involved in the acute infantile form (type A), which is most common in Ashkenazi Jewish populations. There is severe hepatosplenomegaly, a cherry-red spot of the retina, a diffuse reticular infiltration of the lungs, and a rapidly progressive encephalopathy. Hypotonia may be present in the early course, but there is gradual loss of motor function and intellectual deterioration. Death usually occurs by the age of 3.

Type B is more variable in presentation and progression but much less severe than type A. Patients do not have neurologic involvement but present with massive hepatosplenomegaly, often detected on routine physical exam. Survival into adulthood is common.

Type C is less common and has a slower clinical course; it may also involve the nervous system. However, the neurologic manifestations appear later in the course of the disease.

Type D (Nova Scotia variant), which may also involve the CNS, has been reported as a separate type, but many sources now consider it a syngenic variant of type C.

Type E had been distinguished as an adult-onset disorder but is now viewed as type B with late onset.

All of the forms of Niemann-Pick disease, regardless of the gene involved, are characterized by the presence of large macrophages with distended cytoplasm. These large cells have round, clear vacuoles visible under both light microscopy

Figure 10-2. Niemann-Pick disease. Electron microscopy of a foam cell.
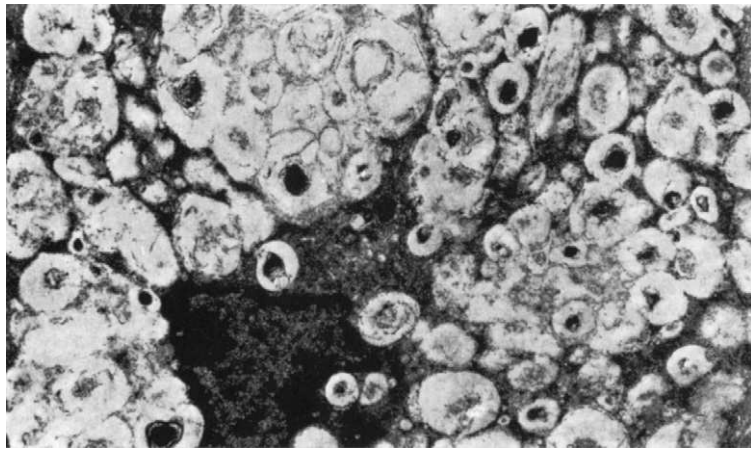
and electron microscopy and have been called *foam cells* (Fig. 10-2), regardless of location. They are often detected on bone-marrow biopsy but also occur in the liver, spleen, and lymph nodes. Involvement of the nervous system occurs in types A, C, and D. Type A shows marked atrophy of the brain with severe gliosis. Types C and D may show atrophy, but the finding is more variable. In all three forms (A, C, and D) there are abundant large neurons with distended cytoplasm and many small, round, clear vacuoles. Histochemical studies performed on frozen sections may demonstrate the presence of neutral lipids. Patients with onset of the disease in infancy, who have severe involvement of the CNS, sometimes show evidence of PNS involvement characterized morphologically by the presence of lamellated inclusions and empty vacuoles in the cytoplasm of Schwann cells and in endoneurial and perineurial fibroblasts.

Farber Lipogranulomatosis

Farber lipogranulomatosis (also termed *ceramidase deficiency* or *Farber disease*) is an autosomal recessive disorder resulting from deficient activity of acid ceramidase, a lysosomal enzyme required for the catabolism of ceramide into sphingosine and fatty acids. Ceramide consequently accumulates in excess in various tissues, including the central and peripheral nervous system. A gene located on chromosome 8p22-p21.3 encodes the acid ceramidase protein.

The characteristic feature of the disease is the development of periarticular and perivascular nodules that are composed of lipid-filled macrophages typically accompanied by a granulomatous inflammatory reaction. The nodules are often first detected in the skin, where they form readily visible subcutaneous nodules. Similar lipogranulomas may also involve the joints, bones, and kidneys. In the CNS, the large neurons of the anterior horns of the spinal cord and their homologues in the brainstem appear distended with lipid inclusions, and are the main structures affected. Peripheral (sensory and autonomic) ganglion cells are also affected. Characteristic inclusions (curvilinear tubular structures) are also seen in capillary endothelial cells in the CNS.

Fabry Disease

Fabry disease (also termed *angiokeratoma corporis diffusum* or *α-galactosidase deficiency*) is a rare, X-linked recessive disorder due to a deficiency of the hydrolase enzyme α-galactosidase. This enzyme is coded on the long arm of the X chromosome (Xq21.33-q22). α-Galactosidase deficiency results in the accumulation of glycosphingolipids, particularly globotriaosylceramide; this forms abnormal intracellular lipid inclusions (foam cells), especially in vascular endothelial and smooth muscle cells.

Clinically, Fabry disease is characterized by the development of angiokeratomas of the skin and mucous membranes, and by corneal changes (cornea vertilata). The disease commonly results in life-threatening pathologic changes in the kidneys, heart, and cerebral blood vessels, leading to renal

or cardiac failure or multiple strokes. Gastrointestinal dysfunction is likewise frequent; this has been attributed to lipid inclusions in the myenteric plexus. Common symptoms suggesting involvement of the PNS are recurrent attacks of severe pain in the hands or feet, especially in the presence of heat, and absence of sweating.

Foam cells are found in the liver, spleen, and lymph nodes as well as in renal and cutaneous epithelial cells. The storage material is sudanophilic, periodic acid-Schiff (PAS) positive, and birefringent under polarized light (with a Maltese cross shape). Under electron microscopy, the inclusions are often seen to have a myelin-like lamellated structure, sometimes in parallel arrays, sometimes in concentric layers, with a periodicity of 5 nm. Some of them are membrane-bound, others not. Some, instead of being lamellated, are in the form of dense, osmiophilic aggregates.

CNS involvement is apparently limited to the amygdala, hypothalamus, hippocampus, entorhinal cortex, and brainstem nuclei. Neurons in these areas have reticular foam cytoplasm with abundant storage material. Storage is also seen in astrocytes, endothelial cells, and smooth muscle cells around blood vessels. In peripheral nerves, inclusions may be found in the cytoplasm of perineurial cells, vascular endothelial cells, and smooth muscle cells in the tunica media of arteries.

Gangliosidoses

All of the *gangliosidoses* are characterized by accumulation of gangliosides, which are composed of one ceramide molecule, up to four hexoses (galactose and glucose), and up to three molecules of sialic acid (*N*-acetylneuraminic acid). Gangliosides stain intensely with myelin stains in histologic sections (such as Luxol fast blue [LFB]), but do not stain appreciably with routine stain, so swollen neurons usually appear to have clear vacuoles on hematoxylin and eosin (H and E; Fig. 10-3A). Under electron microscopy, the perikarya of neurons are seen to contain membranous cytoplasmic bodies. These may have two appearances: (1) circular concentric profiles formed by alternating concentric electron-lucent and electron-dense bands, 5 to 6 nm wide, known as *membranous concentric bodies* (MCBs); and (2) oblong profiles with alternating linear electron-lucent and electron-dense bands, known as *zebra bodies* (Figs. 10-3B and C).

GM2 Gangliosidosis. *GM2 gangliosidosis* (also termed *Tay-Sachs disease, variant B,* and *hexosaminidase A deficiency*) is an autosomal recessive disease formerly known as "amaurotic idiocy" (to emphasize the blindness and intellectual deterioration). It is caused by mutations in the α subunit gene coding for hexosaminidase A (*HEXA*, chromosome 15q23-q24), with deficiencies in hexosaminidase A and S activities. Hexosaminidase A is composed of α and β subunits (encoded by the *HEXA* and *HEXB* genes, respectively). Hexosaminidase B is composed of two β subunits (*HEXB* gene), and hexosaminidase S is composed of two α subunits (*HEXA* gene). Mutations of the α subunit gene, therefore, lead to deficiencies of both hexosaminidase A and S activities.

Tay-Sachs disease occurs predominantly in Ashkenazi Jews, with a high mutation frequency in that population. Onset is in infancy, usually after birth but within the first few months of life. Patients show poor head control and other symptoms of psychomotor decline. In the early stages, the head and brain are enlarged but there is no visceromegaly. Gradual decline occurs, and death usually occurs within 2 years. The neuropathology is that of a neuronal storage disease, with greatly enlarged neurons with distended cytoplasm and large clear vacuoles seen on H and E. The microscopic features are the same as other gangliosidoses (i.e., PAS-positive on frozen sections, PAS-negative on routine sections, strongly LFB-positive, membranous concentric bodies on electron microscopy).

Sandhoff disease (also known as *variant O GM2 gangliosidosis*) results from mutations involving the HEXB gene, causing deficiency of hexosaminidase A and B activities (hexosaminidase S activity is preserved). Sandhoff disease does not show any particular ethnic predominance, and is clinically indistinguishable from Tay-Sachs disease.

Tay-Sachs disease AB variant, which is rare, is clinically and histologically identical with Tay-Sachs disease; however, there is normal hexosaminidase A and B activity. The disease is caused by mutations in the GM2 activator protein (*GM2A*, chromosome 5q32-q33).

GM1 Gangliosidosis. *GM1 gangliosidosis* is an autosomal recessive neuronal storage disease caused by a deficiency of β-galactosidase (gene, *GLB1*; chromosome 3p21.33). As in Tay-Sachs disease, onset is in infancy and there is early onset of
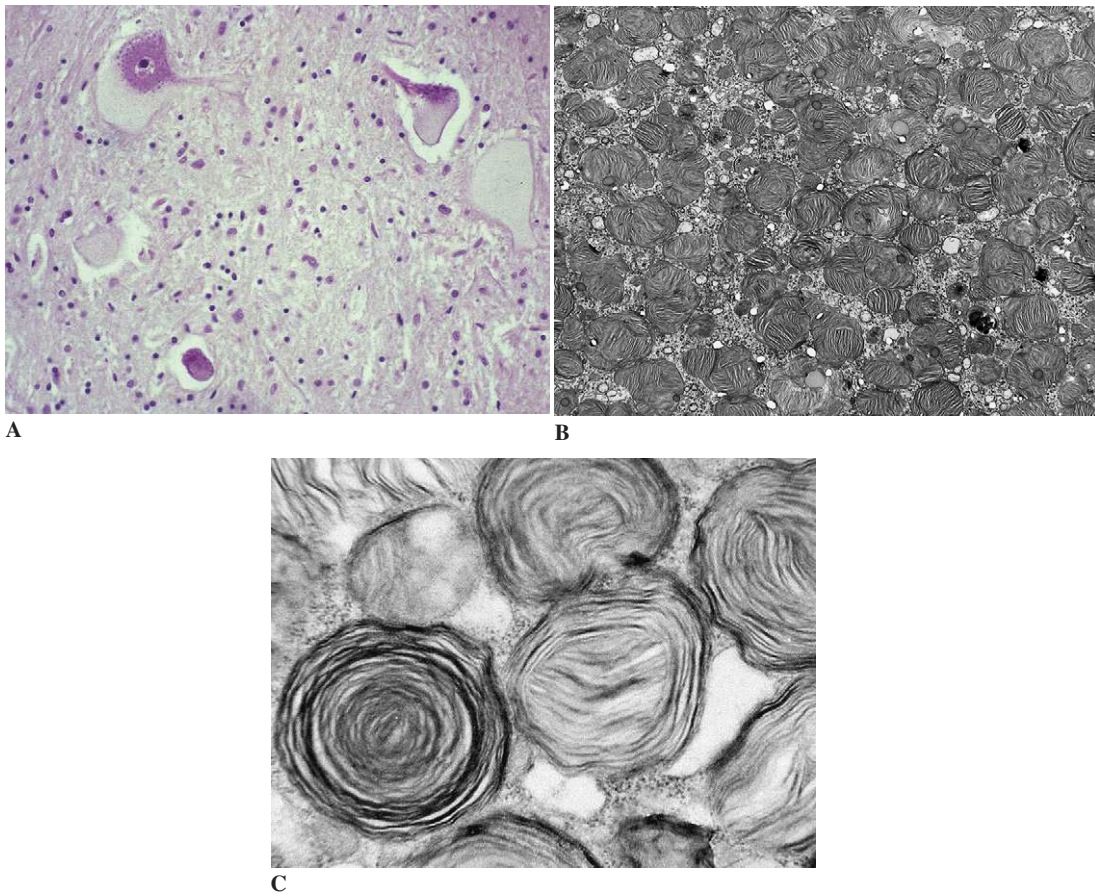
Figure 10-3. Tay-Sachs disease. **A**, Swollen neurons with clear peripheral vacuoles (H and E). **B** and **C**, Membranous cytoplasmic bodies on electron microscopy.

hypotonia and cherry-red spots. However, there are also signs of systemic involvement, including corneal opacities, depression of the nasal bridge, and hepatomegaly, features which are similar to Hurler disease, a mucopolysaccharide storage disorder. The disorder is, therefore, sometimes known as *pseudo–Hurler disease*. The staining properties of the gangliosides are similar to those in Tay-Sachs; however, storage material may also be found in the liver, spleen, kidney, and bone marrow.

Metachromatic Leukodystrophy
and Related Disorders

Metachromatic leukodystrophy is an autosomal recessive disorder resulting from a deficiency of lysosomal arylsulfatase A activity, which catalyzes the catabolism of the sphingolipid galactocerebroside sulfate (a sulfatide) to the corresponding

nonsulfated compound. These lipids are integral components of the myelin sheaths in both the central and peripheral nervous systems; deficiency of enzyme activity creates an excessive accumulation of sulfatides, which in turn results in breakdown of myelin and phagocytosis of its disintegration products. The disease most often occurs due to mutations in the gene for arylsulfatase, located on chromosome 22q13.31-qter. The differences in severity and onset are thought to be related to the residual enzyme activity associated with the two mutations affecting each allele, with the least enzyme activity associated with the late infantile form of the disease. The onset of symptoms in the disease may be during the infantile or juvenile periods or in adulthood. In the late-infantile form, clumsiness and spasticity are often early findings, with onset between 2 and 3 years of age. Progression is relentless, and death usually occurs in early childhood.

Sulfatide deposits accumulate in many tissues. They may be up to 20 or 30 µm in diameter and are PAS-positive and metachromatic (i.e., stain brown with acidic cresyl violet [Fig. 10-4B] and pink with toluidine blue). Under electron microscopy these lysosomal inclusions are seen to have a lamellar structure with a regular periodicity. They may be arranged concentrically, but parallel prismatic bodies or rectilinear "tuffstone" bodies (Fig. 10-4C) are also characteristic.

On gross examination, the brain may be atrophic, especially in longstanding cases. The entire white matter shows loss of myelin with sparing of the subcortical fibers (Fig. 10-4A). Myelin is largely absent throughout the entire centrum semiovale, and gliosis is severe, with scattered macrophages. Metachromasia is identified in the macrophages, which tend to have a perivascular location. In the PNS, there is demyelination and may be some onion-bulb formation. Schwann cells, macrophages, and occasionally axons may contain metachromatic material, and electron microscopy shows the characteristic inclusions (see Fig. 14-24).

Three important variants are known, which involve separate genetic loci:

1. Mutations involving the activator protein saposin B (*prosaposin* gene [*PSAP*], chromosome 10q22.1) lead to a condition that is indistinguishable in clinical appearance from arylsulfatase A deficiency but in which arylsulfatase activity is normal (i.e., metachromatic leukodystrophy with saposin B deficiency).
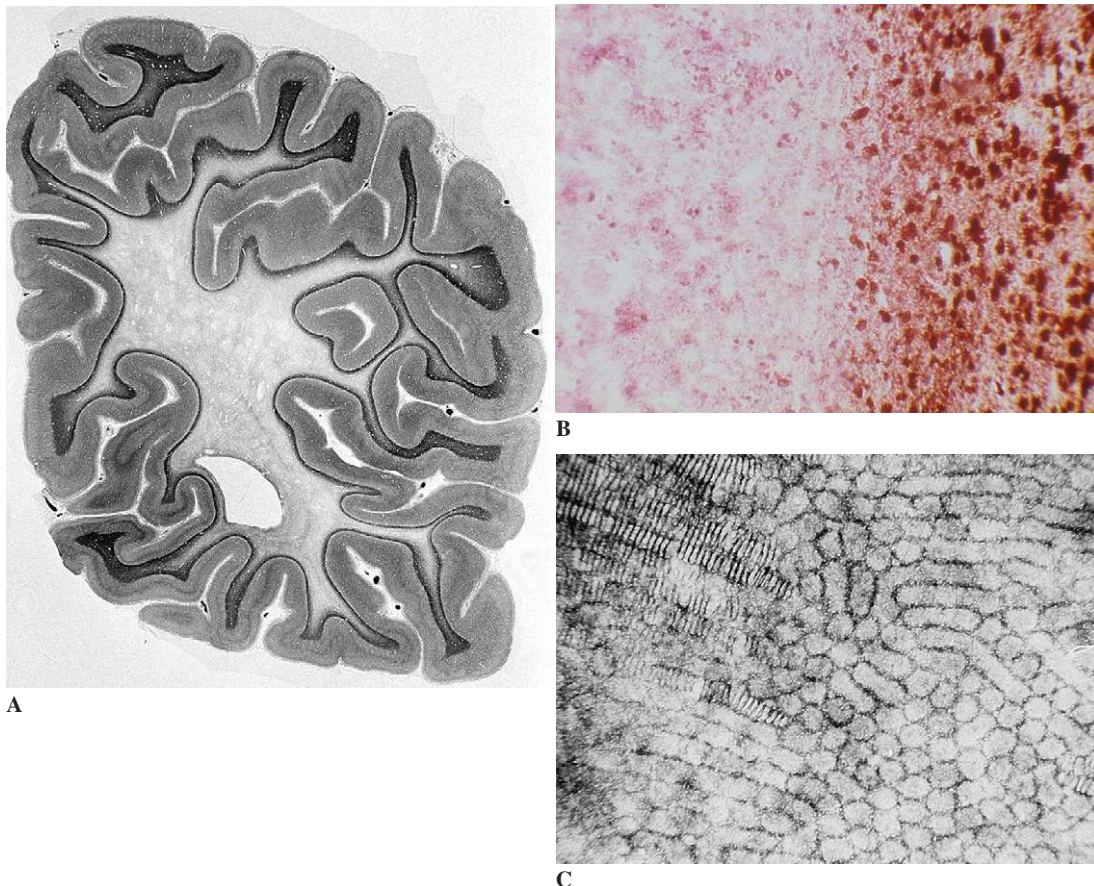
Figure 10-4. Metachromatic leukodystrophy. **A**, Massive demyelination sparing the U fibers in the right parieto-occipital region (Loyez). **B**, Metachromasia of the white matter, which stains brown with acidic cresyl violet. **C**, Sulfatide inclusion by electron microscopy.

2. Multiple sulfatase deficiency (Austin disease) is caused by an absence of activity of arylsulfatases A, B, and C. The sulfatide accumulation is accompanied by an accumulation of mucopolysaccharides, and patients have some facial and bony features that resemble those seen in Hurler disease.
3. Pseudodeficiency of arylsulfatase A is a benign mutation of the arylsulfatase gene, present in up to 2% of some populations.

Mucopolysaccharidoses

The nervous system, especially neurons, are involved only in certain forms of *mucopolysaccharidosis*. In such cases, a systemic disturbance of acid mucopolysaccharides (also known as glycosaminoglycans), which are excreted in the urine, is accompanied by a lipid neuronal storage disorder that involves gangliosides. Because of the secondary nature of the gangliosidosis, this group of diseases is usually excluded at this time from the neurolipidoses as a whole, but it should be stressed that in some forms the neuronal changes dominate the picture.

The histopathologic findings consist of an association of nervous system changes with alterations in the blood vessel walls. In the cerebral cortex and cerebellum the appearance of the swollen neurons is comparable to that seen in gangliosidoses, with the presence of zebra bodies (Fig. 10-5A) and other structures that are intermediary to the membranous cytoplasmic bodies of Tay-Sachs disease. Capillary pericytes may show marked vacuolation (Fig. 10-5B), which corresponds to the excessive accumulation of glycosaminoglycans. Vacuolization is found in the central nervous system, in various visceral organs (including the liver, myocardium, and bone marrow), and in lymphocytes. The vacuoles appear to be of lysosomal origin, as suggested by the demonstration of acid phosphatase.

The mucopolysaccharidoses that involve the CNS to the greatest extent are as follows:

- *Type I mucopolysaccharidosis* (Hurler syndrome: dermatan sulfate and heparan sulfate storage, α-L-iduronidase deficiency, gene locus 4p16.3). Facial and skeletal deformities (gargoylism) and nervous system lesions, which are usually discrete.
- *Type II mucopolysaccharidosis* (Hunter syndrome: dermatan sulfate and heparan sulfate storage, α-iduronate-2-sulfatase deficiency, gene locus Xq28). Similar to Hurler disease, with similar deposition of glycosaminoglycans but X-linked inheritance and absence of corneal opacities.
- *Type III A mucopolysaccharidosis* (Sanfilippo disease: heparan sulfate storage, heparan sulfate N-sulfatase deficiency, gene locus 17q25.3). Histologically similar to types I and II, but only heparan sulfate accumulates in excessive amounts.
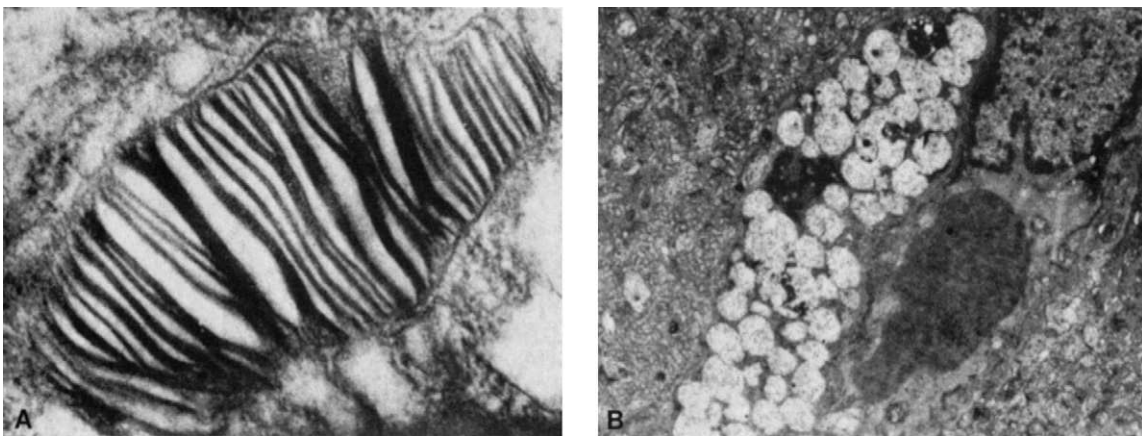
Figure 10-5. Mucopolysaccharidosis. **A**, Zebra body in Hurler disease. **B**, Vacuoles in a pericyte.

Enzymes Involved in Metabolism of Cholesterol and Other Lipids and Lipoproteins

Wolman Disease

Wolman disease (lysosomal acid lipase deficiency) is an autosomal recessive infantile disease with hepatosplenomegaly, gastrointestinal signs, and progressive neurologic deterioration caused by mutations of the gene for lysosomal acid lipase (*LIPA*, chromosome 10q24-q25) with resulting accumulation of cholesterol and triglycerides. Calcification of the adrenals is accompanied by lesions in the intestinal mucosa and by the presence of "foam cells" in the liver, spleen, and lymph nodes. The foam cells are derived from macrophages and have large clear vacuoles. In the CNS, the choroid plexuses, the leptomeninges, and the Purkinje cells are often affected. Death usually occurs before the age of 1 year.

Tangier Disease

Tangier disease (*hypo-α-lipoproteinemia*) is an autosomal recessive, multiorgan disease affecting cells of the lymphoreticular type, cornea, and the peripheral nervous system. It is caused by mutations in the ATP-binding cassette 1 (*ABC1*) gene. This gene is located on chromosome 9q22-q31 and encodes an ATP-binding cassette transporter, an important protein involved in regulating the intracellular transport of cholesterol.

The disease is characterized by near or total absence of circulating alpha lipoproteins. Histiocytes, which may be encountered in lymphoid tissues and bone marrow, transform to foam cells due to cholesterol ester accumulation. Tonsil hypertrophy, hepatomegaly, and splenomegaly are common. Nearly all patients have some degree of neuromuscular dysfunction during the course of the illness and about one third of patients come to medical attention because of polyneuropathy.

Neuropathologic features vary; there are three fairly distinct clinical syndromes. Sural nerve biopsies from patients with peripheral neuropathy characterized by remittent and relapsing asymmetric polyneuropathy have shown striking evidence of segmental demyelination and remyelination and very little overall fiber loss. Patients with a distal symmetric polyneuropathy have loss of large myelinated fibers and a relative increase in very small fibers, with evidence of remyelination and fiber regeneration (sprouting). In patients with a syringomyelia-like illness, mostly middle-aged adults, there is severe loss of small myelinated and unmyelinated fibers, with a tendency for the large myelinated fibers to be relatively spared. Accumulation of lipid droplets in Schwann cells is a constant feature.

Abetalipoproteinemia

Abetalipoproteinemia (*Bassen-Kornzwieg disease*) is a rare, hereditary (autosomal recessive) syndrome characterized by a combination of malabsorption of lipids, a chronic progressive peripheral neuropathy, pigmentary degeneration of the retina, and acanthocytosis (formation of burr cells) affecting red blood cells. Signs of cerebellar dysfunction (intention tremor, nystagmus) are frequently seen in association with peripheral neuropathy characterized by prominent sensory impairment, muscular weakness, and atrophy (leading to kyphoscoliosis and pes cavus in some cases).

The disease results from mutations of a gene on chromosome 4q22-q24 that encodes the microsomal triglyceride transfer protein (MTP). This protein catalyzes transport of lipids between membrane surfaces and is required for assembly of very low density lipoprotein (VLDL) particles in the liver. In the absence of functional MTP, the apolipoprotein is never assembled and released from the liver.

The peripheral neuropathy is characterized morphologically by marked loss of myelinated axons, especially large ones, and involvement of the posterior horns of the spinal cord. Retinal pathology entails loss of photoreceptors and pigmentary retinopathy with mobilization of retinal pigment epithelial cells, which enter the sensory retina to produce brownish pigmentation. The formation of finely granular lipopigments in peripheral nerve and skeletal muscle fibers resembles that seen in vitamin-E or α-tocopherol deficiencies, and tocopherol therapy has been found beneficial for Bassen-Kornzweig disease patients.

Cerebrotendinous Xanthomatosis

Cerebrotendinous xanthomatosis (CTX) is an autosomal recessive disorder of sterol metabolism that

results in extensive lipid deposition, mainly in large tendons (e.g., Achilles tendons and elbow regions) and in the CNS, where it is associated with ataxia, spasticity, premature atherosclerosis, and impaired intellect. CTX generally becomes manifest in young adult life and progresses slowly. It is caused by mutations of the *CYP27A1* gene (chromosome 2q33-qter), which encodes polypeptide 1 of the cytochrome P450, subfamily XXVIIA (required for sterol 27–hydroxylase activity). This enzyme activity is required for hydroxylation of a variety of sterols at the 27 position. In a few cases of CTX, there has been evidence of a peripheral neuropathy, both clinically and on sural nerve biopsies. The changes in the nerves have been those of relative loss of large myelinated fibers and segmental demyelination and remyelination with some onion-bulb formation.

Neuronal Ceroid Liposfuscinosis (Batten Disease, Kufs Disease)

The *neuronal ceroid lipofuscinoses* (NCLs), a group of disorders also called *Batten disease*, are the most frequent group of neurodegenerative diseases in children and are marked by neuronal loss and ubiquitous accumulation of intracellular lipopigments. There is also a rare adult form (*Kufs*

disease). The frequency is as high as 7 per 100,000 live births in some populations. These diseases are autosomal recessive progressive disorders of uniformly fatal outcome and are characterized by intralysosomal accumulation of lipid pigments that are positive for acid phosphatase and autofluorescent under light microscopy.

Infantile, late-infantile, juvenile, and adult forms may be recognized according to the onset of clinical symptoms. While the juvenile form is the most frequent one in Northern Europe and North America, the late-infantile form is the most frequent one in southern Europe and South America. The infantile form, however, predominates in Finland as one of the hereditary diseases of Finnish heritage and, though more rarely, may be encountered worldwide (as may the rare adult form).

The former classification of the NCLs, according to clinical subtypes, has recently been replaced by one based on genetic defects and numbering CLN1 to CLN8 (Table 10-1). In the two early childhood forms (CLN1 and CLN2), two different proteases (palmitoyl protein thioesterase 1 [PPT1] and tripeptidyl peptidase 1 [TPP1], respectively) are the deficient gene products. The other genetically identified forms (CLN3, CLN5, CLN6, and CLN8) are marked by deficiencies of structural transmembrane proteins, perhaps those affecting lysosomal loca-

Table 10-1. Current Classification of NCL (Neuronal Ceroid Lipofuscinosis)

Clinical Types	Chromosome	Gene Product	Genetic Types
INCL Santavuori-Haltia disease	1p32	Lysosomal palmitoyl protein thioesterase I	*CLN1*
LINCL Jansky-Bielschowsky form	11p15	Lysosomal tripeptidyl peptidase I	*CLN2, (CLN1)*
JNCL Batten-Speilmeyer-Vogt disease	16p12	Transmembrane CLN3 protein (battenin)	*CLN3, (CLN1)*
ANCL Kufs disease	Not known	Not known	*CLN4, (CLN1)*
LINCL Finnish variant	13q31–32	Transmembrane CLN5 protein	*CLN5*
EJNCL, LINCL Indian/Czech Gypsy variant	15q21–23	Transmembrane CLN6 protein	*CLN6*
LINCL	Not known	Not known	*CLN7*
"Northern" epilepsy +LINCL Turkish variant	8	Transmembrane CLN8 protein	*CLN8*

INCL = infantile NCL, LINCL = late-infantile NCL, EJNCL = early juvenile NCL, JNCL = juvenile NCL, ANCL = adult NCL.

tion. These proteins have been designated, respectively, the CLN3, CLN5, CLN6, and CLN8 proteins (the CLN3 protein also having been named *battenin*). For in vivo and prenatal diagnoses, biochemical activities of PPT1 and TPP1 may be measured and found severely reduced or absent in CLN1 and CLN2, respectively. CLN4 represents the unknown genotypes, including the adult cases.

NCLs are uniformly fatal disorders. The late infantile form results in death during the second decade of life; juvenile NCL may last to the third or even fourth decade of life, depending on intensity of supportive treatment; and patients who have Kufs disease usually succumb less than 10 years after onset.

In affected children, the clinical tetrad of visual disturbance (ending in blindness from retinal degeneration), ataxia, seizures, and dementia may be encountered in each form, although with a different onset of first symptoms and sequence of subsequent clinical findings. The ocular fundi show thinning of the degenerating retina and brownish pigmentation. However, visual disturbances or blindness are not a clinical component of the adult form (Kufs disease), and the electroretinogram is largely normal.

Brain lesions in NCLs involve predominantly the cortex (cerebral and cerebellar), resulting in almost complete depletion of nerve cells in the infantile form at autopsy, lesser depletion in the late-infantile form, some neuronal depletion in the juvenile form, and little neuronal loss in the adult form. Macroscopically, there is variable brain atrophy that correlates with onset and duration of the disease. It is particularly severe in the infantile and late-infantile forms (Fig. 10-6A), whereas the juvenile NCL cortex may display a brownish hue. Secondary loss of axons and myelin, shrinkage of the white matter, and dilatation of the ventricles and the subarachnoid space are also common.

Two nosologic microscopic features define NCL: (1) Loss of nerve cells, followed by cellular and fibrillar astrocytosis and proliferation of macrophages. (2) The intracellular, especially intraneuronal, accumulation of lipopigments. The latter feature may lead to enlargement of nerve cell perikarya (Figs. 10-6C and D) and proximal segments, albeit usually not to the degree seen in the gangliosidoses. Lipopigments are autofluorescent (Fig. 10-6B) and rich in acid phosphatase. They are PAS-positive and are stained by LFB (Fig. 10-6C). To various degrees, lipopigments may also contain the subunit C of mitochondrial ATP synthase and sphingolipid activator proteins that are demonstrable by immunohistochemistry. Immunohistochemical absence of the genetically deficient tripeptidyl peptidase enzyme protein in late-infantile NCL/CLN2 has been documented.

As the lipopigments in NCL show different ultrastructural patterns, conventional diagnosis of individual NCL forms may be achieved by electron microscopic examination of circulating lymphocytes, in which, as in cells found in numerous other types of sample (skin biopsies, appendectomy specimens, muscle biopsies), lipopigments accrue. A granular pattern may be seen in infantile NCL (Fig. 10-6E), curvilinear bodies are a hallmark of late-infantile NCL (Fig. 10-6F), fingerprint profiles within membrane-bound lysosomal vacuoles are indicative of juvenile NCL (Fig. 10-6G), and genetic late-infantile variants show a mixture of curvilinear and fingerprint profiles within the circulating lymphocytes. In adult NCL, lymphocytes have not been found to be affected by lipopigment formation. Apart from granular material, fingerprint profiles have been identified in neuronal lipopigments (Fig. 10-6H), and curvilinear/rectilinear lipopigment profiles have been identified in skeletal muscle fibers in Kufs disease. Prenatal electron microscopy may reveal granular lipopigments in the infantile type and lamellar inclusions in juvenile NCL within stromal cells of chorion vessels, whereas late-infantile NCL is prenatally marked by curvilinear bodies within amniotic fluid cells.

Figure 10-6. Neuronal ceroid lipofuscinosis (NCL). **A**, Gross appearance. Considerable atrophy of the cerebral hemispheric and cerebellar cortex. **B**, Cerebellar cortex. Presence of autofluorescent pigment in the Purkinje cells (H and E, seen by fluorescence microscopy). **C**, Intraneuronal accumulation of Luxol fast blue positive pigment. **D**, Semithin section, showing intraneuronal accumulation of lipofuscin (toluidine blue). **E–H**, Ultrastructural appearance of the lipofuscin pigment. Granular osmiophilic deposits in infantile NCL (**E**); curvilinear profiles in late-infantile NCL (**F**); fingerprint profiles in juvenile NCL (**G**); fingerprint profiles in granular matrix in adult NCL (**H**).

A
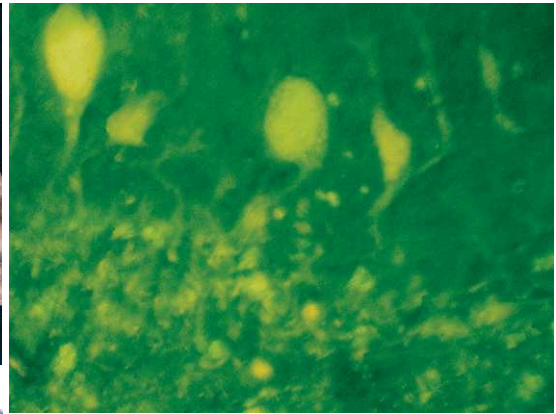
B
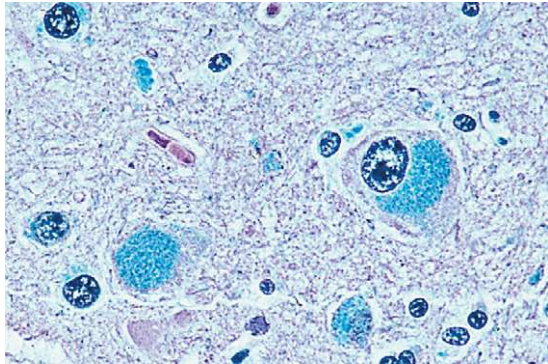
C
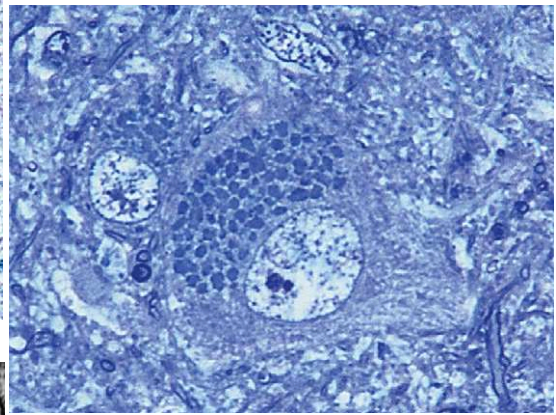
D
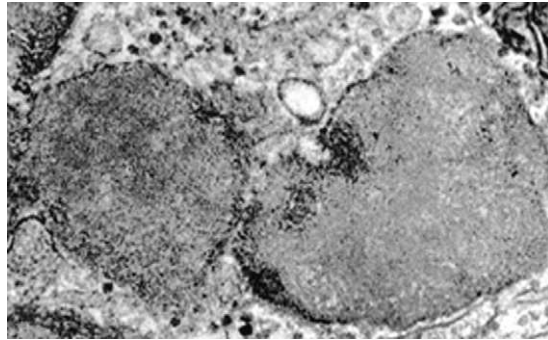
E
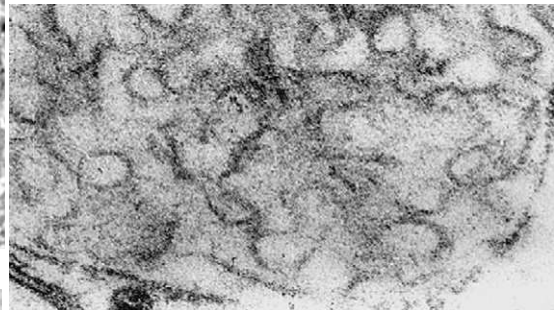
F
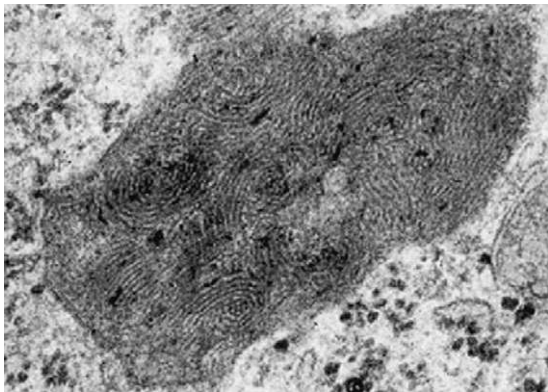
G
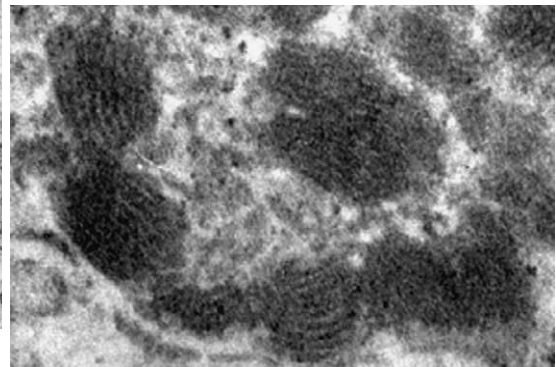
H

Disorders of Peroxisomal Function

Peroxisomes are intracellular organelles with a single membrane and a granular matrix visible under electron microscopy. Initially identified as "microbodies" by electron microscopy, peroxisomes contain catalase; their ability to cleave hydrogen peroxide via the enzymatic activity of catalase allowed their initial localization and is the basis for their name. They are involved in a number of metabolic pathways, including the initial pathway for breakdown of very-long-chain fatty acids (VLCFAs) and the catabolism of several organic acids (i.e., phytanic acid, glutaric acid, pipecolic acid). Defects in peroxisomal function may involve all of the enzymatic functions of the peroxisome due to failure of biogenesis of the organelle (as in Zellweger disease, neonatal Refsum disease, neonatal adrenoleukodystrophy), or may result in the deficiency of a single enzymatic function of the peroxisome.

Zellweger Disease

Zellweger disease (*cerebrohepatorenal syndrome*) is an autosomal recessive malformative syndrome caused by mutations in one of at least six genes involved in the biogenesis of the peroxisome. The six genes identified so far have been termed "peroxins," and mutations in *peroxin-1*, *peroxin-2*, *peroxin-3*, *peroxin-5*, *peroxin-6*, and *peroxin-12* have all been identified in Zellweger disease. Patients are symptomatic at birth, with dysmorphic features and severe hypotonia ("floppy baby"), and often have cataracts, retinitis pigmentosa, deafness, hepatomegaly, small renal cysts, pulmonary hypoplasia, and cerebral malformations. Death usually occurs before the age of 6 months.

Electron microscopy of patients with Zellweger disease has demonstrated an absence of peroxisomes, usually identified by special techniques that localize catalase in the peroxisome of control patients. Absence of peroxisomal function is identified by elevated serum levels of VLCFA, pipecolic acid, and phytanic acid.

The neuropathologic findings in patients with Zellweger disease are principally those of a neuronal migration disorder. The cortex may show polymicrogyria, pachygyria, or subcortical neuronal heterotopias, all findings that are associated with abnormalities of neuronal migration. Closely related, but less severe, disorders are *neonatal adrenoleukodystrophy* (NALD) and *infantile Refsum disease*. These disorders share the early onset and cerebral malformation findings of Zellweger disease but are less severe phenotypes with longer survival. NALD also has the inflammatory demyelination of adrenoleukodystrophy.

Adrenoleukodystrophy and Adrenomyeloneuropathy

Adrenoleukodystrophy (ALD) is an X-linked recessive leukodystrophy caused by mutations in the ALD gene, with a resultant defect in the catabolism of VLCFAs. The gene, located on chromosome Xq28, encodes a member of the ATP-binding cassette, subfamily D, member 1 (ABCD1), which is located in the peroxisome and is involved in transporting VLCFAs into the peroxisome for catabolism. In the absence of functional ABCD1, VLCFAs accumulate in the blood and brain. Accumulation is also evident in the adrenal, and may lead to functional hypoadrenalism.

In the classic juvenile form, young males often present with behavioral problems or adrenal insufficiency (Addison disease). The adrenal insufficiency, even when not the initial presenting symptom, is often associated with tanning. The disorder is rapidly progressive; initial demyelination can be detected in the occipital lobes by magnetic resonance imaging, but eventually progresses to entirely involve both cerebral hemispheres. Demyelination in the CNS is the predominant neuropathologic finding and is extensive and symmetrical (Fig. 10-7). Midline structures (corpus callosum, fornix) and the optic nerves and tracts are severely affected (Fig. 10-7A), and at late stages the demyelination may be accompanied by axonal loss and cavitary leukomalacia with secondary degeneration of the descending pathways. Myelin stains show the complete absence of myelin in the areas of chronic involvement, and the older central portion of the demyelinated lesion shows severe fibrillary gliosis. Scattered macrophages contain myelin degradation material, which stains with neutral lipid stains and is PAS-positive. At the periphery of the chronic lesions, macrophage infiltration is intense and is accompanied by a marked inflammatory infiltrate (Fig. 10-7C).
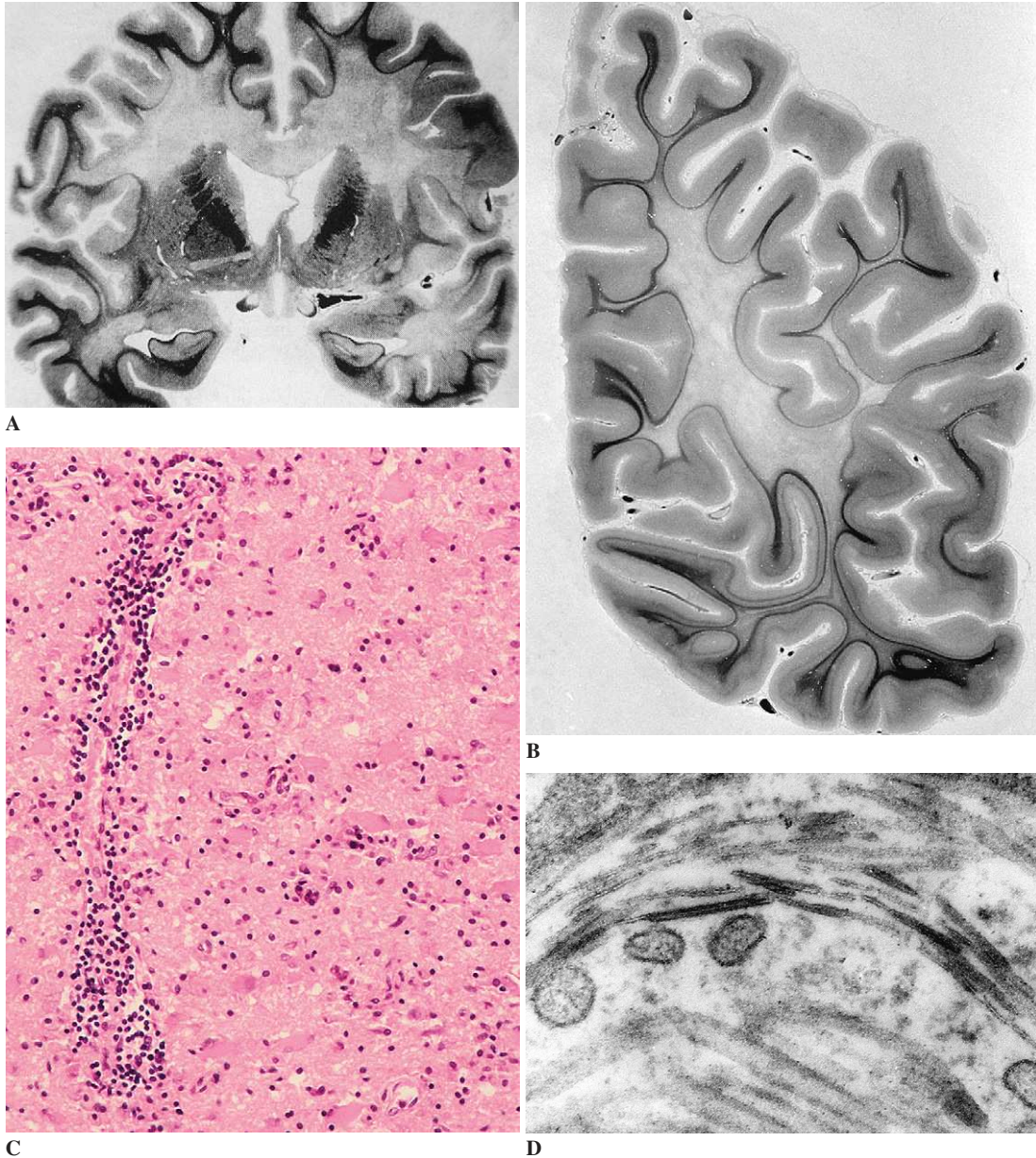
Figure 10-7. Adrenoleukodystrophy. **A**, Coronal section of the cerebral hemispheres at the level of the anterior commissure, showing symmetrical demyelination with marked involvement of the corpus callosum, anterior commissure, and optic tracts (Loyez). **B**, Massive demyelination sparing the U fibers in the right occipital lobe (Loyez). **C**, White matter. Severe myelin loss with macrophages, reactive astrocytosis, and perivascular inflammatory infiltrate (H and E). **D**, Electron microscopy, showing characteristic inclusions in a macrophage of the CNS.

The pathology in peripheral nerve is predominantly a demyelinating neuropathy, with thin myelin sheaths and segmental demyelination on tease fibers. Under electron microscopy, membrane-bound, cleft-like intracytoplasmic inclusions are seen, most typically in cells of the adrenal cortex, interstitial cells of the testis, and Schwann cells (see Fig. 14-23).

Under electron microscopy, storage material can be seen to form cleft-like inclusions composed of two lamellae that measure 2.5 to 3.5 nm in thickness and are separated by a clear space measuring from 4 to 10 nm (Fig. 10-7D). These inclusions are sometimes associated with lipid droplets. They are most readily identified in cells of the adrenal cortex, but may also be found in some macrophages in the CNS, in Schwann cells in peripheral nerves, and in interstitial cells of the testis.

Adrenomyeloneuropathy is the adult form of the disease and occurs in the same families with ALD. These patients present with clumsiness and ataxia, which results from involvement of the long tracts of the spinal cord and peripheral nerve. It may affect either hemizygous males or heterozygous females in families with ABCD1 gene mutations. Adrenal insufficiency is also common, and may be associated with slowly progressive spastic paraplegia.

Refsum Disease

Refsum disease is an autosomal recessive disease caused by a mutation in the gene (*PAHX*, chromosome 10pter-p11.2) encoding the peroxisomal enzyme phytanoyl CoA hydrolase (phytanic acid α-hydroxylase). It is characterized by progressive distal motor and sensory impairment, ataxia of trunk and limb movements, blindness (from pigmentary degeneration of the retina), and deafness of sensorineural type. Additional clinical manifestations, of varying degree, include anosmia, pupillary abnormalities, nystagmus, ichthyosis, skeletal deformities, and a cardiomyopathy that can lead to arrhythmias, cardiac failure, and early death. The disease makes its appearance in late childhood, adolescence, or early adult life, and, untreated, progresses gradually, though with occasional remissions.

The biochemical abnormality is a marked increase in the serum phytanic acid, a branched 20-carbon fatty acid. Accumulation of phytanic acid is due to the deficiency of phytanoyl CoA hydroxylase, the enzyme responsible for the first step in the catabolism of phytanic acid via alpha-oxidation within the peroxisome.

The peripheral nervous system shows a severe demyelinating neuropathy. The nerves (including the spinal nerve roots) are considerably enlarged as compared with normal. Microscopically, there are prominent onion-bulb structures interspersed with collagen fibers, creating a striking onion-bulb pattern. There is also an increase of perineurial and interstitial connective tissue. Axons, both myelinated and unmyelinated, are decreased in numbers. In the CNS, a cerebellar system degeneration is often present with neuronal loss in the inferior olivary nucleus and dentate nucleus and loss of fibers in the cerebellar peduncles. Posterior-column degeneration and loss of neurons in the gracile and cuneate nuclei have also been observed.

Disorders of Metabolism of Glycogen and Other Carbohydrates

Glycogenoses

The *glycogenoses* are glycogen storage diseases, which result in the intracellular accumulation of glycogen. Some, such as McArdle disease and Forbes disease, involve chiefly the skeletal musculature (see Chap. 13); the CNS is affected only exceptionally. Pompe disease (type II glycogenosis), which is caused by acid maltase deficiency (acid α-glucosidase deficiency), however, may involve the nervous system. The neurons of the anterior horns, some brainstem nuclei, the cerebellum, and, to a lesser extent, the cortex may be vacuolated and swollen and may, like the glia, show excessive storage of glycogen when examined by electron microscopy or stained with PAS. Acid maltase deficiency is unique among the glycogen storage diseases; due to the role of the enzyme in intralysosomal degradation of glycogen, its deficiency results in the intralysosomal storage of glycogen. The glycogen is surrounded by a lysosomal membrane, visible under electron microscopy (see Fig. 13-16C) and is associated with acid phosphatase in routine histologic sections. The disease often presents with a "floppy" infant, and is rapidly progressive with death by the age of 1 year.

Lafora Disease and Adult Polyglucosan Body Disease

Lafora disease is an autosomal recessive disorder characterized by progressive myoclonic seizures (see Chap. 12), caused by mutations of the laforin gene (*EPM2*, chromosome 6q24). *EPM2* encodes a protein with an amino acid sequence that suggests a protein-tyrosine phosphatase. The genetic defect results in an abnormality of carbohydrate metabolism, with the accumulation of polyglucosan bodies, the Lafora bodies (see Fig. 1-17), in a number of cell types.

In adults, storage of glucose polymer inclusions (polyglucosan bodies) has been described in the axons of the central and peripheral nervous systems, astrocytic processes, and some of the viscera, and are associated with progressive involvement of central and peripheral motor neurons, sensory disturbances, sphincter disturbances, and dementia. This form of "adult polyglucosan body disease" can be distinguished from the nonspecific presence of corpora amylacea—which may be numerous in the elderly—by the distribution of the inclusions in the cortex (Fig. 10-8B) and in the axons of the peripheral nerves (Figs. 10-8D and E) and by the presence of a diffuse or focal myelin pallor in the cerebral white matter (Fig. 10-8A).

Enzyme Deficiencies Without Intracellular Storage

In addition to enzyme deficiencies that lead to intracellular accumulation of a metabolic product ("storage diseases"), some metabolic disorders are due to a deficiency of the activity of a cytoplasmic enzyme that does not lead to storage or elevation of metabolites. In this category are included neuroaxonal dystrophies, the disorders of DNA repair, and defects in heme biosynthesis (porphyrias).

Neuroaxonal Dystrophies

Infantile Neuroaxonal Dystrophy (Seitelberger Disease and Schindler Disease)

Infantile neuroaxonal dystrophy (INAD) is a recessive autosomal disorder of infancy that is characterized by axonal enlargement with a dystrophic appearance (axonal dystrophy). The disease affects only the nervous system. It produces a wide distribution of spheroid bodies throughout the nervous system, which correspond to the axonal dilatations. The classic form, Seitelberger disease, is characterized by mental retardation, paralysis, and epilepsy. The metabolic basis and gene locus are not identified in these patients, but in a subset of patients with similar clinical and pathologic features (Schindler disease), a deficiency of N-acetyl-α-D-galactosaminidase is present, and in these patients, the disorder maps to the gene locus on chromosome 22q11.

On gross examination, the globus pallidus may be orange-yellow and the white matter has a chalky appearance (Fig. 10-9A). The ventricles may be dilated and there is frequently cerebellar atrophy. Microscopic studies have shown the presence of dystrophic axons, which have given the disease its name and which consist of rounded structures, measuring 10 to 20 μm. These axonal spheroids are argentophilic, weakly eosinophilic, and stain strongly with PAS. They are especially numerous in the gray matter of the spinal cord and the medulla and present in lesser number in the cerebellum, the pontine nuclei, the white matter of the spinal cord, the medulla, and the pons; they are rare in the cerebral hemispheres. Severe and diffuse cerebellar atrophy is common and includes almost total loss of Purkinje cells and granular neurons, as well as glial proliferation.

Axonal swellings are also seen in the peripheral nerves and in the nerve fascicles of the dental pulp, the skin, the conjuctiva, and the perirectal plexuses, thus permitting the diagnosis to be made by biopsy. Under electron microscopy, the axonal swellings are seen to be composed of tubulomembranous material, in contrast to other axonal swellings (Fig. 10-9B).

Neuroaxonal Dystrophy with Iron Accumulation, Type I (Hallervorden-Spatz Disease)

Hallervorden-Spatz disease is an autosomal recessive disorder caused by a mutation in the pentothenate kinase gene *PANKZ*, which is located on chromosome 20p13-p12.3. Onset is in the first or second decade with a survival of 15 to 20 years. Adult cases have been reported. Progressive rigidity is accompanied by involuntary movements
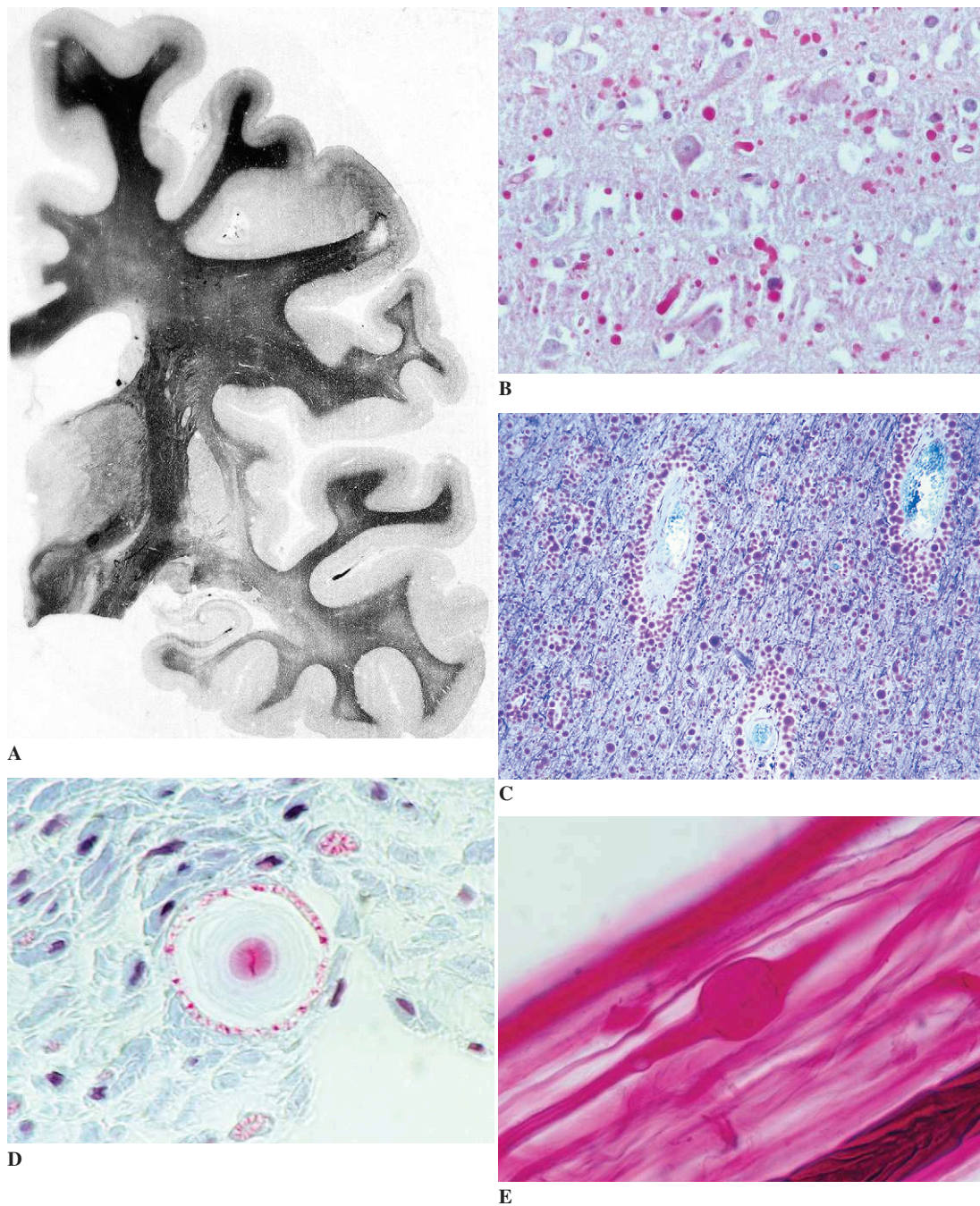
Figure 10-8. Adult polyglucosan body disease. **A**, Presence of multiple foci of myelin pallor in the cerebral white matter (Loyez). **B**, Cerebral cortex. Numerous polyglucosan bodies are present in the neuropil (PAS). **C**, Hemispheric white matter. Accumulation of polyglucosan bodies, especially in the perivascular regions (Cresyl violet–Luxol fast blue). **D** and **E**, Peripheral nerve biopsy. Intra-axonal inclusion stained with trichrome (**D**) and with PAS after teasing (**E**).
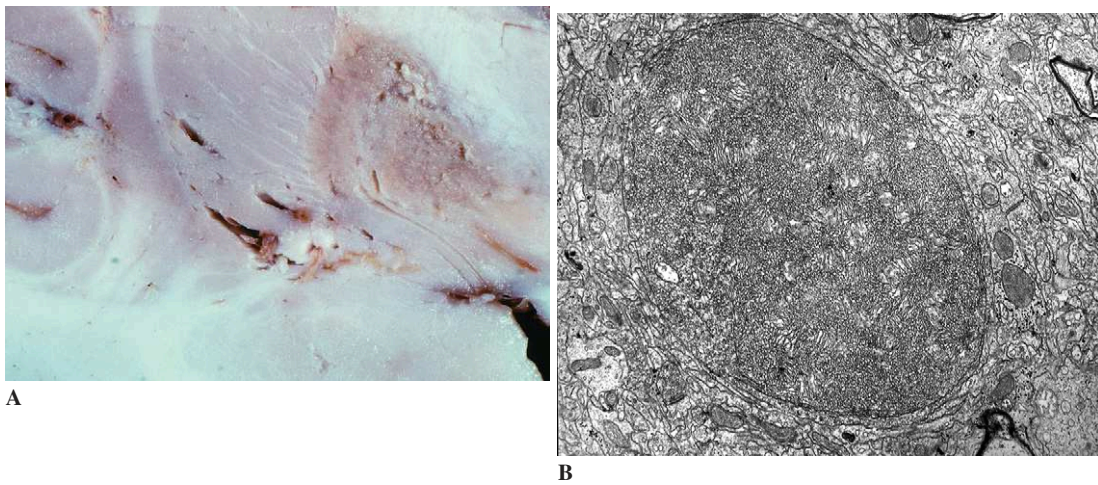
Figure 10-9. Neuroaxonal dystrophy. **A**, Orange-yellow discoloration of the globus pallidus. **B**, Electron microscopy of a swollen axon containing tubulomembranous material.

involving limbs, face, and tongue; mental deterioration; and, later, pigmentary retinopathy. Magnetic resonance imaging enables antemortem diagnosis of the disease, showing iron deposition in the globus pallidus and pars reticulata of substantia nigra. Gross examination of the brain shows orange-yellow discoloration of the globus pallidus and substantia nigra and iron deposition in the basal ganglia. The latter results from intracytoplasmic accumulation of iron pigment in neurons, astrocytes, and macrophages, or free in the parenchyma surrounding the blood vessels. Neuronal loss and gliosis are marked in the globus pallidus and inconstant in the cerebral cortex. The red nucleus and the subthalamus may also be involved. Axonal spheroids are abundant in the globus pallidus and substantia nigra. Ultrastructurally, the spheroids consist of packed membranes, dense bodies, tubules, and mitochondria.

Disorders Associated with Defective DNA Repair

Xeroderma Pigmentosum

Xeroderma pigmentosum is an autosomal recessive disorder that is mainly characterized by an abnormal degree of sensitivity of the skin and eyes to ultraviolet radiation and a greatly increased susceptibility to sunlight-induced malignant epithelial neoplasms. Neurologic abnormalities occur in 18% of patients; among these, the most frequent abnormality (occurring in 80%) is intellectual impairment, which often is progressive. In a smaller proportion of patients, there is evidence of involvement of the PNS (i.e., absence of stretch reflexes, ataxia, muscular wasting, and distal sensory impairment). Examination of peripheral nerves shows both demyelination and axonal degeneration, with endoneurial and perineurial fibrosis. The underlying defect is a lack of adequate mechanisms to protect or repair environmentally induced damage to DNA. This lack is caused by a defective nucleotide excision repair mechanism, required to repair DNA crosslinking of pyrimidine residues. A number of proteins are involved in the nucleotide excision repair mechanism, and mutations in genes encoding these proteins may all give rise to xeroderma pigmentosum.

Ataxia-Telangiectasia

Ataxia-telangiectasia (AT, also known as *Louis-Bar disease*) is a rare, autosomal recessive disorder that combines progressive neurologic symptoms (including cerebellar ataxia) and extrapyramidal and oculomotor disturbances with telangiectatic vascular proliferation in the skin and conjunctiva and defects in the immune system (involving both B-cell and T-cell function). Patients with AT are

prone to neoplastic diseases, particularly non-Hodgkin lymphomas and carcinoma of the stomach. It is caused by a defect in DNA repair. AT cells are abnormally sensitive to ionizing radiation.

Neuropathologic examination shows a constant and usually diffuse atrophy of the cerebellar cortex. It involves predominantly the Purkinje cells and the granular neurons and may be accompanied by neuronal cell loss in the dentate nuclei and the inferior olives. Nerve cell loss in the anterior horns and degeneration of the posterior columns are common, especially in longstanding cases. In the spinal root ganglia, neurons are small, the number of satellite cells is reduced, and the residual satellite cells may show marked nuclear abnormalities, as do the nuclei of Schwann cells in peripheral nerves.

The relevant gene, *ATM*, is located on chromosome 11q22.3 and encodes a phosphatidylinositol-3 kinase protein, a member of the group of proteins that respond to DNA damage by phosphorylating the substrates involved in DNA repair.

Cockayne Syndrome

Cockayne syndrome is a very rare, autosomal recessive disorder with mental retardation and photosensitivity. There are multiple genes that can give rise to Cockayne syndrome. *CKN1* and *ERCC6* are the genes affected in Cockayne syndrome types A and B, respectively. Each is involved in the repair of DNA following UV radiation, but neither is associated with increased incidence of malignancies.

Classic Cockayne syndrome, with a gene locus on chromosome 5 (*CKN1*), is associated with dwarfism, microcephaly, retinitis pigmentosa, deafness, and peripheral nerve involvement. The brain is atrophic, especially the cerebellum and brainstem. The demyelination, which is often subcortical, is a "tigroid" demyelination. Calcifications are present in the basal ganglia and in the dentate nuclei. A demyelinative peripheral neuropathy can be demonstrated electrophysiologically and neuropathologically.

Porphyrias

Porphyrias are a group of disorders of heme biosynthesis. Acute intermittent porphyria is a neurologic disorder characterized by acute psychotic episodes and acute-onset peripheral neuropathy. The disorder is due to a deficiency of porphobilinogen deaminase (uroporphyrinogen-1 synthetase) and chiefly causes a peripheral nervous system axonopathy. In the central nervous system, neuronal chromatolysis in the anterior horn cells and in the motor nucleus of the vagus may be associated with cerebellar lesions.

Mitochondrial Enzyme Deficiencies (Mitochondrial Encephalomyelomyopathies)

Mitochondrial encephalomyelomyopathies (MEs) are clinically heterogeneous disorders with multi-organ involvement. They are caused by dysfunction of the mitochondrial respiratory chain. Most of them involve muscle; morphologic and biochemical analysis of muscle biopsies allow the diagnosis (see Chap. 13). But abnormalities are not always present in skeletal muscle, especially when the CNS is predominantly involved.

Mitochondria contain their own DNA, which encodes 13 polypeptides (subunits of the respiratory chain, complexes I, III, IV, V), 22 tRNAs, and 2 rRNAs. The other subunits of the respiratory chain are encoded by nuclear genes. Mitochondrial disorders may thus be caused by mutations either in the mitochondrial or the nuclear genome; defects of intergenomic signaling may also interfere. There are two main types of mitochondrial (mtDNA) mutations: those that affect mitochondrial protein synthesis in toto and those that affect protein-coding genes. Disorders related to mtDNA mutations are sporadic or due to maternal transmission. Mendelian transmission characterizes nuclear DNA mutations and defects of intergenomic signaling.

Histologically most of the lesions are characterized by sponginess affecting gray and white matter, capillary proliferation, and some degree of neuronal loss and astrocytosis. Some of the diseases may overlap.

Leigh Disease

Leigh disease (also termed *subacute necrotizing encephalopathy*) is seen most often in early
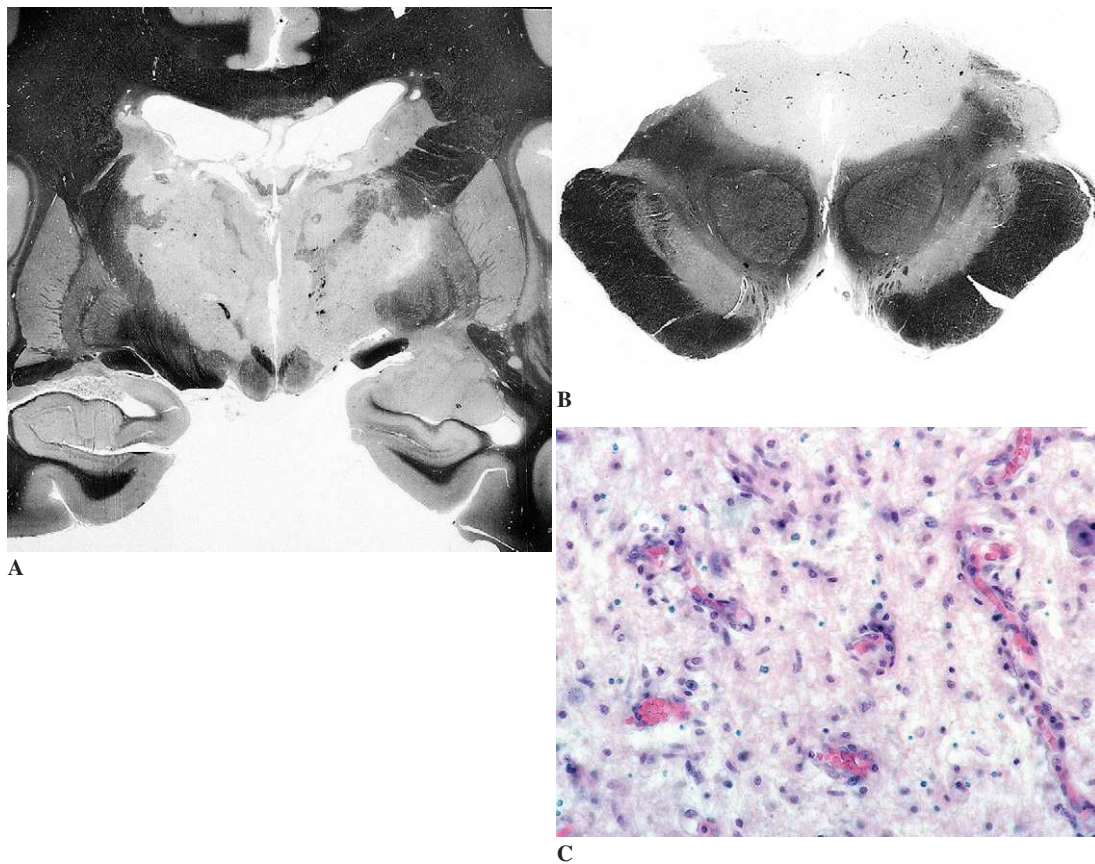
Figure 10-10. Leigh disease. **A**, Necrosis of the walls of the third ventricle and of the basal ganglia (Loyez). Note that the mamillary bodies are spared. **B**, Periaqueductal necrosis (Loyez). **C**, Microscopic appearance. Necrosis, macrophagic reaction, capillary proliferation, and relative neuronal sparing.

childhood, but variants with late onset have been described. The condition is characterized by the presence of symmetrical spongy, necrotizing lesions that affect both the gray and the white matter; they are predominantly located near midline structures. The basal ganglia (especially the putamen), thalamus (Fig. 10-10A), substantia nigra, subthalamic nucleus, tegmentum of the midbrain (Fig. 10-10B), inferior olives, and posterior columns of the spinal cord may be involved. The relative sparing of the neurons, the presence of gliosis, and especially the endothelial proliferation (Fig. 10-10C) closely resemble the lesions of Wernicke encephalopathy (see Chap. 9). Sponginess and demyelination are subsequently replaced by cystic cavitation, necrosis, and cortical pseudolaminar destruction. Sensory neuropathy is seldom recognized. Ultrastructural

studies show alterations of mitochondria, but only in a few cases. The same abnormalities may or may not be present in skeletal muscle.

Recent data have demonstrated the genetic heterogeneity of the disease, which may be related to the following defects:

- X-linked pyruvate dehydrogenase complex deficiency (subunit E1α).
- Abnormalities of the respiratory chain, that is, defects of nuclear genes of complexes I, II, and IV (mutations of assembly genes of cytochrome-*c* oxidase, such as *SURF1*).
- Abnormalities of mtDNA genes coding for ATPase 6 and tRNA (*Lys*).

Enzyme defects have been demonstrated in muscle biopsy material in a low percentage of cases,

and in the brain in an even lower percentage of cases. Congenital lactic acidosis may likewise cause necrotizing lesions in the hemispheric white matter.

Mitochondrial Encephalopathy with Lactic Acidosis and Stroke

Mitochondrial encephalopathy with lactic acidosis and stroke (MELAS) is defined by the association of mitochondrial encephalomyopathy, lactic acidosis, and stroke-like episodes. Other CNS signs include dementia, seizures, and deafness. Pathologically, infarct-like lesions are present in the cerebral cortex and subcortical white matter, often in the parieto-occipital lobes or cerebellum and rarely in the brainstem. The spinal cord may be involved. Calcifications of basal ganglia are common. Enlarged mitochondria—present in pericytes, smooth muscle cells, and endothelial cells of the terminal arterioles—have been considered responsible for the recurrence of transient cerebral ischemia. Ragged red fibers (see Fig. 13-15A) are usually abundant in muscle.

MELAS was first associated with a point mutation in the tRNA $Leu^{(UUR)}$(3243 A-G) gene but has also been associated with mutations in complexes I and IV (*Cox III*). It is usually maternally transmitted.

Myoclonic Epilepsy with Ragged Red Fibers

Myoclonic epilepsy with ragged red fibers (MERRF), also termed Fukuhara disease, is defined by the association of myoclonic epilepsy with ragged red fibers. Other signs include dementia, cerebellar ataxia, and deafness. Pathologically, the central and peripheral nervous systems and skeletal muscle are involved. The topographical distribution of lesions is reminiscent of neuronal system degeneration: degeneration of the dentatorubral and pallidoluysian system; spinal-cord lesions resembling Friedreich ataxia; and degeneration of the substantia nigra, cerebellar cortex, inferior olivary nucleus, locus caeruleus, gracile and cuneate nuclei, and pontine tegmentum. Many ragged red fibers are found in muscle.

MERRF was first associated with point mutations in the tRNA *Lys* gene (8344 A-G; 8356 T-C);

deficiencies in complexes I, III, IV (*Cox II*) have been reported subsequently. It is usually maternally transmitted.

Kearns-Sayre Syndrome

Kearns-Sayre syndrome (KSS) is defined as progressive external ophthalmoplegia and pigmentary retinopathy with onset before 20 years of age. Cardiac conduction block is important for prognosis. The disease progresses slowly and often develops more severe multisystem involvement. In the CNS, its pathologic hallmarks are neuronal loss and spongy to vacuolar myelinopathy of the brainstem and cerebellum. The lesions may extend to the cerebral white matter, with mineralization of basal ganglia and thalamus. Skeletal muscle nearly always displays ragged red fibers (see Chap. 13). Large-scale deletions of mtDNA are present in KSS ("common deletion of 4,977bp"). Most cases are sporadic.

Disorders of Copper Metabolism

Wilson Disease

Wilson disease (also termed *hepatolenticular degeneration*) is an autosomal recessive disorder of copper excretion with variable phenotypic expression. It is related to mutations of the Wilson gene on chromosome 13 (more than 190 mutations known). Its product is ATP7B, a cation-transporting, P-type ATPase with six copper-binding domains that is located in mitochondria. Characteristic brain lesions are found in the basal ganglia. These culminate, in advanced stages, in necrosis of the putamen with cavitation (Fig. 10-11A), whereas the globus pallidus, thalamus, and cerebral cortex are involved to a lesser extent. Less severe lesions consist of a spongy state with glial changes that involve the astrocytic nuclei. These are voluminous, pale, and multilobulated and present the picture of Alzheimer type II glia. More voluminous cells of macrophage/microglial origin with eccentric nuclei—Opalski cells—are also found scattered in the basal ganglia (Fig. 10-11B). Microscopic copper deposits encrust the astrocytes but are difficult to visualize. The disorder is also accompanied by cirrhosis of the liver, elevated copper
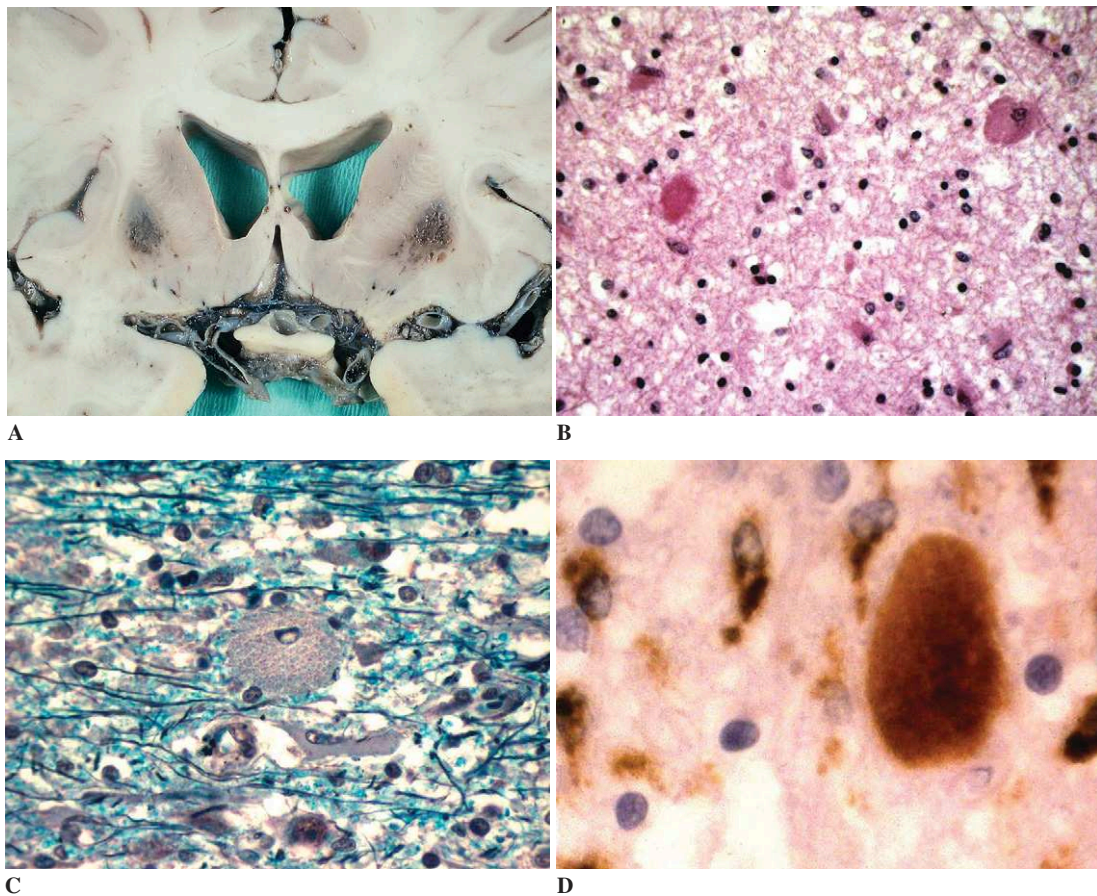
Figure 10-11. Wilson disease. **A**, Bilateral necrosis of the putamen. **B–D**, Opalski cells with eccentric nucleus and granular cytoplasm (**B**, H and E; **C**, Bodian–Luxol stain; **D**, Immunolabeling with the macrophage marker CD68).

levels, and Kayser-Fleischer rings (copper-colored rings at the periphery of the cornea). Mitochondrial dysfunction has been demonstrated in the liver but not in the brain.

Low serum levels of ceruloplasmin are a diagnostic feature of Wilson disease, but this is secondary to the decrease of the fixation of copper on apoceruloplasmin. The ceruloplasmin gene, located on chromosome 3, is intact. In contrast, in the rare cases of hereditary ceruloplasmin deficiency linked to a mutation of the ceruloplasmin gene, the major morphologic feature is the deposition of iron in the basal ganglia, particularly the putamen, thalamus, and dentate nuclei. Opalski cells and Alzheimer type II glia may be associated.

The distribution of iron deposition (putamen, thalamus) is quite different from that in Hallervorden-Spatz disease (globus pallidus, substantia nigra). It is also different from that in other diseases with iron deposition in the brain, such as idiopathic hemochromatosis (in which iron accumulates in the choroid plexus, area postrema, and other areas with defective blood-brain barrier) and subpial cerebral hemosiderosis (a rare consequence of smoldering subarachnoid hemorrhage).

Menkes (Kinky-Hair) Disease

Menkes disease (also termed *kinky-hair disease* or *trichopoliodystrophy*) is an X-linked disorder of copper uptake. The gene (at Xq13.3) codes for the copper-transporting ATPase 7A. There are low levels of copper and ceruloplasmin in the blood.

The disease causes abnormalities in the hair and neuropsychiatric manifestations. Pathologically, there are changes in the hemispheric myelin (temporal lobes) and lesions in the cerebellar cortex (granule and Purkinje cells) and blood vessel walls (thickening and splitting of elastic fibers).

Disorders of Amino-Acid Metabolism

Disorders of amino-acid metabolism are the cause of many syndromes of mental retardation in childhood and may be associated with various neurologic manifestations. Most are autosomal recessive disorders, and are characterized pathologically by a prominent spongiosis or cavitation of the white matter with accompanying gliosis. Different mechanisms are involved in the pathogenesis of the neurologic disorders, as amino acids have a role in neurotransmission, protein and lipid metabolism, and mitochondrial function. A direct toxic effect may be induced by abnormal accumulation of by-products. Diagnosis is usually made by identification of elevated amino acids or their by-products in serum or urine.

Canavan Disease

Canavan disease (also termed *spongy leukodystrophy*) is an autosomal recessive leukodystrophy caused by mutations of the gene encoding the enzyme aspartoacylase (ASPA gene locus 17 pter-p13). Aspartoacylase is the enzyme that cleaves *N*-acetylaspartate into aspartate and acetate, and its absence leads to elevated levels of *N*-acetylaspartate. Missense point mutations involving the aspartoacylase gene are the most common, but deletions have also been detected.

Symptoms include mental deterioration and megalencephaly. The onset is usually in the first 6 months of life, with death occurring by 18 months of age. The abnormality is exclusively in the CNS and consists of a spongy degeneration creating an increased volume of the brain with a soft, gelatinous consistency. The spongiosis often involves the subcortical white matter of the cerebral hemispheres and cerebellum (Fig. 10-12A) with intra-myelinic edema (Fig. 10-12B). Proliferation of Alzheimer type II astrocytes is common, and the

severity of demyelination usually parallels that of the spongiosis. Macrophages are infrequent.

Phenylketonuria

Phenylketonuria, the most common aminoaciduria, is due to absence of phenylalanine mono-oxygenase, which is coded by a gene on chromosome 12q24.1 and hydrolyzes phenylalanine to tyrosine. Elevated levels of phenylalanine result in retardation in neural development, and there is a relative deficiency of tyrosine, which becomes a dietary essential amino acid.

The neuropathologic findings are variable, but include microcephaly; spongiosis of the white matter; smaller-than-normal neurons with poorly developed dendritic trees; and pallor of the myelin of hemispheric and cerebellar white matter, optic tracts, and fornices (resembling the pallor seen in leukodystrophy).

Leucinosis

Maple syrup urine disease (*leucinosis*) is a neonatal disorder caused by a missense mutation of the E_3 subunit of the branched chain oxo-acid dehydrogenase complex. The gene is located on chromosome 19q13.1-13.2; the mutations induce a decrease of decarboxylase activity. Leucinosis is identified by the presence of sotolone in the urine, which has a characteristic caramel odor. Plasma concentrations of branched chain amino acids are increased, with a particularly elevated level of leucine. Leucinosis may cause spongy lesions in the white matter resembling those of Canavan disease but without evidence of myelin breakdown.

Homocystinuria

Homocystinuria is caused by a deficiency of cystathionine β-synthase activity, which normally couples homocysteine to serine to form cystathionine; the relevant gene is located on chromosome 21q22.3. The disease may cause alterations in blood vessel walls, with fibrosis of the intima, degeneration of the elastic fibers, and thromboses.
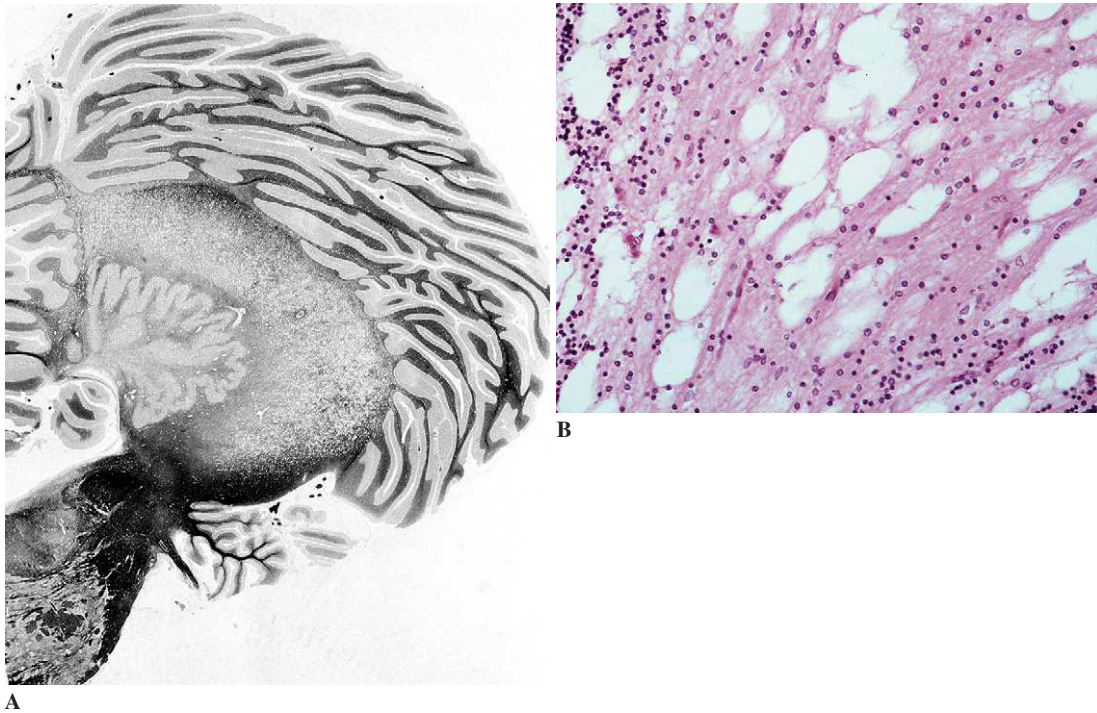
Figure 10-12. Spongy degeneration of the neuraxis (Canavan disease). **A**, Spongiosis of the cerebellar white matter (Loyez). **B**, Microscopic appearance. Intramyelinic edema (H and E).

Foci of cerebral necrosis of vascular origin are often found, also in adults.

Hartnup Disease

Hartnup disease is caused by a disorder of tryptophan absorption and produces a picture that resembles pellagra, with clinical features of dermatitis, dementia, and diarrhea and neuropathologic features of cortical atrophy and neuronal loss, especially in the occipital cortex and cerebellum. The relevant gene is located on chromosome 5p15.

Hyperglycinemia

Hyperglycinemia arises in two forms. In the ketotic form, there is a primary metabolic block, leading to severe acidosis and hyperglycinemia. The nonketotic form is due to a defect of the glycine cleavage enzyme system. Agenesis of the corpus callosum and gyral malformations are associated with vacuolation of the white matter and loss of myelin.

Urea-Cycle Disorders

Urea-cycle disorders are related to hyperammonemia, and result from a defect of conversion of ammonia to urea. The most common deficiency is that of ornithine carbamyltransferase; this is an X-linked disorder. Other forms include arginase deficiency, arginosuccinic aciduria, citrullinemia, and carbamylphosphate synthetase deficiency. Alzheimer type II astrocytes are frequent; in severe cases, the cerebral cortex and the deep gray matter may be involved.

Disorders of Structural Proteins

Unlike the metabolic disorders described thus far, some inherited diseases are caused by genetic mutations of genes encoding structural proteins. No

enzyme activity is known for these proteins; rather, the proteins are believed to play a structural role in the cell. Since they play no known role in cell metabolism, the classification of these disorders as "metabolic" diseases could be questioned; however, they share the genetic inheritance and typical clinical progression of other metabolic diseases, and were classified with the other inherited metabolic diseases prior to the identification of the genes involved.

Alexander Disease

Alexander disease is an autosomal recessive megalencephalic leukodystrophy caused by mutations of the GFAP (glial fibrillary acidic protein) gene. GFAP is the intermediate filament protein of glia, with individual subunits assembled into the 10-nm intermediate filaments. Point mutations are typically found and may be recessively inherited or occur as de novo mutations.

Infantile presentation is the typical clinical form and is characterized by mental retardation, seizures, spasticity, and enlargement of the brain (megalencephaly). Death usually occurs within 10 years of the age of onset. On gross examination, the white matter is softened and friable; the abnormality is especially prominent in the frontal lobes. There is massive demyelination involving the cerebral hemispheres (Fig. 10-13A), cerebellum, and, to a lesser degree, the brainstem and spinal cord. A unique histologic feature that sets Alexander disease apart from other leukodystrophies is a prominent accumulation of Rosenthal fibers. Rosenthal fibers are densely eosinophilic astrocytic processes filled with glial filaments and electron-dense structures composed of α-B-crystallin (Fig. 10-13C). In Alexander disease, they are particularly numerous around blood vessels (Fig. 10-13B), adjacent to the ventricular walls, and in the subpial zone.

Pelizaeus-Merzbacher Disease

Pelizaeus-Merzbacher disease is an X-linked recessive leukodystrophy, caused by mutations involving the proteolipid protein-1 gene (*PLP1*). Proteolipid protein-1 is a structural protein of CNS myelin, and point mutations, deletions, and gene duplications in *PLP1* have all been described in Pelizaeus-Merzbacher disease. In the classic, infantile form, infants have rotary movements of the head and eyes, and develop spasticity of the limbs, cerebellar ataxia, and parkinsonian symptoms during childhood. Death usually occurs in late adolescence. As in other leukodystrophies, the disease is characterized by the loss of myelin in the white matter. Due to the sparing of a few small islands of normal myelin, often in a perivascular distribution, the "striped" appearance of perivascular myelin sparing has been known as a "tigroid leukodystrophy" (Figs. 10-14A, C, and D). The cerebral and cerebellar white matter appears atrophic. Axons are relatively preserved and there is a severe gliosis. The myelin disorder is restricted to the central nervous system; the peripheral nervous system is usually spared, and visceral involvement is absent.

While the usual form of the disease presents in the first three months of life, a connatal form (congenital form of Seitelberger) is characterized by a virtually complete absence of CNS myelin (Fig. 10-14B) and severe symptoms in infancy.

Orthochromatic Leukodystrophies

The *orthochromatic leukodystrophies* are a heterogeneous group constituting a temporary category in which various familial or sporadic cases have been assembled. Some of these are infantile, presenting before the age of 5 and having a rapid course. Others present in adults and have a slow evolution. The latter represent the most frequent leukodystrophies in adults. The lesions involve the CNS only. Demyelination is diffuse, ill-defined, and often irregular (Fig. 10-15); it tends to predominate in the frontal lobes, which accounts for the frequency of psychiatric disorders. Axonal involvement is frequent. Macrophagic reaction is discrete and there is no inflammation.

In a few adult cases, sporadic or familial, the macrophages and glial cells contain a brown, autofluorescent, PAS-positive pigment (pigmentary orthochromatic leukodystrophy of Van Bogaert and Nyssen). Cavitary forms presenting as highly destructive white matter lesions (Fig. 10-16) with increased density and "clustering" of oligodendrocytes have been described in children and in adults.
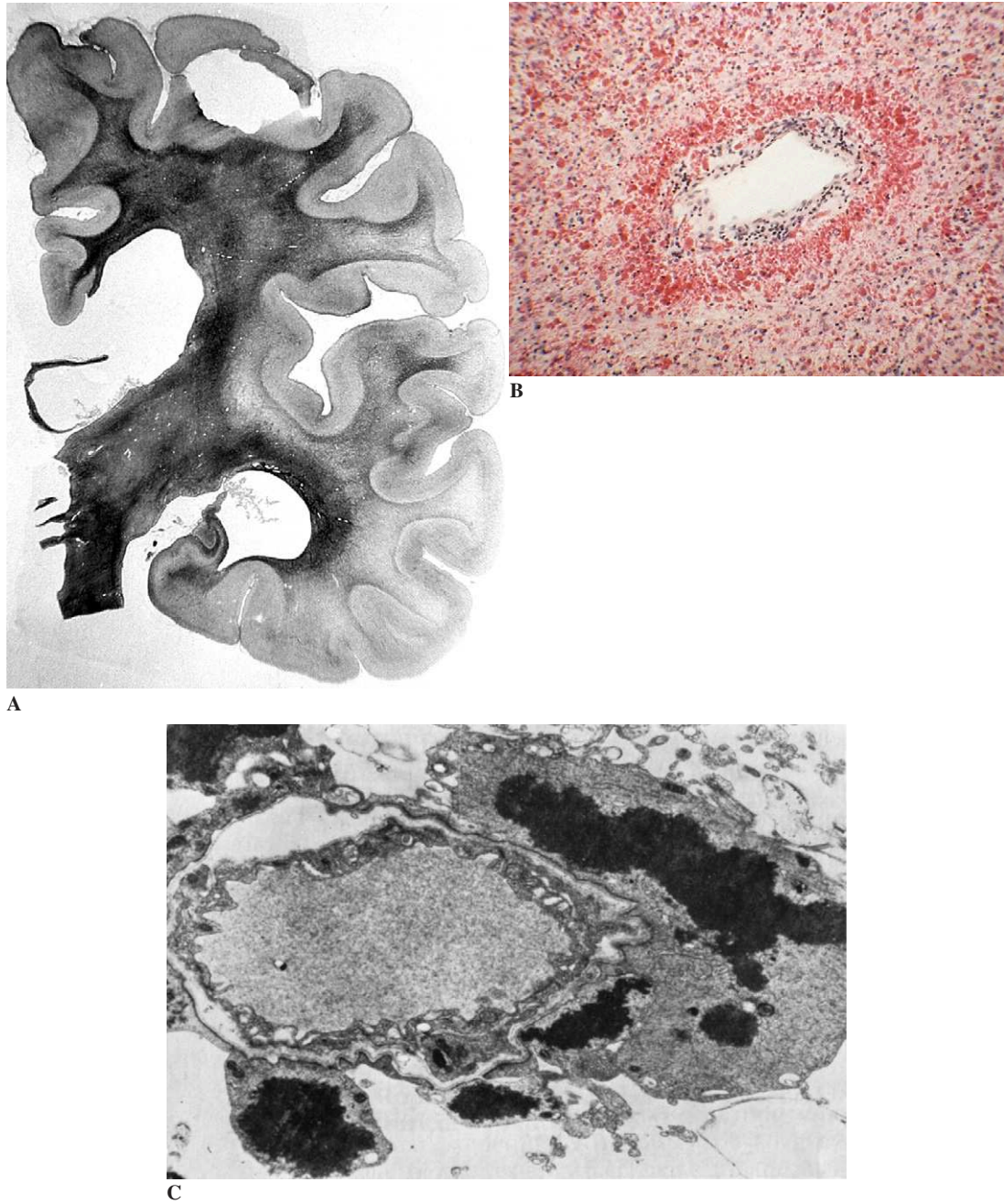
Figure 10-13. Alexander disease. **A**, The massive demyelination of the cerebral hemispheres is less obvious than other demyelinating disease (compare to Fig. 10-7A), because the numerous Rosenthal fibers are stained by the Loyez method. **B**, Hemispheric white matter. Numerous Rosenthal fibers, especially dense around a blood vessel (H and E). **C**, Electron microscopy of Rosenthal fibers, which appear as electron-dense masses in pericapillary astrocytic processes.
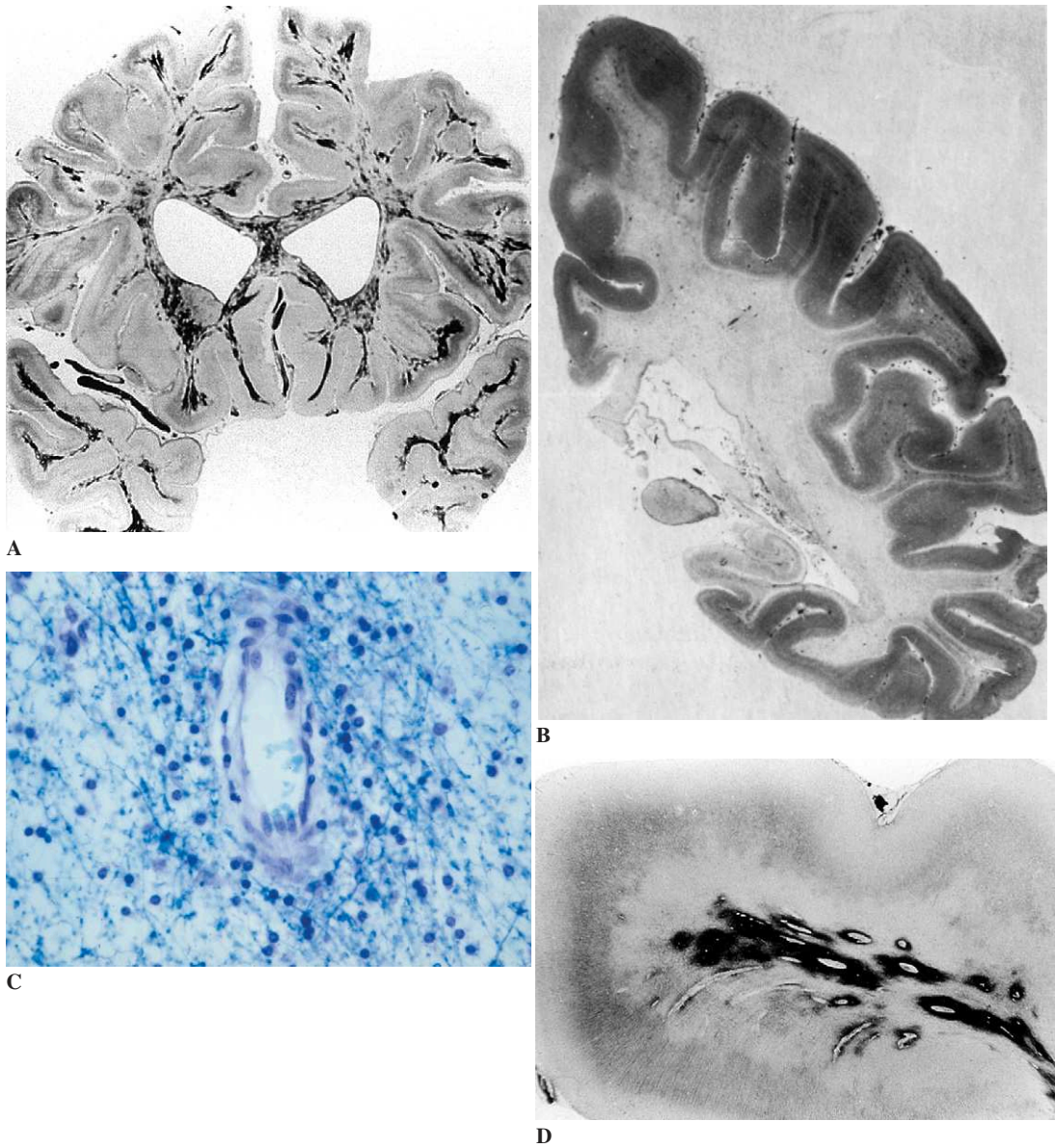
Figure 10-14. Pelizaeus-Merzbacher disease. **A**, Typical infantile form of Pelizaeus-Merzbacher tigroid leukodystrophy (Loyez). **B**, Massive congenital form of Seitelberger (Loyez). **C** and **D**, Microscopic appearance. Relative preservation of the myelin around the blood vessels (**C**, Loyez; **D**, Luxol fast blue–Cresyl violet). (**A**, Courtesy of Doctor Jean Lapresle.)
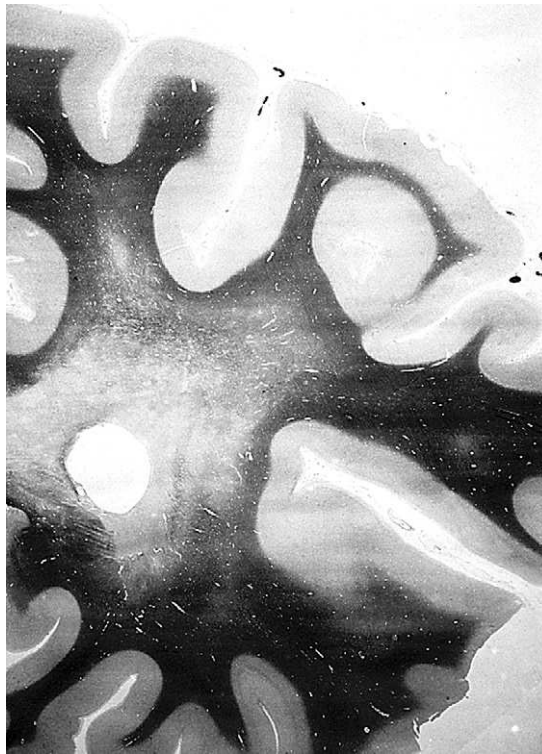
Figure 10-15. Simple, diffuse, orthochromatic leukodys-trophy (Loyez).
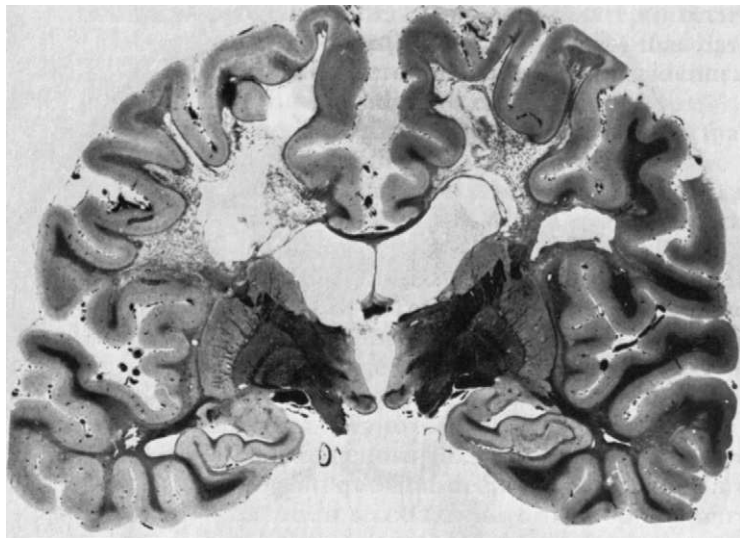
Figure 10-16. Cavitating sudanophilic leukodystrophy (Loyez).

Overlaps between cavitary and pigmentary forms have been observed occasionally. In a subset of young patients with an autosomal recessive disorder termed *leukoencephalopathy with vanishing white matter* (or *childhood ataxia with central hypomyelination*), which is characterized by cavitary orthochromatic leukoencephalopathy with increased oligodendrocyte density, the responsible genes have been identified as translation initiation factors *EIF2B*: *E1F2B1*, *E1F2B2*, *E1F2B3*, *E1F2B4*, or *E1F2B5* (with gene loci of chromosome 12, 14q24, 1, 2p23.3, and 3q27, respectively).

Chapter 11
Congenital Malformations and Perinatal Diseases

Férechté Encha-Razavi, Rebecca Folkerth, and Brian Harding

General Considerations

Congenital malformations are deviations from normal structure that may be recognized at birth. *Primary* malformations are developmental failures due to genetic or chromosomal abnormalities, whereas *secondary* malformations are generally related to destructive ("encephaloclastic") processes due to exogenous causes, such as infections, ionizing radiation, or chemical agents (including drugs). By definition, secondary malformations are not inherited; however, inherited factors can predispose to secondary malformations. Distinction between the two groups of brain malformations is of great importance in genetic counseling of parents and siblings of affected infants.

To date, only a few monogenic causes with mendelian inheritance are identified in relation to CNS malformations. *Autosomal dominant holoprosencephaly* has been linked to chromosome microdeletions, which in turn has led to identification of causal genes (*SHH*, *Zic2*, *TGIF*, *Six6*). Recently, a candidate gene (*POMT1*, coding for *O*-mannosyltransferase 1) has been identified in autosomal recessive type II lissencephaly, and *L1CAM* (on Xq28) has been shown to be the causal gene of an X-linked triventricular hydrocephalus with aqueductal stenosis and thumb deformities, formerly Bicker-Adams syndrome, but now termed HASA (for *h*ydrocephalus, *a*queduct *s*tenosis, *a*dductus thumbs).

In contrast, a large group of CNS abnormalities—the *neural tube defects* (NTDs)—show non-mendelian inheritance and are therefore considered *polygenic* or *multifactorial*. In some disorders, the appearance results from the additive effect of a number of influences (genetic, environmental, or unknown).

Although chromosome disorders are often responsible for mental retardation, CNS malformations are neither constant nor specific in a particular chromosome aberration. For example, chromosome 13 aberrations (monosomy or trisomy) are strongly associated with holoprosencephaly, but not all individuals with chromosome 13 abnormalities have holoprosencephaly. Furthermore, holoprosencephaly has been found with other chromosome aberrations, such as trisomy 18, triploidy, and chromosome 1 partial monosomy. In structural rearrangements and microdeletions, phenotype/karyotype correlations have led to the localization and identification of genes responsible for brain malformations.

The effect of an exogenous factor on brain development depends upon the timing of exposure of the fetus to the insult. Classically, the critical period in teratogenesis of the CNS is from the third to the sixth week of gestation, during which time

injurious agents (e.g., X rays, warfarin, phenytoin, mercury, ethanol) can directly affect neurogenesis, migration, or bulk growth. Later in gestation, exogenous factors (e.g., trauma, ischemia, infection) may damage previously well-formed regions. In particular, the neurotropism of infectious agents such as rubella, cytomegalovirus, *Listeria monocytogenes,* and *Toxoplasma gondii* can, depending on the time of maternofetal infection, result in either maldevelopment mimicking primary malformations or cavitations with mineral deposits from necrotizing inflammation.

Maternal metabolic illnesses, such as diabetes mellitus, may be associated with NTDs via unknown mechanisms. Maternal vitamin A deficiency and overuse can both interfere with normal brain development. Folate supplementation during pregnancy usually prevents NTDs in mothers with previously affected infants.

Whether inherited or acquired, abnormalities of the developing brain nearly always result in the nonspecific clinical finding of microcephaly (defined as a head circumference three standard deviations below the mean). Such a finding may be the first indication of a significant problem, although the increased use of prenatal ultrasound and, more recently, fetal magnetic resonance imaging (MRI) has led to earlier detection of many lesions.

Congenital Malformations

Neurulation Failure

The transformation of the neural plate into the neural tube begins around the ninteenth day and terminates with the closure of the posterior neuropore by the end of the fourth week of gestation. NTDs include a large spectrum of CNS malformations resulting from faulty neurulation. In this setting, neural tube abnormalities are found in association with disorders of the surrounding mesoderm and ectoderm.

NTDs are the most frequent CNS malformations, with an incidence of 1 to 2 per 1,000 live births. The cause is unknown, but both genetic and environmental influences have been invoked, since the risk of recurrence among couples who have had an affected offspring is increased over the general population. There is geographical variation in the incidence of NTDs, with the rates in Ireland and in Punjab, India, for example, reaching 8 per 1,000 live births. Preconceptional multivitamin and folate supplementation reduce the recurrence risk for women with one affected child. Alpha-fetoprotein (AFP) screening of maternal serum, although not specific, may identify pregnancies at risk. Prenatal diagnosis requires ultrasound or MRI examination.

NTDs may either be isolated or accompany syndromes, including chromosome aberrations (e.g., trisomy 13 and 18) and autosomal recessive conditions such as Meckel-Gruber syndrome or Walker-Warburg syndrome.

Cranial NTDs

Exencephaly and *anencephaly* are characterized by absence of the calvarium and abnormalities of the base of the skull, with constant abnormality of the sphenoid bone and shallow orbits causing protrusion of the eyes (Fig. 11-1).

A

B

Figure 11-1. Anencephaly.

Figure 11-2. Exencephaly (**A**) associated with spina bifida aperta (**B**).

In exencephaly (Fig. 11-2), cerebral hemispheres are usually present (though disorganized and rudimentary), whereas in anencephaly they are replaced by vascular tissue with multiple CSF-containing cavities, ependyma-like epithelium, and choroid plexus ("area cerebrovasculosa"). In either case, the brainstem and cerebellum are intact, except in the most severe examples.

Encephalocele (or *meningoencephalocele*) is the herniation of cerebral tissue and/or meninges through a calvarium defect of variable size. In 80% of cases the bone defect occurs in the occipital region and is associated with skin and hair abnormalities (Fig. 11-3). Polymicrogyric cortex may be found in association with meningoencephaloceles.

Meningocele (see following section) is similar to encephalocele, but includes only meningothelial connective tissue, without a central neuroglial component.
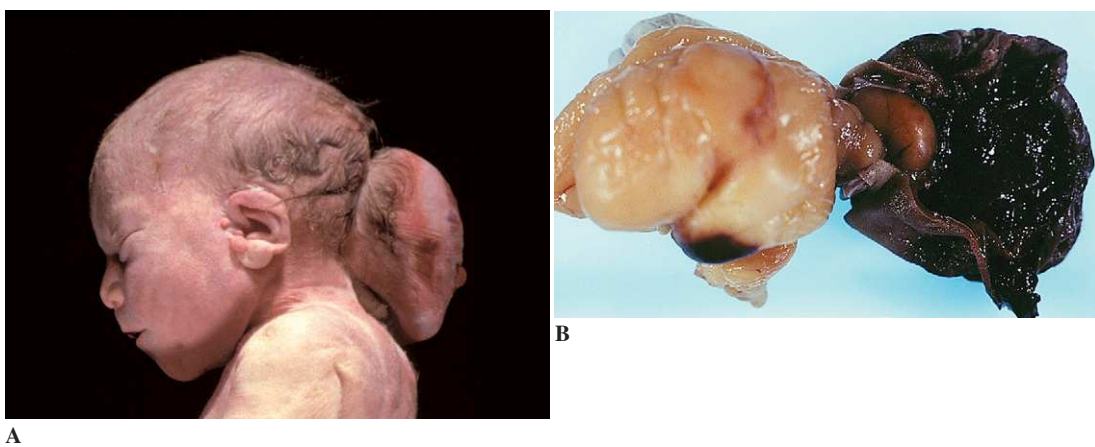
Figure 11-3. Occipital meningoencephalocele in a stillborn infant (**A**) and as a surgical specimen associated with hypovascular meningeal tissue (**B**).

Skin

Spinal apophysis

Spinal canal

Spinal cord

Subarachnoid space

Meninges

Vertebral body

Normal

Neural groove

Skin

Spina bifida aperta

Meninges

Skin

Spinal cord

Meningocele

Skin

Meninges

Spinal cord

Myelomeningocele

Dermal sinus

Skin

Meninges

Spinal cord

Congenital dermal sinus

Skin

Closure defect of posterior vertebral arch

Meninges

Spinal cord

Spina bifida occulta

Figure 11-4. Spinal neural tube closure defects.

Spinal NTDs

Iniencephaly is characterized by spina bifida (failure of closure of posterior vertebral arches) of the rostral cervical vertebrae, either open (*aperta*) or closed (*occulta*), and is usually associated with abnormalities of the brainstem and the medulla (Fig. 11-4).

Meningocele is the herniation of dura and arachnoid through a vertebral defect while the spinal cord remains in the spinal canal. In contrast, *meningomyelocele* is the herniation of the spinal cord into a meningeal sac filled with CSF and sometimes covered by an abnormal epidermis. In spina bifida aperta, no skin or meningeal covering is present. Usually, the spinal cord shows abnormalities such as syringomelia (Fig. 11-5), hydromyelia, and diastematomyelia (partial duplication). In congenital dermal sinus, a communication persists between the skin surface and the subarachnoid space, which can be complicated by recurrent meningitis.

Meningomyelocele is nearly always associated with a small posterior fossa, leading to hindbrain crowding and secondary abnormalities of the brainstem and the cerebellum. These consist of lengthening of the cerebellar peduncles, a Z-shaped deviation of the medulla oblongata, and cerebellar hypoplasia (Fig. 11-6). The cerebellar vermis is displaced caudally into the spinal canal through an enlarged foramen magnum and often has disorganized cortical Purkinje and granule cells. This complex association—termed the *Chiari type II* (or *Arnold-Chiari*) *malformation*—is further characterized by hydrocephalus, sometimes with a microgyric pattern of the cerebral convolutions and subependymal heterotopia.

Disorders of Development of the Prosencephalon

The *prosencephalon*, the most rostral part of the neural tube, gives origin to lateral outgrowths—the telencephalic vesicles—in the fifth week of gestation. The medial part of the original prosencephalon becomes the diencephalon. Optic vesicles arise from the prosencephalon before the closure of the anterior neuropore. The anterior neuropore site becomes the lamina terminalis, where the cerebral hemispheres meet through the decussation of the corpus callosum fibers around the 12th week of gestation. The cerebral hemispheres and the olfactory placodes derive from the telencephalic vesicles. In human beings the olfactory vesicles become obliterated at about 10 weeks and form olfactory bulbs, but they persist in many other vertebrates.

Figure 11-5. Syringomyelia, with expansion of the central canal and compression of the posterior horn and column (Loyez stain for myelin).
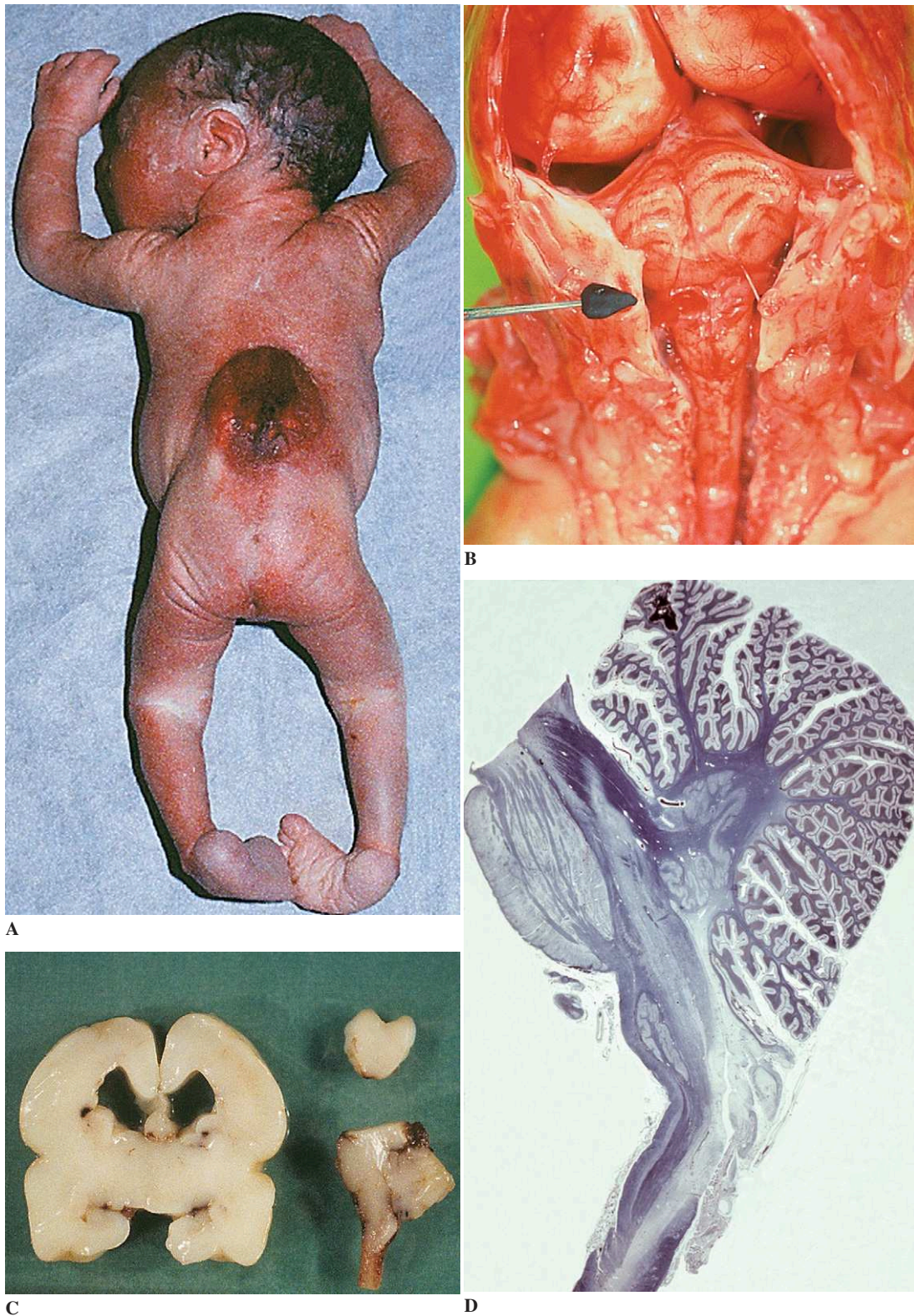
Figure 11-6. Arnold-Chiari malformation. **A**, Dorsolumbar meningomyelocele. **B**, Dorsal view of the posterior fossa, showing cerebellar engagement and Z-shaped deviation of the medulla oblongata. **C**, Coronal section of the cerebral hemispheres and midbrain, showing bilateral ventricular dilatation. **D**, Sagittal section of the brainstem and cerebellum, showing cerebellar vermian herniation and Z-shaped deformity of the medulla oblongata (Loyez stain). (**A** and **B**, Courtesy of Dr. J.C. Larroche.)

Holoprosencephalies

Failure of induction and growth of the prosencephalon results in a spectrum of malformations called *holoprosencephalies*, which are classically associated with midline facial abnormalities such as cyclopia, cebocephaly, ethmocephaly (nose with single nostril), facial median cleft due to the absence of the premaxilla, and hypo- or hypertelorism. This association exists because the prechordal mesoderm is an inducing factor in the development of both the prosencephalon and in the development of the face.

Holoprosencephalies are frequently found in chromosome aberrations involving chromosomes 13 and 18 and in triploidies. They may also occur in either an autosomal recessive or X-linked fashion. Prenatal ultrasonography, performed routinely or in the context of hydramnios or intrauterine growth retardation, may detect the malformation.

The spectrum of holoprosencephalies ranges from complete absence of the prosencephalon to minimal abnormality (isolated absence of the olfactory bulbs and tracts), with numerous transitional forms.

Aprosencephalies are characterized by a rudimentary prosencephalon, leading to extreme micrencephaly. These are very rare.

Alobar holoprosencephaly (Fig. 11-7) consists of an undivided holospheric cerebrum (prosencephalic monoventricle), which may open posteriorly into a dorsal sac-like structure. The thalamic and other diencephalic nuclei are totally or partly fused, with a narrow or absent third ventricle. The corpus callosum and septum pellucidum are absent. The cerebral convolutions may be aberrant and pachygyric. The olfactory bulbs and hypophysis are absent (arrhinencephaly). The cerebellum may be hypoplastic and dysplastic, as may the cerebral peduncles and aqueduct of Sylvius.

Semilobar holoprosencephalies have interhemispheric fissures only in the parieto-occipital regions, contrasting with continuous cortical gyri bridging over the midline in frontal regions (Fig. 11-8). The prosencephalic monoventricle is frontal, divided posteriorly into two temporal and occipital horns. There may be partial fusion of diencephalic structures. Again, olfactory bulbs and tracts are missing.

Lobar holoprosencephaly is characterized by two well-developed hemispheres connected by a bridge of cortical convolution or a thin membrane corresponding to the lamina terminalis. The corpus callosum, however, is still lacking.

Arrhinencephaly, the least severe of the holoprosencephalies, consists of isolated absence of olfactory bulbs and tracts and of the straight sulci along the orbital frontal cortical surface (Fig. 11-9).

Histologic findings in holoprosencephalic brains differ from case to case. However, hypoplastic deep nuclei and cytoarchitectonic abnormalities with subependymal heterotopias are frequently reported.

Abnormalities of Midline Structures

Agenesis of the Corpus Callosum. *Agenesis of the corpus callosum* is a relatively common malformation that may be isolated or associated with other brain or systemic anomalies. It may occur sporadically or as part of chromosome aberration syndrome such as trisomy 18 or trisomy 8. Familial cases have been also reported. Some are incidental findings at autopsy in adults with no neurologic or developmental difficulties. The corpus callosum develops rostrocaudally after the crossing over of the telencephalic commissural fibers between the 11th and 20th weeks of gestation; thus, this abnormality can be seen even in early prenatal ultrasonograms.

In *total agenesis*, the medial surface of the hemispheres shows secondary abnormalities character-

Figure 11-7. Alobar holoprosencephaly.
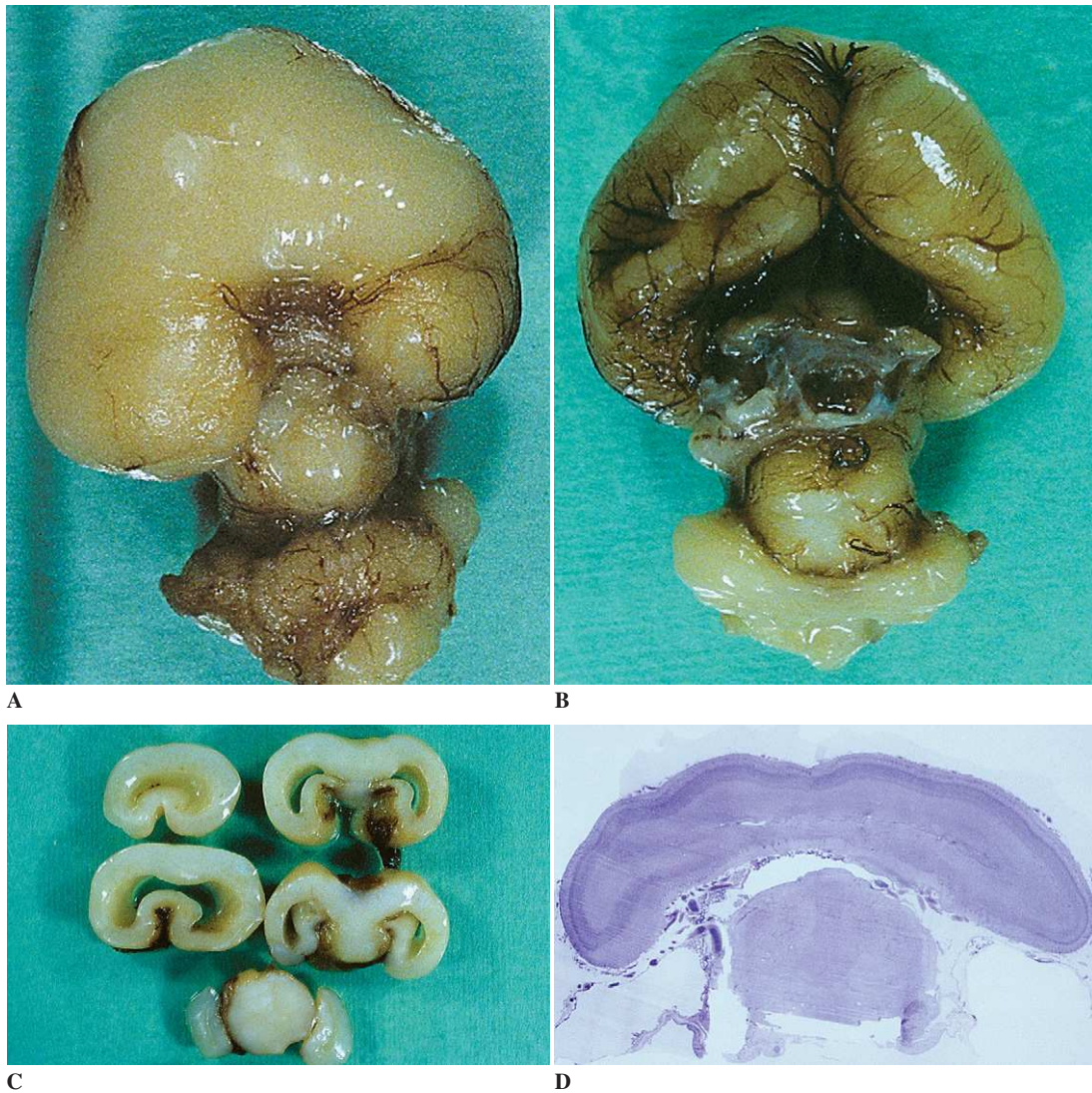
Figure 11-8. Semilobar holoprosencephaly in a 19-week-old fetus. **A**, Basal view. **B**, Dorsal view. **C**, Coronal section. **D**, Microscopic appearance.

ized by aberrant callosal artery and replacement of the normal cingulate gyrus by perpendicular ("radiating") convolutions. On coronal sections, no crossing white-matter fibers are seen and the lateral ventricles show a vertical ("bat-wing") orientation (Fig. 11-10). This most severe form is due to the total absence of callosal fibers or to their inability to cross the midline. In the latter circumstance, remnant callosal fibers form an aberrant antero-posterior tract known as Probst bundle.

Partial agenesis of the corpus callosum is clas-

sically posterior, so that there is a relatively normal genu and anterior body (Fig. 11-11).

Whether total or partial, callosal agenesis may be accompanied by lipomatous tissue, vascular abnormalities, or calcifications at the site of fiber absence.

Anomalies of Septum Pellucidum.   *Cavum septi pellucidi* and *cavum vergae* are seen in fetuses as developmentally normal midline cavities (the former rostral, the latter caudal) lying between the

Figure 11-9. Arhinencephaly.

A

B
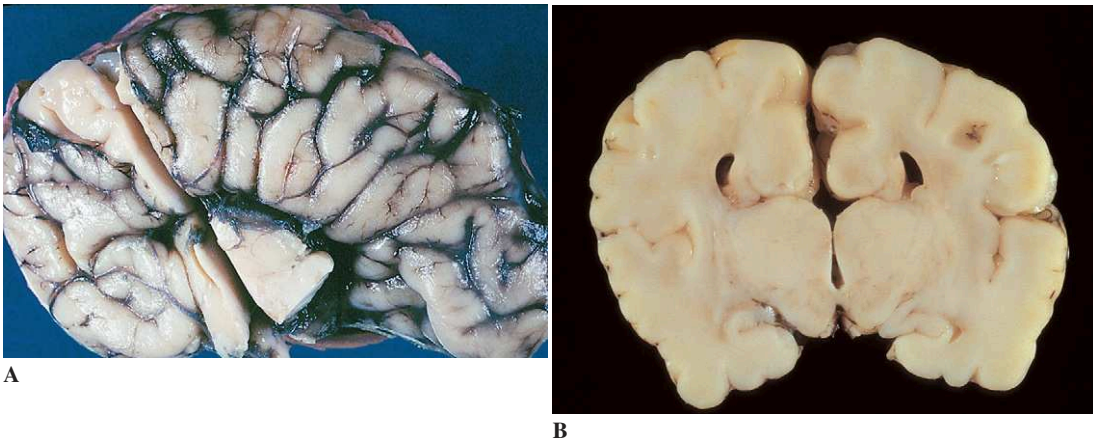
Figure 11-10. Complete agenesis of corpus callosum. **A**, Interhemispheric view. **B**, Coronal section.
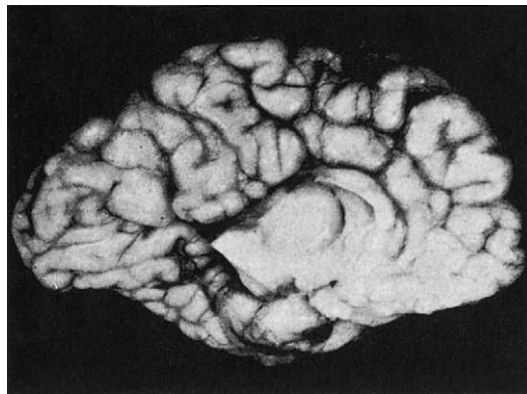
Figure 11-11. Partial agenesis of the corpus callosum.

Figure 11-12. Cavum septi pellucidi.

Figure 11-14. Cerebellar heterotopia.

two leaves of the septum (Fig. 11-12). They tend to be obliterated toward term, but persist postnatally in a minority of individuals.

Agenesis of the septum pellucidum results in a pseudomonoventricle and is usually associated with retinal dysplasia and hypothalamo-hypophyseal and endocrine dysfunctions. In hydrocephalic brains, the destruction of one or both leaves of the septum may lead to such an appearance (Fig. 11-13).

Disorders of Cortical Neurogenesis and Migration

Disorders of normal cortical cell genesis, migration, and maturation lead to a spectrum of cyto-

Figure 11-13. Septal rupture.

architectonic abnormalities, some of which (e.g., lissencephaly and cortical dysplasia) may be visible on gross inspection of the brain while others (e.g., heterotopic neurons in the white matter) may be detectable only on microscopic examination.

Neuronal Heterotopia

Minute (microscopic) *heterotopias*, which consist of small clusters of neurons in the subcortical white matter, are occasional findings in otherwise normal brains. In the cerebellum, heterotopias are more frequent and are mainly found in the tectum and in the dentate nucleus (Fig. 11-14). Their significance is unknown, since they are found in normal fetuses as well as those with chromosome aberrations, including trisomy 18.

Periventricular nodular heterotopias are larger aggregates of neural (and sometimes glial) cells found in the subependymal deep white matter (Fig. 11-15). They represent a failure of migration of immature neuroblasts from the ventricular zone, due, in some cases, to an X-linked mutation in the *Filamin-1* gene. Females, who carry two copies of the gene, have a subset of neuroblasts with an intact gene that is able to migrate normally to the cortex and a randomly X-inactivated subpopulation that is unable to migrate and thus remains in the ventricular regions. Males, who carry one copy of the gene, have complete failure of migration, which may confer prenatal lethality; there are, however, rare occurrences of nodular heterotopia in males who are germline mosaics, a mechanism which is

Figure 11-15. Periventricular nodular heterotopia (Loyez stain for myelin).

also responsible for the existence of phenotypically normal mothers with affected daughters. Isolated periventricular heterotopias may be found on neuroimages obtained in patients with mental retardation and epilepsy, or incidentally in normal subjects.

Polymicrogyria

The term *polymicrogyria* refers to an abnormal cortical pattern, often likened to "Moroccan leather," that results from excessive folding and irregular fusion of adjacent gyri. The leptomeninges covering the polymicrogyric cortex can be abnormally vascularized and may contain heterotopic (i.e., displaced and disorganized) neuroglial tissue.

Although polymicrogyria may be seen in triploidies and in association with pachygyria in the primary metabolic disorder of Zellweger syndrome, it is also seen at the margins of disruptions (see later in the chapter). Its pathogenesis is, there-

fore, unclear, although the gestational timing of its development is considered to be between 17 and 25 weeks.

Unlayered polymicrogyria displays a festoonlike, chaotic pattern of neuronal orientation. It is found in association with the abnormal pattern of temporal lobe sulcation in thanatophoric dysplasia, a disorder caused by mutation in the fibroblast growth factor gene leading also to skeletal growthplate disruption (Fig. 11-16). Focal unlayered polymicrogyria may also be found in Chiari II malformations, encephaloceles, and fetal alcohol syndrome.

The term *four-layered polymicrogyria* refers to the polymicrogyria first described by Bielschowsky in 1915. This is characterized by (1) a superficial acellular molecular layer that infolds and fuses to produce a microsulcus; (2) a second cellular layer comprising neuronal types normally belonging to cortical laminae II and III; (3) a third layer devoid of neurons, containing mostly glial cells; and (4) a fourth layer contiguous with normal layer VI of the adjacent cortex (Fig. 11-17). This microscopic appearance, along with the fact that it may be focal, bordering porencephalic defects, suggests that four-layered polymicrogyria may be a sequela of laminar necrosis of layers IV and V due to early ischemic, toxic, or infectious injury (see later in this chapter).

Pseudo-polymicrogyria or *polygyria* may be seen in cases of severe congenital hydrocephalus. In this setting, the increased sulcation is believed to allow increased surface area for cortical neurons to situate, overcoming somewhat the loss of sulcal depth in the thinned cerebral mantle.

Lissencephaly

Lissencephaly means "smooth brain" and refers to the macroscopic appearance of few or no sulci, apart from the interhemispheric fissure and wideopen sylvian regions. The term is used interchangeably with *agyria*. When smoothness is localized to smaller regions of the brain, the term *pachygyria* is preferred.

Type I Lissencephaly. Classic (type I) lissencephaly is characterized by a markedly thickened cortex overlying a reduced volume of white matter
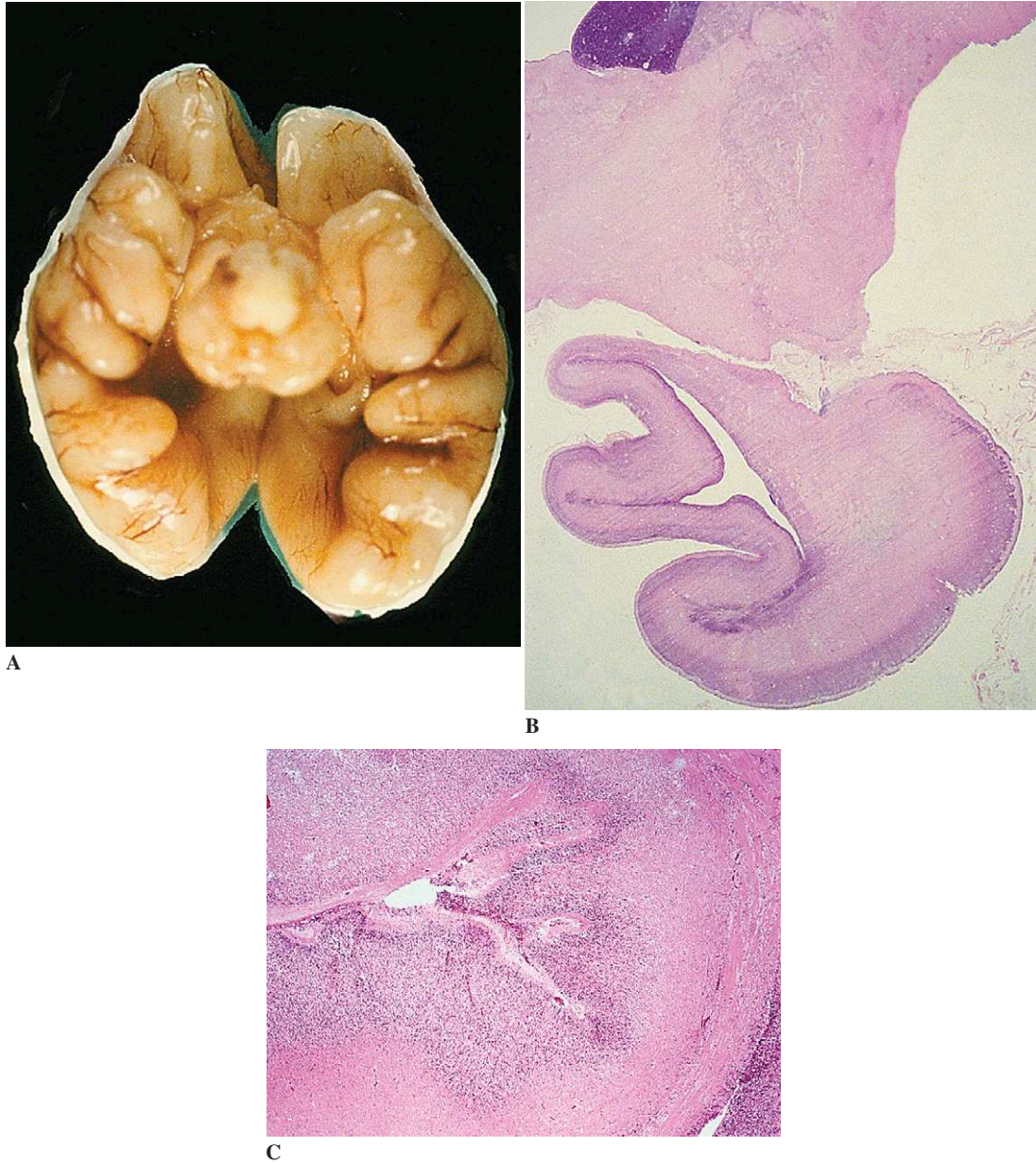
Figure 11-16. Thanatophoric dysplasia. **A**, Basal view. **B**, Temporal sulcus. **C**, Cytoarchitectonic abnormalities.
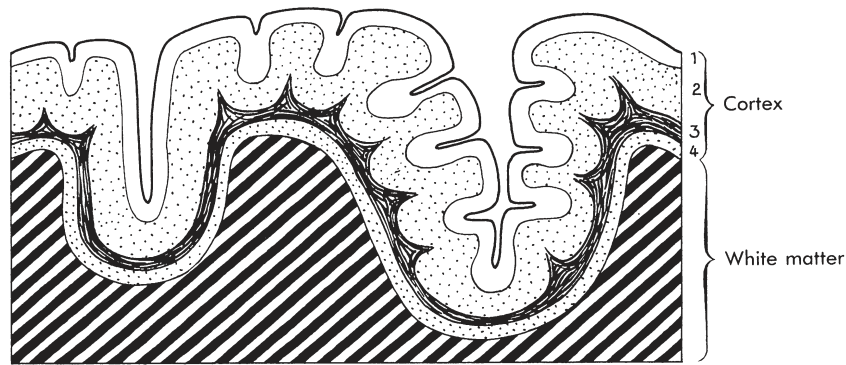
Figure 11-17. Cortical changes in polymicrogyria. (From Crome L, Stern J. Pathology of mental retardation, 2nd ed. Baltimore, Williams & Wilkins, 1972.)

(Fig. 11-18). Ventricular enlargement is also frequent. These macroscopic features, especially the altered white-to-gray ratio, are easily seen on fetal or postnatal MRI. Histologically, the thickened grey matter displays an abnormal horizontal lamination with four layers (rather than the usual six) in a vaguely "inside-out" pattern; that is, the most superficial layer is an acellular molecular layer, followed by a highly cellular zone of large pyramidal neurons, a sparsely cellular layer with numerous myelinated fibers, and a deep, highly cellular layer of disorganized neurons (Fig. 11-19). The remnant periventricular white matter may contain single or grouped heterotopic neurons. Anomalies of the inferior olivary nuclei, cerebellum, and corti-
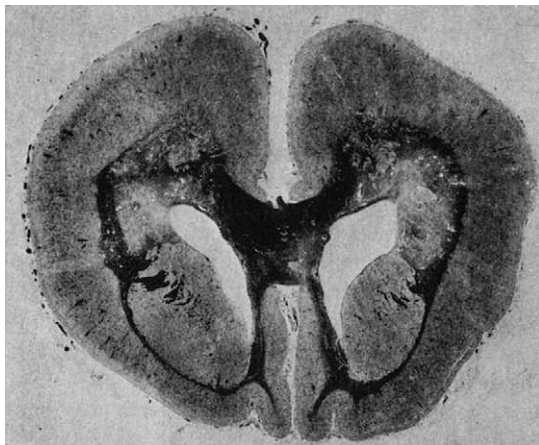
Figure 11-18. Agyria/pachygyria (Loyez stain).

cospinal tracts may be found in association with this migration defect.

Type I lissencephaly has several inheritance patterns and underlying genetic abnormalities. The most common is the autosomal dominant Miller-Dieker syndrome, in which the gene *LIS-1*, located on 17p13, is mutated, leading to altered cytoskeletal dynamics and ineffective migration of neuronal progenitors. This syndrome features craniofacial abnormalities such as microcephaly, bitemporal hollowing, prominent occiput, small jaw, and neurologic impairment (i.e., decreased activity, abnormal tone, profound mental retardation, and seizures). Genetic analysis may disclose microdeletion of the short arm of chromosome 17, allowing prenatal detection of the syndrome.

In X-linked type I lissencephaly, the gene *DCX* encodes the protein doublecortin, also important in normal migration of neuroblasts. In females this mutation results in a band of heterotopic gray matter in the white matter (i.e., a subcortical band heterotopia, in which the neurons have lost one allele through random X-inactivation) beneath a relatively normal-appearing cortex (retaining the normal allele). Male progeny exhibit lissencephaly of four-layer type that is particularly severe in the anterior parts of the brain.

Type II Lissencephaly.   Type II or "cobblestone" lissencephaly (LISII) is a distinct cytoarchitectonic disorder characterized by the obliteration of arachnoid space by numerous clusters of ectopic neurons and glial cells responsible for early hydrocephalus.
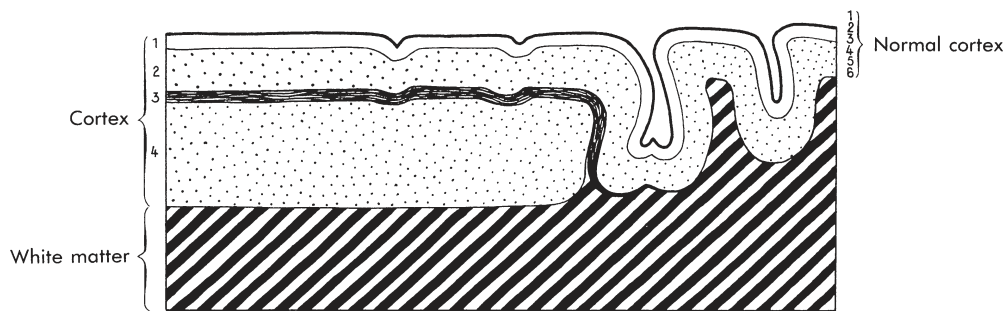
Figure 11-19. Cortical changes in agyria/pachygyria. (From Crome L, Stern J. Pathology of mental retardation, 2nd ed. Baltimore, Williams & Wilkins, 1972.)

In this setting, hydrocephalus may be severe, perhaps detectable by ultrasound as soon as the 18th week of gestation.

LISII has no recognizable pattern of lamination. Instead, there is a superficial, disorganized band of neurons, glia, and vascular connective tissue overlying a band of neurons that probably represents the remnant of the cortical plate. These bands are separated by an ill-defined line thought to represent the normal pial surface. The pathogenesis of this type of lissencephaly is believed to be due to disruption of the pial barrier, allowing migrating cells to grow past their normal cortical destinations.

This type of abnormality is seen in Walker-Warburg syndrome (autosomal recessive oculocerebral dysplasia), autosomal recessive Fukuyama congenital muscular dystrophy, and Finnish "muscle-eye-brain" disease (see Chap. 13). It may also be seen at the margins of disruptions (see later discussion).

Focal Cortical Dysplasia

Focal cortical dysplasia is a localized cortical malformation that is frequently found in surgical lobectomy specimens removed for intractable epilepsy (see Chap. 12). They are characterized by a macroscopically visible expansion of the cortical gyrus that resembles a cortical tuber of tuberous sclerosis. In fact, both focal cortical dysplasia and cortical tubers share microscopic features in common: in both cases the normal layering of the cortex is obscured by randomly scattered "balloon" cells, with abundant eosinophilic cytoplasm and bizarre nuclei and prominent nucleoli. Binucleated ganglion cells, coarse Rosenthal fibers in the back-

ground neuropil, and proliferation of oligodendroglial cells around blood vessels may also be seen. Tuberous sclerosis is distinguished by other typical features of the syndrome, including subependymal nodules, renal angiomyolipomas, subungual fibromas, and adenoma sebaceum of the face.

Disorders of Hindbrain Development

Malformations of the Cerebellum

In fetuses, complete or unilateral hemispheric agenesis of the cerebellum is uncommon. In contrast, hypoplasia is more frequent, found in association with trisomy 18 or with other brain malformations such as holoprosencephaly and Chiari type II malformation.

Agenesis of the vermis, total or partial, is usually associated with a spectrum of abnormalities that is termed *Dandy-Walker malformation* (Fig. 11-20). In this setting, the fourth ventricle expands into the posterior fossa as a cyst-like space covered by a thin meningoependymal sheet. The Dandy-Walker malformation may be isolated or part of other malformative conditions.

Rarely, total agenesis of the vermis is associated with fusion of the cerebellar hemispheres and dentate nucleus across the midline, with hypoplasia of the fourth ventricle (rhombencephalosynapsis). In both conditions, hydrocephalus may occur as a secondary change.

A posterior fossa arachnoid cyst, expanding into the cerebello-medullary cistern and causing hydrocephalus, may mimic Dandy-Walker malformation on fetal ultrasound. In these cases, the
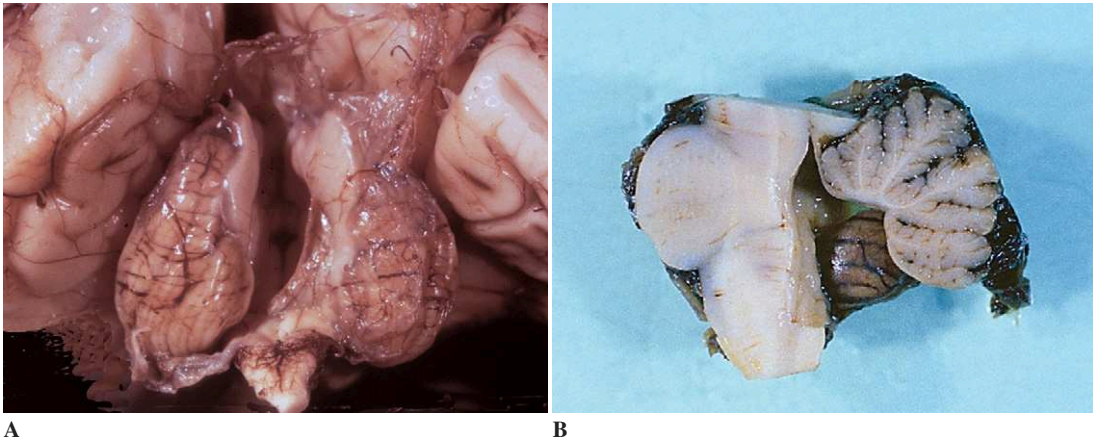
Figure 11-20. Dandy-Walker malformation. **A**, Agenesis of the vermis and cystic dilation of the fourth ventricle, posterior view. **B**, Partial agenesis of the inferior vermis, sagittal section of brainstem and cerebellum.

vermis is present but compressed, and the fourth ventricle is not dilated.

Abnormalities of the Aqueduct of Sylvius

Isolated aqueductal stenosis, in which there is a reduced lumen only, with no histologic changes of the aqueduct otherwise, is rare. It has been reported in association with abnormalities of the pyramidal tracts in an X-linked hydrocephalus with thumb deformities (HASA). Given the experimental induction of inflammation-free aqueductal stenosis with mumps virus in hamsters, the possibility of a viral origin of aqueductal stenosis in humans has been suggested.

Dysplasia of the aqueduct is often found in malformed brains, such as in holoprosencephaly and Walker-Warburg syndrome, as well as in fetal disruption syndromes, including intrauterine strokes (Fig. 11-21).

Occlusion of the aqueduct, which may be infectious, neoplastic, or hemorrhagic, can result in triventricular hydrocephalus. In such cases, the lumen of the aqueduct is of normal size (or dilated) but occluded by necrotic tissue, inflammatory debris, or hemorrhage. The ependymal layer of the aqueduct, as well as other parts of the ventricular system, is disrupted and replaced by reactive gliosis and siderophages. At later stages the aqueduct may be occluded by a glial plug or covered over by a glial septum.
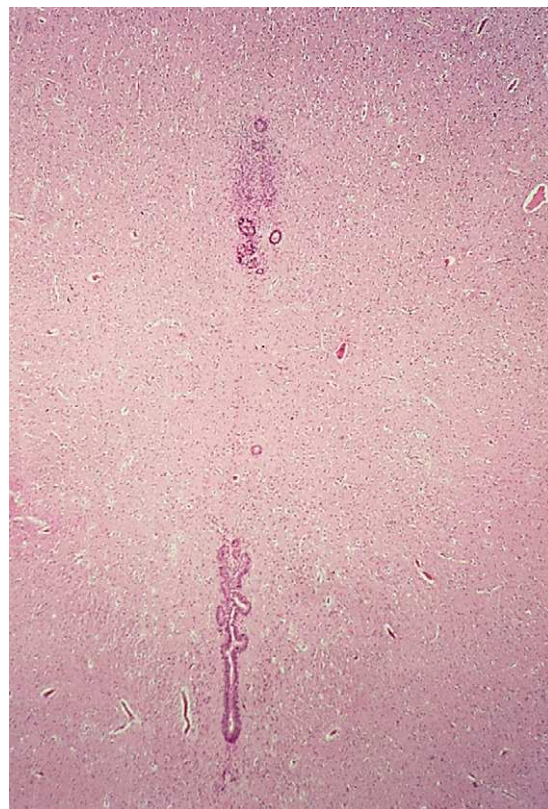
Figure 11-21. Aqueduct atresia.

Disruptions of Developing Brain

The foregoing sections have considered primarily abnormalities of development related to genetic or environmental influences on early organogenesis. The term *disruption* reflects a later (whether intra- or extrauterine) event altering the configuration of a previously normally developed structure or structures. Disruptions often affect both gray matter (i.e., cortical and deep periventricular elements) and white matter at the same time, manifested clinically as *hypoxic-ischemic encephalopathy*. However, their distinct neuropathologic patterns will be discussed separately. Disruptive lesions are reported in association with a variety of situations that cause altered in-utero hemodynamics, from trauma, gas intoxication, and drug abuse, to twin gestations.

Lesions of Developing Gray Matter

Exogenous processes disrupting the normal sequence of neuronal migration and cortical differentiation (encephaloclastic processes) usually act after midgestation. They lead to a spectrum of cortical abnormalities ranging from disturbed cytoarchitecture (often at the margins of cysts, i.e., *porencephalies*) or loss of cortical plate segments ("basket brain") to complete absence of supratentorial brain tissue (hydranencephaly). Lesser degrees of insult may have effects on selective neuronal populations.

Finally, disruptions of germinal matrix and deep nuclei of the diencephalons and brainstem have distinctive features. The vast majority of disruptions feature decreased perfusion (ischemia), low oxygen tension (hypoxia), or both; the two phenomena tend to occur together (hence the commonly used term *hypoxia-ischemia*).

Encephaloclastic Lesions of Developing Neocortex

Porencephaly. *Porencephaly* refers to any defect extending from the brain surface to the ventricle. Usually these are in the sylvian region (Fig. 11-22); they may be bilateral. The margins are smooth and have abnormal gyral architecture, either polymicrogyria or gyri radiating outward from the lips of the defect. The polymicrogyria found at the margins
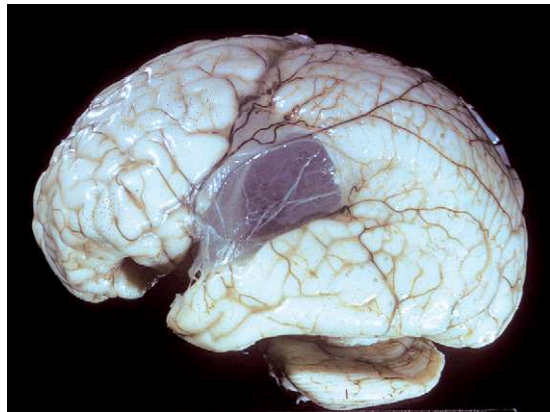
Figure 11-22. Porencephaly.

in some cases is thought to be due to incomplete ischemia in the tissue lying near the defect. Porencephalies lack significant glial scarring.

These features are consistent with an intrauterine insult occurring after neuroblast migration and during gyration (i.e., after 20–24 weeks). The basal ganglia, cerebellum, and brainstem are not affected, although the thalamus and descending white matter tracts may be secondarily atrophic. Clinical manifestations are related to the area of involvement and may include hemiparesis, blindness, and seizures.

Hydranencephaly. The term *hydranencephaly* ("bubble brain") refers to the residua of intrauterine massive hemispheric necrosis. Various insults occurring between 22 and 27 weeks—including trauma; attempted abortion; TORCH (*t*oxoplamosis, *r*ubella, *c*ytomegalovirus, or *h*erpesvirus) infection; and household gas intoxication—have been correlated with hydranencephaly, though most antecedent events are unknown. The extent of destruction dictates the clinical picture, which typically includes spasticity, severe seizures, and vegetative signs; mortality in infancy is high. Since the areas involved are often in the distribution of the carotid arteries, the inferior temporal and occipital lobes tend to be preserved. The basal ganglia are variably affected, but the thalamus and descending tracts are always atrophic. Head enlargement develops in longer-surviving infants as a result of scarring of the aqueduct, which leads to hydrocephalus. Hydranencephaly has been reported in a familial form due to a distinctive proliferative vasculopathy.

Basket Brain.   *Basket brain* is a form of encephaloclasia intermediate between porencephaly and hydranencephaly. The cingulate gyri and medial hemispheric structures are preserved (corresponding to the "handle" of the basket) while the lateral parietal and frontal lobes are cystic bilaterally.

Multicystic Encephalomalacia.   *Multicystic encephalomalacia* differs from porencephaly and hydranencephaly by the occurrence of innumerable cysts separated by glial septa and involving the cortex and white matter in all lobes (Fig. 11-23). Microscopic evidence of resolved infarction and hemorrhage, including macrophages and hemosiderin, can be seen accompanying the marked gliosis, and suggests an insult in the perinatal period (i.e., late gestation to early infancy). As with porencephaly and hydranencephaly, associated events have included maternal suicide attempts, infection, and parturition-related complications such as cord prolapse. In surviving infants, epilepsy and severe motor deficits are common.

Ischemic Strokes.   Perinatal *ischemic strokes*, usually arising in the territory of the middle cerebral artery, can often be seen in the setting of congenital heart disease or in other conditions requiring extracorporeal membrane oxygenation. These strokes are similar to those occurring in adults in terms of their histologic evolution.

Selective Neuronal Necrosis.   The premature infant has a somewhat different profile of neuronal vulnerability to hypoxia-ischemia than that of the full-term baby; this is believed to be due to variations in patterns of cerebral blood flow. For example, the parasagittal regions, which are the border zones between anterior and middle cerebral artery territories, are especially susceptible to hypoxia-ischemia. Injury in these areas gives rise to "basket brain" or lesser degrees of porencephaly, as described previously. The depths of sulci are end-arterial regions, so that neurons there are susceptible to hypoxia-ischemia, which can lead to ulegyria, a mushroom-like appearance of sulcal atrophy with preservation of gyral crests (Fig. 11-24). For unclear reasons, neurons within the deeper cortical layers are more prone to injury than are neurons in upper layers, giving rise to laminar necrosis, a layer of destruction within the cortical ribbon. The pattern of vulnerability depends on the developmental stage; for example, Sommer sector of the hippocampus is vulnerable in the term baby, while the subiculum is susceptible in the premature. Coexistence of neuronal necrosis in predictable patterns, as in pontosubicular necrosis, may be seen, and may be highly associated with white matter necrosis (discussed later).

Encephaloclastic Lesions of Developing Basal Ganglia

In both term and premature infants, thalamic and basal ganglionic neurons may undergo necrosis, resulting in mineralization (or ferrugination) of
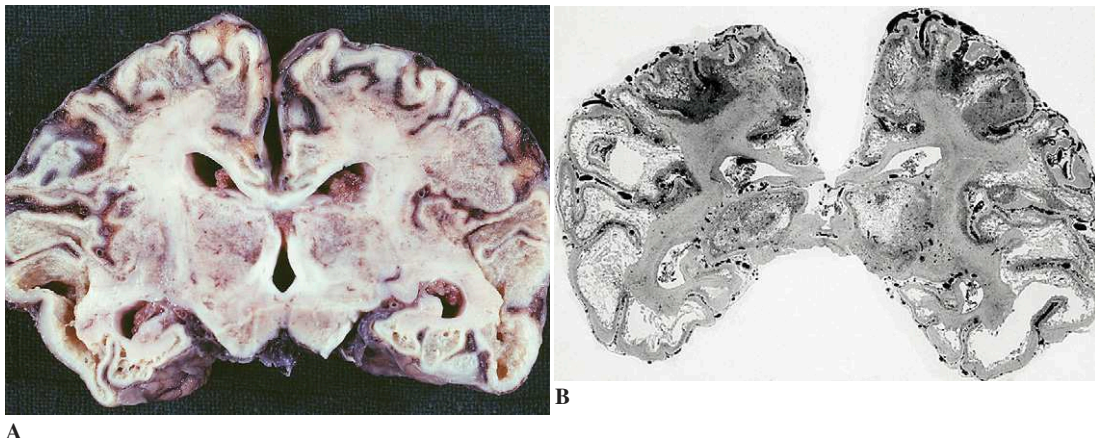
Figure 11-23. Multicystic encephalomalacia in a case of neonatal carbon monoxide intoxication. **A**, Gross appearance. **B**, Appearance with Loyez stain.

A   B
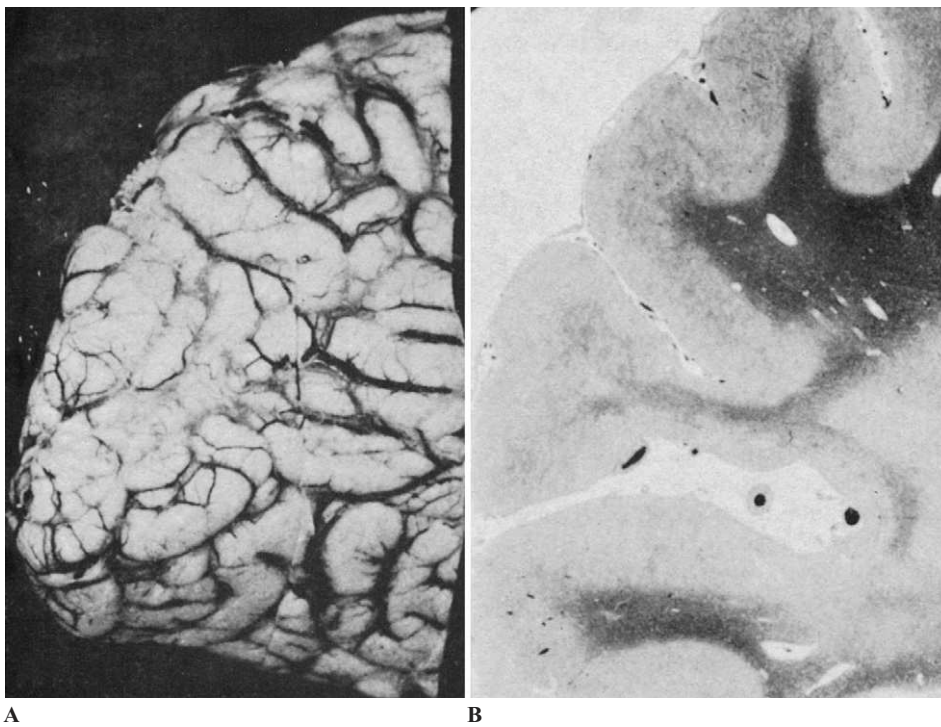
Figure 11-24. Ulegyria. **A**, Gross appearance of medial aspect of occipital lobe. **B**, Microscopic appearance showing atrophy of gyral sulci with relative preservation of gyral crests (Loyez).

individual cells. In babies surviving a year or more, damage to the thalamus and basal ganglia may lead to disturbed architecture known as *status marmoratus* (or *état marbré*), in which aberrant myelination of disoriented axons and glial processes leads to a marbled gross appearance.

Clinical features accompanying status marmoratus classically include static (nonprogressive) bilateral choreoathetosis, motor and intellectual retardation, spastic diplegia, and sometimes epilepsy; the inexact term "cerebral palsy" has been applied to many such affected individuals.

Lesions of the Ganglionic Eminence (Germinal Matrix)

The periventricular gray matter in utero is composed of immature cells (neuroblasts and glial progenitors), proliferation and migration of which peaks between the 18th and 26th gestational week. Because the vessels of this region are remodeling actively during this time and therefore have incompletely formed basal lamina and loosely interdigi-

tated glial end-feet, they are particularly vulnerable to any alterations in hemodynamics.

Not surprisingly, then, *periventricular hemorrhages* represent a common lesion in prematurely delivered babies, who are typically respiratorily compromised and hemodynamically labile. Large, periventricular hemorrhages can result in extensive destruction of precursor cells as well as adjacent mature structures, such as the caudate and internal capsule, and can interrupt the overlying ventricular (ependymal) surface, leading to intraventricular hemorrhage and hydrocephalus. In surviving infants, macrophages resorb the hemorrhage, resulting in periventricular cysts. Hemosiderosis, gliosis, and rosette-like remnants of ependymal cells may remain. In noncavitating, healed lesions, mineralization of cell bodies and processes may persist as markers of injury.

Hemorrhages of the choroid plexus (though not ganglionic eminence lesions) are mentioned here, as they can have the same sequelae (e.g., hydrocephalus) as intraventricular hemorrhages arising from the germinal matrix.

Coexistence of deep (germinal matrix) and surface (cortical plate) disruptions is common in the porencephalies, described earlier. Likewise, *perisylvian polymicrogyria* (sometimes referred to as *schizencephaly* in the older literature) is thought to reflect a combination of disruption of the local glia limitans and cortical plate together with interruption of precursor migration, leading to complex cortical dysplasia and deep gray matter heterotopia.

Lesions of Developing White Matter

In the human, white matter development lags behind gray matter development such that the vulnerable period for the former is the final trimester through the first year of life, that is, the period of myelinogenesis. The most severe form of perinatal white matter damage is periventricular leukomalacia (PVL; Fig. 11-25), in which cystic degeneration of necrotic deep white matter is thought to be the consequence of ischemia (with or without reperfusion) and of cytokine release (potentiated by infection). The vulnerability of the hemispheric white matter is due in part to the previously mentioned anatomic "watersheds" at the depths of sulci, extending into the periventricular regions, coupled in very premature infants with frequently significant hemodynamic and respiratory compromise.

Perinatal Telencephalic Leukoencephalopathy and Periventricular Leukomalacia

Perinatal telencephalic leukoencephalopathy (PTL) is the mildest, and possibly earliest, manifestation of hypoxia-ischemia in the hemispheric white matter. It is characterized neuropathologically by the occurrence of prominent, often hypertrophic astrocytes, "acutely damaged glia" (pyknotic nuclei), capillary cell proliferation, and perivascular "globules," which may mineralize. The term *white matter gliosis* is used interchangeably with PTL and refers to the diffuse proliferation of glial fibrillary acidic protein (GFAP)–positive cells accompanying myelin pallor on LFB stain. PTL may be seen alone or in conjunction with the focal lesions of frank PVL.

PVL is defined as circumscribed regions of tissue loss that measure 0.2 to 1.0 cm and usually occur within 1.5 cm of the lateral ventricular wall in the hemispheric white matter. Generally, these are anterior to the frontal horns, lateral to the atria, or along the occipital horns (see Fig. 11-25). Within 3 to 8 hours of the initiating event, shrinkage of glial cell nuclei is accompanied by vacuolization, eosinophilia, and axon beading or swelling. Astroglial and capillary prominence develop by 12 hours postinjury and are followed by microglial proliferation progressing to macrophage infiltrates over the next few days. Mineralization of disrupted axons and necrotic glial cells and processes at the periphery of the lesion, with associated gliosis, occurs within days to weeks. If large enough, the area will cavitate as macrophages clear the necrotic debris. Because oligodendroglia are among the irreversibly damaged elements, myelination is disrupted, appearing as increased T2-weighted signal on MRI in vivo, and as pallor on myelin-stained autopsy brain sections. If severe, the white matter volume is macroscopically reduced and is marked by hydrocephalus ex vacuo and thinning of the corpus callosum and descending tracts.

The clinical manifestations of perinatal white matter injury tend to be more pronounced in preterm babies, and include spastic diplegia or quadriplegia ("cerebral palsy"). On MRI, cystic cavities may be obvious, along with evidence of delayed or permanently deficient myelination as determined by signal characteristics. In children followed by MRI over time, early cavitations may be seen to be replaced by glial scars with adjacent white matter hypomyelination and hydrocephalus ex vacuo, suggesting a capacity for remodeling in some lesions.

Figure 11-25. Periventricular leukomalacia.

Chapter 12
Neuropathology of Epilepsy

Maria Thom and Francesco Scaravilli

Epilepsy is not a single disease. The term describes the occurrence of repeated seizures that may be generalized, focal, or both. *Myoclonus*, which is a rapid, shock-like, involuntary contraction of a single muscle or muscle group, can be associated with virtually any type of epilepsy. Brain changes associated with epilepsy include both lesions that may cause epilepsy and lesions that are the consequence of epilepsy or of uninterrupted seizures (status epilepticus), although, in some cases, it may be difficult to make the distinction between them.

Epilepsy may be the consequence of a wide range of disorders affecting the brain. These include tumors, trauma, cerebrovascular disorders, inflammatory and infectious diseases, degenerative and genetically determined diseases, metabolic disorders, cortical malformations, hippocampal sclerosis, and aging. Some of these conditions are generalized, others focal; some, such as infectious and inflammatory diseases, could be included in either category, depending on their etiology.

Brain Tumors

Brain tumors (see Chap. 2) are frequently associated with epilepsy, which, in the case of supratentorial tumors, can be the presenting symptom. In these patients, the incidence of epilepsy is 35% for all types of neoplasms and 50% when cerebellar and pituitary neoplasms are excluded. Moreover, in patients with intractable temporal lobe epilepsy, tumors are diagnosed in over 50% of cases, whereas they are diagnosed in only 20% to 45% of patients with extratemporal epilepsy. All primary and secondary brain tumors are potentially epileptogenic; among these, gliomas are most often so, particularly low-grade neoplasms. Supratentorial gliomas associated with epilepsy occur most often in the temporal lobe, followed by the frontal lobe, central portions of the brain, and the occipital and parietal lobes.

Astrocytomas are the most common type of tumor associated with intractable epilepsy. This includes both infiltrative (diffuse) and well-circumscribed tumors. Well-circumscribed, low-grade astrocytomas are more often associated with epilepsy than are diffuse astrocytomas.

Dysembryoplastic neuroepithelial tumor (DNT), a glioneuronal neoplasm (World Health Organization grade 1), is an intracortical, multinodular tumor with heterogeneous cellular composition (see Chap. 2).

DNTs are typically associated with intractable seizures of the partial complex type. Rarely, patients with DNT have no history of preceding epilepsy. The type of epilepsy is usually concordant with the site of the tumor (e.g., complex partial seizures occur with temporal lobe–based tumors). Secondary generalization of the seizures may also occur. The onset of epilepsy may be in childhood, adolescence, or early adulthood; however, DNTs have less often

been discovered in older epileptic patients, even up to the age of 75.

Trauma

Both missile and non-missile head injuries may result in *post-traumatic epilepsy*.

Epilepsy following head trauma occurs either early, during the first few days (early epilepsy) or weeks or months later (late epilepsy). Seizures in the first few hours or days after injury suggest an acute intracranial hematoma (particularly when the hematoma is intradural rather than extradural) and is an important predictor of late seizures. A number of factors influence early epilepsy: age of the patient, severity of the injury, presence and localization of a fracture, and presence of intracranial hematoma. Early epilepsy is more frequent in children younger than 5 years than in older children, and the rates in both age groups are considerably higher than in adults. A fracture of the frontoparietal skull is much more prone to be associated with seizures than one in the occipital bone; the risk in the latter case is not very different from that in individuals with no fracture.

The overall incidence of epilepsy after intracranial surgery has been found to be around 17%, with a higher incidence in patients with a previous history of epilepsy. Seizures occurring more than three months after surgery for glioma are suggestive of tumor recurrence. The incidence of epilepsy varies according to the type of surgery, and is higher after ventricular shunting or after craniotomy for aneurysm than after posterior fossa surgery.

Epileptogenesis results from a number of factors, including gliotic scar, the collagenous component of the scar, and the presence of iron derived from hemoglobin.

Cerebrovascular Disorders

Many forms of cerebrovascular disease (CVD) cause epilepsy. In the elderly, CVD accounts for about 50% of all newly diagnosed epilepsy cases. Epilepsy may occur as an acute or late sequela of a cerebrovascular accident.

The pathology of cerebrovascular disorders is described in Chapter 4. Within this large group of diseases, vascular malformations (arteriovenous and venous malformations, cavernous angiomas, and capillary telangiectasias) stand out as a particularly important group because these lesions are frequently associated with epilepsy. Indeed, the seizure disorder may be the first clinical manifestation which brings the patient to medical attention.

Inflammatory and Infectious Diseases

Seizures in patients with inflammatory disorders may occur as a consequence of generalized encephalopathy, meningitis, a focal lesion of the brain (e.g., cerebral abscess or granuloma), or as the result of any focal lesion that causes scarring of brain tissue. With regard to vasculitides, the incidence of epilepsy increases with the duration or severity of the disease, ranging from 24% to 45%. Infectious diseases are associated with epilepsy in 1% to 5% of patients, the incidence being particularly high in children and in the elderly. There is no obvious increase in risk in the case of aseptic meningitis. In contrast, in the case of encephalitis the risk is increased 10 times and persists at that level for 15 years. However, in patients with encephalitis and associated early seizures the risk is 10% by 5 years and 22% by 20 years postinfection.

Infections of the CNS

Viruses, bacterial organisms, protozoa, fungi, and worms can cause seizures (see Chap. 5), and some correlation may be observed between specific encephalitides and epilepsy. Before the advent of the modern antibiotic era, neurosyphilis was deemed responsible for 15% of adult onset seizures. Among viral agents, herpes simplex is associated with complex partial and generalized seizures. Of the many parasitic infections involving the CNS, neurocysticercosis is the most commonly associated with epilepsy. Among protozoal diseases, seizures are one of the hallmarks of the clinical presentation in malaria. In Chagas disease, the incidence of epilepsy has been evaluated at about 27%; however, the relationship between the trypanosomiasis and epilepsy is indirect, via cardiac embolization of the brain.

Inflammatory Demyelinating Diseases

Although epilepsy is an expression of lesions of the gray matter, it is also a well-known complication in demyelinating diseases. It appears in 5% of individuals with multiple sclerosis and has been attributed to plaques encroaching upon the cortex.

Rasmussen Syndrome

Rasmussen syndrome (RS) is a rare, devastating disorder that is characterized by progressive, unilateral neurological deficit with sudden onset of seizures, usually in childhood, which are refractory to treatment. They are of partial complex type, and become generalized and associated with hemiplegia, hemianopia, and intellectual deterioration.

Macroscopic changes vary from case to case and are predominantly unilateral. They consist of cerebral atrophy, which may be patchy, and dusky discoloration of the cortex (Fig. 12-1A). Histological examination confirms the largely unilateral distribution of the lesions, although bilateral involvement also occurs. Lesions are more diffuse and severe than can be assumed from macroscopic observation. They include thickening of the leptomeninges with mild lymphocytic infiltration and accompanying intraparenchymal cuffing of the vessels by lymphocytes and macrophages (Fig. 12-1B). Microglial nodules and neuronophagia are ubiquitous (Figs. 12-1C and D), and the former are seen also in the white matter. In older lesions, there may also be thinning of the cortex with loss of neurons and spongiosis, severe glial reaction, and less-intense inflammatory changes.

The pathogenesis of RS is unknown. The possibility of an infectious etiology is raised by some studies, which have shown similarities between RS and the epilepsy seen in Kozhevnikov encephalitis, a tick-borne viral encephalitis with intractable seizures seen almost exclusively in Russia. The presence of an infectious ipsilateral uveitis and chorioiditis are also consistent with this hypothesis. Other supporting data include the demonstration by in-situ hybridization of Epstein-Barr virus and cytomegalovirus as reported in some studies, though not confirmed by others.

Autoimmune mechanisms of injury including immune complex deposits and vasculitis have also been postulated. Antibodies to GluR3 have been identified in RS, but these may be nonspecific. More recently, direct T-cell–mediated cytotoxicity against these neurons has been demonstrated.

The observation of cortical dysplasia, tuberous sclerosis, cavernous angioma, and tumors in patients with RS has raised the possibility that these lesions may be instrumental in inducing the seizures and altering the blood-brain barrier; this could, in turn, trigger a viral or autoimmune disorder.

Degenerative and Genetic Disorders

In *degenerative and genetic disorders*, myoclonus is observed and can be associated with various forms of epilepsy. Two groups can be discerned: (1) diseases in which myoclonus is part of a progressive cerebral disorder, and (2) diseases in which myoclonic seizures are the major symptom (i.e., the progressive myoclonic epilepsies).

Diseases in Which Myoclonus Is Part of a Progressive Cerebral Disorder

The group of diseases in which myoclonus is part of a progressive cerebral disorder includes lysosomal storage diseases (e.g., Krabbe disease and Niemann-Pick disease; see Chap. 10), other pediatric degenerative diseases of gray and white matter (e.g., Alpers disease, Canavan disease, and Alexander disease), Creutzfeldt-Jakob disease (see Chap. 6), Alzheimer disease, dementia with Lewy bodies, and progressive supranuclear palsy (see Chap. 8).

Myoclonus is also a consistent and often principal manifestation in mitochondrial cytopathies, in particular in mitochondrial encephalopathy with ragged red fibers (see Chaps. 10 and 13) and in dentatorubropallidoluysial atrophy (see Chap. 8).

In the past, myoclonus with progressive cerebellar ataxia, with or without seizures, was referred to as *Ramsay-Hunt disease*, a disease characterized pathologically by degeneration of the cerebellar dentate nucleus. It appears now that Ramsay-Hunt is not a distinct entity but includes a variety of clinically, biochemically, and genetically heterogeneous conditions.
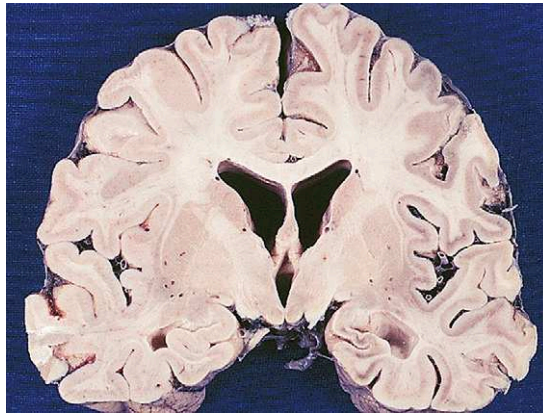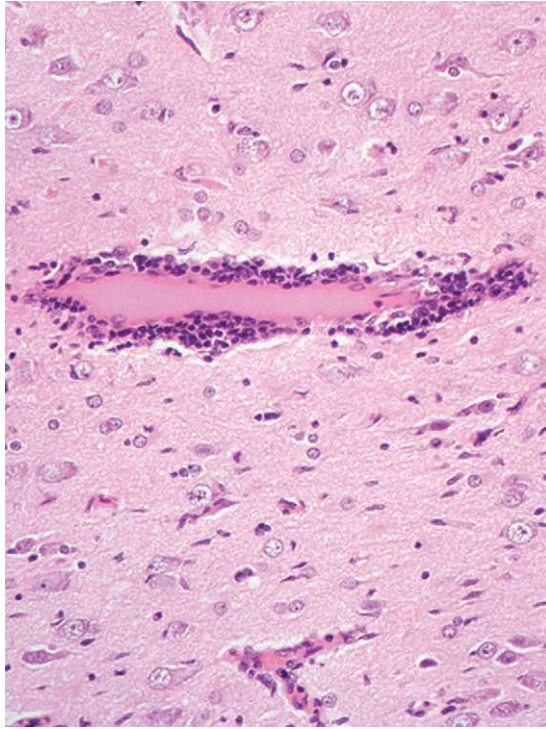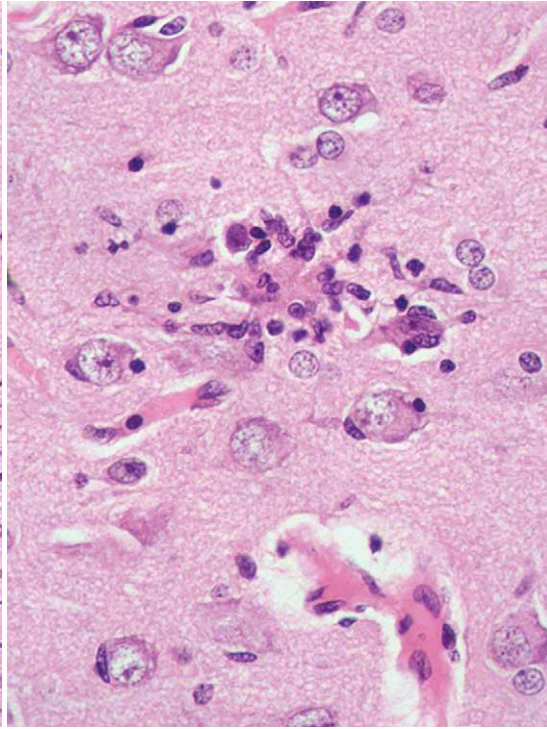
Figure 12-1. Rasmussen encephalitis. **A**, Gross appearance. **B**, Intraparenchymal perivascular cuffing by lymphocytes and macrophages (H and E). **C**, Nodule of neuronophagia (H and E). **D**, Microglial nodule (H and E). **E**, Proliferation of rod cell microglia (immunocytochemistry for CD68).

Progressive Myoclonic Epilepsies

Progressive myoclonic epilepsies are mostly familial disorders. They are characterized by severe epilepsy with prominent myoclonus and progressive neurologic deterioration.

Unverricht-Lundborg Progressive Myoclonus Epilepsy

Unverricht-Lundborg progressive myoclonus epilepsy (also termed *Baltic myoclonus*) is an autosomal recessive disorder. The disease is ubiquitous,

D   **E**
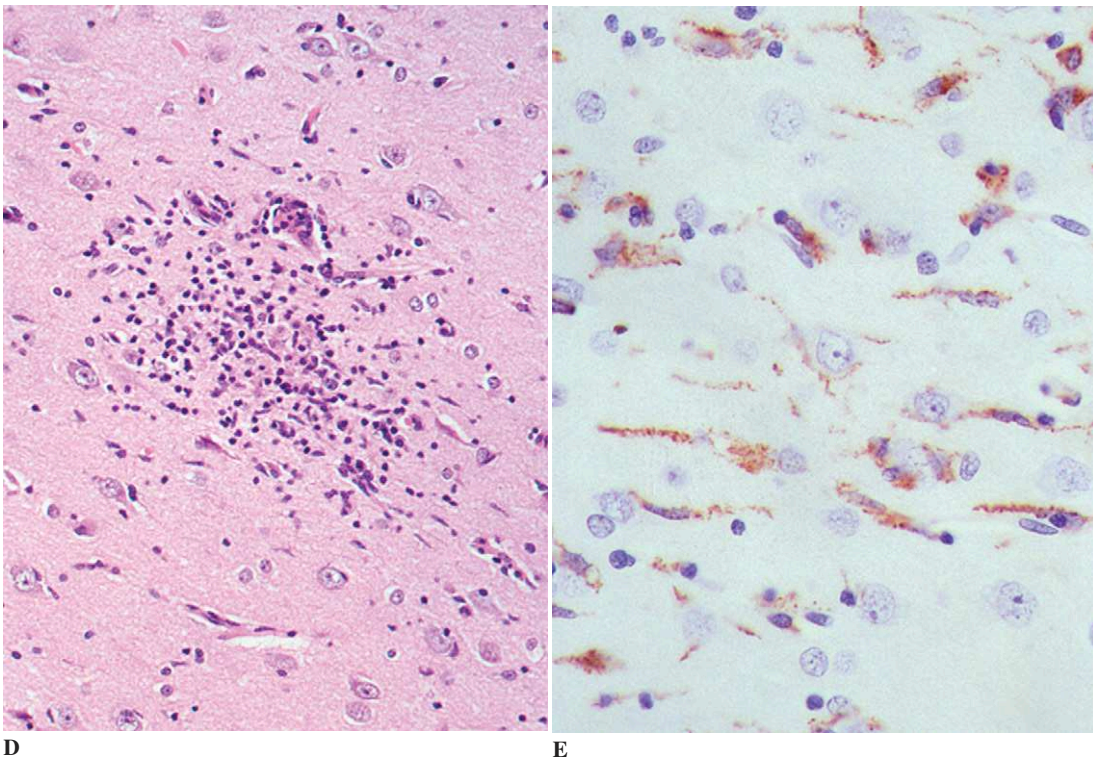
Figure 12-1 continued.

but has its highest incidence in Baltic countries (1 in 20,000 individuals). The gene locus is on the long arm of chromosome 21 (21q22.3) and encodes cystatin B, a cystein protease inhibitor. The disease presents in childhood or adolescence with generalized myoclonic seizures that may progress to generalized tonic seizures. Cerebellar ataxia and pyramidal signs also occur, together with muscle atrophy and depressed tendon reflexes. Intellectual decline may also follow.

Morphological changes in the nervous system are nonspecific. There is nerve cell loss in basal ganglia, thalamus, brainstem, and anterior horns of the spinal cord; in the cerebellum, there is loss of dentate nucleus–neurons and Purkinje cell with proliferation of Bergmann glia. The inferior olives, substantia nigra, and subthalamic nucleus can also be affected. In some patients, examination of sweat glands shows membrane-bound vacuoles.

Lafora Body Disease

Lafora body disease (also termed *familial progressive myoclonic epilepsy with Lafora bodies*)

is a disorder of carbohydrate metabolism. The mode of inheritance is autosomal recessive. The *EPM2A* gene on chromosome 6q23-25 encodes laforin, a protein on the plasma membrane and the endoplasmic reticulum that functions as a dual-specificity phosphatase. Eighty percent of patients with Lafora body disease have mutations in this gene. Onset is usually between 9 and 20 years; however, adult onset is also seen. Symptoms include generalized seizures followed by myoclonus, personality changes, unusual behavior, cerebellar and pyramidal signs, and optic atrophy with visual symptoms.

Neuropathological findings include mild, diffuse, cortical atrophy and neuronal loss in the globus pallidus and dorsomedial nucleus of the thalamus. A characteristic feature of the disease is the Lafora body, a formation ranging from 1 to 30 μm in diameter that is seen in the perikaryon of nerve cells, in axons, and in dendrites (see Fig. 1-17). One or more inclusions may be present in the same cell. Their cores stain intensely with periodic acid-Schiff (PAS) and Alcian blue and are diastase-

and hyaluronidase-resistant. Lafora bodies are metachromatic with methyl violet and toluidine blue. Lafora bodies are ubiquitous in the brain; however, they are most numerous in the central gyrus and anterior frontal region, thalamus, globus pallidus, and substantia nigra. There are only few present in the brainstem, but many are seen in the cerebellum. Outside the central and peripheral nervous system, Lafora bodies are found in the liver, skeletal-muscle, and apocrine sweat glands. The disease leads inexorably to dementia and to death within 10 years.

*Myoclonus Epilepsy with Mutation
of the Neuroserpin Gene*

A third form of progressive myoclonus epilepsy has been recently reported in two North American families. It is characterized by generalized seizures, myoclonus, and progressive neurologic deterioration, with onset in the third decade. The disorder is due to a mutation of the neuroserpin gene, which is located in chromosome 3q26. Neuroserpin is a serine protease inhibitor, a regulator of extracellular proteolytic reactions. As a result of the mutation, there is accumulation of abnormal protein as eosinophilic intracytoplasmic inclusions in neuronal cell bodies and processes throughout the CNS.

Palatal Myoclonus

Palatal myoclonus (or *palatal tremor*) is associated with lesions of the central tegmental tract or dentate nucleus and may be associated with hypertrophy of the inferior olive. These lesions may be either degenerative or due to a wide range of abnormalities including infarction, vascular malformations, tumor, and demyelination.

Metabolic Disorders

Alcohol-related seizures have been known since the time of Hippocrates. Recent studies show that they account for 16% of cases of epilepsy and that alcohol abuse is among the commonest causes of adult-onset epilepsy. However, it is now well-demonstrated that most alcohol-related seizures

result from withdrawal of alcohol. Moreover, alcohol may precipitate fits in epileptic patients and thus may reveal underlying epilepsy in previously asymptomatic individuals.

Seizures may follow both acute and chronic alcohol abuse. Acute neuropathologic changes include cerebral congestion, edema, and petechial hemorrhages; cellular lesions may be reversible and are nonspecific.

Chronic changes that may be related to seizure disorder include brain atrophy and cerebellar degeneration (see Chap. 9). Histological examination may show neuronal swelling or pyknosis, accumulation of lipofuscin, and patchy loss of medium-size pyramidal cells in the superficial and intermediate cortical layers. It is difficult to be certain that any of these changes are directly related to the effects of alcohol on the CNS.

*Morel laminar sclerosi*s is the best-known of the cortical disorders in chronic alcoholism. It is characterized by diffuse atrophy with neuronal loss and gliosis of layers II and III of the frontotemporal cortex. This disease is usually associated with, and probably secondary to, the callosal lesions of Marchiafava-Bignami disease (see Chap. 9).

Seizures are also a common manifestation of hereditary metabolic diseases that involve gray matter.

Cortical Malformations

Malformation of cortical development resulting from a disorder of normal cortical cell genesis, migration, and maturation are discussed in detail in Chapter 11. Those that are of particular importance in causing seizures are discussed in the following sections.

Laminar, Subcortical Band Heterotopia (Double Cortex). This consists of bilateral, often symmetrical bands of gray matter of variable thickness, within the centrum semiovale and separated from the normal-looking cortex by a band of white matter (Fig. 12-2A). The temporal lobe is usually spared. Histologically, heterotopias reveal well-differentiated, randomly oriented, and focally clustered nerve cells (including pyramidal cells) that form bands or aggregates (Fig. 12-2B). The overlying cortex usually has a hexalaminar organization.
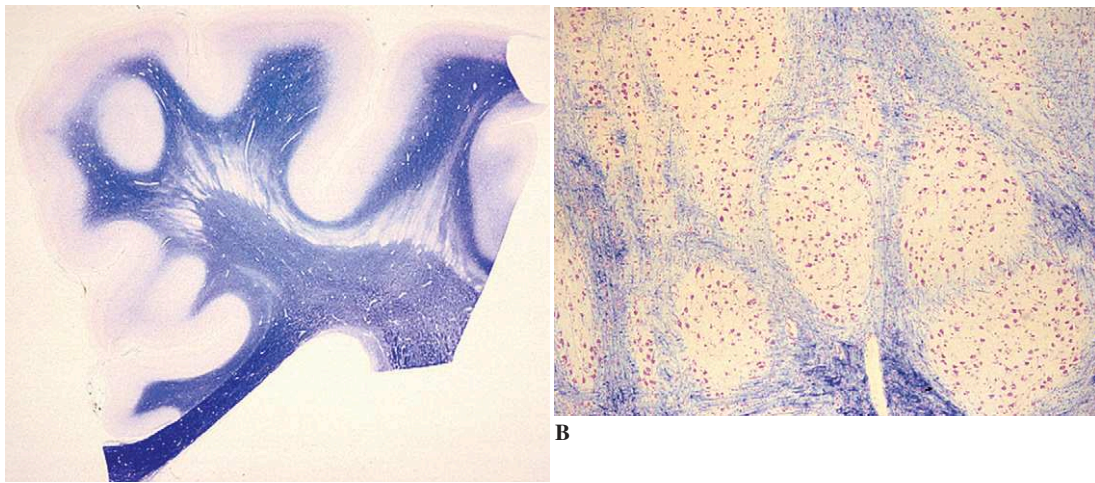
Figure 12-2. Laminar subcortical heterotopia. **A**, Heterotopic tissue separated from the normal cortex by a layer of normally myelinated white matter (Luxol fast blue/cresyl violet). **B**, Nerve cells in the heterotopic gray matter are arranged in irregular aggregates of normal-looking pyramidal cells (Luxol fast blue).

Periventricular Nodular Heterotopia (see Chap. 11)**.**   This is the most common form of heterotopia in adults and appears as discrete and well-defined nodules (2 to 10 mm) beneath the ependymal lining (Fig. 12-3). The trigones and occipital horns of the lateral ventricles are the most commonly affected regions. Histologically, the nodules consist of islands of mature nerve cells resembling cortical neurons, interneurons, and glia. Nodular heterotopia may be an isolated finding or complicate other cerebral malformations, such as microcephaly, agenesis of the corpus callosum, cerebel-

lar hypoplasia, polymicrogyria, agyria, pachygyria, and cortical dysplasia.

Localized or Focal Malformations

Focal Cortical Dysplasia

Focal cortical dysplasia (FCD) may involve any cerebral lobe, but more frequently involves the frontal and temporal lobes around the central sulcus. Macroscopic examination of resected surgical specimens is often unremarkable, although sometimes a smooth cortex lacking sulci, thickening of the gyri, or blurring of the gray matter–white matter border have been reported.

Histological findings include a disorganized, hypercellular cortex with disruption of the normal lamination; persistence of the columnar alignment of nerve cells; heterotopic nerve cells in the molecular layer; and increased numbers of nerve cells in the underlying juxtacortical white matter (Fig. 12-4B). The following cytological abnormalities have been described: bizarre, cytomegalic nerve cells reaching the size of Betz cells; vacuolation and random orientation of abnormal nerve cells (Fig. 12-4A), with increased number of branching and arborization of dendritic processes, as revealed by Bielschowsky stain (dysplastic neurons); and

Figure 12-3. Subependymal/periventricular heterotopia. Section of frontal lobe showing multiple nodules of gray matter above the caudate nucleus.
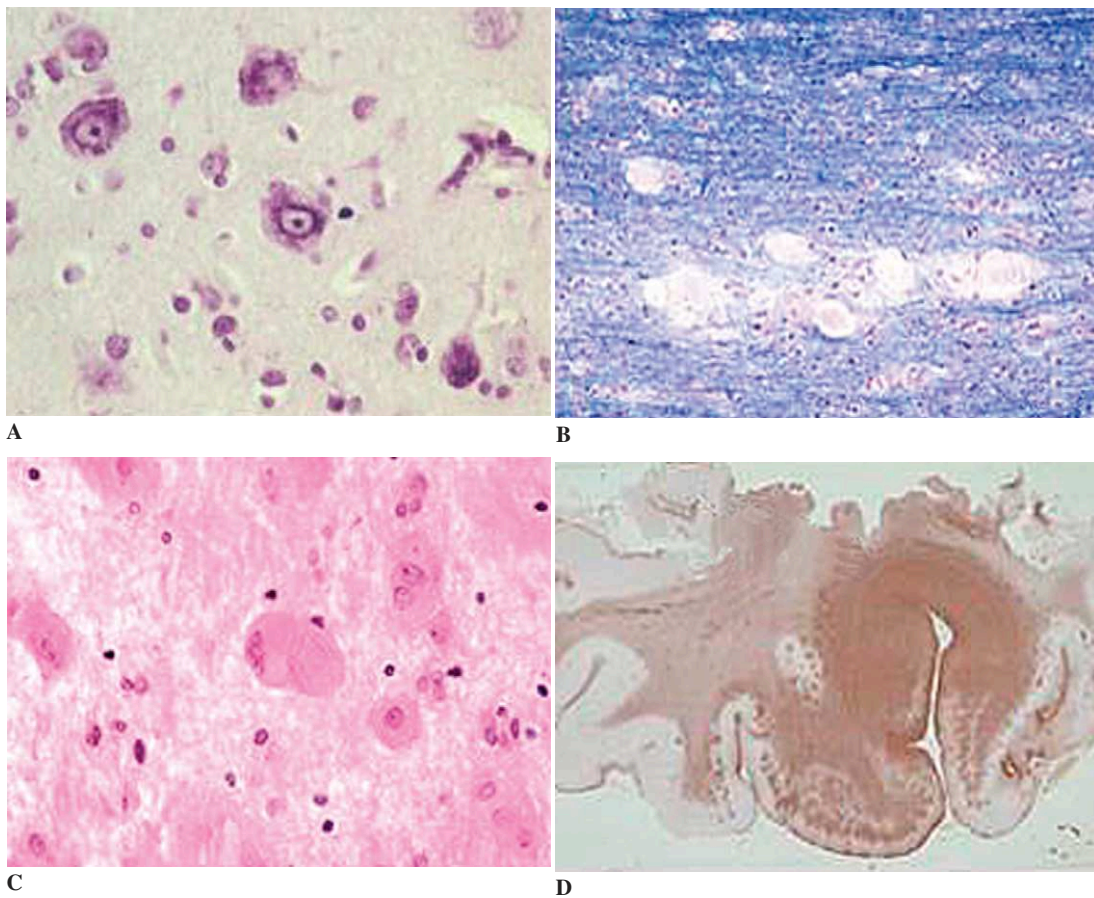
Figure 12-4. Focal cortical dysplasia. **A**, Dysplastic neurons in focal cortical dysplasia. The neurons are enlarged and show apparent thickening of the nuclear membrane. They are irregularly orientated within the cortex (Cresyl violet stain). **B**, Aggregates of balloon cells in the white matter underlying an area of focal cortical dysplasia (Luxol fast blue/Nissl). **C**, Balloon cells in the cortex in a region of focal cortical dysplasia (H and E). **D**, An area of cortical dysplasia with marked gliosis as seen on glial fibrillary acidic protein (GFAP) immunostaining.

ballooned cells (Fig. 12-4B), which have abundant, glassy cytoplasm and an astrocyte-like morphology but show variable glial fibrillary acidic protein (GFAP) positivity and are therefore also called "uncommitted cells" (Fig. 12-4D).

Abnormal nerve cells in areas of FCD show cytoskeletal changes such as coarse intracytoplasmic fibrillary inclusions (which stain with antibodies to high and medium weight phosphorylated neurofilaments, and microtubule-associated protein (MAP) antibody, as well as weakly with anti-ubiquitin antibody). Although these inclusions are reminiscent of neurofibrillary tangles seen in Alzheimer disease, they do not stain with anti-

bodies to paired helical filaments. In addition, dysplastic cortical cells are positive with immature (MAP1B, MAP2C) MAP2 antibody; this may reflect an increased plasticity and remodeling of dendrites in these cells. Dysplastic cells stain also with the embryonal form of the cell adhesion molecule N-CAM (E-NCAM) as well as well as developmental neurofilament nestin and internexin, supporting the hypothesis of maturational failure. Ballooned cells in FCD stain with anti-GFAP antibody, in keeping with electron microscopic evidence of intermediate cytoplasmic filaments. In addition, some cells contain neuronal markers and even dual labeling has been elicited, thus reflecting

an intermediate glial and neuronal differentiation. On the other hand, the proliferation index of these cells is low.

Additional histological features reported in FCD include subpial layers of myelinated axons, reactive gliosis, subpial fibrillary (Chaslin) gliosis, loss of axons, and an increased number of corpora amylacea. Low-grade tumors (pilocytic and fibrillary astrocytomas, DNTs, gangliogliomas, and meningoangiomatoses) have been reported adjacent to cortical malformations. Less commonly reported features are inflammatory, degenerative, or destructive lesions. It should be mentioned also that hippocampal sclerosis and Rasmussen's encephalitis may occur in combination with FCD.

FCD has features reminiscent of tuberous sclerosis (TS). However, the following characteristics should help distinguish between the two disorders: patients with FCD show no systemic or cutaneous stigmata of TS, absence of subependymal lesions or calcifications, and no family history of TS, and the onset of epilepsy tends to occur at an older age than in TS. In addition, tubers in TS tend to be multiple and distributed throughout the cerebral hemispheres and are macroscopically recognizable, whereas lesions in FCD are more often solitary. Histology of tubers shows a paucicellular cortex with bizarre nerve cells, but with relatively more atypical glial cells at the corticomedullary junction. A peculiar "wheatsheave" arrangement of astrocytes in the subpial region is typical of tubers. However, differentiation from FCD is not always possible by histology alone and genetic analysis should be carried out when there is uncertainty.

Microdysgenesis

Microdysgenesis (MD) is not visualized either by imaging or naked-eye examination. The spectrum of histological features described includes presence of unipolar or bipolar nerve cells in the subpial layer; an excess of nerve cells in the molecular layer, either singly or in nodules; an indistinct boundary between laminae I and II; protrusion of nerve tissue into the pia; persistence of columnar alignment of cortical nerve cells in some cases; and increased numbers of heterotopic cells in the white matter. The cytoarchitectural abnormalities may represent remnants of the embryonic preplate and abnormally migrated neurons.

It has been postulated that MD represent a morphological hallmark that correlates with epilepsy, rather than being its specific cause. Increased numbers of heterotopic nerve cells in the frontal-lobe white matter have also been seen in patients with post-traumatic epilepsy.

Hippocampal Sclerosis

The occurrence of abnormalities in hippocampal structure in patients with epilepsy has been known since the early 19th century. *Ammon's-horn sclerosis* is the most common lesion seen in temporal lobe resections for intractable partial complex seizures arising in the temporal lobe. Its incidence ranges from 47% to 70% of all cases of temporal lobe epilepsy. The disease presents in early childhood, and patients have no family history of epilepsy. A history of febrile seizures in infancy or early childhood is reported in 75% of cases.

The most striking pathological change is seen in the CA1 region, also known as *Sommer's sector*, in which some neuronal loss is always present and may be total. Changes may also involve CA3 and CA4 (the hilum of the dentate gyrus). CA2 and the dentate gyrus also may be somewhat involved, but much less severely. Cell loss is accompanied by reactive gliosis, whose severity is comparable to that of the neuronal loss. Hippocampal sclerosis may be unilateral, though involvement has been reported in 18 % to 60% of the patients.

It has been recently observed that a number of patients with hippocampal sclerosis have additional changes of the laminar organization of the fascia dentata (Fig. 12-5). The abnormality may present either as *dispersion*, in which the layer is wider than normal, or as *duplication*. Dispersed granule cells may be aligned in columns, have elongated and bipolar shape, and may extend into the molecular layer. These abnormalities have been considered as the result either of an alteration of cell migration or as evidence of neuronal plasticity.

It is not always clear whether the hippocampal sclerosis precedes the onset of epilepsy, and if so, if it progresses following repeated seizures. In some patients with temporal lobe epilepsy, seizures progressively worsen over time. Several prospective MRI studies have shown progression to
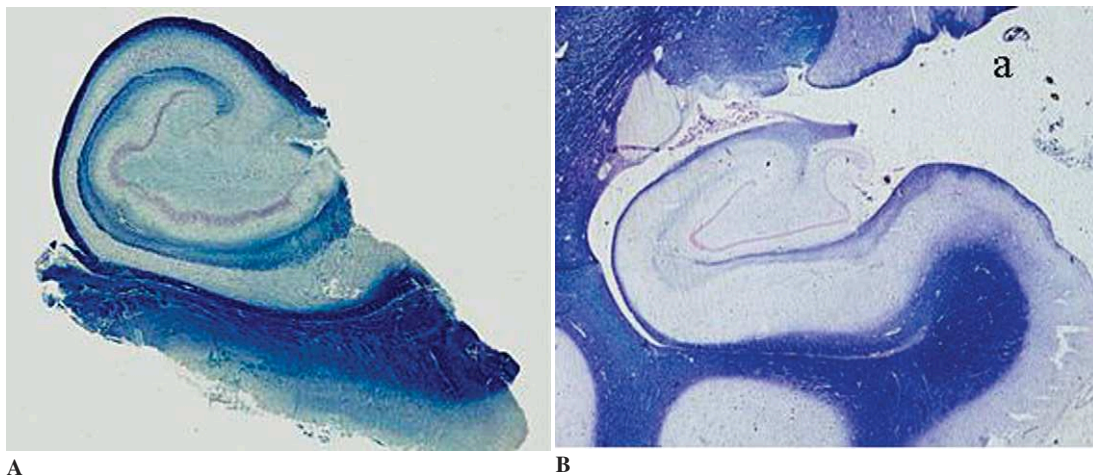
Figure 12-5. Hippocampal sclerosis. **A**, A surgical specimen from a patient with chronic temporal lobe epilepsy and hippocampal sclerosis. The CA1 region shows narrowing that corresponds to marked neuronal loss and gliosis. **B**, The widening of the granule cell layer can be appreciated by comparison with a normal control.

hippocampal sclerosis in patients with convulsive status epilepticus; excitotoxicity has been proposed as a pathogenetic mechanism of injury.

Combination of severe lesions in patients with temporal lobe epilepsy and hippocampal sclerosis may occur. These additional lesions include congenital malformations, gliomas and ganglion cell cortical scars, neoplasms, inflammation, developmental cysts, and vascular lesions.

Status Epilepticus

Status epilepticus (SE) is a condition of seizure activity, which is either continuous or intermittent, but without intervening recovery for a period greater than 60 minutes for adults and 30 minutes for children. It is a medical emergency with high morbidity and mortality, even after the introduction of appropriate drugs and emergency treatment. SE may occur both in epileptic patients and in those without a previous history of epilepsy. In the latter case it follows cerebrovascular accident, drug overdose, tumor, trauma, cardiac arrest, or alcohol withdrawal.

Various morphological changes have been associated with SE, including chromatolysis of cortical pyramidal neurons of layer II and III; hippocampal cell loss or ischemic changes, sometimes with acute gliosis; and loss of cerebellar Purkinje and granule cells. Children are more susceptible than adults to these insults.

Sudden and Unexpected Death in Epilepsy

Death in epileptic patients may occur as a result of a concomitant disease, a brain disorder that also causes the seizures (secondary epilepsy), status epilepticus, an accident as a result of a seizure, or suicide, or can be *sudden and unexplained death in epilepsy* (SUDEP). To satisfy the definition of SUDEP, no anatomically or toxicologically demonstrable cause of death can be found postmortem. Known accidental deaths during a seizure (e.g., by suffocation, aspiration, or drowning) are excluded from the SUDEP group.

SUDEP accounts for 5% to 30% of epilepsy deaths. It tends to affect younger patients. In most cases there is a long history of generalized seizures, although it may occur in partial seizures. In many cases, the epilepsy is not well controlled.

Neuropathological changes at post mortem include cerebral edema, old contusions, vascular malformations, old infarcts, hippocampal sclerosis, tumors, and gray matter heterotopia.

Various theories have been brought forward to explain SUDEP, including cardiac arrhythmia

and hypoxemia or apnea following seizure. The former theory seems to be more widely accepted than the others and has the support of experimental work.

Aging and Epilepsy

The incidence of epilepsy appears to increase significantly after the age of 60. The most common cause of epilepsy in this age group is cerebrovascular disease, whereas neurodegenerative disorders account for a smaller number of cases. On the other hand, idiopathic epilepsy still accounts for a significant proportion of the cases. These figures represent an increased incidence in the elderly and could be the consequence of a change in the susceptibility of the old brain to epileptogenesis, a hypothesis that is supported by experimental data on animals. A further possible cause could be a mutation of mitochondrial DNA (known to take place with advancing age) and the consequent abnormality in neuronal oxidative phosphorylation.

Changes Secondary to Epilepsy

Nerve Cell Loss

Nerve cell loss in epilepsy is a frequent event. Histologically, changes include also nonspecific gliosis (the classical example of which can be seen in the hippocampus) and Chaslin's subpial gliosis. The loss of neurons seems to affect the same regions and neuronal subgroups that are vulnerable to status epilepticus. It can affect any region of the brain and be associated with all types of epilepsy.

Cerebellar Atrophy

Cerebellar atrophy with epilepsy consists of loss of Purkinje cells, preservation of the baskets, and proliferation of Bergmann glia. This pathology has been considered as the consequence of a number of pathogenetic mechanisms including phenytoin toxicity (see Chap. 9), as confirmed by reports of permanent ataxia after the withdrawal of the drug and

by experimental studies. However, in view of the small number of cases with lesions compared with the large number of patients treated, it seems unlikely that the drug plays a direct role in the cerebellar damage.

Cerebral Hemiatrophy

Cerebral hemiatrophy consists of reduction in size of one cerebral hemisphere. Acute and chronic forms of this lesion have been described. Changes consist of nerve cell loss in a laminar distribution, involving layer III and, less often, layers II and V, with associated gliosis. In some severe cases, the whole thickness of the cortex may be involved. Some areas, such as the calcarine cortex, are sometimes spared, whereas the hippocampus is invariably involved.

Contralateral Cerebellar Atrophy

Contralateral cerebellar atrophy is observed in patients with cerebral hemiatrophy and tends to be associated with longstanding, diffuse, severe contralateral lesions of the cerebral hemisphere. One may distinguish three types of lesions: (1) reduction in size of the cerebellar hemisphere without significant cortical changes; (2) cerebellar cortical degeneration involving predominantly the granular layer and thinning of the molecular layer; and (3) lobular sclerosis, in which loss of Purkinje cells is the most characteristic finding.

Surgical Management of Chronic Epilepsy

In approximately one third of patients with epilepsy, seizures remain uncontrolled despite trials with a variety of antiepileptic drugs. In these patients, surgical intervention may offer the opportunity of a reduction or even elimination of the seizures.

Most patients who may benefit from surgery have lesional or secondary epilepsy. Excellent outcomes following temporal lobectomy in patients with hippocampal sclerosis have been reported, with over two thirds of patients becoming seizure-free and many showing quality-of-life

improvements. The benefits of surgery in the resection of localized lesions as DNT and vascular malformations are also well documented. In cases with multiple lesions, surgery does not seem to alter significantly the frequency of seizures unless all lesions are removed. In malformations of cortical development, seizure-free outcomes are achieved in around 40% of cases, although this varies according to the type of lesion and the length of the follow-up period. For the treatment of temporal lobe epilepsy, a temporal lobectomy is the standard treatment. Operative procedures include "en bloc" resection of the anterior temporal lobe versus selective resection of the amygdala and hippocampus.

Chapter 13
Skeletal Muscle Diseases

Hart Lidov, Umberto De Girolami, and Romain Gherardi

General Considerations

Neuromuscular pathology must always be evaluated in a multispecialty context; the integration of clinical features (age of onset, clinical picture, course), electrophysiological recordings, and in some instances, neuroimaging constitute information which permits the formulation of most likely clinical diagnostic hypotheses preceding the biopsy. The object of the biopsy is to confirm, extend, or perhaps disprove these initial hypotheses. Determining the need for a muscle biopsy, ensuring its performance, and formulating the interpretation can best be accomplished through collaboration between the neurologist and neuropathologist.

Biopsy of Skeletal Muscle

Site of the Biopsy

Uniformity in muscle biopsy site is frequently the best approach; nevertheless, biopsy of a severely involved or "end-stage" muscle, and conversely of minimally involved muscle, should be avoided. Magnetic resonance imaging (MRI) is also now being used to guide the choice of biopsy sites. It is important not to biopsy the region of a prior electromyographic needle puncture, which may be the site of a focal necrotic inflammatory reaction and therefore give misleading information.

Techniques

Choice of Technique

The choice of appropriate techniques in the evaluation of a muscle biopsy is made in the context of the clinical setting. Biopsies are performed in circumstances ranging from known systemic disease (which may or may not manifest with neuromuscular deficit—e.g., vasculitis, sarcoidosis) to primary neuromuscular disorders. Unfortunately, clinical manifestations frequently do not permit such a clear-cut distinction prior to the biopsy; indeed, the goal of the biopsy is to discriminate between these possibilities.

At one end of the spectrum, the diagnosis may be obtained satisfactorily with "routine" histopathological techniques performed on formalin-fixed, paraffin-embedded tissue. This is adequate for the study of interstitial lesions, such as inflammation and vasculitis.

At the other extreme, precise analysis of morphology, immunocytochemical expression of muscle-specific proteins, and even ultrastructural study may be necessary for the definitive diagnosis of a neuromuscular disease.

Therefore, in cases of suspected neuromuscular disease, it is proper to begin the muscle biopsy evaluation by studying precisely oriented, frozen cross-sections of muscle stained with H and E, the modified Gomori trichrome stain, periodic acid-Schiff (PAS), and oil red O, as well as a battery of muscle enzyme histochemical reactions, including NADH-TR (NADH tetrazolium reductase), cytochrome-*c* oxidase (COX), and ATPase at acid and alkaline pHs. The study can be complemented by (1) immunocytochemistry for specific structural proteins or immunologic markers, (2) electron microscopy, which is essential for the identification of certain structural abnormalities; and (3) study, in rare instances, of terminal motor innervation. It is also the rule to keep frozen tissue for biochemical studies, particularly in metabolic diseases or for the molecular diagnosis of hereditary disease (Western Blot, Southern Blot, polymerase chain reaction [PCR]).

Muscle Enzyme Histochemistry

Assessment of muscle pathology largely relies on histoenzymatic reactions aimed at detecting endogenous enzymatic activities of muscle fibers, which convert soluble substrates into insoluble precipitates. Particular methods employ specific substrates to demonstrate specific enzymes, such as myosin ATPase, COX, many of the lysosomal enzymes, and the enzymes of the glycolytic pathway. These methods require frozen, unfixed tissue sections in which the native enzymatic activities are preserved.

In muscle pathology this study has several objectives, as discussed in the following subsections.

Analysis of Different Fiber Types (Table 13-1). One of the defining characteristics of type 1 (slow-twitch) muscle fibers and type 2 (fast-twitch) muscle fibers is that the myosin ATPases in these two fiber types have different optimal pH. Advantage can be taken of this difference by preincubating tissue at pH 4.3 or 9.4, respectively; as a result, the histochemical reaction selectively demonstrates type 1 or type 2 fibers. The ATPase activity of type 1 fibers is weak at alkaline pH (9.4), but strong at acidic pH (4.3); thus, the type 1 fibers appear pale at pH 9.4 and dark at pH 4.3, and the reverse is true

Table 13-1. Chief Enzyme Histochemical Characteristics of the Different Types of Muscle Fibers

Enzyme Reactions	Fiber Type 1	Fiber Type 2A	Fiber Type 2B
NADH-TR	+++	++	+
ATPase 9.4	+	+++	+++
ATPase 4.6	+++	0	+
ATPase 4.3	+++	0	0

NADH-TR = NADH tetrazolium reductase, O = no reaction, + = weakly reactive, ++ = moderately reactive, +++ = strongly reactive.

of type 2 fibers. This distinction can be further refined by carrying out the ATPase reaction at pH 4.6, which permits differentiation of type 2A and type 2B fibers (Fig. 13-1). A small percentage of fibers appear dark—that is, strongly reactive at both acid and basic pH—and these are designated *2C fibers*. They are interpreted as fetal/pathological fibers, since this pattern of lack of pH sensitivity appears to be a normal feature of fibers expressing some forms of myosin early in development, as well as of some fibers that may be regenerating in the context of a myopathy.

Type 1 fibers, which are rich in oxidative enzymes, stain strongly by NADH-TR and succinic dehydrogenase (SDH), whereas type 2 fibers are relatively weakly stained. One caveat regarding this fiber type differentiation is that there is an apparent "concentration" of organelles in atrophic
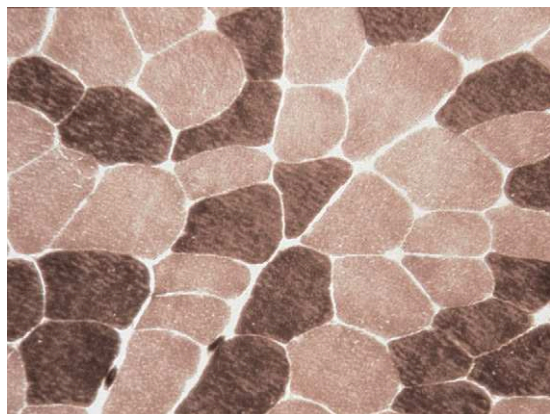
Figure 13-1. Frozen section of a normal muscle with ATPase reaction at 4.6. Mosaic pattern of the different fiber types.

fibers, and a tendency for all small atrophic fibers to stain darkly with oxidative reactions.

Demonstration of Subcellular Organelles. The acid phosphatase reaction reveals lysosomal hyperactivity. Mitochondria are reactive for NADH-TR, SDH, and COX, whereas the T-tubule system and other membranous organelles are only reactive for NADH-TR.

Detection or Specification of Certain Structural Abnormalities. NADH-TR reveals structural anomalies associated with focal mitochondrial loss or with a disorganized distribution of such structural abnormalities as target fibers, cores, lobulated fibers, or "moth-eaten" fibers.

Documentation of Specific Enzymatic Defects. Myophosphorylase deficiency can be identified in McArdle disease; myoadenylate deaminase deficiency can be identified in certain myalgia/cramp syndromes.

Immunohistochemistry

Immunohistochemical reactions are now used routinely in muscle pathology. They can be performed on frozen sections and, for the identification of some proteins, on paraffin sections. They may be used for the purposes described in the following subsections.

Identification of the Different Fiber Types. Immunohistochemistry for fast myosin, which is expressed in type 2 fibers, is an excellent means for fiber typing on paraffin or frozen sections.

Detection of Muscle Regeneration. The neural cell adhesion molecule (NCAM) isoform CD56/Leu19 is a marker of human satellite cells, which are mononucleated muscle precursor cells that normally reside beneath the basal lamina of muscle fibers. They account for more than 10% of myonuclei in young people and about 2% to 3% in adults. Postnatal muscle growth and regeneration result from activation, proliferation, and fusion of satellite cells into muscle fibers. Increased expression of NCAM by muscle fibers is useful to assess muscle regeneration following injury.

Other. Immunohistochemical methods can also be used to detect structural proteins and constitute an important diagnostic tool in the muscular dystrophies. They are also useful in characterizing the cells in inflammatory myopathies (see later in this chapter).

Normal Appearance on Frozen Section

Much information is gained from the initial histological examination of the overall architecture of the muscle biopsy. In cross section, the muscle fibers are polygonally shaped, fairly uniform in size, and have little intervening space between them. Neuromuscular spindles are recognized as round structures (about 50–100 μm in diameter) with intrafusal fibers and contained by a connective tissue capsule. The nuclei of muscle fibers are ordinarily located next to the subsarcolemma, although even in specimens without any apparent neuromuscular disease as many as 3% to 5% percent of fibers may have more centrally located or internalized nuclei. Endomysial connective tissue normally consists of thin, delicate, almost imperceptible strands between the fibers and in the capillary network. The perifascicular connective tissue, or perimysium, contains small arteries, arterioles, veins, and nerve twigs, but in the adult, it is normally devoid of adipocytes. The fascia or epimysium, situated at the periphery of several fascicles, contains neurovascular bundles and adipose tissue.

A motor unit (i.e., a single motoneuron and its innervated myocytes) comprises muscle fibers of the same histochemical type. These fibers are not adjacent, but normally are spatially dispersed in a muscle fascicle over a distance of several millimeters. On histochemical reactions, the muscle appears as a mosaic of the two fiber types (see Fig. 13-1). In the adult, the number of types 1, 2A, and 2B fibers are roughly comparable in the muscles that are usually studied (i.e., type 1, 30–40%; type 2A, 20–30%; type 2B, 40–50%; type 2C, 1–2%). The percentages of each fiber type vary not only with the particular muscle studied but also according to sex, age (Table 13-2), and physical state, making it necessary to evaluate the results in comparison to normative data of closely matched controls.

The appearance of normal muscle, as just described, applies only to adults; in biopsies from

Table 13-2. Mean Diameters of Muscle Fibers According to Age

Age	Diameter (μm)
Newborn	12
1 year	16
10 years	40
Adult female	30–70
Adult male	40–80

infants and very young children, muscle fibers are round and only become fully polygonal later in development. As the mean fiber diameter is a function of age, analysis of muscle biopsies in infants and children requires comparison to normal values for age (see Table 13-2). Nevertheless, variability of fiber diameter is not a function of age, (i.e., excessive variation in fiber diameter is abnormal even in infants). Normally there may be increased variability in fiber size and shape near tendinous insertions (sites that should be avoided in biopsy) and in certain muscles such as the extraocular muscles, diaphragm, and paraspinal muscles.

Basic Reactions

Changes in Muscle Fibers

Before considering the spectrum of pathologic change in muscle fibers, one must be cognizant of the histologic artifacts that may occur and avoid interpreting these as significant alterations. Foremost among these is "freeze artifact," the formation of spaces due to intramyocytic microcrystal ice formation. This is the result of improper freezing of the muscle tissue. Tissue fixed with formaldehyde and destined for paraffin embedding can become distorted during fixation and is rarely properly oriented. Paraffin sections commonly show contraction artifacts and preclude fine morphological analysis of muscle fibers; however, they remain valuable to assess interstitial and vascular inflammatory changes.

Variations in Size and Shape

The first parameters evaluated are the uniformity of muscle fiber size (diameter) and shape. Fibers should be relatively uniform in size, although the mean diameter increases up to ages of 12 to 15. If a significant population of smaller or larger fibers is present, the condition is described as "excessive variation in fiber size." Fibers that have lost the polygonal contour and are smaller than normal and triangular in shape, "small angulated fibers," are not a normal feature. "Hypercontracted fibers" (see Fig. 13-11B), which are characterized by a distinctly round appearance amid a background of somewhat smaller polygonal fibers and by moderate hyperchromasia, are an abnormality. They are particularly frequent in muscular dytrophies, but they can occur in biopsies of patients with no other evidence of neuromuscular disease.

Atrophy and Hypertrophy

Hypertrophy consists of increase in size of the muscle fibers, often associated with loss of their usual polygonal outline. Some observers have reported that physiological hypertrophy of type 2 fibers may be seen in athletes, but definitive data on the muscle biopsy changes in response to training is lacking. In pathological skeletal muscle, hypertrophied fibers are a compensatory change, and are often accompanied by structural changes such as internalized nuclei and split fibers (Fig. 13-2).

Atrophic fibers may be rounded in myopathic processes; they may be angulated in neurogenic processes. In the end stages of atrophy, the atrophic fibers form "nuclear bags" (i.e., clusters of nuclei within muscle cells largely devoid of myofibrillary material; see Fig. 13-7C). In the late stages of both myopathic and neurogenic processes, the muscle becomes "end-stage" and categorizing the shape of atrophic fibers becomes a fruitless effort.

Once atrophic fibers are identified, their distribution—either randomly scattered or grouped together in clusters—is significant. *Fascicular* or *group atrophy*, a hallmark of denervation, consists of aggregates of atrophic fibers that occupy part of a fascicle. This process differs from perifascicular atrophy, as seen in dermatomyositis, in which atrophic fibers line the edges of the fascicles and transition to atrophy is gradual. Randomly scattered atrophic fibers are less characteristic of a particular pathologic process; when they involve both
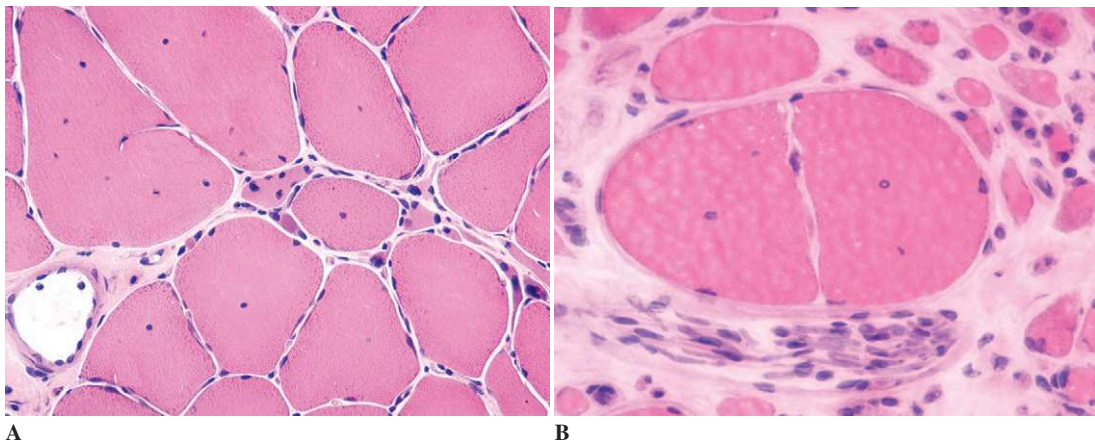
Figure 13-2. Variation in size and shape of the muscle fibers. **A**, Small angulated fibers contrasting with hypertrophic fibers with internalized nuclei. **B**, Hypertrophic, split muscle fiber with central nuclei in muscular dystrophy.

fiber types, they may represent early stages of denervation.

Atrophy may select a particular fiber type. *Type 1 atrophy* (Fig. 13-3) is usually seen in myotonic dystrophy and in congenital myopathies, perhaps due to developmental arrest. *Type 2 atrophy* (which mainly involves type 2B fibers) is very frequent and is seen in a variety of conditions, including immobilization, chronic debilitating disorders, and steroid treatment.

Predominance or Deficiency of a Fiber Type

The proper proportion of type 1 to type 2 fibers, or more precisely type 2A to 2B fibers, is dependent
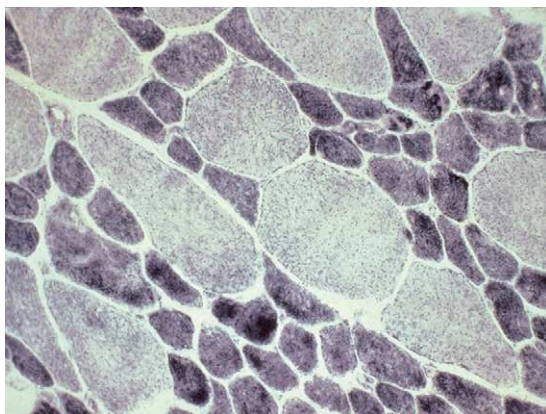
Figure 13-3. Type 1 predominance and type 1 atrophy in a case of congenital myopathy (NADH-TR).

on the specific muscle biopsied. For the most frequently biopsied sites (i.e., the deltoid, quadriceps, biceps, and gastrocnemius muscle), an abnormal predominance of fiber type is recognized when the proportion of fibers exceeds 55% type 1 or 80% type 2 fibers. Type 1 fiber predominance can be seen in congenital myopathies (see Fig. 13-3). Type 2 fiber predominance is found in amyotrophic lateral sclerosis. Cases of "central hypotonia" often show aberrations of fiber type proportions in the absence of overt denervation. Type 2B deficiency, sometimes total, and/or the presence of type 2C fibers may be seen in certain myopathic processes.

The mechanism underlying the establishment of fiber type is not well understood. It has been stated that fiber type is determined by the innervating motor neuron; however, embryologic studies also suggest that myofibers generated at different times in development have an autonomous genetically regulated program to develop into specific fiber types.

Structural Anomalies of Muscle Fibers

Nuclear Anomalies. Central displacement of the nuclei (*internalized nuclei*) is considered abnormal when present in over 5% percent of the fibers (see Fig. 13-2). The biologic basis of this phenomenon is not clear; it is a marker of fibers which have regenerated or are in the process of regeneration. Relatively unremarkable-appearing nuclei may be internalized in hypertrophic fibers, possibly

representing a preliminary stage in the process of fiber splitting. Nuclei tend to be arranged in chains in longitudinal section, especially in myotonic dystrophy. Nuclear inclusions may be seen in certain disorders such as inclusion body myositis and oculopharyngeal muscular dystrophy.

Split Fibers.   *Split fibers* are especially seen in hypertrophic fibers. In cross section, splitting presents as a fissure originating from the surface of a muscle fiber. This fissure may be branched or contain a capillary (see Fig. 13-2). It may become more ill-defined in the center of the fiber or extend to another edge of the fiber. Multiple splits may lead to grouping of angulated muscle fibers of the same histochemical type, a phenomenon sometimes termed *myopathic grouping*. The mechanism of splitting is not settled. It should be discounted when seen in the neighborhood of myotendinous junctions.

Necrotizing Changes.   Fiber degeneration is the hallmark of dystrophic, inflammatory, or toxic myopathic processes. Conversely, the presence of necrotic and degenerating fibers should cast doubt on a diagnosis of a neurogenic process, although it may also be seen in the end stages of neurogenic atrophy. In H and E preparations, necrotic fibers show a homogenization and glassy appearance of the cytoplasm and poor staining. In longitudinal sections there is pallor and loss of striations. There is also loss of staining with PAS and NADH-TR. Gradually, fibers become vacuolated, followed by invasion of inflammatory cells across the basement membrane (Fig. 13-4A). Later, admixtures of macrophages, T (predominantly T8) lymphocytes, and regenerating myoblasts arising from neighboring muscle fibers may be seen within the muscle tube. This stage ends with the migration of inflammatory cells toward the adjacent blood vessels. The fact that necrotic phenomena are often segmental is best seen in longitudinal sections (Fig. 13-4B). Centromyocytic necrosis, presenting as a collection of inflammatory cells surrounded by normal sarcoplasm, is often seen in polymyositis.

Basophilic Fibers.   These fibers correspond to regenerating muscle fibers and are rich in RNA. The fibers have a basophilic cytoplasm, express NCAM, may be either weakly striated or non-striated, and possess vesicular nuclei with prominent nucleoli. Regeneration may result in complete restitution of the muscle fiber or leave sequelae such as variation in the shape and size of fibers. Regenerating fibers are either scattered randomly or occur in small clusters.

Target Fibers.   *Target fibers* may be detected in standard preparations (see Fig. 13-7B), but are particularly well seen with NADH-TR. True target fibers are particularly but not exclusively seen in type 1 fibers. They are composed of three concentric zones: (1) a central, pale zone that lacks oxidative enzyme activity; (2) a dark, annular, intermediate zone that is rich in oxidative enzymes; and (3) a normal peripheral zone. They are often found in denervation. A "targetoid" fiber is one in which the intermediate zone is absent, and is considerably less specific of denervation.

Moth-Eaten Fibers.   *Moth-eaten fibers* are recognized in oxidative enzyme preparations. They appear as ill-defined zones of enzyme loss, giving a disorganized aspect to the intermyofibrillary network. They are not specific and are seen in a wide range of conditions, including inflammatory myopathies, malignant hyperpyrexia, and denervation.

Inclusions and Other Uncommon Findings: Ring Fibers (Ringbinden) and Lateral Sarcoplasmic Masses.   Striated annulets (ringbinden or ring fibers) are formed by myofibrils that are normal in structure but abnormally arranged so as to be perpendicular to the muscle fiber axis as seen on cross section. Lateral sarcoplasmic masses present as delicately granulated, nonstriated clear areas that are filled with oxidative enzymes and are situated between the sarcolemmal membrane and a central myofibrillary zone of normal appearance (Fig. 13-5). These two abnormalities may be seen in myotonic dystrophy and other dystrophies and myotonic disorders.

Vacuoles.   *Vacuoles* are clear, intramyocytic spaces seen in H and E stain and may have variable pathological significance. Their contents are best demonstrated after a battery of special stains, and sometimes can be characterized only with electron microscopy. They occur in the following varieties:
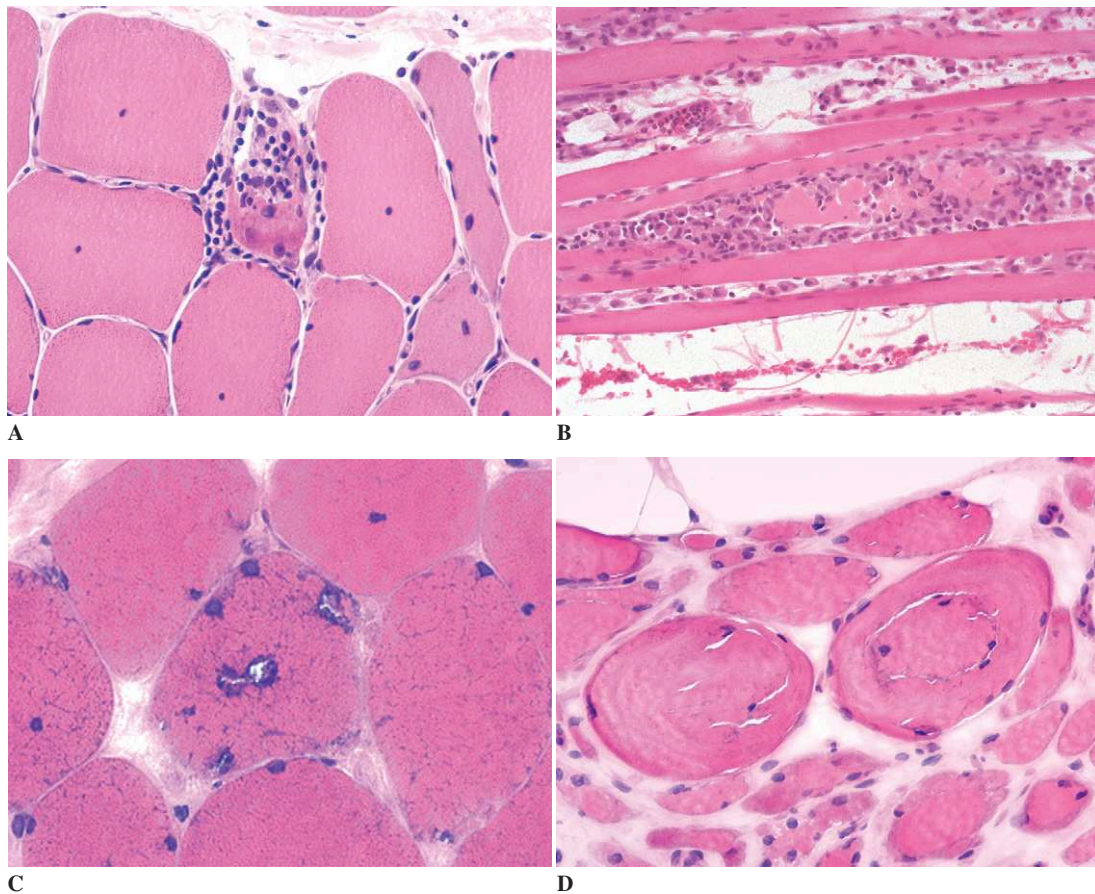
Figure 13-4. Structural anomalies of muscle fibers. **A**, A necrotic fiber is invaded by inflammatory cells. **B**, Centromyocytic necrosis is shown on longitudinal section. **C**, Rimmed vacuole. **D**, Whorled fibers or "coiled fibers" with central disorganization of the myofilaments.

- *Vacuoles formed in nonlysosomal storage diseases.* These contain, for example, glycogen in McArdle disease and lipids in carnitine deficiency.
- *Vacuoles formed in lysosomal storage diseases.* These are recognized by the acid phosphatase reaction and by identification of the stored material (e.g., glycogen in Pompe disease, autofluorescent lipopigment in ceroid lipofuscinosis).
- *Autophagic vacuoles with lysosomal hyperactivity.* These are revealed by the acid phosphatase reaction (e.g., chloroquine myopathy).
- *Rimmed vacuoles* (see Fig. 13-4C). These are seen in inclusion body myositis. Their outer border is granular and basophilic on H and E and reddish with Gomori trichrome, and by electron microscopy is seen to consist of membranous debris and intermediate filaments.
- *Vacuoles produced by dilatation of the internal membrane systems*, as in periodic paralysis. These include microvacuoles, produced by dilatation of the T transverse tubular system and seen amid healthy regions of the sarcoplasm next to zones of recent segmental necrosis; and accumulation of sarcotubular material in sarcotubular myopathy, which can be identified at the ultrastructural level.
- *Vacuoles resulting from the disappearance of myofibrils*. These are seen, for example, in dermatomyositis and critically ill–patient myopathy (in which the vacuole content may have a reticulated honeycomb appearance).
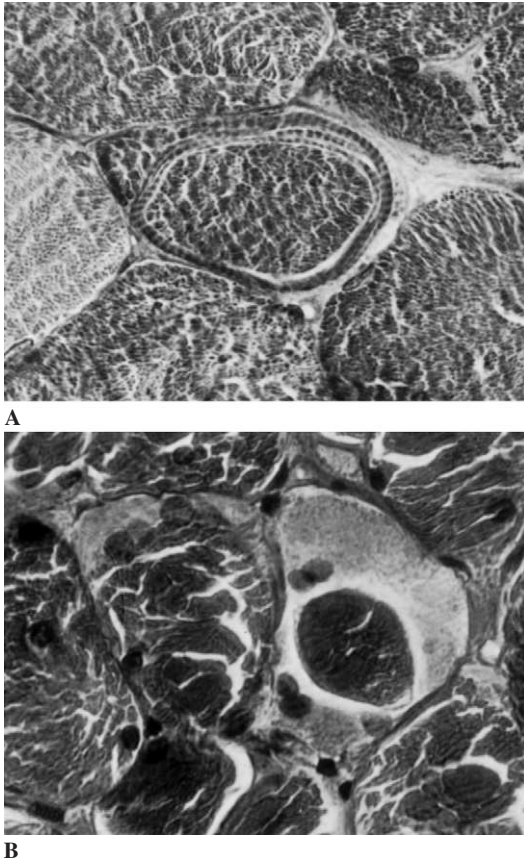
Figure 13-5. A, Striated annulet (ring fiber). **B**, Lateral sarcoplasmic masses.

"Ragged Red Fibers." *Ragged red fibers* are subsarcolemmal and/or intermyofibrillary aggregates and are the hallmark of mitochondrial myopathy. They appear reddish with Gomori trichrome (see Fig. 13-15A), hence the name, and bluish with H and E. These aggregates, which are essentially formed by abnormal mitochondria, are filled with oxidative enzymes and therefore stain strongly with the NADH-TR and SDH reactions. Ultrastructurally, they are associated with accumulation of glycogen and, especially, of lipids. Although strongly indicative of mitochondrial myopathy when found before the age of 60, scattered ragged red fibers may also be found in muscle tissue of elderly individuals in nonmitochondrial disorders. Conversely, their absence does not exclude the diagnosis of a mitochondrial cytopathy.

Tubular Aggregates.   Appearing as well-limited zones that are usually subsarcolemmal and stain blue with H and E and red with Gomori trichrome, *tubular aggregates* affect mainly type 2 fibers. They are strongly positive with NADH-TR but are SDH-negative. By electron microscopy, their appearance is that of aggregates of tubules arranged in an organ-pipe pattern. These structures are not specific, but are often encountered in dyskalemic paralysis and represent the chief histological skeletal muscle anomaly seen in the myalgia/cramps syndrome associated with tubular aggregate myopathy (see later in this chapter).

Interstitial Changes

Some of the changes seen in the interstitial tissue may have diagnostic significance and establish the etiology of the process with certainty (e.g., sarcoidosis, polyarteritis nodosa, amyloidosis). Increased endomysial connective tissue (*endomysial fibrosis*) is less specific but suggests muscular dystrophy. In end-stage muscle of whatever cause, there is infiltration and replacement of muscle by fibrous and adipose connective tissue.

Discrete inflammatory cellular infiltrates may be seen in a variety of conditions, including, to some extent, in muscular dystrophies such as dystrophinopathies and dysferlinopathies, and (more floridly) in inflammatory myopathies such as dermatomyositis, polymyositis, and inclusion body myositis. The topography and also the cellular composition of the inflammatory infiltrates are important clues to their etiologic basis.

Muscle Diseases

Two broad diagnostic categories of muscle disease are recognizable on muscle biopsy, namely, *neurogenic muscle disease* and *myopathic muscle disease* (Table 13-3). These major subdivisions denote fundamental differences in the pathogenesis of the muscle disorder, namely (and respectively) whether the process is denervative or whether it primarily involves the muscle fiber itself.

Neurogenic Muscle Disease

This group encompasses a large number of neurologic illnesses that secondarily affect the muscle fiber.

Table 13-3. Prototypic Myopathic and Neurogenic: Differential Histological Features

Myopathic Processes	Neurogenic Processes
Considerable variation in fiber size	Nests of atrophic fibers
Rounded fibers	Angular fibers
Increase in number of nuclei	Pseudomultiplication of nuclei due to cytoplasmic atrophy
Internalized nuclei	No internalized nuclei
Necrotic and basophilic fibers	No necrotic or basophilic fibers
Cytoplasmic alterations in contractile proteins	Target fibers
Conspicuous interstitial fibrosis	Minimal interstitial fibrosis
Inflammatory cellular infiltrates	No inflammatory cellular infiltrates

The precise locus of the damage to the innervating neuron, whether the anterior horn cell itself, the axon, or the intramuscular terminal nerve twigs, usually cannot be determined from the muscle pathology alone.

Denervation Atrophy

As a result of denervation, skeletal muscle fibers undergo progressive atrophy. The first detectable change is angular muscle atrophy. Small angulated fibers scattered throughout the biopsy may be apparent only with close examination; they are both type 1 and type 2 fibers, as may be assessed by ATPase reactions or fast myosin immunocytochemistry, and show a marked increase of oxidative enzyme activity. At a later stage, the atrophied fibers are grouped in small nests and, still later, in islands, giving the picture of fascicular atrophy (Fig. 13-6). In the absence of reinnervation, the atrophied fibers form nuclear bags (Fig. 13-7).

Grouping of Fibers of the Same Histochemical Type (Type Grouping)

Denervated fibers recover their normal size when reinnervated by collateral sprouting from unaffected motor axons. As the enzyme histochemical type of a muscle fiber depends on the innervating motoneuron, the fiber may recover its previous
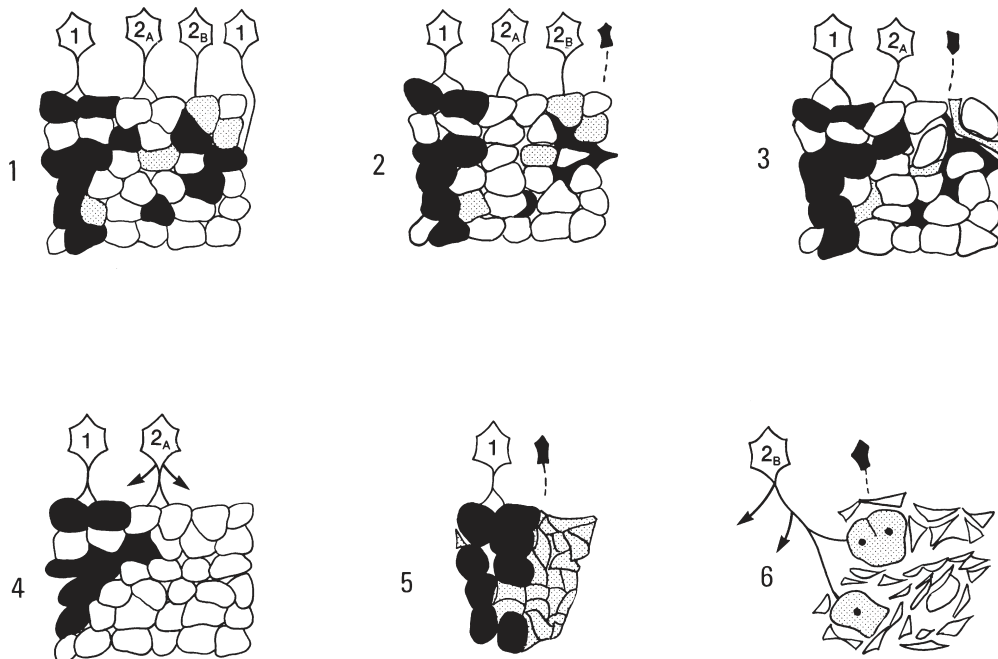
Figure 13-6. Mechanisms of denervation. 1, Normal muscle with checkerboard pattern of motor units. 2, Angular muscle fiber atrophy following motor unit involvement. 3, Nest-like angular muscle fiber atrophy (small group atrophy), resulting from the involvement of two contiguous motor units. 4, Collateral reinnervation of denervated muscle fibers, with formation of a giant type 2A motor unit ("type grouping"). 5, Fascicular atrophy secondary to atrophy of the giant motor unit. 6, Pseudomyopathic changes in chronic atrophy.
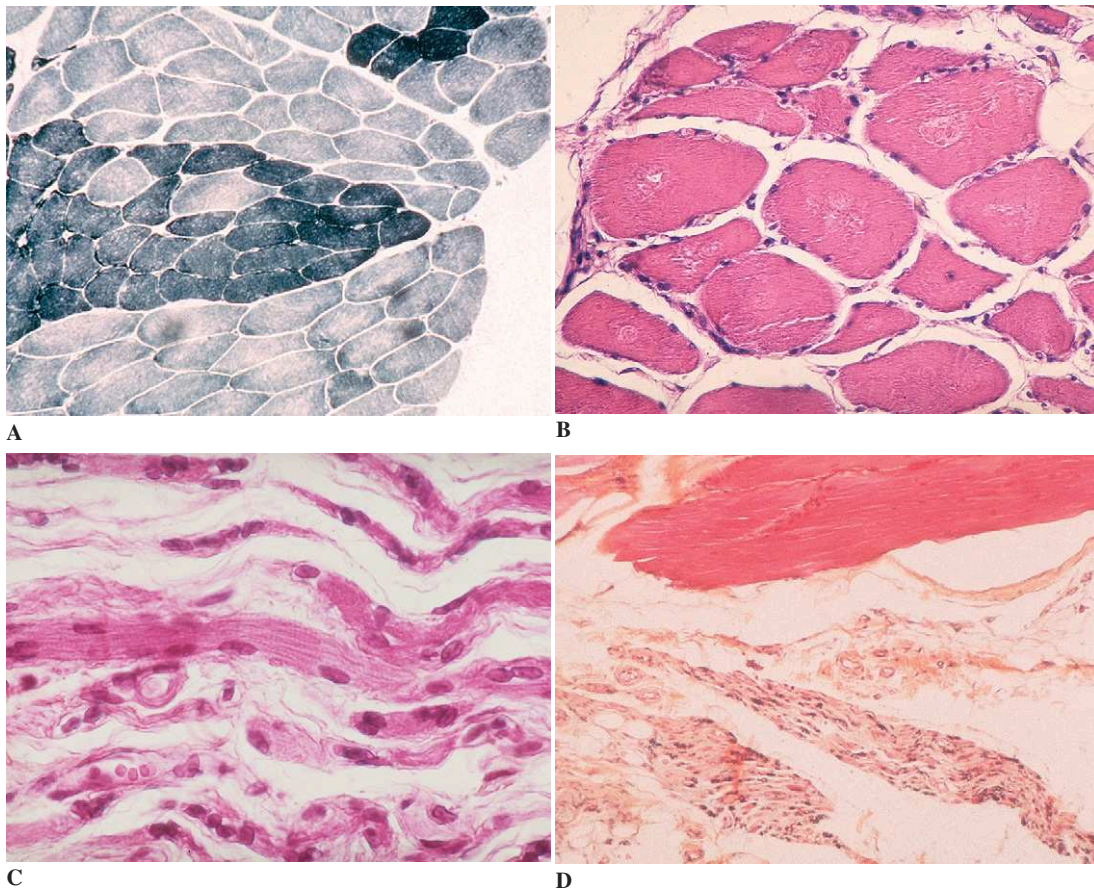
Figure 13-7. Neurogenic atrophy; morphological appearances. **A**, Type grouping (ATPase at pH.4.6). **B**, Simple angular atrophy and target fibers. **C**, Atrophic fibers forming "nuclear bags," i.e., clusters of nuclei within muscle cells largely devoid of myofibrillary material. **D**, Fascicular atrophy.

size but the fiber type may change. Since the sprouting axons will reinnervate aggregates of atrophic fibers in the same vicinity, this leads to the formation of patches of contiguous fibers of the same enzyme histochemical type. Repeated cycles of this process result in the progressive pathological enlargement of motor units composed of a single fiber type and thus, gradually, to the formation of giant motor units. As a result, there is progressive disappearance of the normal checkerboard appearance of the muscle fibers. In ATPase stain, the appearance of large, contiguous fields of fibers of a single fiber type is striking and is called *fiber type grouping* (see Fig. 13-6). Fiber type grouping is virtually pathognomonic of denervation (Fig. 13-7A). Fibers at this stage may be of uniform normal diameter; however, if the axon innervating these fibers is also damaged, this results in atrophy of

muscle fibers clustered together (*group atrophy*). The latter finding is apparent on H and E staining (Fig. 13-7D). Pseudogroupings of myopathic nature may occur when multiple fiber splits are present.

It is not firmly established what the ideal number of contiguous fibers should be to be certain that one is dealing with genuine type-grouping, but the presence of fibers of a given fiber type, surrounded by nearest neighbors all of the same fiber type—so-called "enclosed fibers"— may be used as a rough guide. Furthermore, the assessment is complicated if one is dealing with a muscle sample where one fiber type predominates.

Target Fibers

Target fibers may be very common in denervation. Their presence is not well understood but is typi-

cally ascribed to attempts at reinnervation. They are best visualized in oxidative enzyme preparations, as in NADH-TR. In paraffin sections they may, however, also be recognized with H and E (see Figure 13-7B), especially with the Gomori trichrome stain.

Neurogenic Atrophy in Infants

In *infantile spinomuscular atrophy* (juvenile form *Werdnig-Hoffmann disease SMA1*), muscle biopsy demonstrates numerous hypotrophic type 1 and type 2 fibers with rounded (not angulated) outlines. This form of atrophy is associated with groups of hypertrophic fibers, predominantly of type 1 (Fig. 13-8). There may be relatively little capacity to reinnervate denervated muscle fibers in these patients, and as a result, fiber type grouping is seldom seen. In the juvenile form of the disease (Kugelberg-Welander disease SMA3), more typical findings of denervation may be seen.

Acute and Chronic Neurogenic Processes

The histologic findings described give some sense of the tempo of the process; therefore, a distinction can sometimes be drawn between acute and chronic processes.

The hallmark of acute denervation is atrophy, manifest as small, angulated random muscle fiber atrophy.
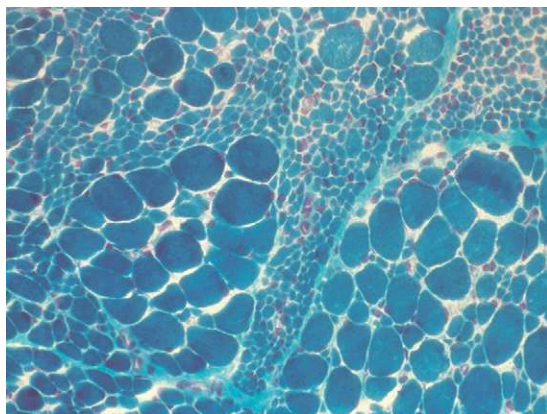
Figure 13-8. Neurogenic atrophy in an infant with Werdnig-Hoffmann disease (SMA1). Numerous hypotrophic fibers with rounded outlines are associated with groups of hypertrophic fibers (Masson trichrome).

With time, the denervated atrophic fibers may be reinnervated and regain their former size, but ATPase histochemistry will reveal fiber type grouping, which implies a later stage of the process.

In slowly evolving denervation or in prolonged chronic denervation, in addition to typically neurogenic changes muscle fiber hypertrophy, with excessive numbers of central nuclei, split fibers, and interstitial fibrosis—"pseudomyopathic" changes—may be found, including scattered perivascular mononuclear cellular infiltrates and necrotic fibers.

Neuromuscular Transmission Defects

Neuromuscular transmission defects are diseases that present clinically with a myasthenic syndrome characterized by weakness and fatigability that may be generalized but may be most obvious in extraocular and eyelid muscles. The basic mechanism of injury is dysfunction of the neuromuscular junction resulting in impaired neuromuscular transmission.

The diseases may be separated into acquired, autoimmune myasthenic syndromes (e.g., myasthenia gravis and Lambert-Eaton syndrome) and congenital myasthenic syndromes.

Myasthenia Gravis

Myasthenia gravis (MG) is due to an antibody-mediated autoimmune response to nicotinic acetylcholine receptors (AChR) localized on the postsynaptic part of the neuromuscular junction. MG may be associated with other autoimmune disorders. Thymus hyperplasia is found in 70% of patients with MG and thymomas in 15% to 20%.

The diagnosis is usually obtained by clinical examination; electrophysiological examination showing the characteristic decremental electromyography (EMG) response to successive nerve firings; pharmacological tests, particularly prostigmine test; and detection of AchR antibodies in serum.

Muscle biopsy is generally not necessary to establish the diagnosis except, in seronegative cases, to eliminate other diseases with similar clinical presentation, namely mitochondrial cytopathies. Lymphocytic infiltrates (lymphorrhages)

and mild, nonspecific alterations of the muscle fibers (e.g., type 2 atrophy) may be seen. Ultrastructural study of the neuromuscular junction shows widening of the synaptic cleft and simplification of the postsynaptic membrane with atrophy and flattening of the postsynaptic folds.

Lambert-Eaton Syndrome

Lambert-Eaton syndrome is also an acquired autoimmune disorder. It typically presents as a paraneoplastic syndrome in association with a small-cell carcinoma of the lung. Patients develop antibodies against voltage-gated calcium channels on the presynaptic nerve terminal in neuromuscular junctions. Muscle biopsy is not contributory to diagnosis.

Congenital Myasthenic Syndromes

The *congenital myasthenic syndromes* (CMSs) are a heterogeneous group of disorders caused by genetic abnormalities of the proteins of the neuromuscular junction. Given the large number of these proteins, an increasing number of new mutations will likely be discovered in the future.

These conditions affect mainly children but may also occur in adults. Clinical symptoms and electrophysiological findings are those of myasthenia, but serologic tests for AchR antibodies are negative.

According to the site of the defect, one may distinguish *presynaptic* CMS, *synaptic* CMS, or *postsynaptic* CMS. A number of entities have been described thus far.

Presynaptic CMS includes paucity of synaptic vesicles, reduced quantal release, and (in CMS with episodic apnea) endplate choline acetyltransferase deficiency.

Synaptic CMSs are due to an endplate acetylcholinesterase deficiency.

Postsynaptic CMS includes mutations in AchR-subunit genes that increase (in fast-channel syndrome) or decrease (in slow-channel syndrome) the synaptic response to Ach (the primary kinetic abnormality may or may not be associated with AchR deficiency); primary AchR deficiency, with or without minor kinetic abnormality; and myasthenic syndrome with plectin deficiency.

In some CMS a specific diagnosis can be made by histologic or EMG study, but in others CMS muscle biopsy of an intercostal muscle is required. The biopsy allows in vitro electrophysiology, immunocytochemistry, and ultrastructural and immuno-electron microscopic study. If these tests point to a specific defect, then molecular genetic analysis become feasible and allows for a more precise diagnosis.

Myopathies

Diseases affecting primarily the skeletal muscle may be acquired (i.e., toxic or inflammatory) or genetically determined.

Genetically Determined Diseases of Skeletal Muscle

This group of diseases may be classified into three main categories: (1) *muscular dystrophies*, which are progressive myopathies typically characterized by degeneration and regeneration of muscle fibers (exception: myotonic muscular dystrophies); (2) *congenital myopathies*, which typically have a very early onset, tend to have a nonprogressive or very slowly progressive course, and show peculiar myopathologic alterations that allow a specific morphological diagnosis; and (3) *metabolic myopathies*, including mainly glycogen, lipid-storage, and mitochondrial cytopathies.

A classification system taking into account the specific molecular defects responsible for the myopathy is emerging. These molecular defects may involve structural proteins or, less often, enzymes. With a greater understanding of the underlying pathobiology of the genetically determined muscle diseases, the current practice of subdividing these illnesses under the categories muscular dystrophies, congenital myopathies, and metabolic myopathies, may prove arbitrary.

Muscular Dystrophies

The *muscular dystrophies* are, classically, a group of genetically determined myopathies marked clinically by chronic and progressive weakness and by markedly elevated serum creatinine kinase. The last two decades have witnessed a revolution in the
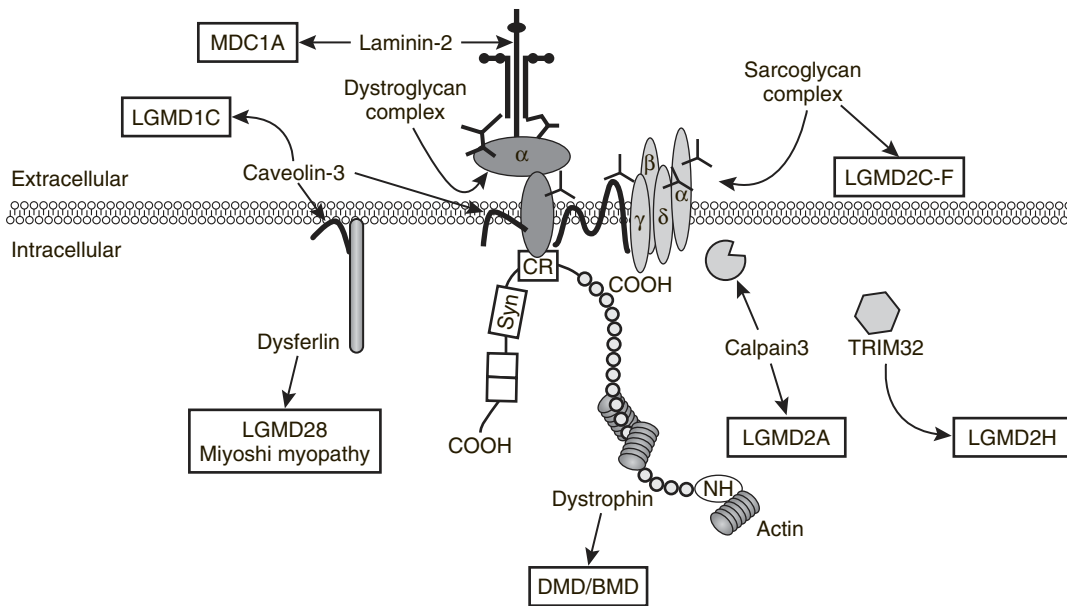
Figure 13-9. Diagram of the cytoskeletal proteins involved in the pathogenesis of muscular dystrophies (Modified from Dalkilic & Kunkel, 2003).

understanding of the genetic and molecular basis of the muscular dystrophies.

The majority of these have been shown to be the result of mutations in the genes encoding functionally related cytoskeletal proteins of the muscle fiber. These form a link between cytoskeletal actin and the extracellular matrix (Fig. 13-9) and include extracellular matrix proteins (merosin, collagen VI), transmembrane and membrane-associated proteins (dystrophin, sarcoglycans, dystroglycans, caveolin-3, α5- and α7-integrins, dysferlin), intracellular proteases (calpain-3), cytoplasmic proteins associated with organelles and sarcomere (titin, telethonin, fukutin), and nuclear membrane proteins (lamin, emerin; Fig. 13-10). It seems likely

Figure 13-10. Diagram of the nuclear proteins involved in the pathogenesis of muscular dystrophies (Modified from Dalkilic & Kunkel, 2003).

that this complex of cytoskeletal proteins stabilizes the muscle fiber plasma membrane (the sarcolemma) against the mechanical stress of repeated cycles of contraction and relaxation. The absence of dystrophin or of other components of this mechanical link robs the muscle of this protective effect and results in clinical disease. This complex is also increasingly recognized to transduce survival signals. The respective roles of the "structuropathies" and of the "signalopathies" associated with disruption of the complex are not yet fully determined.

The muscular dystrophies are now classified according to the gene and/or protein involved in the causation of the disease. This classification is still incomplete but is most appropriate to incorporate our evolving understanding of the genetic and molecular biology of the muscular dystrophies. It also takes into account the mode of genetic transmission (X-linked, autosomal dominant, autosomal recessive) and the clinical aspects of the illness.

X-Linked Muscular Dystrophies

DUCHENNE MUSCULAR DYSTROPHY. *Duchenne muscular dystrophy* (DMD) is the paradigmatic muscular dystrophy, as well as the foundation for many recent advances in the understanding of the muscular dystrophies. The gene that

is mutated is the DMD gene, a large gene (about 2700 kb) that encodes the 427-kDa muscle-cytoskeletal protein dystrophin. (This is presently the largest gene identified in the human genome.) DMD is inherited as an X-linked recessive disease, that is, involving males and transmitted by females; however, about one third of DMD cases result from spontaneous mutations. Females are generally asymptomatic carriers. Manifesting carriers presumably reflect skewed inactivation of the X chromosome carrying the intact copy of the DMD gene.

The myopathy is of early onset in the muscles of the pelvic limb-girdle and presents a pseudohypertrophic appearance in the calves. Creatine phosphokinase is characteristically markedly increased into the range of >10,000 IU. The heart may be involved. The course is rapid, leading to death in young adulthood.

The appearance of the muscle biopsy may differ dramatically depending on the age of the patient at the time of biopsy. In the moderately affected boy biopsied in late childhood, the skeletal muscle shows striking variation in fiber size, with atrophic fibers mixed with rounded hypertrophic fibers, centronucleation, swollen fibers with opaque sarcoplasm, so-called "hypercontracted fibers," foci of small basophilic fibers, myophagocytosis, and scattered inflammatory infiltrates. Also distinctive is progressive increase in endomysial connective tissue (Figs. 13-11A and B). As muscle degeneration proceeds, there is gradual infiltration of the muscle by adipose tissue. Poor enzyme histochemical fiber differentiation is often seen in ATPase reactions.

The appearance at either end of the natural history of the disease is a variation on this basic pattern:

- At an early stage of the disease, typically at about age 2, the biopsy will show rounded fibers and small numbers of degenerating and regenerating fibers. Endomysial fibrosis is subtle if present, and fatty infiltration of the endomysium is not seen.
- When biopsy is performed at the end of the age spectrum or at autopsy, it may show abnormalities largely consisting of fat and abundant fibrosis with only scattered surviving muscle fibers (Fig. 13-11F). At this stage, CK is often paradoxically much lower than at any time in the antecedent years.

Demonstration of dystrophin deficiency is mandatory for a diagnosis of DMD.

- Immunocytochemistry that normally demonstrates dystrophin in its characteristic subsarcolemmal distribution, usually shows a total absence of expression in DMD contrasting with normal expression of spectrin used as control of membrane integrity. A weak expression may be found with monoclonal antibodies to the N terminus or to the rod domain but never to the C terminus (Figs. 13-11C and D), allowing distinction with Becker dystrophy (see later in this chapter). Female carriers will show a mosaic of dystrophin positive and negative fibers.
- Western blotting on muscle homogenate tissue identifies a markedly decreased amount or absence of dystrophin molecule.
- Finally, genetic tests are increasingly used to directly identify mutations in the DMD gene. The genetic information can also be used for carrier identification and for prenatal diagnosis in subsequent at-risk pregnancies.

Becker Muscular Dystrophy.   While DMD is produced by mutations that usually result in near-absolute loss of dystrophin, *Becker muscular dystrophy* (BMD) results from mutations associated with preservation of some dystrophin, albeit abnormal either in amount (underexpression) or molecular size (either truncated proteins, or in rare instances, larger-than-normal dystrophin, neither of which function normally).

Clinically, this type of myopathy is rather similar to DMD, but its onset occurs later and its course is longer and has a considerably wider variation in severity. Severe forms of BMD may be hardly better than DMD, whereas mild cases may permit ambulation until late in life. Even milder forms, identified only by molecular testing, may involve nothing more than cramps and an elevated serum CK.

In keeping with this clinical variability, the appearance on muscle biopsy is variable, with qualitatively the same features seen in DMD but, in some instances, with much less severe findings. Dystrophin immunochemistry in Becker-dystrophy patients is characterized by variation in labeling intensity both between fibers and within the same
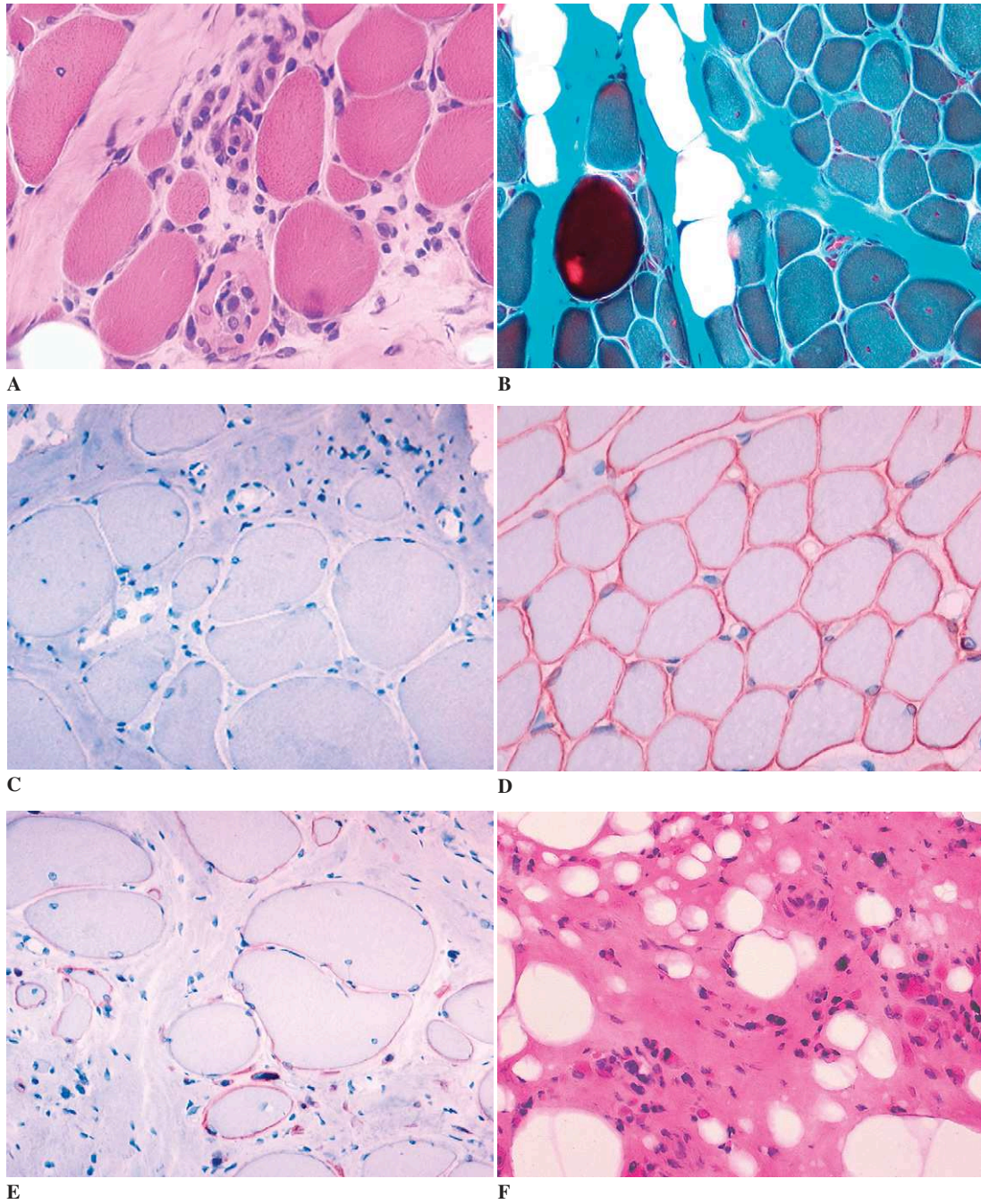
Figure 13-11. Duchenne muscular dystrophy. Morphological appearance. **A**, Necrotic fibers with myophagocytosis and foci of small basophilic fibers, variation in fiber size, atrophic fibers mixed with rounded hypertrophic fibers, and centronucleation. **B**, "Hypercontracted fiber" and increased endomysial connective tissue. **C** and **D**, Total absence of expression of dystrophin on immunocytochemistry using antibody to the C terminus using an antibody to, compared to a normal control (**D**). **E**, Immunocytochemistry (**C**) α-sarcoglycan shows partial loss of expression. **F**, Morphological appearance of the muscle at a late stage of the disease. Only scattered surviving muscle fibers are present within fibrosis and ingrowth of adipocytes.

fiber. It is important to use antibodies to different regions of the dystrophin molecule to avoid false-negative results. This observation always must be confirmed by Western blotting and genetic studies.

EMERY-DREIFUSS MYOPATHY. *Emery-Dreifuss myopathy* is the less common X-linked muscular dystrophy. Important features that distinguish it clinically from DMD are the later age of onset, prominent contractures, and cardiac involvement. The early muscle contractures characteristically involve elbows, Achilles tendons, neck extensors, and scapulohumeroperoneal muscles. Disturbances in cardiac conduction often lead to death by the fifth decade. The muscle biopsy shows dystrophic changes but is not otherwise distinctive; it may show atrophy of type 1 fibers and considerable endomysial fibrosis. The diagnostic study is immunocytochemistry for emerin, a nuclear protein that is mutated in this disease. Emerin is a membrane-spanning component of the molecular skeleton that supports the nuclear membrane; it is expressed in all cells. Absent immunocytochemical expression of emerin can be assessed in muscle and other tissues, such as skin.

Emerin is associated with the intermediate filament lamin A/C. There are also autosomal forms of Emery-Dreifuss syndrome, due to mutations in the lamin A/C gene (see Fig. 13-10).

Autosomal Dystrophies

LIMB-GIRDLE MUSCULAR DYSTROPHIES. *Limb-girdle muscular dystrophies* (LGMDs) are a heterogeneous group myopathies of autosomal recessive or, less commonly, autosomal dominant inheritance (Table 13-4). These autosomal dystrophies have clinical and myopathologic features that overlap somewhat with those of DMD or BMD, except that they may occur in females. Although less common than DMD in most countries, LGMDs are as common as DMD in some regions of the world (e.g., North Africa).

Onset of LGMD is most often in the second or third decade of life, but may range from childhood to adulthood. Patients often present with predominant limb-girdle involvement. Two chief patterns of weakness are recognized, one with scapulo-humeral and the other with pelvic-femoral distribution. Myopathy involving the quadriceps is a

Table 13-4. Classifications and Characteristics of Limb Girdle Muscle Dystrophies

Subtype	Gene Product	Gene Localization	Characteristic Feature
Limb Girdle Dystrophies: Autosomal Dominant			
LGMD 1A	Myotilin	5q31	Nasal dysarthric speech
LGMD 1B	Lamin A/C	1q21	Dilated cardiomyopathy, conduction defects
LGMD 1C	Caveolin-3	3p25	Childhood onset, cramps, rippling muscle disease
LGMD 1D		6q23	
LGMD 1E		7q7–9	
Limb Girdle Dystrophies: Autosomal Recessive			
LGMD 2A	Calpain-3	15q15	Scapular winging; may have contractures and facial weakness late
LGMD 2B	Dysferlin	2p12	Proximal or distal weakness
LGMD 2C	γ-Sarcoglycan	13q12	Scapular winging, calf hypertrophy, possibly dilated cardiomyopathy
LGMD 2D	α-Sarcoglycan	17q21	Scapular winging, calf hypertrophy, possibly dilated cardiomyopathy
LGMD 2E	β-Sarcoglycan	4q12	Scapular winging, calf hypertrophy, possibly dilated cardiomyopathy
LGMD 2F	δ-Sarcoglycan	5q33	Scapular winging, calf hypertrophy, possibly dilated cardiomyopathy
LGMD 2G	Telethonin	17q11-12	Anterior distal weakness, rimmed vacuoles
LGMD 2H	TRIM32	9q31-q34.1	Slowly progressive, facioscapulohumeral
LGMD 2I	Fukutin-related protein	19q13.3	Calf hypertrophy, dilated cardiomyopathy
LGMD 2J	Titin	2q31	Proximal and distal weakness; anterior tibial wasting

variant. There may be calf hypertrophy. Cardiac involvement may be present but is not prominent. Intellectual function is normal. The CPK may range from the upper limit of normal to several hundred times normal.

At muscle biopsy, the appearance is that of muscular dystrophy without any distinctive histological characteristics. At first, biopsy only shows irregularities in fiber size and a mild excess of centronucleated fibers. Eventually, evidence of muscle degeneration becomes moderate to severe. There is progressive rounding of fibers, increasing variation in fiber diameter, centronucleation, muscle fiber degeneration and regeneration, and fatty replacement. Mild, inflammatory infiltrates may be seen. Hypertrophic fibers subsequently show splitting and various other cytoplasmic changes that include whorled fibers, moth-eaten fibers, and lobulated fibers. Endomysial fibrosis follows.

Molecular genetics has revolutionized the understanding of these diseases. The illnesses are now classified according to their pattern of inheritance (i.e., autosomal dominant or recessive) and chromosomal locus or linkage. The standard nomenclature assigns the prefix LGMD, followed by 1 (autosomal dominant) or 2 (autosomal recessive), followed by a letter (A, B, C, etc.) to subclassify the disorders. For many of LGMDs, the mutated gene and abnormal or absent protein have been identified; these LGMDs may be named according to the deficient protein (e.g., sarcoglycanopathies, dysferlinopathies, caveolinopathy, myotilinopathy; see Table 13-4). For these proteins, specific antibodies have become available commercially, allowing immunocytochemical diagnosis of a number of LGMDs. Sarcoglycans, as well as dysferlin (the protein involved in LGMD 2B), normally have a sarcolemmal distribution at the light microscopic level as observed with antidystrophin antibodies and absent in disease states. Because they normally form a complex of dystrophin-associated proteins, sarcoglycans and dystroglycan expression may be altered secondary to the loss of one of the other members of the complex (Fig. 13-11E). These partial secondary losses are difficult to interpret. Thus, confirmation of a specific defect by molecular genetics remains mandatory.

Miyoshi myopathy (also termed *distal myopathy*) has been shown to be a distal form of dysfer-

linopathy resulting from a mutation in the same gene as that involved in LGMD 2B. Miyoshi myopathy usually begins in adulthood with distal atrophy of the upper limbs. It has a slowly progressive course. Posterior muscles are predominantly affected in lower limbs. Marked elevation of CK (10–150 times normal) is characteristic. Muscle biopsy shows the nonspecific features of a dystrophy and, frequently, inflammatory infiltrates. As in LGMD 2B, the diagnosis relies on immunocytochemistry or Western blotting for dysferlin. Myoshi distal myopathy is to be distinguished from Nonaka distal myopathy, which is characterized by predominant tibial muscle involvement and rimmed vacuoles.

CONGENITAL MUSCULAR DYSTROPHIES. *Congenital muscular dystrophy* (CMD) is a category of muscle illness that is part of the differential diagnosis of the hypotonic infant; muscular contractions and joint deformities may also be seen. CMDs may be subdivided into (1) merosin- (laminin 2)-negative, (2) merosin-positive, and (3) CMD associated with CNS malformations. The latter two CMDs are genetically heterogeneous.

Merosin-negative CMD. This form is typically associated with contractures; CK elevation to more than 10 times normal; diffuse MRI changes in the cerebral white matter; and dystrophic features at muscle biopsy with increased endomysial connective tissue, degenerating and regenerating fibers, and, frequently, inflammatory infiltrates. Merosin immunocytochemistry shows absence of the normal expression of the α2 subunit of laminin (merosin) in the basement membrane. It can also be performed on skin biopsies. It seems likely that a partial merosin-deficient state may have a milder clinical course than total absence of the protein.

Merosin-positive CMD. A heterogeneous group of patients with dystrophic muscle biopsies in the neonatal period show apparently normal immunolabeling for merosin.

CMD with CNS malformations. A third class of CMD consists of the cases which are associated with overt malformations of the CNS. In this category are Fukuyama congenital muscular dystrophy, which is caused by mutation in fukutin-related protein and involves predominantly Japanese patients; muscle-eye-brain disease, which affects Finnish patients and is caused by an enzymatic

defect in *O*-mannose β-1,2-*N*-acetylglucosaminyl-transferase; and Walker-Warburg syndrome.

Fukutin-related protein being a putative glyco-syl transferase, a unifying hypothesis is that the multiple lesions in these diseases may all result from the failure to correctly glycosyslate compo-nents of the membrane cytoskeleton, specifically α-dystroglycan, or of the extracellular matrix, with consequent deleterious effects on both muscle and the developing brain.

Fascioscapulohumeral Myopathy (Lando-uzy-Dejerine). *Fascioscapulohumeral myopa-thy* begins in adolescence. Its slow evolution is compatible with prolonged survival. It predomi-nantly involves the face, the scapular girdle (with the notable exception of the deltoid muscle), and the perihumeral musculature. Peroneal involve-ment is frequent; indeed, scapuloperoneal myopa-thy belongs to the same nosological group.

There are three main histological features: (1) a pseudoneurogenic appearance due to the presence of atrophied angular fibers arranged in small nests; (2) a dystrophic form with whorled fibers, moth-eaten fibers, and, especially, lobulated fibers (well-seen with the NADH-TR reaction as irregularities of the intermyofibrillary network); and (3) a pseudomyositic appearance due to the presence of inflammatory cellular mononuclear infiltrates. Considerable histological differences are seen from one muscle to the next. Endomysial fibrosis, of variable intensity, is frequent.

Fascioscapulohumeral myopathy is due to a large deletion in the telomeric region of the long arm of chromosome 4, which normally contains more than 11 repeats of 3.3 kb. No transcript has been identified and the underlying mechanism is poorly understood. DNA deletion at 4q35 is diagnostic.

Oculopharyngeal Dystrophy. *Oculopha-ryngeal dystrophy* is an uncommon muscular dystrophy, usually autosomal dominant and charac-terized by the late-life appearance of external oph-thalmoplegia with severe dysphagia. Discrete limb-girdle involvement may be present. Muscle biopsy demonstrates rare "rimmed vacuoles," intranuclear inclusions, and, occasionally, type 1 fiber predominance. Necrotic fibers are not typical; ragged red fibers are occasionally seen. Ultrastruc-tural studies show intranuclear tubulofilamentous inclusions measuring 8 μm in diameter, not found in the cytoplasm.

The genetic defect in this disease has been shown to be an expanded trinucleotide repeat in the poly (A) binding protein nuclear 1 (PABPN 1). Although immunocytochemistry has shown PABPN 1 to be present in the intranuclear inclu-sions, the confirmatory diagnostic study is identifi-cation of the expanded GCG repeat.

Myotonic Dystrophies and Nondystrophic Myotonias. *Myotonic dystrophies*, still classified among muscular dystrophies for historical reasons, have entirely different genetic abnormalities and pathogenic mechanisms of muscle injury. The current classification of these heterogeneous myotonic disorders is given in Table 13-5.

Dystrophic Myotonias. *Myotonic dystrophy* (also termed DM, DM1, or *Steinert disease*) is seen in young subjects. It includes characteristic facial involvement with distal limb amyotrophy, myotonia, and systemic manifestations. The latter include frontoparietal baldness, posterior cataracts, endocrine disturbances dominated by gonadal hypoplasia, and cardiac involvement. Neonatal myotonic dystrophy affects children who have inherited the genetic anomaly from their mother and is manifested by severe hypotonia with facial, oropharyngeal, and respiratory involvement.

Histologic lesions vary greatly in different patients and in different muscles. Characteristic anomalies include selective atrophy of type 1 fibers and a considerable increase of internalized nuclei. Some of the atrophied fibers may be reduced to nuclear bags or have the appearance of pseudoneu-rogenic angular fibers. Sarcolemmal nuclei show, in longitudinal section, an arrangement in chains at various depths of the sarcoplasm. Striated annulets (ringbinden) and numerous lateral sarcoplasmic masses are after present. Endomysial fibrosis and evidence of degeneration and regeneration are modest.

The mutation in myotonic dystrophy is the unstable expansion of a CTG repeat that is in the 3′ untranslated region of the "DM protein kinase" (DMPK) gene on chromosome 19. How this abnormality produces the myopathy is unclear, but mechanisms that have been considered are alter-ations in the level of expression of DMPK and

Table 13-5. Characteristic Genetic, Clinical, and Pathologic Features of Channel-Disease Myotonia

Disease Name	Gene Name and Locus	Gene Product and Functional Change	Symptoms	Pathology
Myotonia congenita (Becker dystrophy)	CLCN1 7q35	Chloride channel 1; loss of function	Recessive, childhood onset, transient weakness	Muscle hypertrophy
Thomsen disease	Same as above	Chloride channel 1; gain of function	Dominant, second-decade onset	Mild hypertrophy; myofibrillar disarray; loss of 2B fibers
Potassium-aggravated myotonia	SCN4A 17q23	Sodium channel α-subunit; gain of function	Dominant, variable onset, no weakness	
Paramyotonia congenital	SCN4A 17q23	Sodium channel α-subunit; gain of function	Dominant, childhood onset, cold-induced stiffness, weakness	
Hypokalemic periodic paralysis	CACNL1A3	Calcium channel	Dominant, second-decade onset, episodic weakness triggered by carbohydrates or exercise, no myotonia, improved by potassium	Tubular aggregates, debris-filled vacuoles
	SCN4A 17q23	Sodium channel α-subunit; loss of function		
	KCNE3 11q13-14	Potassium channel β-subunit; loss of function		
Hyperkalemic periodic paralysis	SCN4A 17q23	Sodium channel α-subunit; loss of function	Dominant, childhood onset, episodic weakness, triggered by rest after exercise, no paramyotonia	Tubular aggregates, debris-filled vacuoles
Malignant hyperthermia (King-Denborough syndrome; Barnes syndrome)	RYR, CACNA1S, SCN4A	Ryanodine receptor; calcium channel; sodium channel α-subunit	Lethal hyperthermia in response to inhalation anesthetics, no weakness	Can be associated with central core myopathy

flanking genes and toxicity of long CUG-repeat RNA. The latter may induce aberrant mRNA splicing affecting chloride channel 1 expression and, consequently, chloride conductance. In addition, DMPK is localized to the neuromuscular junction and sarcoplasmic reticulum, and there is the suggestion that there may be an alteration in Ca++ homeostasis and excitation contraction coupling.

Another dystrophic myotonia (DM2 or *proximal myotonic myopathy*) has been recently identified. In DM2, in contrast to DM1, type 2 fibers are predominantly affected. The underlying genetic defect consists in expansion of CCTG repeats affecting the ZNF9 gene in chromosome 3.

NONDYSTROPHIC HEREDITARY MYOTONIAS. Among the *nondystrophic hereditary myotonias*, Thomsen disease is the best known though least common. It is transmitted as an autosomal domi-

nant trait. The autosomal recessive variant is known as *Becker myotonia*. Considerable myotonia is associated with diffuse muscular hypertrophy presenting in childhood. The muscle lesions in the various nondystrophic myotonias usually consist of discrete irregularity of fiber caliber and rare centralized nuclei. Type 2A fibers may be hypertrophic, while type 2B fibers are sometimes absent. Both of these diseases are associated with mutations in a chloride channel (CLCN1), but in the first, there is dominant negative effect, and in the latter a loss of function, hence recessive. Patients with potassium-aggravated myotonia and congenital paramyotonia both have mutations in the sodium channel α subunit. The light-microscopic features of the muscle biopsy may be similar to those seen in Thomsen and Becker disease.

RELATED DISORDERS. Related classes of disease are *hyperkalemic periodic paralysis* and

hypokalemic periodic paralysis. The former may include myotonia. Both are dominantly inherited. Both may have mutations in a sodium channel subunit, but hypokalemic periodic paralysis is more often associated with a loss-of-function mutation in a calcium channel. Both diseases show gradually increasing vacuolation; ultrastructurally, these vacuoles are expansions of the T-tubule system and sarcoplasmic reticulum. Tubular aggregates may be seen and are related to the SR.

There are also rare myopathies characterized by cramps and prominent tubular aggregates. By light-microscopy, the aggregates are red with the modified Gomori trichrome stain. They are also reactive with NADH, so the distinction from "ragged red fibers" and mitochondrial myopathy is important. The tubular aggregates do not exhibit cytochrome *c* oxidase or succinic dehydrogenase activity (which are specific for mitochondria) and ultrastructurally are quite different from ragged red fibers. The genetic mutation is not known, but the clinical similarities of the periodic paralyses allows for speculation that an ion channel may be involved.

Congenital Myopathies

In general, the clinical course of patients with *congenital myopathies* differs from that of those with muscular dystrophies in that the disease is either nonprogressive or very slowly progressive. However, this distinction is inconstant. Some of these myopathies are first manifest as neonatal hypotonias, whereas others are first detected later, showing retarded motor development and/or muscle weakness of variable distribution. There is frequent association with skeletal dysmorphism. Muscle enzymes are normal or subnormal. All modes of inheritance are found among the congenital myopathies, and indeed, many have multiple patterns of inheritance, with the particular pattern often being of prognostic significance. The congenital myopathies are, for the most part, characterized by specific structural anomalies in the muscle.

Advances in understanding of the underlying molecular basis of these diseases will hopefully aid in a more precise classification. For the time being, this heterogeneous group is still subdivided on the basis of the principal structural abnormalities.

Congenital Myopathies with Structural Anomalies

NEMALINE MYOPATHY. *Nemaline myopathy* is a heterogeneous group of genetically diverse disorders characterized by the presence of intracytoplasmic rodlets that are visible by light microscopy (reddish on modified Gomori trichrome, often grouped within hypotrophic type 1 fibers; Fig. 13-12) and by electron microscopy (electron-dense structures, measuring 1 to 3 μm in length and 0.3 μm in diameter, extending from actin filaments, and in the neighborhood of, or in continuity with, Z discs). The number of affected fibers is highly variable and is not correlated with the clinical severity of the disease. Type 1 fibers often predominate. Both dominant and recessive forms and variants with infantile (most severe), childhood (most common), and adult onset have been described. Nemaline myopathy is associated with genetic defects of thin filament–associated molecules including tropomyosin, nebulin, and actin. Nemaline rods can also occur as a secondary phenomenon in other myopathies (dystrophies, inflammatory, mitochondrial), and even as an acquired response to tenotomy, neoplasia, and weightlessness.

CENTRONUCLEAR OR MYOTUBULAR MYOPATHY. *Centronuclear myopathy* is characterized by the presence of a centrally placed nucleus in a majority of abnormally small fibers. This appearance gives an "immature" look to the fibers and has led to the
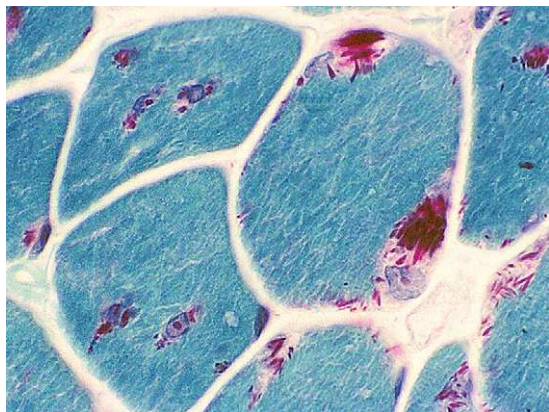
Figure 13-12. Nemaline myopathy. Presence of intracytoplasmic rodlets that appear reddish on modified Gomori trichrome.

suggestion that it represents a developmental arrest of muscle fibers at an early fetal stage (myotubular stage), but there is no persuasive evidence to support this concept. At least three forms of the disease are recognized: (1) a severe X-linked infantile form, (2) a milder, childhood form that seems to occur both in autosomal dominant and recessive forms, and (3) a mild, adult form that is dominantly inherited. The severe infantile X-linked form appears to be caused by mutations in the gene for myotubularin, a tyrosine phosphorylase. Some of the later-onset variants have been associated with mutations in the MYF6 muscle-specific transcription factor. Oculomotor palsies are frequent. Typically, a large number of central sarcolemmal nuclei present in 50% to 90% of fibers are associated with excessive oxidative enzyme activity (with loss of ATPase activity) in the central myocytic zones. The intermyofibrillary network often has a radial appearance that is well-seen in NADH histochemistry and in semithin plastic sections. Frequently observed are a predominance and selective hypotrophy of type 1 fibers. In the dominant adult form, the type 1 fibers remain smaller than normal for age, while the type 2 fibers are normal or even hypertrophic (Fig. 13-13). Either type 1 or both fiber types have a central cluster of nuclei mixed with a core of granular debris and in longitudinal sections may have central chains of nuclei.

CENTRAL CORE DISEASE.   *Central core disease* is a form of myopathy that usually has autosomal dominant inheritance and results from mutations of the *RYR1* gene in chromosome 19. The *RYR1* gene encodes for the ryanodine receptor, which is involved in calcium homeostasis. Other forms have been associated with β-myosin heavy chain mutations. This form of myopathy is characterized by the presence of areas devoid of mitochondrial oxidative and phosphorylase activity within type 1 fibers (Fig. 13-14). These zones, which are rounded in cross-section, correspond to cylindrical axes extending throughout the length of the fiber. Ultrastructurally, they show streaming, disruption, and sometimes disorganization of the contractile apparatus and Z bands. There is a strong predominance of type 1 fibers; biopsies are sometimes described as *uniform type 1*. The central core resembles that seen in target fibers in reinnervation, but the latter involves both muscle fiber types. A few isolated, angular, atrophic fibers may also be seen.

Central core disease may be associated with an increased incidence of the sometimes fatal malignant hyperthermia reaction in response to certain general anesthetics.

Other congenital "core myopathies" include conditions referred to descriptively as *multicore*, *minicore*, or even *multiminicore* myopathy, some of which have shown to be associated with mutations of either *RYR1* (like central core disease) or a selenoprotein encoding gene.

Congenital Fiber-Type Disproportion.   *Congenital fiber-type disproportion* (CFTD) myopathy,
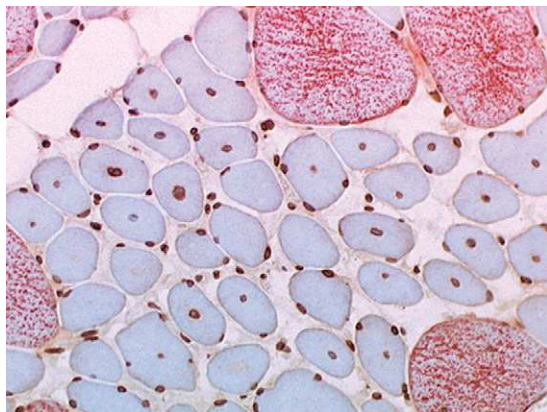
Figure 13-13. Centronuclear myopathy. Atrophy and centronucleation of type 1 fibers, whereas type 2 fibers are normal (fast myosin).
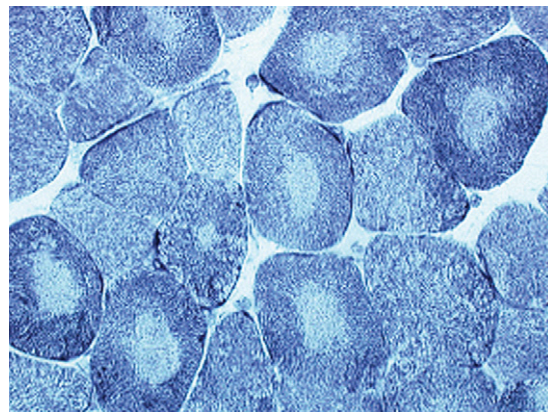
Figure 13-14. Central core disease (NADH-TR).

which has a benign prognosis, was originally identified because of the distinctive histologic appearance of small (hypotrophic) and excessively numerous type 1 fibers (fiber type disproportion). However, this appearance is far from specific, since it may be seen in other congenital myopathies and in myotonic dystrophy type 1 (DM1). Thus, the nosologic identity of this condition is uncertain.

Desmin Myopathy. *Desmin myopathy* cannot be classified satisfactorily as a muscular dystrophy, a congenital myopathy, or a metabolic myopathy; rather, it belongs to a new group of *protein storage myopathies*. Some cases are likely to be identical to what has been described as *cytoplasmic body myopathy*, *spheroid body myopathy*, or *myofibrillar myopathy*. The disease manifests predominantly by distal muscle weakness and cardiopathy. It is mainly characterized by intracytoplasmic granulofilamentous protein accumulations that include desmin (the muscle-specific intermediate filament protein) and αB-crystallin, a desmin-associated chaperone molecule. Ectopic dystrophin expression as small intracellular vacuoles is common. Ultrastructurally, the aggregates can have dense cores as well as a filamentous clear halo.

The condition is probably etiologically heterogeneous; it involves at least two genes, the desmin gene and the αB-crystallin gene. In some cases, abnormal desmin aggregates likely represent a secondary phenomenon.

Metabolic Myopathies

Mitochondrial Myopathies. Primary mitochondrial disorders constitute a group of systemic conditions that are highly variable from the clinical standpoint and are related to mitochondrial enzyme deficits (see Chap. 10). Mitochondrial cytopathies may result from mutations of either the mitochondrial DNA or the nuclear DNA. Mitochondrial DNA is a 16.5-kb DNA encoding for 22 transfer RNA, 2 ribosomal RNA, and 13 mRNA for respiratory-chain proteins. The other 67 polypeptides implicated in the mitochondrial respiratory chain are encoded by the nuclear DNA. Many cases appear to be sporadic, but autosomal (dominant or recessive) mendelian transmission, and especially nonmendelian maternal transmission by the mitochondrial genome, are sometimes present. Maternal inheritance is only a feature of mutations of mitochondrial DNA.

Among a wide range of clinical manifestations, external ophthalmoplegia, heart conduction block, short stature, deafness, diabetes, and epilepsy are particularly suggestive of mitochondrial cytopathy. Initial detection of these diseases is mainly based on elevated lactate-to-pyruvate ratio in blood and on CSF and muscle biopsy.

These disorders are inconstantly associated with intramyocytic accumulation of abnormal mitochondria, which are detectable by light microscopy, particularly in the modified Gomori trichrome stain, as "ragged red fibers" (Fig. 13-15A). The presence of ragged red fibers in a muscle biopsy is a major diagnostic feature, but it is neither specific nor invariable. The number of ragged red fibers is highly variable within a biopsy sample and from one muscle to another. The same subsarcolemmal accumulations are seen with NADH histochemistry, although SDH is the only oxidative reaction specific for mitochondria. Histoenzymatic demonstration of COX (complex IV of the mitochondrial respiratory chain) deficiency is extremely useful in assessing mitochondrial dysfunction. In most patients with mitochondrial DNA mutations, COX reaction shows a pattern of reactivity in which selected, randomly distributed fibers are totally COX-negative (Fig. 13-15B). Concomitant with mitochondrial disease and altered glycogen and lipid metabolism, there may be accumulations of lipids, glycogen, or both. Electron microscopy may show mitochondria with structural abnormalities (e.g., involving cristae) that are concentrically arranged, honeycombed, or contain paracrystalline inclusions (Fig. 13-15C).

Molecular studies of the mitochondrial genetic material and biochemical studies of the mitochondrial electron transport chain enzymes can be performed on either muscle biopsy samples or lymphocytes. Clinicopathological correlations are complicated by the fact that the same biochemical deficit may be responsible for a highly variable clinical picture. Conversely, identical clinical manifestations may be caused by different enzyme abnormalities. Deletions of mitochondrial DNA are often seen in Kearns-Sayre syndrome.

While a general biochemical classification continues to evolve, there is a practical advantage in referring to a few distinct clinical forms (Table 13-6).
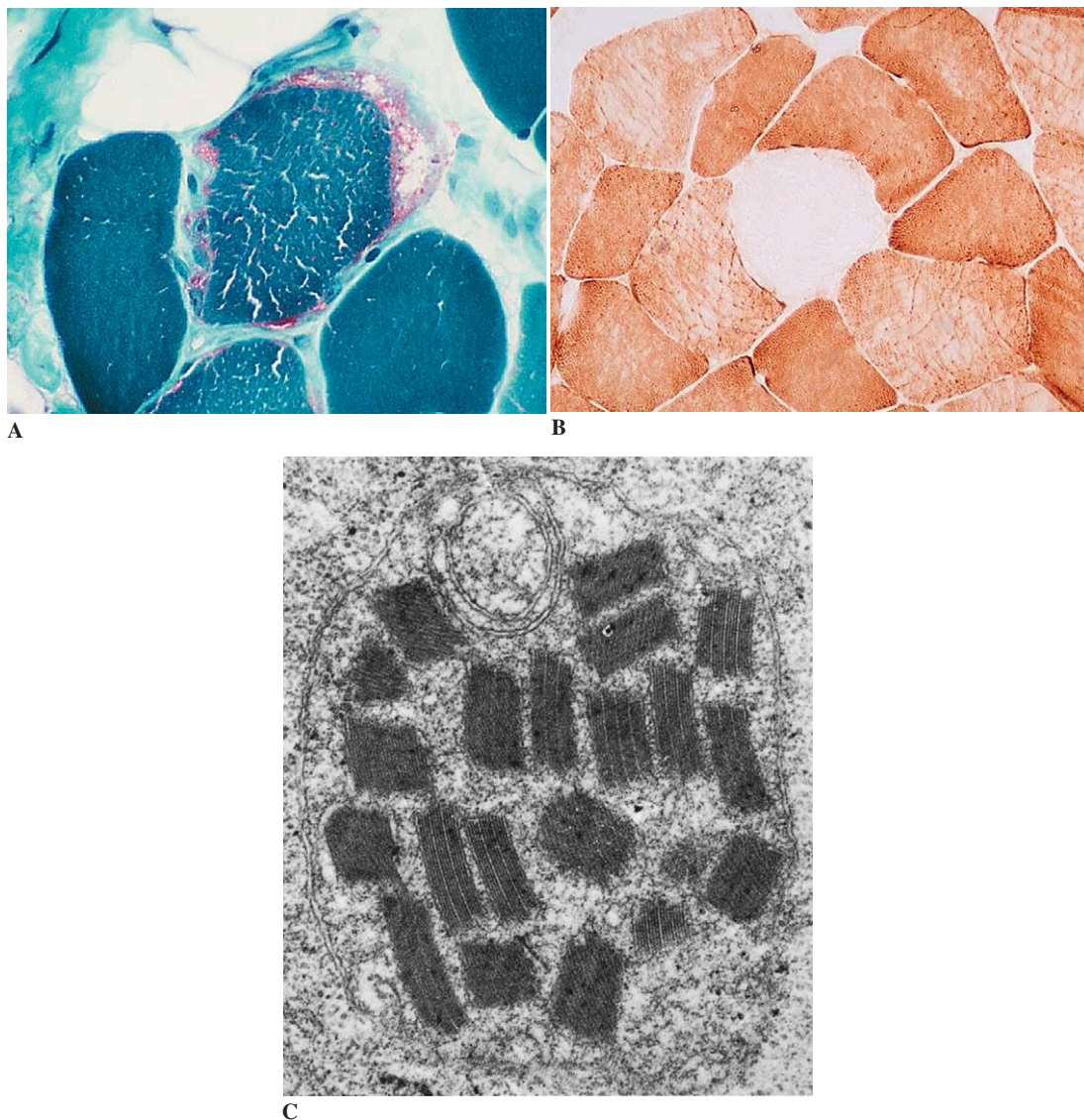
Figure 13-15. Mitochondrial cytopathies. **A**, Ragged red fiber (Gomori trichrome). **B**, COX-negative fiber. **C**, "Parking-lot" type of paracrystalline inclusion seen by electron microscopy.

- The oculocraniosomatic syndrome (ophthal-moplegia plus, Kearns-Sayre syndrome).
- MERRF (myoclonus epilepsy with ragged red fibers).
- MELAS (mitochondrial myopathy, ence-phalopathy, lactic acidosis, and stroke-like episodes).
- MNGIE syndrome (mitochondrial myopathy, neurogastrointestinal encephalomyopathy).
- Leigh disease, or subacute nercotizing encephalomyelopathy.
- Leber's hereditary optic neuropathy (in which muscle biopsy is typically normal).

Acquired mitochondrial myopathy may occur in patients treated with zidovudine (AZT), an anti-viral nucleoside analog interfering with mtDNA replication.

Table 13-6. Selected Mitochondrial Myopathic Syndromes

Syndrome	Genetics	Clinical Features	Pathology
Kearns-Sayre syndrome	Single large mtDNA deletion most common mutation type (80%); identical in Pearson syndrome and progressive external opthalmoplegia	Progressive external ophthalmoplegia; pigmentary degeneration of retina; heart block; mitochondrial myopathy; weakness (proximal, symmetric); multiple CNS deficits	Variation in muscle fiber size; ragged red fibers common (COX+ and COX−)
MELAS (mitochondrial calcification, encephalomyopathy, lactic acidosis, stroke)	mtDNA point mutations	Encephalopathy; seizures; hemiplegia; pigmentary retinopathy; myopathy; exercise intolerance; proximal symmetric weakness	Ragged red fibers (COX+); focal necrosis in basal ganglia and cerebral hemispheres.
MERRF (myoclonic epilepsy, ragged red fibers)	mtDNA point mutations	Late-adolescence onset; myoclonus; polyneuropathy; myopathy; hearing loss; optic atrophy	Ragged red fibers (COX−)

COX = cytochrome-*c* oxidase.

Lipid Myopathies

CARNITINE DEFICIENCY.   Three main forms of *carnitine deficiency* are known:

(1) *Muscle carnitine deficiency* causes a limb-girdle myopathy presenting in the second decade of life. Muscle biopsy reveals vacuolar myopathy. Lipid storage appears as droplets stained with Sudan black. This storage is localized in type 1 fibers and is accompanied by mitochondrial abnormalities. Muscle carnitine levels are low, but serum levels are normal.

(2) *Systemic carnitine deficiency* may become evident early in life in the form of acute metabolic episodes, in the course of which the myopathy may be detected only as a secondary phenomenon.

(3) *Secondary partial carnitine deficiency* may be associated with cachexia, liver pathology, chronic hemodialysis, or another form of myopathy, especially mitochondrial myopathy. Carnitine deficiency, and the consequent lipid-storage myopathy, may also be drug-induced (i.e., secondary to valproate anticonvulsant therapy).

CARNITINE PALMITYL TRANSFERASE DEFI-CIENCY.   *Carnitine palmityl transferase deficiency* is manifested from early childhood by episodes of cramps with myoglobinuria occurring after prolonged effort. Hyperlipidemia may be present. Between these episodes of rhabdomyolysis, muscle biopsy is usually normal. Lipid storage, which is detected in less than one third of cases, is less

evident than in carnitine deficiency. The enzyme deficit is demonstrable in skeletal muscle, leukocytes, and cultured fibroblasts.

OTHER MYOPATHIES WITH LIPID ACCUMULA-TION.   A form of lipid myopathy with congenital ichthyosis, as well as various lipid and lipid-glycogen myopathies with mitochondrial abnormalities, have been described. *Ceroid lipofuscinosis* is characterized by the accumulation of autofluorescent lipopigment in various tissues and is recognized by the accumulation of curvilinear inclusions at the ultrastructural level. This lysosomal disorder does not produce a clinical myopathy; the manifestations are essentially due to CNS involvement (see Chap. 10).

Glycogenoses

In the *glycogenoses*, striking aggregates of glycogen accumulate within the muscle fiber and are demonstrable in PAS-stained sections. These observations should be complemented with ultrastructural and biochemical studies. The presence of granular glycogen that is infiltrated into the contractile apparatus may be used as a rough guide to increased glycogen. From the morphological viewpoint, it is important to differentiate the type of muscle glycogenoses according to the site of glycogen accumulation, that is, mainly lysosomal (i.e., type II; Pompe disease) or cytoplasmic (types III, IV, V, and VII). A further distinction is the presence of abnormal fibrillary glycogen (polyglu-

cosan) in type IV and of phosphofructokinase deficiency.

POMPE DISEASE.   Two very different forms of *Pompe disease* (type II glycogenosis; acid maltase deficiency) exist: the *hypotonic and cardiomegalic* form in the neonate, which is rapidly fatal, and the *myopathic* form in children and adults. In adults, acid maltase deficiency presents typically as a limb-girdle dystrophy with respiratory involvement, making its appearance in middle life. Muscle biopsy reveals vacuolar myopathy (Fig. 13-16A). The vacuoles involve a highly variable proportion of muscle fibers, usually of type 1. They may be small and scanty. They contain PAS-positive inclusions (Fig. 13-16B) that are digested by amylase and show a strong acid-phosphatase reaction. Electron microscopy (Fig. 13-16C) demonstrates that the abnormal storage often extends beyond the

lysosomes to involve the cytosol. The diagnosis is established by biochemical assay.

FORBES DISEASE.   Characterized by the accumulation of dextrin, *Forbes disease* (type III glycogenosis; deficit of the debranching enzyme amylo-1,6 glucosidase) is usually evidenced in childhood; nonmyopathic manifestations predominate.

MCARDLE DISEASE.   *McArdle disease* (type V glycogenosis; myophosphorylase deficiency) is usually recognized in the adult because of painful cramps, which are sometimes associated with myoglobinuria and occur during short and intense bouts of physical exertion. With subsequent effort, the cramp, which is electrically silent, is followed by a characteristic "second-wind" phenomenon. The curve of hyperlactacidemia, normally obtained with effort, is flat. Muscle biopsy inconstantly
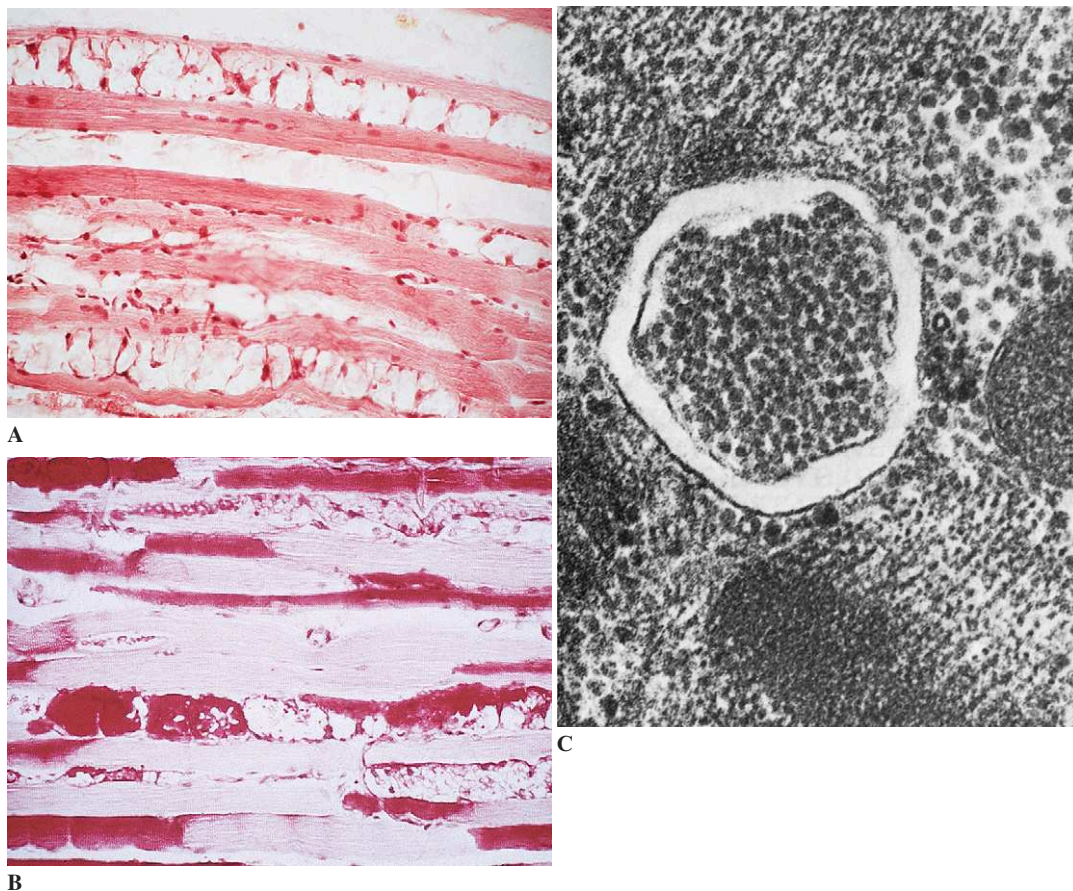
Figure 13-16. Pompe disease. Large, "empty" vacuoles on H and E (**A**), are strongly stained by PAS (**B**). **C,** Electron microscopy shows lysosomal storage. (**C,** Courtesy of Dr. M. Baudrimont.)

shows subsarcolemmal vacuoles with PAS-positive contents. The diagnosis is made with enzyme histochemical preparations (i.e., by the negativity of the phosphorylase reaction) and biochemical assay.

TARUI DISEASE. The clinical picture in *Tarui disease* (type VII glycogenosis; phosphofructokinase deficiency) is similar to that of McArdle disease and is associated with moderate hemolytic anemia. Phosphorylase activity is normal. The diagnosis is made either biochemically or on the basis of enzyme histochemistry.

RARE GLYCOGENOSES. Among these, a group of disorders characterized by the accumulation of glucose polymers (polyglucosan bodies) is recognized; they include type IV glycogenosis, Lafora disease, and polyglucosan myopathy (see Chap. 10).

Endocrine Myopathies. Although muscle weakness is often observed in various endocrine disorders, the corresponding histological changes usually show little specificity.

STEROID MYOPATHY. *Steroid myopathy* is seen in Cushing disease or as a result of prolonged corticosteroid therapy. An acute form may occur in status asthmaticus when treatment with curare and high doses of steroids is necessary. Steroid myopathy is manifest by type 2 (especially type 2B) muscle atrophy. Lipid and/or glycogen storage, as well as vacuolar myopathy, may also be seen.

THYROID MYOPATHY. In hyperthyroidism, the muscle biopsy is ordinarily unremarkable. The muscle biopsies of patients with thyrotoxic periodic paralysis, seen mainly in Japan, show the picture of dyskalemic vacuolar myopathy. In hypothyroidism, abnormalities in the muscle biopsy are more frequent; these include myopathic changes, type 2 fiber atrophy, glycogen storage, and accumulations of basophilic acellular material in the connective tissue.

Myalgia/Cramps Syndromes. A large number of well-recognized muscle disorders may be manifest primarily as painful myopathies, which are continuously present or are accentuated by physical exertion and which may be accompanied by cramps. These include the glycogenoses, some of the lipidoses, and the toxic and endocrine myopathies. In practice, the muscle biopsy in these predominantly myalgic syndromes is often disap-

pointing and shows only nonspecific changes, such as moderate atrophy of type 2 fibers. Such is often the case in fibromyalgia rheumatica.

Two disorders that are essentially characterized by a *myalgia/cramps syndrome* and that have a documented myopathology are *myoadenylate deaminase deficiency* and *myopathy with tubular aggregates*.

MYOADENYLATE DEAMINASE DEFICIENCY. The enzyme myoadenylate deaminase converts adenosine monophosphate into ammonia and inosine monophosphate. Deficiency of this enzyme is common in the general asymptomatic population or may be seen in well-characterized muscle disease, such as polymyositis, muscular dystrophy, or denervation. In patients with *myoadenylate deaminase deficiency*, muscle histology and standard enzyme histochemistry are normal. A negative enzyme histochemical myoadenylate deaminase reaction is found in affected individuals. As is evident from these observations, the relationship between the enzymatic abnormality and the clinical syndrome is difficult to ascertain.

MYOPATHY WITH TUBULAR AGGREGATES. *Myopathy with tubular aggregates* is characterized by painful intolerance on muscular exertion and presents in adulthood. Tubular aggregates are found in type 2 fibers.

Malignant Hyperpyrexia Syndrome. *Malignant hyperpyrexia syndrome* is a hereditary disease, transmitted as an autosomal disease, that is manifested in the course of general anesthesia with halothane and/or succinylcholine as a severe general syndrome that includes hyperpyrexia and rhabdomyolysis. Although, as mentioned previously, it is sometimes associated with a well-defined myopathy (e.g., central core disease or a myotonic syndrome), in most cases, muscle biopsy performed during the latent phase is either normal or shows only minor nonspecific abnormalities.

Toxic Myopathies

In the wide variety of drug-related and chemical toxic myopathies (Table 13-7), both the clinical manifestations and histological appearances are highly variable. The picture may be that of a rhabdomyolysis, a subacute necrotizing myopathy, a hypokalemic myopathy, a myositis that may be part

Table 13-7. Conditions Associated with
Toxic Myopathies

Rhabdomyolysis
  Alcohol
  Heroin
  Amphetamines
  Methadone
  Barbiturates
  Amphotericin B
  Carbon monoxide

Subacute Necrotizing Myopathy
  Alcohol
  Clofibrate
  ε-Aminocaproic acid
  Emetine
  Azidothymidine (AZT)

Hypokalemic Myopathy
  Diuretics
  Laxatives
  Liquorice

Inflammatory Myopathy
  D-Penicillamine
  Cimetidine
  Procainamide

Vacuolar Myopathy with Lysosomal Hyperactivity
  Chloroquine
  Perhexiline maleate
  Type 2 fiber atrophy
  Corticosteroids

of systemic lupus erythematosus, or a painless proximal myopathy. It may show various functional manifestations, such as a myalgia/cramp syndrome or myotonia, both of which may be induced by serum triglyceride-reducing drugs ("statins"). Chloroquine neuromyopathy gives rise to a most characteristic picture: progressive proximal muscle weakness is associated with vacuolar myopathy, seen on muscle biopsy; the vacuoles often predominate in type 1 fibers, are partially filled by PAS-positive material, and are strongly reactive for acid phosphatase, indicating a lysosomal origin (autophagic vacuoles). Lysosomal overactivity may also be seen in the absence of vacuoles. Electron microscopy of muscle and nerve shows the presence of membranous whorlings, myelin figures, and curvilinear inclusions, the latter persisting many years after cessation of treatment.

Rhabdomyolysis

Rhabdomyolysis is characterized by concomitant necrosis of a large number of muscle fibers followed by their presumably synchronous regeneration Inflammation is often remarkably minimal. Postnecrotic intramyocytic calcifications are encountered in rare instances. Rhabdomyolysis may follow a traumatic or ischemic cause such as crushing, excessive exercise, or compression within an anatomical compartment, particularly in the setting of acute intoxication (generally due to alcohol or psychotropic drugs). It may also be found in conjunction with a metabolic myopathy (e.g., a glycogenosis of the McArdle or Tarui type; a deficiency of carnitine palmityltransferase; malignant hyperpyrexia; or a potassium, phosphorus, or magnesium deficiency), a hemoglobinopathy (e.g., drepanocytosis), or an inflammatory muscle disease (e.g., a viral myositis).

Inflammatory Myopathies

Inflammatory myopathies are acquired myopathies that are characterized by muscle fiber inflammation, usually associated with destruction of the myocytes. They may be divided into two groups, according to whether the causative agent is a known infectious agent or the inflammatory process is believed to be an autoimmune phenomenon.

Inflammatory Myopathies Caused by Microorganisms

Viral Myositis

The most frequent acute myosites are due to (1) an influenza virus, which may cause acute benign myositis or severe rhabdomyolysis, and (2) an enterovirus, which in particular may be responsible for Bornholm disease or epidemic myalgia (Coxsackie B).

Polymyositis is often associated clinically with all types of human and animal retroviral infections, but does not seem to result from direct invasion of muscle fibers.

In the setting of *AIDS*, muscle involvement can be classified into four groups.

1. *HIV-associated myopathy*, which may be the presenting manifestation of the infection and is similar to seronegative polymyositis. HIV antigens may be detected in endomysial and perivascular macrophages, and muscle fibers strongly express MHC-1 molecules.
2. *AZT myopathy*, a toxic mitochondrial myopathy frequently associated with an inflammatory component. This condition is associated with myalgias that improve rapidly after AZT withdrawal. Muscle biopsy typically shows AZT-fibers (ragged red fibers with marked shrinkage of myofibrils) and COX-negative fibers.
3. *Muscle involvement linked to immunodeficiency*, including pyomyositis, toxoplasmic polymyositis, and primary muscle lymphoma.
4. A variety of other conditions, including HIV-cachectic myopathy, acquired nemaline myopathy, and recurrent myoglobinuria.

Bacterial Myositis

Bacterial myositis may be a complication of a skin injury (muscle abscess or gas gangrene caused by a clostridium) or part of a pyomyositis. The latter condition, which is seen in severely debilitated patients in intensive care units and is also observed in tropical countries (tropical pyomyositis), may present as a spontaneous, acute, suppurative infection culminating in the formation of abscesses in one or several skeletal muscle groups. It is caused by strict anaerobic organisms.

Parasitic Myositis

The most frequent *parasitic myositis* is trichinosis, which is secondary to the ingestion of meat infested with *Trichinella spiralis*. The latter may be diagnosed in muscle biopsy when encysted larvae are demonstrated (Fig. 13-17).

Toxoplasma cysts may be detected in muscle biopsies of severely immunocompromised patients. This reflects systemic reactivation of the parasite encysted in brain, retina, myocardium, and skeletal muscle (Fig. 13-18).

Fungal Myositis

Instances of fungal myositis are rare.
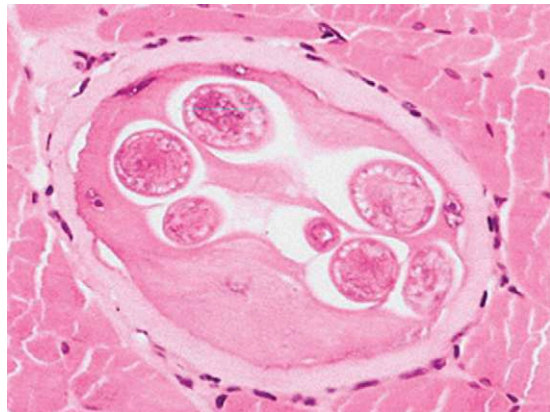
Figure 13-17. Trichinosis. Encysted larvae in a muscle cell.

Idiopathic Inflammatory Myopathies

The *idiopathic inflammatory myopathies* are subacute or chronic diseases that involve both adults and children. They ave been the subject of evolving classification schemes. Dermatomyositis, polymyositis, inclusion-body myositis, and systemic vasculitis with muscle involvement are the most common forms.

Dermatomyositis

In *dermatomyositis* (DM), proximal muscular weakness, often painful and of acute or subacute onset, is typically associated with cutaneous signs dominated by erythema of the face and the

Figure 13-18. Toxoplasmosis. Toxoplasma cyst in a muscle cell.

extremities that results in a purplish-blue discoloration of the eyelids and in periungual hyperemia. Dysphagia, arthralgia, constitutional symptoms, and elevated levels of serum muscle enzymes are frequent. Dermatomyositis is associated with visceral cancer in 15% of adult patients; therefore, DM occurring in adulthood, especially in the elderly, should be considered as a possible paraneoplastic manifestation. In children, dermatomyositis is often accompanied by a systemic vasculitis. DM may be difficult to distinguish from systemic lupus erythematosus with muscle involvement.

Muscle biopsy is the definitive diagnostic test for DM. Myopathologic features of DM are most characteristic and reflect primary involvement of microcirculation mediated by humoral processes with secondary ischemic changes of muscle fibers.

Myofiber alterations include (1) progressive atrophy of marginal layers of myofibers (perifascicular atrophy; Fig. 13-19A) that is preceded by local reexpression of MHC class 1 antigens (Fig. 13-19B); (2) ischemic punched-out vacuoles that occur subsequent to focal myosin loss (Fig. 13-19C); and (3) microinfarcts consisting of foci of contiguous necrotic or regenerating fibers (Fig. 13-19D).

Microvascular changes include (1) early capillary deposition of the complement C5b-9 membranolytic attack complex; (2) subsequent destruction of endothelial cells (free basement membranes), with focal loss of capillaries predominating in perifascicular areas; and (3) endothelial hyperplasia with detection of tubuloreticular inclusions (interferon-γ).

Inflammatory infiltrates include (1) septal perivascular infiltrates (without fibrinoid necrosis; Fig. 13-19E) and endomysial infiltrates predominating in perifascicular areas; (2) a mixture of mononuclear cells including B cells, T cells with % CD4+ > % CD8+, and macrophages (Fig. 13-19F); and (3) no CD8+ lymphocytic invasion of nonnecrotic myofibers.

Polymyositis

Polymyositis (PM) is a syndrome of diverse causes that may occur separately or in association with other connective tissue diseases or retroviral infections (see earlier in this chapter). PM manifests by symmetrical muscle weakness of subacute or chronic onset in adulthood with, or more often without, myalgia. There are no skin changes. CK levels are usually increased and the EMG findings are consistent with myositis. Since PM has no unique clinical features, its diagnosis is one of exclusion.

PM is a CD8+ T-cell–mediated and MHC1-restricted autoimmune myopathy. In contrast with DM, PM is not associated with capillary loss, perifascicular atrophy, or other ischemic changes. Inflammatory infiltrates are mainly composed of CD8+ T cells (Fig. 13-20B) and are found in endomysium, where they initially surround individual healthy-appearing muscle fibers. Then, together with macrophages, they attack and invade them focally, tunnel to the center of the fibers, and, finally, destroy them (Fig. 13-20A). Muscle cells die by perforin-mediated necrosis. The autoinvasive T cells exhibit selective gene rearrangement of their T-cell receptors. It is likely that the accumulated cytotoxic CD8+ T cells that use their TCR to recognize peptide antigens presented by MHC1 molecules at the surface of muscle fibers have been subjected to antigen-driven expansion, these T-cell clones being specific of as yet unknown muscle autoantigens. Widespread and strong MHC1 reexpression by muscle fibers constitutes a major immunopathologic feature of PM (Fig. 13-20C). It is associated with reexpression of the nonclassic MHC antigen HLA-G. MHC1 expression may be detected even in the absence of endomysial inflammatory cells, as is observed in patients with inactive PM following therapy. The possibility of an association with a connective tissue disease is raised when the disease is associated with perivascular lymphocytic infiltrates (Fig. 13-20D).

Inclusion Body Myositis

Inclusion body myositis (IBM) is a sporadic disease mainly affecting adult males over 50 years old. Onset is insidious and painless and is typically reported as an increasing difficulty with everyday tasks requiring proximal or distal limb muscles. Early involvement of quadriceps muscles, remarkable involvement of distal limb muscles, mainly deep finger flexors and foot extensors, and selective and often asymmetrical amyotrophy are typically present. CK levels are normal or slightly
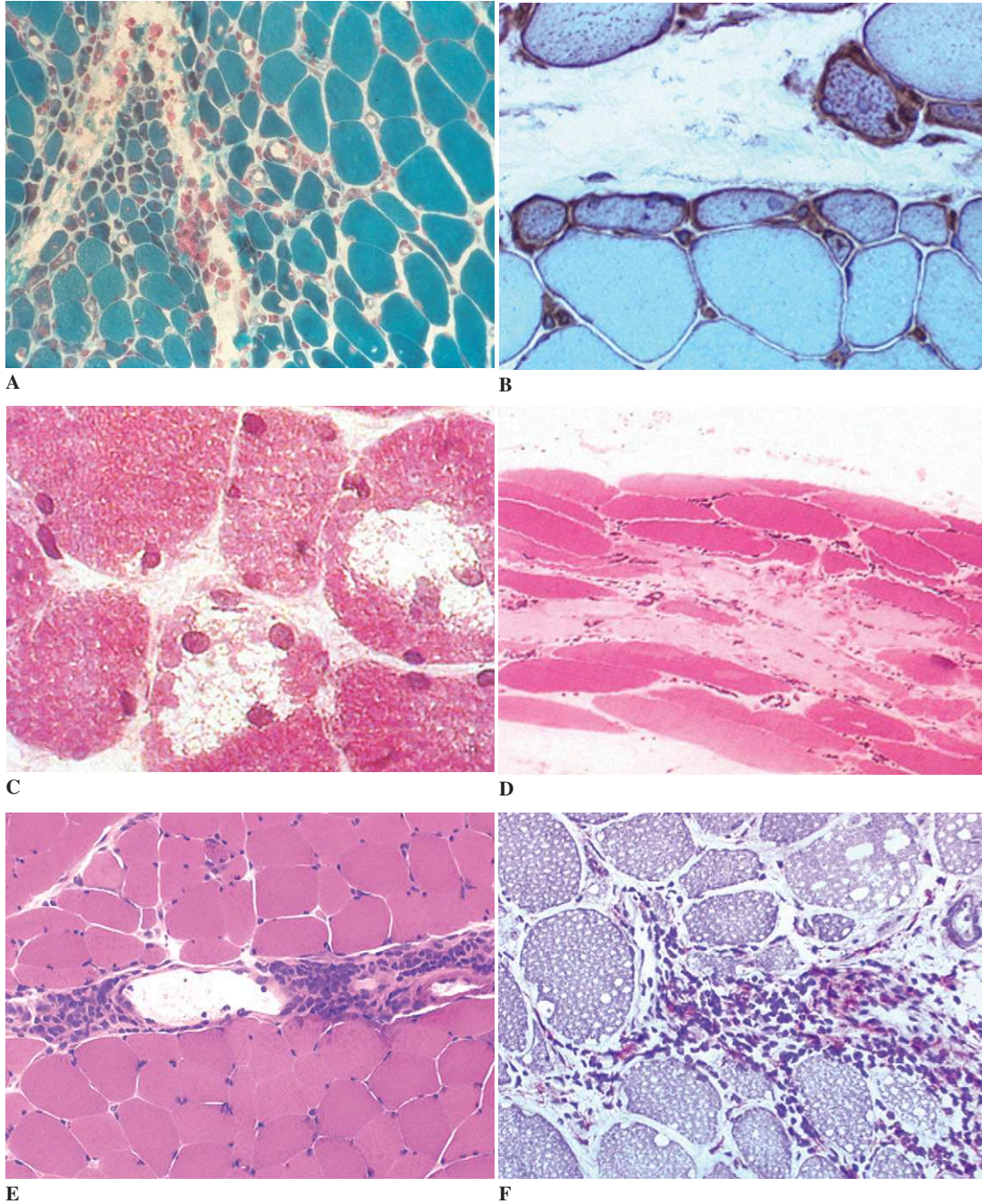
Figure 13-19. Dermatomyositis. **A**, Perifascicular atrophy. **B**, Expression of MHC class 1 antigens by the peripheral myofibers. **C**, Ischemic "punched-out" lesion due to focal myosin loss. **D**, Microinfarct. **E**, Perivascular septal inflammatory infiltrate. **F**, Immunocytochemistry for CD4 showing predominant CD4 lymphocytes within the inflammatory infiltrate.
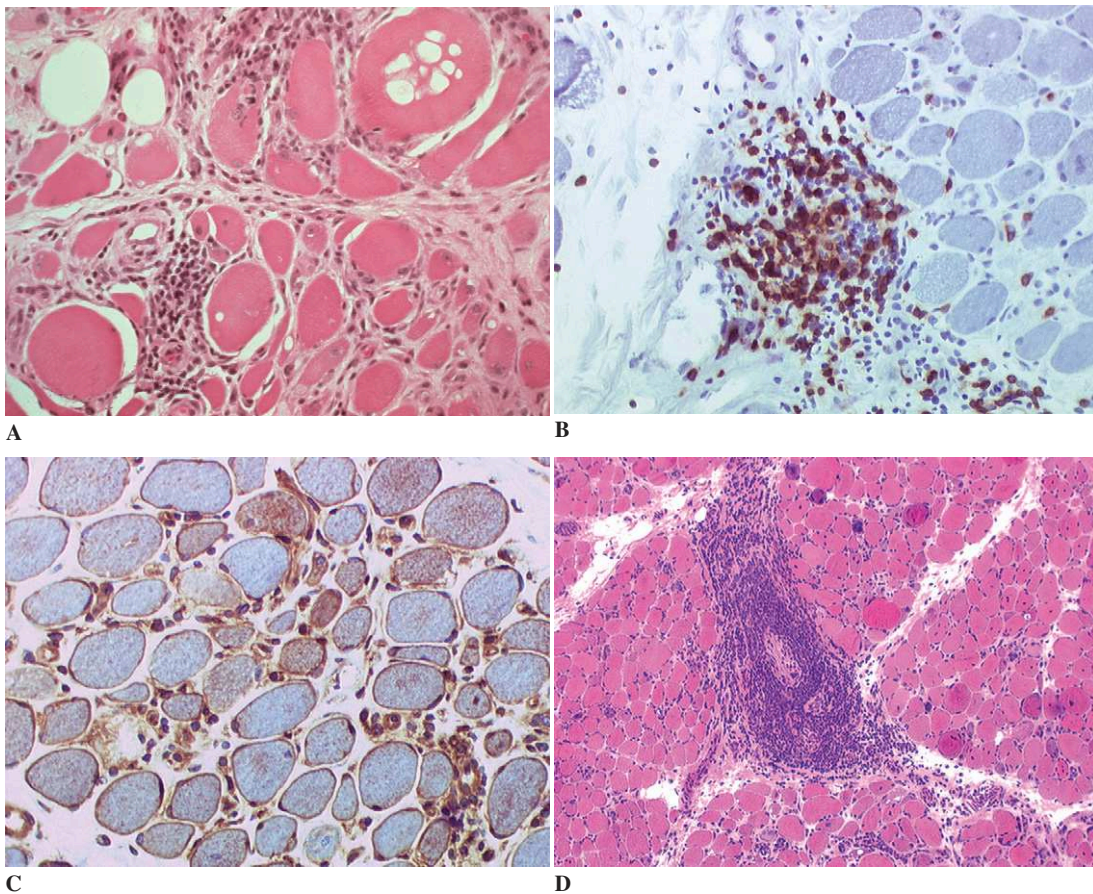
Figure 13-20. Polymyositis. **A**, Inflammation in the endomysium surrounding individual muscle fibers, some of which appear vacuolized and invaded by inflammatory cells. **B**, Immunocytochemistry for CD8 showing predominant CD8 cytotoxic lymphocytes within the inflammatory infiltrate. **C**, Immunocytochemistry for MHC1 showing widespread expression by muscle fibers. **D**, Lymphocytic vasculitis in a case of polymyositis associated with systemic lupus erythematosus.

elevated. The EMG may show a mixed myogenic and neurogenic pattern. Progression of IBM is slow and relentless, and patients often do not respond to immunosuppressive treatment. Reevaluation of muscle biopsy for possible signs of IBM should be performed in patients with presumed polymyositis resistant to steroids.

Typical muscle biopsy findings are required for the diagnosis of IBM. They may not be observed at the time of the first biopsy and may need to be searched in additional muscle biopsies. The characteristic myopathologic picture consists in the coexistence of rimmed vacuoles located anywhere in the muscle fibers and a multifocal inflammatory process (i.e., focal invasion of MHC1-expressing muscle fibers by CD8+ T cells). Rimmed vacuoles

are not specific and are insufficient in themselves to establish the diagnosis of IBM. Other features that may be seen in IBM include small groups of atrophic fibers, eosinophilic cytoplasmic inclusions, accumulation of Alzheimer-associated proteins in vacuolated muscle fibers (e.g., β-amyloid and its precursor protein, ubiquitin; prion protein; apolipoprotein E; hyperphosphorylated tau protein), mitochondrial abnormalities (ragged red fibers, COX-negative fibers, secondary mtDNA mutations), and ultrastructural demonstration of characteristic cytoplasmic and intranuclear tubulofilaments that measure 15 to 21 nm in diameter. An oligoclonal pattern of the TCR gene is observed in IBM. Whether the accumulated proteins provide autoantigens remains to be demonstrated.

Hereditary Inclusion Body Myopathy

It is now recognized that there is a heterogeneous group of patients with hereditary myopathies who have muscle biopsy findings that are similar to those in IBM, including rimmed vacuoles and immuno-cytochemical and ultrastructural findings (though they tend to have less prominent inflammation).

The clinical features, pattern of weakness, and age of onset differ from the IBM myositis. Both autosomal dominant and recessive pedigrees have been reported. One form, notable for sparing of the quadriceps and found in the Persian Jewish population, is caused by mutation in the GNE gene (UDP-*N*-acetylglucosamine 2-epimerase) on chromosome 9p12-p11. A Japanese form (Nonaka myopathy), also caused by allelic mutations of this gene, shows distal weakness. The autosomal dominant forms, seen in Swedish families, are characterized by muscle weakness with a deterioration of muscle function starting between 30 and 50 years of age. Muscle atrophy is most prominent in pectoralis muscles and, in contrast to the recessive form, involves the quadriceps muscles. This form is linked to 17p13.1.

An unusual constellation of autosomal dominant inclusion body myopathy, Paget disease, and premature frontotemporal dementia has been reported in several families with mutations at 9p13.3-p12.

Sarcoidosis

Interstitial epithelioid and giant cell granulomas may be seen in the muscle of patients with *sarcoidosis*, particularly at postmortem examination and irrespective of clinical manifestations referable to muscle involvement. A possibly related condition, termed g*ranulomatous polymyositis*, has a similar histologic picture but is unassociated with any extramuscular clinical or histological evidence of sarcoidosis.

Nodular Focal Myositis

Nodular focal myositis may be seen in various connective-tissue diseases, but is especially frequent in longstanding rheumatoid arthritis. It is characterized by the interstitial infiltration of lym-

phocytes and plasma cells, which form compact nodules measuring 1 to 2 mm in diameter that are situated near a small artery or arteriole but without invasion of the vessel wall. There may or may not be changes in the adjacent muscle fibers. An identical picture known as *lymphorrhages* is sometimes seen in myasthenia gravis.

Eosinophilic Myositis and Fasciitis

Eosinophilic myositis is defined by the presence of inflammatory cellular infiltrates containing eosinophils in the muscle, and can be associated with degenerative lesions of the muscle fibers. In addition to parasitic diseases of muscle and to systemic vasculitis (especially Churg-Strauss syndrome), the main cause is hypereosinophilic syndrome, a rare multisystem disorder in which muscle involvement includes eosinophilic polymyositis and eosinophilic fasciitis.

Eosinophilic fasciitis (also termed *Shulman syndrome*) is characterized by a subcutaneous induration that spares the face and fingers, stiffening of the joints, and a raised blood eosinophil count. Scleroinflammatory lesions predominate in the fascia but may extend into the dermis or muscle. In the tissues, eosinophilia is often well-circumscribed or absent. The lymphocyte and plasma cell infiltrates are mostly perivascular.

Macrophagic Myofasciitis

Macrophagic myofasciitis (MMF) is a recently recognized entity defined by stereotyped deltoid muscle biopsy findings that include perimuscular infiltration by large macrophages with a finely granular, PAS-positive content; a lymphocytic infiltrate; and inconspicuous muscle fiber damage (Fig. 13-21). MMF mainly manifests at adulthood by chronic fatigue and diffuse myalgias forming a syndrome that meets criteria for the so-called chronic fatigue syndrome. Macrophages of MMF contain intracytoplasmic osmiophilic crystalline inclusions composed of aluminum and similar to aluminum hydroxide, a Th2 immunostimulatory compound frequently used as a vaccine adjuvant. MMF is now recognized as a lesion secondary to long-term, local persistence of vaccine-derived aluminum hydroxide in muscle.
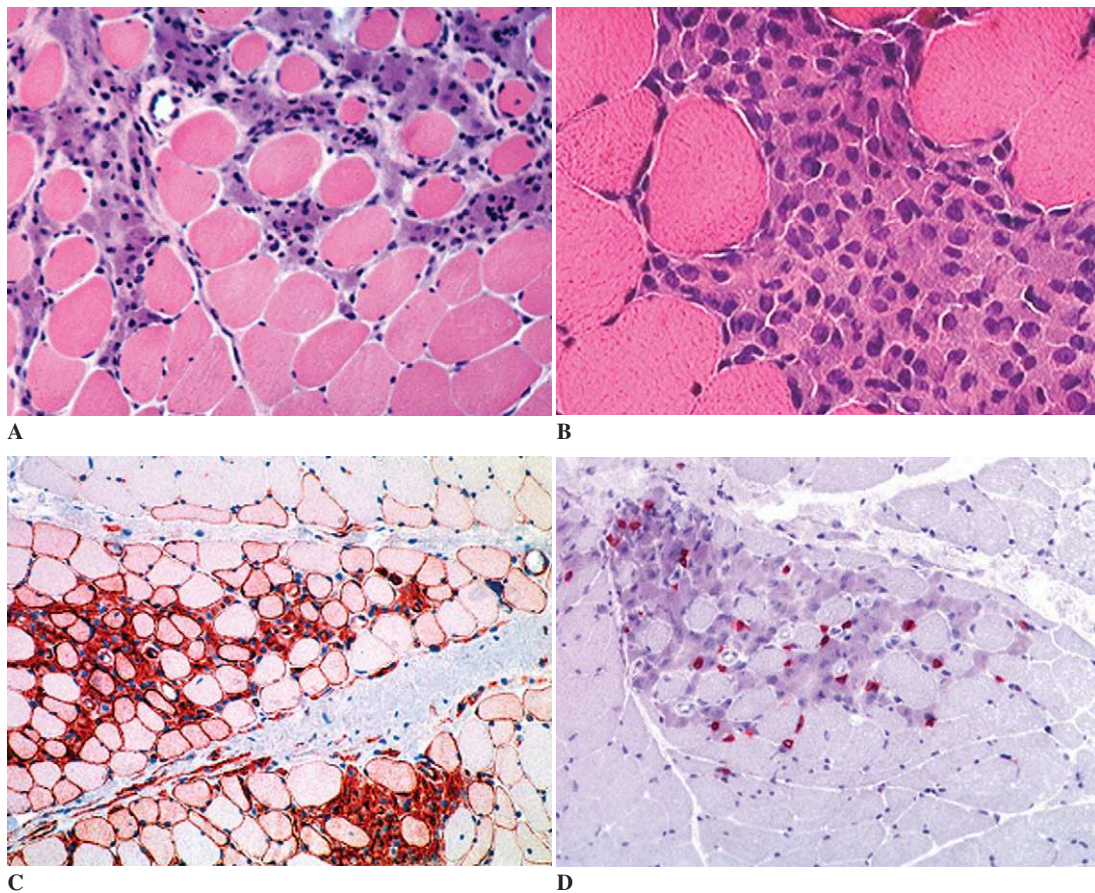
Figure 13-21. Macrophagic myofasciitis. **A**, Interstitial infiltration by large macrophages with a basophilic cytoplasm. **B**, Higher magnification shows the finely granular cytoplasmic content of the macrophages. **C**, Immunocytochemistry for CD68 clearly shows the perifascicular infiltration of the muscle by macrophages. **D**, Immunocytochemistry for T lymphocytes shows the presence of lymphocytes within the infiltrate.

Localized Myositis

Noninfectious myositis localized to a portion of the muscle, to one particular muscle, or to one muscle group essentially includes orbital myositis, sclerosing segmental polymyositis, inflammatory pseudomotor (focal) myositis, and proliferative myositis.

Vasculitis Involving Skeletal Muscle

In the systemic vasculitides (see Chap. 14), nerve and muscle biopsy may establish the diagnosis (Fig. 13-22). The lesions in skeletal muscle consist of small, inflammatory cellular infiltrates adjacent to
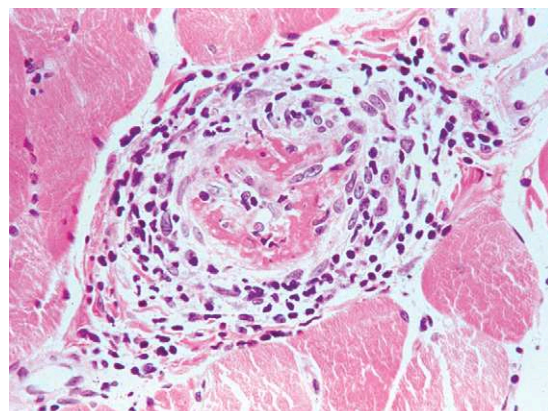
Figure 13-22. Polyarteritis nodosa (PAN).

the involved blood vessels, nonspecific type 2 atrophy, or evidence of denervation atrophy related to concomitant peripheral nerve involvement. Focal infarction of muscle is sometimes seen that involves part of a fascicle. The affected muscle fibers have lost their tinctorial affinity and at their periphery inflammatory cells may be seen, including acute inflammatory cells.

Cholesterol Emboli

Within the framework of ischemic myopathies may be included *cholesterol emboli*, which are often the source of systemic manifestations due to microinfarction of multiple organs. Cholesterol crystals migrate from aortic atheromatous plaques and occlude small arteries, especially those of lower-limb muscles, after which they may be surrounded by reactive changes and inflammatory cell infiltrates, including macrophages.

Chapter 14
Peripheral Nerve Diseases

Jean-Michel Vallat, Douglas Anthony,
and Umberto De Girolami

Peripheral Nerve Biopsy

Site of the Biopsy

A peripheral nerve biopsy is taken ordinarily from a purely sensory nerve of sufficient caliber to yield meaningful information. The choice in practice is limited to two nerves in the lower limb: the sural nerve (a branch of the medial popliteal nerve) and the musculocutaneous (superficial peroneal) nerve (a branch of the lateral popliteal nerve). In the absence of selective sensory involvement, the musculocutaneous nerve is sometimes chosen because the underlying peroneus brevis muscle may also be sampled with a single surgical incision. In case of selective involvement of the limb girdle, it is at times possible to perform a biopsy of a sensory superficial branch of the crural nerve; when the neuropathy is restricted to the upper limbs, a sensory superficial branch of the radial nerve of the forearm may be biopsied.

Methods

Immediately after removal, the biopsy specimen must be processed so that the proper studies can be carried out. These include routine histology, electron microscopy, and teased fiber preparations. Tissue must also be set aside and cryostat sections quick frozen for chemical analyses.

Qualitative and Chemical Analysis

Routine Histology. Fixation in 10% formaldehyde followed by paraffin embedding is commonly employed. This technique enables the study of abnormalities of interstitial tissues, including an evaluation of the integrity of blood vessels, the assessment of the presence of inflammatory cells, and a search for abnormal substances (e.g., amyloid). The stains most commonly employed for this study include H and E, elastic tissue stains, Masson trichrome, silver impregnation for reticulin, myelin stains, silver impregnations and myelin stains for axons, and Congo red for amyloid deposits. Immunohistochemical stains suitable for paraffin-embedded tissue may also be used.

Plastic Embedding. Plastic embedding following immediate fixation in 2.5% buffered glutaraldehyde allows for semithin (1-μm-thick) transverse and longitudinal sections, which is the method of choice for examining the fine structural details of both myelinated and unmyelinated fibers (Figs. 14-1A, B, and C). It also allows, when necessary, to proceed to electron microscopy. In special cases, immunoelectronmicroscopy may be performed in order to identify specific proteins at the ultrastructural level.

Dissociation of Fibers (Nerve Teasing). This technique consists of the separation of single

315
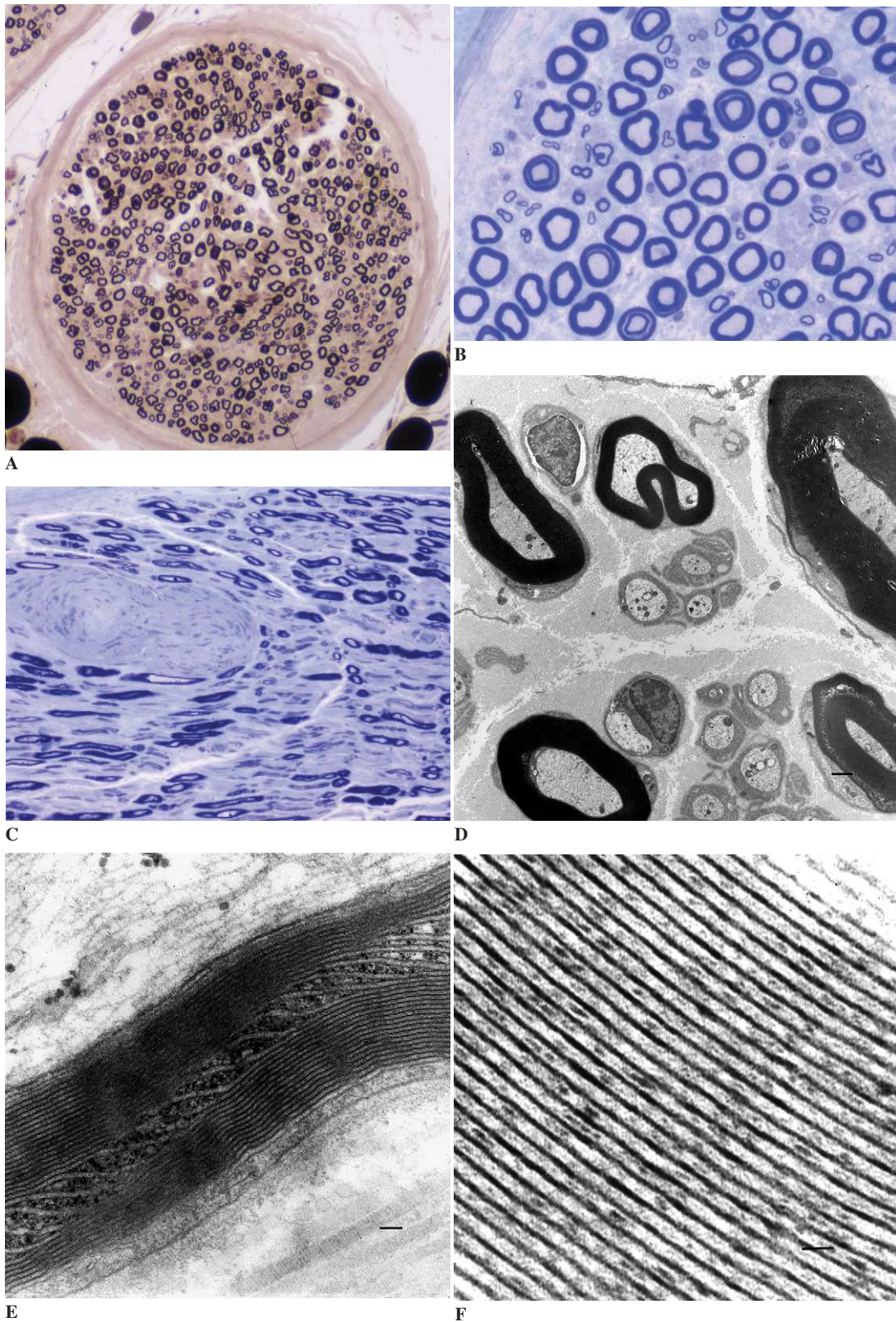
Figure 14-1. Normal morphologic appearance of peripheral nerve. **A** and **B**, Semithin transversal section. **C**, Semithin longitudinal section with Renaut body. **D–F**, Ultrastructural appearance: appearance at low magnification (**D**); higher magnification, showing myelin sheath with Schmidt-Lanterman incisure (**E**); still higher magnification showing structure of myelin lamellae (**F**).

myelinated fibers (around 1 cm long), after alde-hyde fixation and osmication, by teasing them apart with fine needles under visualization with a dis-secting microscope. Light-microscopic examina-tion of the teased fibers clearly shows the relative positions of nodes of Ranvier and is very helpful in discriminating between lesions characteristic of demyelination or axonal involvement and those typical of degeneration.

Frozen Sections for Immunofluorescence and/or Chemical Analysis.   Direct immunofluorescence studies can be carried out using specific antibodies to identify abnormal deposits of immunoglobulins in endoneurium or in myelinated fibers. Various markers can be employed (also on paraffin sec-tions) to identify different types of inflammatory cells (T and B lymphocytes, macrophages, etc.) as well as amyloid deposits.

It is also important to have frozen tissue avail-able when testing for metabolic or chemical disorders.

DNA Extraction.   DNA can be extracted from either paraffin-embedded or frozen tissue. This allows for the reclassification of archival material. Abnormalities of genes coding for myelin proteins can thus be sought.

Morphometric Analysis

From a practical standpoint, morphometric studies are time-consuming and require a substantial investment in equipment. Ordinarily, it is clearly not justified to employ such techniques, which tend to be reserved for research purposes. A trained observer can often give a reliable opinion as to the density of myelinated fibers, an estimate of the degree of loss of large or small fibers, and the pres-ence and the severity of demyelinating and/or axonal lesions.

Quantitative Analysis on Dissociated Fibers. The object of these studies is to quantify, using computer-assisted statistical methods, the intern-odal distances on single nerve fibers. The mean internodal distance and the standard deviation around the mean are both calculated. The data are usually represented by a plot of internodal dis-tances against the mean diameter of the fibers for a number of myelinated fibers.

Quantitative Study on Semithin Sections and on Electron Micrographs.   Morphometric analysis of cross-sections of the nerve may be carried out either after photography or directly by image analysis.

Myelinated fibers. The diameter of myelinated fibers ranges from 2 to 12 μm in a bimodal distri-bution with peaks at 3–6 μm and 9–12 μm. There are more small myelinated fibers than large ones. In young adults, the average is 7000–10,000 fibers/mm^2 of endoneurial surface; there are marked age-dependent variations. The number of fibers decreases progressively with age.

The ratio between size of the axon and number of myelin lamellae, which tends to be linear, can only be established by EM examination. The "*g*" ratio, or ratio of axonal diameter/total diameter, is commonly used to evaluate the severity of the demyelinating lesions.

Electron-microscopic examination of unmyeli-nated fibers. This is time-consuming and costly and is not generally carried out on a routine basis. It also requires special expertise to reliably identify unmyelinated fibers. The diameter of these axons ranges from 0.2 μm to 2.5 μm in a unimodal distri-bution with a peak at 1.4–1.6 μm. The density of unmyelinated fibers ranges from 20,000/mm^2 to 35,000/mm^2. The ratio of unmyelinated fibers to myelinated ones is about 4 to 1.

Other parameters may also be quantified, such as the thickness of the perineurium and the extent of proliferation of endoneurial connective tissue.

Normal Anatomy

Connective Tissue Sheaths of Peripheral Nerve

The nerve fibers of peripheral nerve trunks are sep-arated from each other and compartmentalized in bundles or fascicles by organized connective tissue sheaths. Individual myelinated and unmyelinated nerve fibers are embedded in a meshwork of deli-cate connective tissue termed the *endoneurium*. Bundles of nerve fibers within each fascicle are held together by multiple concentric layers of spe-cialized connective tissue termed the *perineurium*. The vascular bundles that travel along with periph-eral nerves and give rise to their vascular supply lie within layers of fibroadipose connective tissue that surround one or multiple fascicles; these layers are termed the *epineurium*.

In addition to the myelinated and unmyelinated fibers, their Schwann cells, and collagen fibers, the endoneurial compartment contains capillaries, mast cells, fibroblasts, and Renaut bodies. Endoneurial capillaries have tight junctions, as do those in the brain and spinal cord, thus forming and effective blood-nerve barrier analogous to the blood-brain barrier. Renaut bodies (see Fig. 14-1B) occur at sites of potential entrapment, such as in the median nerve at the wrist and the ulnar nerve at the elbow. Absent in the fetus, they increase in number with age. They are made up of cells showing perineurial differentiation. Their precise function is not known, but a cushioning effect has been speculated.

Axons (Nerve Fibers)

The ratio of myelinated to unmyelinated fibers and the diameter of the fibers vary considerably from nerve to nerve, depending on the number of sensory/autonomic fibers of the various modalities and on the number of motor axons within a given nerve. In this regard, the most extensive body of quantitative data is from the sural nerve. As mentioned previously, unmyelinated nerve fibers are about four times as numerous as myelinated nerve fibers (Fig. 14-1D).

Myelin Sheaths

In myelinated fibers, the *myelin sheath* extends from one end of the axon to the other, that is, from just beyond the neuronal cell body to just before the axon terminal. Myelin is produced by and situated within the Schwann cells that line up along the axon. The myelin sheath is not a continuous structure throughout the length of the axon but is interrupted at regular intervals along its length, namely, at those points where one Schwann cell ends and the next begins. The space between two adjacent Schwann cells is referred to as a *node of Ranvier*. The stretch of myelin between one node of Ranvier and the next is referred to as an *internode*. The length of an internode is fairly constant along the axon and is proportional to the diameter of the axon. Each internode is subserved by a single Schwann cell, whereas several axons are within the purview of one Remak cell in unmyelinated axons (see later

in this chapter). The myelin sheath is made up of very regular concentric lamellae with a periodicity of 12 nm to 17 nm, forming major dense lines separated by electronlucent zones in which one or two interperiod lines can be observed (Figs. 14-1E and F). Discontinuity in the compaction of the lamellae is seen at the Schmidt-Lanterman incisures (see Fig. 14-1E). The major dense lines open periodically, allowing invaginations of Schwann cell cytoplasm to penetrate between them.

Myelinated Axons

Axons vary in diameter from 3 μm to 10–12 μm. They are surrounded by a 7- to 8-nm-thick membrane termed the *axolemma*, which communicates directly with the internal mesaxon. The axolemma has the same ultrastructural characteristics as the cytoplasmic membranes of Schwann cells; it is lined by a basal lamina which passes from one Schwann cell to the next without interruption at the nodes of Ranvier. The axoplasm contains longitudinally oriented mitochondria, a smooth endoplasmic reticulum, multivesicular bodies, neurofilaments, and neurotubules. Neurofilaments have a mean diameter of 10 nm, whereas neurotubules, which have a central lumen, have a diameter of around 20 nm.

Schwann Cells

Schwann cells can be distinguished from endoneurial fibroblasts by the presence of a basement membrane. Their elongated nuclei are found roughly equidistant from two adjacent nodes of Ranvier. The cytoplasm, located between the inner lamella of the myelin sheath and the axon and between the outermost myelin lamella and the cell membrane, is almost always very sparse. Found mainly around the nucleus, this cytoplasm contains endoplasmic reticulum, a Golgi apparatus, mitochondria, sometimes a centriole, and complex multilamellar lipid membranous granules (π, or granules of Reich).

Unmyelinated Fibers

Unlike myelinated fibers, multiple unmyelinated axons are usually enclosed by a single Schwann cell (Remak cell); they are closely packed and separated from each other by a thin layer of cytoplasm.

General Reactions of Peripheral Nerve to Disease

The general reactions of peripheral nerve to injury can be separated into two types: those which involve primarily the axon and those that preferentially involve the myelin sheath. Combinations of the two are common.

Primary Axonal Degeneration

There are four principal types of axonal degeneration (Fig. 14-2). By and large, all forms ultimately result in denervation of muscle fibers when the process affects motor axons.

Types of Axonal Degeneration

Wallerian Degeneration. *Wallerian degeneration* is the response of the distal part of an axon to transection of the nerve. In the early stages, it is characterized morphologically by breakdown of the axon and its myelin sheath. There follows a reparative stage, which consists of proliferation of Schwann cells within the tube formed by the original schwannian basal lamina. The Schwann cell groups that form constitute the *Büngner bands*. Regeneration through the sprouting of axons from the proximal stump of the sectioned nerve begins almost at once after axotomy, but progresses slowly

(1 to 3 mm per day). These sprouts, usually two to five per sectioned axon, may enter the Büngner bands. This process results in the morphologic appearance of clusters of small, thinly myelinated groupings of regenerating clusters or regenerating fibers (clusters; Fig. 14-3).

Dying-Back Neuropathy (Distal Axonopathy). This type of axonal injury is characteristic of a group of neuropathies, with fairly symmetrical, subacute or chronic degeneration that first affects the most distal portions of the axon, followed by progressively more proximal degeneration. The longest and largest fibers are first involved (length-dependent vulnerability). The central axonal extensions from sensory neurons undergo degeneration concomitant with that of their peripheral extensions; degeneration of the posterior columns, for example, starts from the upper end of the spinal cord. For some time, the conduction velocity remains near normal owing to a retention of a significant proportion of normal fibers, but values drop in the very late stages of the disease.

The pathogenesis of this commonly observed phenomenon in nerve biopsy samples (particularly prominent in toxic neuropathies) is still poorly understood. There is some evidence to support the hypothesis that the dying-back process is related to abnormalities of fast axonal transport.

The neuropathologic picture is characterized by a reduction in the number of myelinated fibers

Figure 14-2. The different types of nerve degeneration. (From Asbury AK, Johnson PC. Pathology of peripheral nerve. Philadelphia, WB Saunders, 1978, p. 51, with permission.)
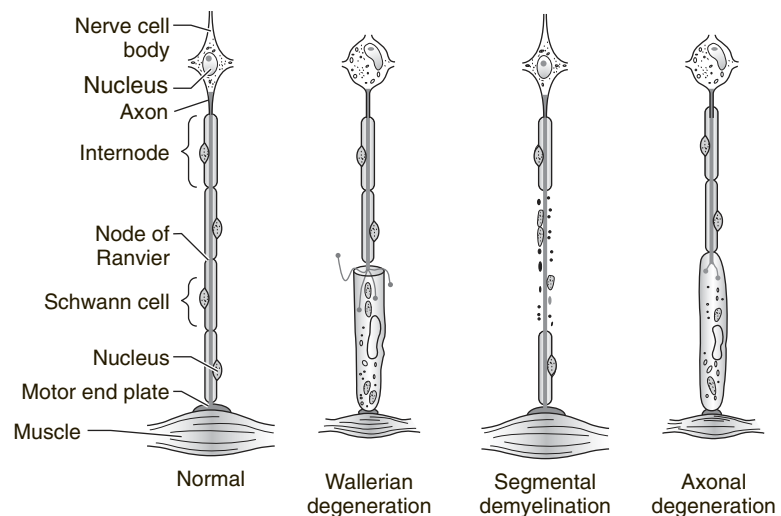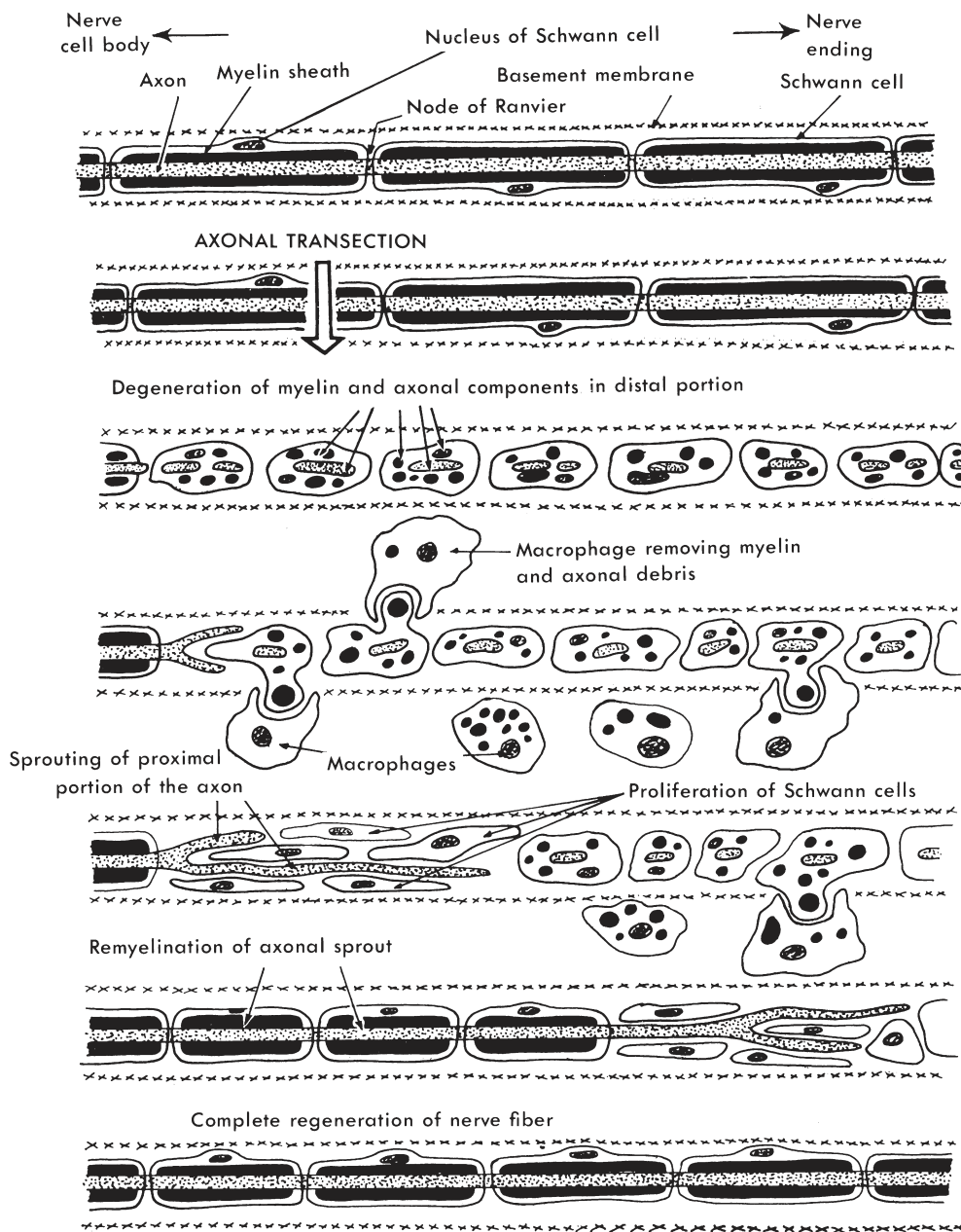
Figure 14-3. The main stages of wallerian degeneration and regeneration of a myelinated peripheral nerve fiber. (Redrawn and modified from Bradley WG. Disorders of peripheral nerves. Oxford, Blackwell, 1974.)

with evidence of regeneration, including axonal sprouting.

Neuronopathy. *Neuronopathy* is a category of axonal neuropathy wherein the primary abnormality is thought to be in the neuronal cell body, with a more or less synchronous injury to the axon, thereby rendering regeneration impossible. Neuronopathies, as neuronal degenerations in the gray matter of the cerebral cortex and elsewhere, characteristically are slowly progressive and sequentially involve selective populations of neurons.

Sensory neurons are more often affected than motor neurons in neuronopathic toxic injuries (e.g., pyridoxine intoxication and injuries by circulating antibodies, such as paraneoplastic neuropathy). The reasons for this predilection of sensory systems are not known, but have been postulated to be related to the lack of vascular barrier in dorsal root ganglia, which may permit direct access of toxins to the cell. Furthermore, preferential involvement of populations of selected neurons within dorsal root ganglia is well-recognized, as it occurs in neuropathies that preferentially involve either small neurons (e.g., Fabry disease) or large neurons (e.g., sensory paraneoplastic neuropathy, Friedreich ataxia, abetalipoproteinemia). Another proposed mechanism of cell injury is uptake of noxious substances in the free sensory terminals. These lack the blood-nerve barrier, thereby allowing absorbed substances access to the perikaryon through retrograde axonal transport ("suicide transport").

Abnormalities of Axonal Caliber. *Axonal caliber* is related to, among other things, the number of neurofilaments and neurotubules contained in the axon.

In human pathology, axonal atrophy, in most cases, is regarded as secondary to a reduction of neurofilament synthesis. It chiefly affects the large fibers because they are richest in neurofilaments (caliber-dependent vulnerability). Axonal atrophy is manifest as a loss of the circular outline of the fiber and a reduction of axonal caliber. In prolonged insults, secondary demyelination may occur and be severe enough to mimic a primary chronic demyelinating process. Axonal atrophy in the elderly has been documented in Charcot-Marie-Tooth disease, in uremic neuropathy, in diabetic neuropathy, in neuropathy associated with myeloma, and in various toxic neuropathies.

Axonal swelling resulting from focal or multifocal accumulation of neurofilaments and other organelles is characteristic of hereditary neuropathies (e.g., hereditary giant axonal neuropathy; Fig. 14-4A) and of toxic neuropathies (e.g., glue-sniffing neuropathy; Fig. 14-4B).

Morphological Appearances of Acute/Chronic Degeneration and Regeneration in Axonal Neuropathies

Morphological appearances of acute and chronic degeneration and regeneration in axonal neuropathies vary depending on the course of the disease, the interval between biopsy and the onset of the disease, and the site of the nerve sample along the length of the fiber.

In the early stages of the process, myelinoaxonal degeneration may be seen by light microscopy as *ovoids*, that is, axonal fragments surrounded by disintegrating myelin (Figs. 14-5A and B). This form of degeneration is sometimes difficult to distinguish from crush artifact. It is best appreciated by electron microscopy (Fig. 14-5C) and in teased nerve preparations (Fig. 14-5D). In addition, teasing permits

A   B
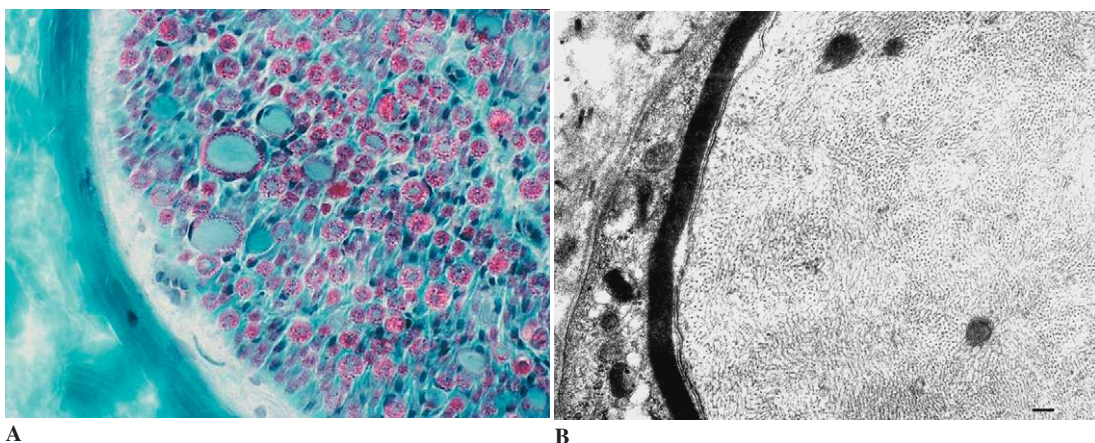
Figure 14-4. Axonal swelling. **A**, Light microscopy in a case of hereditary giant axonal neuropathy. **B**, Electron microscopy in a case of hexane neuropathy. Note accumulation of neurofilaments.
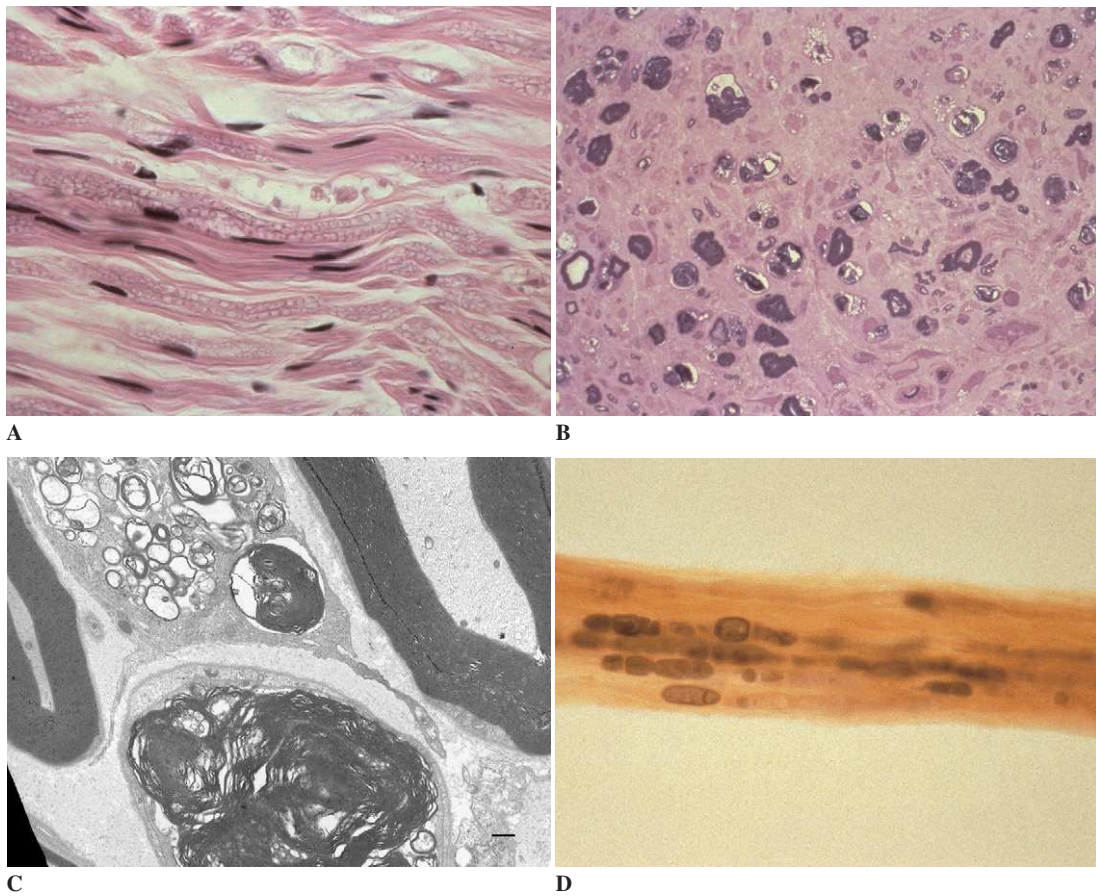
Figure 14-5. Acute wallerian degeneration. **A,** Paraffin-embedded section. **B,** Semithin section. **C,** At ultrastructural examination. **D,** Teasing preparation.

identification of the earliest lesions, which consist of myelin retraction on either side of the nodes of Ranvier followed by myelin irregularity and fragmentation in each internode. Phagocytosis of degenerated nerve fiber fragments by Schwann cells and by circulating mononuclear phagocytes is seen to better advantage in longitudinal sections and by electron microscopy (see Fig. 14-5C). Early axonal sprouting may also be seen. The earliest changes that attend axonal degeneration are best detected by electron microscopy as disruption of the myelin sheath associated with abnormalities within the axon, including clustering and swelling of organelles. The lesion becomes identifiable by light microscopy when the sprouting axonal extensions are myelinated and form clusters of small, closely packed fibers, which are well seen in semithin cross sections (*regeneration clusters*; Fig. 14-6). Teasing may also demonstrate myeli-

nated axonal sprouts with internodes that are regularly spaced but too short for the diameter of the fiber.

In the chronic or late stages of axonal degeneration, the principal morphologic features consist of a loss of myelinated axons and an increase in endoneurial connective tissue (Fig. 14-7). The presence of regenerating clusters is good presumptive evidence that the underlying pathologic process is due to axonal degeneration. Teased nerve fiber preparations may demonstrate the different stages of degeneration and regeneration, which indicates an ongoing process.

Primary Segmental Demyelination

Primary segmental demyelination is a process that takes place when the primary site of injury is on
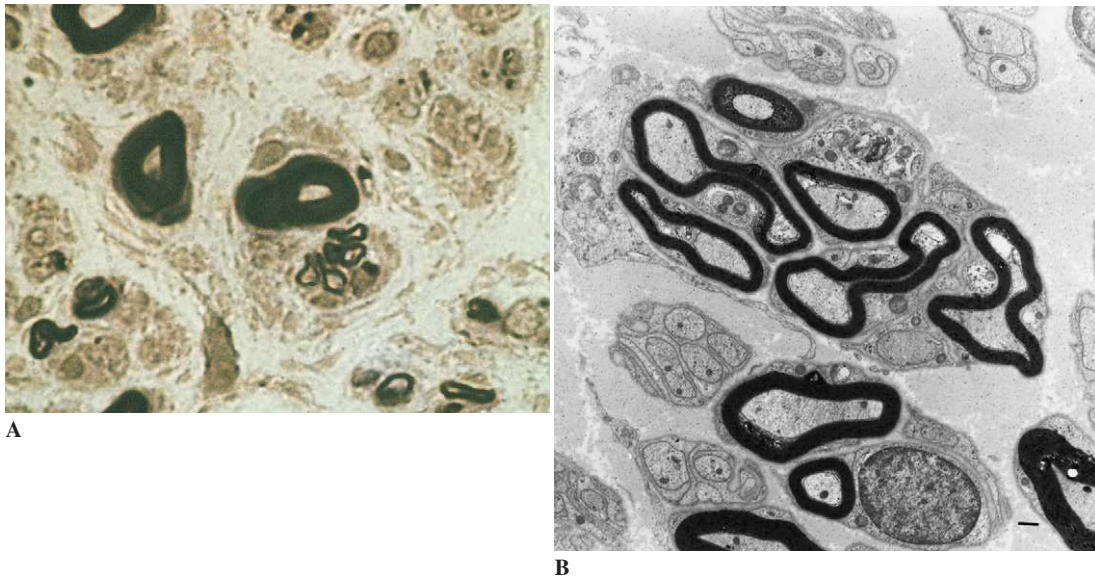
Figure 14-6. Bundles of small, closely packed fibers ("regeneration clusters"). **A,** Semithin cross-section. **B,** Electron microscopy.
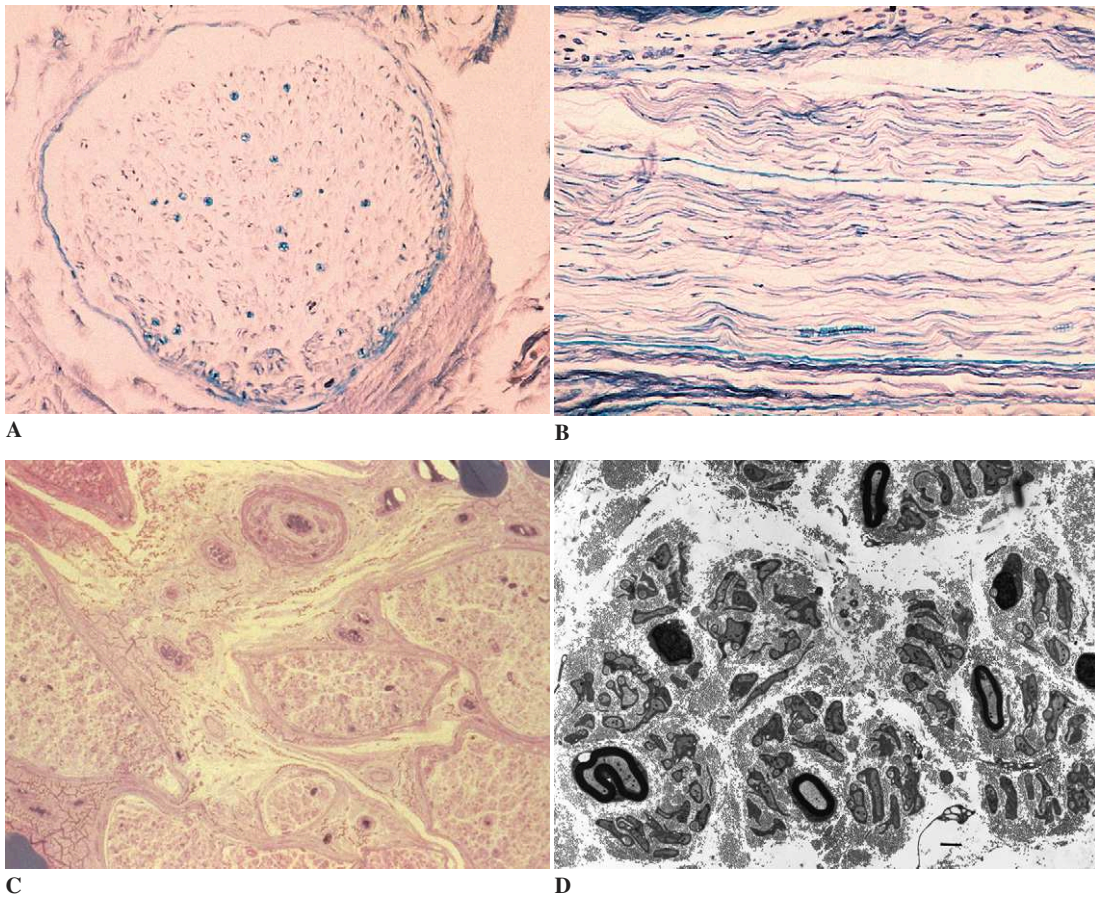
Figure 14-7. Severe chronic axonal neuropathy. Chronic wallerian degeneration on transverse (**A**) and longitudinal (**B**) sections (Bodian silver impregnation combined with Luxol fast blue) and on semithin section (**C**). **D**, Ultrastructural examination showing severe rarefaction of myelin fibers in a case of autosomal recessive CMT2.

the myelin sheath. When a motor axon is affected, because the axon remains intact, denervation muscle atrophy does not ensue.

Acute Segmental Demyelination and Remyelination

Primary involvement of the myelin sheaths or the Schwann cells causes segmental demyelination with relative sparing of the axon. This process involves the myelin internodes discontinuously along the length of the fiber, affecting some in sequence while sparing others. The process begins paranodally. Schwann cells and mononuclear phagocytes are responsible for phagocytosis of degenerated myelin fragments. Widening of the nodes of Ranvier and denuded stretches of demyelinated internodes affecting most fibers within a nerve causes conduction blocks and a reduction in the speed of peripheral nerve conduc-

tion. Myelin loss involving only very short segments of the fiber (i.e., stretches less than 15 μm long) may be followed by remyelination initiated by the Schwann cell responsible for the affected internode (if it has survived). When the extent of myelin internodal loss is greater than 15 μm, remyelination is achieved by selected, newly proliferated Schwann cells, which form small, intercalated internodes. In teased nerve preparations, the characteristic appearance of a fiber that has undergone remyelination after segmental demyelination consists of internodes of unequal size; the remyelinated internodes are shorter than normal and have a myelin sheath that is thinner than that of the adjoining, unaffected internodes (Fig. 14-8). In semithin sections and when the cross section traverses a remyelinated internode, these fibers appear to be hypomyelinated (i.e., the myelin sheaths are disproportionately thin in comparison to the axon diameter; Fig. 14-9A).
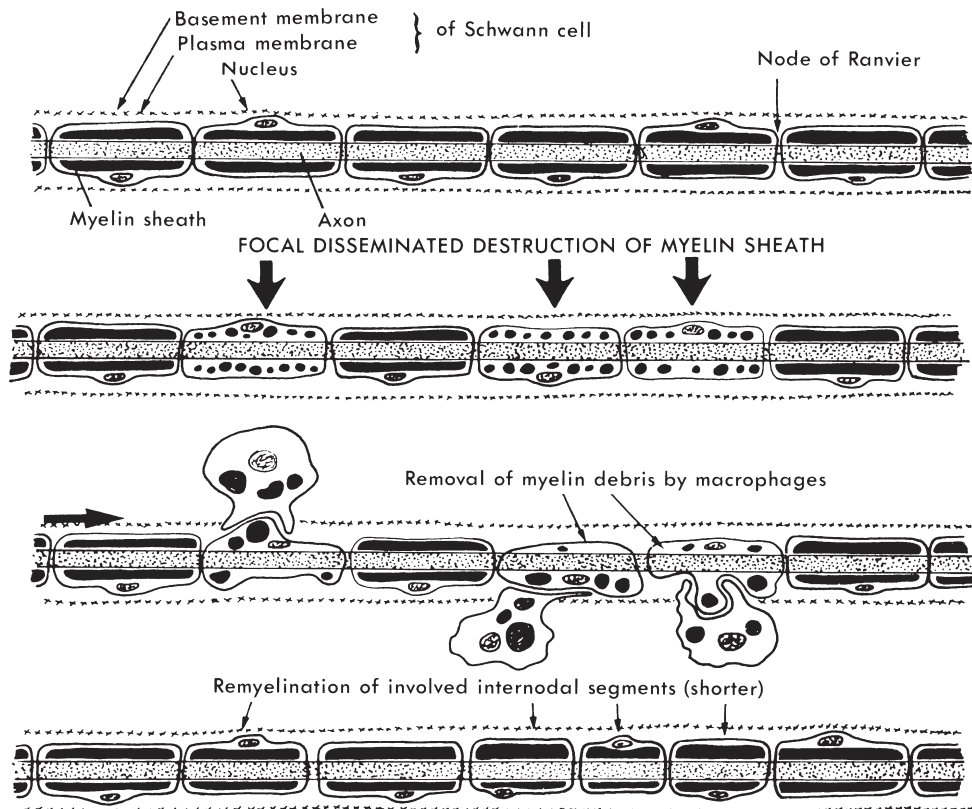
Figure 14-8. The main stages of segmental demyelination and remyelination of a myelinated peripheral nerve fiber. (Redrawn and modified from Bradley WG. Disorders of peripheral nerves. Oxford, Blackwell, 1974, p. 142.)
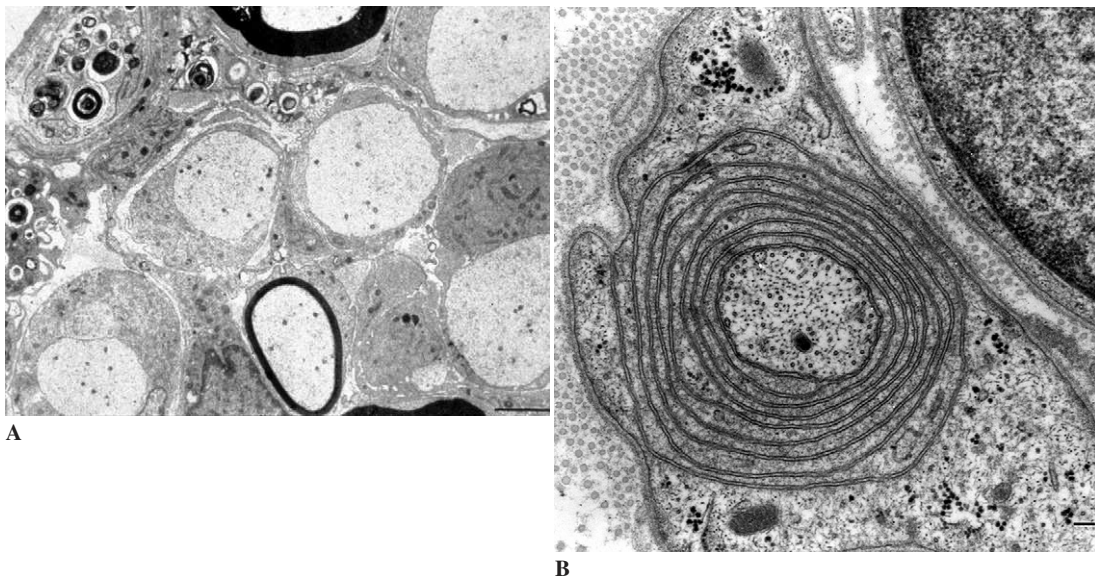
Figure 14-9. Ultrastructural appearance of abnormal myelination. **A,** At low magnification, numerous fibers are non-myelinated or hypomyelinated. **B,** Incomplete compaction of myelin.

Other Myelin Lesions

During myelination and with remyelination, one may observe incomplete compaction of the outermost myelin lamellae at the ultrastructural level (Fig. 14-9B). Here, the spacing between the lamellae is abnormally wide. In pathologic circumstances, this widening of myelin lamellae may stem from abnormalities and genetically determined mutations of certain proteins in compact myelin, such as myelin protein zero (P_0). This phenomenon may also be observed in neuropathies associated with monoclonal gammopathy (often of immunoglobulin M [IgM] type with anti-MAG [myelin-associated glycoprotein] or antiglycolipid activity).

Hypomyelination and hypermyelination—abnormally thin or abnormally thick myelin sheathing—is seen in genetically determined neuropathies. Hypermyelination is an excess of myelin lamellae relative to the diameter of the axon, often producing redundant, abnormally folded loops of myelin in various configurations. These lesions, referred to as *tomacula*, are characteristic of certain genetically determined entrapment peripheral neuropathies (e.g. hereditary neuropathy with liability to pressure palsies—HNPP—see later in this chapter). Tomacula are occasionally seen in conditions other than HNPP such as sporadic chronic neuropathy in childhood, neuropathy associated with alcoholism, and benign monoclonal gammopathy. In the majority of families, the disorder is inherited as an autosomal dominant trait and affected individuals have a deletion of a large portion of chromosome 17p11.2. In congenital hypomyelinating neuropathies, myelin is abnormally thin for the patient's age.

Schwannian Onion-Bulb Proliferation

Repeated episodes of segmental demyelination and remyelination culminate in *schwannian onion-bulb proliferation* (Fig. 14-10). This process is the result of proliferation of Schwann cells and of basement membrane deposits arranged concentrically around a relatively intact axon, which may be completely denuded of myelin or may have a thin myelin sheath relative to the diameter of the axon (Figs. 14-11A, B, and C). There is also an increase of collagen in the endoneurium, which often has a loose, sometimes metachromatic appearance. The early stages of onion-bulb formation may be demonstrable only by electron microscopy (Fig. 14-11D).
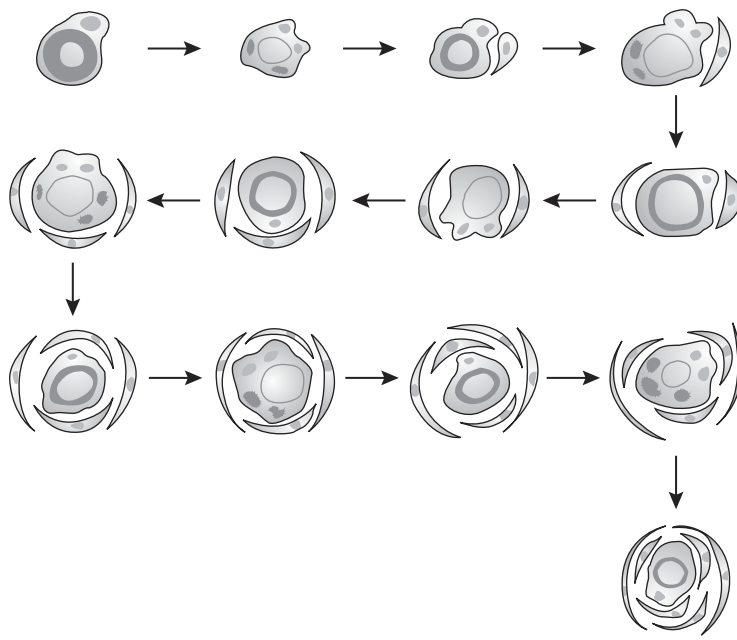
Figure 14-10. Process of formation of an onion bulb. (From Bradley WG. Disorders of peripheral nerves. Oxford, Blackwell, 1974, p. 144).
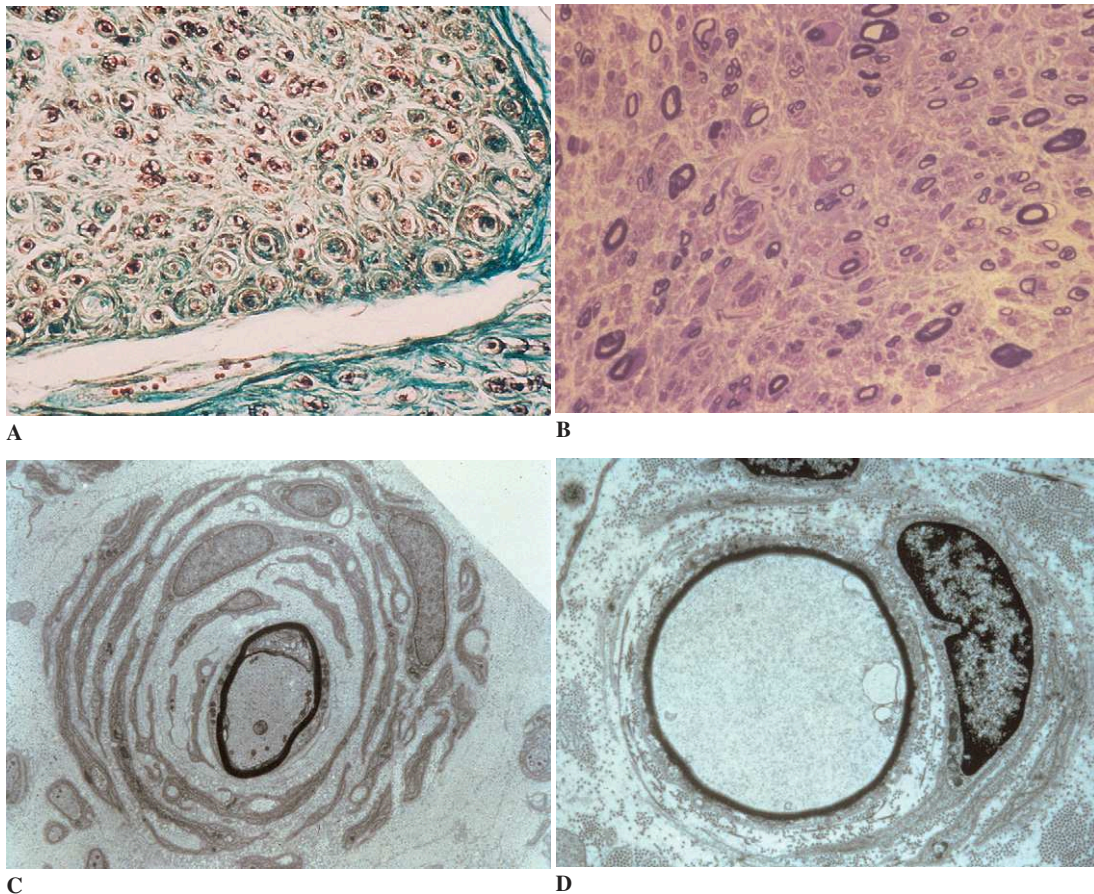
Figure 14-11. Onion bulbs. **A**, Microscopic appearance in hypertrophic neuropathy. **B**, Onion bulbs on semithin section. **C**, Ultrastructural appearance: proliferation of Schwann cells and of basement membrane concentrically around an intact axon. **D**, Early stage of onion-bulb with a few layers of concentrically arranged Schwann cell processes surrounding a thinly myelinated axon.

Peripheral Nerve Diseases

Inflammatory Polyneuropathies

Immunopathologic Disorders of Unknown Cause

Guillain-Barré Syndrome. *Guillain-Barré syndrome* (GBS; also termed *acute inflammatory demyelinating polyneuropathy*) is a polyneuropathy that can be the primary manifestation of a neurologic illness or may occur in the setting of systemic disorders, including infections (e.g., by cytomegalovirus, Epstein-Barr virus, mycoplasma, hepatitis viruses, HIV), vaccinations, surgery, pregnancy, immunosuppression, and cancer. Immune-mediated nerve damage is believed to be the cause of the peripheral nerve lesions, but the precise pathogenesis of the illness is incompletely understood.

Nerve biopsy is only rarely needed to establish the diagnosis of GBS, although in a few severe cases, in the presence of electrically silent nerves, histological examination of biopsy specimens can determine the type and extent of lesions. Biopsy may also identify the very rare, purely axonal forms of GBS (acute motor axonal neuropathy and acute motor and sensory axonal neuropathy) and assess the relative extent of the demyelinating and axonal lesions.

In the acute phases of the disease, lesions typically show disseminated foci of segmental demyelination that predominate in the perivenular regions and are associated with endoneurial edema with mononuclear cellular inflammatory infiltrates. The demyelination is induced by mononuclear cells. This characteristic feature is revealed by electron microscopy. Macrophages cross the basal lamina and displace the Schwann cell cytoplasm; their processes surround the myelin sheaths and insert themselves between the outer myelin lamellae (Fig. 14-12); and the myelin sheaths are thus progressively destroyed, so that macrophages are in contact with the axon. Perhaps independently of this process, myelin sheaths undergo vesicular degeneration. Axonal degeneration is also sometimes seen in teased nerve preparations.

Autopsy studies have shown that the inflammatory lesions tend to predominate in the proximal regions of the peripheral nervous system. For this
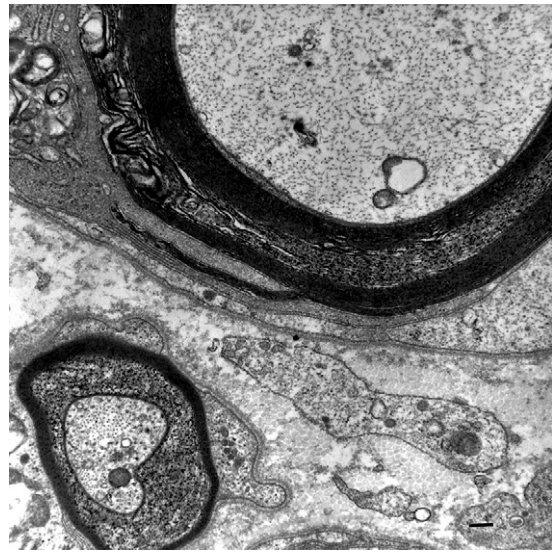
Figure 14-12. Guillain-Barré syndrome. A tongue-like macrophage extension inserts itself between the outer myelin lamellae.

reason, sural nerve biopsies may be less informative than desired. The infiltrate is composed of histiocytes and, especially of T lymphocytes in which the T4-to-T8 ratio is identical with that seen in the blood.

Subacute/Chronic Inflammatory Demyelinating Polyradiculoneuropathy. As with GBS, lesions occurring in *subacute/chronic inflammatory demyelinating polyradiculoneuropathy* (CIDP) vary considerable in degree of severity. The demyelination is segmental and irregular and tends to predominate in the nerve roots. Inflammatory infiltrates are usually minimal or absent.

Light-microscopic examination of epon-embedded nerve sections shows some loss of myelinated fibers. Some of the remaining axons are totally devoid of myelin, while others are surrounded by a thin sheath of myelin, probably indicative of remyelination. The process of segmental demyelination and remyelination is well shown with tease-fiber preparations. Ongoing demyelination is best seen on electron-microscopic examination. Onion-bulb formations—the characteristic concentric whorling of Schwann cell cytoplasm with skeins of basal membrane surrounding

normally myelinated or thinly myelinated axons—are striking, both in plastic sections and by electron microscopy. Regenerating clusters, indicative of concomitant axonal involvement and interpreted as secondary to chronicity, are also seen. There is often also significant involvement of unmyelinated fibers.

Sarcoidosis. *Sarcoidosis* is a T-cell–mediated inflammatory response to unknown antigenic stimulation. There is a wide range of clinical and pathological manifestations of the disease when it affects the peripheral nervous system.

Noncaseating granulomas with giant cells may be seen in the nerves, chiefly in the epineurium. Inflammatory infiltrates invade the endoneurium, following connective tissue septae and blood vessels; a necrotizing vasculitis occurs in some cases. Multifocal heterogeneous axonal loss is the rule. Demyelination is very rare.

Neuropathies Due to Infections

Leprosy. A wide variety of polyneuropathies and nerve lesions are found in all forms of *leprosy*.

Multibacillary (lepromatous) form. In lepromatous leprosy, there is nearly always widespread involvement of cutaneous sensory nerves even in patients with no clinical signs of neuropathy. Most cases show signs of modest inflammation with a widespread infiltration of the endoneurium, perineurium, and epineurium by numerous macrophages (Fig. 14-13A). The cytoplasm of these macrophages is filled with *Mycobacterium lepri* (*Hansen*) bacilli (Fig. 14-13B), sometimes collected in large aggregates (globi). The microorganisms are abundant, especially in the Schwann cell cytoplasm of unmyelinated cells. On ultrastructural examination, bacilli predominate in macrophages and Schwann cells but may also be seen in axons and in the cytoplasm of endothelial cells. Individual bacteria or groups of organisms are surrounded by a clear electronlucent halo (Fig. 14-13C). In some cases, there is a marked proliferation of neu-

trophils, as is the case in the paucibacillary form of the disease.

Paucibacillary (tuberculoid) form. In tuberculoid, leprosy bacilli are either completely absent at light-microscopic examination or are extremely rare. Granulomatous infiltrates predominate and consist of T lymphocytes with some B cells, plasma cells, Langhans giant cells, and histiocytes (Fig. 14-14). In some cases, necrosis may occur, producing abscesses. Marked distortion of the walls of capillaries and small vessels is also found. Axons, Schwann cells, and myelin are lost and there is fibrosis of the perineurium and endoneurium; the nerves adjacent to the foci of granulomatous inflammation undergo nodular thickenings and become abnormally firm.

Intermediate form. The nerve lesions in these patients are characterized by varying amounts of inflammatory infiltrates and leprosy bacilli. Organisms, often in a state of disintegration, can be demonstrated ultrastructurally in the cytoplasm of Schwann cells, as well as in macrophages.

AIDS. Several different types of peripheral nerve involvement have been described in patients with AIDS. Apart from toxic iatrogenic polyneuropathies, which are increasingly frequent, a number of polyneuropathies can be related to HIV infection, though none of these appear to be the direct result of viral attack. Nevertheless, in situ hybridization and immunocytochemical methods have detected viral antigen in mononuclear endoneurial cells.

Polyradiculoneuritides (GBS or CIDP) have been observed mainly in the early stages of the disease. These HIV-related inflammatory polyneuropathies are more frequently associated with pleocytosis in the CSF than with GBS or CIDP in the absence of HIV infection.

Distal, painful, sensory neuropathies have been described in the late stages of the disease and attributed to involvement of the dorsal root ganglia with apoptosis of neurons of unknown cause.

Necrotizing vasculitis identical to that seen in polyarteritis nodosa may be found in some cases of multiple mononeuropathy.
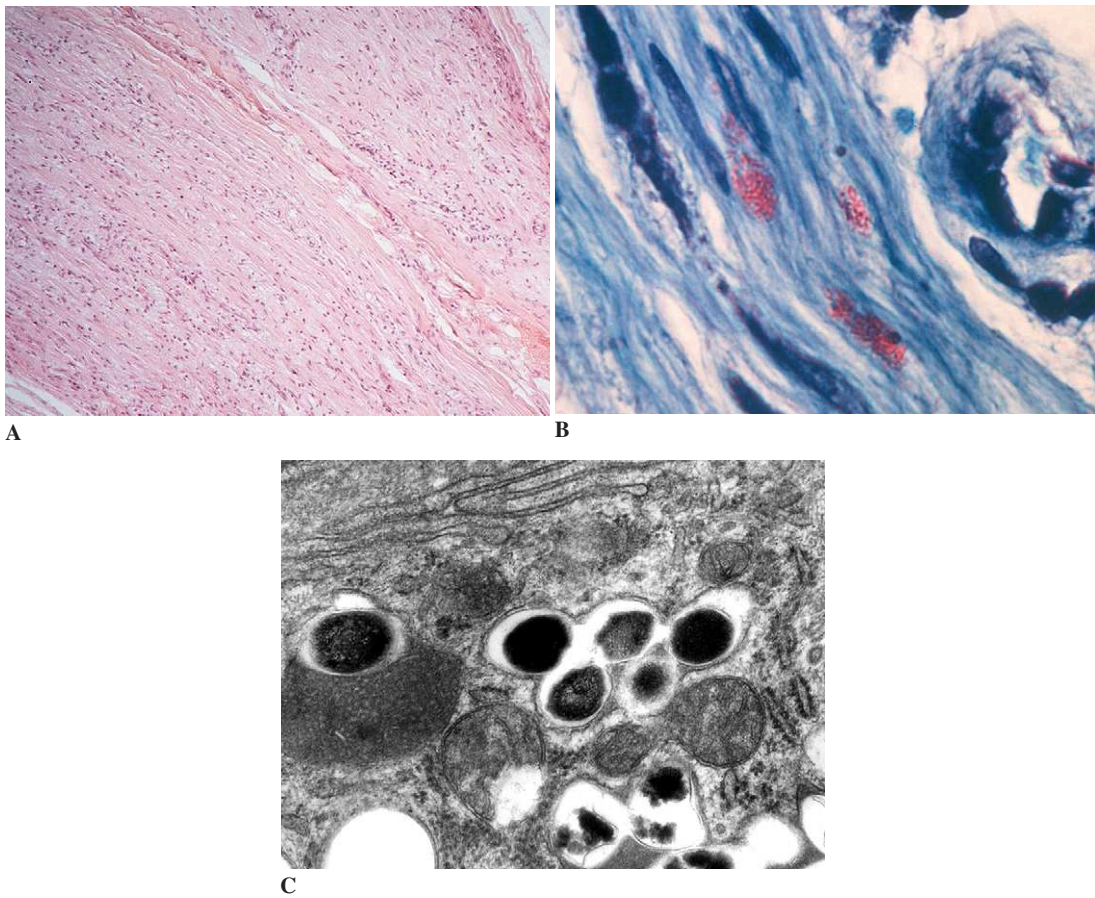
Figure 14-13. Multibacillary (lepromatous) leprosy. **A**, Infiltration of the endoneurium by numerous macrophages. **B**, The cytoplasm of these macrophages is filled with lepra bacilli well-demonstrated on Ziehl-Nielsen stain. **C**, Ultrastructural examination shows a group of bacteria surrounded by electronlucent halo.
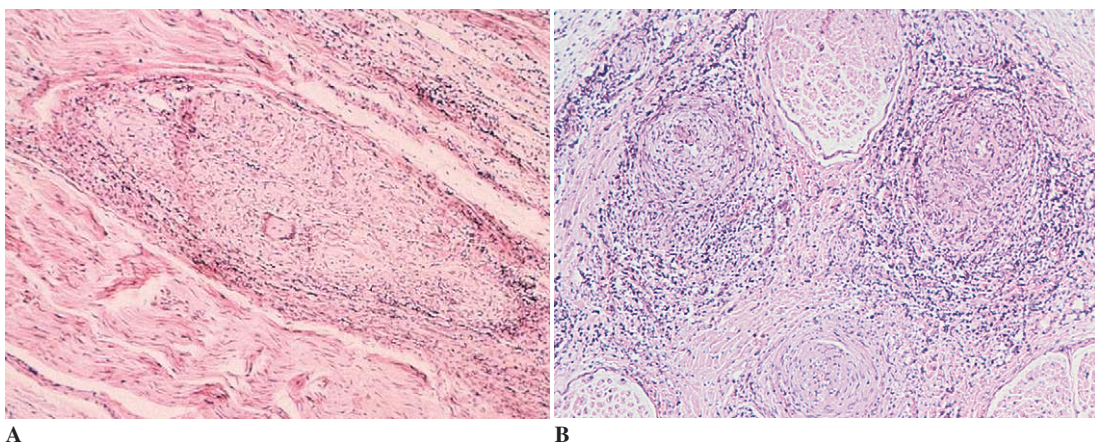
Figure 14-14. Paucibacillary (tuberculoid) leprosy. **A**, Granulomatous inflammatory infiltration of the endoneurium with Langhans-type giant cell. **B**, Note, on transverse section, inflammation and fibrosis of the perineurium and endoneurium.

A subset of HIV-infected patients develop persistent CD8 hyperlymphocytosis and a Sjögren-like syndrome (known as *diffuse infiltrative lymphocytosis syndrome*) associated with multivisceral CD8 T-cell infiltration. Nerve biopsy has shown marked angiocentric CD8 infiltrates without mural necrosis and abundant expression of HIV p24 protein in macrophages.

Some patients with AIDS develop polyneuropathy induced by cytomegalovirus. A particularly dreaded complication is a painful meningomyeloradiculitis that affects the lumbosacral regions. The characteristic viral inclusions are seen on light-microscopic examination, highlighted by immunocytochemistry; by electron microscopy, viral particles are found in Schwann cells, macrophages, endothelial cells, and fibroblasts.

Tick-Bite Meningoradiculoneuritis (Lyme Disease). Signs of acute axonal involvement are found in peripheral nerve biopsies in the meningoradiculoneuritic or secondary stage of *Lyme disease*. There may also be a prominent lymphocytic and plasma cell reaction around blood vessels in the endoneurium (Fig. 14-15), perineurium, and epineurium. The inflammatory-cell infiltrates have been found to be mainly of the B type. No demyelinating lesions or dissociation of myelin lamellae by inflammatory cells, as seen in GBS, have been seen in Lyme disease. Vessel walls are free of fibrinoid necrosis or inflammatory infil-

trates. *Borrelia burgdorferi* has yet to be detected in nerve lesions.

Vasculitic Neuropathies

The term *vasculitis* is used to describe a heterogeneous set of inflammatory diseases of blood vessels characterized by lesions consisting of a cellular inflammatory infiltrate permeating the wall of blood vessels. The presence of an associated fibrinoid necrosis of the wall defines the entity of *necrotizing vasculitis*. Vasculitis usually involves the blood vessels of the epineurium. Parenchymatous lesions secondary to vascular involvement usually take the shape of a predominantly axonal type of degeneration. Infarction of an entire peripheral nerve is rare. The usual appearance is that of rarefaction of nerve fibers, due to multifocal ischemic nerve fiber loss at multiple levels along the length of the fiber and secondary distal wallerian degeneration. The lesions are typically heterogeneous from one fascicle to the next and/or within the same fascicle (centrofascicular depopulation). The clinical picture most suggestive of a vasculitis-induced neuropathy is that of a multiple mononeuritis (sometimes also called *mononeuritis multiplex*); a polyneuropathy is also seen.

Two types of vasculitis are most commonly associated with nerve and/or muscle disease; these are described in the following sections.

Figure 14-15. Tick-bite neuropathy, perivascular mononuclear cell infiltrate.

Systemic Vasculitis Affecting Middle Caliber Arterioles. The classic lesions of *polyarteritis nodosa* (PAN) involve the arteries of small- and middle-caliber arterioles (70–200 μm). The vasculitis is characterized by medial fibrinoid necrosis, polymorphonuclear panarterial cellular inflammatory infiltrates (see Fig. 13-22), and vascular thrombosis. It is typical to find lesions of different ages. Hepatitis B surface antigen is often detectable.

The Churg-Strauss syndrome (allergic angiitis with granulomatosis) occurs in asthmatic patients who have received prolonged treatment with corticosteroids. The lesions are similar to those of PAN, but differ by the great abundance of eosinophils in the cellular infiltrates, by the frequency with which both veins and capillaries are also involved, and by

the presence of extravascular granulomas in some cases.

Patients with rheumatoid arthritis may have peripheral nerve lesions identical to those seen in PAN, except that they involve the microcirculation and the lesions are often especially rich in plasma cells. Less often, a necrotizing panarteritis can also occur in other collagen diseases (e.g., systemic lupus erythematosus, Sjögren syndrome).

A distinctive necrotizing or non-necrotizing granulomatous angiitis involving large- and middle-caliber blood vessels is seen in patients with Wegener granulomatosis and other granulomatous angiitides; in these conditions, characteristic lesions may be seen in muscle and nerve biopsies.

Microvasculitis Affecting Blood Vessels Less Than 70 μm in Diameter. Peripheral nerve microvasculitis that affects mainly the postcapillary venules but also the arterioles, capillaries, and small veins is characteristic of hypersensitivity angiitides. It may follow various antigenic exposures, (i.e., a drug, a heterologous protein [Zeek angiitis], an infectious agent like hepatitis B virus, or a neoplastic antigen). It may also supervene in the course of a systemic disease. The lesions are usually all of the same age. Two types are recognized, probably caused by diverse pathogenic mechanisms:

(1) In *leukocytoclastic vasculitis,* various degrees of vessel wall necrosis are associated with cellular infiltrates composed of more or less altered polymorphonuclear neutrophils. This lesion is typically seen in skin biopsies but may on occasion be demonstrable on neuromuscular biopsies.

(2) *Lymphocytic microvasculitis* is a non-necrotizing vasculitis characterized by infiltration of the vessel wall by mononuclear cells. Lesions of this type are not infrequent in peripheral nerve biopsies in a variety of clinical settings. The role of these vascular lesions in the pathogenesis of associated nerve lesions is uncertain. Nevertheless, the presence of sizable numbers of chronic inflammatory cells in the endoneurial or epineurial compartments, angiocentric or otherwise, must be regarded as pathological. This is the picture seen in a collagen vascular disease (e.g., rheumatoid arthritis,

systemic lupus erythematosus, Sjögren disease, or scleroderma) or with carcinoma, especially when muscle lesions of the same type are also present.

Neuropathies Associated with Hematologic Diseases and Neoplasms

Paraneoplastic Neuropathies

Patients with carcinoma or a lymphoma may develop polyneuropathy at the time of diagnosis, before, or months or even years later. In cases of paraneoplastic sensorimotor polyneuropathy, axonal lesions involving fibers of all kinds may be observed on nerve biopsy; sometimes, perivascular lymphocytic infiltrations are seen. Typical CIDP may also be observed.

The paraneoplastic sensory neuropathy (Denny-Brown) is characterized by extensive loss of neurons in the spinal sensory ganglia with secondary degeneration of their axons in the posterior spinal nerve roots and posterior columns of the spinal cord. Lymphocytic infiltrations indicating a prominent inflammatory component of the disorder have been found in peripheral nerves in some cases (see Chap. 9).

Neuropathies Associated with Malignant Lymphomas

Patients with *non-Hodgkin malignant lymphomas* (NHMLs) may develop a distal sensorimotor polyneuropathy. Malignant B-cell or T-cell proliferation may be demonstrated in nerve biopsies by immunolabeling of the infiltrates on paraffin or frozen sections using specific antibodies. The patchy distribution of the lesions in this condition should be borne in mind, underscoring the fact that a negative biopsy does not exclude the possibility of lymphomatous infiltrates in the nerve.

Widespread polyradiculoneuropathies have also been seen in cases of NHML and are designated as *neurolymphomatosis*. It is not yet clear whether the heavy, diffuse cell infiltration of the PNS in these diseases is due to dysimmune and inflammatory mechanisms or to lymphomatous proliferation, as few of these biopsies have been studied by immunocytochemistry.

Monoclonal Gammopathies

General Considerations

Involvement of peripheral nerve is frequent in patients with *monoclonal gammopathies*.

Patients with the osteosclerotic form of myeloma with monoclonal IgG are at greatly increased risk for the development of peripheral neuropathy in comparison to those with multiple (osteolytic) myeloma. In some studies, neuropathological examination of nerves in myeloma-associated neuropathy with light and electron microscopy has shown both distal axonal degeneration and demyelination and remyelination. Perivascular collections of lymphocytes (endoneurial and/or perineurial) have been observed.

Anti-MAG activity of a monoclonal IgM may require nerve biopsy for immunohistochemical confirmation. By direct immunofluorescence and immunoperoxidase techniques, labeled antibodies to the respective monoclonal IgM deposits may be identified along the myelin sheaths. It has been estimated that approximately 50% of all the patients with IgM monoclonal gammopathy and peripheral neuropathy have monoclonal IgM antibodies that bind to MAG. In some of the patients who do not have IgM that binds to MAG, the IgM reacts as an antibody to glycoproteins other than MAG or to glycolipids; in others, no PNS antigen toward which the IgM might be directed has been identified.

Nerve biopsy is ordinarily not needed in patients with IgM/anti-MAG syndrome or in those with the POEMS syndrome (also termed *Crow-Fukase syndrome*)—a complex of *p*eripheral neuropathy, *o*rganomegaly (hepatosplenomegaly, lymphadenopathy), *e*ndocrinopathy (which can be multiple), *M* protein (IgG), and *s*kin changes (thickening, hyperpigmentation, hypertrichosis).

Specific Changes in Patients with Monoclonal Gammopathy–Associated Polyneuropathy

Widening of Myelin Lamellae. This lesion consists of a 23-nm spacing between the separated leaflets of the intermediate line, which contains an electronlucent material. The ultrastructural features of the dense lines remain unchanged. These widened lamellae are associated with dilatation of the outer mesaxon and are mainly located on the outer part of the sheath (Fig. 14-16). In some fibers, the widenings are restricted to the outermost lamellae, and careful examination is required to notice it. Such features are indicative of a dysglobulinemia, and in a patient with polyneuropathy of unknown origin should prompt the search for a monoclonal peak by appropriate immunological investigations.

Widenings of myelin lamellae are observed in Waldenström macroglobulinemia and in monoclonal gammopathy of unknown significance (MGUS; Fig. 14-16A). In very few patients with IgA (Fig. 14-16B) or IgG monoclonal gammopathies and polyneuropathy, identical widenings of the myelin lamellae have been described. This abnormal widening has been seen on occasion, in the absence of a dysglobulinemic neuropathy.

Uncompacted Myelin Lamellae. Myelin lamellae can be found not to be normally flattened and joined together, but separated from each other (see Fig. 14-9B); they may also be seen as stacks of Schwann cell cytoplasm. This unusual alteration of myelin is encountered in the POEMS syndrome, though it is not specific to any one disease and has also been observed in cases of acute and chronic inflammatory demyelinating polyneuropathy.

Endoneurial Deposits. In a few cases, amyloid deposits have been observed in the course of polyneuropathy associated with either multiple myeloma or Waldenström macroglobulinemia. Finding filaments 7 nm to 8 nm in diameter in various planes on ultrastructural examination is particularly informative. In these instances, the amyloid is derived from kappa and lambda light chains.

The presence and specificity of immunoglobulin deposits can only be established by ultrastructural and immunopathological investigations. Minute deposits may not be detectable on light-microscopic examination using any of the current immunopathological techniques. The ultrastructural appearance of these deposits is quite variable; they may be observed as fingerprints, fibrils, granules, microtubules, or with no defined structure (Fig. 14-17). Such deposits are not specific of any monoclonal dysglobulinemia. They have been described in MGUS (IgM, IgGm, or IgA), myeloma, and Waldenström macroglobulinemia.
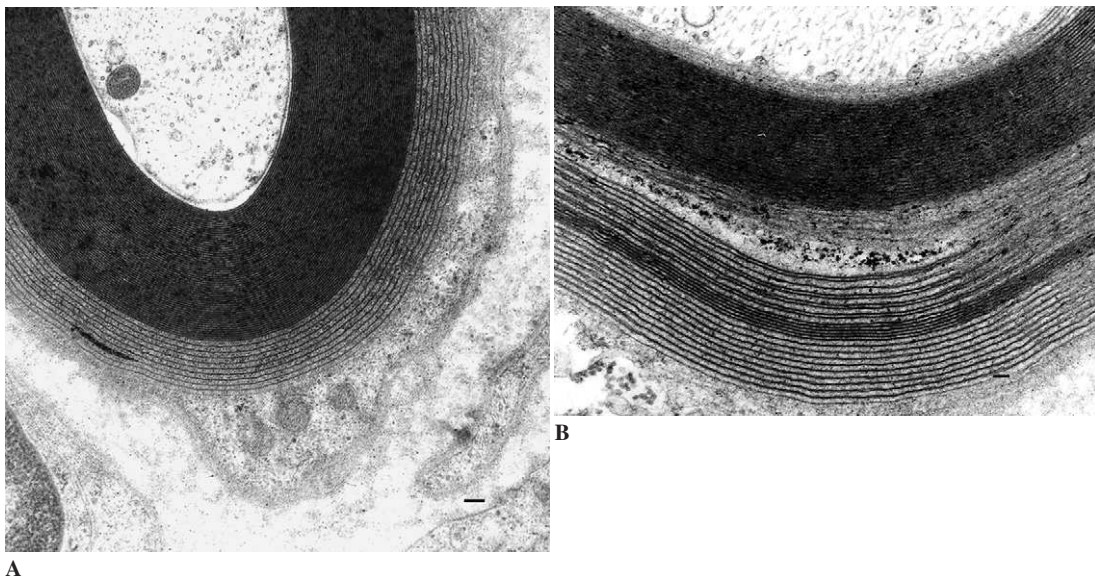
Figure 14-16. Widening of peripheral myelin lamellae. **A,** A case of monoclonal gammopathy of undetermined significance. **B,** A case of IgA monoclonal gammopathy.

Cryoglobulinemias

Cryoglobulins are circulating immunoglobulins that precipitate when cooled to 4° C and redissolve when warmed to body temperature (37° C). Cryoglobulinemias are classified into three distinct categories,

Figure 14-17. Myeloma neuropathy. Electron-dense endoneural deposit of IgG.

depending on the particular immunoglobulin or combination that is present. They can either be *isolated monoclonal*, as found in paraproteinemia (type 1—around 25% of cases); *mixed*, including a monoclonal component (type 2—around 25% of cases); or *polyclonal* (type 3—around 50% of cases). Cryoglobulins may occur idiopathically (in *essential cryoglobulinemia*) or secondary to some specific disease. They are said to be symptomatic in less than one third of cases.

The clinical manifestations of cryoglobulinemia include purpura, weakness, arthralgia or arthritis, fever, glomerulonephritis, Raynaud phenomenon, and neurologic involvement. The latter can present as peripheral neuropathy, vasculitic encephalopathy, or both.

The specific type of cryoglobulinemia needs to be determined. If it is type 1, antinerve activity (antiglycolipids and anti-MAG) should be sought; a few cases have been observed of IgM cryoglobulinemia (type 1) with anti-MAG activity. On both electrophysiological and histological grounds, the neuropathy appears to be demyelinating, just as neuropathies induced by an IgM paraproteinemia with anti-MAG activity.

If the cryoglobulinemia is of type 2 or 3, axonal lesions will be associated with widespread

vasculitis affecting medium and small epineurial vessels and, more rarely, endoneurial vessels. In such cases, the presence of axonal lesions in a nerve biopsy requires the careful examination of multiple sections through the nerve fragment, as deposits or vasculitis tend to be multifocal or nodular. The relationship between vasculitis and circulating cryoglobulins is not clear; globulin deposits in vessel walls have not been observed in such cases.

A necrotizing vasculitis is observed in 22% of patients who are infected with hepatitis C virus and are suffering from peripheral neuropathy associated with a mixed cryoglobulinemia.

Direct Invasion of Nerve by Neoplasm

Nerve invasion by neoplasm is demonstrated not infrequently in the course of autopsy studies of individuals with disseminated disease (Fig. 14-18). Patients may or may not have had clinical manifestations, but when they do, the polyneuropathy presents as a painful polyneuropathy, multiple mononeuropathy, or radiculopathy. Peripheral nerve biopsy is rarely necessary under these circumstances, but when appropriate, it may reveal the nature of the malignant tumor.

Metabolic and Nutritional Neuropathies

Functional and structural changes in peripheral nerve develop in response to various metabolic
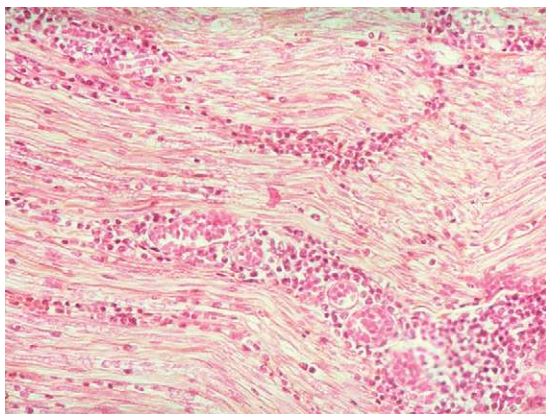
Figure 14-18. Invasion of nerve by neoplastic cells in a case of chronic lymphocytic leukemia.

alterations caused by either endogenous disorders or exogenous agents. The most common of these processes are discussed in the following sections.

Diabetes

The prevalence of peripheral neuropathy in patients with *diabetes mellitus* depends on the duration of the disease; up to 50% of diabetic patients develop peripheral neuropathy clinically after 25 years of diabetes, and nearly 100% have conduction abnormalities electrophysiologically.

Several distinct clinicopathologic patterns of diabetes-related peripheral nerve abnormalities have been recognized. The most common peripheral neuropathy is a symmetric neuropathy that involves distal sensory and motor nerves. Another manifestation of diabetic neuropathy is dysfunction of the autonomic nervous system; this affects 20% to 40% of diabetics, nearly always in association with a distal sensorimotor neuropathy. Some patients, especially elderly adults with a long history of diabetes, develop a peripheral neuropathy that manifests itself as a disorder of individual peripheral or cranial (oculomotor nerve) nerves or of several individual nerves in an asymmetric distribution (*multiple mononeuropathy* or *mononeuropathy multiplex*).

In patients with *distal symmetric sensorimotor neuropathy*, the predominant pathologic finding is an axonal neuropathy. As with other chronic axonal neuropathies, there is often some segmental demyelination. There is a relative loss of small myelinated fibers and of unmyelinated fibers, but large fibers are also affected. Endoneurial arterioles show thickening, hyalinization (Fig. 14-19A), intense periodic acid-Schiff positivity in their walls, and extensive reduplication of the basement membrane (Fig. 14-19B). Whether the lesions are due to ischemia or metabolic derangement is unclear. The pathogenesis of mononeuropathies in adult-onset diabetes is thought to involve vascular insufficiency that causes ischemic injury of the peripheral nerve.

Other Metabolic Neuropathies

As many as 65% of patients with renal failure have clinical evidence of peripheral neuropathy before dialysis (*uremic neuropathy*). This is typically a
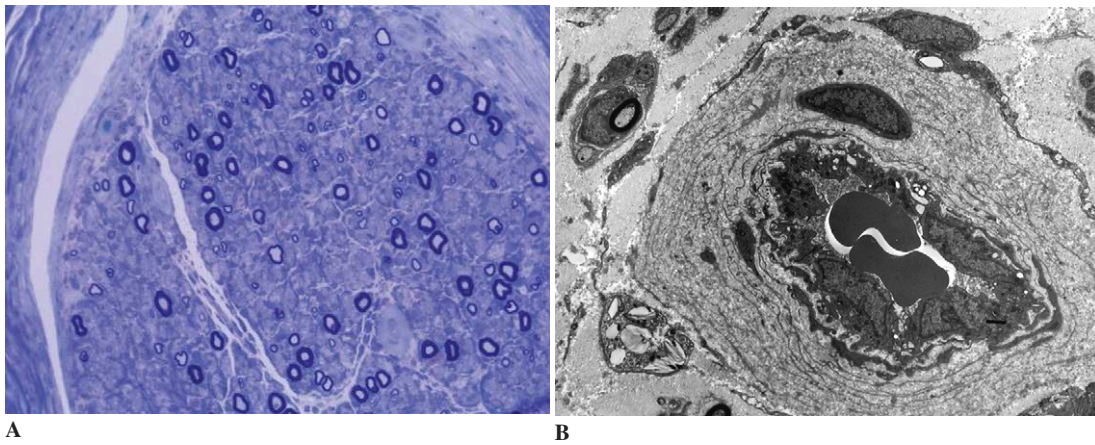
Figure 14-19. Diabetic neuropathy. **A**, Rarefaction of small myelinated fibers on semithin section. **B**, Microangiopathy with marked duplication of the basement membrane.

distal, symmetric neuropathy that may be asymptomatic or may be associated with muscle cramps, distal dysesthesias, and diminished deep-tendon reflexes. In these patients, axonal degeneration is the primary event, with degenerating fibers and fiber loss; occasionally there is secondary demyelination. Regeneration and recovery are common after dialysis.

Peripheral neuropathy can also develop in patients with chronic liver disease, chronic respiratory insufficiency, and thyroid dysfunction. Thiamine deficiency is characterized by axonal neuropathy, a clinical condition termed *neuropathic beriberi*. Axonal neuropathies also occur with deficiencies of vitamins B$_{12}$ (cobalamin) and B$_6$.

Toxic Neuropathies

Peripheral neuropathies can occur after exposure to industrial or environmental chemicals, biologic toxins, or therapeutic drugs. Prominent among the environmental chemicals are heavy metals, including lead and arsenic. In addition, many organic compounds are known to be neurotoxic.

Diphtheria Toxin

Peripheral nerve involvement results from the effects of the diphtheria exotoxin and begins with paresthesias and weakness; early loss of proprioception and vibratory sensation is common.

The earliest changes are seen in the sensory ganglia, where the incomplete blood-nerve barrier allows entry of the toxin. There is selective demyelination of axons that extends into adjacent anterior and posterior roots as well as into mixed sensorimotor nerves.

Accidental and Industrial Exposures

Among the heavy metals and the organophosphates, arsenic, thallium, alkyl mercury, and triorthocresylphosphate have been incriminated as causative agents of peripheral neuropathies.

Arsenic

The metallic element *arsenic* has been known for centuries to be highly toxic, and has frequently been used with homicidal or suicidal intent. Apart from encephalopathy (see Chap. 9), a mixed sensory and motor neuropathy is a well-known and often disabling sequela of both acute and chronic arsenical intoxication. The characteristic neuropathological feature of this neuropathy is a distal axonopathy, with secondary breakdown of myelin, in the most distal parts of the longest nerves. The largest fibers are more severely affected than the small ones.

Lead

In adults, *lead* poisoning has generally occurred as a result of occupational exposure; in children, it

usually ensues from ingestion of dust and fragments of the lead-containing paint that formerly was extensively used. Lead intoxication in adults most frequently results in the development of a peripheral neuropathy, while in children encephalopathy occurs more frequently (see Chap. 9). Despite the numerous clinical descriptions of lead-induced polyneuropathy, very little is known about its neuropathologic features in humans; the most commonly observed lesion is axonal degeneration rather than segmental demyelination.

Organophosphorus Compounds

Organophosphorus compounds have been extensively used in industry and agriculture as insecticides, modifiers of plastics, petroleum additives, lubricants, antioxidants, and flame retardants. A biologic effect of many of them is to phosphorylate acetycholinesterase (AChE), which leads to irreversible inhibition of function of this enzyme and, consequently, severe symptoms of excessive cholinergic activity within a day or less of acute exposure to the compound. Death from respiratory paralysis can occur during this acute phase of the intoxication; but if the patient survives this phase, recovery ensues and there are no delayed effects. Some organophosphorus compounds, however, also have the effect of inducing a delayed polyneuropathy that is not due to inhibition of AChE but correlates with inhibition of another esterase, neurotoxic esterase.

Hexane and Related Compounds

The six-carbon aliphatic compounds n-hexane and methyl-*n*-butyl ketone, used as industrial solvents, produce striking toxic effects on the PNS. The ensuing polyneuropathy, which involves the distal parts of both sensory and motor nerves, is characterized by focal swelling of axons to some two to three times their normal diameter (see Fig. 14-4B). The myelin sheaths surrounding these swollen axonal segments are thinned and there is retraction of myelin at the nodes of Ranvier, with some segmental demyelination. Electron microscopy of the axonal swellings demonstrates that they contain accumulations of 9–10-nm neurofilaments.

Complications of Therapeutic Agents

Drug-induced neuropathies with prevailing or notable segmental demyelination include those associated with treatment with amphophilic cations; these include perhexiline maleate, amiodarone, and chloroquine. The neuropathy caused by the first two drugs is a subacute polyneuropathy, whereas chloroquine causes a neuromyopathy. The diagnosis may be apparent from the study of semithin sections, based on the presence of numerous dense cytoplasmic inclusions in the Schwann cells and endothelial cells. It is confirmed by electron microscopy, which demonstrates polymorphic lysosomal inclusions, some of which have a paracrystalline or a plurilamellar reticular appearance (Fig. 14-20). The accumulated lipids include gangliosides and phospholipids.

Many commonly used drugs may cause polyneuropathy, predominately axonal. These include: vincristine, *cis*-platinum, the nitrofurantoin compounds, metronidazole, isoniazid, disulfiram, almitrine, and pyridoxine.

Traumatic Neuropathies

Peripheral nerves are commonly injured in the course of trauma. Lacerations result from cutting
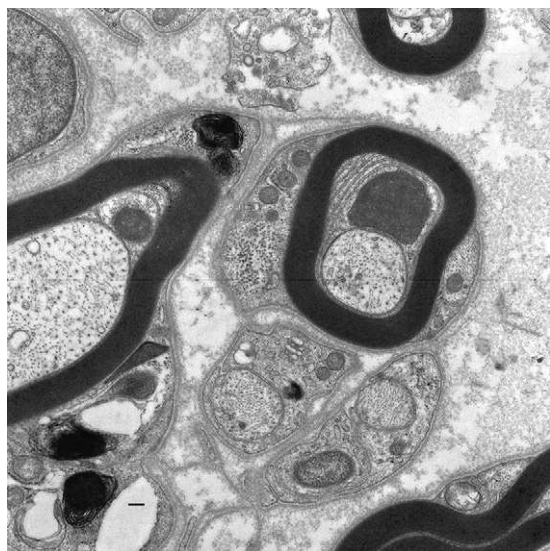
Figure 14-20. Amiodarone neuropathy. Multiple lipid inclusions in Schwann cells.

injuries and can complicate fractures when a sharp fragment of bone lacerates the nerve. Avulsions occur when tension is applied to a peripheral nerve, often as the result of a force applied to one of the limbs. The direct severance of nerves is associated with hemorrhage, and there is transection of the connective tissue planes. Regeneration of peripheral nerve axons does occur, albeit slowly. Regrowth may be complicated by discontinuity between the proximal and distal portions of the nerve sheath as well as by the misalignment of individual fascicles. Axons, even in the absence of correctly positioned distal segments, may continue to grow, resulting in a mass of tangled axonal processes known as a *traumatic neuroma* (also termed a *pseudoneuroma* or *amputation neuroma*). Within this mass, small bundles of axons appear randomly oriented; each, however, is surrounded by organized layers containing Schwann cells, fibroblasts, and perineurial cells.

Compression neuropathy (also termed *entrapment neuropathy*) occurs when a peripheral nerve is compressed, often within an anatomic compartment. *Carpal-tunnel syndrome* is the most common entrapment neuropathy and results from compression of the median nerve at the level of the wrist within the compartment delimited by the transverse carpal ligament. Additional compression neuropathies include involvement of the ulnar nerve at the level of the elbow, the peroneal nerve at the level of the knee, and the radial nerve in the upper arm as seen after sleeping with the arm improperly positioned ("Saturday night palsy"). Another form of compression neuropathy is found in the foot, affecting the interdigital nerve at intermetatarsal sites. This problem, which occurs more often in women than in men, leads to foot pain (*metatarsalgia*). The histologic findings of the lesion (Morton neuroma) include evidence of chronic compressive injury.

Hereditary Neuropathies

The *hereditary neuropathies* include a group of heterogeneous, typically progressive, and often disabling syndromes that affect peripheral nerves. Some are inherited diseases affecting peripheral nerves only and are classified based on whether they predominantly affect the motor and sensory modalities (hereditary motor and sensory neu-

ropathies) or the sensory and autonomic modalities (hereditary sensory and autonomic neuropathies). In addition to these hereditary neuropathies, which are limited to peripheral nerve disease and its complications, there are a number of inherited systemic diseases which have peripheral neuropathy as one of the symptoms. In general, these systemic hereditary diseases are classified on the basis of the metabolic fundamental problem, such as diseases of lipid metabolism.

Hereditary Motor and Sensory Neuropathies

Hereditary Motor and Sensory Neuropathy, Type I

The most common hereditary peripheral neuropathy is *Charcot-Marie-Tooth* (CMT) disease, hypertrophic form (also termed *hereditary motor and sensory neuropathy, type I*, or HMSN I), which usually presents in childhood or early adulthood. Patients may be asymptomatic, but when they seek medical attention it is often with symptoms of distal muscle weakness, atrophy of the calf (peroneal muscular atrophy), or secondary orthopedic problems of the foot (e.g., pes cavus). The disorder is usually autosomal dominant. Although it is slowly progressive, the disability of sensorimotor deficits and associated orthopedic problems such as pes cavus are usually limited in severity and a normal life span is typical.

The disease is genetically heterogeneous, and subgroups of genetically distinct forms have been identified as types IA, IB, and IC. In most pedigrees (known as HMSN IA or CMT1A), there is a duplication of a large region of chromosome 17p11.2-p12 resulting in "segmental trisomy" of the duplicated region. A separate genetic locus on chromosome 1 involves myelin protein zero, but produces an identical clinical and pathological phenotype (HMSN IB). A third set of pedigrees shows no linkage to either of these sites (type IC). In addition, some pedigrees have a genetic locus on the X chromosome, with mutations in the gene for the gap-junction protein connexin-32.

CMT1 is a demyelinating neuropathy, both by nerve conduction velocity studies and pathologically. Histologic examination shows the consequences of repetitive demyelination and

remyelination, with multiple onion bulbs (more pro-nounced in distal than in proximal nerves). The axon is often present in the center of the onion bulb, and the myelin sheath is usually thin or absent. In some biopsies, nearly every axon is surrounded by an onion bulb. The redundant layers of Schwann cell hyperplasia surrounding individual axons are asso-ciated with enlargement of individual peripheral nerves that may be individually palpable, which has led to the term *hypertrophic neuropathy*. In the lon-gitudinal plane, individual segments of the axon may show evidence of segmental demyelination. These findings support the view that the primary cause is disruption of the maintenance of myelin, and that these forms are primarily demyelinating neuropathies, both pathologically and electrophysi-ologically. In the later stages of the disease, axonal loss also occurs, involving the most distal portions of axons. Autopsy studies of affected individuals have shown degeneration of the posterior columns of the spinal cord.

Hereditary Motor and Sensory
Neuropathy, Type II

Hereditary motor and sensory neuropathy, type II (HMSN II) is a neuronal form of autosomal domi-nant Charcot-Marie-Tooth disease that presents with signs and symptoms similar to those of HMSN I, although nerve enlargement is not seen and the disease presents at a slightly later age. This form is less common than HMSN I and in some families the disease (designated CMT2A) is linked to chro-mosome 1p36.2. It is caused by a mutation in the KIF1B gene, which encodes a molecular motor of the kinesin superfamily. Additional, less common loci have been identified and involve mutations in the lamin A/C gene (2B1) and a locus on chromo-some 19q13.3 (2B2).

Nerve biopsy specimens show loss of myeli-nated axons as the predominant finding (Fig. 14-7D). Segmental demyelination of internodes is infrequent. These findings indicate that the site of primary cellular dysfunction is the axon or neuron.

Hereditary Motor and Sensory
Neuropathy, Type III

Hereditary motor and sensory neuropathy, type III (HMSN III; Dejerine-Sottas disease) is a slowly

progressive, autosomal recessive disorder that begins in early childhood, when it is manifested by delay in such developmental milestones as the acquisition of motor skills. Unlike in HMSN I and HMSN II, in which muscular atrophy is limited to the leg, both trunk and limb muscles are involved in Dejerine-Sottas disease. On physical examina-tion, enlarged peripheral nerves can be detected by inspection and palpation. The deep tendon reflexes are depressed or absent and nerve conduction velocity is slowed. Families have been identified with mutations of different genes, but in each pedi-gree, the mutation has involved genes involved in the formation and maintenance of myelin. The genes identified thus far in Dejerine-Sottas disease include peripheral myelin protein 22, myelin protein zero, and periaxin.

Morphologically, the size of individual periph-eral nerve fascicles is increased, often dramatically, with abundant onion bulb formation as well as seg-mental demyelination. There is usually evidence of axonal loss, and the remaining axons are often of diminished caliber. These findings are most severe in the distal portions of the peripheral nervous system; however, autopsy studies have shown that similar findings may be present in spinal roots.

Congenital hypomyelinating neuropathy is a term that has been used to designate a diffuse sym-metrical polyneuropathy that is evident at birth or becomes manifest shortly thereafter. It is charac-terized pathologically by nearly complete absence of myelin in the presence of normal axons and is closely related clinically to Dejerine-Sottas disease. Patients with this disease are sometimes referred to as having *congenital Dejerine-Sottas disease* (congenital HMSN III), and sometimes as having *congenital hypomyelinating neuropathy* (CMT 4E). The mutated gene is located on chro-mosome 10q21.1-q22., and has been identified as the early growth response 2 gene (*EGR2*).

Tomaculous Neuropathy

Tomaculous neuropathy (also termed *hereditary neuropathy with liability to pressure palsies*, HNPP) is transmitted as an autosomal dominant trait and is characterized by recurrent attacks of mononeuropathy (single or multiple) that are char-acteristically brought on by pressure (such as that affecting the ulnar nerve when the elbow rests on

a table for an extended period), traction, or stretching. There is generally some recovery, which may require weeks or months; with repeated attacks, some permanent sensory or motor dysfunction may remain.

Examination of peripheral nerve biopsies shows either focal enlargements of the myelin sheath, either involving entire internodal segments or confined to the paranodal regions (Figs. 14-21A and B). These enlargements create a sausage-like appearance in the longitudinal plane referred to as *tomacula* (from the Latin *tomaculum*, "sausage"), and the disorder has been known as *tomaculous neuropathy*. Morphometric examinations have regularly shown decreased numbers of large, myelinated fibers with relatively normal numbers of smaller myelinated fibers and scattered, small, onion-bulb structures.

The tomaculous swellings, when examined by electron microscopy, have been shown to be made up of greatly thickened and abnormally folded myelin sheaths (Fig. 14-21C); axons enclosed by these abnormal myelin structures often appear to be contracted.

Neuropathy Associated with Hereditary Ataxia

A neuropathy with clinicopathological features closely resembling those in HMSN I and II is regularly found in the most frequently encountered form of genetically determined progressive ataxia, Friedreich ataxia (see Chap. 8).

Giant Axonal Neuropathy

Giant axonal neuropathy is characterized by greatly enlarged axons in the CNS and PNS and a gradually progressive sensorimotor neuropathy that begins in early childhood. A pattern of autosomal recessive inheritance occurs in most affected pedigrees. The disease becomes manifest generally as an awkwardness of gait with a tendency to fall. Increasing motor instability ensues and is associated with sensory loss that affects mainly deep sensibility and proprioception (with less involvement of sensations for light touch, pain, and temperature). The disease progresses gradually but relentlessly, and clinical manifestations of dysfunction of the CNS become evident in the form of nystagmus, visual impairment with optic atrophy, dysarthria, and intellectual deterioration. Most affected individuals have an unusual appearance of the hair, variously described as frizzy or kinky.

The distinctive neuropathological feature of this disorder is greatly enlarged axons (20–50 μm in diameter; see Fig. 14-4A). Overlying the enlarged portion of the axon, the myelin sheath is either greatly thinned or absent, and electron microscopy
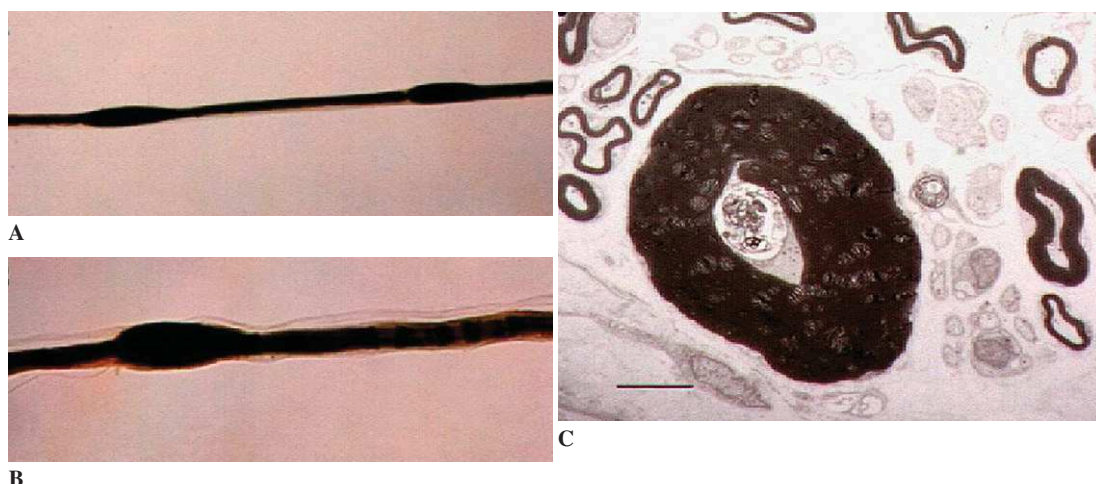
Figure 14-21. Tomaculous neuropathy. **A** and **B**, Scattered focal swellings of individual myelin sheaths with a sausage-like appearance in the longitudinal plane, seen on teasing preparations. **C**, By electron microscopy, the swellings are seen to be made up of greatly thickened and abnormally folded myelin sheaths.

shows that the enlarged portions of the axons are filled with masses of densely packed intermediate filaments 9 nm in diameter, frequently arranged in whorl-like patterns. In addition to the changes in the peripheral nerves, there are striking abnormalities in the CNS, including enlarged axons (spheroids) and amorphous masses of glial fibrillary protein in the form of Rosenthal fibers. Aggregates of intermediate filaments also occur in fibroblasts and glia, and the accumulation of aggregates of intermediate filaments occurs in cultures of fibroblasts from patients. The gene responsible for giant axonal neuropathy, *GAN*, is located on chromosome 16q24.1 and encodes gigaxonin, a cytoskeletal-associated protein.

Infantile Neuroaxonal Dystrophy

Infantile neuroaxonal dystrophy is an autosomal recessive disorder characterized by a relentlessly progressive global deterioration of cerebral function that begins during early infancy after a normal neonatal period and leads to death in childhood. Weakness is profound and associated with hypotonia and muscular wasting, and there is an exaggeration of muscle-stretch reflexes. The outstanding neuropathological finding is the presence of enlarged axons (spheroids) at all levels of the CNS (see Chap. 10), and frequently on nerve biopsies, although they are less frequent than in CNS.

Hereditary Sensory and Autonomic Neuropathies

The *hereditary sensory and autonomic neuropathies* mainly affect sensation and are accompanied by varying degrees of autonomic nervous system dysfunction. The most widely accepted classification of these hereditary neuropathies combines them in an overall category of hereditary sensory and autonomic neuropathies (HSAN) and divides this into several subtypes based on inheritance and the clinical manifestations: *HSAN type I* (predominantly sensory; autosomal dominant), *HSAN type II* (predominantly sensory; autosomal recessive), and *HSAN type III* (predominantly autonomic; autosomal recessive). Other forms, including various types of congenital indifference to pain, have also been described.

HSAN Type I

HSAN I (also termed *familial ulceromutilating acropathy of Thevenard*, *dominant*) is characterized by dominant inheritance and very slow progression. Painless injuries to the feet, with ulcerations of the skin and damage to joints, are typical. Dysfunction of the autonomic nervous system is not prominent. Neuropathologic examination has shown extensive loss of neurons in spinal sensory ganglia, with secondary axonal loss in the posterior roots and posterior columns of the spinal cord and preservation of motor neurons and anterior roots. There is also severe loss of myelinated fibers in peripheral nerve fibers of all sizes, with increased collagen.

The relevant gene is the *SPTLC1* gene, which is located on chromosome 9q22 and encodes serine palmitoyltransferase, an important enzyme in sphingolipid synthesis. This enzyme catalyzes the formation of 3-oxoshanganine from serine and palmitoyl-CoA, an initial step in the formation of sphingolipids.

HSAN Type II

Autosomal recessive inheritance is the main distinguishing feature of HSAN II, and the predominant clinical feature is impairment of pain perception (insensitivity to pain) resulting in painless injuries. Nerve biopsy studies show widespread loss of myelinated fibers of all sizes; unmyelinated fibers are only slightly decreased. A striking vacuolation of the cytoplasm of endoneurial fibroblasts has also been reported.

HSAN Type III

HSAN III (also termed *familial dysautonomia* or *Riley-Day syndrome*) is characterized by severe autonomic nervous system dysfunction present at birth, as evidenced by absent lacrimation and abnormal reactions to anxiety (lability of blood pressure, salivation, excessive sweating, and erythematous blotching of the skin). The syndrome is inherited as an autosomal recessive trait and tends to occur in children of Ashkenazi-Jewish parentage. Integral components of the syndrome include early-appearing lack of pain perception and lack of fungiform papillae in the tongue. Sural-nerve biopsy

shows a great decrease in the numbers of unmyelinated fibers and of large and small myelinated fibers. Teased fibers show some with shortening of the internodal length, but no segmental demyelination or remyelination and no onion-bulb structures. Autopsy studies have reported shrinkage and neuronal loss in dorsal root ganglia, sympathetic ganglia, and the intermediolateral cell column of the spinal cord, suggesting that the primary abnormality is in neurons of the autonomic and spinal sensory ganglia and that the changes seen in peripheral nerve specimens are secondary to the axonal degeneration that results from neuronal death.

The gene for familial dysautonomia is located on chromosome 9q31 and encodes an inhibitor of kappa light polypeptide gene enhancer in B cells, a kinase-complex associated protein known as IKBKAP. The role of this gene product in the nervous system is not fully understood. More than 99.5% of the alleles in families with the mutation share a common ancestral haplotype, supporting the view that the ethnic basis of the disease is due to a founder effect.

Other Types of HSAN

Some cases of hereditary sensory neuropathy, with or without autonomic dysfunction, cannot readily be classified under any of the previously mentioned categories. They differ from one another in the details of their clinical expression as well as in their pattern of neuropathological changes.

Amyloid Neuropathies

Familial Amyloid Polyneuropathies

Peripheral neuropathy may occur due to deposition of amyloid in peripheral nerve. There are two major categories of amyloid neuropathies: familial amyloid polyneuropathies and sporadic amyloidosis (see also discussion of amyloid in Chap. 4).

The familial amyloid neuropathies are characterized predominantly by the deposition of amyloid within the peripheral nervous system. Most kindreds exhibit mutations of the transthyretin (TTR) gene, located on chromosome 18q11.2-q12.1. More than 20 forms of mutant TTR have been identified. Rarer forms of amyloid neuropathies are characterized by the deposition of different amyloid-forming proteins, namely, a variant of apolipoprotein A1 in familial amyloid polyneuropathy (Type III), and a mutant form of gelsolin in the Finnish form of familial amyloid polyneuropathy (Type IV). Clinically, these are sensorimotor and autonomic polyneuropathies with predominant deficiency of heat and pain sensation.

In all cases, the lesions are acellular deposits situated in the endoneurium and in the blood vessel walls. They are stained by Congo red (Fig. 14-22), are birefringent by polarized light, and are composed of characteristic, nonbranching 7-nm fibrils visible by electron microscopy. Parenchymatous involvement is essentially axonal and typically affects mainly small myelinated and unmyelinated fibers. The amyloid fibrils are composed of transthyretin (TTR), a serum protein in the prealbumin electrophoretic range that has a role in transporting thyroxine and retinol. The presence of TTR can be demonstrated in tissue by immunoperoxidase methods.

Acquired Amyloid Neuropathies

Acquired amyloidosis may occur in association with immunocyte (B-cell) dyscrasias ("primary amyloidosis") or as reactive systemic amyloidosis ("secondary amyloidosis"). The amyloid in the immunocyte dyscrasias is of AL type (amyloid light chain amyloid, i.e., composed of fragments of immunoglobulin light chains, most often lambda chains), while the amyloid deposits in reactive
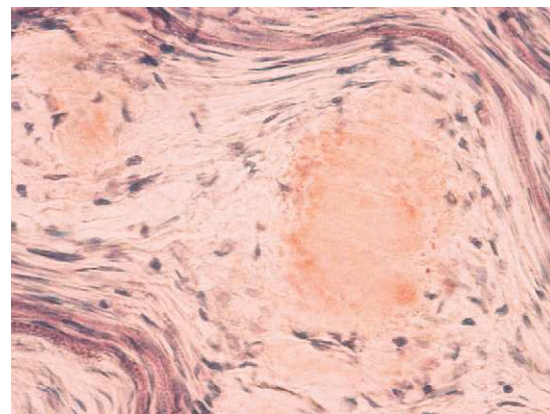
Figure 14-22. Interstitial amyloid deposit in peripheral nerve (Congo red).

systemic amyloidosis is of AA type (amyloid-associated amyloid, i.e., composed of a fragment of the serum protein nonimmunoglobulin). The amyloid deposits, whether familial TTR-derived, AL, or AA type, are often discrete and may be demonstrated by immunocytochemical techniques. They must be distinguished from abnormal globulin deposits that do not have the features of amyloid. AL amyloidosis may infiltrate the skeletal musculature and the transverse carpal ligament (flexor retinaculum), causing carpal tunnel syndrome.

Porphyria

Polyneuropathy of acute or subacute evolution is characteristic of three varieties of dominantly inherited disorders of heme metabolism, namely, *acute intermittent porphyria*, *variegate porphyria*, and *hereditary coproporphyria*. The polyneuropathy may be asymmetrical and tends to involve motor fibers more than sensory fibers. The neurologic aspects are the same in all of the three varieties of porphyria in which they are encountered.

The primary axonal neuropathy associated with all forms of the disease with peripheral neuropathy has a distribution that suggests a dying-back process; an impression confirmed by electrophysiologic observations. Unmyelinated axons are

Table 14-1. Neuropathies in Disorders of Lipid Metabolism

Lipid Disorders with Predominant Involvement of the PNS
Refsum disease
Bassen-Kornzweig disease (abetalipoproteinemia)
Tangier disease
Lipid Disorders with Predominant Involvement of the CNS
Metachromatic leukodystrophy
Adrenoleukodystrophy
Krabbe disease
Nieman-Pick disease
Neuronal ceroid lipofuscinosis
Lipid Disorders with Predominant Systemic Involvement
Fabry disease
Cerebrotendinous xanthomatosis

affected as well as large and small myelinated fibers. In severe cases of long standing, secondary changes in the spinal cord and sensory ganglia (e.g., central chromatolysis and ascending degeneration in the posterior columns in the presence of affected posterior roots) are regularly encountered, as is atrophy of denervated musculature. The relationship of the disorder of heme metabolism and of the porphyrin accumulations to the development of the lesions in the nervous system is still unknown.

Figure 14-23. Adrenomyeloneuropathy. Cleft-like inclusions in the cytoplasm of a Schwann cell. (Courtesy of Dr. J. M. Powers.)
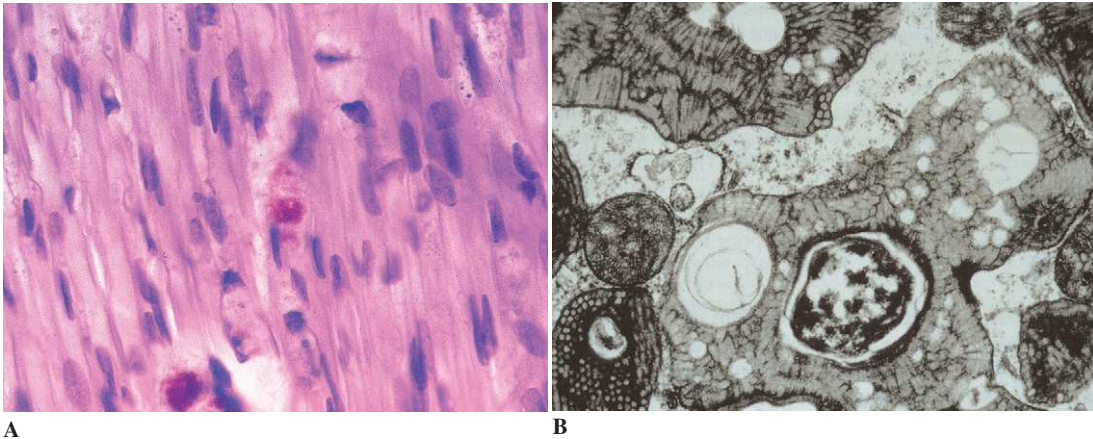
Figure 14-24. Metachromatic leukodystrophy. **A**, Presence of metachromatic material (appearing red on toluidine blue stain) in macrophages in the peripheral nerve. **B**, By electron microscopy this material has a characteristic "tuffstone" appearance.

Disorders of Lipid Metabolism

A number of the systemic disorders of *lipid metabolism* may present with prominent involvement of the nervous system (see Chap. 10). In some of these diseases (e.g., Refsum disease, Bassen-Kornzweig syndrome, and Tangier disease), peripheral nerve involvement may be the presenting sign. In other conditions, particularly the leukodystrophies (metachromatic leukodystrophy, adrenoleukodystrophy, or Krabbe disease) or in Nieman-Pick disease, involvement of the CNS is usually the predominant feature. Other conditions, such as Fabry disease or cerebrotendinous xanthomatosis, present as systemic disorders in which the CNS and PNS may be involved among many other organs. In many cases, biopsy of the polyneuropathy may show diagnostic deposits or intracellular inclusions of abnormal lipid (Table 14-1; Figs. 14-23 and 14-24). The neuropathology of these diseases including the changes in peripheral nerves, are described in detail in Chapter 10.

Chapter 15
Diseases of the Pituitary Gland

Vânia Nosé and E. Tessa Hedley-Whyte

General Considerations

The pituitary is the endocrine gland that controls the release or inhibition of hormones from the hypothalamus and the peripheral endocrine glands. It has two major components, anterior and posterior.

The *anterior* pituitary is composed of epithelial cells with secretory granules containing trophic hormones. It is controlled by hypothalamic hormones that stimulate or inhibit the release of the anterior pituitary hormones (Table 15-1). The *posterior* pituitary contains axons arising from nerve cells in the supraoptic and paraventricular nuclei of the hypothalamus, and glial cells.

The first step in approaching pituitary pathology is to appreciate the close association of clinical and laboratory information with histopathologic findings. Routine histology and immunohistochemistry, hormonal immunohistochemistry, and electron microscopy usually enable one to classify the normal pituitary cells and their neoplasms and to identify tumors not composed primarily of adenohypophyseal cells. Molecular pathology techniques, such as molecular genetics, have characterized transcription factors and genes important in the development of the anterior pituitary.

The Normal Pituitary

The *adenohypophysis* and the *neurohypophysis* form the human pituitary gland. The adeno-hypophysis develops from an evagination of the primitive stomateal ectoderm, Rathke pouch. The neurohypophysis originates from the infundibular process of the diencephalon. The pituitary can be recognized by the third month of fetal development, and the hormone-producing cells of the anterior gland can be recognized as early as the fifth week of gestation (Table 15-2). The adult gland weighs 400 mg to 600 mg and is located in the sella turcica.

The anterior pituitary constitutes approximately 70% to 80% of the pituitary gland and is composed of the pars distalis, pars intermedia, and pars tuberalis. It can also be roughly subdivided into a central mucoid wedge and lateral acidophilic wings (Fig. 15-1). The "intermediate lobe," vestigial in humans, is composed of gland-like spaces (which are remnants of Rathke cleft) intermixed with adrenocorticotropic hormone (ACTH)–secreting cells. The anterior pituitary cells are arranged in cords surrounded by a rich network of capillaries. The anterior pituitary cells are characterized by their tinctorial properties in H and E stained preparations, by their immunoreactions (indicating function), and by their ultrastructural features. The distribution of the various cell types is uneven (see Table 15-2). Routine H and E staining reveals that the acidophil cells are concentrated in the lateral wings, basophilic cells are concentrated in the mucoid center, and chromophobe cells are diffusely spread in a horizontal section across the pituitary (Fig. 15-2A). The sustentacular-like cells in the

Table 15-1. Major Hypothalamic Hormones and Their Effect on Anterior Pituitary Hormones

Hypothalamic Stimulatory Hormones	Affected Pituitary Hormones
Corticotropin-releasing hormone (CRH): released from paraventricular neurons, supraoptic and arcuate nuclei, and limbic system	Adrenocorticotropic hormone (ACTH): basophilic/corticotrophs. ACTH is product of propiomelanocortin (POMC) gene
	Melanocyte-stimulating hormone (MSH): alternate product of POMC gene
	Endorphins: also products of POMC genes
Growth hormone–releasing hormone (GHRH)	Growth hormone (GH): acidophilic/somatotrophs
Gonadotropin-releasing hormone (GnRH): mostly released from preoptic nucleus	Luteinizing hormone (LH) and follicle-stimulating hormone (FSH): gonadotrophs
Thyrotropin-releasing hormone (TRH): released from anterior hypothalamic area	Thyroid-stimulating hormone: thyrotropes
Prolactin-releasing factors: including serotonin, acetylcholine, opiates, and estrogens	Prolactin (PRL): lactotrophs
Hypothalamic Inhibitory Hormones	
Somatostatin (GIH)	Inhibits the release of growth hormone (GH)
Prolactin-inhibiting factors (PIF): including dopamine	Inhibits the release of prolactin (PRL)

adenohypophysis (stellate cells) are distinct from the epithelial cells and stain for S-100 protein and glial fibrillary acidic protein.

The anterior pituitary produces and releases six hormones which are under the control of different stimulatory and inhibitory hypothalamic releasing factors (see Table 15-1).

The posterior pituitary constitutes 20% to 30% percent of the gland and is composed of the infundibulum or median eminence, the infundibular stem or pituitary stalk and the posterior lobe of the pituitary gland (neurohypophysis). The neurohypophysis is part of a neurosecretory unit and stores oxytocin and vasopressin hormones associated with the carrier protein neurophysin. The neurohypophysis is composed of nerve fibers, axon terminals, and pituicytes, the glial cells of the posterior lobe.

Lesions of the Pituitary Gland

Lesions of the pituitary consist of a wide variety of distinct conditions (Table 15-3). The signs and symptoms of pituitary lesions are due to hormonal hyperfunction, hormonal hypofunction, or local mass effects, including compression of surrounding structures.

Hyperfunction is due to excess secretion of trophic hormones. The cause is most commonly a functional adenoma, less frequently hyperplasia, and rarely a pituitary carcinoma. Nonpituitary tumors and hypothalamic diseases are rare causes of hyperpituitarism. The syndromes match the hormone produced by the lesion; the most common are gigantism (acromegaly), due to the overproduction of growth hormone; Cushing disease (pituitary-dependent hypercortisolism) due to the

Table 15-2. Cells of the Anterior Pituitary: Cell Types in Fetal Development and Cell Percentages and Locations in Adults

Cell Types	Weeks of Gestation	Cell % (Adults)	Location
Corticotroph-ACTH	5	10–20	Mucoid edge
Somatotroph-GH	8	40–50	Lateral wings
Alpha-subunit	9	Variable	Diffuse throughout
Thyrotroph-TSH	12	5	Anterior mucoid edge
Gonadotroph-FSH/LH	12	10	Diffuse throughout
Lactotroph-PRL	12	10–30	Lateral wings
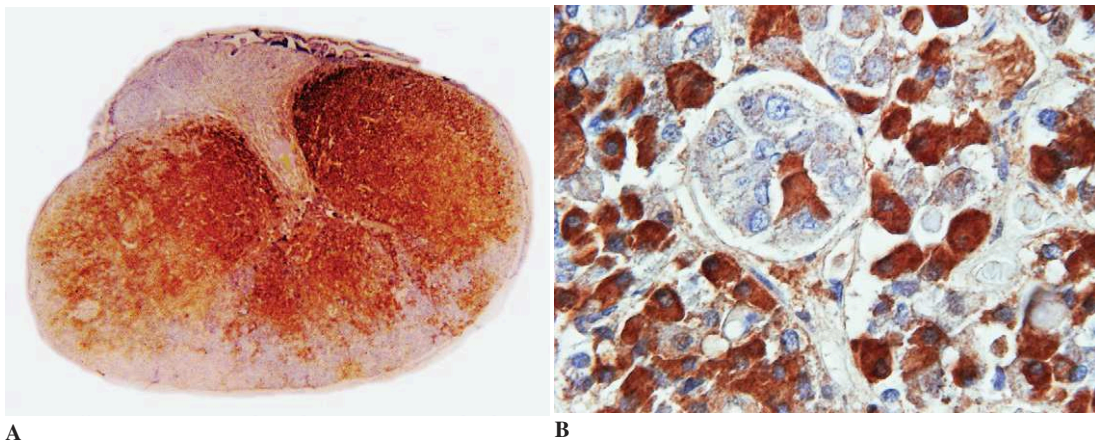
Figure 15-1. Normal pituitary. **A**, Whole mount horizontal section demonstrating the anterior, intermediate, and posterior lobes of the pituitary. The section reveals the normal distribution of the growth hormone producing cells in the lateral lobes of the anterior pituitary. **B**, A high-power picture with detail of normal growth hormone-producing cells. (Immunohistochemistry for growth hormone.)

overproduction of adrenocorticotrophic hormone; galactorrhea and ovulatory disturbances in hyperprolactinemia in women. and decreased libido and erectile dysfunction in men; and hyperthyroidism or hypothyroidism in patients with pituitary-dependent thyroid-stimulating hormone (TSH)

excess. Overproduction of gonadotrophic hormones rarely causes well-defined clinical signs.

Hypofunction is caused by deficiency of trophic hormones due to lesions within the sella turcica with destruction of the hormone-producing cells (Table 15-4). The most common cause is a pituitary
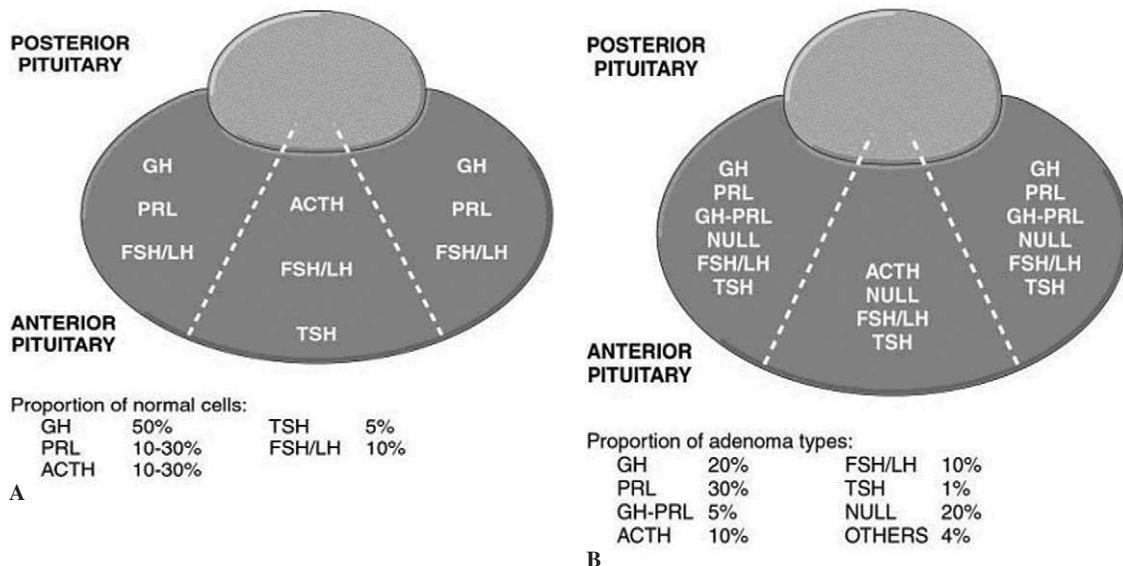
Figure 15-2. A, Cell-type distribution in anterior normal pituitary (horizontal section). Note the distribution and proportion of growth hormone producing cells (see Fig. 15-1A). **B**, Distribution of pituitary adenomas (horizontal section). The locations of subtypes of pituitary adenomas correspond to the location and distribution of the cells in the normal pituitary shown in (**A**).

Table 15-3. Lesions of the Pituitary and Sellar Region

Benign Neoplasms		Malignant Neoplasms	
Pituitary adenoma	Neurilemomma	Pituitary carcinoma	Metastatic carcinoma
Atypical pituitary	Paraganglioma	Chordoma	Metastatic carcinoma to
adenoma	Glomangioma	Germ cell tumors	pituitary adenoma
Meningioma	Hemangioma	Hemangiopericytoma	Leukemia
Craniopharyngioma	Hemangioblastoma	Postirradiation sarcoma	Metastatic lymphoma
Granular cell tumor	Myxoma	Osteosarcoma	Plasmacytoma
Gangliocytoma	Fibrous dysplasia of bone	Hemangiosarcoma	Fibrosarcoma
Ganglioglioma	Histiocytosis X	Malignant histiocytosis	Melanoma
Ganglioneuroma	Giant cell tumor of bone	Chondrosarcoma	Malignant peripheral nerve
Glioma	Schwannoma	**Infectious Diseases**	sheath tumor
Paraganglioma	Teratoma	Bacterial abscess	Syphilis
Osteoma		Tuberculosis	Cysticercosis
Chondroma		Fungal abscess	Hyatid cyst
Inflammatory Disorders		**Systemic Diseases**	
Xanthomatous	Giant cell granuloma	Hemosiderosis/	Amyloidosis
hypophysitis	Granulomatous hypophysitis	hemochromatosis	Sarcoidosis
Lymphocytic		Mucopolysaccharidoses	
hypophysitis		**Physical Injury**	
Vascular Lesions		Trauma	
Pituitary infarction	Aneurysm	Radionecrosis	
Pituitary apoplexy	Vascular malformation	**Empty Sella Syndrome**	
Cysts/Malformations		Primary	
Rathke cleft cyst	Mucocele	Secondary	
Arachnoid cyst	Dermoid cyst		
Epidermoid cyst	Hamartoma		
Choristoma	Congenital malformations		

adenoma; inflammatory diseases are a less common cause. The loss of the hormone producing cells and consequent absence of the trophic hormones leads to hypopituitarism, with thyroid, gonadal, and adrenal dysfunction. Patients may also show signs

Table 15-4. Major Causes of Hypopituitarism

Pituitary Diseases
Pituitary adenomas and carcinomas
Pituitary surgery and radiation
Autoimmune diseases and hypophysitis
Infiltrative and metabolic lesions
Pituitary infarction and apoplexy
Sheehan syndrome
Genetic diseases
Empty sella syndrome
Pituitary cysts
Hypothalamic Diseases
Mass effect: benign and malignant tumors
Radiation for CNS and nasopharyngeal malignances
Infiltrative lesions
Trauma with fracture of skull base
Infections

of isolated anterior pituitary hormone deficiency such as hypothyroidism or hypogonadism.

The clinical syndrome associated with the neurohypophysis is usually diabetes insipidus, due to antidiuretic hormone secretion abnormalities. The other posterior pituitary hormone, oxytocin, rarely causes a significant clinical syndrome.

Due to its location adjacent to a variety of normal structures, the *local mass effects* of an adenoma can manifest as sellar expansion, bone erosion, disruption of the diaphragma sellae, and compression of the optic chiasm, with bitemporal hemianopsia, elevated intracranial pressure, headaches, seizures, obstructive hydrocephalus, and cranial nerve palsies.

Hyperpituitarism, Pituitary Adenomas, and Hyperplasia

Functional pituitary adenomas are the most common cause of hyperpituitarism. They represent 10% to 20% of intracranial neoplasms in neuro-

Table 15-5. Immunohistochemical Classification of Adenohypophyseal Tumors

Adenoma Type	Principal Immunoreactivity	Secondary Immunoreactivity
Somatotrophic	GH	PRL, α-SU, TSH, FSH, LH
Lactotrophic	PRL	α-SU
Combined features of GH and PRL	GH, PRL	α-SU, TSH
Corticotrophic	ACTH	LH, α-SU
Thyrotrophic	TSH	α-SU, GH, PRL
Gonadotrophic	FSH, LH, α-SU	PRL, GH, ACTH
Plurihormonal	Plurihormonal	—
Null cell	Hormone immunonegative	—

ACTH = adrenocorticotropic hormone; FSH = follicle-stimulating hormone; GH = growth hormone; LH = luteinizing hormone; PRL = prolactin; SU = subunit; TSH = thyroid-stimulating hormone.
Source: *WHO–Histological Typing of Endocrine Tumors, 2000.*

surgical series. Incidental adenomas are found in up to 25% of autopsies. Pituitary adenomas are benign, usually monoclonal, well-circumscribed neoplasms surrounded by a reticulin pseudocapsule. These tumors are found primarily in women in all age groups, mostly between the third and sixth decades of life, while childhood pituitary adenomas are extremely rare.

The clinicopathologic classifications of pituitary adenomas are complex and are based on histology and immunohistochemistry (Table 15-5), ultrastructure (Table 15-6), endocrine activity (Table 15-7), imaging and operative findings (Table 15-8).

While the great majority of these lesions remain benign, a small number show invasive behavior and a small proportion become malignant. The pattern of growth can be expansive, grossly invasive, or, rarely, metastasizing (see Table 15-8). The location of the adenomas within the pituitary has a basically similar distribution to that of the normal anterior pituitary cells (Fig. 15-2B).

Peptide-Hormone-Producing Adenomas

Prolactin Cell Adenoma (Prolactinoma)

The majority of *prolactinomas* are composed of diffuse, uniformly round, periodic acid-Schiff (PAS)–negative, chromophobic cells (as seen by routine histologic staining) with a paucity of secretory granules. Prolactinomas are composed of a homogeneous population of small cells with no pleomorphism and have a tendency to contain microcalcifications and psammoma bodies (Fig. 15-3). The prolactin (PRL) immunoreactivity in the

sparsely granulated tumors is paranuclear in the region of the Golgi apparatus. The rarer, densely granulated PRL cell adenoma shows diffuse cytoplasmic prolactin positivity.

PRL-secreting tumors in males are usually macroadenomas, while in females they are usually

Table 15-6. Ultrastructural Classification of Adenohypophyseal Tumors

Tumor Type	Variants
Growth hormone cell adenoma	Densely granulated Sparsely granulated
Prolactin cell adenoma	Densely granulated Sparsely granulated
Adenomas with growth hormone and prolactin cell differentiation	Mixed GH-PRL cell adenoma Mammosomatotroph cell adenoma Acidophil stem cell adenoma
ACTH cell adenoma	Densely granulated Crooke cell variant Sparsely granulated
TSH cell adenoma	—
FSH-LH cell adenoma	Male type Female type
Null cell adenoma	Nononcocytic Oncocytic
Other adenomas	Silent "corticotroph" subtype 1 Silent "corticotroph" subtype 2 Silent adenoma subtype 3 Plurimorphous adenomas, e.g., GH-PRL-TSH, PRL-ACTH Unclassified

ACTH = adrenocorticotropic hormone; FSH = follicle-stimulating hormone; GH = growth hormone; LH = luteinizing hormone; PRL = prolactin; TSH = thyroid-stimulating hormone.
Source: *WHO–Histological Typing of Endocrine Tumors, 2000.*

Table 15-7. Functional Classification
of Adenohypophyseal Tumors

Endocrine Hyperfunction
   Acromegaly/gigantism, elevated growth hormone levels
   Hyperprolactinemia and sequelae
   Cushing syndrome, elevated ACTH and cortisol levels
   Hyperthyroidism with inappropriate secretion of TSH
   Significantly elevated FSH/LH and/or alpha subunit levels
   Multiple hormonal overproduction
Clinically Nonfunctioning
Functional Status Undetermined
Endocrine Hyperfunction Due to Ectopic Sources
   Clinical acromegaly secondary to ectopic GRH
      overproduction
   Cushing syndrome secondary to ectopic CRH
      overproduction

ACTH = adrenocorticotropic hormone; CRH = corticotropin-
   releasing hormone; FSH = follicle-stimulating hormone;
   GRH = growth hormone releasing hormone; LH =
   luteinizing hormone; TSH = thyroid-stimulating hormone.
Source: *WHO–Histological Typing of Endocrine Tumors,
   2000.*

microadenomas. Dopamine-agonist therapy pro-
duces involution, atrophy, tumor-growth arrest, and
microcalcifications in prolactinomas.

   PRL-secreting tumors have to be differentiated
from other lesions producing prolactinemia, as by
interference of dopamine release by compression
of the pituitary stalk. The serum levels of prolactin
with stalk compression is usually less than 300 ng/
mL, whereas the serum level of prolactin in patients
with a prolactin-secreting tumor is usually above
1000 ng/mL.

Table 15-8. Imaging and Surgical Classification
of Adenohypophyseal Tumors Based on Location,
Size, and Growth Pattern

Location
   Intrasellar
   Extrasellar (extension into surrounding structures:
      suprasellar, nasopharynx, sphenoid sinus, cavernous
      sinus, etc)
   Ectopic
Size
   Microadenoma
   Macroadenoma
Growth Pattern
   Expansive
   Grossly invasive to dura, bone, nerves, or brain
   Metastasizing (craniospinal or systemic)
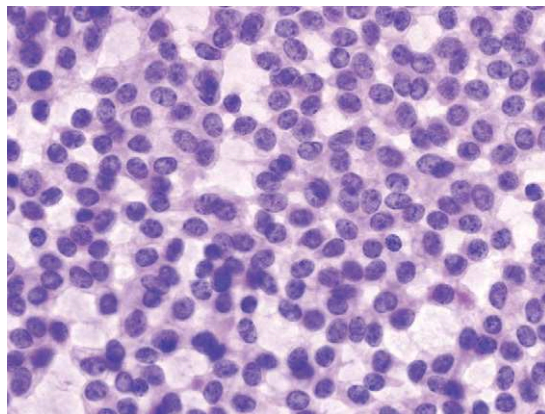
A
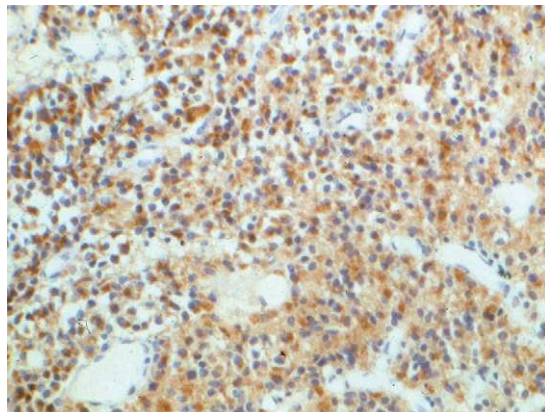
B

Figure 15-3. Prolactinoma. **A**, This adenoma is composed
of sheets of uniform small cells with a densely staining
nucleus and little cytoplasm (H and E). **B**, The tumor cells
stain uniformly for prolactin.

Growth Hormone Cell Adenomas

Clinical or immunohistochemical evidence of
growth hormone (GH) production occurs in around
30% of pituitary adenomas. This class includes
GH-only pituitary adenomas, GH and PRL pituitary
adenomas, and plurihormonal pituitary adenomas
producing GH. These adenomas are the major cause
of acromegaly (gigantism; Table 15-9).

GH-Only Pituitary Adenomas. GH-producing
tumors have a diffuse homogeneous cell population
of round to oval cells. The majority of the cells in
these tumors are acidophilic by routine H and E
staining. Because the GH molecule lacks a carbo-

Table 15-9. Causes of Acromegaly (Gigantism)

Excess Growth Hormone Secretion
  Pituitary Origin (approximately 98%)
    GH cell adenoma (approximately 60%)
    Mixed GH cell and PRL cell adenoma (approximately 20%)
    Mammosomatotroph cell adenoma (approximately 10%)
    Plurihormonal adenoma
    GH cell carcinoma
    Multiple endocrine neoplasia I with GH cell adenoma
    McCune-Albright syndrome with adenoma
  Ectopic Sphenoid or Parapharyngeal Sinus Pituitary Adenoma
  Extrapituitary Origin
    Pancreatic islet cell tumor
Excess Growth Hormone Releasing Hormone Secretion
  Central Ectopic (<1%)
    Hypothalamic hamartoma, choristoma, ganglioneuroma
  Peripheral Ectopic (1%)
    Bronchial carcinoid, pancreatic islet cell tumor, small cell lung cancer, adrenal adenoma, medullary thyroid carcinoma, pheochromocytoma
Excess Growth Factor Activity

GH = growth hormone; PRL = prolactin.

hydrate component, PAS stains are uniformly negative. These tumors also have two different keratin patterns that correlate with the presence or absence of the alpha subunit and are associated with differing prognoses. Immunohistochemistry for GH shows a variable expression. If the tumor is sparsely granulated, the immunoexpression of GH is weak, whereas if the tumor is densely granulated, there is strong immunoreactivity.

Mixed GH Cell/PRL Cell Adenomas. Patients with acromegaly can also have evidence of hyperprolactinemia, due to the production of both hormones (Fig. 15-4). The mixed GH cell/PRL cell adenomas contain two different cell types, well characterized by both their distinctive ultrastructural appearances and immunohistochemistry. These lesions are not aggressive.

Mammosomatotrophic Cell Adenomas. These rare tumors are characterized by dual immunopositivity and by a monomorphous cell population.

Unlike those in mixed bicellular tumors, these cells exhibit both lactotroph and somatotroph differentiation in the same cell when viewed by electron microscopy.

Acidophil Stem Cell Adenomas. These rare adenomas are clinically nonfunctioning or may simulate prolactinoma because of stalk compression. Acromegaly with elevation of GH is very unusual. These tumors are thought to represent stem cells of the acidophilic line. By routine H and E stains they are chromophobic, and the cells have a vacuolated cytoplasm. Both GH and PRL are detected in the same cell by immunohistochemistry and by electron microscopy; the tumor cells show features intermediate between those of GH and PRL cells.

Plurihormonal Adenomas. These adenomas are characterized by the production of multiple hormones. They produce not only GH but prolactin, one or more of the glycoprotein hormones, and the alpha subunit of the glycoprotein hormones. The plurihormonal adenomas may be functioning, partially functioning, or silent. One or more cell types (as detected by electron microscopy) can form these tumors. The *monomorphous* type is composed of one cell type that can produce multiple hormones. The *plurimorphous* type is composed of at least two cell types, each with distinct immunohistochemical and electron microscopic characteristics. Some plurimorphous adenomas may represent collision tumors.

ACTH-Producing Adenomas

A large number of lesions underlie the overproduction of ACTH. The most common is ACTH-dependent Cushing syndrome, caused by a basophilic ACTH-producing pituitary adenoma with adrenal cortical hyperplasia (Table 15-10). ACTH-independent Cushing disease is less frequent.

Corticotroph Cell Adenomas. *Corticotroph cell adenomas* represent approximately 20% of the pituitary adenomas and occur more often in women than men. Most corticotroph cell adenomas are microadenomas and arise in the central mucoid wedge of the anterior pituitary, where most of the
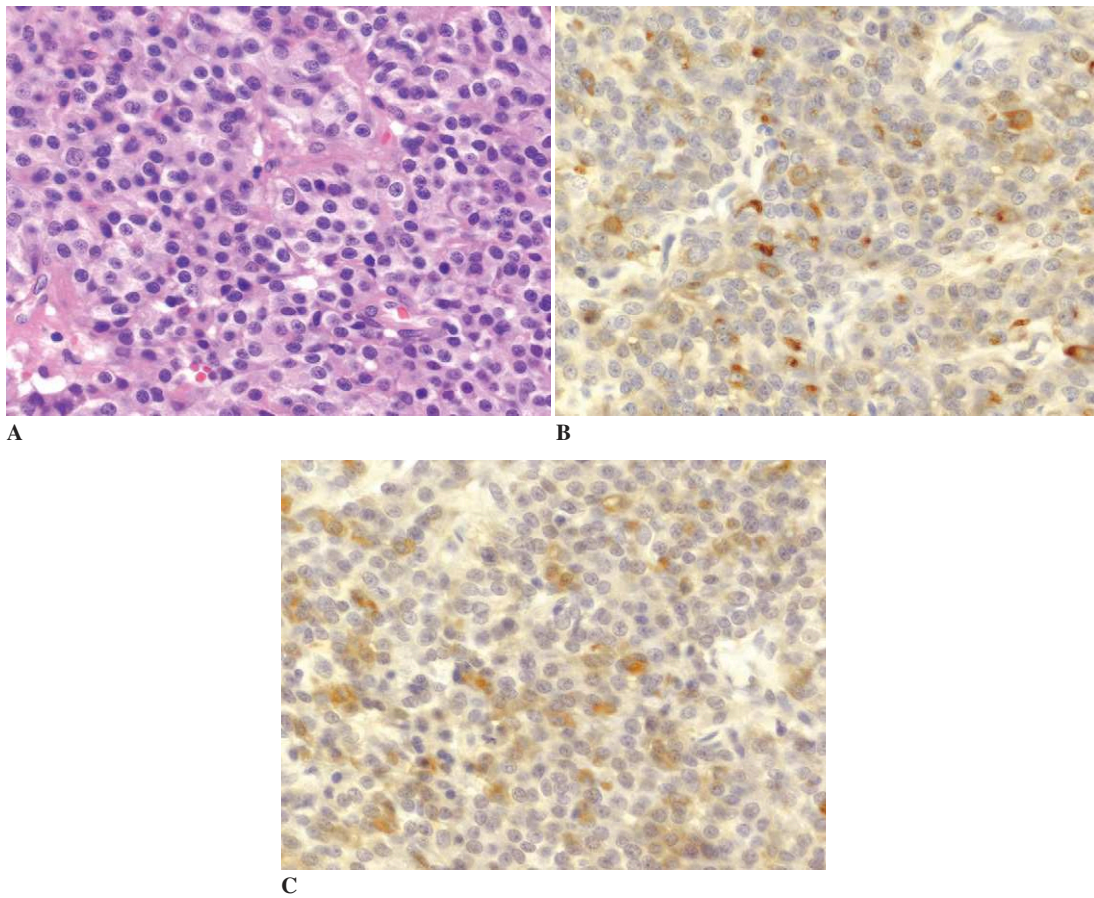
Figure 15-4. Mixed growth-hormone-producing adenoma. This patient had acromegaly. The tumor is composed of uniform small cells with only a small amount of cytoplasm (**A**). Most of the tumor cells stain positively for both human growth hormone (**B**) and prolactin (**C**).

Table 15-10. Causes of Cushing Syndrome

ACTH-Dependent Cushing Syndrome
   Cushing disease—pituitary adenoma/carcinoma
   Ectopic ACTH syndrome
   Ectopic CRH syndrom
ACTH-Independent Cushing Syndrome
   Adrenal adenoma
   Adrenal carcinoma
   Micronodular hyperplasia
   Macronodular hyperplasia
   Primary pigmented nodular adrenocortical disease
Pseudo-Cushing Syndrome
   Major depressive disorder
   Alcoholism

ACTH = adrenocorticotropic hormone; CRH = corticotropin-releasing hormone.

normal ACTH-producing cells are located. Posteriorly located adenoma are uncommon; they are thought to derive from intermediate lobe corticotrophs and are usually silent. ACTH-producing macroadenomas are rare and often invasive. Microscopically, the tumors are composed of monotonous cells with basophilic and PAS-positive cytoplasm. The presence of ACTH or other propiomelanocortic derivatives can be demonstrated by immunohistochemistry (Fig. 15-5). These adenomas have teardrop-shaped neurosecretory granules with variable electron density and cytokeratin accumulation in the perinuclear region, simulating the Crook hyaline change of normal corticotrophs. Diffuse Crook hyalinization of ACTH adenomas is rare, and is associated with larger neoplasms (macroadenomas) and with invasion.
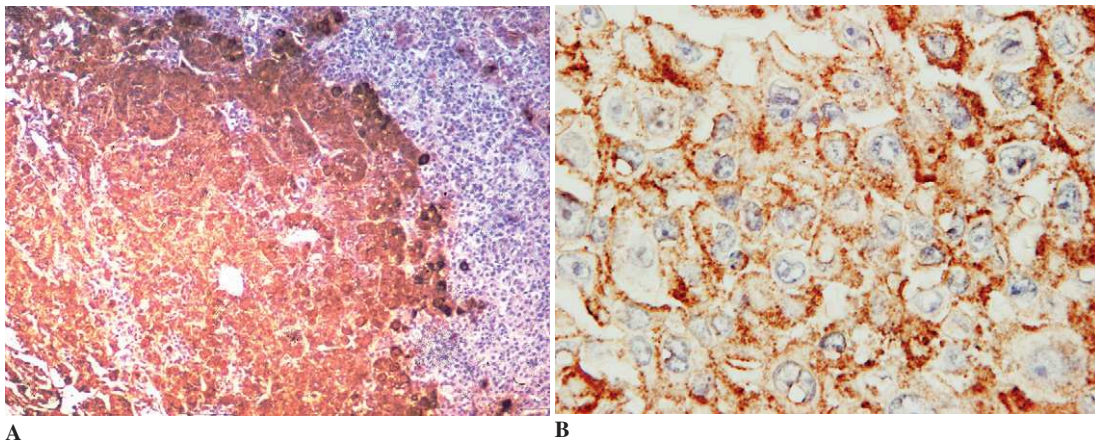
Figure 15-5. A, Adrenocorticotropic hormone (ACTH)–producing adenoma, on the left, with well-defined borders between itself and the normal pituitary. **B**, Higher-power view of the ACTH-producing adenoma (immunohistochemistry for ACTH).

Silent Corticotroph Adenomas. *Silent corticotroph adenomas* are macroadenomas which are endocrinologically nonfunctioning but immunoreactive for ACTH. Most likely, these neoplasms elaborate abnormal endocrinologically inactive products or fail to release the hormone. Some patients have a mildly elevated serum ACTH. Silent corticotroph adenomas are composed of basophilic to chromophobic cells immunoreactive with ACTH or other propiomelanocortin derivatives similar to that of usual corticotroph cell adenoma.

Gonadotroph Cell Adenoma

The normal follicle-stimulating hormone/luteinizing hormone (FSH/LH) cells are basophilic and PAS-positive, but the adenomas derived from these cells are chromophobic and only faintly PAS-positive, with positive granules located at the periphery of their cytoplasm. There is marked variability of immunoexpression in these tumors. Some tumors demonstrate diffuse positive immunoreactivity for the beta subunits of FSH and LH, with or without immunoreactivity for the alpha subunit, and some tumors fail to demonstrate immunoreactivity for these hormones (Fig. 15-6). Gonadotroph adenomas exhibit ultrastructural diversity. These tumors are believed to be nonfunctional because of a failure to appropriately combine the alpha and beta subunits of the glycoprotein hormones to make the active hormone.

Most of the gonadotroph adenomas become evident because of mass effect on the surrounding structures. Some tumors are diagnosed in the elderly after a long history of hypogonadism. These macroadenomas less frequently invade surrounding structures, and recur less often than the other macroadenoma subtypes (Table 15-11).

Thyrotroph Cell Adenoma

TSH-producing tumors are rare, often invasive macroadenomas that can present with either hyperthyroidism or hypothyroidism. They represent approximately 1% of pituitary adenomas. The majority of these tumors have polygonal cells that are chromophobic by routine H and E stains and faintly PAS-positive. Immunohistochemistry shows the tumor cells to be positive for both β-TSH and the α subunit of the glycoprotein hormones. Most of these lesions are located in the anterior mucoid wedge, where the thyrotroph cells are usually concentrated. Electron microscopy shows peripherally placed, sparse secretory granules.

Pituitary Adenoma with Neuronal Metaplasia

Rare GH-producing pituitary adenomas and other, even rarer types of pituitary adenomas may contain ganglion cells. The neurons react with neuronal markers such as neurofilament protein as well as epithelial markers and the hormonal immunoprofile
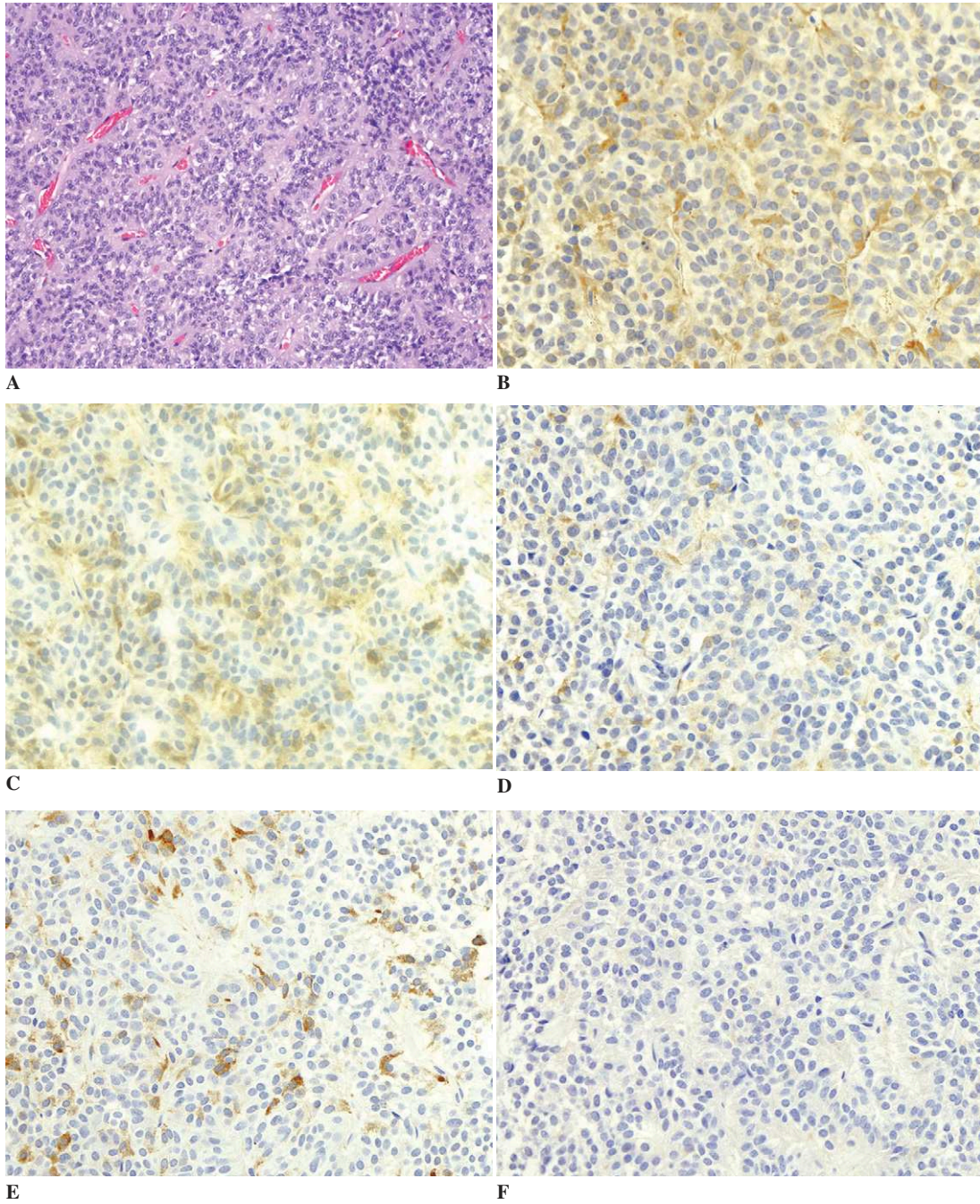
Figure 15-6. Gonadotrophic adenoma. Note that the tumor cells are arranged in a papillary fashion around fine capillaries (**A**). A variable number of tumor cells stain for the common α subunit (**B**) as well as the β subunits of LH (**C**), TSH (**D**), and FSH (**E**), but are all negative for prolactin (**F**).

Table 15-11. Clinical Presentations of Gonadotroph Adenomas

Neurologic Symptoms/Mass Effect
Visual impairment, headache, hemianopsia, and seizures
CSF rhinorrhea
Other
Incidental Finding
Hormonal Symptoms
Oligomenorrhea or amenorrhea, premenopausal woman
Ovarian hyperstimulation (FSH increased), premenopausal woman
Precocious puberty (intact LH secreted), prepubertal boy
Symptoms of hormonal deficiencies

FSH = follicle-stimulating hormone; LH = luteinizing hormone.

of the adenoma cells. These ganglion cells may be scant or may represent the great majority of tumor cells, and may or may not be accompanied by neuropil. The ganglion cells are thought to represent neuronal metaplasia of adenoma cells; this view is supported by immunocytochemical and ultrastructural demonstration of cells with transitional features between neurons and pituiticytes. Alternatively, the presence of neurons in an adenoma might represents a developmental malformation.

Adenomas not Associated with Hormone Production

Adenomas not associated with hormone production (*null cell adenomas*) account for approximately one third of all pituitary adenomas. They show no clinical evidence of hormonal production and are characterized by absent or scant hormone immunoreactivity and by ultrastructural features of cells without specific differentiation. These lesions include a heterogeneous group of adenomas, despite their similar clinicopathologic features. Due to the lack of hormonal overproduction, they tend to present with symptoms and signs associated with compression and, if there is extensive normal pituitary tissue destruction, hypopituitarism. Some patients may have mild hyperprolactinemia if there is pituitary stalk compression by the adenoma. The pathologic diagnosis of null cell adenoma is based on the morphologic features, hormonal immunoprofile, and electron microscopy. Most null cell adenomas are silent gonadotrophic adenomas with minimal glycoprotein expression, such as β-FSH, LH, or α-subunit immunoreactions. Some of the null cell adenomas have oncocytic changes (oncocytomas), indicating a large concentration of mitochondria.

Ectopic Adenomas

Ectopic adenomas are extremely rare. They are derived from pituitary cells in the pharynx and can occur in the sphenoid sinus, mouth, nasal cavity, or suprasellar region. These ectopic adenomas can be hormonally producing tumors or null cell adenomas.

Invasive Pituitary Adenomas

Pituitary adenomas are classified as *invasive* if invasion of the dura, adjacent bone, cavernous sinus, or sinus mucosa can be demonstrated either on the basis of imaging or operative findings. There are no light or electron microscopic features distinguishing noninvasive adenomas from invasive and aggressive adenomas. Mitoses are more often present in invasive tumors than in noninvasive lesions, and p53 immunohistochemical expression is higher in invasive adenomas.

Atypical Adenomas

An adenoma with intermediate clinicopathologic characteristics between a typical adenoma and pituitary carcinoma is defined as an *adenoma with atypical morphologic features suggestive of aggressive behavior*. These are macroadenomas with invasive behavior and frequent recurrences that demonstrate their potential for aggressive behavior. Atypical pituitary adenomas have increased mitotic activity, possibly including occasional atypical mitosis, with a proliferative MIB-1 index greater than 3 percent (Fig. 15-7) and, often, p53 over-expression with or without p53 gene mutation (Table 15-12).

Pituitary Carcinoma

Adenohypophyseal neoplasms with craniospinal spread and brain invasion and metastases to
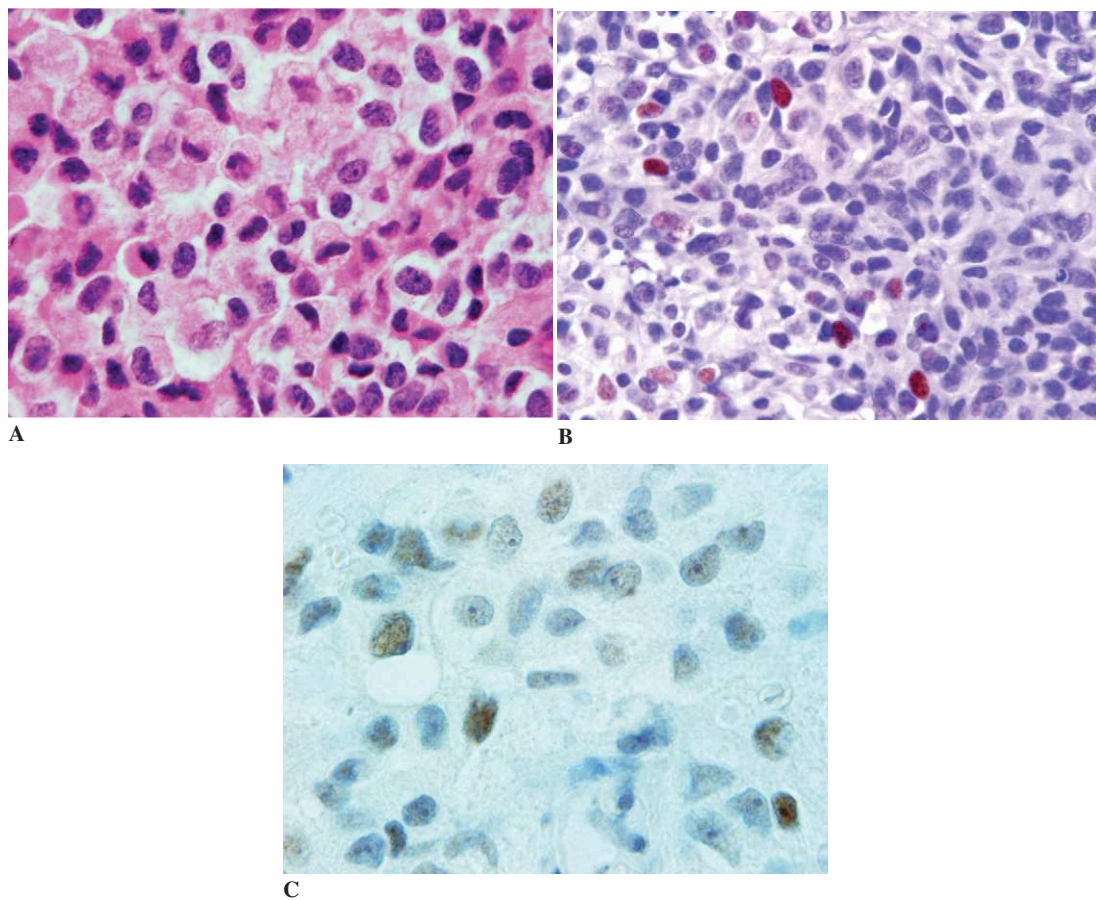
Figure 15-7. Atypical pituitary adenoma with recurrence. **A**, Histologic appearance. **B**, High MIB-1 index adenoma cell nuclei. **C**, Adenoma cell nuclei with positivity for p53.

extracranial sites are designated *pituitary* or *adenohypophyseal carcinomas*. They are extremely rare. Metastatic potential distinguishes pituitary carcinoma from the other adenohypophyseal tumors. The metastases are usually to lymph nodes, bone, liver, or skull (Fig. 15-8). Pituitary carcinomas are more frequently hormonally inactive; however, prolactin-producing and ACTH-producing carcinomas have been described.

It is not possible to make a diagnosis of pituitary carcinoma on histology alone. Most carcinomas do not show much cellular pleomorphism or

Table 15-12. Differences Between Pituitary Adenomas, Atypical Adenomas, and Pituitary Carcinomas

Tumor Characteristics	Adenoma	Atypical Adenoma	Carcinoma
Mitosis	Rare	Few	Present
MIB-1 labeling index	0–3%	>3%	High
p53	Negative	0–15%	100%
Tumor size	Micro/macro	Macro	Macro
Gross invasion	Possible	Probable	Required
Metastases	No	No	Required

LH = luteinizing hormone.

A   **B**
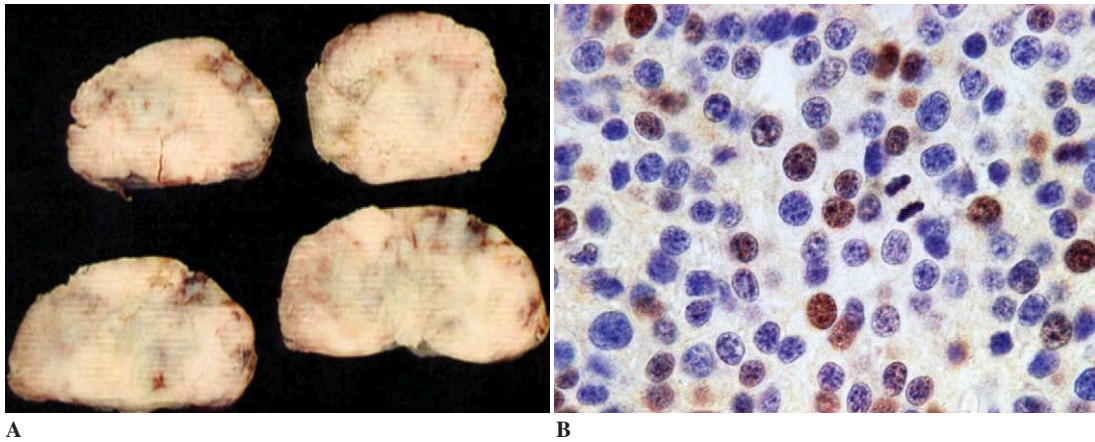
Figure 15-8. Metastases of pituitary carcinoma. **A**, Gross appearance. **B**, Histologic appearance is similar to that of pituitary adenomas with high proliferative activity, as seen by MIB-1 and presence of mitosis.

nuclear atypia. However, they have increased mitotic activity (see Fig. 15-8), high MIB-1 labeling index, and p53 immunoreactivity (see Table 15-12) when compared with typical and atypical adenomas.

Pituitary Hyperplasia

A rare cause of pituitary hyperfunction is *pituitary hyperplasia*. It may cause a clinical syndrome such as acromegaly, Cushing syndrome, or hypothyroidism. By definition, pituitary hyperplasia is an increase in number of one or more specific anterior pituitary cell types; it is distinct from neoplasia. Anterior pituitary hyperplasia can be classified as *primary* (idiopathic) hyperplasia, *secondary* hyperplasia (due to lack of negative feedback stimulation and end organ failure), or *tertiary* hyperplasia (due to hypothalamic hormone stimulation). Idiopathic pituitary hyperplasia is probably due to hypothalamic dysfunction with excess of hypothalamic hormone production (Table 15-13).

Hyperplasia is usually focal but can be nodular or diffuse. The diagnosis is based on histologic findings of expansion of the acinar architecture, seen with a reticulin stain. Immunohistochemistry can help in identifying the hyperplastic cell type. The differential diagnosis from adenoma can be difficult (Table 15-14).

Table 15-13. Pituitary Hyperplasia

Prolactin Cell (Lactotroph Cell)
  Physiologic: pregnancy and estrogen therapy
  Secondary to decreased dopamine release to anterior
    pituitary from hypothalamus, secondary to
    suprasellar-space-occupying lesions
  Hypothyroidism (thyroid stimulating hormone effect)
Growth Hormone Cell (Somatotroph Cell)
  Primary hyperplasia: hypothalamic hamartoma or
    ectopic sources of growth hormone releasing
    hormone
  Primary hyperplasia: Neuroendocrine neoplasia by
    gonadotropin releasing hormone excess
  Mammosomatotroph cell hyperplasia in McCune-
    Albright syndrome
  Adrenocorticotropin (Corticotropin Cell)
  Secondary hyperplasia: glucocorticoid insufficiency in
    untreated Addison disease
  Primary hyperplasia: excessive secretion of
    corticotropin-releasing hormone by ectopic or
    neuroendocrine neoplasms or gangliocytic hamartoma
  Idiopathic
**Luteinizing Hormone/Follicle-Stimulating Hormone
  (Gonadotroph Cell)**
  Secondary hyperplasia: hypogonadism, Klinefelter
    syndrome, Turner syndrome
Thyroid-Stimulating Hormone (Thyrotroph Cell)
  Secondary hyperplasia: primary hypothyroidism

Table 15-14. Pituitary Adenoma and Hyperplasia

	Adenoma	Hyperplasia
Pattern of Growth	Diffuse	Nodular and diffuse
Normal Pituitary	Compressed	No distinction from normal
H and E Stain	Loss of acinar pattern, one cell population	Acinar pattern maintained and distinct cells
Reticulin Stain	Disruption of the acinar pattern, pseudocapsule	Preserved pattern with expanded acini
Immunohistochemistry	Specific hormone strong reactivity	Specific hormone weak reactivity

Hypopituitarism and Inflammatory and Vascular Lesions

Hypopituitarism is caused by deficiency of the pituitary trophic hormones due to a variety of causes. With the loss of up to 50% of the pituitary cells, the patient may be asymptomatic; when more than 80% of the anterior pituitary cells are destroyed, hypopituitarism becomes evident.

Inflammatory Lesions

Inflammatory lesions of the pituitary can cause hypopituitarism, mass effect, and/or diabetes insipidus. These inflammatory lesions are divided into *primary* (idiopathic) and *secondary* lesions (Table 15-15).

Primary or Idiopathic Inflammatory Lesions

Lymphocytic Hypophysitis. *Lymphocytic hypophysitis* is a chronic process that is particularly associated with pregnancy or the post-partum

Table 15-15. Inflammatory Lesions of the Pituitary Gland

Primary or Idiopathic
Lymphocytic hypophysitis
Granulomatous hypophysitis
Xanthomatous hypophysitis
Giant cell granuloma
Secondary
Infections: pneumocystis, toxoplasma, cytomegalovirus, meningitis, syphilis, brucellosis, fungi, mycobacteria
Systemic diseases: sarcoidosis, Wegener granulomatosis, Takayasu disease, Crohn disease
Adenoma undergoing necrosis
Ruptured Rathke cleft cyst

period; it is a cause of pituitary insufficiency of pregnancy. The clinical presentation is that of panhypopituitarism and often headache. Decompressive biopsy is part of the treatment. The adenohypophyseal interstitium and the acini are infiltrated by lymphocytes and plasma cells with occasional histiocytes. Lymphoid follicles with well-developed germinal centers are seen (Fig. 15-9). Fibrosis may be found in chronic phases.

Lymphocytic hypophysitis is an autoimmune disease both humoral and cellular-mediated, with the development of antipituitary antibodies and a lymphoplasmacytic infiltrate.

Granulomatous Hypophysitis. *Granulomatous hypophysitis* is a rare, chronic, inflammatory disease of unknown pathogenesis. Unlike lymphocytic hypophysitis, granulomatous hypophysitis occurs equally in both sexes. The usual clinical presentation is a variable degree of adenohypophyseal failure, hyperprolactinemia, headache with nausea and vomiting, and diabetes insipidus. Microscopically, granulomatous hypophysitis is characterized by large collections of histiocytes, occasional multinucleated giant cells and by a lymphoplasmacytic infiltrate (Fig. 15-10). It must be differentiated from other causes of granulomatous inflammation such as tuberculosis, fungi, and sarcoidosis.

Xanthomatous Hypophysitis. *Xanthomatous hypophysitis* is a rare idiopathic entity that may represent a reactive process. It occurs in young women, who present with a combination of menstrual irregularities, diabetes insipidus, headache, and nausea with a localized lesion in the pituitary. Histologically, the adenohypophysis is infiltrated by foamy histiocytes, immunoreactive for CD68, and immunonegative for CD1a and S-100 protein.

Figure 15-9. Lymphocytic hypophysitis. The anterior pituitary tissue is almost replaced by a lymphocytic infiltrate.

Giant Cell Granuloma of the Pituitary. *Giant cell granuloma* of the pituitary is another rare cause of hypophysitis. It occurs in both sexes and is not associated with pregnancy. Histologically, the pituitary is infiltrated by noncaseating granulomas with occasional Schaumann bodies. Systemic evidence of sarcoidosis or other diseases has to be excluded.

Secondary Hypophysitis

A variety of systemic diseases and infections can also cause hypophysitis (see Table 15-15).
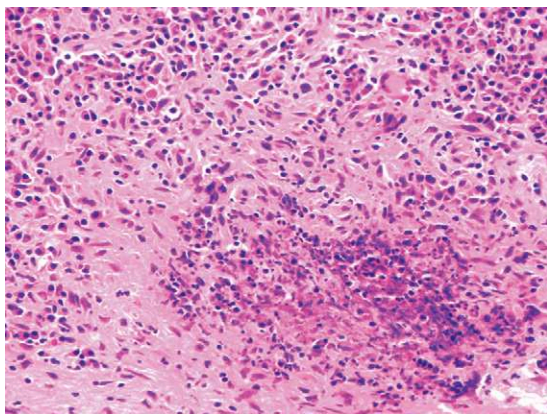
Figure 15-10. Granulomatous hypophysitis. There is a well-formed granuloma in the anterior pituitary with epithelioid cells and fibroblasts with some scattered multinucleated giant cells at the periphery.

Vascular Lesions of the Pituitary

Pituitary Infarction

Diverse diseases can cause ischemic necrosis of the pituitary gland, including hemorrhagic shock, thrombocytopenia and other coagulopathies, head injury, massive cerebrovascular accidents, and heparin therapy. This condition is followed by hypopituitarism.

Pituitary Apoplexy

Pituitary apoplexy is a medical emergency presenting with acute headache and sometimes visual loss secondary to hemorrhage or infarction, usually of a pituitary macroadenoma. It can be seen also in the setting of an enlarged pituitary gland during pregnancy.

Sheehan Syndrome

Sheehan syndrome is hypopituitarism in women following delivery of a baby and is due to ischemic necrosis of the pituitary gland secondary to hypotension from post-partum hemorrhage. The posterior pituitary is spared due to its independent blood supply. There is a rim of normal viable adenohypophyseal cells at the periphery of the gland, with almost total necrosis of the gland. Subsequent fibrosis follows the necrosis.

Hereditary and Developmental Disorders

Persistence of Rathke-Pouch Remnants

Rathke-pouch remnants are small nests of squamous cells in the posterior lobe adjacent to the cleft. They can be found in 30% of normal human pituitaries at autopsy. The nests have no hormonal function and are an unlikely origin of a neoplasm, although it has been postulated that craniopharyngiomas may arise from these remnants.

Persistence of Cleft of Rathke Pouch

Persistence of the cleft of Rathke pouch is a frequent developmental abnormality without
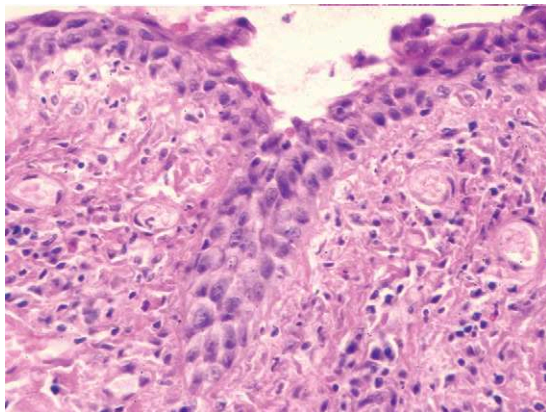
Figure 15-11. Rathke pouch cyst. Note the multilayered cuboidal epithelium lying on a connective tissue base.

significant functional or clinical problems. It is a colloid-filled space between the anterior and posterior pituitary that can give rise to Rathke's-cleft cysts. These cysts are usually small, but when large they can be symptomatic either from pressure or hypopituitarism (including diabetes insipidus). When suprasellar extension is present, headaches and visual fields defects can occur.

Each cyst contains watery to mucinous fluid and is lined by columnar epithelium or ciliated cuboidal epithelium with occasional goblet cells. Squamous metaplasia, xanthomatous inflammation, and amyloid deposition can be seen (Fig. 15-11).

Cysts

Arachnoid cysts (congenital or acquired) and *dermoid* or (more commonly) *epidermoid* cysts originating from ectopic or implanted epithelial cells can be found in the sella or parasellar regions. These cysts present with mass effect from suprasellar extension or hypopituitarism due to pituitary compression.

Pituitary Aplasia and Hypoplasia

Congenital absence of the pituitary is rare and is usually associated with hypoplasia of the adrenals, thyroid, and gonads. Even if the anterior pituitary is not formed, the posterior pituitary may be present. Pituitary hypoplasia is an incomplete development of the pituitary gland as a result of atrophy or a developmental defect. It may be associated with anencephaly, where the number of cells may be normal but the ACTH-producing cells are decreased and have poorly developed organelles.

Empty Sella Syndrome

Empty sella syndrome is an anatomic description of the appearance of the sella turcica. Empty sella syndrome can be primary or secondary. The primary empty sella syndrome is a developmental disorder due to incomplete development of the diaphragma sella. The arachnoid membrane invaginates and compresses the pituitary. This condition is usually asymptomatic; however, imaging studies may reveal an enlarged sella that mimic a pituitary adenoma. Secondary empty sella syndrome occurs after resection, irradiation, necrosis, or infarction of a pituitary adenoma.

Other Lesions

Pituitary Diseases in Familial Syndromes

Pituitary adenomas are integral components of the *type 1 multiple endocrine neoplasia syndrome* (MEN1). MEN1 is inherited as an autosomal dominant disorder. The gene responsible is located on chromosome 11q13; it is a suppressor gene and produces a protein called *menin*. An abnormality of this gene is related to hyperplasia and neoplasia of the pituitary gland, pancreas, and parathyroid gland (Table 15-16). The pathophysiological findings in MEN1-associated pituitary adenomas are related to genetic events involving the *MEN1* gene. Both copies of the gene have to be mutated for the development of pituitary neoplasia: one copy has the inherited mutation, and the other copy acquires a mutation. Other genes may be mutated and some hormonal factors may be involved, both in the formation of adenomas and in the hormone production of pituitary adenomas associated with MEN1. The pituitary adenomas in the MEN1 syndrome are usually hormonally active, with a preponderance of prolactin and/or growth hormone production.

Table 15-16. Classification of and Pituitary Involvement in Multiple Endocrine Neoplasias

Multiple Endocrine Neoplasia Syndrome Type 1
  Primary hyperparathyroidism (>90 percent)
  Pituitary tumors (10–20%)
    Prolactinoma
    Growth hormone-secreting
    Corticotropin-secreting
    Non-hormone-secreting
  Enteropancreatic tumors (60–70%)
    Gastrinoma (Zollinger-Ellison syndrome)
    Insulinoma
    Vasoactive-intestinal polypeptide-secreting
    Glucagonoma
    Pancreatic polypeptide-secreting
    Non-hormone-secreting
  Other
Multiple Endocrine Neoplasia Syndrome Type 2A
  Medullary thyroid cancer (>90 percent)
  Pheochromocytoma (40–50%)
  Parathyroid hyperplasia (10–20%)
  Cutaneous lichen amyloidosis
Multiple Endocrine Neoplasia Syndrome Type 2B
  Medullary thyroid cancer
  Pheochromocytoma
  Other
    Mucosal neuromas
    Intestinal ganglioneuromas
    Marfanoid habitus
Familial Medullary Thyroid Cancer (Variant of MEN Type 2A)
  Medullary thyroid cancer
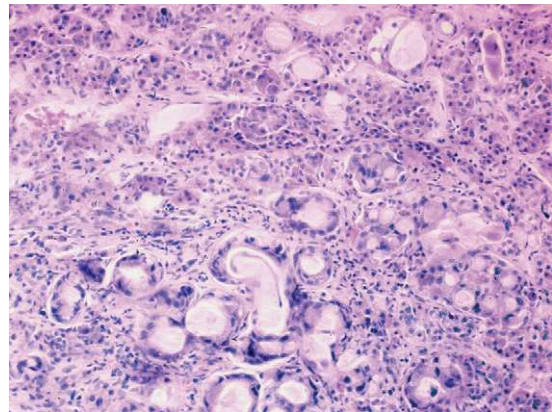
Figure 15-12. Metastatic carcinoma to the pituitary gland. The atypical glandular cells are surrounded by pituicytes, seen in the upper portion of the figure. The patient had widely metastatic breast cancer.

Tumors of the Hypothalamus, Neurohypophysis, and Sellar Region

The region of the sella has a variety of tissues and cell types, including central and peripheral nervous system, endocrine, germinal, epithelial, meningeal, mesenchymal and hematopoietic cells. Besides the great variety of neoplasms that can occur in this region, the neoplasms can mimic each other, clinically and morphologically. Immunohistochemistry is, most of the time, necessary for the differential diagnosis of the lesions in this region (see Table 15-17).

Craniopharyngioma

Craniopharyngiomas are uncommon neoplasms but are the second most common neoplasm of the sellar region (after pituitary adenomas) and the most common suprasellar neoplasm in children. The vast majority of craniopharyngiomas are in the suprasellar region. The usual symptoms are headache and visual changes such as diplopia. Craniopharyngiomas are usually cystic, irregular, nodular masses of firm tissue with yellow-brown viscid contents often described as "crank-case oil" (Fig. 15-13A). The fluid contains large numbers of cholesterol crystals. Pseudostratified columnar cells palisade around stellate cells, forming the adamantinomatous pattern. The basaloid epithelium keratinizes without maturing, giving rise to

Metastatic Neoplasms to the Pituitary Gland

Metastatic neoplasms to the pituitary gland are rare (Fig. 15-12). The metastases are usually from carcinomas in patients with widespread systemic metastases. Metastatic sarcomas are extremely rare. Metastases occur more often to the posterior lobe because of the systemic arterial blood supply and present with diabetes insipidus. The most common primary sites of origin in women are breast, lung, and stomach; in men, lung and prostate. Occasional metastases of melanoma and germ cell tumors to the pituitary are seen. The anterior lobe may be the only region involved by metastatic tumor; in such cases the differential diagnosis from a pituitary adenoma has to be considered and often requires immunohistochemistry (Table 15-17).

Table 15-17. Immunoreactivity of Tumors of the Pituitary and Sellar Region

Tumor	Pituitary Hormones	EMA	CK	S100 Protein	SYN	Chromogranin	CEA	PLAP	LCA	Vimentin
Pituitary adenoma	+ (Null cell −)	ACTH +	ACTH + GH ±	−	+	Null cell > LH/FSH, TSH	−	−	−	−
Metastatic carcinoma	−	+	+		±	±	±	±	−	±
Myeloma	−	±	−	−	−	−	−	−	±	−
Germinoma	−	−	10% +	−	−	−	−	+	−	15% +
Granular cell tumor	−	−	−	+	−	−	±	−	−	+
Chordoma	−	+	+	+	−	−	+ 10%	−	−	+

ACTH = adrenocorticotropic hormone; CEA = carcino-embryonic antigen; CK = cytokeratin; EMA = epithelial membrane antigen; LCA = leukocyte common antigen; PLAP = placental alkaline phosphatase; SYN = synaptophysin.
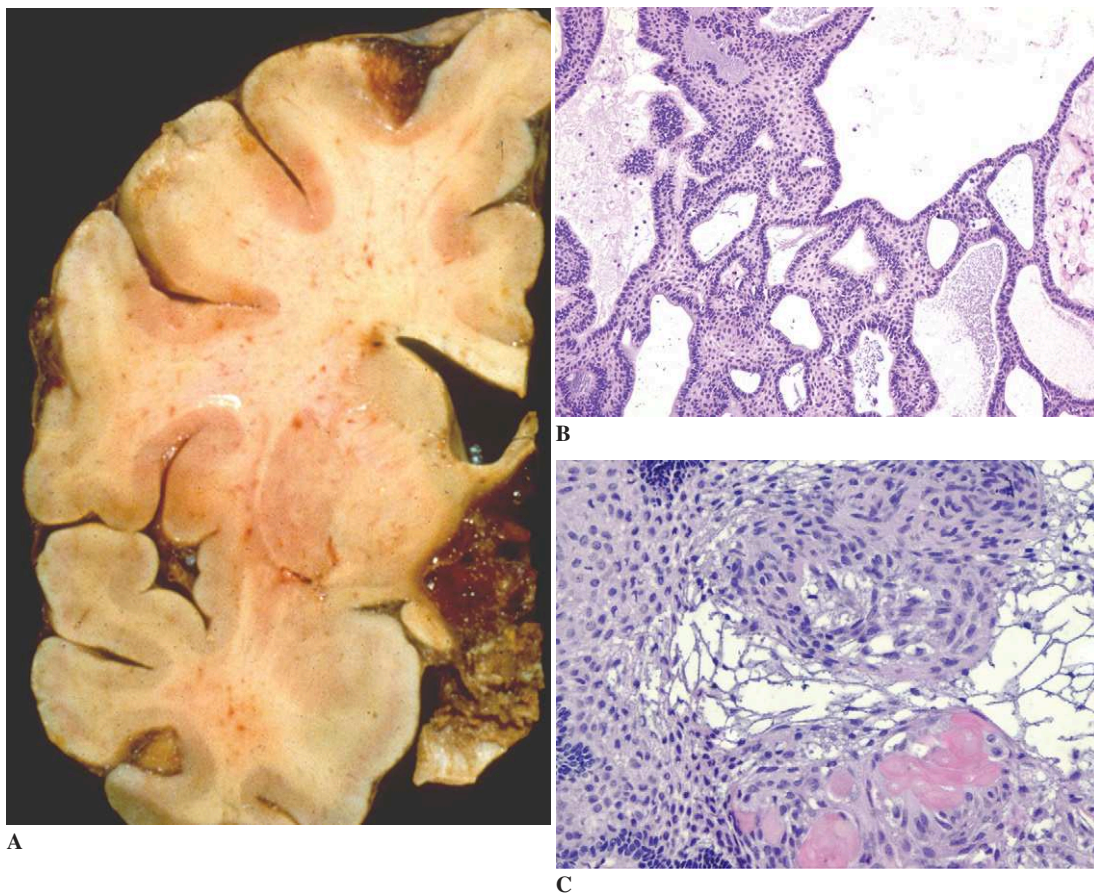
Figure 15-13. Craniopharyngioma. **A**, Gross appearance. The coronal section of the brain at the level of the hypothalamus shows a craniopharyngioma occupying the region of the hypothalamus. **B** and **C**, Microscopy showing the adamantino-matous pattern with the basaloid epithelium (**B**) and the lacy type of epithelial maturation with keratin nests (**C**).

nests of keratin in the tumor. A squamous cell pattern can be intermixed with the adamantinomatous, forming a mixed pattern (Figs. 15-13B and C). The tumors frequently contain calcific debris, cholesterol clefts, and foreign-body giant cells.

Papillary craniopharyngioma is a distinct neoplasm that differs from the classic form by the absence of the histologic features of the classic type and by an older age incidence. Radical excision is rarely curative and may lead to hypothalamic dysfunction and psychological abnormalities as well as hypopituitarism. Recurrence is common.

Granular Cell Tumors

Granular cell tumors are benign tumors of the neurohypophysis or distal pituitary stalk with uncertain histogenesis. The great majority of these neoplasms are small, slow-growing tumors and most are asymptomatic. They may be found incidentally in 1% to 17% of autopsies if careful sectioning of the pituitary is performed. Macroscopically they are firm, well-demarcated, nonencapsulated lesions. The characteristic histologic findings are similar to those for granular cell tumors of other locations.

Chordoma

Chordomas of the sellar region, clivus, and sphenoid bone account for about half of all chordomas, corresponding to the most cranial portion of the notochord. Visual-field changes are the most common presentation, and bony destruction of the sella and clivus is frequent.

The *myxoid multilobular neoplasm* has characteristic histologic features. It is composed of cords of physaliferous cells (Fig. 15-14), with vacuoles that contain mucin. The extracellular matrix is alcian-blue positive.

Germ Cell Tumors

Germ cell tumors are usually located in the midline and are derived from residual germ cells. Germ cell tumors of the pituitary are rare and include germinomas (Fig. 15-15), embryonal carcinomas, endodermal sinus tumors, teratomas, and choriocarcinomas. The histologic findings are similar to the corresponding tumor found elsewhere.
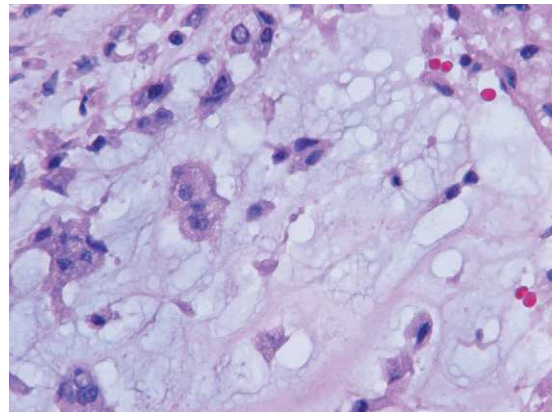
Figure 15-14. Chordoma. The neoplasm derived from notochord, and has similar histologic appearance.

Plasmacytoma

A difficult histologic differential diagnosis from pituitary adenoma is a *plasmacytoma* of the sellar region (Fig. 15-16). The majority of sellar plasmacytomas will evolve into systemic multiple myeloma.

Hamartoma (Choristoma)

Hamartomas or *choristomas* are rare and usually located in the hypothalamus. Hamartomas are lesions attached to the tuber cinereum or the mamillary bodies, located usually behind the pituitary stalk. They may present with visual-field defects or
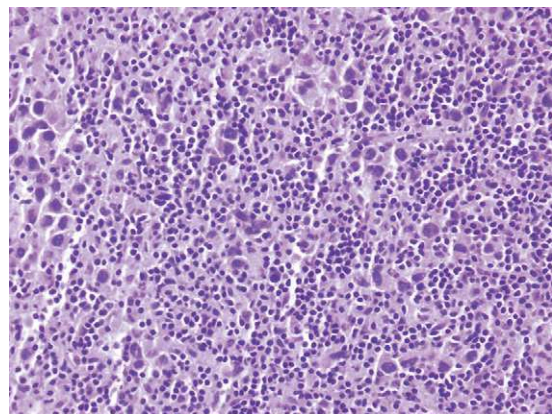
Figure 15-15. Germinoma. The picture shows a densely cellular tumor composed mostly of lymphocytes interspersed with some much larger cells having clear cytoplasm and prominent nucleoli.
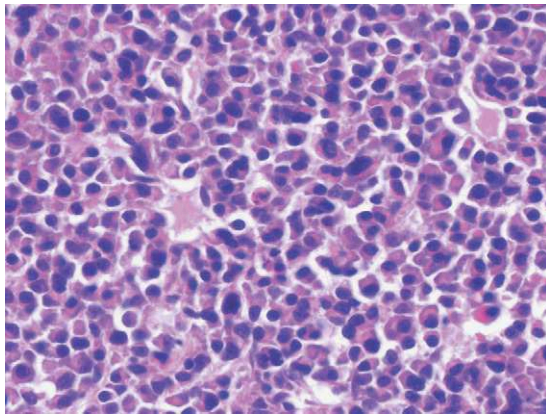
Figure 15-16. Plasmacytoma. This is a rare neoplasm of the pituitary, which usually occurs in association with systemic multiple myeloma. The picture shows pleomorphic atypical plasma cells.

endocrinologic disturbances such as precocious puberty. The association of neuronal hamartomas and growth-hormone-producing pituitary adenomas has suggested that the growth hormone releasing factor has a paracrine effect. Hamartomas and choristomas are firm, round masses formed by mature neurons in clusters separated by unmyelinated axons.

Other Tumors

Other primary neoplasms in the region of the sella turcica are rare and include meningiomas, paragangliomas, oligodendrogliomas, ependymomas, gliomas, esthesioneuroblastomas, histiocytosis X, fibromas, sarcomas, giant cell tumors of bone, osteosarcomas, melanomas, vascular tumors, and lymphomas, amongst others (see Table 15-4).

Appendix

Brief Survey of Neuropathologic Techniques

Homa Adle-Biassette, Jacqueline Mikol, and Jacques Poirier

The practice of neuropathology depends on a number of specialized techniques, most of which are derived from those used in general pathology and histology.

Methods of Removal

Autopsy

Autopsy of the nervous system cannot be regarded as an isolated procedure; findings should be correlated with those of the general autopsy. It must be performed without delay, since the central nervous system (CNS) is very rapidly altered by postmortem autolysis. Since the CNS tissue is delicate and enclosed within hard bony structures (skull and spine), dissection is complex and requires special training.

Removal of the Spinal Cord

The spinal cord can be approached after evisceration (anterior approach) or via the posterior approach, at the beginning of the autopsy, when the entire length of the spinal cord and dorsal root ganglia need to be examined. These two procedures include the following steps:

A. Posterior Approach
1. The body is turned face down.

2. The skin and underlying soft tissues are incised along the spinous processes from the external occipital protuberance to the base of the sacrum.
3. The soft tissues are freed, first with the knife and then with the scraper, to bare the vertebral laminae on either side of the spinous processes. The prosector should angle the blade of the saw so as to cut as far laterally as possible from the posterior spinous processes.
4. The vertebral laminae are then sectioned along the entire length of the spine.
5. The spinous processes, together with their connecting tendinous aponeuroses, are lifted and pulled off throughout their entire length.
6. The cervical spinal cord is sectioned with a scalpel as high up as possible.
7. The spinal cord is then carefully removed by lifting the dura at each segmental level. This is done by working carefully from the top down, using an ordinary forceps, while systematically cutting the spinal nerve roots and dissecting outer dorsal root ganglia down to the cauda equina with a scalpel or scissors.

B. Anterior Approach
The bodies of the vertebrae are peeled off and the pedicles of the vertebrae are cut along the length of the cord. The anterior vertebral arch

is then lifted and then the spinal cord is removed as described previously.

Once the cord is removed, the dural sheath is opened longitudinally with scissors to permit better penetration by the fixative and thus avoid possible shrinkage and distortion of the underlying cord.

The spinal cord is then laid out flat and immersed in 10% formalin.

Removal of the Brain

Removal of the brain entails the following steps:

1. The body is turned face up.
2. The scalp is incised along a coronal plane from one pinna to the other.
3. The scalp is freed and reflected forward to the supraorbital ridges and backward to the external occipital protuberance.
4. The cranial cavity is pried open with the electric saw.
5. The skull cap thus obtained is lifted by exerting firm traction from front to back, using the wedge of the autopsy hammer inserted in the center of the cut frontal bone. Normally the dura should remain intact.
6. The dura is incised first longitudinally (approximately 2 cm on either side of the midline and from front to back) and then in a semicircular fashion, along the edge of the bony cut.
7. The anterior attachment of the falx cerebri is incised down to the crista galli.
8. The olfactory bulbs are lifted off and gently dissected off the base of the skull.
9. The frontal lobes are very gradually raised and freed from front to back by systematically sectioning the anterior connecting structures (optic nerves, internal carotid arteries, pituitary stalk) with scissors.
10. The tentorium cerebelli is incised along its attachment at the edge of the upper border of the petrous bone.
11. The posterior connecting structures (cranial nerves, vertebral arteries) are sectioned while, with the left hand, the prosector supports the brain, which will otherwise tend to topple backward.
12. The brain is then delivered; with one hand the prosector continues to support the brain while placing the palm of the other hand on the ventral surface of the pons, inserting the index finger to

the left and the middle finger to the right of the medulla. If the spinal cord has not been removed beforehand, it will, of course, be necessary to section the upper cervical cord with a long, thin scalpel. The cut end of the medulla is then delivered, following which the prosector inserts two fingers under each cerebellar hemisphere. With the one hand the prosector is then able to lift the entire brain, and it only remains for the dura of the posterior fossa to be incised for the brain to be completely freed.

13. The brain is weighed.
14. A string is tied around the basilar artery and the brain is immediately immersed in 10% formalin, its base facing up, within a receptacle large enough to allow it to float and thus avoid future distortion resulting from possible postmortem compression. If meningeal swabs or portions of the brain itself need to be cultured (particularly in case of suspected infectious disease), specimens should be secured before immersion of the brain in formalin. Similarly, if the case is part of a protocol, selected samples should be taken and, if necessary, frozen before fixation.

Removal of the pituitary gland is also part of any routine autopsy.

Removal of Portions of the Peripheral Nervous System and Samples of the Skeletal Musculature

The removal of samples of skeletal muscle and peripheral nerves is both easy and essential, although it is well-known that, because of various artifacts, histopathologic examination of autopsy material gives less valuable information than examination of biopsies. In obtaining these samples it is, of course, necessary to avoid multiple skin incisions and disfigurement of the body.

Special Procedures

Removal of the spinal cord, brain, and samples of peripheral nervous system and of skeletal musculature is part of a complete routine autopsy. However, in some cases this must be supplemented by the examination of certain areas of the body that are not normally scrutinized in a routine autopsy procedure. This includes, for example, removal of the eyes, examination and sampling of the base and the vault of the skull, removal of the inner ear in

the temporal bone, and removal en bloc of the cervical spine to include the vasculature of the neck. It is crucial to stress that special consent for research must be obtained, if necropsy study of these areas is to be performed.

Surgical Specimens

Neurosurgical specimens must be immediately placed in fixative after their removal by the neurosurgeon.

Rapid sectioning of frozen tissue and smear preparations permit a general diagnostic assessment to be made within a few minutes. This service can be very useful to the surgeon, so long as the interpretative shortcomings of the procedure are recognized by all involved.

Biopsy Procedures

Muscle Biopsy

Muscle biopsy is a minor surgical procedure, but it is important to stress the strict and meticulous technical care with which it must be performed (see Chap. 13). Muscle tissue is indeed very delicate, and if it is not removed with all necessary precautions the correct interpretation of histologic lesions may be considerably hampered by the presence of numerous artifacts (see Chap. 13). The operation is performed under local anesthesia, care being taken not to inject the local anesthetic beneath the level of the investing aponeurotic fascia. The incision must be generous enough to permit easy dissection of the muscle. After the deep fascia and perimysium have been incised, the muscle is dissected by following the plane of cleavage of the muscle bundles in a direction parallel to that of the fibers. A segment of muscle measuring about 2 cm in length by 1 cm in thickness (smaller in young children) is then isolated, care being taken to avoid traction, and sectioned at either end (Fig. A-1).

Peripheral Nerve Biopsy

Biopsy of a sensory peripheral nerve (see Chap. 14) is most commonly performed on the sural nerve in its retromalleolar portion. It may also be done on the musculocutaneous (superficial peroneal) nerve, at the junction of the middle and inferior thirds of the lateral surface of the lower leg. This permits concomitant sampling of the peroneus brevis muscle. In the latter case, a skin incision is made 1 cm anterior to the line that joins the head of the fibula to the external malleolus (Figs. A-2A and B). Sampling of a whole nerve segment measuring approximately 2 cm in length, (see Fig. A-2A) or of a number of fascicles only (see Fig. A-2B), must be done by sectioning it proximally first. Peripheral nerve biopsy causes permanent hypoesthesia of the dorsum of foot and sometimes paresthesias.

Brain Biopsy

Brain biopsy in non-neoplastic diseases is performed only in highly selected cases. This is a

A   **B**
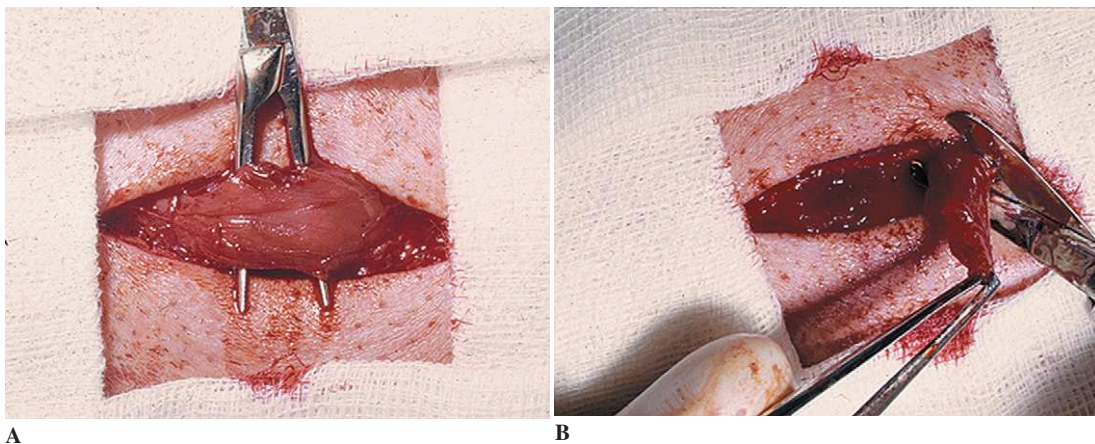
Figure A-1. Muscle biopsy. **A,** Dissection and isolation. **B,** Removal of muscle fragment.
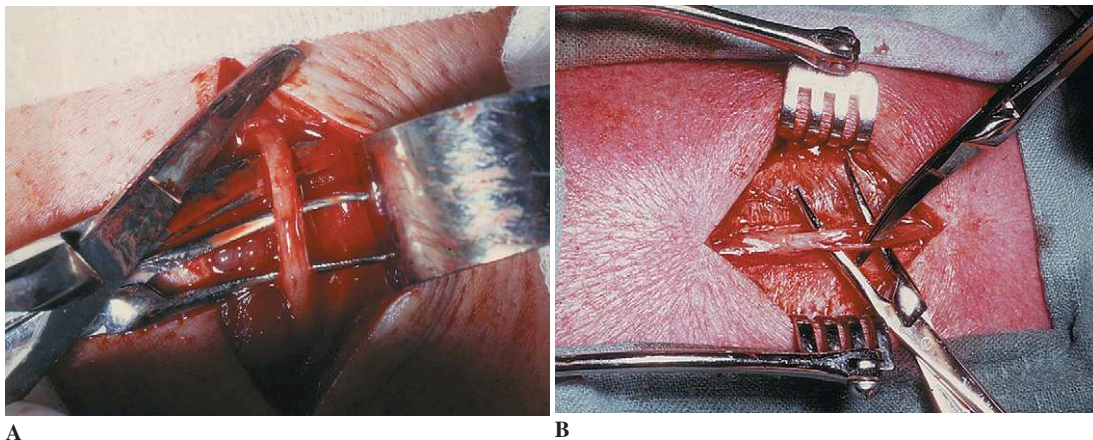
Figure A-2. Peripheral nerve biopsy. **A,** Dissection of a fragment of the superficial branch of the musculocutaneous nerve of the leg. **B,** Removal of nerve segment.

neurosurgical procedure. After administration of the local anesthetic and incision of the scalp, a small disc of bone is drilled with the lobotomy trephine, the dura is incised, and a small fragment of cortex and underlying white matter is removed with the scalpel or a cutting curette. Following this procedure the bone disc is replaced and the scalp is closed. The biopsy is most often taken from the right frontal or occipital lobe. The risk of hemorrhage, infection, reactive edema, or post-traumatic epilepsy is very limited.

Stereotactic Biopsy

Stereotactic biopsy samplings are obtained with a trocar after a series of guidemarks have been obtained by CT scan or MRI. The indications for stereotactic biopsy, most often involve expanding space-occupying lesions, especially tumors.

Other Biopsy Procedures

In some neurologic disorders, particularly neurolipidoses, rectal biopsy is sometimes performed to examine the ganglion cells of Meissner's plexus. Likewise, it is possible to examine these structures in the appendix. Skin and conjunctival biopsies may also provide additional information in some cases (e.g., capillary blood vessel walls, terminal nerve endings, cellular inflammatory infiltrates). Skin biopsy can also be used to obtain fibroblast cultures, allowing, in many cases, genetic analysis.

Cerebrospinal Fluid Cytologic Examination

Cytology is a simple and rapid method of diagnosis. Cytologic study allows for the study of neoplastic and inflammatory processes spreading through the CSF pathways.

Fixation of Tissues

Formalin is the almost universal fixative used in neuropathology. The most frequently employed formalin solutions are those at 10%. Ten percent formalin is prepared by mixing 10 ml of commercial formalin with 90 ml of water. Neutral formalin (calcium formalin) is often recommended and is obtained by pouring powdered calcium carbonate into the fixative container. An alternative method is the use of marble chips in the formalin solution. Buffered formalin-zinc is frequently used for tumors and alcohol-formalin-acetic acid for muscle.

The amount of fixative to be used depends on the amount of tissue to be fixed and should correspond to approximately 15 to 20 times the volume of tissue. Thus, for the brain as a whole, 5 to 6 liters of a 10% formalin solution is required for optimum results; the fixative may be changed periodically.

Good fixation requires a minimum amount of time, depending on the size of the tissue (e.g., 2–3 weeks for a whole brain). On the other hand, the preservation of tissues in formalin is almost indefinite, provided that the fluid—which turns yellow

with age—is changed from time to time and provided that the container is well-sealed to avoid evaporation. Fixation that has been prolonged for a considerable time will jeopardize some staining procedures and immunohistochemical techniques.

Gross Examination of the Central Nervous System

Gross dissection of the CNS (brain and spinal cord) is most often performed only after two to three weeks of formalin fixation, though some laboratories prefer to cut the brain sooner. Fresh tissue for microbiological, toxicological, or molecular studies or for brain banking must be obtained before fixation at the time of autopsy.

Inspection of the Brain and Spinal Cord

The brain and spinal cord are carefully examined, and any abnormal features are recorded on schematic diagrams and photographed.

Brain Cutting

Usual Protocol

The usual protocol includes the following steps:

1. *Severing the cerebral hemispheres from the brainstem*. The arachnoid membrane, which usually obscures the structures of the interpeduncular fossa and the floor of the third ventricle, is first delicately cleared with forceps or fine scissors. The blood vessels of the circle of Willis are then dissected and the rostral part of the midbrain through the cerebral peduncles is divided with a scalpel along a plane parallel to the base of the brain.
2. *Coronal hemispheric slices*. The brain is placed on a board, with the base facing the prosector and the occipital lobes to the right. The first section is through the mamillary bodies; all subsequent sections are absolutely parallel coronal slices approximately 1 cm thick from the frontal to the occipital poles (Figs. A-3 and A-4, pp. 370, 371).

3. *Horizontal sections through the brainstem and cerebellum*. Without separating the cerebellum from the brainstem, horizontal sections approximately 1 cm thick are cut from the cerebral peduncles to the medulla (Fig. A-5, p. 372). In some laboratories the preferred practice is to disconnect the cerebellum from the brainstem by cutting through the cerebellar peduncles before proceeding to the horizontal sections of the brainstem. The cerebellar hemispheres are cut in the sagittal plane in serial parallel sections at 0.5 cm intervals, beginning at the vermis and then proceeding to the right and left of midline.
4. *Transverse sections through the spinal cord*. The spinal cord is placed flat on a board and transverse sections, approximately 1 cm thick, are made using a fresh razor blade held by forceps (Fig. A-6, p. 374).
5. *Documentation*. After the various hemispheric, brainstem, and spinal cord slices have been examined with the naked eye and a magnifying glass, the lesions are recorded on standard stenciled diagrams outlining the main areas of the central nervous system and gross photographs are taken.

Sectioning in the Axial Plane of Computerized Tomography or MRI

In some cases it may be of interest to compare axial CT scans or MRI images to neuropathologic data. The brain is then sectioned in the same plane as by imaging.

Histologic Sampling

After the slices have been examined grossly, the tissue is sampled for histologic study. In making this selection, the neuropathologist is guided by the clinical data, the general autopsy findings, the gross study of the slices, and the type of histologic technique to be applied to the tissues. The samples are then carefully identified and labeled.

Embedding, Sectioning, and Staining Methods

The indications, advantages, and disadvantages of the various embedding, sectioning, and staining

A

B

C
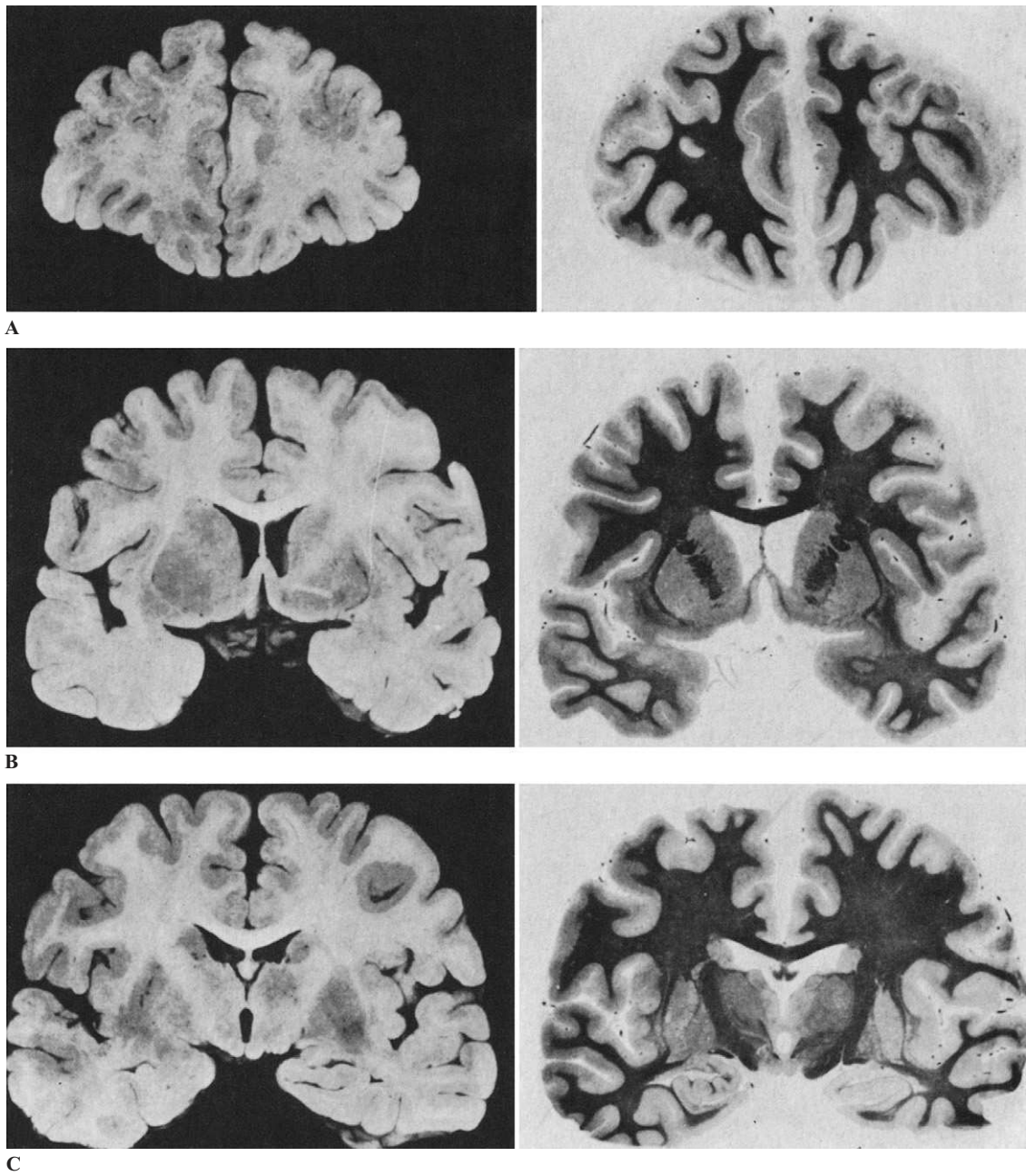
Figure A-3. Coronal sections through the cerebral hemispheres: Gross appearance after fixation (*left*); myelin stain of corresponding slices after celloidin embedding (*right*). **A**, Frontal poles. **B**, Section through the rostral portion of the basal ganglia. **C**, Section through the mamillary bodies.

techniques are reviewed here solely in the context of neuropathologic practice. For details on embedding and sectioning techniques, the reader is referred to general reference works on histologic methods. Table A-1 (p. 375) provides a listing of stains that can be used with paraffin embedding, celloidin embedding, and frozen sections.

Paraffin Embedding

Advantages

In most neuropathology laboratory, paraffin embedding is the embedding method of choice for autopsy and biopsy samples. It is rapid and
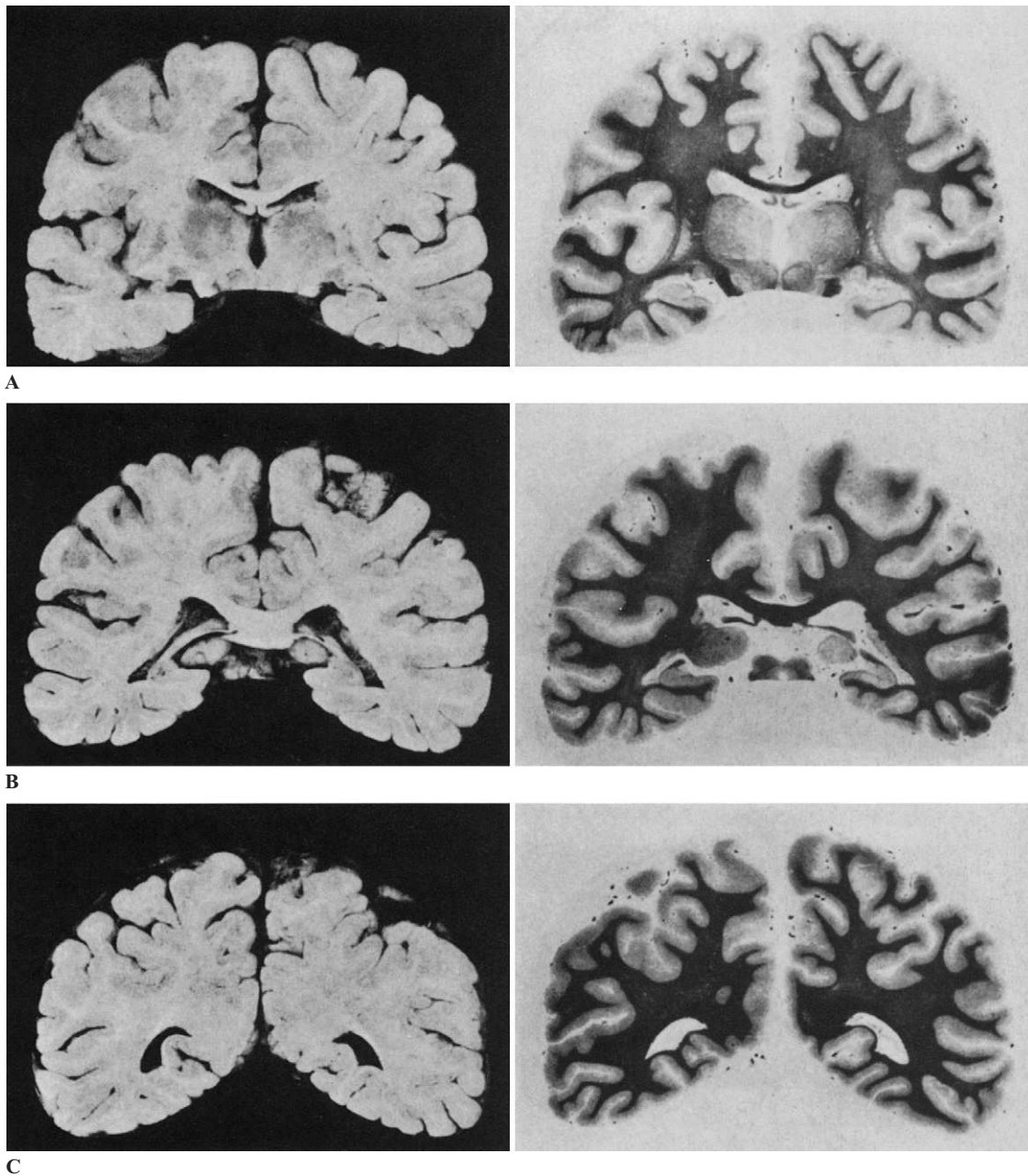
Figure A-4. Coronal sections through the cerebral hemispheres: Gross appearance after fixation *(left)*; myelin stain of corresponding slices after celloidin embedding *(right)*. **A**, Section through the red nuclei, lateral geniculate bodies, and thalami. **B**, Section through the splenium of the corpus callosum, pulvinars, and trigones. **C**, Posterior section through the occipital horns.

allows for relatively thin sections (5–7 µm) as well as step serial sections. Many stains and immunostains can be performed on paraffin sections. It is now also possible to embed in paraffin large blocks of brain tissue and cut "giant" (whole-brain) sections.

Disadvantages

Paraffin embedding requires preliminary treatment with alcohol and toluene, which are lipid solvents. It requires that the tissues be heated during part of the procedure in an oven at a temperature of 56°C
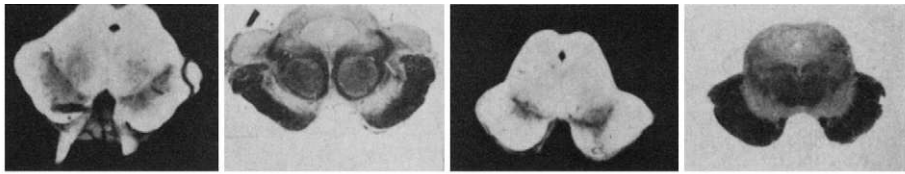
A

B
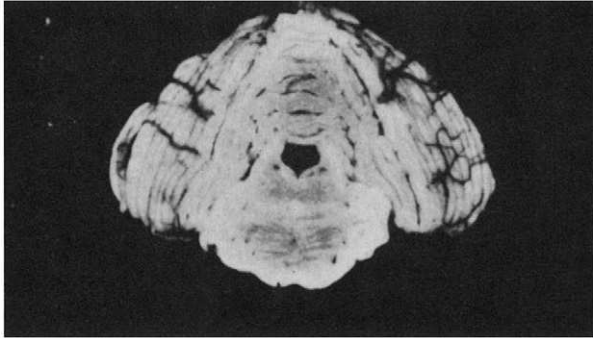
C
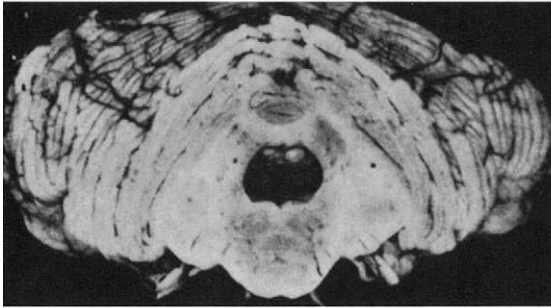
D
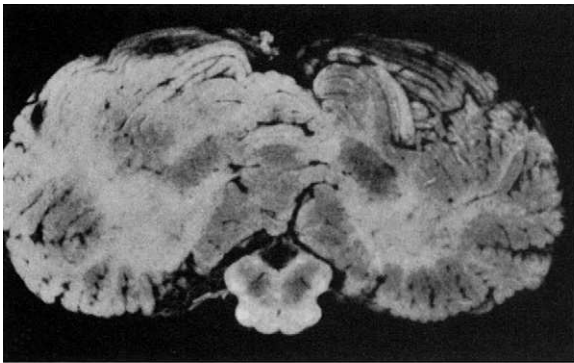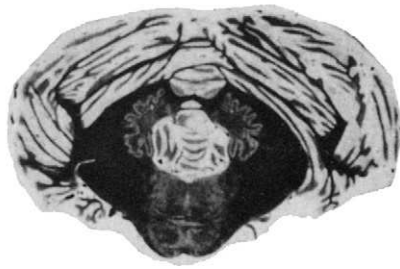
E
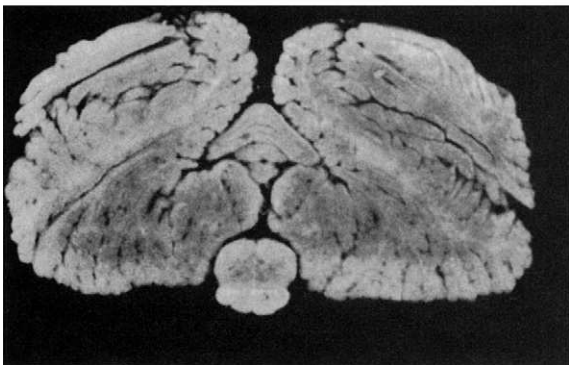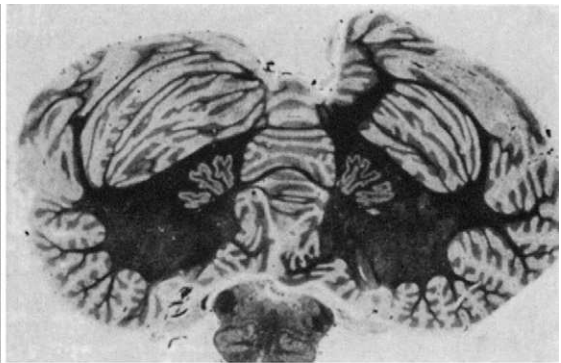
F
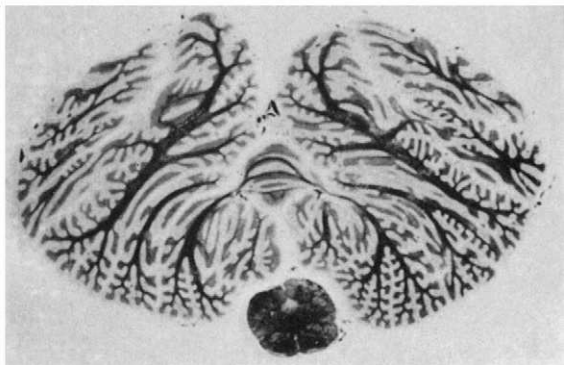
Figure A-5. Coronal sections through the brainstem and cerebellum: Gross appearance after fixation *(left)*; myelin stain of corresponding slices after celloidin embedding *(right)*. **A**, Rostral portion of the midbrain (cerebral peduncles, red nuclei, superior corpora quadrigemina, and exits of third cranial nerves). **B**, Caudal portion of the midbrain (dentatorubral decussation, inferior corpora quadrigemina). **C**, Upper pons and superior cerebellar vermis. **D**, Midpons and cerebellar hemispheres with dentate nuclei. **E**, Upper medulla and cerebellar hemispheres with dentate nuclei and inferior vermis. **F**, Lower medulla and inferior portion of cerebellar hemispheres.

(for the paraffin to be melted). Nervous tissue tolerates this level of temperature poorly, and this results in some artifacts.

Celloidin Embedding

Advantages

Celloidin embedding used to be the method of choice in neuropathology, and very few laboratories around the world still use it. It permits the embedding and sectioning of very large blocks, such as a whole cerebral hemisphere or even an uncut whole brain. The embedding process is very slow and takes place at room temperature, reducing artifactual changes. It provides sections that can be handled easily without having to adhere to the slides. Serial sections can be performed to best advantage.

Disadvantages

The procedure is time-consuming and expensive. At present, celloidin is not available in many countries and its use has been prohibited for safety reasons (i.e., mixture with explosive ether alcohol).

Frozen Sections

Advantages

In the preparation of frozen sections the tissues are not processed through fat solvents, thus preserving many cell constituents that are otherwise destroyed by paraffin or celloidin embedding and thereby permitting the application of special techniques (histochemistry, histoenzymology, immunocytochemistry). Frozen sections can be examined under the microscope very soon after the tissue is obtained (i.e., after a few minutes); this is of practical importance when rapid histologic diagnosis is required (e.g., in intraoperative consultations of brain biopsies).

Disadvantages

Frozen sections are usually not as thin as those obtained after paraffin embedding. The technique also is fraught with its own set of artifactual problems, and the preparations are less permanent than embedded specimens.

Special Techniques

Electron Microscopy

For electron microscopy, immediate fixation is necessary. This is done with a buffered glutaraldehyde in solution at 0°C, followed by postfixation in osmic acid. The complex techniques involved in the processing of tissue for electron microscopy are beyond the scope of this manual.

Immunohistochemistry

All immunohistochemical methods have as a common aim the visualization on histologic sections of antigenic sites that have become immunoreactive with antibodies with which the sections have been incubated. These techniques may be equally applied to dissociated cells, as in the CSF. There are numerous technical variants that are based on the demonstration of different antigens. One may resort either to immunofluorescence or to immunoenzymatic techniques. Recent progress in immunologic procedures has resulted in the current availability for immunohistochemical diagnosis not only of the usual antibodies obtained with polyclonal antisera, but also of numerous monoclonal antibodies obtained by the hybridoma technique. The specificity of monoclonal antibodies may sometimes be superior to that of polyclonal antisera, but their sensitivity may be inferior. Many procedures may be used to retrieve the antigens. Immunohistochemical methods have replaced many of the traditional staining methods used in the past (see Table A-1).

A

B

C

C_2

C_6

T_6

L_2

L_5

S_2
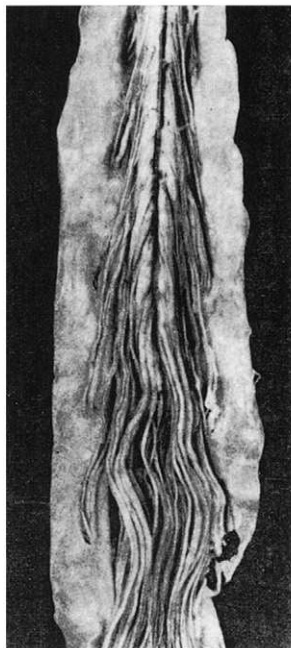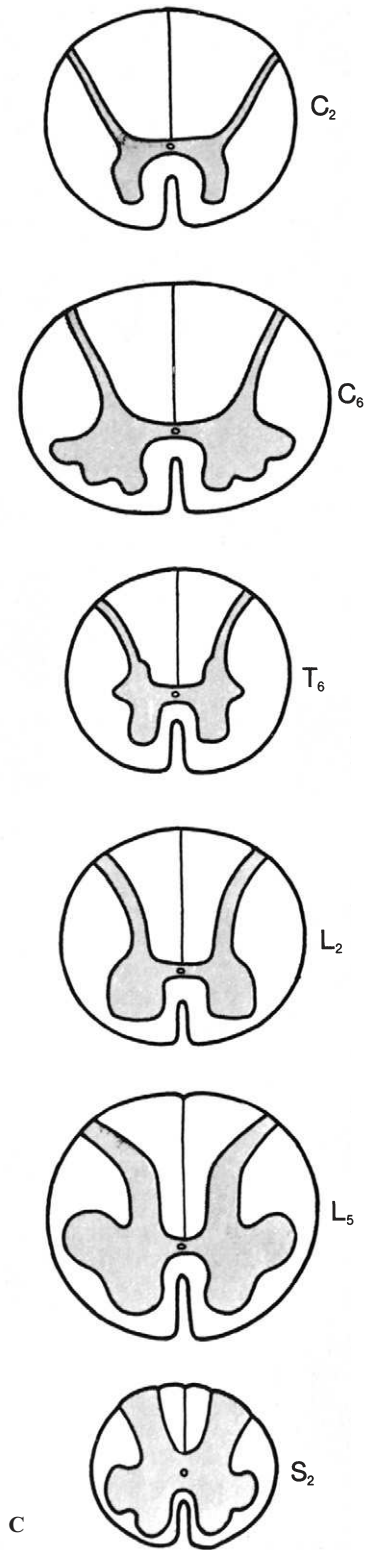
Figure A-6. Gross appearances of the spinal cord. **A**, Cervicothoracic cord. Note the thin thoracic roots (except for T1), compared to the cervical roots. **B**, Lower part of spinal cord. Note exits of L1 roots from the dura at the level of the conus medullaris. **C**, Diagrammatic depiction of the gray and white matter of the spinal cord sectioned at various levels.

Table A-1. Traditional Staining Methods

			Paraffin	Celloidin	Frozen Section
General Histological		Hematoxylin-eosin (H and E)	++	++	++
Stains		Masson trichrome	+	−	−
		Van Gieson stain	+	+	+
Nerve Cell Stains	Nissl bodies	Thionin (Nissl variant)	±	++	−
		Cresyl violet	++	+	++
	Neurofibrils	Bielschowsky	±	−	++
		Gallyas	++	−*	+
	Axons	Bodian	++	±	−
		Gros	−	−	++
Myelin Stains		Loyez	±	++	+
		Woelcke	+	++	++
		Luxol fast blue (LFB)	++	+	+
Glial Cell	Astrocytes	Hortega lithium carbonate	−	−	++
Stains*		Holzer	+	−	++
		Mallory *PTAH*	+	+	+
	Microglia	Silver carbonate	−	−	+
Connective and	Collagen fibers	Masson trichrome	+	−	−
Vascular Tissue		Van Gieson	+	+	+
Stains	Reticulin fibers	Perdrau; Wilder; Gordon-Sweets; Gomori; Laidlaw; Foot	++	±	−
	Elastic fibers	Orcein; Weigert-Hart; Verhoeff; resorcin-fuchsin	++	+	+

PTAH-phosphotungstic acid/hematoxylin.
* Traditional methods, now largely supplanted by immunocytochemistry.

In-Situ Hybridization

In-situ hybridization refers to the utilization of nucleic acid probes (DNA or RNA) to demonstrate and localize within cells or tissues nucleic acid sequences that show base pairing with the probe. The probes used are most often double-stranded DNA, less often single-stranded DNA or messenger RNA. Marking of the probes may be affected with radioactive isotopes, such as ^{3}H, ^{32}P, or ^{35}S, or with nonradioactive compounds, such as biotin ("cold probes"). With the former, demonstration is made by autoradiography; with the latter, by different means, for example, by the avidin-biotin complex technique. Counting the silver grains in autoradiographs allows semiquantitative analysis.

Histoblot and PET Blot

Histoblot and paraffin embedded tissue (PET) blot are mainly used in prion protein research. Based on a combination of immunohistochemistry and Western blot, they allow sensitive detection of the scrapie prion protein isoforms (PrP^{Sc}) and the analysis of their general distribution in different areas of the central nervous system. A nitrocellulose membrane is used instead of a glass slide as a mount for tissue sections. This porous membrane allows optimal proteolysis of the cellular isoform of the prion protein (proteinase K) and protein denaturation (guanidine thiocyanate), enhancing the immunoreactivity. Histoblot was at first described using cryostat sections but PET sections can also be performed on processed tissue. Both are more sensitive than immunohistochemistry, which, on the other hand, offers better cellular and subcellular resolution.

Other Techniques

Neurochemical studies must be performed on fresh, unfixed material, for example, biopsy samples or necropsy tissue that are frozen without delay.

For virologic studies, particularly when intended for tissue culture, sampling is performed in a sterile fashion on the brain in situ, after aseptic removal of the skullcap and dura.

Artifacts

Neural tissue may display various artifacts. These may be caused by terminal changes (i.e., terminal circulatory and asphyxial disturbances), the conditions of removal and fixation, or embedding, sectioning, and staining procedures.

Gross Artifacts

Large bullous cavities with clear-cut edges ("Swiss-cheese artifact"), visible to the naked eye, are the result of postmortem putrefaction due to the proliferation of gas-forming organisms consequent to inadequate or late fixation (Fig. A-7).

Inadequate fixation is likewise responsible for the pinkish appearance (pink spots) and soft consistency of the white matter when the formalin solution has been of insufficient concentration. Conversely, fixation that is greater than required, either because the formalin was excessively concentrated or because the duration of fixation was unduly prolonged, may be responsible for a yellowish, parchment-like appearance of the cortex. Both defects make the application of most histologic techniques difficult or impossible.

The picture of congestion with vascular dilatation is most frequently the result of terminal asphyxial disturbances. The so-called "respirator brain" is swollen and soft and cannot be fixed or studied histologically in a meaningful manner.
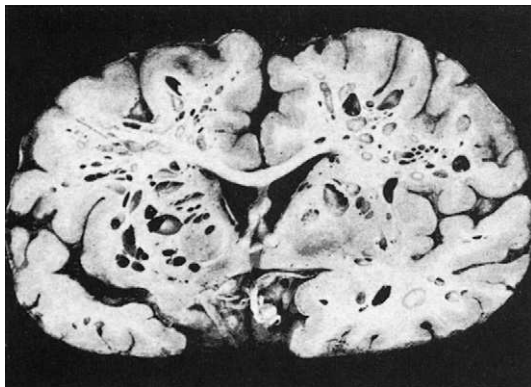
Figure A-7. Gas-forming bullae ("Swiss-cheese brain") due to inadequate fixation.
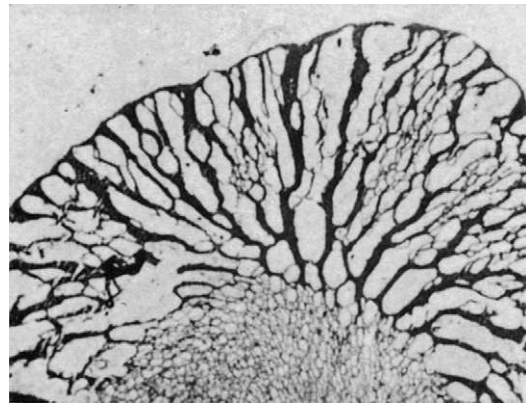
Figure A-8. Microscopic picture of multiple cavitations resulting from freezing artifact.

Microscopic Artifacts

All the light microscopy artifacts encountered in general histology can also be seen in neuropathology. Some, however, are more specific to brain sections.

Multiple microscopic elongated cavities, often predominating in the cortex, are sometimes seen as the result of excessive freezing of the tissues (Fig. A-8).

Nerve cell retraction, with clear pericellular spaces, is very frequently seen in paraffin embedded tissues and is related to the temperature to which the paraffin has been heated. The same applies to the apparent dilatation of the perivascular spaces, which need to be differentiated form possible edema.

Dark neurons result form neuronal retraction with nuclear shrinkage and basophilia. They are frequently found in material removed by cerebral biopsy and are related to the traumatizing conditions of tissue removal or to over-rapid fixation.

Pale, ballooned neurons may be caused by excessive washing of the nervous tissue fragments with water before fixation. An artifact consisting of cellular pallor with conglutination of the neurons in the cerebellar granular layer (*état glacé* or *conglutination artifact*) is the result of a postmortem autolytic change, particularly when the body has not been refrigerated properly; it predominates in the lateral lobes.

Bibliography

In view of the scope of this introductory manual, a full bibliography is not provided. For further details, the reader is referred to the following comprehensive texts and major reviews.

Pathology of the Central Nervous System

Davis RL, Robertson DM (eds.). Textbook of neuropathology. 3rd ed. Baltimore, Williams & Wilkins, 1997.

Ellison D, Love S. Neuropathology. London, Mosby, 1998.

Esiri MM, Oppenheimer DR. Oppenheimer's diagnostic neuropathology: A practical manual. Oxford, Blackwell, 1996.

Garcia JH (ed.). Neuropathology: The diagnostic approach. St. Louis, Mosby, 1997.

Graham DI, Lantos PL (eds.). Greenfield's neuropathology. 7th ed. London, Arnold, 2002.

Nelson JS, Parisi JE, Schochet SS. Principles and practice of neuropathology. St. Louis, Mosby, 1993.

Tumor Pathology

Bigner DD, McLendon RE, Bruner JM. Russell and Rubinstein's pathology of tumors of the nervous system. 6th ed. London, Arnold, 1998.

Burger PC, Scheithauer BW, Vogel FS. Surgical pathology of the nervous system and its coverings, 4th ed. New York, Churchill Livingstone, 2002.

De Angelis LM. Medical progress: Brain tumors. N Engl J Med 2001;344:114–123.

Ironside JW, Moss TH, Louis DN, Lowe JS, Weller RO. Diagnostic pathology of nervous system tumors. London, Churchill Livingstone, 2002.

Kleihues P, Cavenee WK (eds.). Pathology and genetics of tumors of the nervous system. Lyon, ARC Press, 2000.

Lopes MB, Vandenberg SR, Scheithauer BW. Histopathology, immunochemistry and ultrastructure of brain tumors. In: Kaye AH, Laws ER Jr (eds.). Brain Tumors. An Encyclopedic Approach. Edinburgh, Churchill Livingstone, 1995, pp. 125–162.

Trauma

Geddes JF, Whitwell HL. Head injury in routine and forensic pathological practice. In: Love S (ed.). Current Topics in Pathology: Neuropathology, Vol. 95. Berlin, Springer-Verlag, 2001, pp. 101–124.

Prion Diseases

Budka H, Aguzzi A, Brown P, et al. Neuropathological diagnostic criteria for Creutzfeldt-Jakob disease (CJD) and other human transmissible spongiform encephalopathies (prion diseases). Brain Pathol 1995;5:459–466.

DeArmond SJ, Ironside JW. Neuropathology of prion diseases. In: Prusiner SB (ed.). Prion Biology and Diseases. Cold Spring Harbor, NY, Cold Spring Harbor Laboratory Press, 1999, pp. 585–652.

Gambetti P, Parchi P, Peterson RB, Chen SG, Lugaresi E. Fatal familial insomnia and Creutzfeldt-Jakob disease: Clinical, pathological and molecular features. Brain Pathol 1995;5:43–51.

Ghetti B, Dloughy SR, Giaccone G, et al. Gerstmann-Sträussler-Scheinker disease and the Indiana kindred. Brain Pathol 1995;5:61–75.

Degenerative Diseases

Dickson DW. Neurodegeneration: The molecular pathology of dementia and movement disorders. Basel, Switzerland, ISN Neuropath Press, 2003.

Developmental Pathology

Crome L, Sterne J. Pathology of mental retardation, 2nd ed. Baltimore, Williams & Wilkins, 1972.

Friede RL. Developmental neuropathology, 2nd ed. New York, Springer-Verlag, 1996.

Larroche JC. Fetal and perinatal brain damage. In: Wigglesworth JS, Singer DB (eds.). Textbook of Fetal

and Perinatal Pathology, 2nd ed. Tokyo, Blackwell, 1998.

Inherited Metabolic Diseases

Scriver RC, Beaudet AL, Sly WS, Valle D (eds.). The metabolic bases of inherited disease. New York, McGraw-Hill, 2001.

Muscle and Nerve Pathology

Asbury AK, Thomas PK (eds.). Peripheral nerve disorders, 2nd ed. Oxford, Butterworth-Heinemann, 1995.

Bouche P, Vallat J-M. Neuropathies périphériques. Polyneuropathies & mononeuropathies multiples. Paris, Doin, 1992.

Bradley WG. Disorders of peripheral nerves. Oxford, Blackwell, 1972.

Carpenter S, Karpati G. Pathology of skeletal muscle, 2nd ed. Oxford, Oxford University Press, 2001.

De Recondo J, De Recondo AM. Pathologie du muscle strié. De la biologie cellulaire à la thérapie. Paris, Médecine-Sciences Flammarion, 2001.

Dyck PJ, Thomas PK. Peripheral neuropathy, 3rd ed. Philadelphia, WB Saunders, 1993.

Emery AEH. Neuromuscular disorders: Clinical and molecular genetics. Chichester, England, Wiley, 1998.

Engel AG, Franzini-Armstrong C (eds.). Myology. 2nd ed. New York, McGraw-Hill, 1994.

Karpati G (ed.). Structural and molecular basis of skeletal muscle diseases. Basel, Switzerland, ISN Neuropath Press, 2002.

Midroni G, Bilbao JM. Biopsy diagnosis of peripheral neuropathy. Boston, Butterworth-Heinemann, 1995.

Richardson EP Jr, De Girolami U. Pathology of the peripheral nerve. Philadelphia, WB Saunders, 1995.

Pituitary

Lloyd RV. Surgical pathology of the pituitary gland. In: Major Problems in Pathology, Vol. 27. Philadelphia, WB Saunders, 1993.

Scheithauer BW, Horvath E, Kovacs K, Lloyd RV. Tumors of the adenohypophysis. In: Solcia E, Kloppel G, Sobin LH (eds.). Histological Typing of Endocrine Tumors. (World Health Organization. International Histological Classification of Tumors), 2nd ed. Berlin, Springer Verlag, 2000, pp. 15–29.

Index

Note: Page numbers followed by "f" indicate figures; those followed by "t" indicate tables.